

UNCLASSIFIED

AD 281 851

*Reproduced
by the*

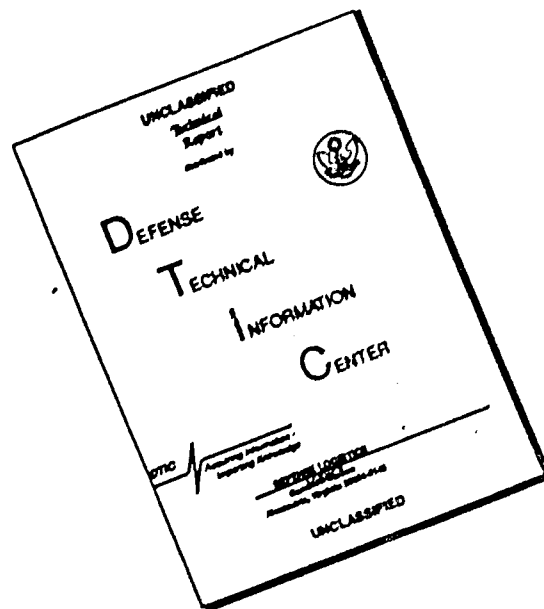
ARMED SERVICES TECHNICAL INFORMATION AGENCY
ARLINGTON HALL STATION
ARLINGTON 12 VIRGINIA



UNCLASSIFIED

NOTICE: When government or other drawings, specifications or other data are used for any purpose other than in connection with a definitely related government procurement operation, the U. S. Government thereby incurs no responsibility, nor an obligation whatsoever; and the fact that the Government may have formulated, furnished, or in any way supplied the said drawings, specifications, or other data is not to be regarded by implication or otherwise as in any manner licensing the holder or any other person or corporation, or conveying any rights or permission to manufacture, use or sell any patented invention that may in any way be related thereto.

DISCLAIMER NOTICE



THIS DOCUMENT IS BEST QUALITY AVAILABLE. THE COPY FURNISHED TO DTIC CONTAINED A SIGNIFICANT NUMBER OF PAGES WHICH DO NOT REPRODUCE LEGIBLY.

281 851

March 1962

Report No. 0411-10F

APPENDIXES A THROUGH G IN SUPPORT OF
STUDY OF MECHANICAL PROPERTIES
OF SOLID-ROCKET PROPELLANTS

Contract AF 33(600)-40314 S. A. No. 1

Period Covered:

30 January 1961 through 30 January 1962

Aerojet-General

CORPORATION

SOLID ROCKET PLANT • SACRAMENTO CALIFORNIA

COPY NO. 25

ASTIA

March 1962

Report No. 0411-10F

APPENDIXES A THROUGH G IN SUPPORT OF
STUDY OF MECHANICAL PROPERTIES
OF SOLID ROCKET PROPELLANTS

Contract AF 33(600)-40314 S. A. No. 1

Period Covered: 30 January 1961 through 30 January 1962

Aerojet-General CORPORATION
SOLID ROCKET PLANT . SACRAMENTO, CALIFORNIA

TABLE OF CONTENTS

APPENDIXES

Appendix

Analytical Determination of Generalized, Linear Viscoelastic Stress-Strain Relations From Uniaxial, Biaxial, and Triaxial Experimental Creep and Relaxation Data	A
Survey and Development of Methods for the Determination of Strains in Solid Propellants	B
Parameter Calculations of Simple Propellant Grains for Temperature Cycling, Pressurization, and Acceleration	C
Stress Analysis of Propellant Grains Using Displacement Equations	D
Finite Difference Solution of Ordinary and Partial Differential Equations	E
Studies Relating to Structural Analysis of Solid Propellants	F
Investigation of the Failure of Solid Fuels Under Combined Stresses	G

APPENDIX A

ANALYTICAL DETERMINATION OF GENERALIZED,
LINEAR VISCOELASTIC STRESS-STRAIN
RELATIONS FROM UNIAXIAL, BIAXIAL, AND
TRIAXIAL EXPERIMENTAL CREEP AND RELAXATION DATA

by

Harry H. Hilton
Professor of
Aeronautical and Astronautical Engineering
University of Illinois
Consultant, Aerojet-General Corporation

1. GENERALIZED LINEAR ISOTROPIC VISCOELASTIC STRESS-STRAIN RELATIONS

The stress-strain relations for a linear, isotropic, viscoelastic material at constant temperature can be decomposed into volumetric ones and deviatoric (change in shape) ones, which may be written in the respective forms

$$P'\{\sigma\} = Q'\{\epsilon\} \quad (1.1)$$

$$P\{S_{ij}\} = 2Q\{E_{ij}\} \quad (1.2)$$

where

$$\left. \begin{aligned} P &= \sum_{n=0}^r a_n \frac{\partial^n}{\partial t^n} & P' &= \sum_{n=0}^{r'} a'_n \frac{\partial^n}{\partial t^n} \\ Q &= \sum_{n=0}^s b_n \frac{\partial^n}{\partial t^n} & Q' &= \sum_{n=0}^{s'} b'_n \frac{\partial^n}{\partial t^n} \end{aligned} \right\} \quad (1.3)$$

The a_n , a'_n , b_n , and b'_n are related to the material properties and the r , r' , s , and s' depend upon the complexity of the actual material behavior.

The relations between the stress and strain deviators (S_{ij} and E_{ij}) and mean stress (σ) and mean strain (ϵ) are

$$S_{ij} = \sigma_{ij} - \bar{\sigma}_{ij} \sigma \quad (1.4)$$

$$E_{ij} = \epsilon_{ij} - \delta_{ij} \epsilon \quad (1.5)$$

with

$$3\epsilon = \epsilon_{ii} , \quad 3\sigma = \sigma_{ii} \quad (1.6)$$

The differential time operators P , P' , Q and Q' are generally unequal and functions of the material properties. These operators are also related to the complex shear and bulk moduli through their Fourier transforms. From creep and relaxation experimental data, it is considerably simpler to compute these complex moduli rather than the material property constants a_n , a'_n , b_n , and b'_n . Since the ultimate aim is to use the relations of Equations (1.1) and (1.2) in stress analysis, it matters little whether the operators P through Q' are known directly or if the corresponding complex moduli are determined. Either procedure is equivalent to the other and leads to identical results. Furthermore, in many problems where the elastic-viscoelastic analogy can be used,^{1,2,3,6,7,8,9} only the complex moduli need to be known.

Stress-strain relations, such as those of Equations (1.1) and (1.2), are fundamental ones since they represent the separate, basic changes in shape and in volume. Consequently, it is mandatory to determine both deviatoric and volumetric behavior. If uniaxial or multiaxial creep and/or relaxation experiments are conducted, which result in neither pure deviatoric nor pure volumetric changes, additional experimentation under either hydrostatic pressure or pure shear must be undertaken. As it will be shown subsequently, all pertinent material properties can be determined

from such pairs of experimental data, i.e. for example hydrostatic pressure and uniaxial tension or pure shear, or pure shear and uniaxial tension, etc. Each set of loading combinations must, however, be interpreted in terms of the fundamental deviatoric and volumetric stress-strain relations.

Linear viscoelastic behavior can be characterized in terms of generalized Kelvin or Maxwell models and either representation completely duplicates the other. Gross¹¹ has discussed in detail the equivalence of these various representations in terms of both differential and integral stress-strain equations and has formulated the various relations which describe the interchangeability of the various characterizations.

As a matter of convenience the generalized Kelvin model is chosen for the purposes of this paper. Depending on the particular material behavior, either of two types of generalized models shown in Figures 1 and 2 may be used. The number of constituent elements or parameters may be finite or infinite. In Model A (Figure 1) the behavior under constant load is characterized by an initial elastic deformation corresponding to the shear modulus G_0 (where $S_{ij}(0) = 2 G_0 E_{ij}(0)$) and a final ($t \rightarrow \infty$) finite deformation corresponding to a final shear modulus G_∞ (where $S_{ij}(\infty) = 2 G_\infty E_{ij}(\infty)$) given by

$$1/G_\infty = \sum_{n=0}^N (1/G_n) \quad (1.7)$$

The initial behavior of Model B, under a constant load is

identical to that of Model A, but the final ($t \rightarrow \infty$) deformations will be infinite. If the material is known to creep indefinitely then Model B should be used for its description. On the other hand if the material creeps only to a finite strain, then its behavior can be represented by Model A. An equivalent approach in terms of generalized Maxwell models can also be used and will lead to the same results. The above discussion has been directed toward deviatoric deformations (changes in shape) as described by Equation (1.2). A parallel approach can be presented for volumetric deformations by using Models A and B and replacing G_k by K_k (bulk moduli) and η_k by η_{vk} (volumetric viscosity).

2. COMPLEX MODULI FOR GENERALIZED MODEL A

If a stress deviator S_{ij} is applied to Model A then each individual element will be stressed by the same amount, but the corresponding strain deviators E_{ij} in each element will differ. The individual stress-strain relations for each element with time independent material properties can be written as follows

Elastic element

$$E_{ij}^e = S_{ij} / 2G_0 \quad (2.1)$$

Kelvin elements

$$E_{ij}^n = \frac{1}{2\eta_n} \int_0^t e^{(t'-t)/\tau_n} S_{ij}(t') dt' \quad (2.2)$$

where

$$\tau_n = \eta_n / G_n \quad (2.3)$$

The total deviatoric strain for Model A is given by the sum of the individual components, or

$$E_{ij} = \sum_{n=0}^N E_{ij}^n \quad (2.4)$$

and can be obtained directly from Equations (2.1) and (2.2).

The Laplace transform of a function $F(t)$ will be denoted by $\bar{F} = \bar{F}(p)$ and is defined by

$$\bar{F} = \int_0^{\infty} F(t) e^{-pt} dt \quad (2.5)$$

Taking the Laplace transform of Equation (2.4) yields

$$\bar{E}_{ij} = \bar{S}_{ij} / 2\bar{G} \quad (2.6)$$

where

$$\frac{1}{\bar{G}} = \frac{1}{G_0} + \sum_{n=1}^N \frac{1}{\eta_n} \left(p + \frac{1}{\tau_n} \right)^{-1} \quad (2.7)$$

If in Equation (2.7) the substitution $p = i\omega$ is made then $\bar{G}(p)$ becomes $\bar{G}(i\omega)$, the complex modulus. Equation (2.7) can be put in a more convenient form by reducing it to a common denominator and factoring the resulting numerator in terms of the roots β_n of the numerator polynomial. It can then further be reduced by partial fractions, so that Equation (2.7) becomes

$$\bar{G} = \frac{G_0 \prod_{n=1}^N (p + \beta_n)}{\prod_{n=1}^N (p + \alpha_n)} = G_0 \left[1 + \sum_{n=1}^N \frac{B_n}{p + \alpha_n} \right] \quad (2.8)$$

where $\beta_n = 1/\tau_n$ and the α_n and B_n are related to the G_0 , τ_n and η_n . In the elastic-viscoelastic analogy the equivalent shear modulus \bar{G} is used in either form (2.8) and there is no need, at this stage, to express the α_n and B_n in terms of the model constants G_0 , τ_n , and η_n . It is to be noted that Model A is always characterized by $2N + 1$ independent constants or parameters no matter which of the representations of Equation (1.2), (2.7) or (2.8) are used.

Similarly, an equivalent bulk modulus for Model A can be defined as

$$\bar{K} = \frac{K_0 \prod_{m=1}^M (p + \beta'_m)}{\prod_{m=1}^M (p + \alpha'_m)} = K_0 \left[1 + \sum_{m=1}^M \frac{B'_m}{p + \alpha'_m} \right] \quad (2.9)$$

and the stress-strain relation for viscoelastic volumetric deformation (1.1) in terms of Laplace transforms is

$$\bar{\epsilon} = \bar{\sigma} / \bar{K} \quad (2.10)$$

3. COMPLEX MODULI FOR GENERALIZED MODEL B

The stress-strain relations for the generalized Model B can be constructed in the same manner as was done in the

previous section except that the relation for the viscous element must be added to Equations (2.1) and (2.2). The viscous element stress-strain relations are

$$\dot{E}_{ij}^{N+1} = \frac{1}{2\eta_{N+1}} \int_0^t S_{ij}(t') dt' \quad (3.1)$$

The total strain deviator for Model B is given by Equation (2.4) if N is changed to N + 1. Again taking the Laplace transform with Equations (2.1), (2.2) and (3.1) substituted in Equation (2.4), one obtains

$$\frac{1}{\bar{G}} = \frac{1}{G_0} + \frac{1}{p\eta_{N+1}} + \sum_{n=1}^N \frac{1}{\eta_n} \left(p + \frac{1}{\tau_n}\right)^{-1} \quad (3.2)$$

If one again reduces Equation (3.2) to a common denominator and factors the numerator, and then reduces the result by partial fractions, the equivalent shear modulus can be written in the form

$$\bar{G} = \frac{G_0 p \prod_{n=1}^N (p + \beta_n)}{\prod_{n=1}^{N+1} (p + \alpha_n)} = G_0 p \sum_{n=1}^{N+1} \frac{B_n}{p + \alpha_n} \quad (3.3)$$

In the same fashion an equivalent bulk modulus for Model B becomes

$$\bar{K} = K_0 p \sum_{m=1}^{M+1} \frac{B'_m}{p + \alpha'_m} \quad (3.4)$$

In either of Equations (3.3) or (3.4) there are $2N + 2$ independent constants or parameters which represent the behavior of Model B.

It is to be noted that the foregoing model analysis applies to nonhomogeneous media as well where $G = G(x)$ and $K = K(x)$ with $x = x_i$, ($i = 1, 2, 3$) the space coordinates. In those cases where the moduli are time dependent as well as space dependent a piece-wise time analogy may be used in viscoelastic stress analysis^{6,7} and these moduli are represented by average space functions over small time intervals. Generally, for the sake of simplicity experimental determination of material properties are carried out on homogeneous specimen at constant temperature and results thus obtained can be readily applied, through proper interpretation, to nonhomogeneous materials at variable temperature.

4. MODEL FITTING TO CREEP AND RELAXATION DATA

Experimental data is generally collected for creep and/or relaxation conditions. In the creep test after an initial build-up the stress is held constant and the strain is measured. (Figure 3) In the relaxation test the procedure is reversed by the application of an initial strain (or deformation) and the measurement of stress. (Figure 4) In either case, the material properties in terms of \bar{G} and \bar{K} are determined from solving Equations (2.6) and (2.10) for the particular loading conditions and fitting them to the experimental data. The procedure will next be outlined in detail for several representative conditions.

4.1 UNIAXIAL RELAXATION FOR INCOMPRESSIBLE MATERIALS

Under uniaxial relaxation conditions the strain in the loaded direction is

$$\epsilon_x = \begin{cases} f(t) & 0 \leq t \leq t_0 \\ \epsilon_x^0 & t \geq t_0 \end{cases} \quad (4.1)$$

where $f(t)$ is a prescribed function indicated on Figure (4) and ϵ_x^0 is the constant value of the strain. Since most straining of specimens is usually conducted at a constant rate this function takes the form

$$f(t) = \epsilon_x^0 t / t_0 \quad (4.2)$$

All the stress components except σ_x vanish in the uniaxial test.

From Equations (2.6), (2.10), (1.3), (1.4), and (1.5) one obtains for the uniaxial incompressible relaxation test

$$\bar{\sigma}_x = \bar{E} \bar{\epsilon}_x \quad (4.3)$$

where $\bar{E} = \bar{E}(p) = 3 \bar{G}(p)$ is the incompressible equivalent Young's modulus.

The Laplace transform for the ϵ_x of Equation (4.1) is

$$\bar{\epsilon}_x = \int_0^{t_0} f(t) e^{-pt} dt + \frac{\epsilon_x^0}{p} e^{-pt_0} \quad (4.4)$$

and for the $f(t)$ of Equation (4.2) it becomes

$$\bar{\epsilon}_x = \frac{\epsilon_x^0}{t_0 p^2} (1 - e^{-t_0 p}) \quad (4.5)$$

The stress can be obtained from the inversion of Equation (4.3) and for the strain of Equation (4.5) it becomes

$$\frac{\sigma_x(t)}{\epsilon_x^0} = F(t) - H(t - t_0) F(t - t_0) \quad (4.6)$$

where $H(t-t_0)$ is a unit step function with properties

$$H(t-t_0) = \begin{cases} 0 & 0 \leq t \leq t_0 \\ 1 & t \geq t_0 \end{cases} \quad (4.7)$$

The function $F(t)$ is the inverse transform of $\bar{E}/t_0 p^2$ and can be obtained by reducing this product to partial fractions:

For Model A

$$F(t) = \frac{E_0}{t_0} \left[t + \sum_{n=1}^N \frac{B_n}{\alpha_n^2} (-1 + \alpha_n t + e^{-\alpha_n t}) \right] \quad (4.8)$$

For Model B

$$F(t) = \frac{E_0}{t_0} \sum_{n=1}^{N+1} \frac{B_n}{\alpha_n} (1 - e^{-\alpha_n t}) \quad (4.9)$$

where $E_0 = 3 G_0$ is the initial incompressible elastic Young's modulus.

The relaxation stress can then be obtained from Equations (4.6), (4.8) and (4.9).

For Model A

$$\frac{t_0 \sigma_x(t)}{E_0 \epsilon_x^0} = \begin{cases} t + \sum_{n=1}^N \frac{B_n}{\alpha_n^2} (-1 + \alpha_n t + e^{-\alpha_n t}) & 0 \leq t \leq t_0 \\ t_0 + \sum_{n=1}^N \frac{B_n}{\alpha_n^2} [t_0 \alpha_n + (1 - e^{\alpha_n t_0}) e^{-\alpha_n t}] & t \geq t_0 \end{cases} \quad (4.10)$$

For Model B

$$\frac{t_0 \sigma_x(t)}{E_0 \epsilon_x^0} = \begin{cases} \sum_{n=1}^{N+1} \frac{B_n}{\alpha_n} (1 - e^{-\alpha_n t}) & 0 \leq t \leq t_0 \\ \sum_{n=1}^{N+1} \frac{B_n}{\alpha_n} (e^{\alpha_n t_0} - 1) e^{-\alpha_n t} & t \geq t_0 \end{cases} \quad (4.11)$$

The constants B_n and α_n can be determined in the following fashion

- (a) From the test data decide whether Model A or B is to be used.
- (b) Select a value of N , which determines the size of the model and fixes the number of B_n and α_n to be determined.
- (c) In the region $t \geq t_0$, fit the proper Equation (4.10) or (4.11) to the relaxation data at least at $2N + 1$ points for Model A and at least $2N + 2$ points for Model B, or by the method of least squares.
- (d) Since Equation (4.10) can be written in the form

$$\frac{\sigma_x(t)}{\epsilon_x^0} = A_0 + \sum_{n=1}^N A_n e^{-\alpha_n t} \quad t \geq t_0 \quad (4.12)$$

and Equation (4.11) in the form

$$\frac{\sigma_x(t)}{\epsilon_x^0} = \sum_{n=1}^{N+1} A'_n e^{-\alpha_n t} \quad t \geq t_0 \quad (4.13)$$

the fitting of these equations to the relaxation data determines the A_n or A'_n and α_n .

(e) For Model A, the constants E_0 and B_n can be found from Equations (4.10) and (4.12) as

$$E_0 = A_0 - t_0 \sum_{n=1}^N \frac{A_n \alpha_n}{1 - e^{-\alpha_n t_0}} \quad (4.14)$$

$$B_n = \frac{A_n t_0 \alpha_n}{E_0 (1 - e^{-\alpha_n t_0})} \quad (4.15)$$

(f) For Model B, the constants E_0 and B_n are found

from the following equations:

$$E_0 B_n = \frac{A'_n t_0 \alpha_n}{e^{-\alpha_n t_0} - 1} \quad (4.16)$$

The modulus E can then be determined from Equation

(4.9) to be

$$E = p t_0 \sum_{n=1}^{N+1} \frac{A'_n \alpha_n}{(e^{-\alpha_n t_0} - 1)(p + \alpha_n)} \quad (4.17)$$

Now consider a uniaxial loading with $\epsilon_x = \epsilon_x^0$

($t \geq 0$) Substituting Equation (4.17) into

Equation (4.3) and inverting, yields

$$\frac{\sigma_x(t)}{\epsilon_x^0} = t_0 \sum_{n=1}^{N+1} \frac{A'_n \alpha_n e^{-\alpha_n t}}{e^{\alpha_n t_0} - 1} \quad (4.18)$$

Evaluation of Equation (4.18) at $t = 0$ gives the desired value of the elastic modulus E_0 , that is

$$\frac{\sigma_x(0)}{\epsilon_x^0} = E_0 = t_0 \sum_{n=1}^{N+1} \frac{A'_n \alpha_n}{e^{\alpha_n t_0} - 1} \quad (4.19)$$

From Equations (4.11) and (4.12), it can be seen that regardless of the value of N , under constant strain Model A relaxes in an infinite time to a stress value $\left[E_0 \left(1 + \sum_{n=1}^N B_n / \alpha_n \right) \epsilon_x^0 \right]$, while Model B relaxes to a zero stress.

4.2 UNIAXIAL RELAXATION OF COMPRESSIBLE MATERIALS

For the same uniaxial conditions as outlined in Section 4.1, but for a compressible material, the stress-strain relations (4.3) now changes to

$$\bar{\sigma}_x = \frac{3 \bar{G} \bar{\epsilon}_x}{1 + \bar{G} / \bar{K}} = \bar{E}_c \bar{\epsilon}_x \quad (4.20)$$

Most materials that exhibit creep and relaxation properties generally do so predominantly while changing shape, with comparatively little inelastic volumetric action. In particular, it has been experimentally observed that solid propellant grains do not ; rally creep volumetrically and consequently, if they are compressible, they are at most elastically

compressible. Under these conditions, the equivalent bulk modulus \bar{K} reduces to K_0 , the elastic bulk modulus. The compressible equivalent Young's modulus \bar{E}_c for a deviatorically viscoelastic and elastically compressible material then becomes

$$\bar{E}_c = \frac{3 K_0 \bar{G}}{K_0 + \bar{G}} \quad (4.21)$$

and from Equation (2.8) for Model A it is

$$\bar{E}_c = \frac{3 K_0 G_0 \prod_{n=1}^N (p + \beta_n)}{K_0 \prod_{n=1}^N (p + \alpha_n) + G_0 \prod_{n=1}^N (p + \beta_n)} = \frac{E_{co} \prod_{n=1}^N (p + \beta_n)}{\prod_{n=1}^N (p + \gamma_n)} \quad (4.22)$$

By partial fractions, Equation (4.22) can be reduced to

$$\bar{E}_c = E_{co} \left[1 + \sum_{n=1}^N \frac{C_n}{p + \gamma_n} \right] \quad (4.23)$$

The constants γ_n and C_n are related to K_0 , G_0 , α_n and β_n , but these identities are not needed since for viscoelastic stress analysis it is sufficient to know \bar{E} in terms of E_{co} , C_n and γ_n . The quantity E_{co} is the compressible initial Young's modulus and is defined by

$$E_{co} = \frac{3 K_0 G_0}{K_0 + G_0} \quad (4.24)$$

The repetition of the same process for Model B gives

$$\begin{aligned}
\bar{E}_c &= \frac{3K_0 G_0 p \prod_{n=1}^N (p + \beta_n)}{K_0 \prod_{n=1}^{N+1} (p + \alpha_n) + G_0 p \prod_{n=1}^N (p + \beta_n)} \\
&= \frac{E_{co} p \prod_{n=1}^N (p + \beta_n)}{\prod_{n=1}^{N+1} (p + \gamma_n)} = E_{co} p \sum_{n=1}^{N+1} \frac{C'_n}{p + \gamma_n} \quad (4.25)
\end{aligned}$$

with E_{co} defined by Equation (4.24). It must be understood that the β_n in Equation (4.22) are not equal to the β_n in (4.25) and that the same lack of equality exists for the γ_n in these two equations.

Furthermore, while the results of a relaxation test can determine the elastic Young's modulus E_{co} they will not yield values for the bulk modulus K_0 . The latter must be determined from separate hydrostatic compression or tension tests or from results of pure shear tests used in conjunction with uniaxial results.

Due to the similarity of Equations (4.23) and (4.25) to the corresponding uniaxial incompressible ones, the procedure previously outlined in Section 4.1 is identical in this case, except that now the unknowns are E_{co} , C_n or C'_n and γ_n . Once these constants are determined and K_0 is established from a separate test, then Equation (4.21) may be used to determine \bar{G} .

4.3 UNIAXIAL CREEP OF INCOMPRESSIBLE MATERIALS

Under uniaxial creep conditions, the stress in the loaded direction is (Figure 4)

$$\sigma_x(t) = \left\{ \begin{array}{ll} f_1(t) & 0 \leq t \leq t_0 \\ \sigma_x^0 & t \geq t_0 \end{array} \right\} \quad (4.26)$$

with all other stress components equal to zero. If the loading proceeds at a uniform rate then

$$f_1(t) = \sigma_x^0 t / t_0 \quad (4.27)$$

The Laplace transform of Equation (4.26) and (4.27) is again obtained in the manner as defined before by Equation (4.4) and is

$$\bar{\sigma}_x = \frac{\sigma_x^0}{t_0 p^2} (1 - e^{-t_0 p}) \quad (4.28)$$

The creep strain may be obtained from Equation (4.3) by substituting (4.28) into the latter and inverting the transforms, which results in

$$\frac{\epsilon_x(t)}{\sigma_x^0} = F'(t) - H(t-t_0) F'(t-t_0) \quad (4.29)$$

The function $F'(t)$ is the inverse transform of $(1/\bar{E} p^2 t_0)$ and is obtained by the partial fraction technique outlined previously.

For Model A

$$\frac{1}{\bar{E}} = \frac{1}{E_0} \left[1 + \sum_{n=1}^N \frac{D_n}{p + \beta_n} \right] \quad (4.30)$$

$$E_o t_o F'(t) = t + \sum_{n=1}^N \frac{D_n}{\beta_n^2} (-1 + \beta_n t + e^{-\beta_n t}) \quad (4.31)$$

For Model B

$$\frac{1}{E} = \frac{1}{E_o} \left[1 + \frac{D_{N+1}}{p} + \sum_{n=1}^N \frac{D_n}{p + \beta_n} \right] \quad (4.32)$$

$$E_o t_o F'(t) = t + \frac{1}{2} D_{N+1} t^2 + \sum_{n=1}^N \frac{D_n}{\beta_n} (-1 + \beta_n t + e^{-\beta_n t})$$

The creep strains can then be obtained from Equations (4.29), (4.31) and (4.33)

Model A

$$\frac{E_o t_o \epsilon_x(t)}{\sigma_x^o} = \begin{cases} t + \sum_{n=1}^N \frac{D_n}{\beta_n^2} (-1 + \beta_n t + e^{-\beta_n t}) & 0 \leq t \leq t_o \\ t_o + \sum_{n=1}^N \frac{D_n}{\beta_n^2} [\beta_n t_o + (1 - e^{-\beta_n t_o}) e^{-\beta_n t}] & t \geq t_o \end{cases} \quad (4.34)$$

Model B

$$\frac{E_o t_o \epsilon_x(t)}{\sigma_x^o} = \begin{cases} t + \frac{1}{2} D_{N+1} t^2 + \sum_{n=1}^N \frac{D_n}{\beta_n^2} (-1 + \beta_n t + e^{-\beta_n t}) & 0 \leq t \leq t_o \\ t_o + D_{N+1} (t_o t - \frac{1}{2} t_o^2) + \sum_{n=1}^N \frac{D_n}{\beta_n^2} [\beta_n t_o + (1 - e^{-\beta_n t_o}) e^{-\beta_n t}] & t \geq t_o \end{cases} \quad (4.35)$$

The various constants D_n , E_o , and β_n are determined from the curve fitting technique outlined in Section 4.1, except that now the creep rather than the relaxation curve is used. Since the same model should fit both relaxation and creep data, these two tests serve as a check on the choice of model, i.e. the assumed value N and on the applicability of linear viscoelastic relations over a given stress and/or strain range.

It is also of interest to note from Equations (4.34) and (4.35) that as $t \rightarrow \infty$ Model A exhibits a finite creep strain equal to $\left[\epsilon_x^o \left(1 + \sum_{n=1}^N D_n / \beta_n \right) \epsilon_o^{-1} \right]$ while Model B creeps indefinitely regardless of the choice of the value of N .

4.4 UNIAXIAL CREEP OF COMPRESSIBLE MATERIALS

For a material which behaves linearly viscoelastically for changes in shape and linearly elastically for changes in volume, the equivalent compressible Young's modulus is given

by Equation (4.24). It is seen that the effect of elastic volumetric compressibility on uniaxial relations is to only conceptually alter Equations (4.30) to (4.35) by changing E_0 to E_{CO} . Of course, the constants D_n are now functions of G_0 , K_0 , δ_n , and β_n . However, again only the quantities E_{CO} , D_n and β_n in Equations (4.30) or (4.32) need to be determined to specify the material behavior. Hence, the procedure is the same as before.

4.5 BIAXIAL RELAXATION AND CREEP OF INCOMPRESSIBLE MATERIALS

Biaxial creep and relaxation experiments are usually conducted on thin strips loaded in one direction in their plane (along x-axis) and clamped along two edges ($\epsilon_y = 0$). (See Figure 5) It is customary to measure σ_x and ϵ_x . If in this problem one deals with the average stresses at the center of the plate, then the analysis is considerably simplified since one need not find the spacial variations of the stresses in the plate. Further, due to the thinness of the plate, one can assume that

$$\sigma_z = 0 \quad (4.36)$$

The Laplace transform viscoelastic stress-strain relations (2.6) can now be applied at the center of the plate and they will be of the form

$$\bar{\sigma}_x - \bar{\sigma} = \mathcal{L} \bar{G} \bar{\epsilon}_x \quad (4.37)$$

$$\bar{\sigma}_y - \bar{\sigma} = 0 \quad (4.38)$$

$$-\bar{\sigma} = 2\bar{G}\bar{\epsilon}_z \quad (4.39)$$

From Equation (4.38) one obtains

$$\bar{\sigma} = \bar{\sigma}_y = \frac{1}{2} \bar{\sigma}_x \quad (4.40)$$

which when substituted into Equation (4.37) yields

$$\bar{\sigma}_x = 4\bar{G}\bar{\epsilon}_x \quad (4.41)$$

Equation (4.41) is similar to Equation (4.3) and, consequently, the discussion and results for uniaxial creep and relaxation applies here as well. It is to be noted that for the incompressible material $E_0 = 3G_0$ and the coefficient $4G_0$ equals $4E_0/3$ which is the correct value of $E_0/(1-\nu^2)$ for an incompressible material.

4.6 BIAXIAL RELAXATION AND CREEP OF COMPRESSIBLE MATERIALS

Biaxial viscoelastic stress-strain relations for the conditions outlined in Section 4.5 can be derived from Equation (2.6) by setting $\bar{\epsilon} \neq 0$ for compressible materials. For the transforms of the normal stresses and strains these now become

$$\bar{\sigma}_x - \bar{\sigma} = 2\bar{G}(\bar{\epsilon}_x - \bar{\epsilon}) \quad (4.42)$$

$$\bar{\sigma}_y - \bar{\sigma} = -2\bar{G}\bar{\epsilon} \quad (4.43)$$

$$- \bar{\sigma} = 2\bar{G}(\bar{\epsilon}_z - \bar{\epsilon}) \quad (4.44)$$

$$\bar{\sigma} = K_o \bar{\epsilon} \quad (4.45)$$

From Equations (4.44) and (4.45) one obtains

$$(K_o + 4\bar{G})\bar{\epsilon}_z + (K_o - 2\bar{G})\bar{\epsilon}_x = 0 \quad (4.46)$$

and substitution of Equation (4.44) and (4.46) into (4.35) leads to

$$\bar{\sigma}_x = \frac{4\bar{G}(K_o + \bar{G})}{K_o + 4\bar{G}} \bar{\epsilon}_x = \bar{E}_{ic} \bar{\epsilon}_x \quad (4.47)$$

It is to be noted that the quantities on the right hand side of Equation (4.47) can be expressed in terms of an equivalent Young's modulus \bar{E} and equivalent Poisson ratio $\bar{\nu}$, such that

$$\bar{E}_{ic} = \frac{\bar{E}}{1 - \bar{\nu}^2} \quad (4.48)$$

A relation similar to Equation (4.48) also holds for the initial elastic values by introducing zero subscripts instead of bars in Equation (4.48).

The modulus \bar{E}_{1c} can be determined by substitution of either Equation (2.8) or (3.3) into Equation (4.47). For Model A, \bar{E}_{1c} becomes after reduction to a common denominator

$$\bar{E}_{1c} = \frac{4G_o \prod_{n=1}^N (p + \beta_n) \left[K_o \prod_{n=1}^N (p + \alpha_n) + G_o \prod_{n=1}^N (p + \beta_n) \right]}{\prod_{n=1}^N (p + \alpha_n) \left[K_o \prod_{n=1}^N (p + \alpha_n) + 4G_o \prod_{n=1}^N (p + \beta_n) \right]} \quad (4.49)$$

$$\bar{E}_{1c} = \frac{E_{loc} \prod_{n=1}^{2N} (p + \lambda_n)}{\prod_{n=1}^{2N} (p + \delta_n)} = E_{loc} \left[1 + \sum_{n=1}^{2N} \frac{F_n}{p + \delta_n} \right] \quad (4.50)$$

The expressions (4.47) and (4.50) are conceptually identical to that of Equation (4.20), (4.22) and (4.23) and, therefore, the same procedure as outlined for uniaxial creep and relaxation can be applied here.

The same scheme can be applied to a \bar{G} for Model B and \bar{E}_{1c} then reduces to

$$\bar{E}_{1c} = \frac{E_{loc} p \prod_{n=1}^{2N+1} (p + \lambda_n)}{\prod_{n=1}^{2N+2} (p + \delta_n)} = E_{loc} p \sum_{n=1}^{2N+2} \frac{F_n'}{p + \delta_n} \quad (4.51)$$

which is equivalent to Equations (4.25) in the uniaxial case.

Once the quantities E_{loc} , F_n' and δ_n are determined from the curve fitting of creep and/or relaxation data, \bar{E}_{1c} is known. The bulk modulus K_o must be determined from separate volumetric experiments and the equivalent shear modulus \bar{G} may be found from Equation (4.47) to be

$$2\bar{G} = \bar{E}_{1c} - K_o + \left(\bar{E}_{1c}^2 - K_o \bar{E}_{1c} + K_o^2 \right)^{1/2} \quad (4.52)$$

4.7 TRIAXIAL RELAXATION AND CREEP OF INCOMPRESSIBLE MATERIALS

Relatively simple experiments under triaxial stress conditions are usually conducted on thin circular plates bonded to rigid supports along both faces and loaded in the direction perpendicular to the faces. (Figure 6) If the radius is large compared to the thickness, then one can assume that at the center of the plate ($x = y = z = 0$)

$$\sigma_x = \sigma_y \quad (4.53)$$

$$\epsilon_x = \epsilon_y = 0 \quad (4.54)$$

It is customary to measure $\bar{\sigma}_z$ and $\bar{\epsilon}_z$.

For an incompressible material, the normal strain vanishes due to Equation (4.54). From the stress-strain relations (2.6) it is seen that under these conditions all the normal stresses must also vanish. Consequently, this type of experiment under the assumptions (4.53) and (4.54) is of no value in determining stress-strain relations for incompressible materials.

More realistic analysis for incompressible materials based on spatially variable stress and strain fields, is so complex as to destroy the simplicity of this type of tri-axial experiment.

4.8 TRIAXIAL RELAXATION AND CREEP OF COMPRESSIBLE MATERIALS

The conditions described in Section 4.7 can also be applied to a material with deviatoric viscoelastic properties and volumetric elastic ones. The transform relations then become

$$\bar{\sigma}_x = \bar{\sigma}_y = (K_o - 2\bar{G}) \bar{\epsilon} \quad (4.55)$$

$$\bar{\sigma}_z = \frac{1}{3}(K_o + 4\bar{G}) \bar{\epsilon}_z = \bar{E}_{2c} \bar{\epsilon}_z \quad (4.56)$$

The modulus \bar{E}_{2c} can be determined from Equations (2.8) and (3.3)

Model A

$$\bar{E}_{2c} = E_{2oc} \left[1 + \sum_{n=1}^N \frac{F_n}{p + \alpha_n} \right] \quad (4.57)$$

Model B

$$\bar{E}_{2c} = E_{2oc} \left[1 + \sum_{n=1}^{N+1} \frac{F_n}{p + \alpha_n} \right] \quad (4.58)$$

with

$$E_{2oc} = \frac{1}{3} (K_o + 4G_o) = \frac{(1-\nu) E_o}{(1+\nu)(1-2\nu)} \quad (4.59)$$

The procedure for determining E_{2oc} , F_n and α_n is identical to that outlined for the uniaxial conditions. Once these quantities are established and K_o is found from a separate volumetric test, \bar{G} can be computed from Equation (4.56).

5. INTEGRAL VISCOELASTIC STRESS-STRAIN REPRESENTATION

Instead of the differential stress-strain relations of Equations (1.1) and (1.2), it is also possible to write integral representation of the type

$$S_{ij} = 2 \int_{-\infty}^t \psi(t-t') \frac{\partial E_{ij}(t')}{\partial t'} dt' \quad (5.1)$$

$$\sigma = \int_{-\infty}^t \psi_v(t-t') \frac{\partial \epsilon(t')}{\partial t'} dt' \quad (5.2)$$

$$E_{ij} = \frac{1}{2} \int_{-\infty}^t \phi(t-t') \frac{\partial s_{ij}(t')}{\partial t'} dt' \quad (5.3)$$

$$\epsilon = \int_{-\infty}^t \phi_v(t-t') \frac{\partial \sigma(t')}{\partial t'} dt' \quad (5.4)$$

For elastic volumetric deformations Equations (5.2) and (5.4) can be simplified by

$$\psi_v = \frac{1}{\phi_v} = K_0 \quad (5.5)$$

For zero initial conditions, which are those used in the uniaxial and multiaxial tests previously described, the application of the Laplace transform to Equations (5.1) and (5.3) results in

$$p \bar{\psi}(p) = \frac{1}{p \bar{\phi}(p)} = \bar{G}(p) \quad (5.6)$$

Equation (5.6) allows for the immediate computation of the relaxation and creep functions $\psi(t)$ and $\phi(t)$ by inversion of the modulus \bar{G} , the latter being determined by the methods discussed in Section 4.

It is, of course, also possible to determine the creep and relaxation function directly but, again, the same care must be exercised to properly interpret the experimental conditions. As an illustrative example, uniaxial relaxation will be considered.

5.1 UNIAXIAL RELAXATION OF INCOMPRESSIBLE MATERIALS

For the usual initial relaxation conditions, $E_{ij}(t) = 0$ for $t < 0$, Equation (5.1) may be integrated by parts to yield

$$S_{ij}(t) = 2 E_{ij}(t) \Psi(0) - 2 \int_0^t \frac{\partial \Psi(t-t')}{\partial t'} E_{ij}(t') dt' \quad (5.7)$$

For incompressible materials in uniaxial loading Equation (5.7) reduces to

$$\sigma_x(t) = 3 \epsilon_x(t) \Psi(0) - 3 \int_0^t \frac{\partial \Psi(t-t')}{\partial t'} \epsilon_x(t') dt' \quad (5.8)$$

Two types of strain-time histories are of interest:

$$\epsilon_x = \left\{ \begin{array}{ll} 0 & t < 0 \\ \epsilon_x^0 & t \geq 0 \end{array} \right\} \quad (5.9)$$

$$\epsilon_x = \left\{ \begin{array}{ll} 0 & t < 0 \\ \epsilon_x^0 t/t_1 & 0 \leq t \leq t_1 \\ \epsilon_x^0 & t \geq t_1 \end{array} \right\} \quad (5.10)$$

If the strain is applied as a step function (5.9), then Equation (5.8) becomes

$$\frac{\sigma_x(t)}{\epsilon_x^0} = 3 \psi(t) \quad (5.11)$$

which indicates that in this case the relaxation function can be determined directly from the relaxation stress.

On the other hand, if the ramp function (5.10) is used for the strain, then Equation (5.8) yields

$$\frac{\sigma_x(t)}{\epsilon_x^0} = \frac{3}{t_1} \int_0^{t_1} \psi(t-t') dt' \quad t \geq t_1 \quad (5.12)$$

and the simplicity of Equation (5.11) is now lost. In an actual experiment, the strain will be of the type given by Equation (5.10) rather than Equation (5.9).

5.2 UNIAXIAL RELAXATION OF COMPRESSIBLE MATERIALS

In a medium with elastic compressible dilatation and under uniaxial conditions, Equation (5.7) reduces to

$$\left[1 + \frac{\psi(0)}{K_0}\right] \sigma_x(t) = 3\epsilon_x(t)\psi(0) - 3 \int_0^t \frac{\partial \psi(t-t')}{\partial t'} \left[\epsilon_x(t') - \frac{\sigma_x(t')}{3K_0}\right] dt' \quad (5.13)$$

The solution for the unknown relaxation function $\psi(t)$ in Equation (5.13) from experimentally determined values of

σ_x and ϵ_x is complex, since it appears as the kernel of the integral equation, regardless of the definition for ϵ_x . The ψ function can, however, be generated numerically from

the experimental data and Equation (5.13). The initial value $\psi(0)$ can be expressed in terms of the initial Young's modulus by setting $t = 0$ in Equation (5.13)

$$\psi(0) = \frac{E_{oc}}{3 - E_{oc}/K_o} = G_o \quad (5.14)$$

and it is seen to be positive since generally $K_o > E_{oc}$. The modulus E_{oc} can be readily determined if the initial strain $\epsilon_x(0)$ is non zero (such as, for instance, the step function of Equation (5.9)), since it then equals the ratio $\sigma_x(0)/\epsilon_x(0)$. However, if $\epsilon_x(0) = 0$ then $\sigma_x(0)$ also vanishes for materials with initial instantaneous response and the modulus can be determined experimentally only by the limit process

$$E_{oc} = \lim_{t \rightarrow 0} [\sigma_x(t) / \epsilon_x(t)] \quad (5.15)$$

from experimentally determined uniaxial stress and strain time data.

Similar procedures can also be used for the formulation of creep functions from uniaxial creep data.

5.3 MULTIAXIAL RELAXATION AND CREEP

Similar procedures may be constructed for the determination of creep and relaxation functions from multiaxial experiments, but extreme care must be exercised to properly interpret such test results since the fundamental functions of Equations (5.1) to (5.4) do not appear explicitly in the

multiaxial stress-strain relations. This is evident from the relations derived in Section 4 for the moduli, where \bar{G} generally appears in experimentally inseparable combinations with the elastic bulk modulus K_0 .

Finally, it must be pointed out that while Equations (5.5) and (5.6) give exact relations between creep and relaxation functions and the corresponding moduli, the determination of the modulus \bar{G} is inherently dependent on the a priori selection of a particular model and number of parameters in that model. While the procedures outlined in Sections 5.1 and 5.2 lead to the formulation of these functions in a somewhat more general fashion without being possibly restricted by the choice of a model, the price of such generalization seems large. The relative simplicity of the model fitting is lost and in most instances the creep functions cannot be directly determined analytically. They can be computed numerically and analytical expressions can be curve fitted to these numerical results if desired. Such a typical numerical computation of the relaxation function is carried in Reference 10.

As more experimental data becomes available and is analyzed, it will be possible to reach conclusions as to the preferable choice of methods for direct formulation of either \bar{G} or ϕ and ψ and as to the accuracy of the two approaches. In any case Equations (5.5) and (5.6) can always be used to determine the moduli from creep or relaxation functions and vice versa.

REFERENCES

1. Bland, D. R., The Theory of Linear Viscoelasticity, Pergamon Press, New York, 1960.
2. Lee, E. H., Radok, J. R. M., and Woodward, W. B., "Stress Analysis for Linear Viscoelastic Materials", Trans. of the Soc. of Rheology, Vol. 3, pp. 41-59, 1959.
3. Morland, L. W., and Lee, E. H. "Stress Analysis for Linear Viscoelastic Materials with Temperature Variation", Trans. of the Soc. of Rheology, Vol. 4, pp. 233-263, 1960.
4. Williams, M. L., "The Strain Analysis of Solid Propellant Rocket Grains", J. of the Aerospace Sciences Vol. 27, pp. 574-586, 1960.
5. Williams, M. L., Blatz, P. J., and Schapery, R. A., "Fundamental Studies Relating to Systems Analysis of Solid Propellants", California Institute of Technology Report No. GALCIT SM 61-5, 1961.
6. Hilton, H. H., Hassan, H. A., and Russell, H. G., "Analytical Studies of Thermal Stresses in Media Possessing Temperature Dependent Viscoelastic Properties", WADC TR 53-322, 1953.
7. Hilton, H. H., and Russell, H. G., "An Extension of Alfrey's Analogy to Thermal Stress Problems in Temperature Dependent Linear Viscoelastic Media", J. of the Mechanics and Physics of Solids, Vol. 9, pp. 152-164, 1961.
8. Hilton, H. H., and Murthy, P. N., "The Analysis of Elastic or Viscoelastic Finite Length Thick-Walled Cylinders Encased by Elastic Shells and Exposed to Internal Pressure, Thermal Cycling or Vertical Storage", Aerojet-General Corporation Report No. SP 61-1, 1961.
9. Hilton, H. H., "Anisotropic, Nonhomogeneous, Linear Viscoelastic Analysis", Aerojet-General Corporation Report SD-16, 1961.
10. Lee, E. H., and Rogers, T. G., "Solution of Viscoelastic Stress Analysis Problems Using Measured Creep or Relaxation Functions", Brown University, Division of Applied Mathematics, Interim Tech. Rept. No. 1, 1961.

11. Gross, B., Mathematical Structure of the Theories of Viscoelasticity, Hermann and Cie, Paris, 1953.
12. Jones, J. W., Daniel, D., and Johnson, D. A., "Propellant Viscoelastic Characterization in Creep and Stress Relaxation Tests", 20th Meeting Bulletin, JANAF-ARPA-NASA Panel on Physical Properties of Solid Propellants, Vol. 1, pp. 193-200, 1961.
13. Freudenthal, A. M., "The Phenomenon of Stress-Relaxation, Proc. ASTM, Vol. 60, pp. 986-999, 1960.

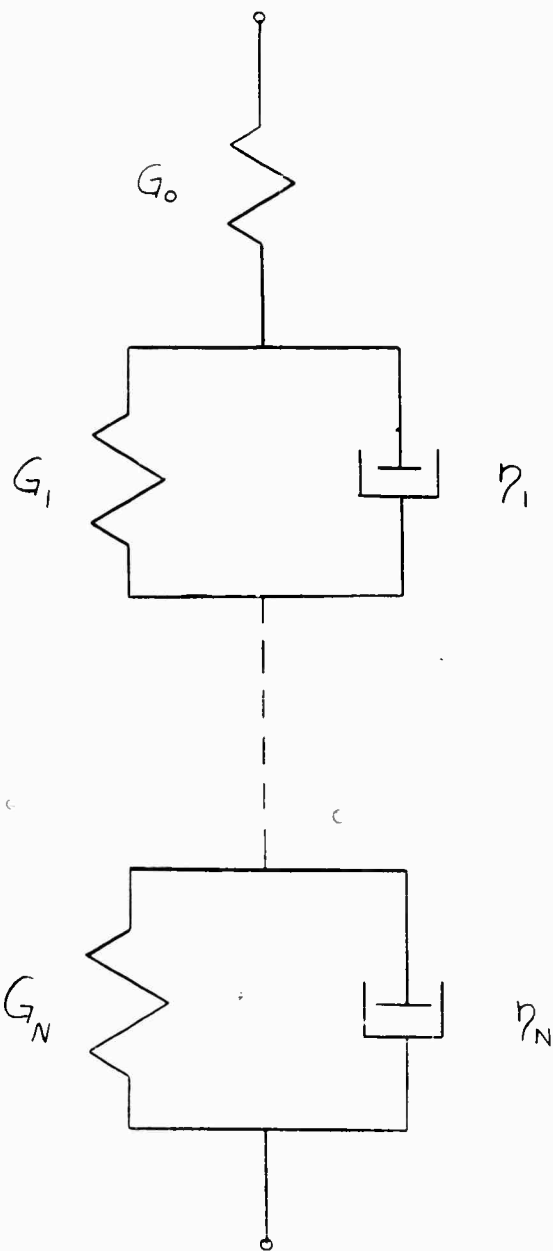


FIGURE 1 - Generalized Kelvin Model A with Initial Elastic Deformation and Finite Creep Strains

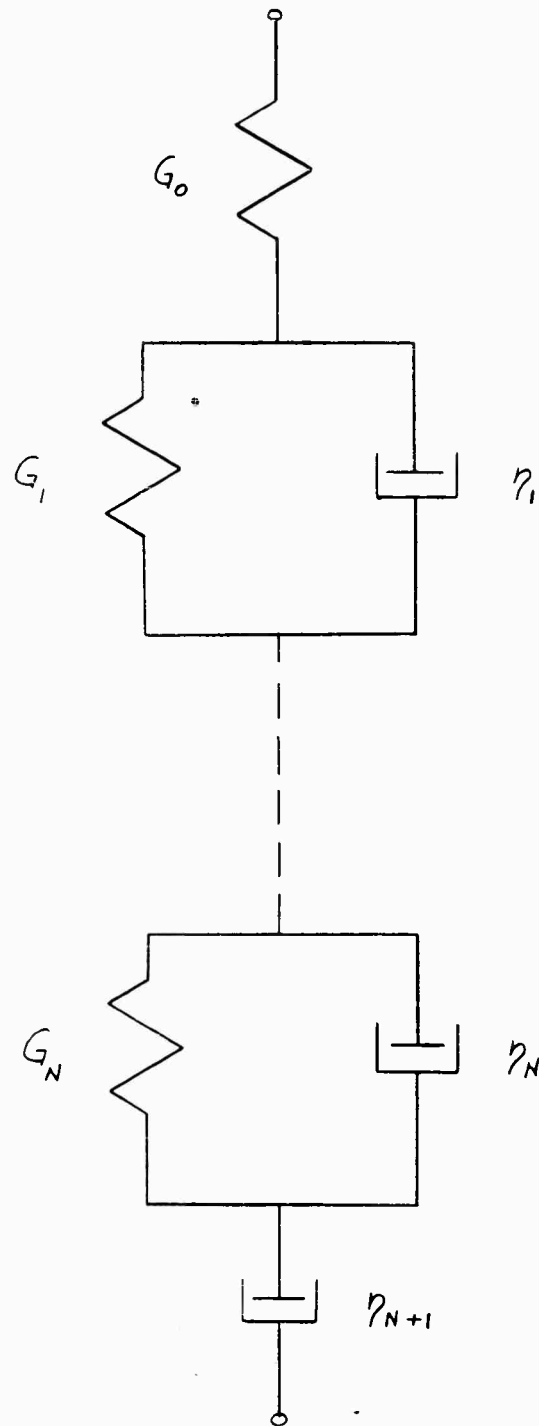


FIGURE 2 - Generalized Kelvin Model B with Initial Elastic Deformation and Unlimited Creep Strains

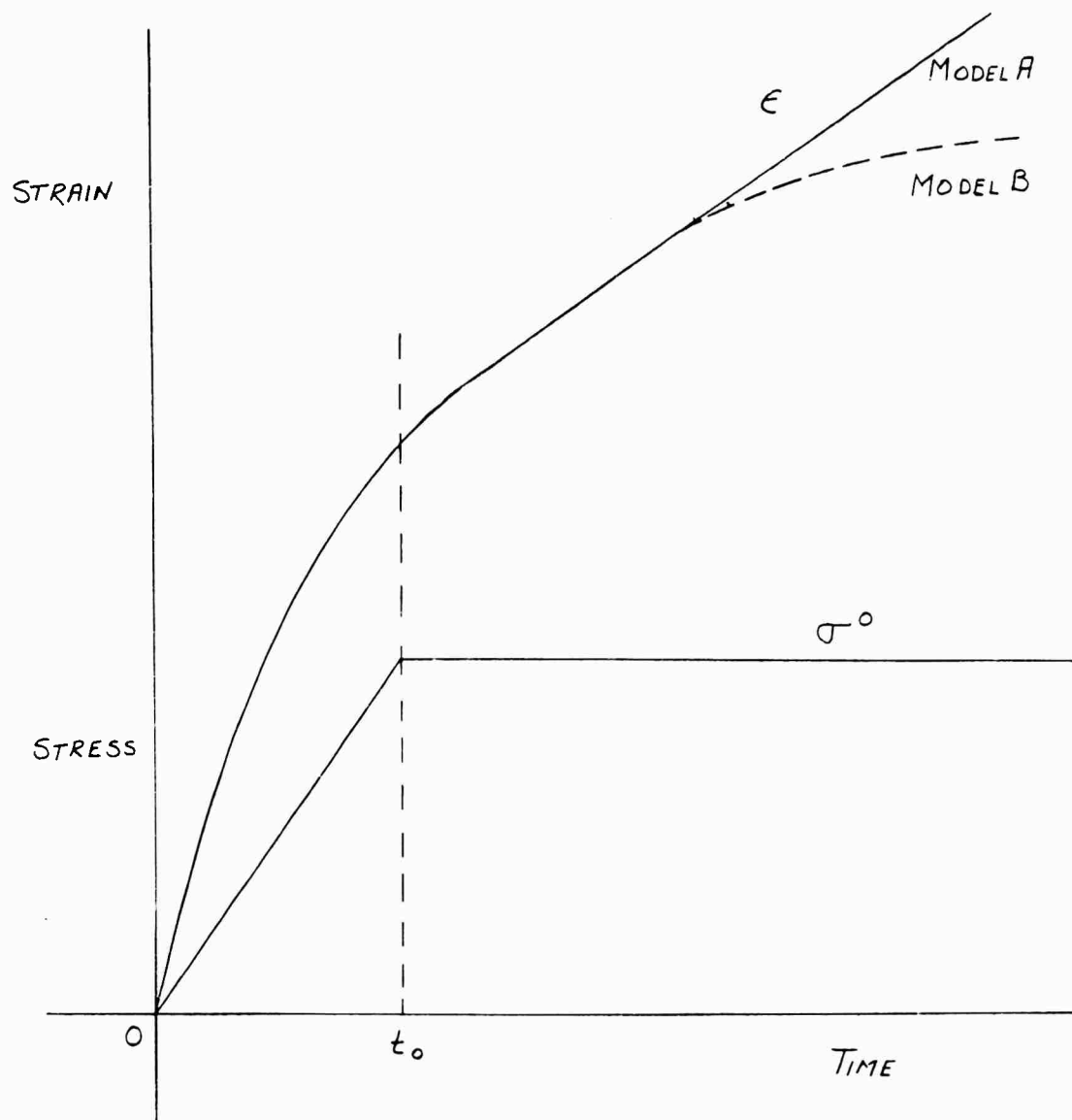


FIGURE 3 - Typical Creep Data

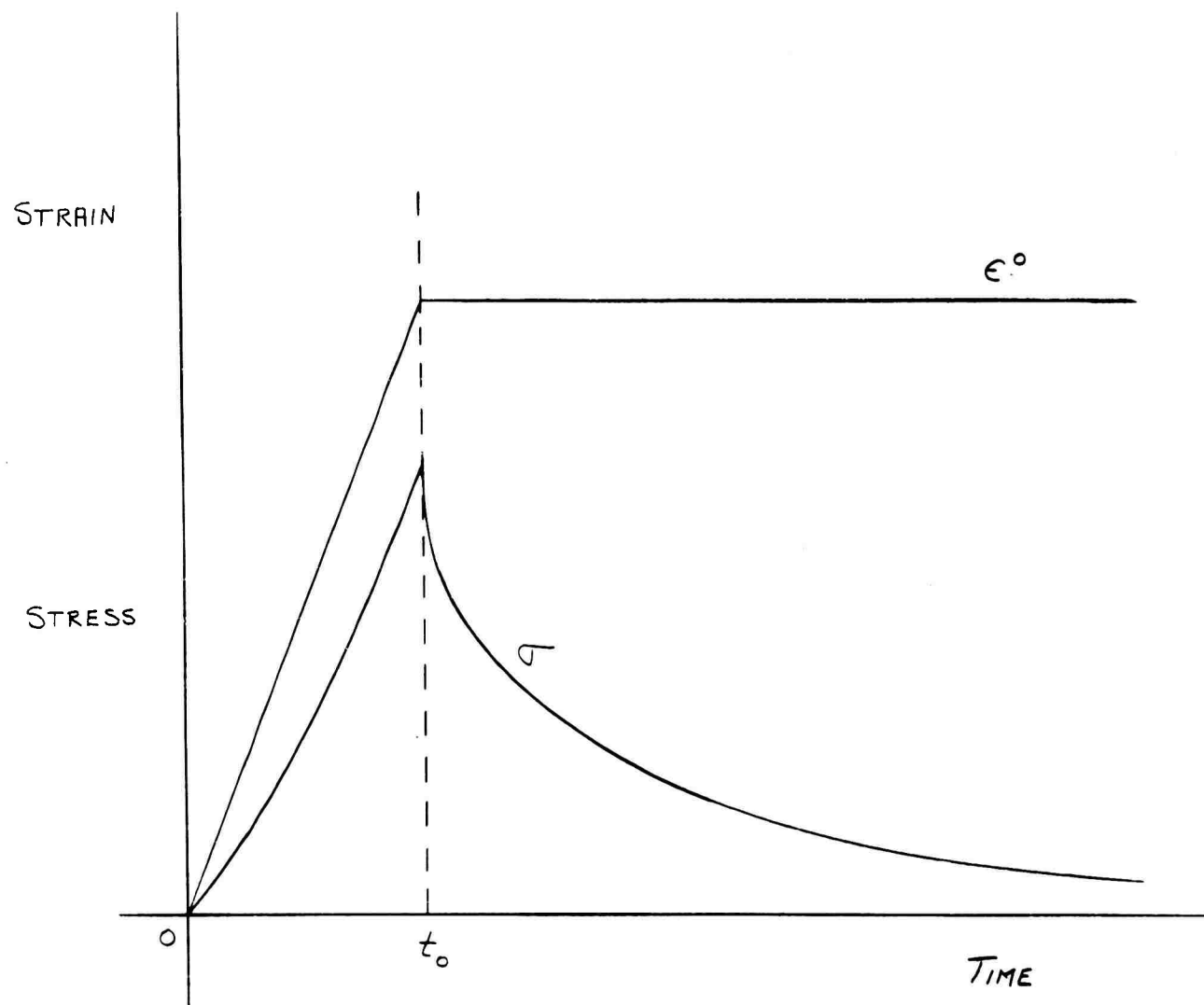


FIGURE 4 - Typical Relaxation Data

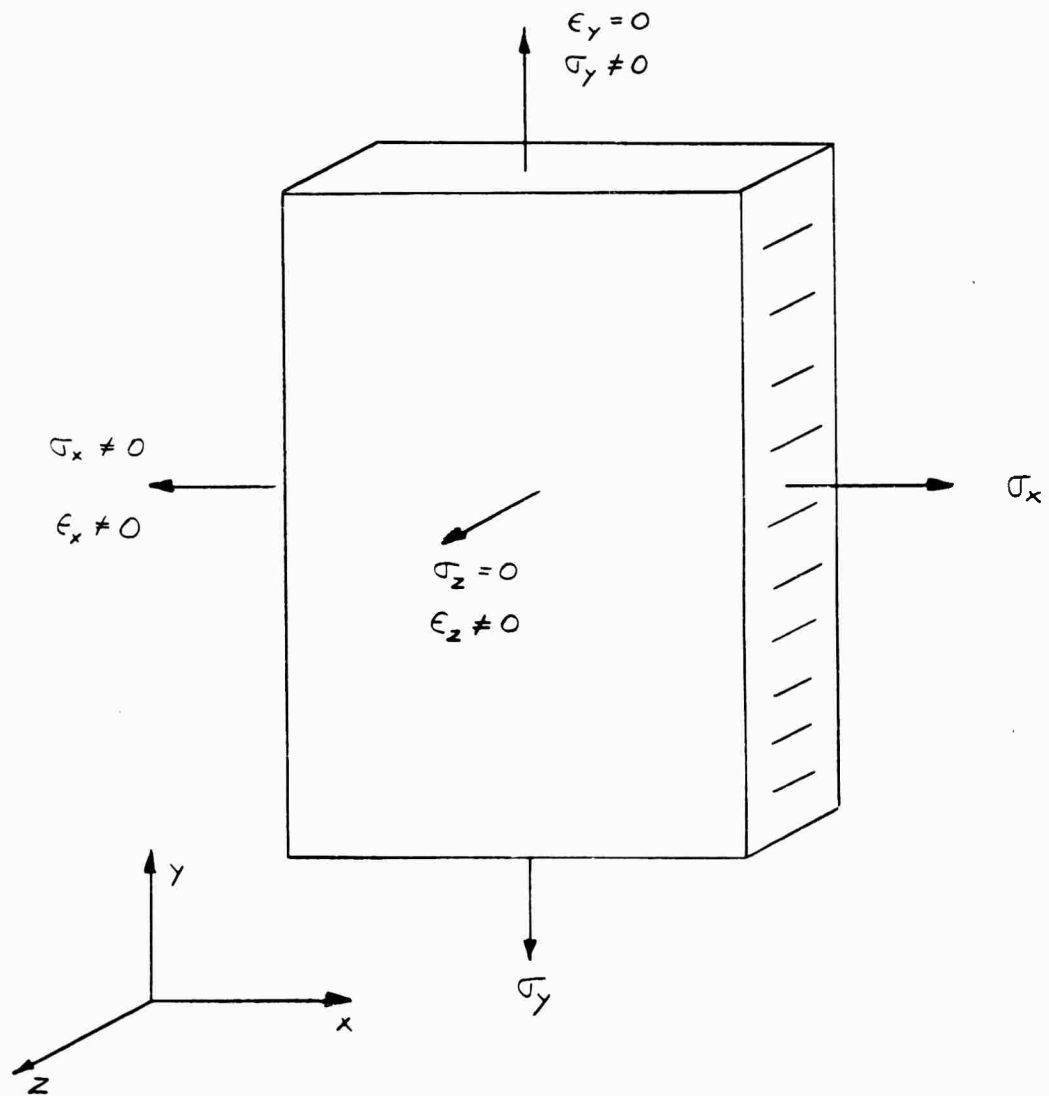


FIGURE 5 - Biaxial Creep and Relaxation Loading

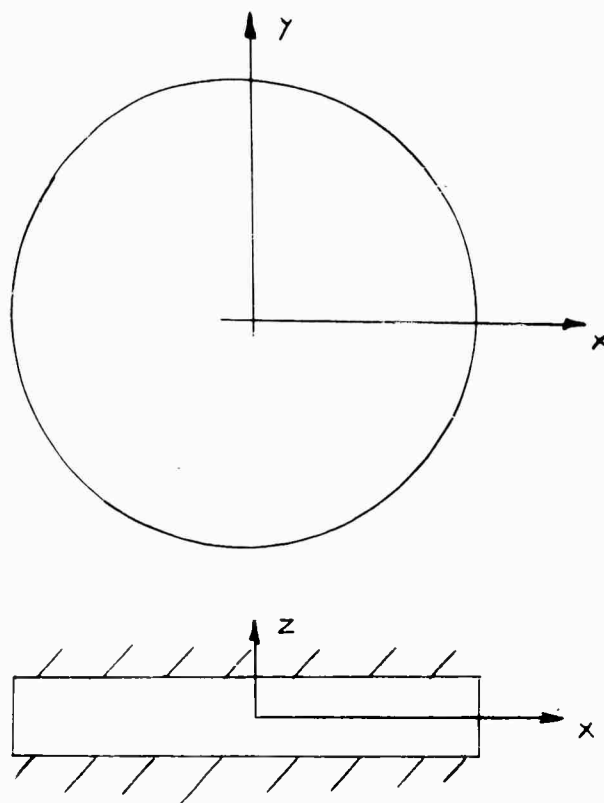


FIGURE 6 - Triaxial Creep and Relaxation

APPENDIX B

SURVEY AND DEVELOPMENT OF METHODS FOR THE
DETERMINATION OF STRAINS IN SOLID PROPELLANTS

by

A. J. Durelli and V. J. Parks
Stress Analysis Laboratory, Civil Engineering Department
The Catholic University of America

LIST OF ILLUSTRATIONS

<u>Figure</u>		<u>Page</u>
1	Isochromatic Pattern of a Urethane Rubber Beam with an Electric Wire Gage Cemented to its Bottom Side, when Subjected to Bending.	4
2	Models Number 1 and 2 (Table 1) Loaded in the Polariscopes to Show The Extent of Reinforcement by a Strain Gage.	5
3	Sketch Showing Location of Standard Wire or Foil Strain Gages Embedded in Capsules.	13
4	Five Plastic Models with Embedded Strain Gages	15
5	Sketch of a Boroscope to Determine Strains on the Inside Surface of a Propellant Grain in Storage.	20
6	Isochromatic Fringe Patterns of a Rocket Grain Model Subjected to 400 Psi Pressure.	29
7	Test Set Up To Apply A Uniform Pressure To The Outer Periphery of A Rocket Grain Model.	30
8	Isochromatic Fringe Pattern of a CR-39 Grain Model Subjected To 520 Psi Uniform Pressure Along the Outer Periphery.	31
9	Test Set-Up for Applying a Uniform Drop in Temperature To A Rocket Grain Model Bonded on the Outer Periphery to a Steel Ring. The Dial Gage Measures The Change in Core Diameter.	32
10	Isochromatic Fringe Patterns of a Urethane Rubber Grain Bonded to a Steel Ring on its Outer Periphery and Subjected to Four Levels of Decreasing Temperature.	33
11	Impressions Made before and after Loading by Rubber Characters Cemented to a 3" Disk of Propellant Loaded in Diametral Compression.	37

SURVEY AND DEVELOPMENT OF METHODS FOR THE
DETERMINATION OF STRAINS IN SOLID PROPELLANTS

I. INTRODUCTION

This is the final report on a research program directed towards the development of an experimental method to determine strains on the inside, or core, surface of solid rocket propellants when the rocket is subjected to thermal loading such as occurs in storage. Of particular interest are the strains in fillets where failure is likely to occur. A desirable feature would be the remote recording of strains.

There exists today an imposing array of experimental methods designed to measure strains. Most of the methods were designed to measure strains in the commonly used engineering materials (steel, concrete, wood, etc.). One approach to the solution of the problem is the adaptation of one of these "engineering-material" methods to the measurement of strains on the relatively soft rubber-like surface of the rocket propellant. Another approach is to choose a method that had already been used to measure strains on soft materials and extend its application to the present problem. In the first approach noted above, the difficulty lies usually in the reinforcement effect produced by the presence of the gage, an effect which will be discussed below; in the second approach difficulties arise in the application of simple optical devices to complicated geometries and to field conditions. A third approach that suggests itself is

the development of some entirely new principle for the measurement of strain. Several rather novel methods are noted in this report, however, all of them can be indirectly related to existing methods, and exhibit some of the same difficulties noted above.

The following section discusses the reinforcement effect produced by most of the known gages. This section is followed by five other sections in which various strain measurement methods are discussed, and in which the experimental studies conducted and their application to the analysis of strains in the rocket propellant are indicated. The final section attempts to evaluate the various methods by comparing them to each other and suggests refinements of the more promising methods.

II. THE REINFORCEMENT EFFECT

If any relatively rigid device is mounted on or in a lower modulus-of-elasticity medium, like the propellant material, to record change in length, these changes in length will generally be distorted by the presence of the device.

This can be illustrated by consideration of a simple, tensile specimen of propellant material with a long, thin wire embedded at the center of the specimen in the direction of loading, and assuming a bond between wire and medium. Neglecting end effects, the relationship of the strain in the direction of loading without the wire (ϵ_n) to the corresponding strain with the wire (ϵ_r) which is common to both wire and propellant, can be shown to be

$$\epsilon_r = \epsilon_n \frac{A_p E_p}{A_p E_p + A_w E_w} \quad (2.1)$$

where A and E represent cross sectional area and Young's modulus and the subscripts p and w refer to the propellant and wire. Since the area of the wire is small, the serious reinforcement effect is produced when Young's modulus of the wire is many times Young's modulus of the propellant, (e.g., $E_w = 30,000,000$ psi, $E_p = 1,000$ psi). The same reasoning can be applied to cases where the gradients of stresses are present, like the edge of a beam under bending. In these cases the reinforcement effect is even more pronounced.

The disturbance effect in practice is usually greater than the one suggested by the above relationship because of the influence of the ends of the rigid device. (Fig. 1)

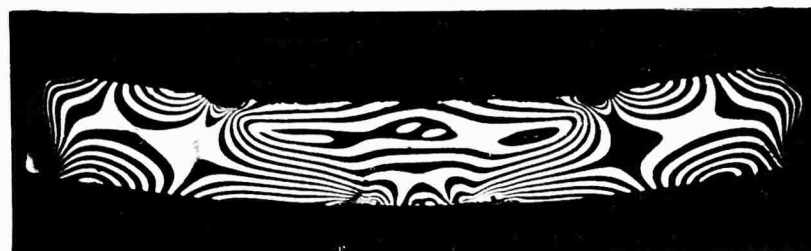
III. ELECTRICAL STRAIN GAGES

A. Resistance Type Gage on the Surface.

1) Design of Specimens

The electrical resistance strain gage is by far the most popular device for measuring strain today. Both the wire and foil type have been developed extensively, applied to different types of problems and associated to different kinds of equipment. It is also common practice to record remotely the response of these gages. With this background of development it seems that it would be desirable to extend the usefulness of this type of gage to the case of solid propellant materials.

The Pattern without the Gage would be a
Series of Equally-Spaced Lines with the Same
Contour as the Top and Bottom Sides



C-I Wire Strain Gage
in this Area on Edge

Note Higher Order
Fringes at Ends of Gage

Fig . 1 ISOCHROMATIC PATTERN OF A URETHANE RUBBER BEAM WITH AN ELECTRIC
WIRE GAGE CEMENTED TO ITS BOTTOM SIDE, WHEN SUBJECTED TO BENDING

As shown in the previous section, the foil or wire gage on propellant will reinforce the vicinity of the gage so that the gage will not record the strain that would have been produced had the gage not been there. If this relationship between the recorded (or measured) strain and the true strain (the strain that would have been at the point had the gage not been there) can be determined, then the gage can still give a meaningful record. The relationship, to be most useful, should be the same regardless of strain biaxiality and should be the same from gage to gage.

To facilitate this study in the laboratory it was decided to mount some of the gages to be studied on specimens of urethane rubber (Hysol 4485) a material which has approximately the elastic properties of the propellant ($E = 490$ psi, $\nu = 0.47$), which is available in sheet form and can be easily machined to various test specimen shapes. A series of eight shapes (see Table I) was designed with varying complexity with respect to load and geometry. The simplest is a uniaxial, tensile specimen to be loaded by dead weight. The most complicated is a typical rocket grain cross section, star-shaped configuration cemented on the outer periphery to a steel ring to be loaded by a decrease in temperature. The series of models allowed the study of the reinforcement relationship in strain fields which have different ratios of principal strains. It also allowed the study of the reinforcement when the model was subjected only to forces or displacements as opposed to the more complex loading by thermal effects where the elastic constant of the material may vary.

TABLE I

Series of Models
Designed to Evaluate the Applicability of Electrical Resistance
Strain Gages to the Measurement of Strains in Low-Modulus Materials

Number	Model	Loading
1	Rectangular strip with $1\frac{1}{4}$ " x $\frac{3}{8}$ " cross section	Uniaxial tension
2	Disk, 3" diameter x $\frac{3}{8}$ " thick	Diametral compression
3	Ring, 8" O.D. x 5" I.D. x $\frac{3}{8}$ " thick	Uniform pressure on O.D.
4	Ring, 8" O.D. x 5" I.D. x $\frac{3}{8}$ " thick	Uniform displacement on O.D.
5	Ring, 8" x O.D. x 5" I.D. x $\frac{3}{8}$ " thick cemented to a $\frac{1}{16}$ " x $\frac{3}{8}$ " steel ring	Decrease in temperature
6	Star perforation on an 8" O.D. disk, $\frac{3}{8}$ " thick	Uniform pressure on O.D.
7	Star perforation on an 8" O.D. disk $\frac{3}{8}$ " thick	Uniform displacement on O.D.
8	Star perforation on an 8" O.D. disk $\frac{3}{8}$ " thick, cemented to a $\frac{1}{16}$ " x $\frac{3}{8}$ " steel ring	Decrease in temperature

2) Testing and Results

Two types of gages were tested. One, a foil type (Budd C5-121) $1/8"$ x $1/8"$ x $0.00015"$ thick on plastic backing (total thickness = $0.001"$) and two, a wire type (Baldwin A-7) $1/4"$ x $3/32"$ x $0.0015"$ diameter wire cemented between two layers of paper (total thickness = $.004"$).

Three types of cements were used, an epoxy (Budd #B-3, ordinary rubber cement and the model material itself (Hysol 4485).

The testing was restricted to the first two types of specimens in Table I, the uniaxial tension specimen and the disk subjected to diametral compression. A specimen of each type is shown in Fig. 2, which illustrates the reinforcement effect photoelastically.

In all the testing conducted on the various combinations of specimens, cement and gage, the relationship of the load to the recorded strain was, except for one case, linear. Thus, for any load, or more directly for any stress there was a given amount of recorded electrical output directly proportional to strain. The results of the tests can then be characterized by a number giving the numerical relationship between the strain that would have been there if the gage had not been there (true strain), and the recorded value of strain (measured strain). These values for all the tests conducted are shown in Table II.



Model 1 with
CG-121 Foil Gage



Model 2 with C-1 Wire Gage
Load Was Applied Both
Parallel and Perpendicular to Gage

Fig. 2 MODELS NUMBER 1 AND 2 (TABLE 1) LOADED IN THE POLARISCOPE TO SHOW
THE EXTENT OF REINFORCEMENT BY A STRAIN GAGE.

TABLE II

Results from Gages on Tensile Specimens (Type 1 in Table I)

Gage	Gage Type	Gage Position	Model Number	Cement	<u>True Strain</u> <u>Measured Strain</u>
1	C6-121	Parallel to Load	I	B-3	39
2	C6-121	" " "	I	B-3	67
3	C6-121	Perpendicular to Load	I	B-3	22
4	C6-121	" " "	I	B-3	57
5	C6-121	Parallel to Load	II	B-3	18
6	C6-121	" " "	II	B-3	16
7	C6-121	" " "	III	B-3	16
8	C6-121	" " "	IV	B-3	18
9	C6-121	" " "	II	B-3	25
10	C6-121	" " "	IV	B-3	29
11	C6-121	" " "	IV	B-3	27
12	A-7	" " "	I	B-3	125
13	A-7	" " "	II	4485	263
14	A-7	" " "	III	"	130
15	A-7	" " "	IV	"	345
16	C6-121	" " "	II	rubber cement	35

TABLE II cont'd.
Results from Two Gages on One Disk (Type 2 in Table I)

Gage	Gage Type	Gage Position	Model Number	Cement	<u>True Strain</u> Measured Strain
17	C6-121	At center, to load	V	B-3	19
18	C6 -121	" ⊥ to load	V	B-3	7
17	C6-121	" ⊥ " "	V	B-3	10
18	C6-121	" to load	V	B-3	13

The ratios of true to measured strain when compared help to establish several points.

- a) When the results from gages 1, 2, and 5 through 11 are compared, it is evident that the same set of conditions do not always produce the same results. This must be due to uncontrollable factors. The most likely variable is the amount of cement used to bond the gages. Gages 2 and 4 were bonded with an appreciable amount of cement. It was believed that this produced the low amount of measured strain and it was hoped that, with practice, an improved cementing technique using less cement would produce a uniform ratio. However, as the subsequent ratios show although the value of the ratio was decreased it was not constant. The 4485 cement and the A-7 gages showed the same difficulties.

- b) The rubber cement was found unsatisfactory. Probably, this was due to relaxation of the cement. The gage response decreased when a constant load was left on the specimen.
- c) The tests on the disk when compared to the tensile specimen tests suggested that the strain ratio also changed with a change in the strain pattern. This suggestion was substantiated when the disk was rotated 90° and reloaded to exchange the position of the gages. The same gages, now in different positions, had new strain ratios; indicating that, in general, when a cemented gage is subjected in turn to two strain fields with different proportions of primary to secondary strain then the ratio of true to measured strain due to reinforcement in each case can be different.

3) Discussion

From a consideration of the difficulties indicated above, it is felt that with the present state of the art the wire or foil resistance strain gage cannot be expected to give an accurate indication of strain when mounted directly on the propellant. The gages may still be used to determine strains within the crude range indicated by the variations of ratios in Table II. A more accurate estimate of

strain, however, may be obtained, if some means is available to calibrate each gage individually after it had been cemented. For instance by applying a known load to the propellant after the gage has been mounted. If the rocket motor could be pressurized, for example, and some means such as photoelastic analysis were available to relate strains to pressures, then the gages could be calibrated for the pressure loading. (This photoelastic method is described more fully in Section V). The thermal loading being a somewhat similar effect could be expected to give the same pattern of strains and so the same calibrations. For this purpose it is recommended that the C6-121 strain gage and B-3 cement be used following the manufacturer's mounting instruction.

B. Embedded Strain Gage Capsules

The electrical resistance strain gage is used in another method which attempts to circumvent the reinforcement problem. The development of this method was started by the investigators in a previous research program directed to measurement of pressures in soils. However, the principles and objectives are the same. One or several standard electrical resistance gages are embedded in a material of essentially the same elastic properties as the material to be studied, and in a sufficiently large volume of the material so that the over-all response is not appreciably affected by the local reinforcement of the gage. (Fig. 3). The unit or capsule is then calibrated by applying known strains and recording the responses of the gage. Finally, the capsule is mounted in the material to be analyzed at the point of interest.

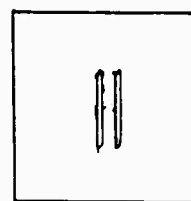
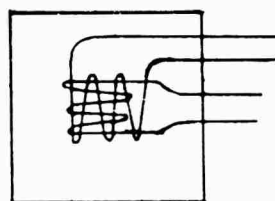
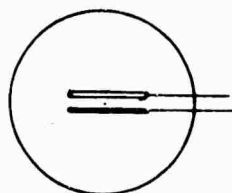


Fig. 3. SKETCH SHOWING LOCATION OF STANDARD WIRE OR FOIL STRAIN GAGES EMBEDDED IN CAPSULES.

Several capsules are shown in Fig. 4. The calibration of a number of these capsules (all 1" in diameter by 1" long) is shown in Table III. Note that the true-strain-over-measured-strain ratio is here a quantity that can be measured in the laboratory before the capsule is inserted in the propellant.

To completely validate the method, it is necessary that either: (1) the strain gage be embedded in a capsule of the actual propellant; or, (2) that the gage be embedded in a capsule of a material with the same mechanical and thermal properties of those of the propellant; or, (3) that the capsule be inserted with mechanical properties stiffer and more flexible than the propellant, and the influence of a change in these on the calibration of the capsule be determined.

Although it seems possible with this method to record the strain in a small fillet, it will be better suited to measure interior strains.

C. Helical and Hydraulic Strain Gages

Two variations of this method are being studied by other investigators under the same sponsorship as the one of this program. In one study use is made of a specially designed helical strain gage wire. The helical configuration will reduce the reinforcement effect, and may not require the previous embedding in a capsule. The helix could be left floating in the propellant. The technique to do this properly may be quite difficult.

The second study used a small, hollow, metal, cylindrically-shaped bellows. The corrugations were on the curved surface to allow appreciable



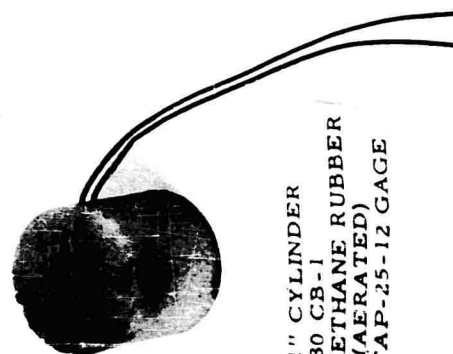
2" D x 2 3/4" CYLINDER
8530 CH-2
URETHANE RUBBER
FABX-25-12 TWO GAGE ROSETTE



1" x 1" CYLINDER
8530 CH-2
URETHANE RUBBER
FABX-25-12 TWO GAGE ROSETTE



1" SPHERE
90% - SAND
10% - 8530 CB-1
URETHANE RUBBER
ONE AB-7 GAGE



1" x 1" CYLINDER
8530 CB-1
URETHANE RUBBER
(AERATED)
ONE FAP-25-12 GAGE

1" SPHERE
POLYURETHANE FOAM
ONE A-7 GAGE

Fig. 4 FIVE PLASTIC MODELS WITH EMBEDDED STRAIN GAGES

TABLE III

RESULTS OBTAINED FROM CAPSULES WITH EMBEDDED STRAIN GAGES

CAPSULE	MATERIAL	GAGE TYPE	GAGE POSITION	RESPONSE TO PRESSURE LOAD $\mu\text{in/in/psi}$	TRUE STRAIN MEASURED STRAIN
1	(8530-CH2) (Urethane)	(FABX-25-12) 2 gages	Parallel to load Perpendicular to load	50* -37*	
2	"	"	Parallel to load Perpendicular to load	55* -29	
3	"	"	Parallel to load Perpendicular to load	(out) -32	
4	Polyurethane Foam	"	Parallel to load Perpendicular to load	15.1 -4.5	4.6
5	8530-CB-1**	FAP-25-12	Parallel to load	40	9.0
6	8530-CH2**	FAP-25-12	" " "	49*	
7	10% sand 90% 8530-CB-1	"	" " "	(not tested)	
8	90% sand 10% 8530-CB-1	"	" " "	6*	
9	90% sand 10% 8530-CB-1	AB-7	" " "	12*	
10	(8530-CB-1) (Urethane)	(FABX-25-12) (2 gages)	" " " Perpendicular to load	35 21	7.5

* Values taken in a previous program

** Aerated Urethane rubber.

axial motion. The inside of the bellows constituted a chamber which was filled with fluid. A small tube leading from the bellows allowed the recording of vibrations in the fluid due to changes in the axial length of the bellows, which, in turn, allowed determination of the strains.

D. Capacitance Type Gage.

Rather late in the development of this program, when it was realized that none of the methods originally considered would give a measure of strain without some important limitations it was decided to investigate the feasibility of a capacitor gage.

A capacitor gage has the immediate advantage that only the material to be measured need span the base length, and therefore, the reinforcement effect is minimized. Capacitor gages have been used primarily as transducers to measure various types of displacement phenomena at high speeds and high frequency. In general the resistance type gage has proved simpler for static strain measurement. However, in the present case where the resistance type gage produced considerable reinforcement, but where the advantage of an electrical signal for remote recording is desirable, the capacitor gage may be a useful method.

A number of thin metal plates (about $3/16"$ x $3/16"$) with attached coaxial cable were embedded in urethane rubber at from $1/8"$ to $1/2"$ apart. In two of the embedments actual propellant material was placed between the plates. In another, just two wires were embedded. Measurable values were obtained from all the samples with a capacitance bridge. An increase in capacitance was noted with compressive strains.

The preliminary models and measurements indicate some promise for the method although it is obvious that additional thought must be given to design, manufacture, and measurement circuits.

Two possible designs are: (1) plates of thin foil or deposited metal and, (2) a double pronged plug that could be stuck in the surface of the propellant at the point where strains are required. The prongs could be about 1/4" long and 1/32" in diameter, and held outside the propellant so as to allow relative motion.

E. Conducting Rubber Method

Another possible method of obtaining a remote electrical signal from strain in the propellant, without reinforcing the area where strain is measured, is the use of conducting rubber threads mounted on the propellant surface. If resistance could be measured, as with the metal resistance gages, then strain could be recorded in this manner. No laboratory work was expended on the development of this method.

IV. BOROSCOPE.

The principles of measuring strains with optical means are well-known. Several instruments are designed to record strains on tensile specimens under load.

The adaptation of an optical method to the measurement of strains on the propellant requires several steps.

1. A method of making observable marks on the propellant and development of a method to locate and focus on the marks with an optical system.
2. Design of the optical system to transmit the mark to an observer outside the rocket.
3. Design of a measuring device to record the true length between marks.

The difficulty with marking the propellant is due to the porous nature of the material. Any scribe marks or cuts on the material, which do not close

up, show a ragged appearance. Filling the scribed marks with ink also proved unsuccessful. After sanding the propellant surface with 180 grit emery cloth, it was found that India ink has sufficient body to produce a clear, if still somewhat ragged line. It is believed that fair precision can be obtained if the point to be analyzed is sanded and marked with a cross of India ink about 3/8" long. The optical system can then be used to determine the lengths from tip to tip of the cross.

It is suggested however that previously to the marking of the surface, this be smoothed by a very thin layer (about 0.002 in.) of latex or of urethane rubber. The India ink lines or the scribed lines could then be placed more precisely on the surface of the rubber. The thickness of this layer would be so small or the properties of the layer of rubber and those of the propellant are so very close, that no change in strain condition would be expected.

The development of Items 2 and 3 were proposed to people in the scientific instrument field. The Gaertner Scientific Company, Chicago (Mr. E. Gordon Watson) are confident that they can manufacture a horescope of about 35" as shown in Fig. 5.

The instrument would have a mounting ring to set down over the point to be analyzed and fix the focal distance. A bulb in the head would provide light. A 45° mirror would transmit the image through the tube. A system of standard Gaertner relay lenses would bring the image to the eyepiece. The eyepiece would be a standard Gaertner Filar eyepiece micrometer with revolution counter. This unit has a hairline mounted on a calibrated screw that can traverse the field and note the distance between any two points. The eyepiece micrometer has 4000 divisions, which will allow a sensitivity of approximately $\pm .00025$ in/in. (assuming an accuracy of ± 1 division).

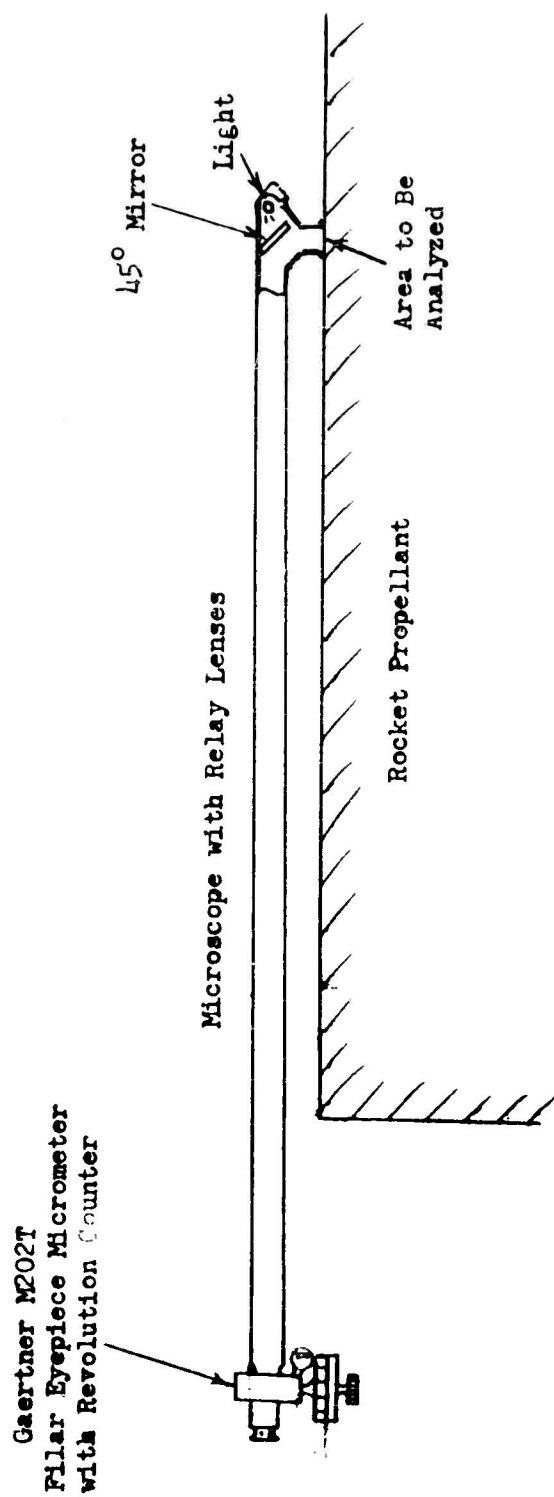


Fig. 5. SKETCH OF A BOROSCOPE TO DETERMINE STRAINS ON THE INSIDE SURFACE OF A PROPELLANT GRAIN IN STORAGE.

Rotating the eyepiece would allow measurement of length in any direction in the field.

The boroscope method as proposed has two limitations. First, it does not allow simultaneous remote reading, which no microscope method can do without individual microscopes for each point and an elaborate transmittal system. Second, it requires straight-line access to the point of analysis along the surface of the propellant. Gaertner feels they can design a step-shaped microscope, however, the amount of step would have to be specified. The more elaborate method of a flexible transmission of the image by the methods of fiber optics, it is felt, is untenable at the present time.

V. EMBEDDED PELLETS.

A variation of the previous method, using X-Rays as the "optical" device, is now being developed under the sponsorship of the Office of Naval Research.* Small steel spheres are embedded in the solid propellant and the distance between spheres recorded before and after loading with an X-ray scanner. The method has been proved very accurately in laboratory models. It remains to be proven, however, how practical it may be in the actual rocket when measurements are taken in the field.

*Principal Investigator: L. U. Rastrelli, Southwest Research Institute, San Antonio, Texas.

VI. CORE DISPLACEMENT MEASUREMENTS USED TO DETERMINE STRAINS.

Under the conditions of linear behavior of the material and constant boundaries, the strain (and stress) at one point in a body will be some multiple of the strain (and stress) at any other part of the body, despite variations in the magnitude of load. Where this is so, a displacement between any two points on the body will have a fixed linear relationship with any strain or stress in the body irrespective of variations in the magnitude of the load.

Thus, if it were possible to measure accurately the distance across the core surface of a rocket motor, and if the relationship between the change in this distance and the strains or stresses, in a fillet, could be determined, then under the above mentioned conditions it would be possible to determine the strains or stresses in a fillet from a measurement of the change in length of the core diameter.

Methods of displacement measurement exist, which are relatively easy to use and of sufficient accuracy to determine the change in diameter of the grain core when the rocket is subjected to thermal loads in storage. (Some of these methods have been developed by other investigators under the same sponsorship as the one of this program).

It is possible to relate these displacement measurements to the strains or to the stresses in different ways. Essentially what is proposed is a calibration procedure which could be conducted in actual grains, or scaled down grains, or as it will be shown below, in small size photoelastic models.

If the calibration is made on scaled down models of any sort then the relationship becomes one of model analysis. Consider then, four cases where the model is a scaled down version of a portion of the rocket grain and made of a material which may be different than the propellant.

Cases 1 and 2 For the portion of a rocket grain which is subjected to internal pressure and in a state of plane stress (case 1) or a state of plane strain (case 2) the relationships between core displacements, strains and stresses on propellant and model is given by:

$$\begin{aligned}\epsilon_p &= \frac{\delta_p}{D_p} \cdot \frac{D_m}{\delta_m} \epsilon_m \\ \sigma_p &= \frac{\delta_p}{D_p} \cdot \frac{D_m}{\delta_m} \cdot \frac{E_p}{E_m} \sigma_m\end{aligned}\quad (6.1)$$

where the subscripts p and m refer to the propellant and model respectively,

- ϵ = the strain at corresponding points on the propellant and model
- δ = the actual change in length of the core diameter
- D = the core diameter
- σ = the stress at corresponding points on the propellant and model
- E = Young's modulus

and assuming Poisson's ratios for propellant and model are approximately the same. (For the usual range of propellants and model materials this assumption is valid).

Case 3 For a portion of a rocket grain which, is subjected to a uniform steady thermal loading, is restricted on the outer boundary, and is in a state of plane stress the comparable relationships will be:

$$\begin{aligned}\epsilon_p - \alpha_p \Delta T_p &= \left[\left(\frac{\delta_p}{D_p} - \alpha_p \Delta T_p \right) / \left(\frac{\delta_m}{D_m} - \alpha_m \Delta T_m \right) \right] (\epsilon_m - \alpha_m \Delta T_m) \\ \sigma_p &= \left[\left(\frac{\delta_p}{D_p} - \alpha_p \Delta T_p \right) / \left(\frac{\delta_m}{D_m} - \alpha_m \Delta T_m \right) \right] \frac{E_p}{E_m} \sigma_m\end{aligned}\quad (6.2)$$

where the terms and assumptions are as above and in addition:

α = the coefficient of thermal expansion (where α is not a constant over the temperature range the thermal strain terms must take the form $\int_{T_1}^{T_2} \alpha \Delta T$)

ΔT = the change in temperature over which δ, ϵ and σ are measured (for a drop in temperature the value is negative)

Note here that ϵ and δ are the actual measured quantities on grain and model.

In the case of the strains, the significant quantity is the $(\epsilon - \alpha \Delta T)$ term since it represents the stress-producing strain.

Case 4. For a portion of the grain which is subjected to a uniform steady thermal loading, is restricted on the outer boundary, and is in a state of plane strain the comparable relationships will be:

$$\begin{aligned}\epsilon_p - (1 + \nu) \alpha_p \Delta T_p &= \left[\left(\frac{\delta_p}{D_p} - (1 + \nu) \alpha_p \Delta T_p \right) / \left(\frac{\delta_m}{D_m} - (1 + \nu) \alpha_m \Delta T_m \right) \right] \left[\epsilon_m - (1 + \nu) \alpha_m \Delta T_m \right] \\ \sigma_p &= \left[\left(\frac{\delta_p}{D_p} - (1 + \nu) \alpha_p \Delta T_p \right) / \left(\frac{\delta_m}{D_m} - (1 + \nu) \alpha_m \Delta T_m \right) \right] \frac{E_p}{E_m} \sigma_m\end{aligned}\quad (6.3)$$

where the terms and assumptions are as above and in addition:

ν = Poisson's ratio of both propellant and model material.

In all four cases it has been assumed that each model, corresponding to the grain being analyzed, was in the same conditions as the grain with respect to the loading and with respect to the state of plane stress or plane strain. However, it is sometimes possible to use one of the four model analyses mentioned above in association with the other three cases.

It has been shown* that the photoelastic stress and strain pattern produced by a thermally loaded two-dimensional model (case 3) can be simulated by a mechanical deformation on the outer boundary of the type $u_r = Kr$ where u_r is the radial displacement, K is a constant, and r is the distance of the point at the boundary from the center. The approach is justified if the thermal loading is thought of as a displacement on the outer boundary of the type $u_r = \alpha \Delta T r$.

In the model analysis of case 1 it has been shown** that the same photoelastic pattern is obtained by loading either the inside or outside of the rocket grain cross section with a uniform pressure. Further, the pattern obtained is approximately the same as the ones obtained by the two methods mentioned in the above paragraph. This happens because the application of a uniform pressure on the outer boundary of a rocket grain with a large web produces approximately a uniform displacement of the outer boundary. (An example of this is shown later).

It follows, then, that for large web grain analysis the model analyses for cases 1 and 3 can be used interchangeably.

Further if the analysis is restricted to transversal stresses, strains

*Photothermoelastic Analyses of Bonded Propellant Grains by I. M. Daniel and A.J. Durelli, Experimental Mechanics, March, 1961.

**Experimental Means of Analyzing Stresses and Strains in Rocket Propellant Grains,
by A. J. Durelli presented to the Society for Experimental Stress Analysis at Philadelphia in May 1961. (To be published in Experimental Mechanics).

and displacements, use can be made of the fact that the stress distribution for a plane stress problem is the same as the stress distribution for the corresponding plane strain problem. This allows the application of any stress ratio computed for either of the two-dimensional plane stress models (cases 1 and 3) to the plane strain counterpart, or with the approximation permitted by the large web of the grain to either case 2 or 4.

This application, however, only holds for stress ratios. The strain ratios are not in general equal in the plane stress and corresponding plane strain field. To apply the two dimensional analysis to the plane strain case it would be necessary to analyze for the strains at the point of interest, compute the stresses with the plane stress form of Hooke's law, substitute these into the plane strain form of Hooke's law and compute the strain. Since one of the "strains" of interest is the displacement across the hole, it would be necessary to use the corresponding strains on the model. These would be the strains along a radial line from the tip of the core to the outer boundary. These strains would have to be reduced to stress and the "plane-strain" strains computed as above, and then these quantities integrated to find the displacement across the web of the grain. Assuming no outer boundary displacement, the core displacement could then be calculated.

This is a tedious method of analysis and for the purposes here may be avoided by one further assumption. If only free boundary strains are considered, the strain ratios will be the same for both plane stress and plane strain, since these strains are in the same state of biaxiality. The core displacement can be considered as a free boundary strain, since it is completely determined by the strains about the core, which are all free boundary strains.

In summary, a two-dimensional plane stress photoelastic analysis of the pressure or thermal type can be applied to either thermal or pressure loading of a rocket grain portion under plane-stress or plane-strain, assuming Poisson's

ratio is approximately the same in the photoelastic model and in the propellant and the web thickness is large, to determine the free boundary fillet strains from a displacement measurement of the core.

Three tests were conducted in developing the model analysis phase of the method. All three tests were on two-dimensional plane-stress models. Photoelastic patterns and core displacements were obtained. In the first and second, pressure loads were applied to CR-39 models. In the third a thermal loading was applied to a urethane rubber model cemented on the outside to a steel ring. The second and third models had the same geometry and so gave similar results. In all three examples the results were applied to a portion of a rocket grain subjected to a uniform, steady thermal loading and in a state of plane strain (case 4), however, the results can be applied to any of the other 3 cases.

For the first and second tests the propellant part of eqn. (6.3) was equated with the model part of eqn. (6.1) to give;

$$\epsilon_p - (1 + \nu) \alpha_p \Delta T_p = \left(\frac{\delta_p}{D_p} - (1 + \nu) \alpha_p \Delta T_p \right) \frac{D_m}{\delta_m} \epsilon_m$$

In photoelastic analysis the equation for free boundary strains is:

$$\epsilon_m = \frac{2nF}{E_m} \quad (6.4)$$

Where F is the model fringe value
 n is the fringe order at the point of interest
 and E_m is Young's Modulus of the model material

The expression of strain in the prototype can then be written as

$$\epsilon_p - (1 + \nu) \alpha_p \Delta T_p = \left(\frac{\delta_p}{D_p} - (1 + \nu) \alpha_p \Delta T_p \right) \left(\frac{2n F D_m}{E_m \delta_m} \right) \quad (6.5)$$

where the first parenthesis on the right side of the equation contains field measured quantities and the second parenthesis contains the model laboratory measured quantities. Note that n and δ_m are taken at any convenient model

load, and for accuracy at several convenient loads. The strain ϵ_p is then the strain produced by a change in temperature ΔT . δ_p must be measured over this same range.

The first model is shown in Fig. 6. The model was loaded with a uniform pressure on the outer periphery. The material is CR-39 and the required properties are $F=180$ psi/fringe and $E=350,000$ psi. The model core diameter is 4.04". If the bottom of the fillet where the strain is the highest is chosen as the point of analysis, then for the load shown in the figure, $n=6.1$ fringes.

One-ten-thousandth dial gages were used to measure the displacement of the core surface. This displacement for the 400 psi pressure was 0.0105". Eq. (6.5) then reduces to

$$\epsilon_p - (1+\nu)\alpha_p \Delta T = 2.41 \left(\frac{\delta_p}{D_p} - (1+\nu)\alpha_p \Delta T \right) \quad (6.6)$$

The second test set-up is shown in Fig. 7. The model was subjected to a uniform pressure on the outer periphery to produce the pattern shown in Fig. 8. Note, incidentally, that this model has an "optimized" fillet contour which means that the fillets were designed (using photoelastic means) to have a uniform fringe over a long portion of the edge, and so reduce the peak strain. The measured quantities are $n=10.0$ at the fillet, $\delta_m = 0.0145$ " (a clip-type strain gage was used here to measure deflections) and $D_m = 4.40$ ". The model material constants are the same as before and the equation for the peak strain in this design therefore is:

$$\epsilon_p - (1+\nu)\alpha_p \Delta T = 3.12 \left(\frac{\delta_p}{D_p} - (1+\nu)\alpha_p \Delta T \right) \quad (6.7)$$

The loading of the third model is shown in Fig. 9. The model was bonded to an outer steel ring and the assembly placed in a cold chamber. The temperature was lowered and the fringe pattern shown in Figure 10 was obtained. Note that the



Dark Field



Light Field



Enlargement of Area at 9 O'Clock on Light Field -

Fig. 6 ISOCHROMATIC FRINGE PATTERNS OF A ROCKET GRAIN MODEL SUBJECTED TO 400 PSI PRESSURE.

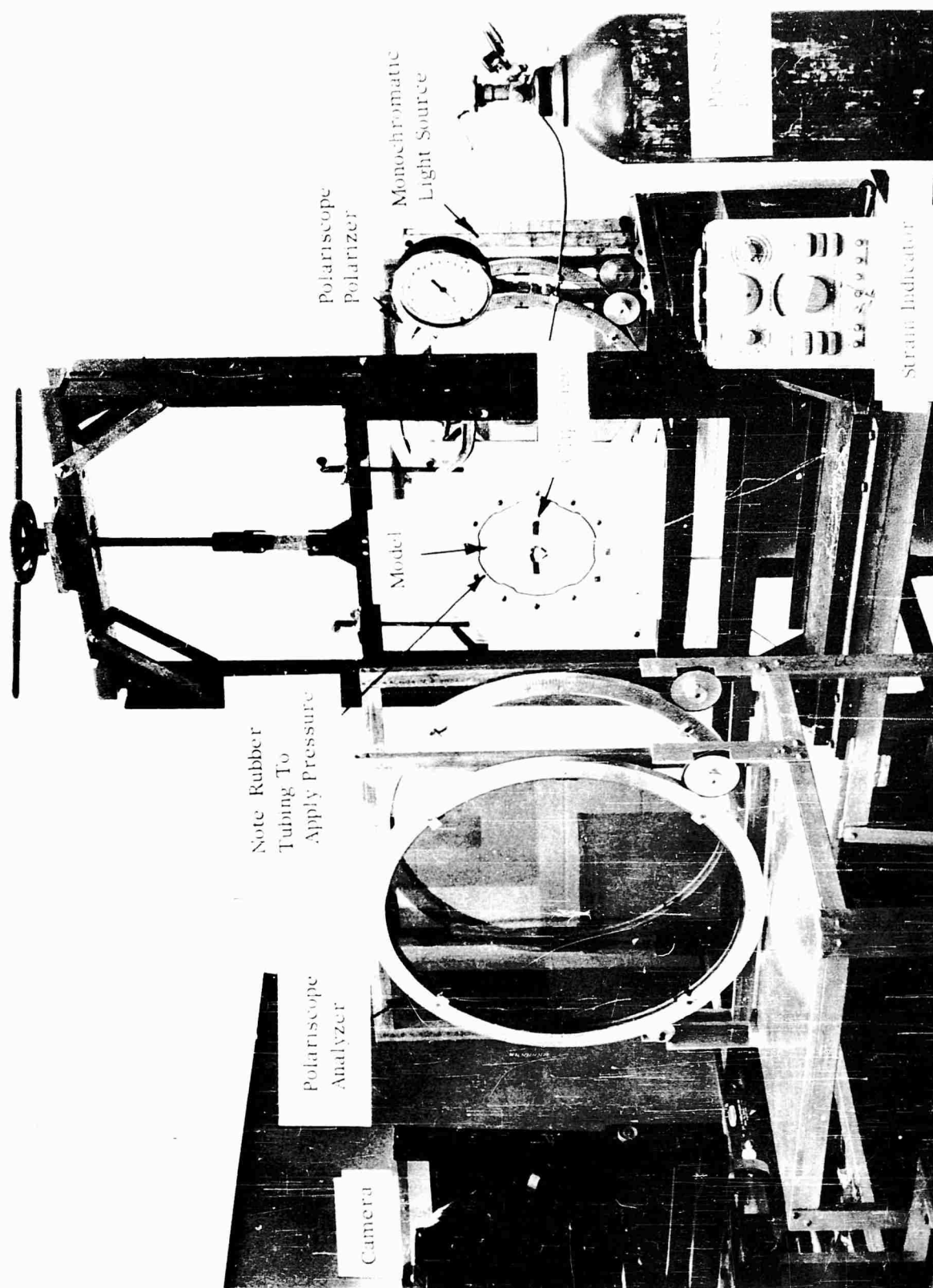


Fig. 7 TEST SET UP TO APPLY A UNIFORM PRESSURE TO THE OUTER PERIPHERY OF A ROCKET GRAIN MODEL



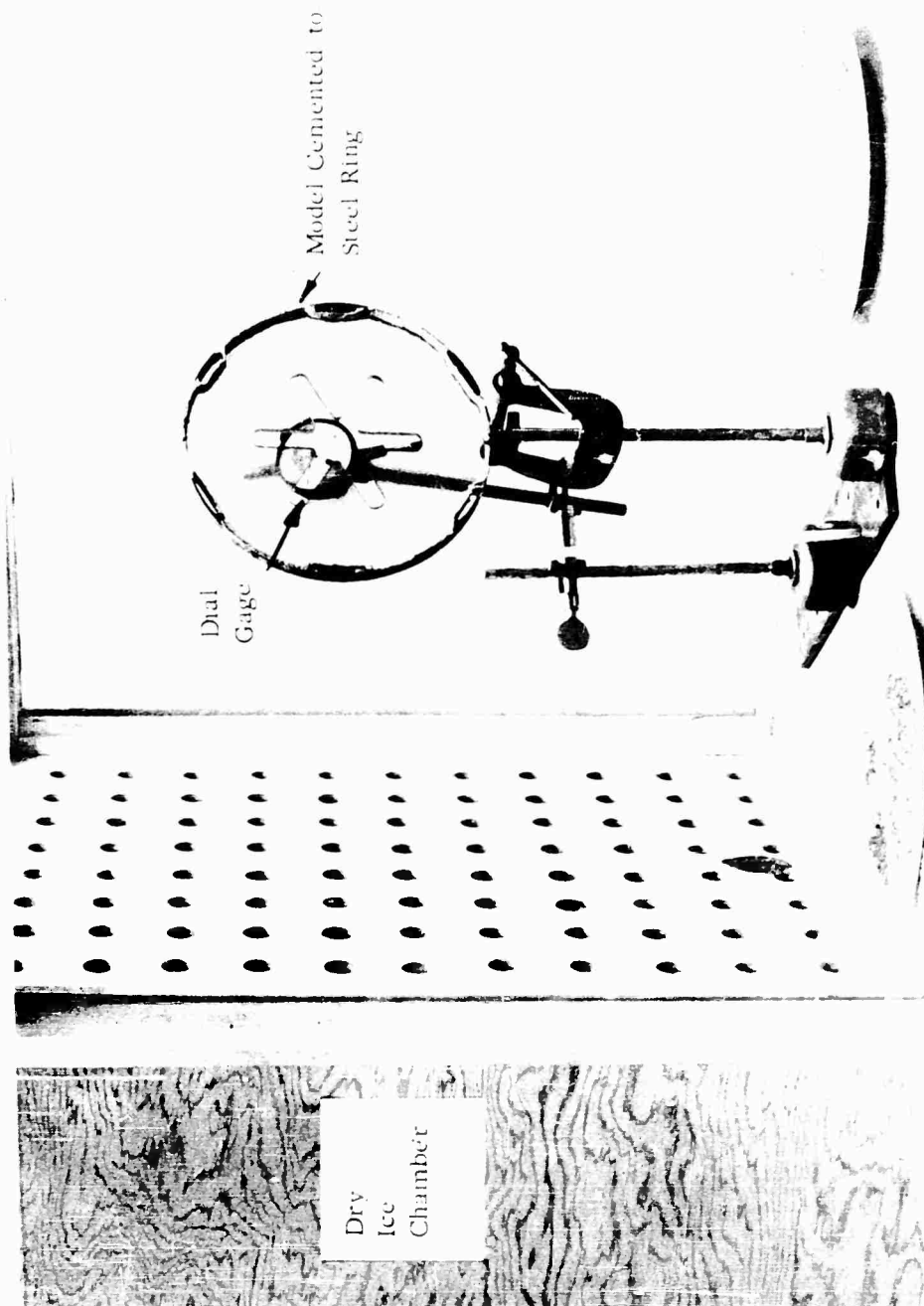
Light Field



Dark Field

Fig. 8 ISOCHROMATIC FRINGE PATTERN OF A CR-39 GRAIN MODEL SUBJECTED TO 520 PSI
UNIFORM PRESSURE ALONG THE OUTER PERIPHERY.

Fig. 1. Test set-up for applying a constant load to a specimen. The load is applied by a steel ring which is cemented to the specimen. The change in cone diameter is measured by a dial gage.



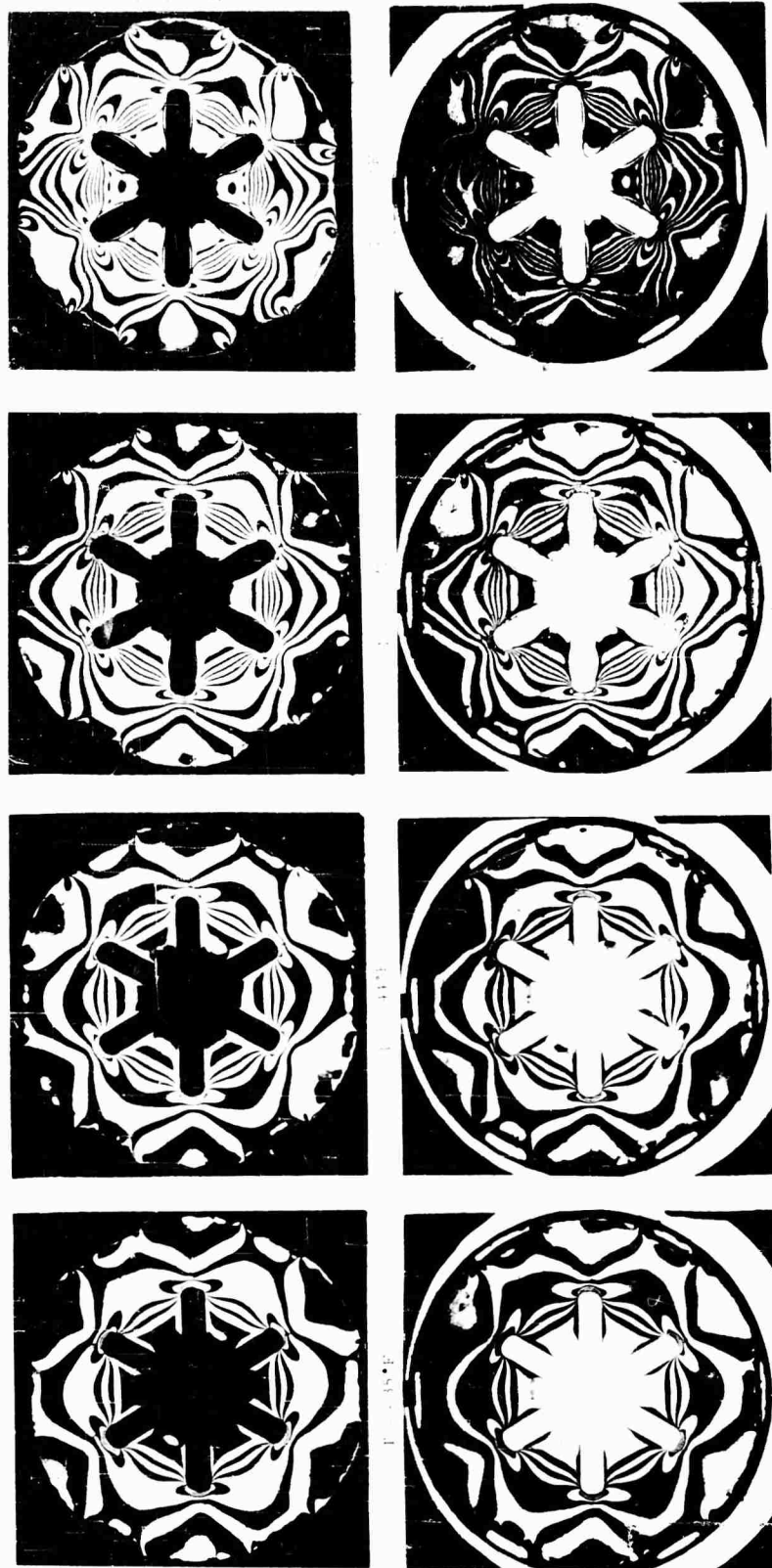


Fig. 10 ISOCHROMATIC FRINGE PATTERNS OF A URETHANE RUBBER GRAIN BONDED TO A STEEL RING ON ITS OUTER PERIPHERY AND SUBJECTED TO FOUR LEVELS OF DECREASING TEMPERATURE.

patterns shown in Figures 8 and 10 are essentially the same.

Here the model analysis equation combines the model terms in Eqn. 6.2 with the propellant terms in Eqn. 6.3,

$$\epsilon_p - (1+\nu)\alpha_p \Delta T_p = \left[\left(\frac{\delta_p}{D_p} - (1+\nu)\alpha_p \Delta T_p \right) / \left(\frac{\delta_m}{D_m} - \alpha_m \Delta T_m \right) \right] (\epsilon_m - \alpha_m \Delta T_m) \quad (6.8)$$

The fringe pattern in the model will be proportional to the stress-related strain so that

$$\epsilon_m - \alpha_m \Delta T_m = \frac{2 n F}{E_m} \quad \text{and}$$

$$\epsilon_p - (1+\nu)\alpha_p \Delta T_p = \left(\frac{\delta_p}{D_p} - (1+\nu)\alpha_p \Delta T_p \right) \left(\frac{2 n F D_m}{E_m (\delta_m - \alpha_m \Delta T_m D_m)} \right)$$

Here the model properties change with temperature and it is necessary to have values of the constants at the temperature at which the analysis is conducted. The model material used in this instance was urethane rubber. At -44°F . the measured values and the material constants were:

$$\begin{aligned} n &= 9.0 \\ \delta_m &= .045'' \\ F &= 1.40 \text{ psi/fringe} \\ E &= 330 \text{ psi} \\ \alpha_m &= 104 \times 10^{-6} \text{ in/in/}^\circ\text{F} \\ \Delta T_m &= -119^\circ\text{F} \end{aligned}$$

As before $D_m = 4.40''$ and the resulting expression is

$$\epsilon_p - (1+\nu)\alpha_p \Delta T_p = 3.36 \left(\frac{\delta_p}{D_p} - (1+\nu)\alpha_p \Delta T_p \right) \quad (6.9)$$

The variation between the expressions obtained from thermal loading (6.9) and pressure loading (6.7) can be ascribed primarily to experimental errors and, to

some extent, to the variation in the boundary conditions used in the two methods.

A further simplification that can be made in this method is to assume that the central triangular-shaped sections contribute little to the rigidity of the geometry and to compute δ_m directly from Lamé's solution for a thick ring under external pressure.

It has been pointed out that the assumption of linear viscoelastic behavior of the propellant does not hold for some propellant materials at high strains when the so-called "dewetting" occurs. For this case it is suggested that a more elaborated model analysis be conducted with the propellant material itself as the model material and a thermal loading similar to the one outlined above. The loading would have to be continued to failure and the simple strain displacement relationship shown above would be replaced with an experimentally obtained curve for any point of interest. The curve will be a strain-displacement curve with the temperature as a parameter. The use of the actual propellant would require a different experimental method for the model, possibly one of the techniques discussed in Section VIII. If the experimental method used gave a whole-field analysis then any point of interest could be chosen to draw a curve, and the complete analysis could be a family of curves for various points. This analysis could then be applied to any size grain of similar geometry.

VII. REPLICA TECHNIQUES

A recognized method of strain measurement which has several advantages but does not present the possibility of remote reading is the replica technique. Here, a plaster, plastic, or low fusion temperature metal impression is made of the area to be analyzed before and after loading, and the two impressions compared under a microscope to note variations in length between random marks (or, if necessary, scratches made before loading). The replica technique is essentially a laboratory method, but is mentioned here for the sake of completeness.

A modification of this technique has been suggested. The surface of the propellant might be coated with ink and an impression of the surface be taken before and after loading that could be observed with a measuring microscope.

Several printing and writing inks were tried in this program, however, none gave a consistent, satisfactory image.

Another variation of this method would be for soft rubber lines to be cemented to the model and inked so that an impression of the lines could be obtained. Essentially the rubber lines would act like an ordinary office rubber stamp.

To illustrate the method strips of a rubber stamp were cut up and cemented with Hysol 4485 on the horizontal and vertical diameters of a 1" thick by 3" diameter disk of propellant material. The characters were inked with stamp pad ink and an impression made on paper. The disk was then loaded along the vertical diameter producing compressive displacement of .150" and another impression of the characters was made. The impressions with the position of the characters with respect to the load are shown in Fig. 11.

VIII SURFACE COATINGS

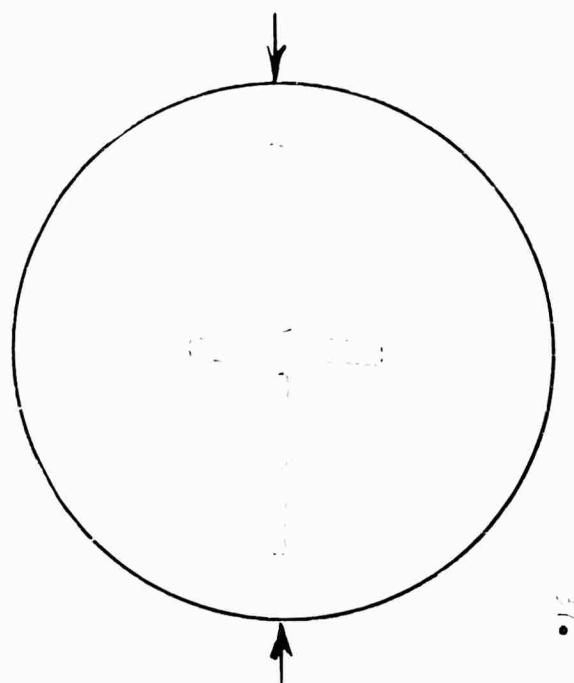
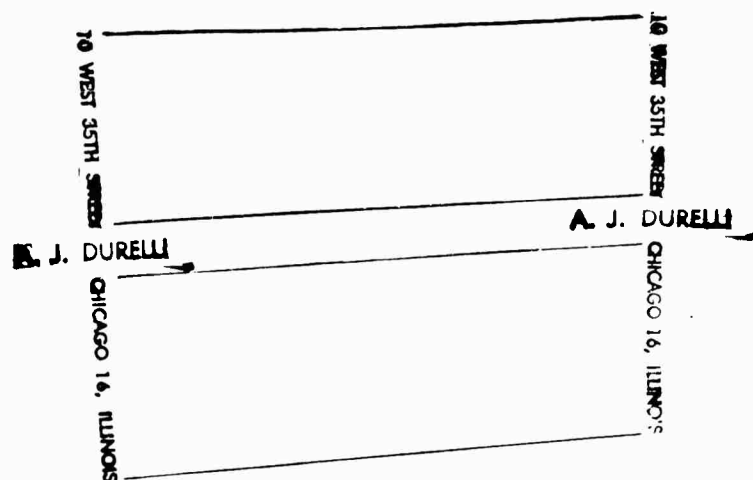
There are at least three methods of whole-field strain determinations of a surface that warrant consideration. None of them unfortunately is well suited for determining strains in sharp fillets. However, the methods would find application when the propellant has a flat end of the same geometry as the general cross-section of the grain, and is accessible to view. Here the strains at the cross-section of the fillet would give a good approximation of the strains in the fillets in the central portion of the rocket.

The Grid Method. A sharp set of lines is marked on, or cemented to, the flat surface and photographed before and after loading. Measurements on the photographs, using a comparator, can give the strain at any desired point.

The Moire Method. A very dense grid of uniformly-spaced parallel lines must be printed on or bonded to the flat surface and a master pattern of the same sort on glass or film laid over it. Any displacement of one grid in respect

Impression From
Unloaded Disk

Impression From
Loaded Disk



Position of Characters on Disk

Fig. 11 IMPRESSIONS FROM RUBBER STAMP CHARACTERS ON AN UNLOADED AND LOADED PROPELLANT DISK

to the other produces interference fringes that can be interpreted as loci of points with the same displacements in the direction perpendicular to the grid line direction. From the displacements the strains can be obtained by differentiation.

Birefringent Coatings. Birefringent coatings have also been considered.

By cementing the coatings to the propellant surface and recording the fringe pattern or color pattern photographically the shear strains can be determined. More elaborate analysis should be used to obtain the complete strain field. For sufficient sensitivity the birefringent coating thickness should be of the order of 0.100". Urethane rubber rather than the more common epoxies is recommended because of its low modulus of elasticity.

IX SUMMARY

The objective of the reported research program was two-fold:

(1) To survey the field of experimental stress analysis to evaluate those methods which seem applicable to the determination of strains on the inside surface of live propellants when the rocket is in storage; (2) To develop those methods which seem more promising to determine those strains. Several methods have been reviewed but none of them can be considered completely satisfactory. Most of these methods may find application to some particular phase of the problem, but likely none can be considered as an all-purpose method. In the report recommendations for further development of several of these methods are made. The authors feel that within the assumptions and limitations explained in the body of the report, the determination of strains, from measurement of diameter changes of the core, deserves special further investigation. They also recommend that the idea of encapsulating strain gages in the actual propellant be further developed.

ACKNOWLEDGEMENTS.

The research reported here was conducted from July 1, 1961 to January 31, 1962 under the sponsorship of Aerojet General Corporation. Dr. James H. Wiegand, Head of the Mechanical and Ballistic Properties Laboratory was the monitor of the program.

The cooperation and encouragement of Professor Frank Biberstein, head of the Civil Engineering Department of the Catholic University of America is gratefully acknowledged. Mr. P. Laura and C. van der Zon contributed to the development of the experimental work.

APPENDIX C

PARAMETER CALCULATIONS OF SIMPLE PROPELLANT GRAINS
FOR TEMPERATURE CYCLING, PRESSURIZATION, AND
ACCELERATION

by

A. Messner and D. Schliessmann

Structural Design and Analysis Department
Aerojet-General Corporation

USE OF THE SOLUTIONS

To obtain relative data such as effect of end bonding a motor or of increasing segment length, etc., use the data as presented. When the absolute magnitude of the stresses and strains are of interest, proceed as follows.

Determine the following dimensions and loading conditions to be analyzed.

outer radius of propellant	B
inner radius of propellant	A
length of the propellant	L
pressure	P
cure temperature-storage temperature	ΔT
acceleration in number of g's	n
modulus of propellant	E

calculate $\frac{B}{A}$, $\frac{L}{B}$, $\frac{P}{500}$, $\frac{\Delta T}{79}$, $\frac{n}{10}$

Look up the appropriate solution for the particular geometry (end bonding, $\frac{B}{A}$, $\frac{L}{B}$) interpolate where required.

- a) For pressurization multiply results by $\frac{P}{500}$
- b) For temperature multiply results by $\frac{\Delta T}{79}$
- c) For acceleration use solution with appropriate B and multiply results by $\frac{n}{10}$

A list of the solutions presented and the figure numbers is given on Pages 7 and 8.

PROPERTIES AND LOADING CONDITIONS USED IN ANALYSIS

The following mechanical properties, constants, and loading conditions were used throughout the analysis:

Linear Coefficient of Thermal Expansion for Case	$\alpha_c = 589 \times 10^{-8} \text{ in. / in}^\circ\text{F}$
Linear Coefficient of Thermal Expansion for Propellant	$\alpha_p = 630 \times 10^{-7} \text{ in. / in}^\circ\text{F}$
Poisson's Ratio of Case	$\gamma_c = .3$
Poisson's Ratio of Propellant	$\gamma_p = .5$
Modulus of Elasticity of Case	$E_c = 30 \times 10^6 \text{ psi}$
Modulus of Elasticity of Propellant	$E_p = 1000 \text{ psi}$
Thickness of Case to Diameter Ratio	$\frac{t}{D} = .00195 \text{ in. / in}$
Pressure Loading	$P = 500 \text{ psi}$
Acceleration Loading (axial)	$A = 10 \text{ g}$
Temperature Cycling	$\Delta T = -79^\circ\text{F}$

(This is equivalent to a cure shrinkage of .5% in linear dimension)

LIST OF SOLUTIONS

LOAD CONDITION	GEOMETRY	$\frac{L}{B}$	STRESSES	$\frac{B}{A}$	FIGURE
Pressurization ↑ ↓ Pressurization	No end bonding	2	Interface	2, 3 & 4 ↑ ↓	1
	No end bonding	4			2
	No end bonding	8			3
	One end bonded	2	Interface		4
		2	End		5
		4	Interface		6
		4	End		7
		8	Interface		8
	One end bonded	8	End		9
	Both ends bonded	2	Interface		10
		2	End		11
		4	Interface		12
		4	End		13
		8	Interface		14
	Both ends bonded	8	End		15
Temperature Cycling ↑ ↓ Temperature Cycling	No end bonding	2	Interface	2, 3 & 4 ↑ ↓	16
	No end bonding	4			17
	No end bonding	8			18
	One end bonded	2	Interface		19
		2	End		20
		4	Interface		21
		4	End		22
		8	Interface		23
	One end bonded	8	End		24
	Both ends bonded	2	Interface		25
		2	End		26
		4	Interface		27
		4	End		28
		8	Interface		29
	Both ends bonded	8	End		30
Acceleration ↑ ↓ Acceleration	No end bonding	2	Interface	2, 3 & 4 ↑ ↓	31
	No end bonding	4			32
	No end bonding	4			33
	No end bonding	8			34
	One end bonded	2	Interface		35
		2	End		36
		4	Interface		37
		4	End		38
		8	Interface		39
	One end bonded	8	End		40

LIST OF SOLUTIONS (Continued)

LOAD CONDITION	GEOMETRY	$\frac{L}{B}$	STRESSES	$\frac{B}{A}$	FIGURE
Acceleration	Both ends bonded	2	Interface	2, 3 & 4	41
		2	Fwd end		42
		2	Aft end		43
		4	Interface		44
		4	Fwd end		45
		4	Aft end		46
		8	Interface		47
		8	Fwd end		48
Acceleration	Both ends bonded	8	Aft end	2, 3 & 4	49

CONFIGURATIONS OF GEOMETRIES ANALYZED

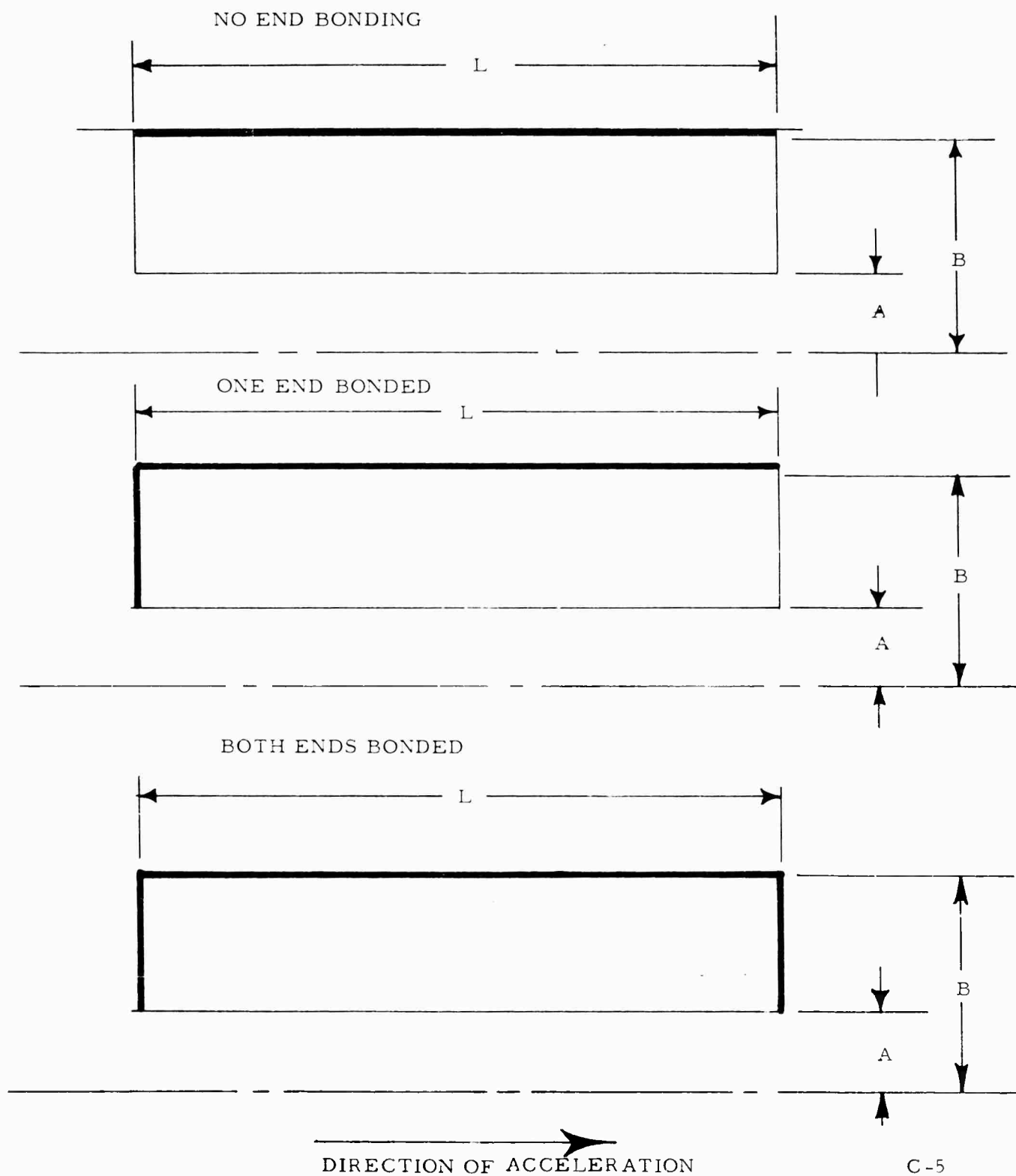
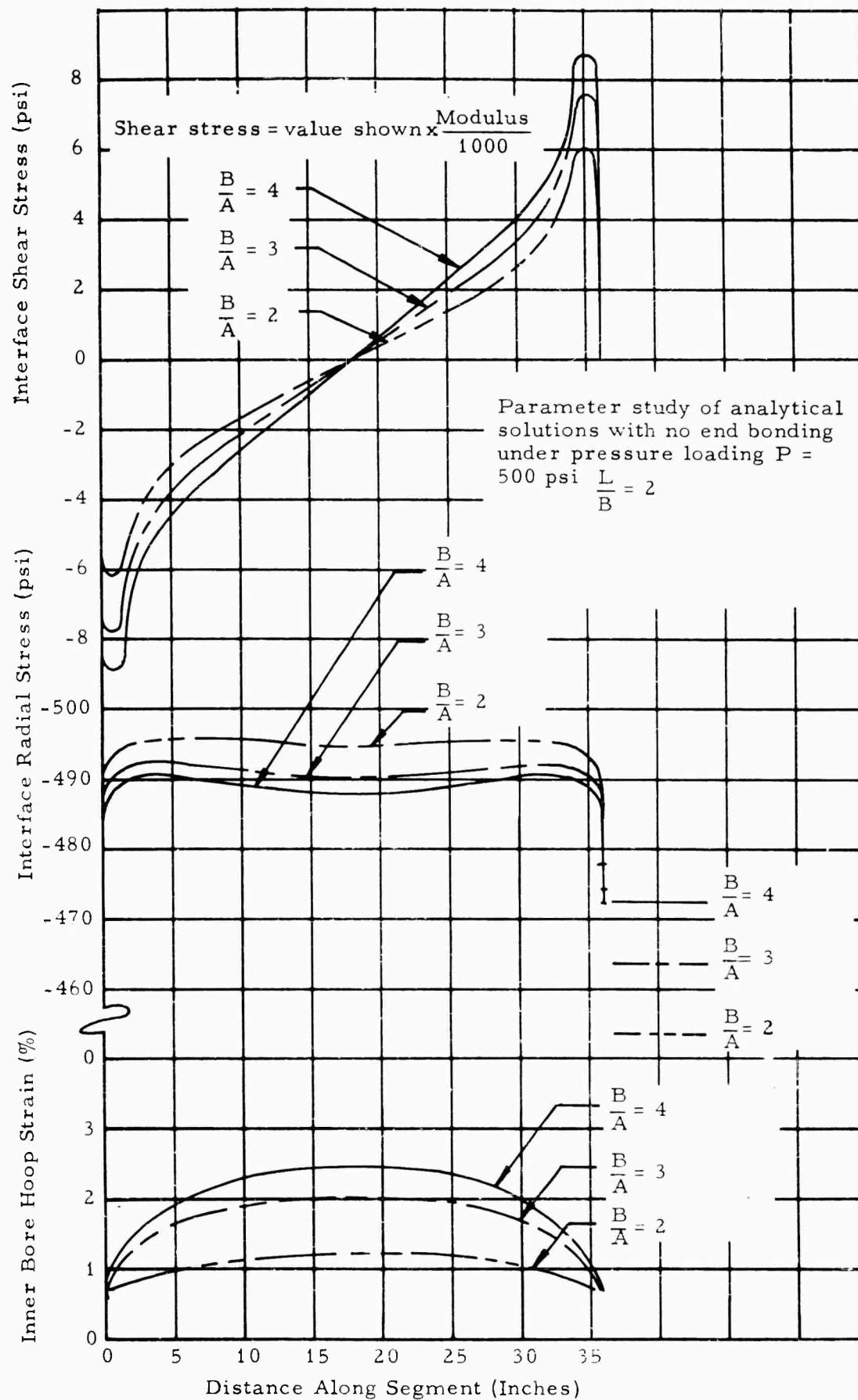


FIGURE 1



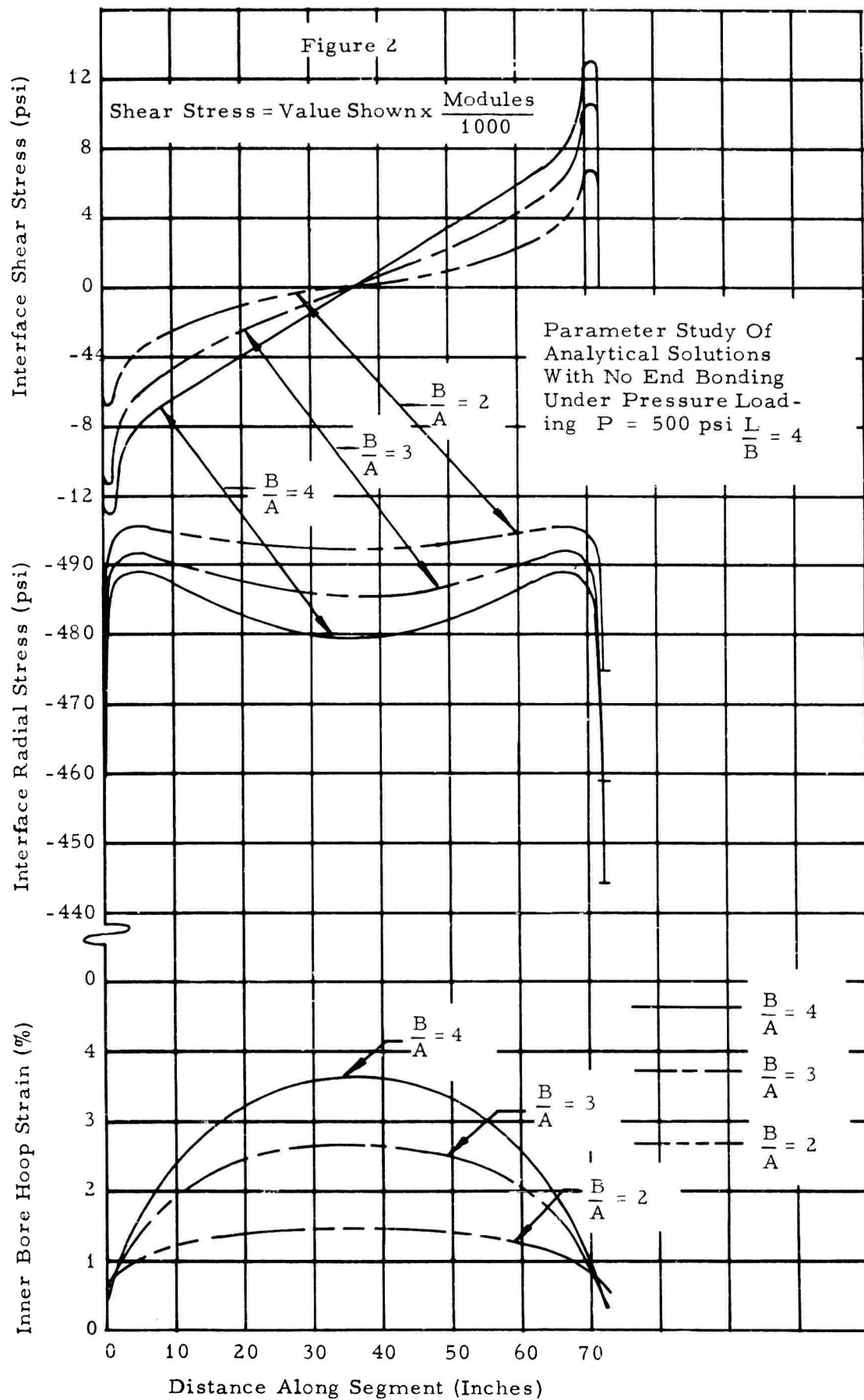
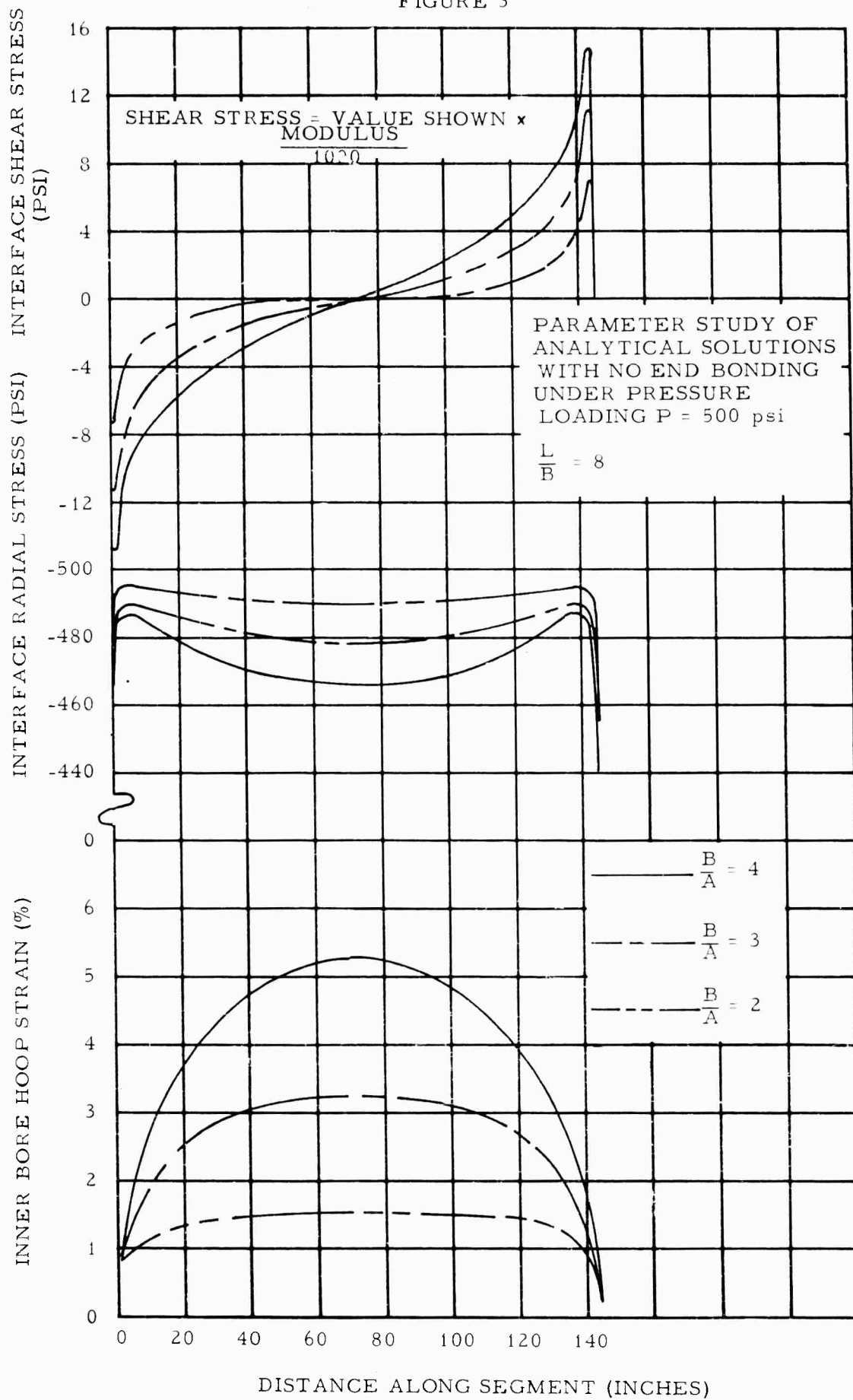


FIGURE 3



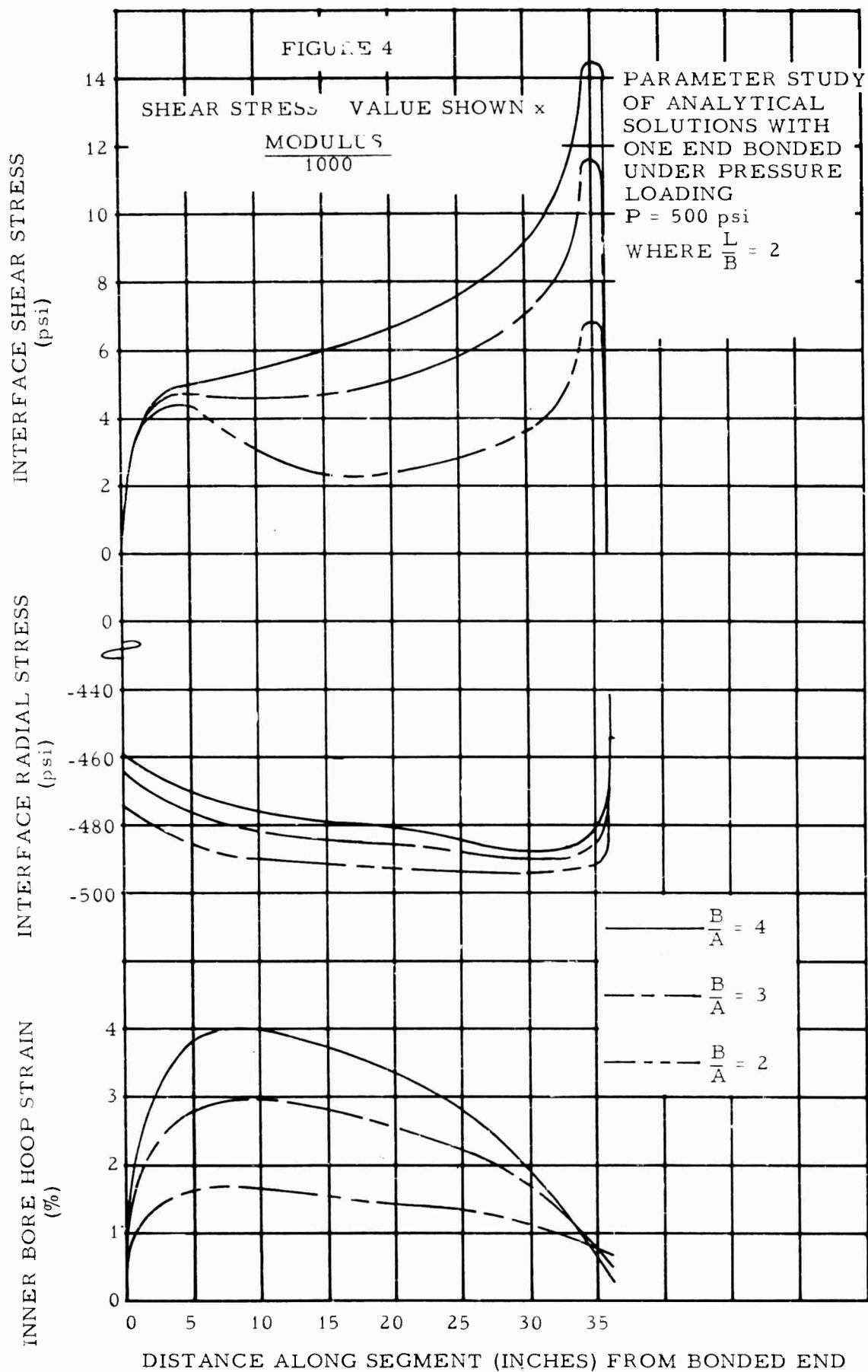


FIGURE 5

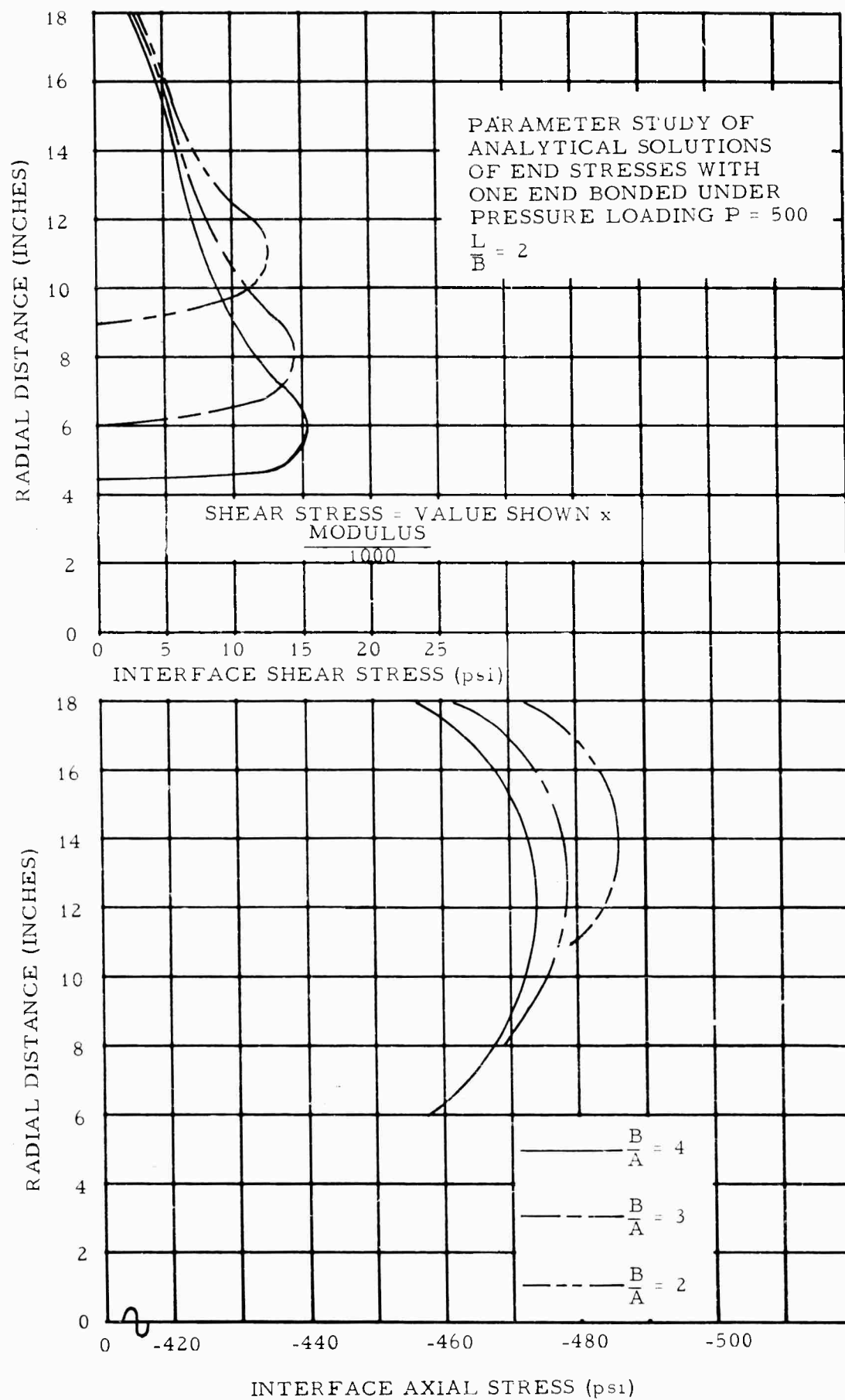


FIGURE 6

PARAMETER STUDY OF
ANALYTICAL SOLUTIONS
WITH ONE END BONDED
UNDER PRESSURE LOADING

$P = 500 \text{ psi}$ WHERE $\frac{L}{B} = 4$

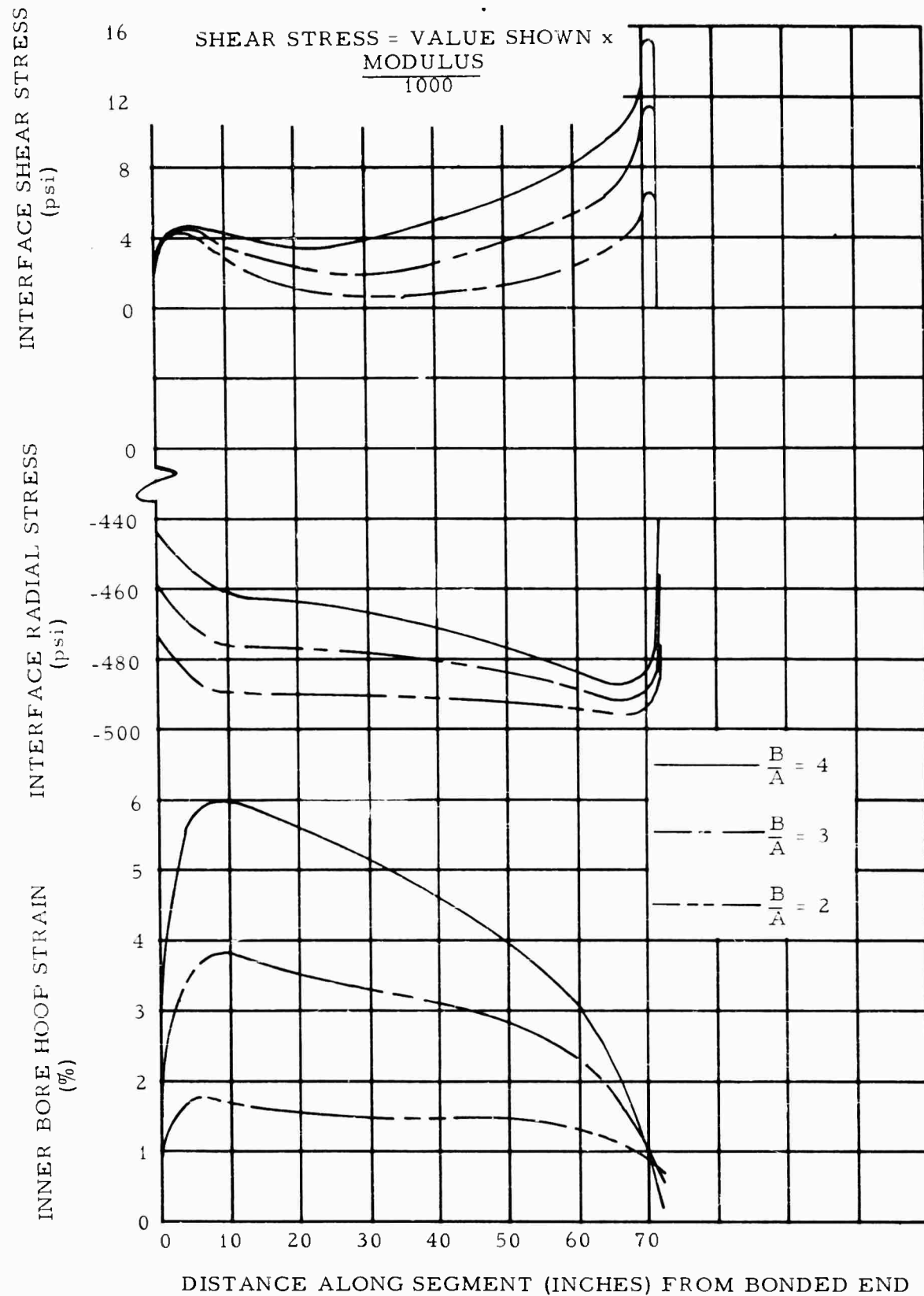


FIGURE 7

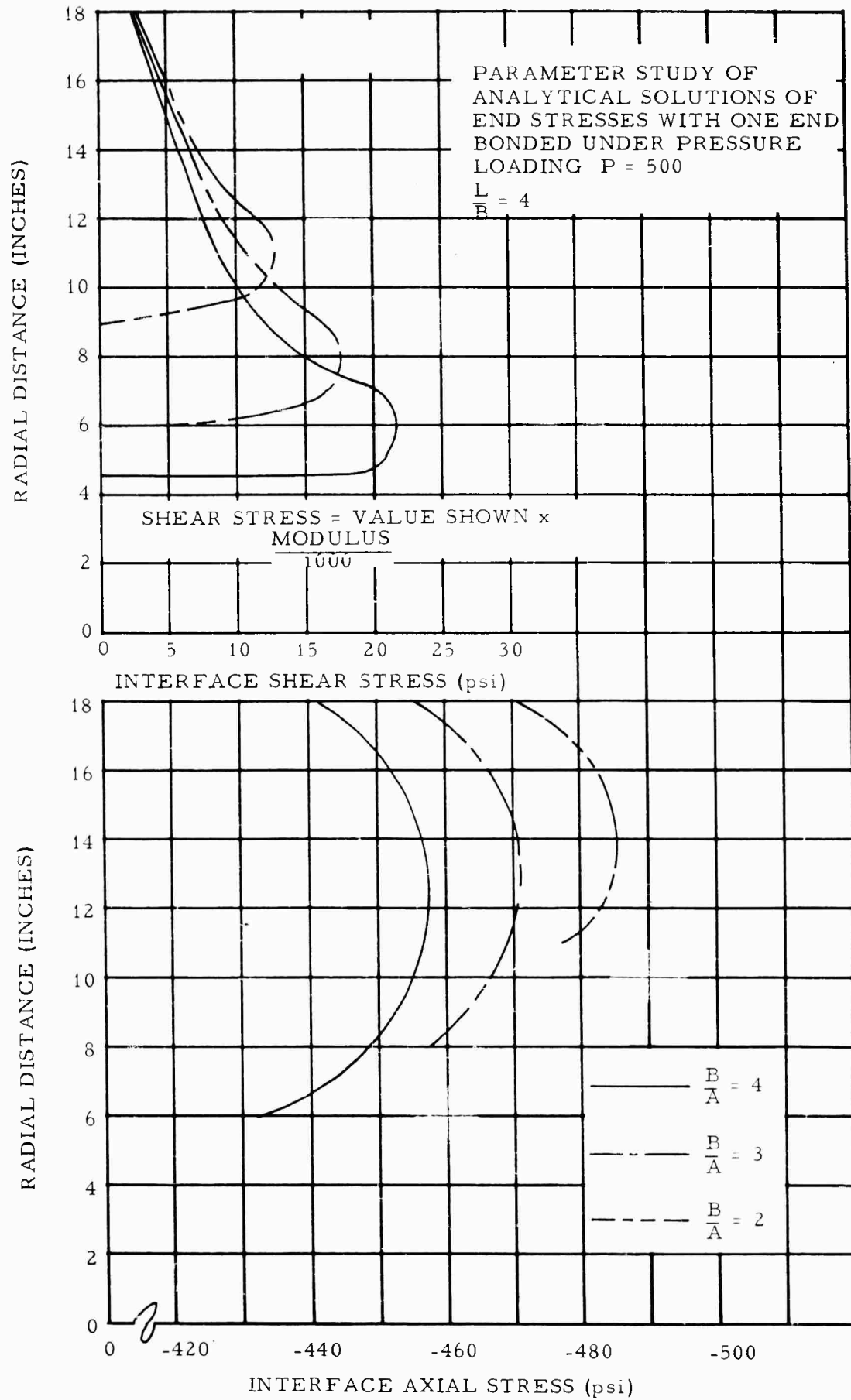
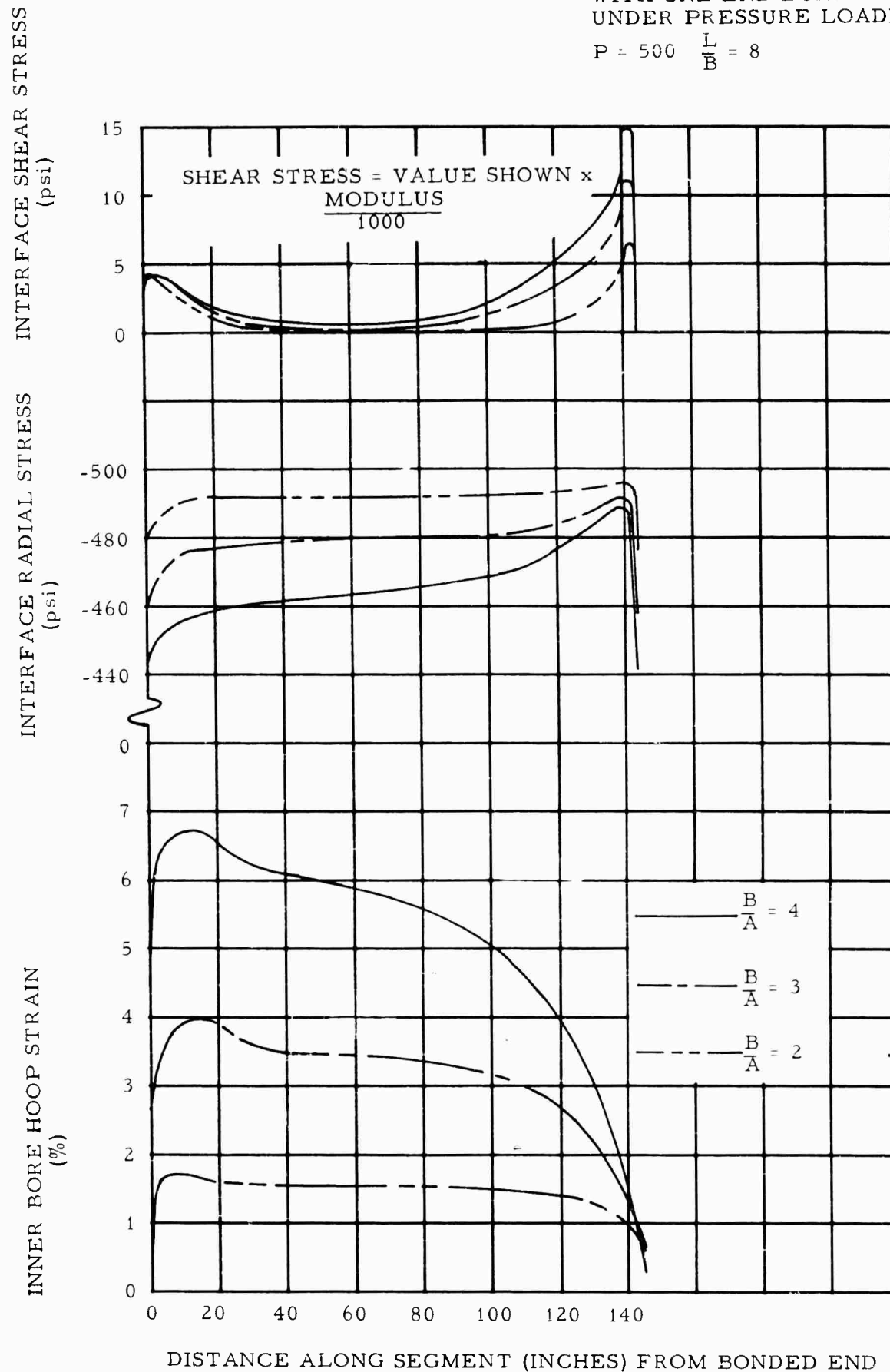
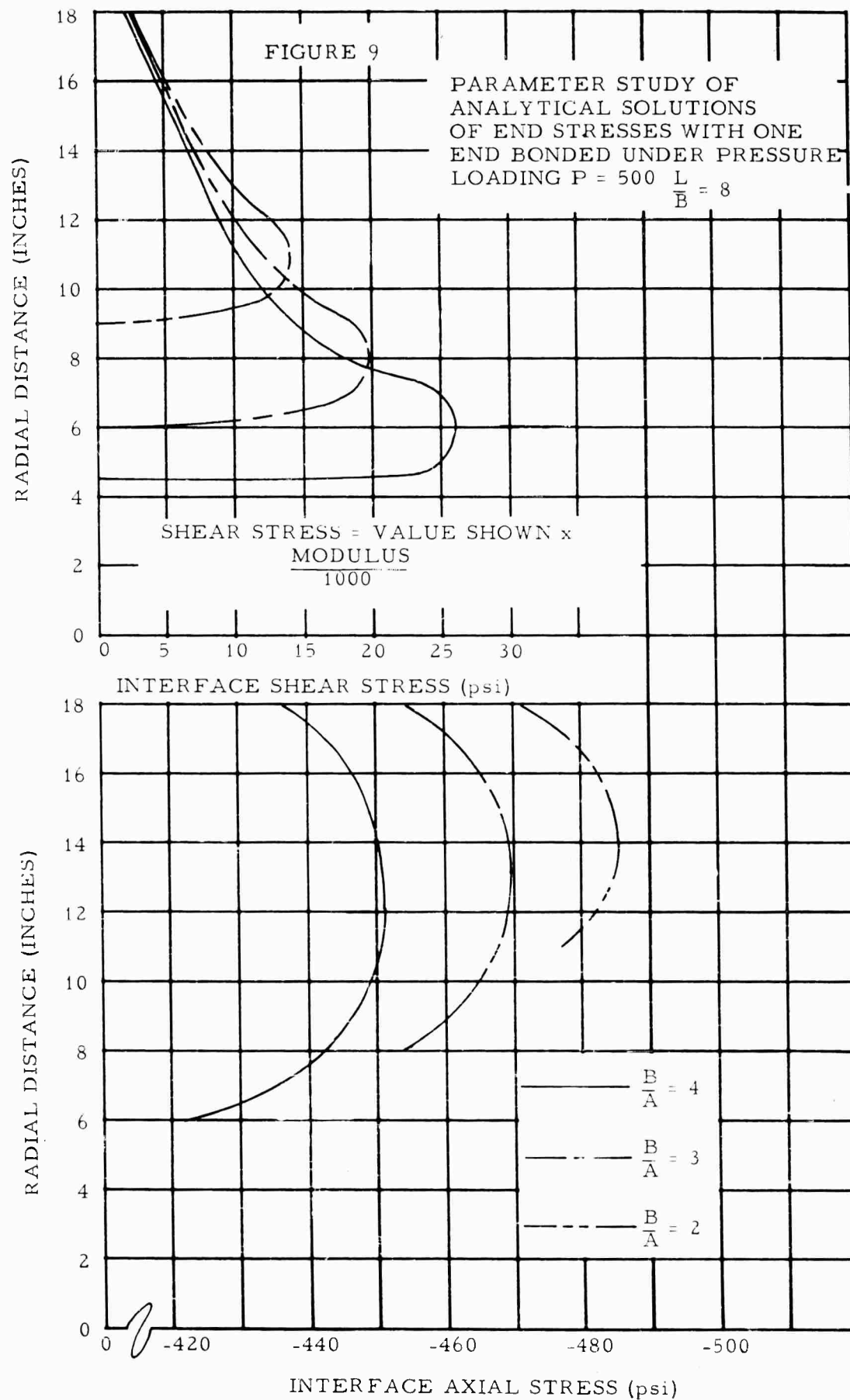


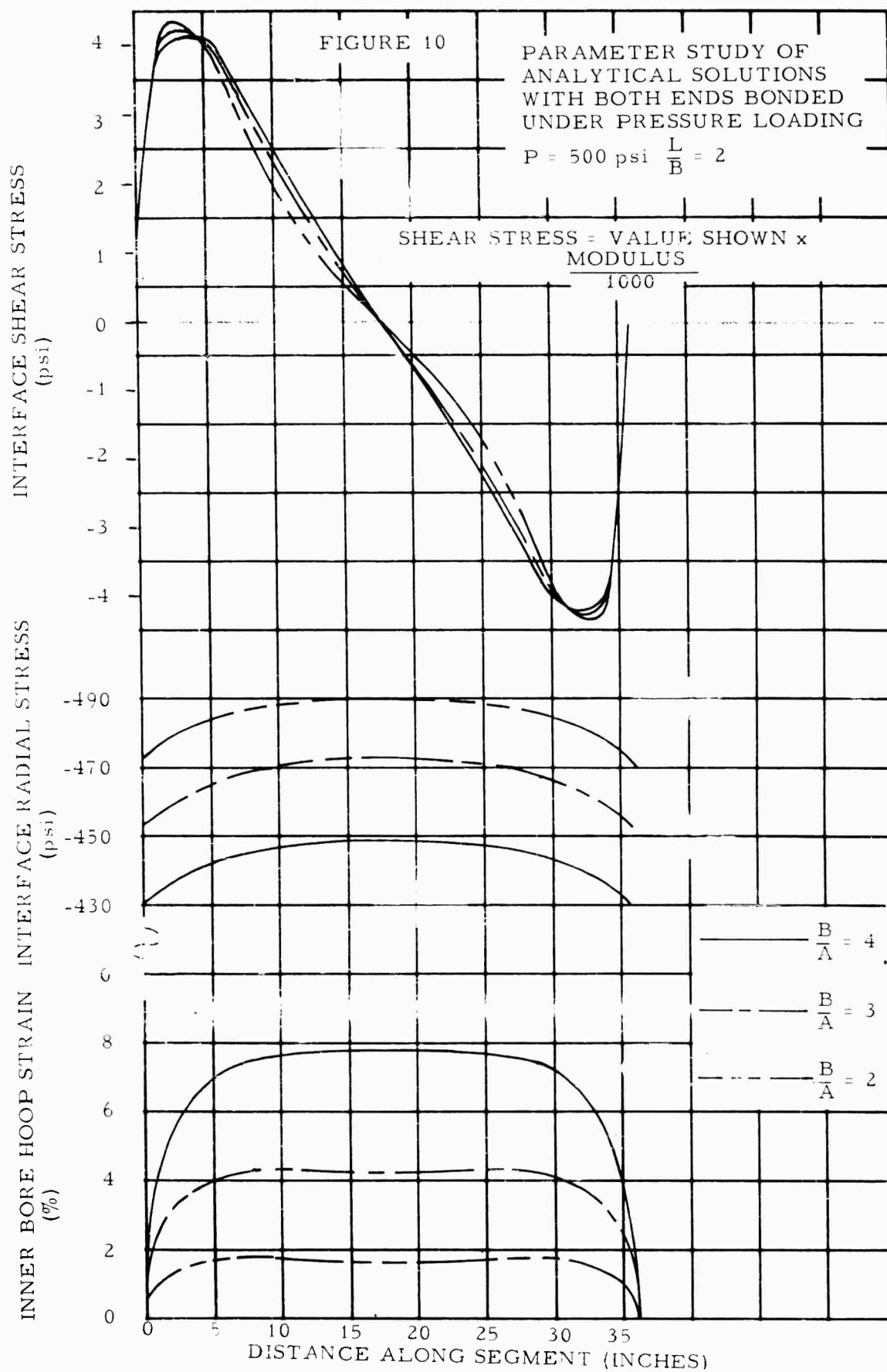
FIGURE 8

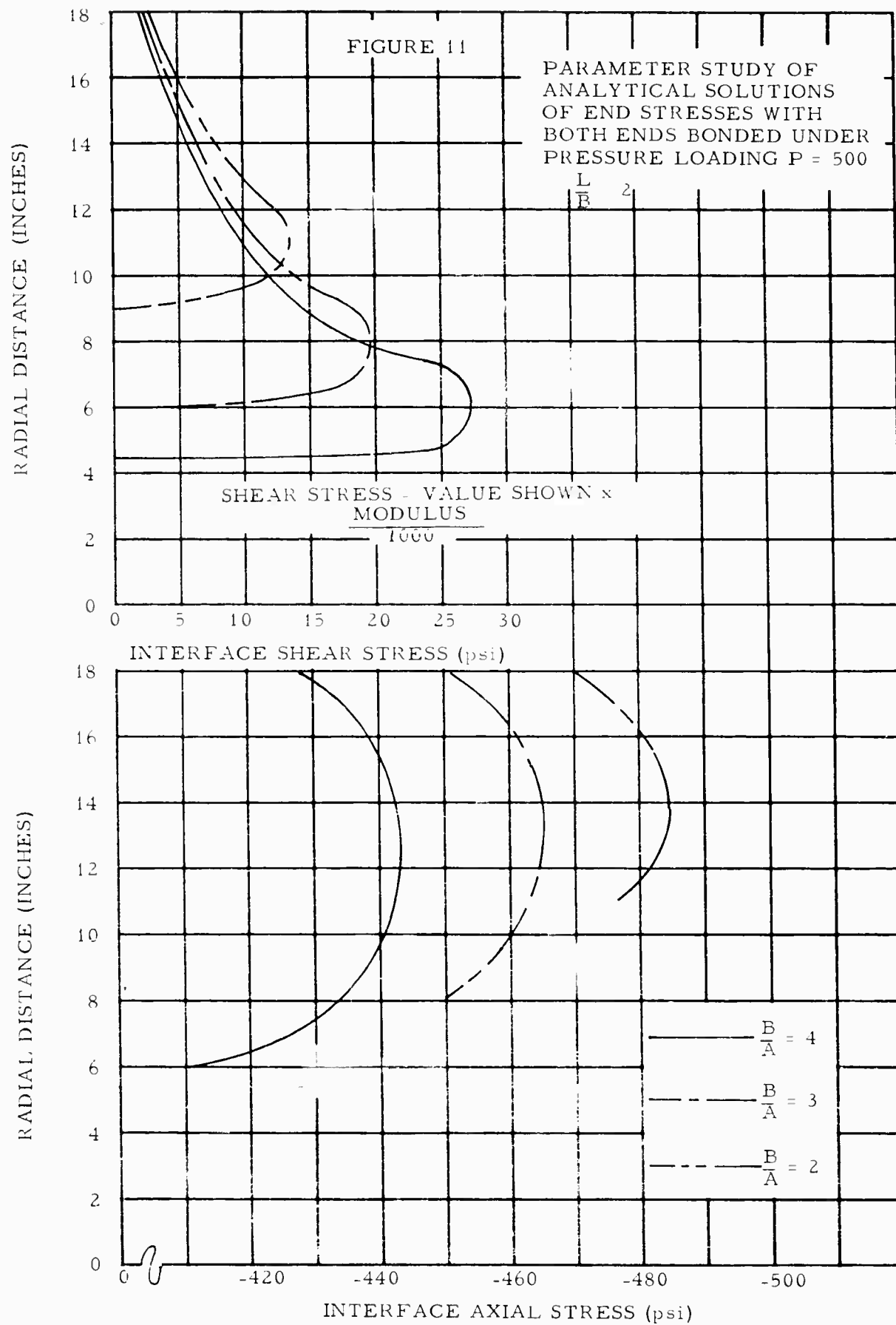
PARAMETER STUDY OF
ANALYTICAL SOLUTIONS
WITH ONE END BONDED
UNDER PRESSURE LOADING

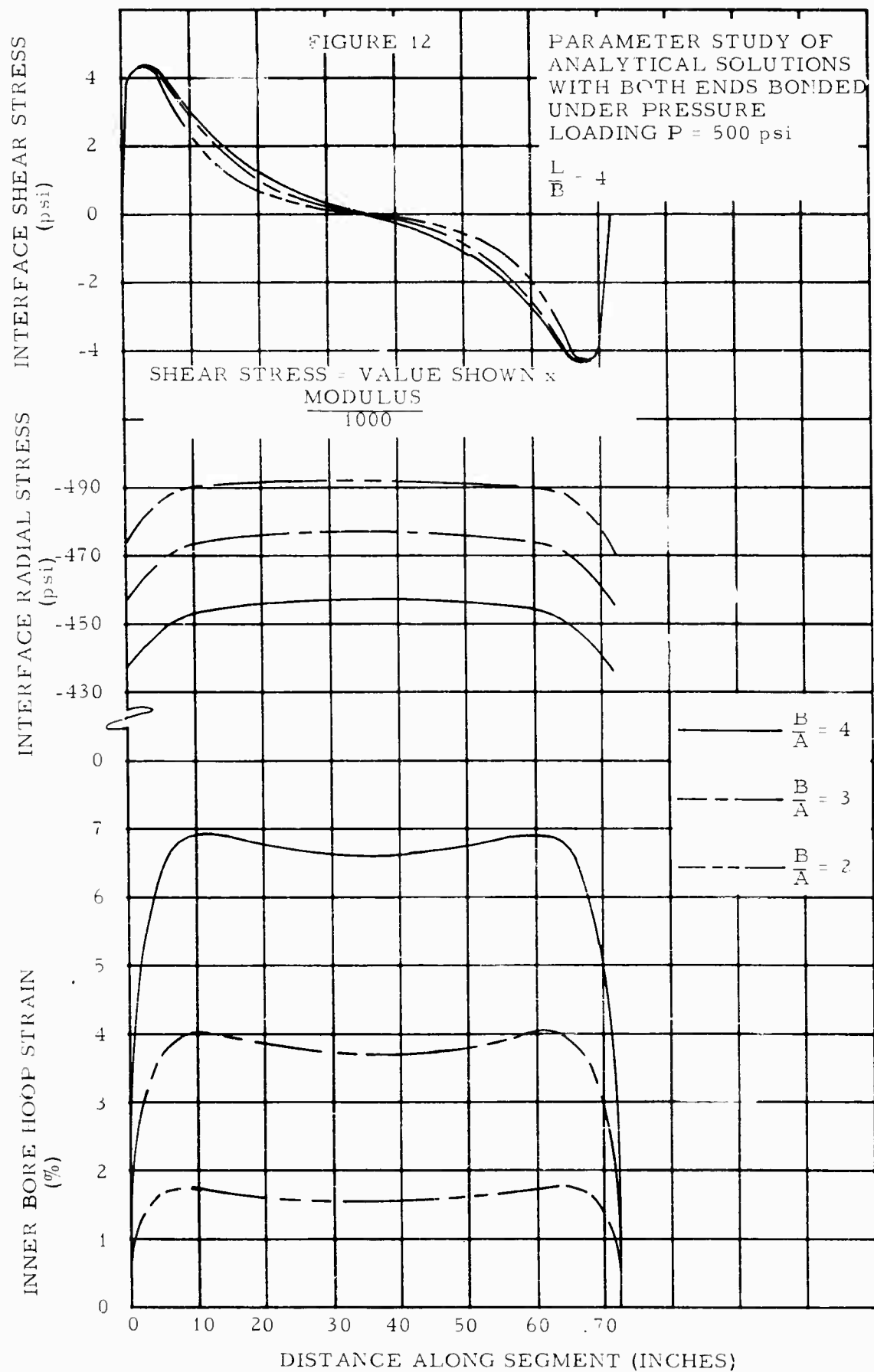
$$P = 500 \quad \frac{L}{B} = 8$$

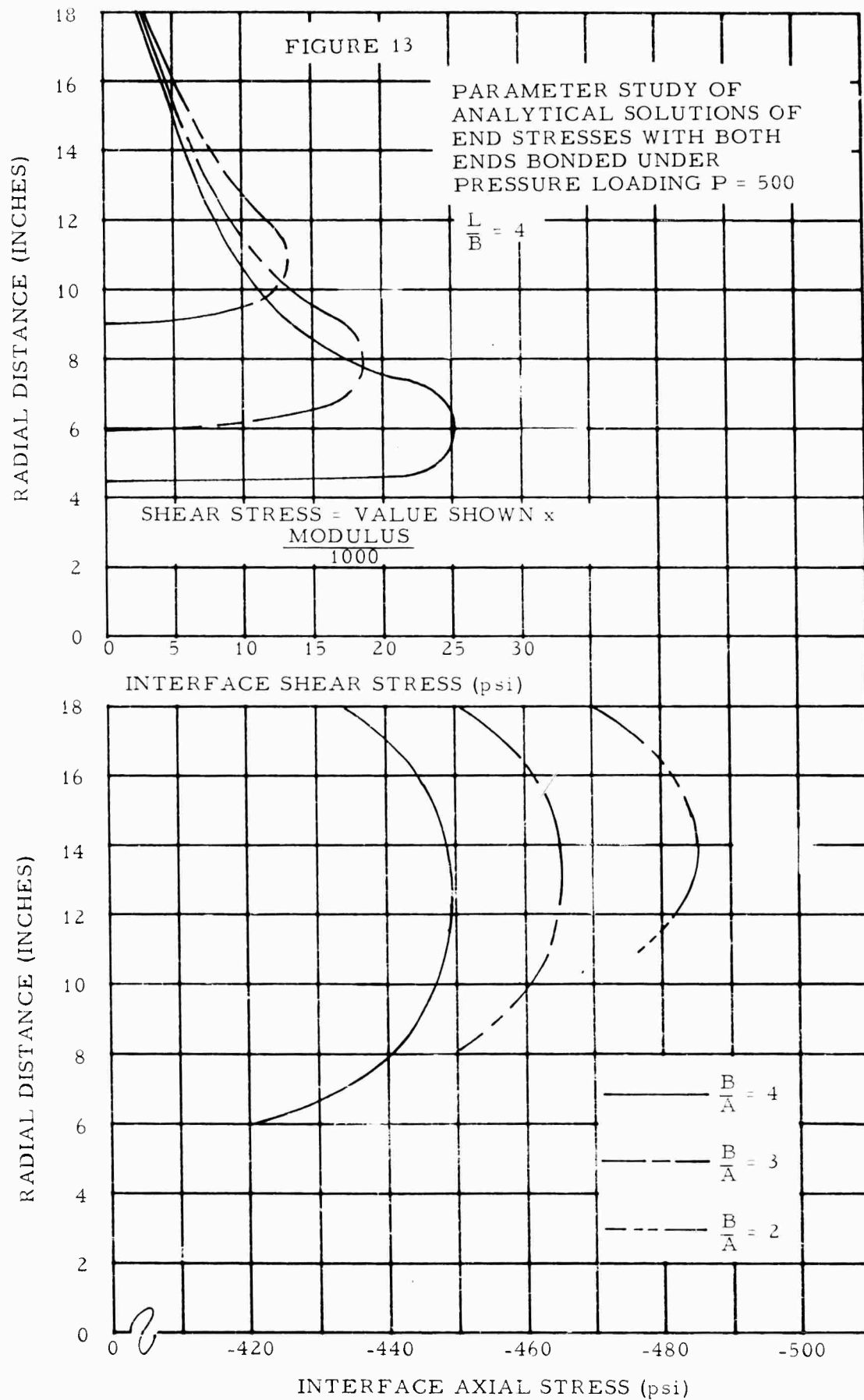


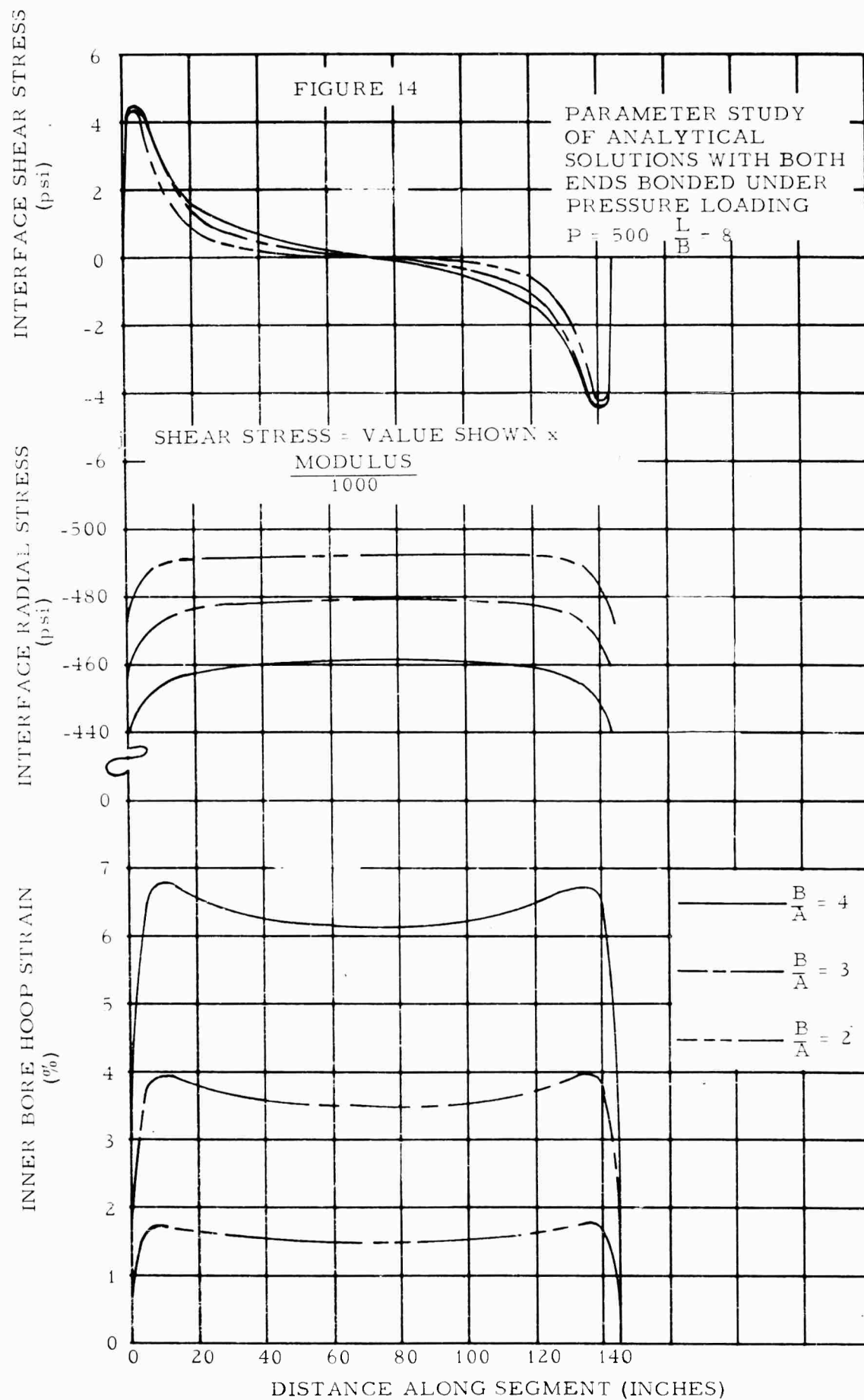


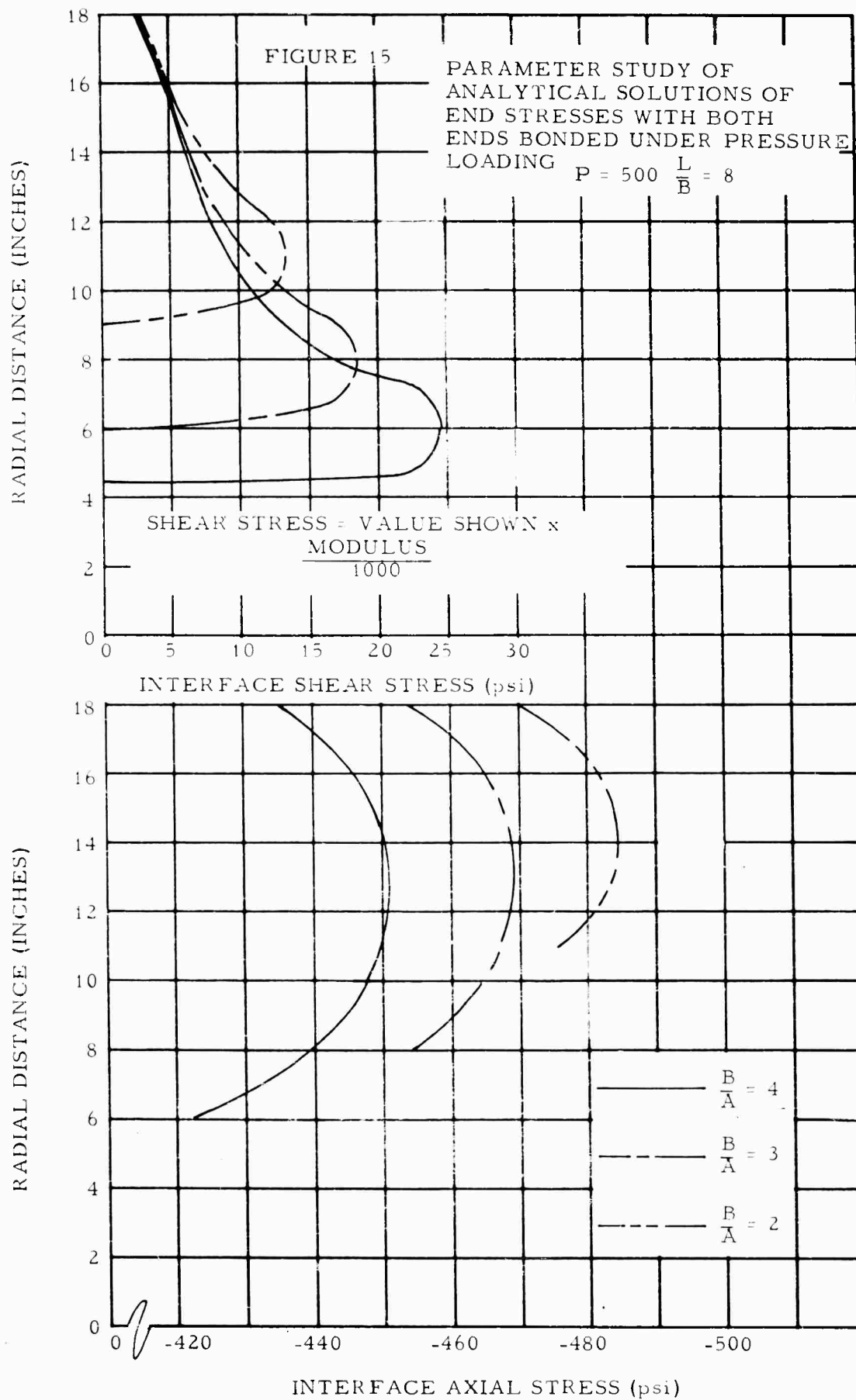


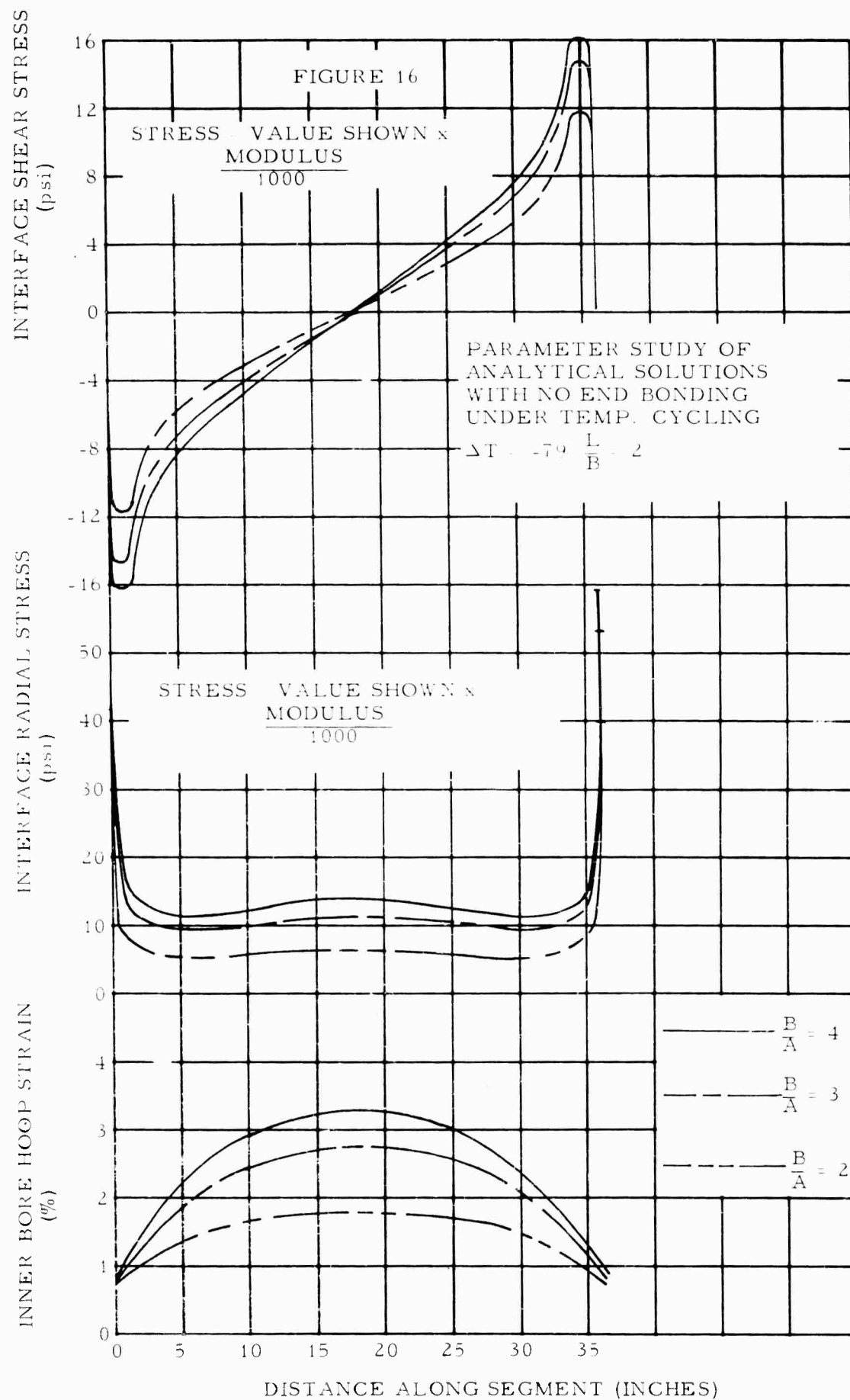


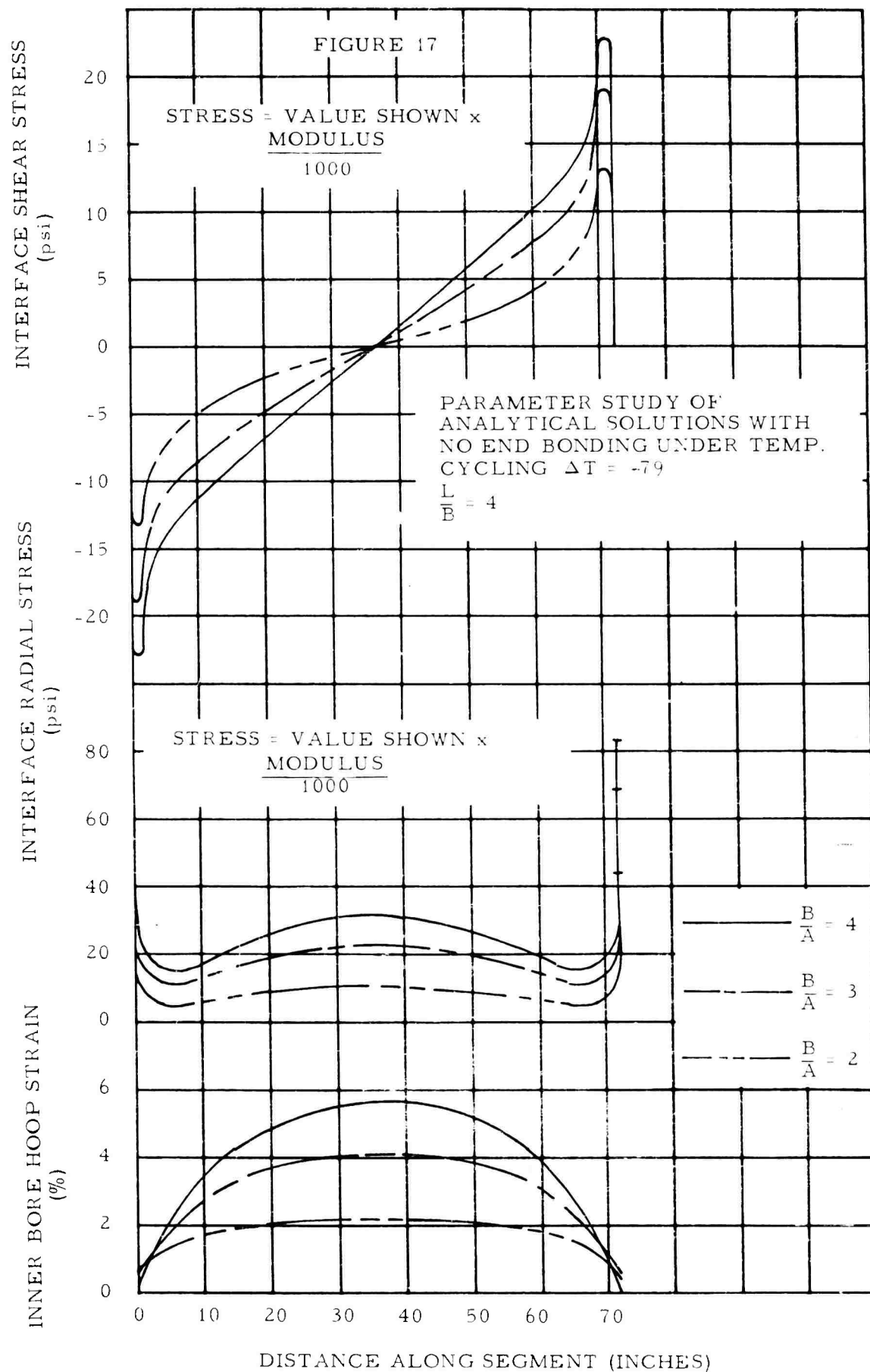


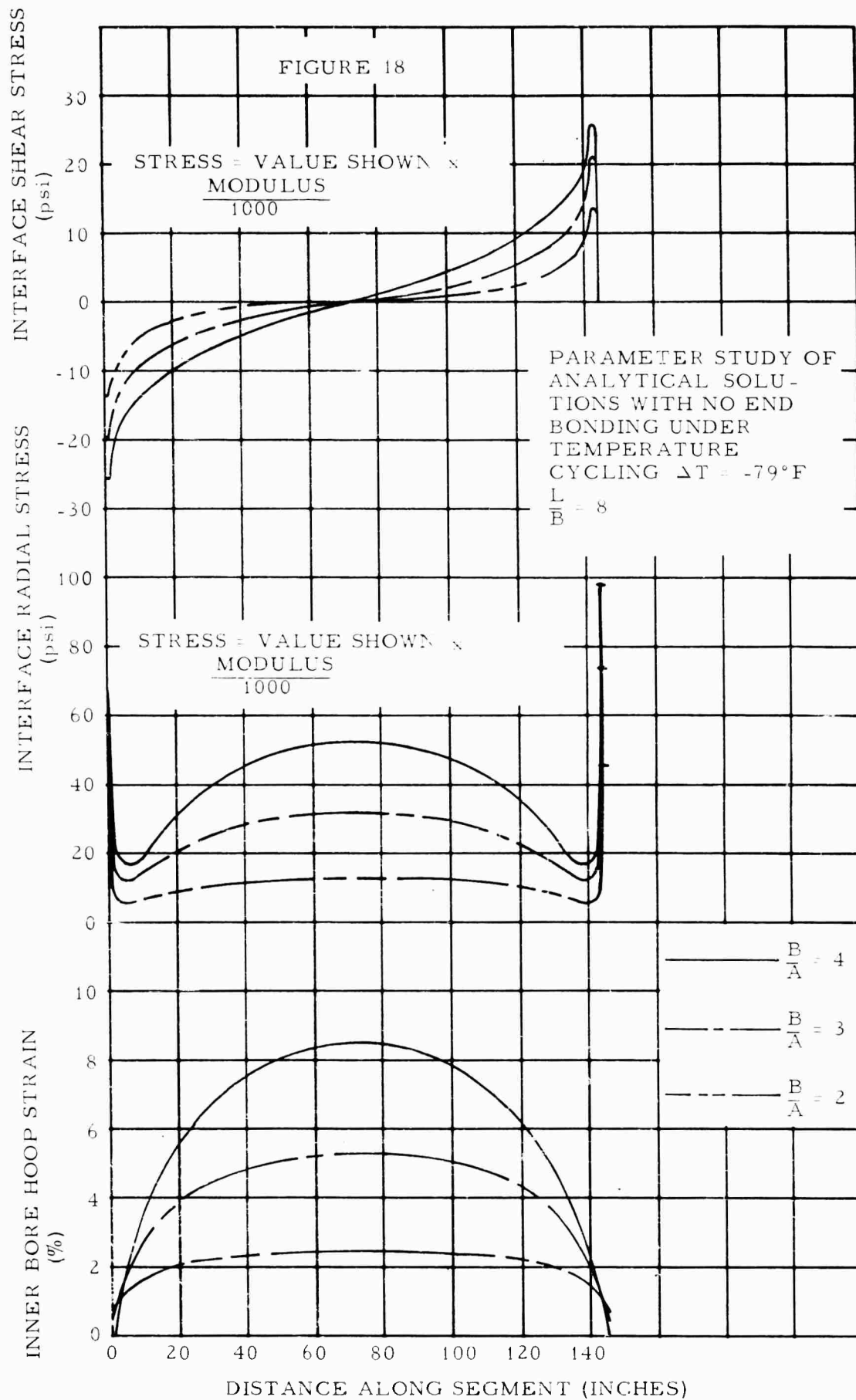


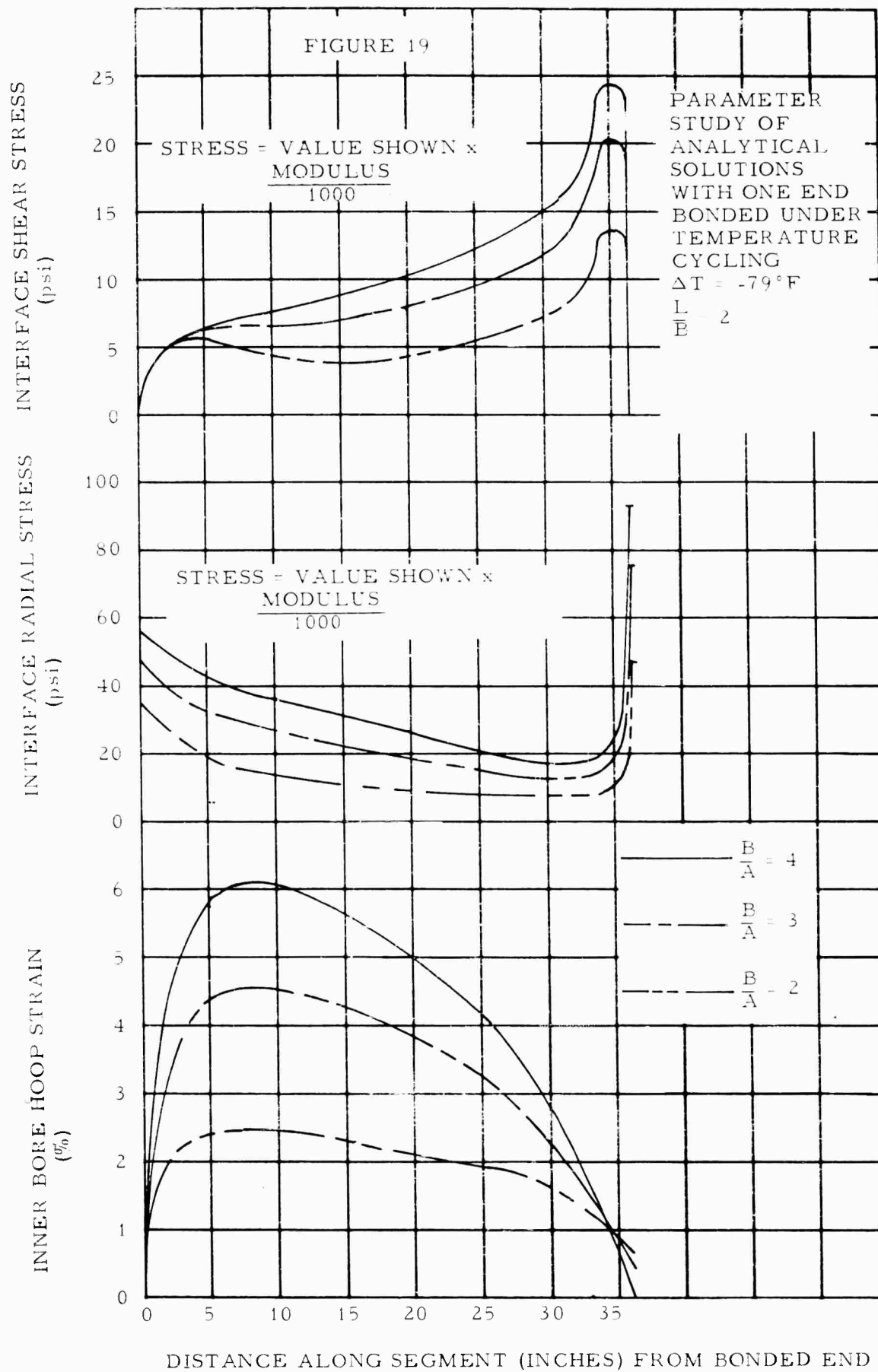


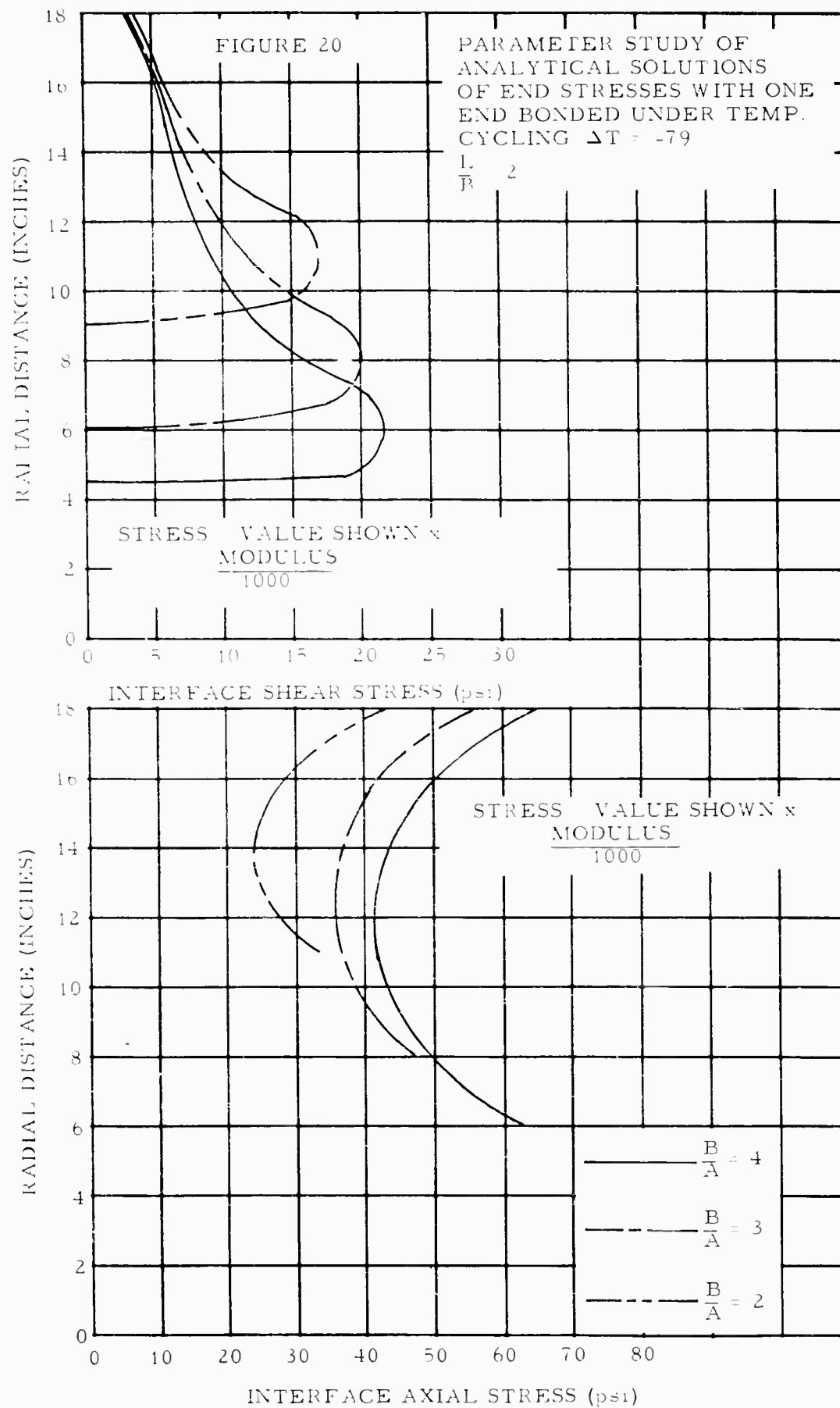


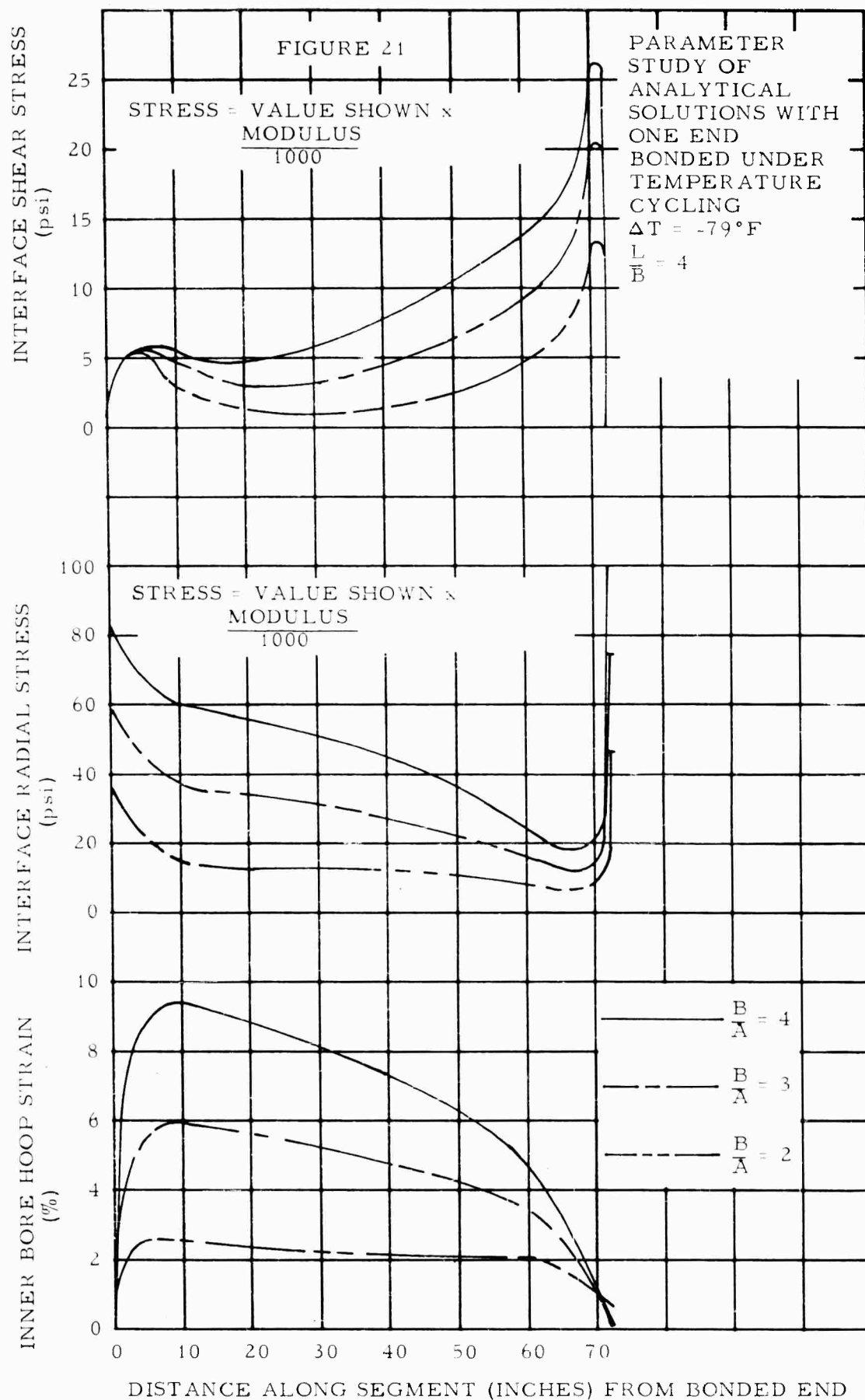












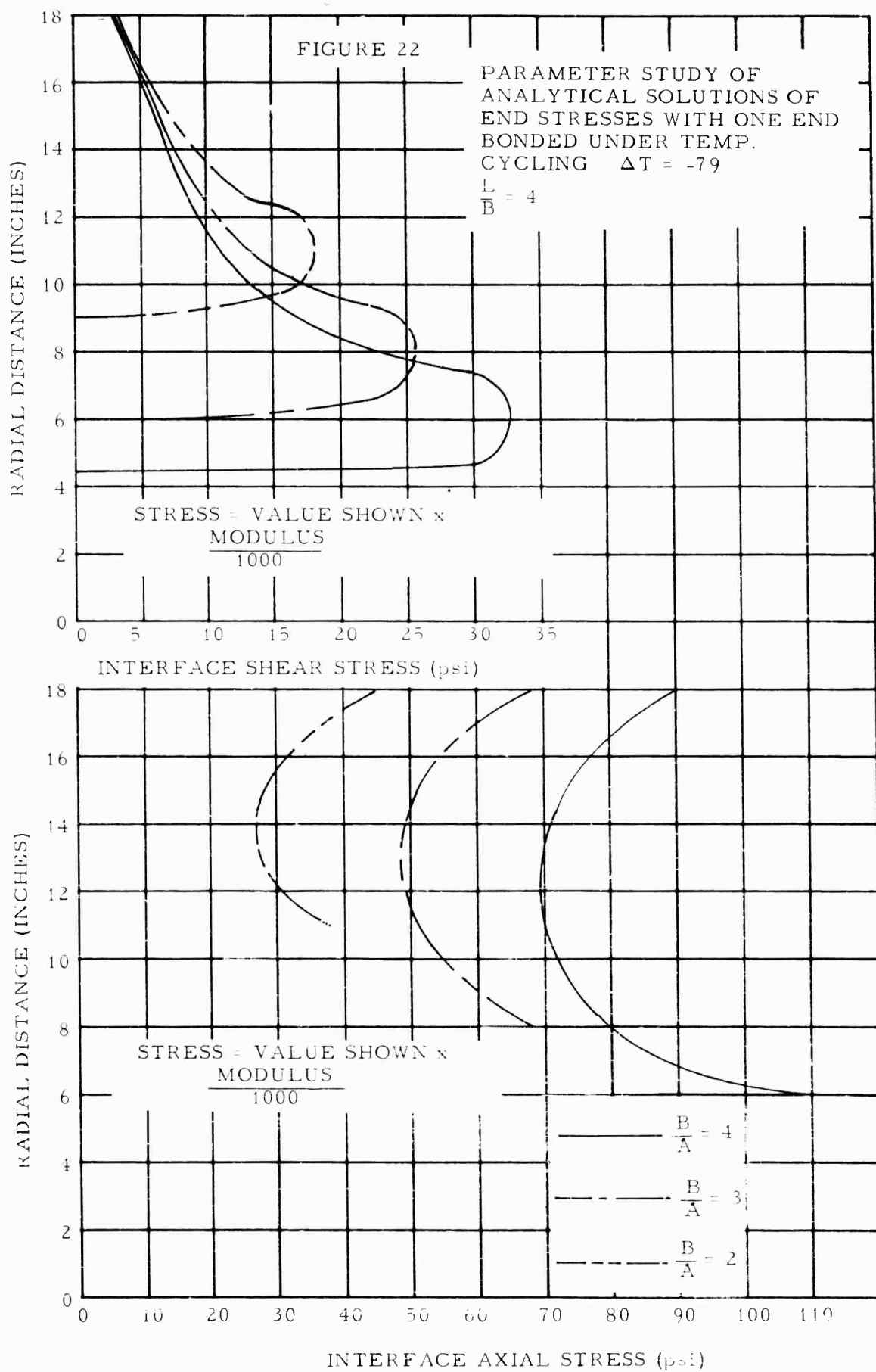
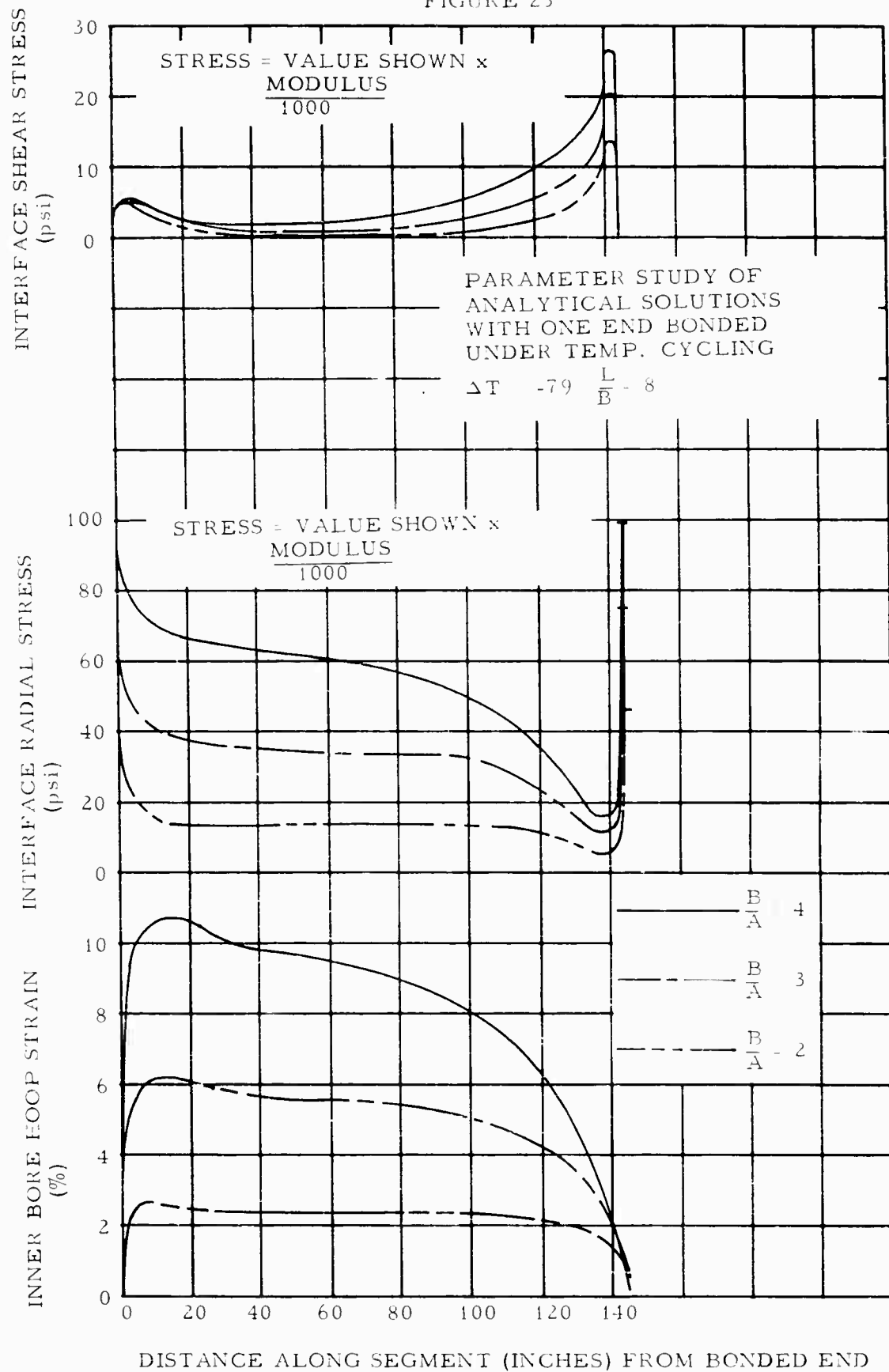
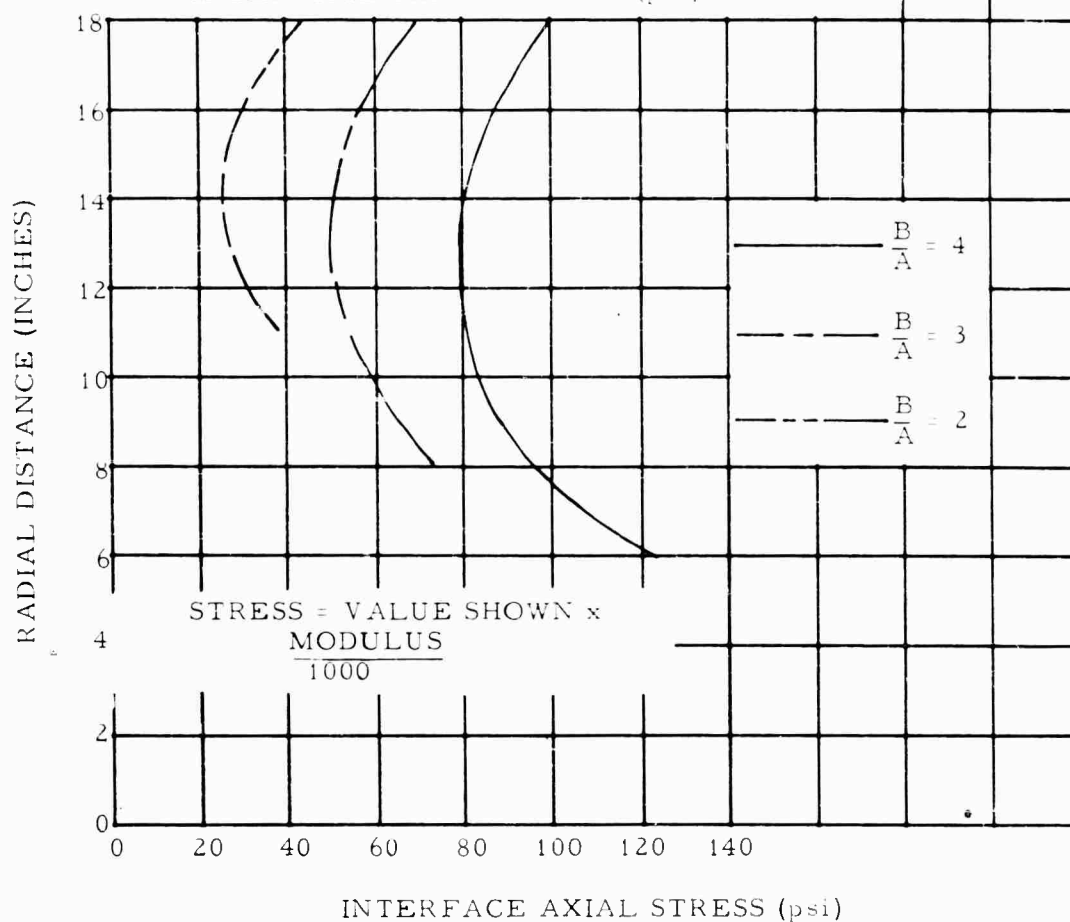
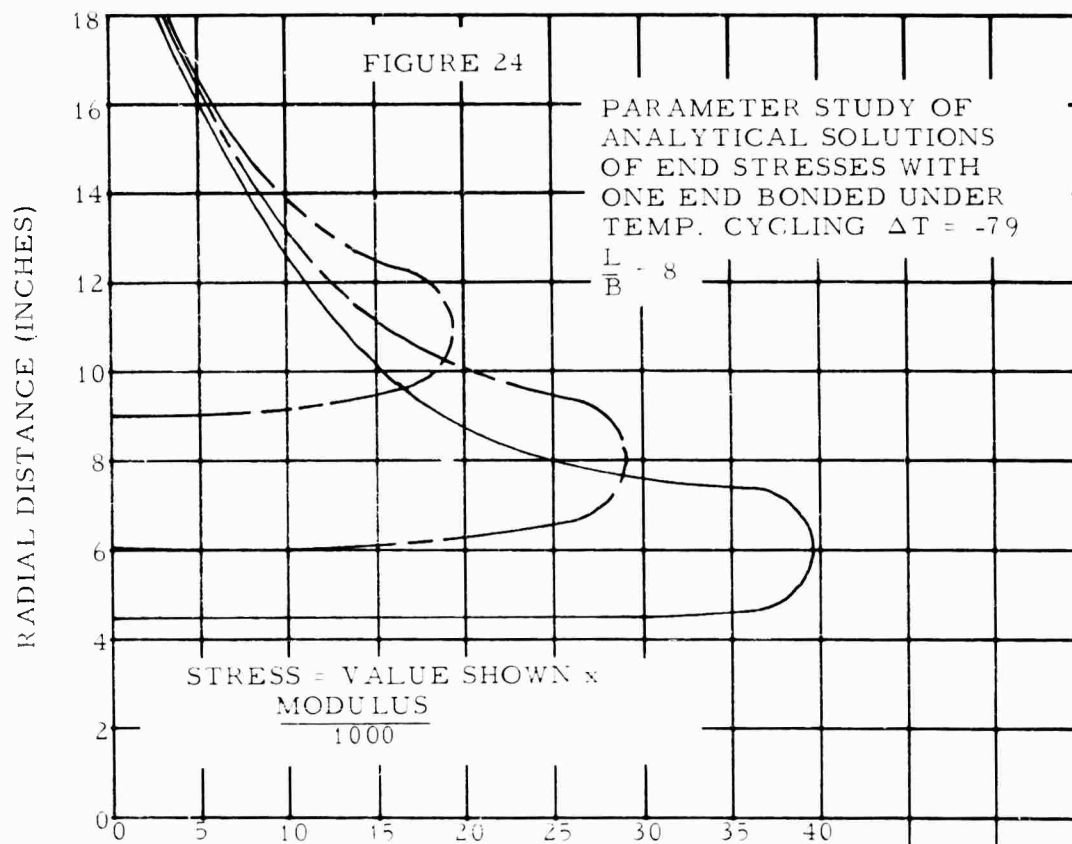
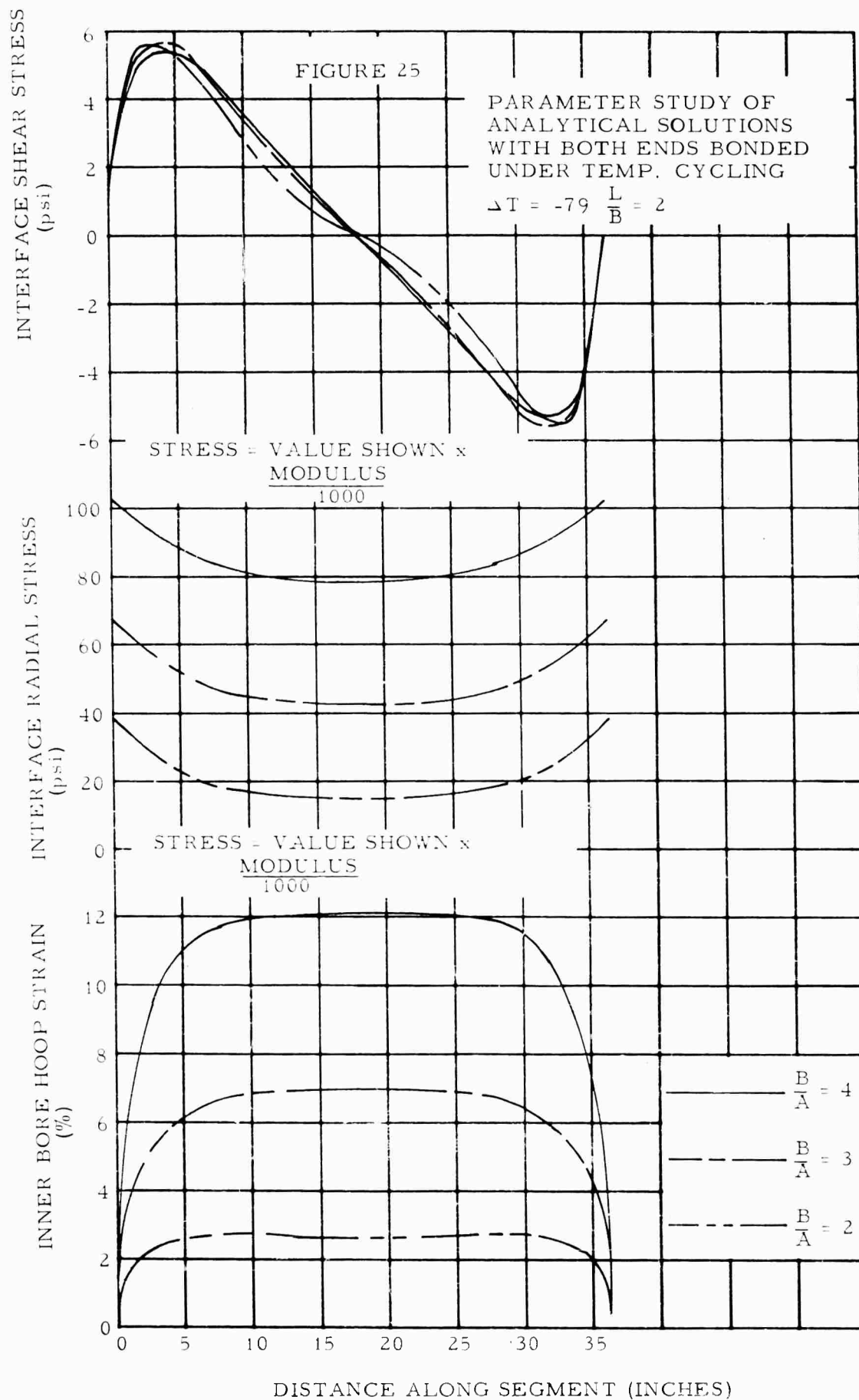
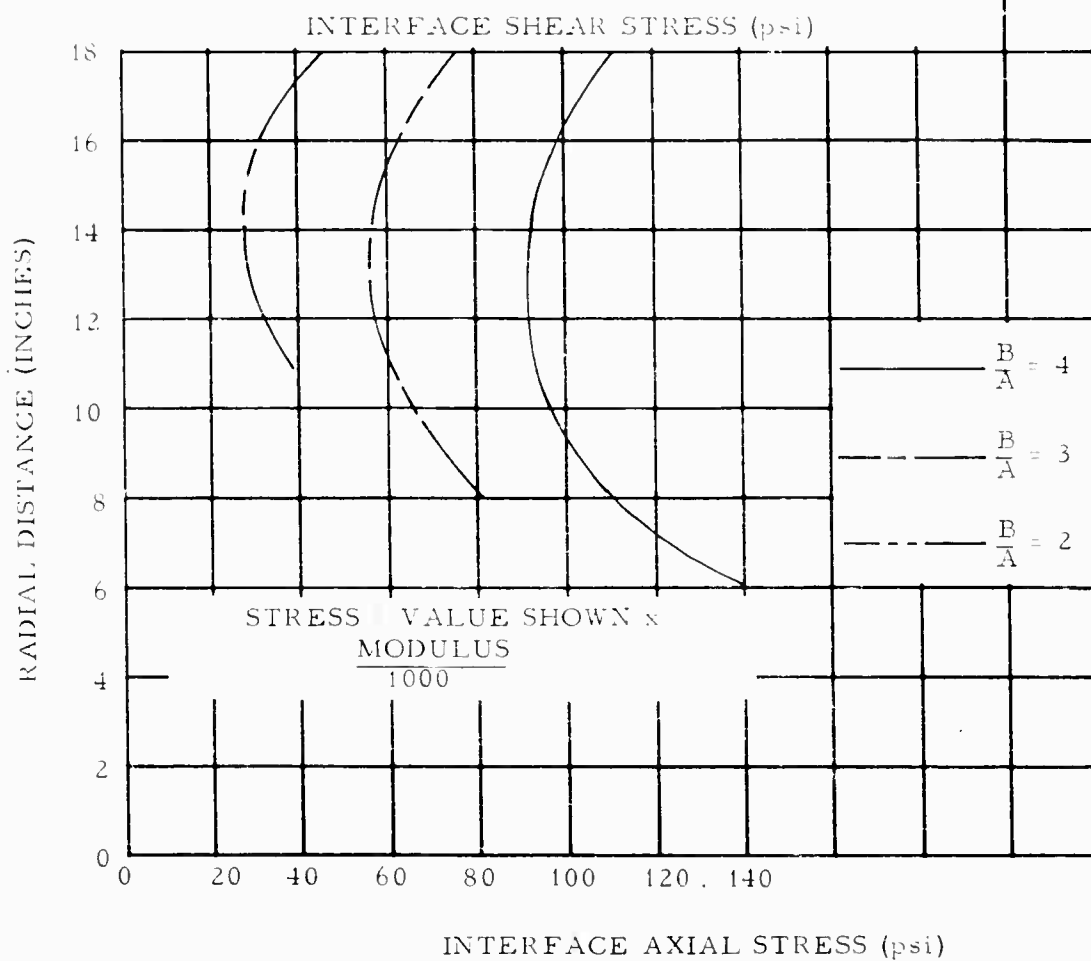
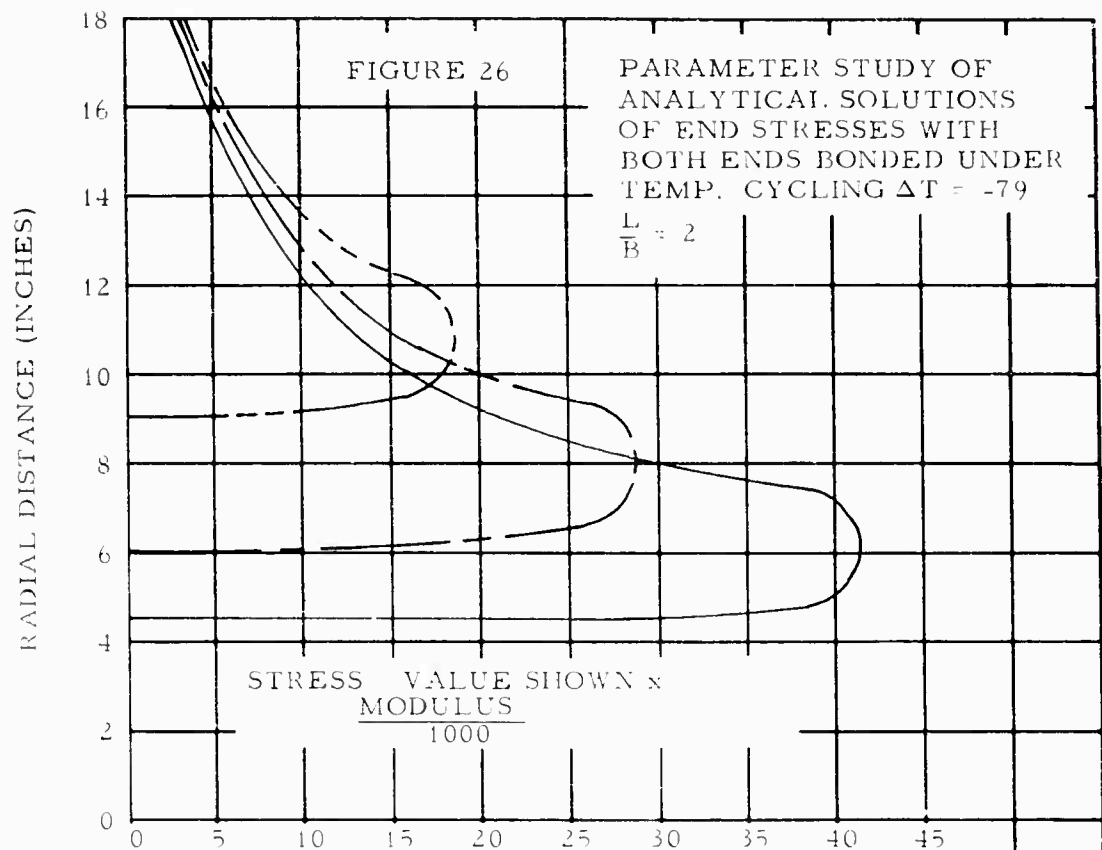


FIGURE 23

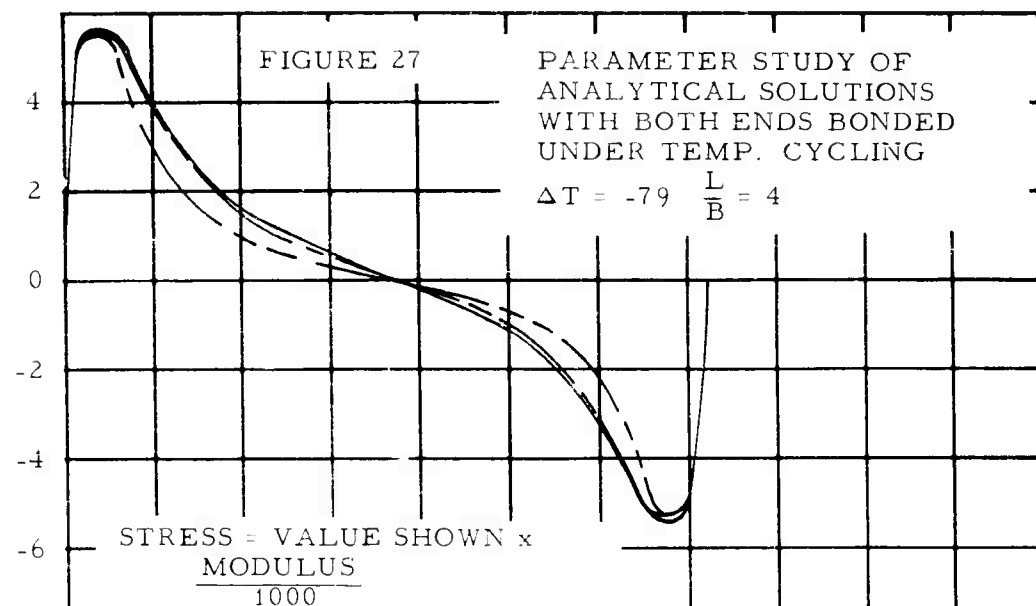




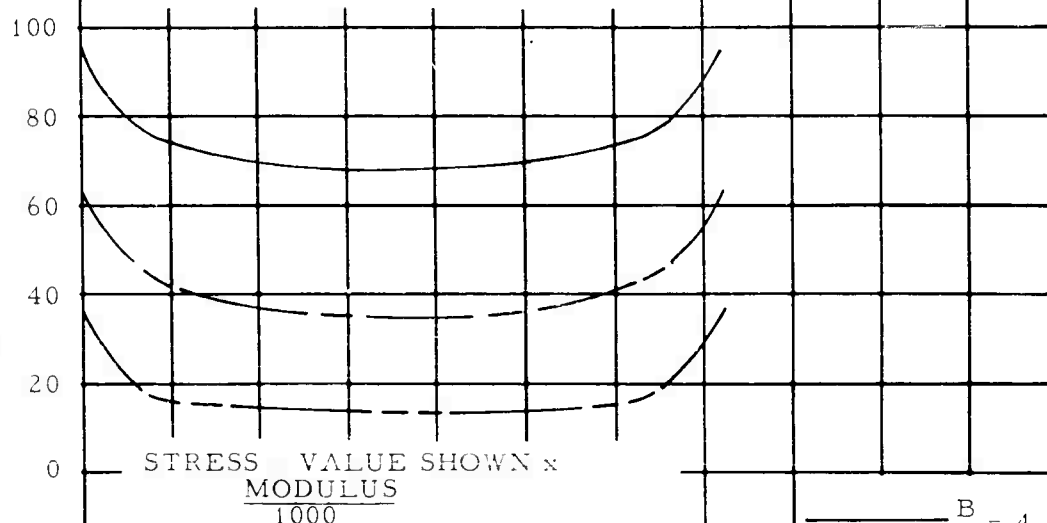




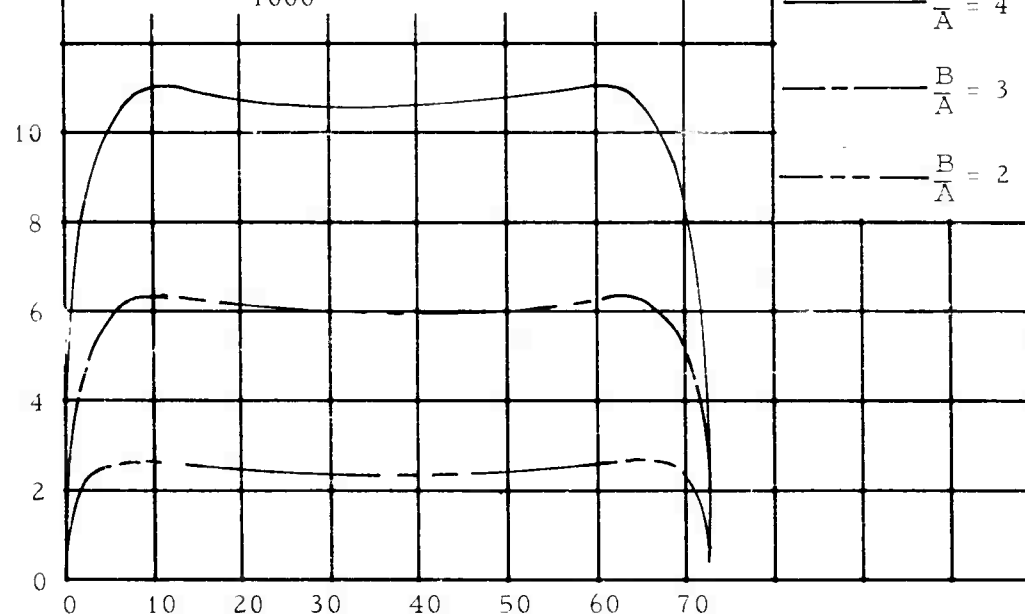
INTERFACE SHEAR STRESS
(psi)



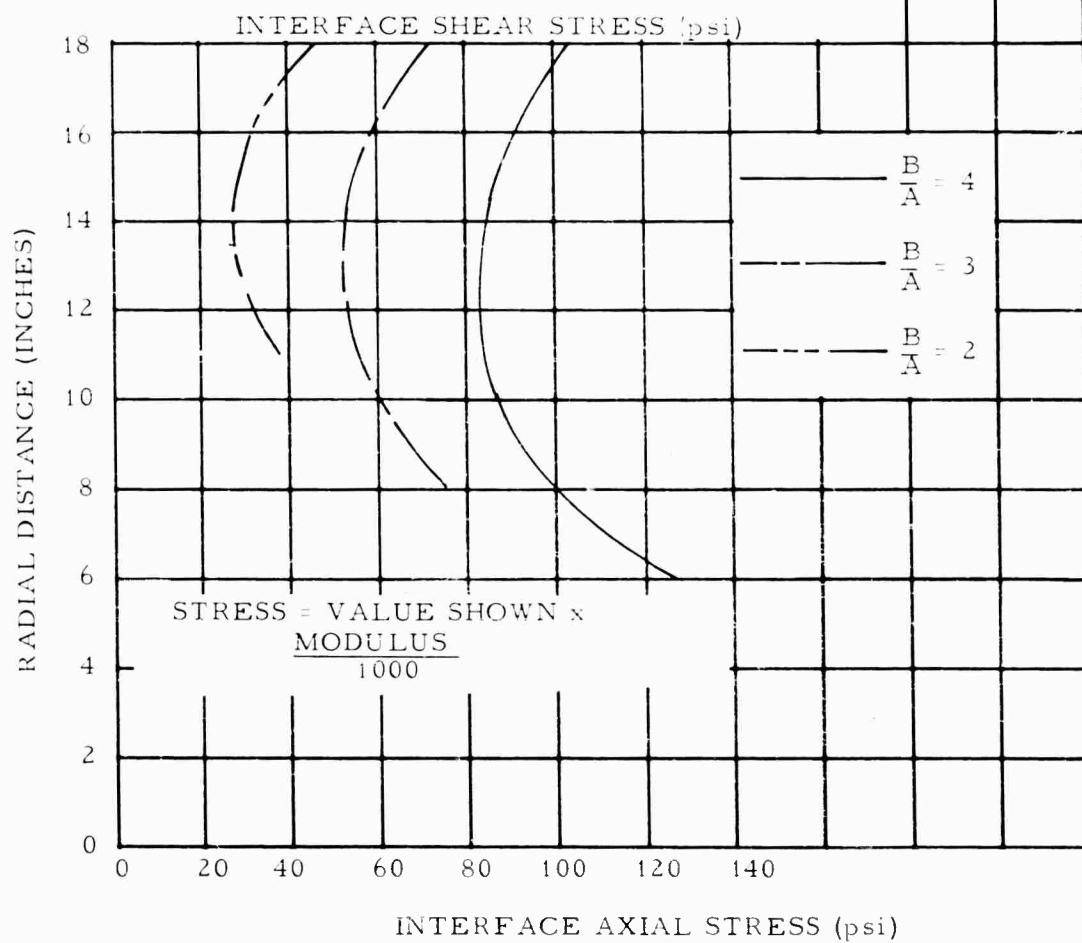
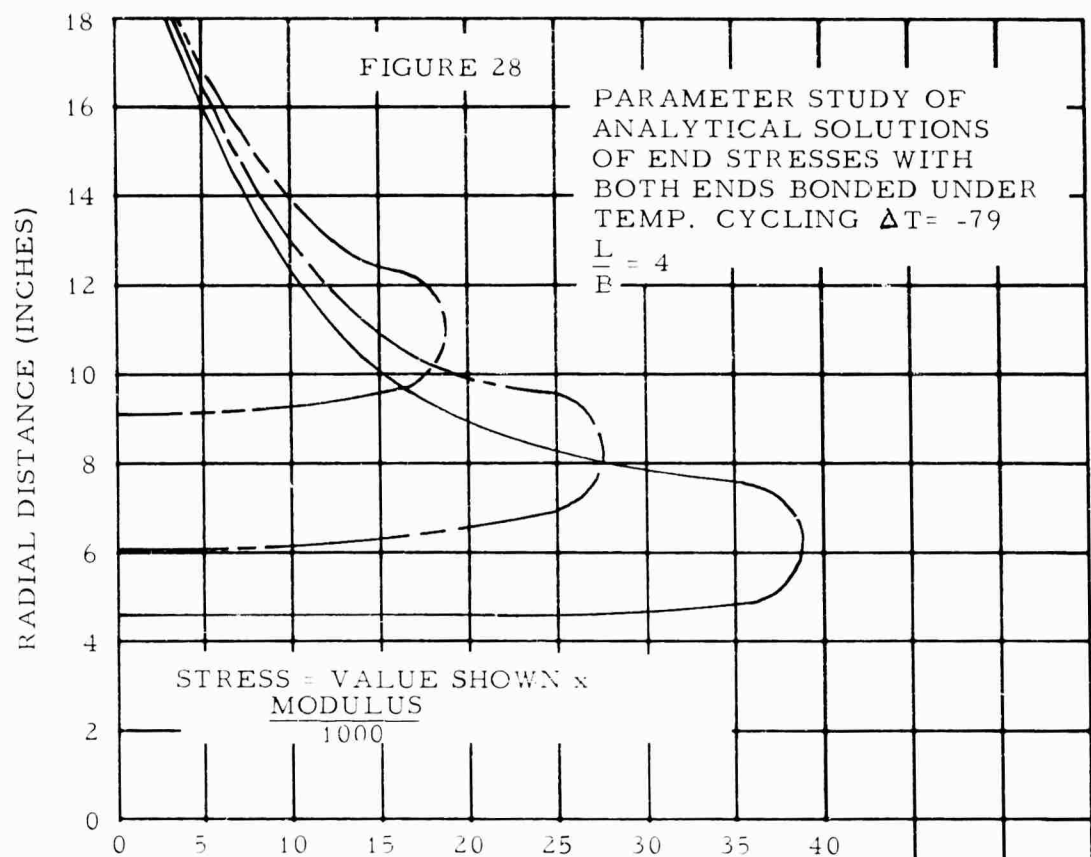
INTERFACE RADIAL STRESS
(psi)

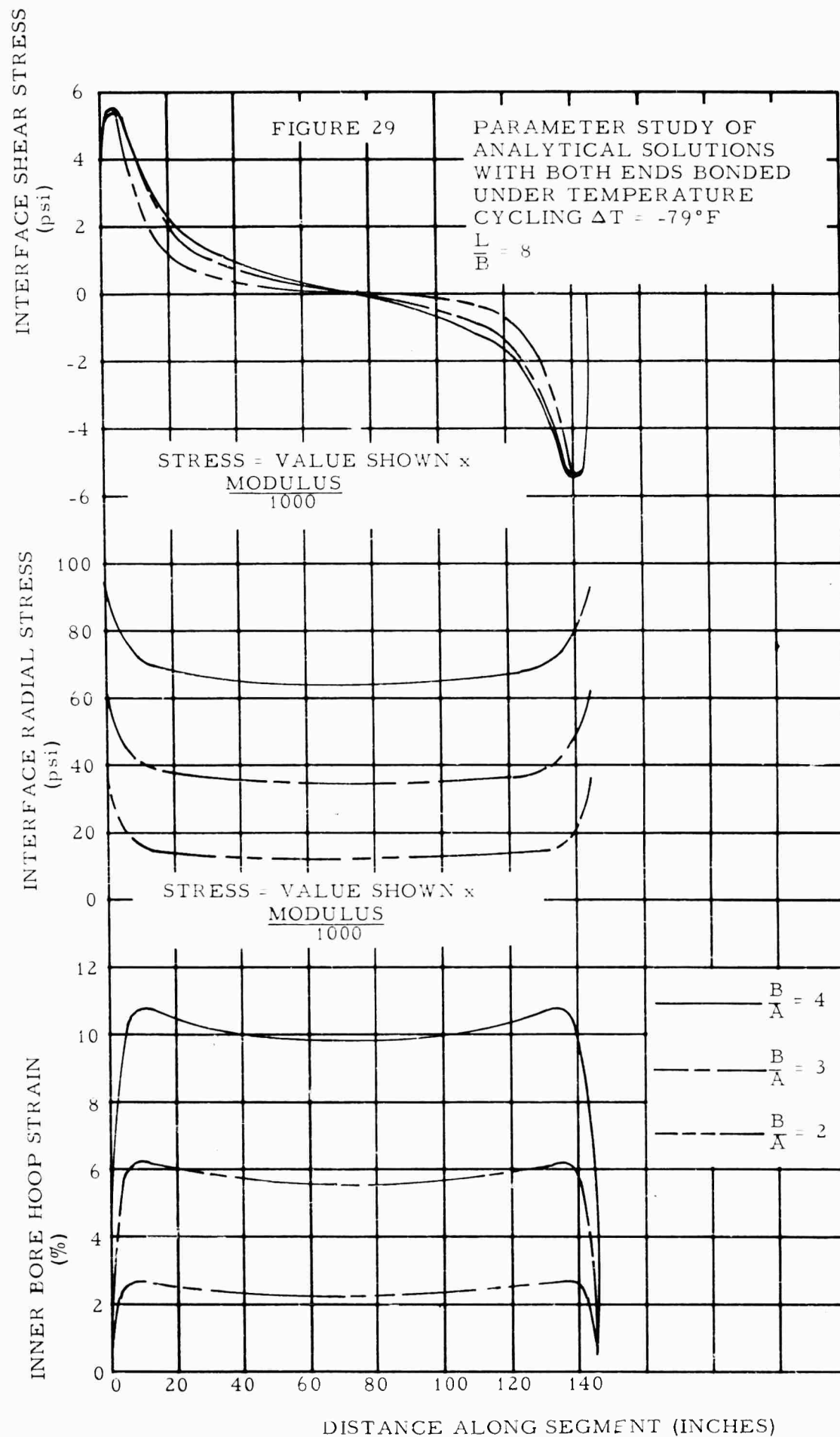


INNER BORE HOOP STRAIN
(%)



DISTANCE ALONG SEGMENT (INCHES)





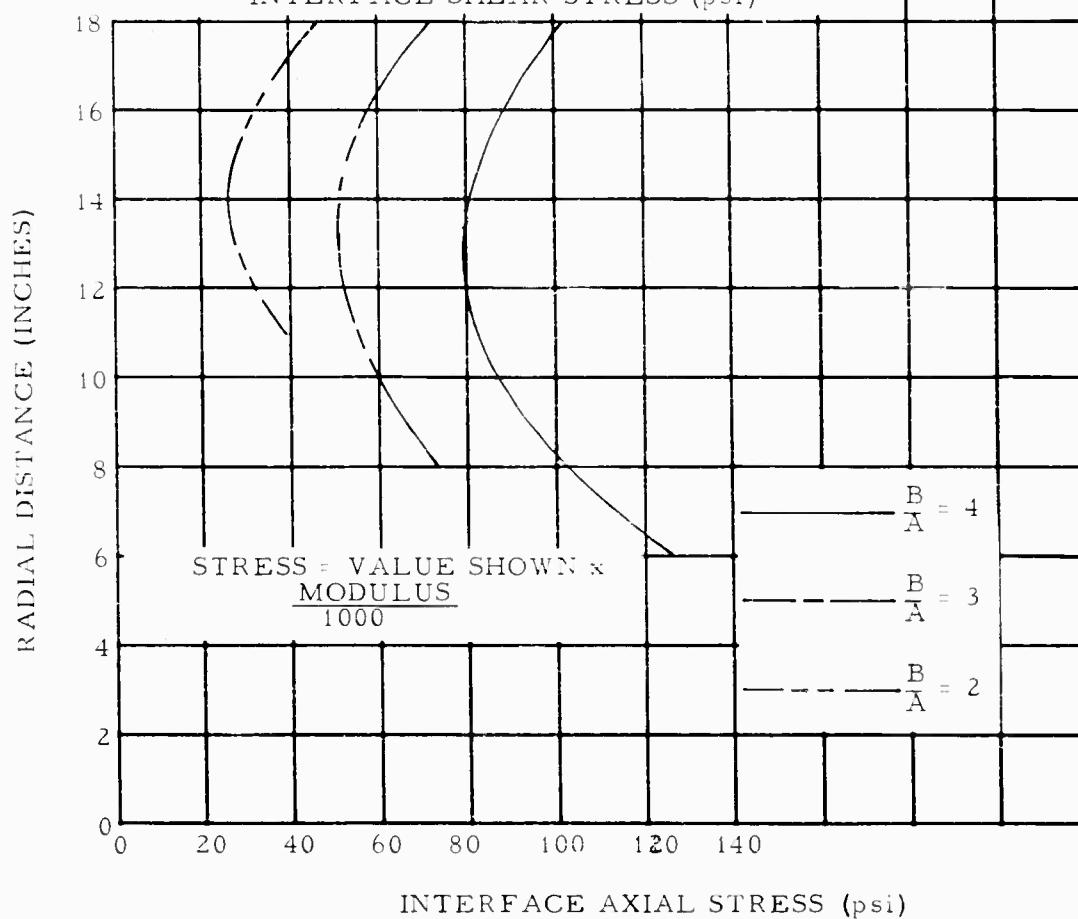
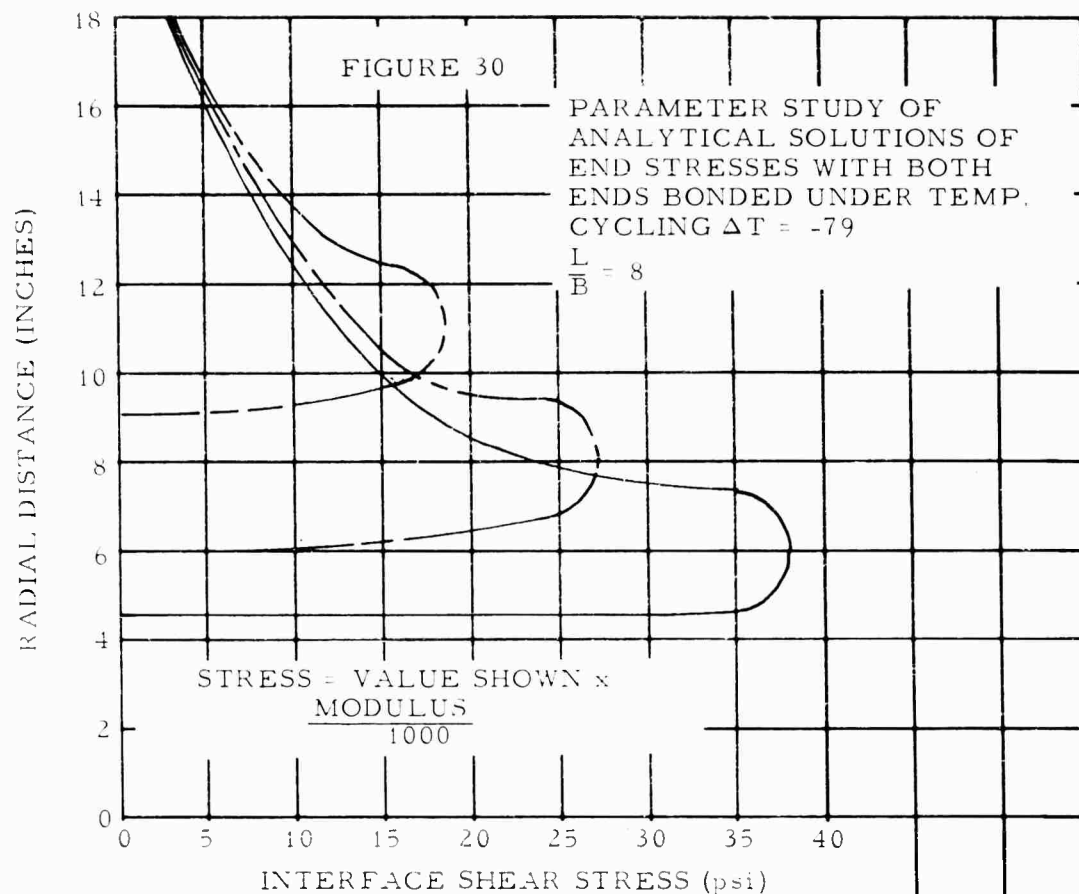
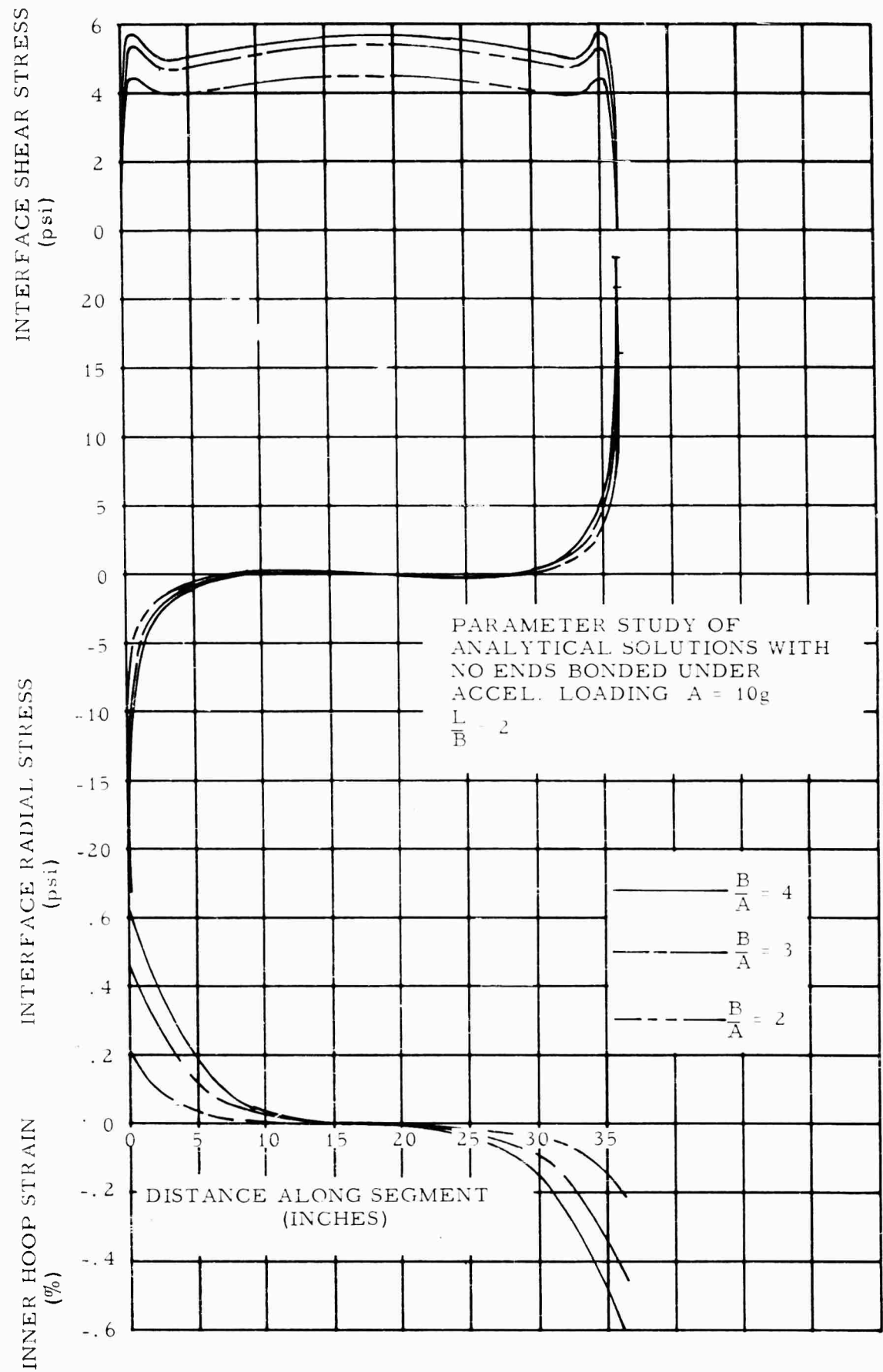


FIGURE 31

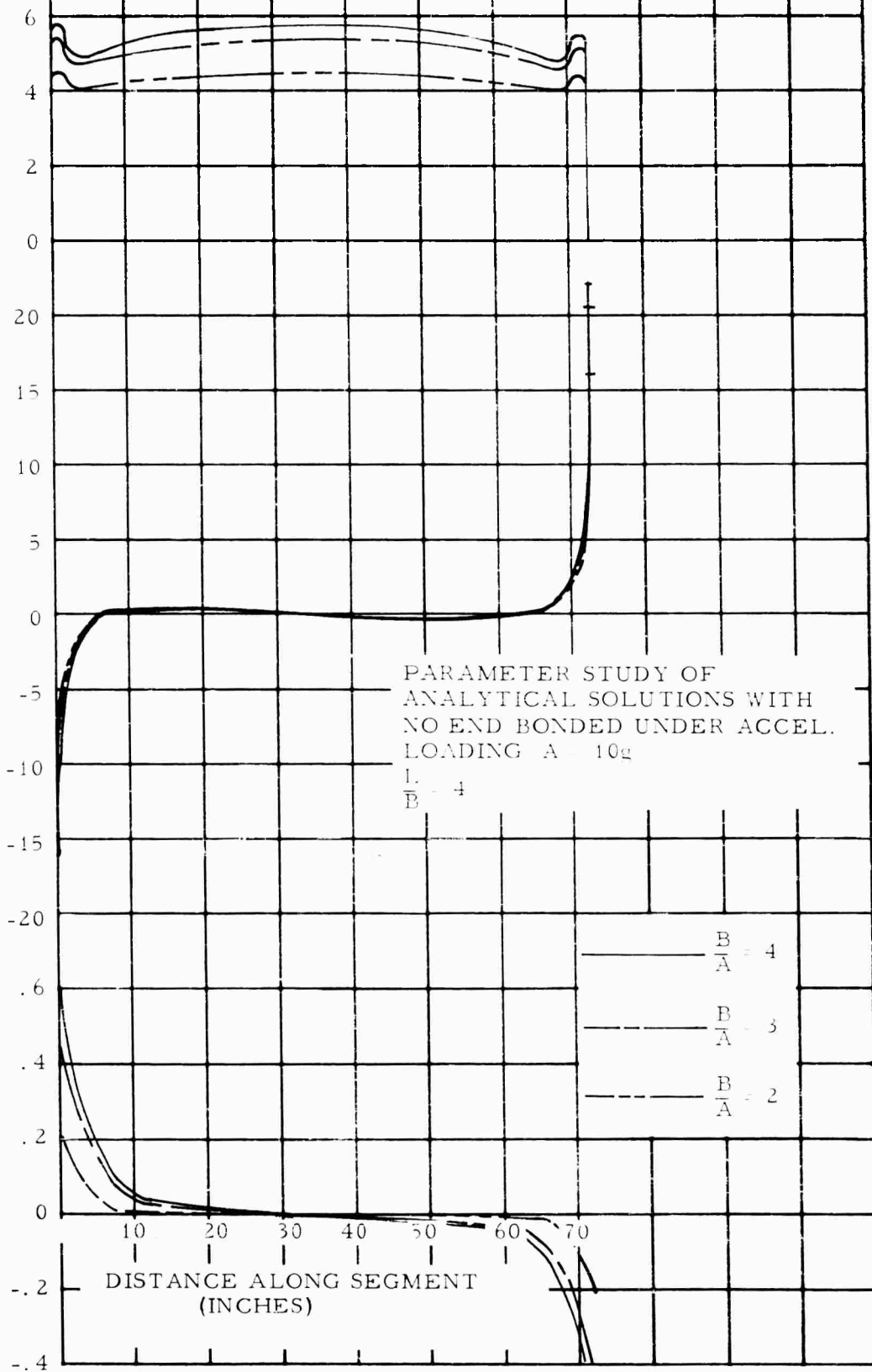


INTERFACE SHEAR STRESS
(psi)

INTERFACE RADIAL STRESS
(psi)

INNER BORE HOOP STRAIN
(%)

FIGURE 32



INTERFACE SHEAR STRESS
(psi)

25
20
15
10
5
0

INTERFACE RADIAL STRESS
(psi)

120
80
40
0
-40
-80
-120

INNER BORE HOOP STRAIN
(%)

1.5
1.0
.5
0
-1.0
-1.5

DISTANCE ALONG SEGMENT
(INCHES)

FIGURE 33

PARAMETER STUDY OF
ANALYTICAL SOLUTIONS
WITH NO END BONDING
UNDER ACCEL. LOADING

A = 10g $\frac{L}{B} = 4$ $\frac{B}{A} = 3$

— B = 72
- - - B = 36
- - - B = 18

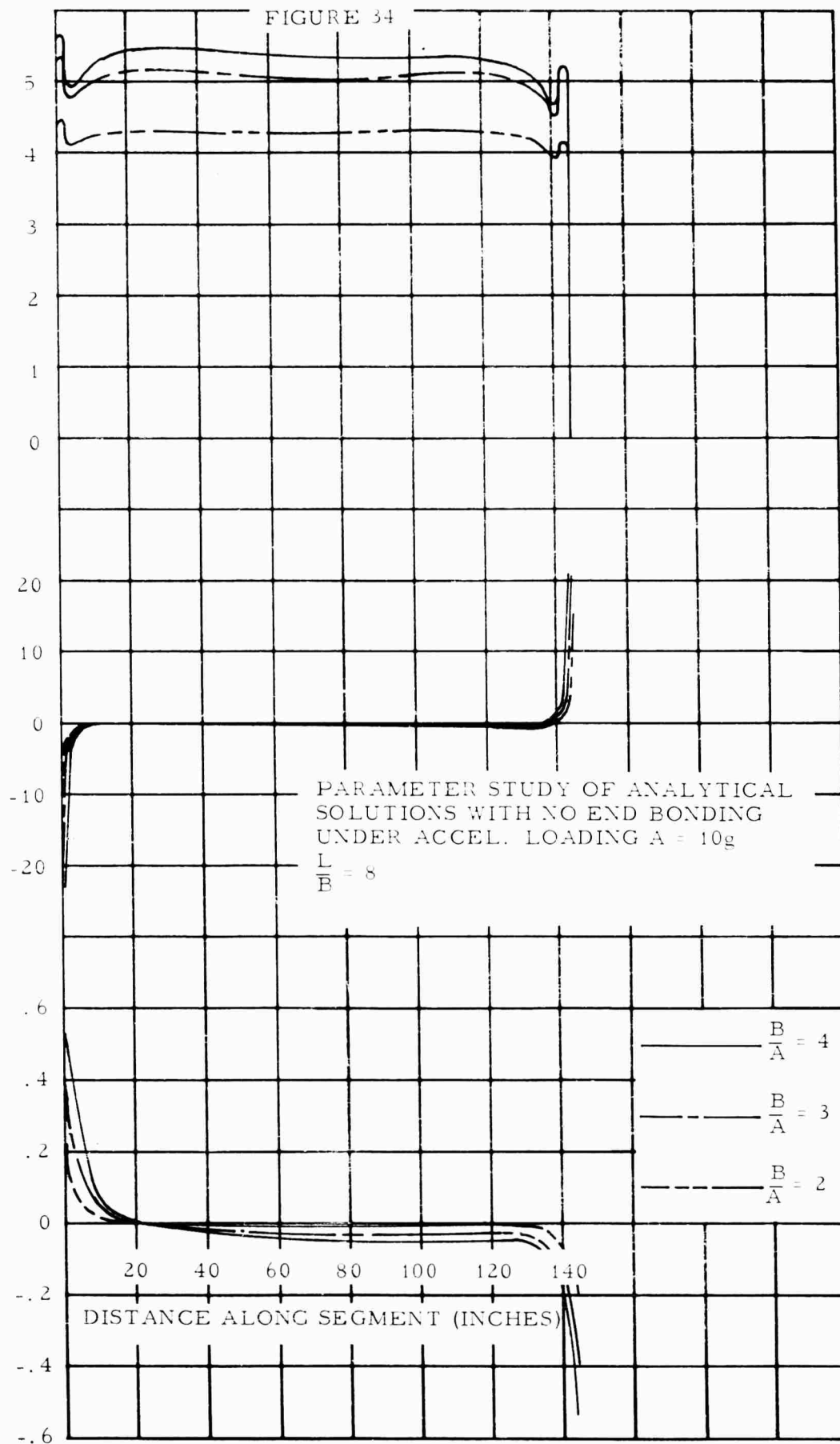
70
140
280

INTERFACE SHEAR STRESS
(psi)

INTERFACE RADIAL STRESS
(psi)

INNER BORE HOOP STRAIN
(%)

FIGURE 34

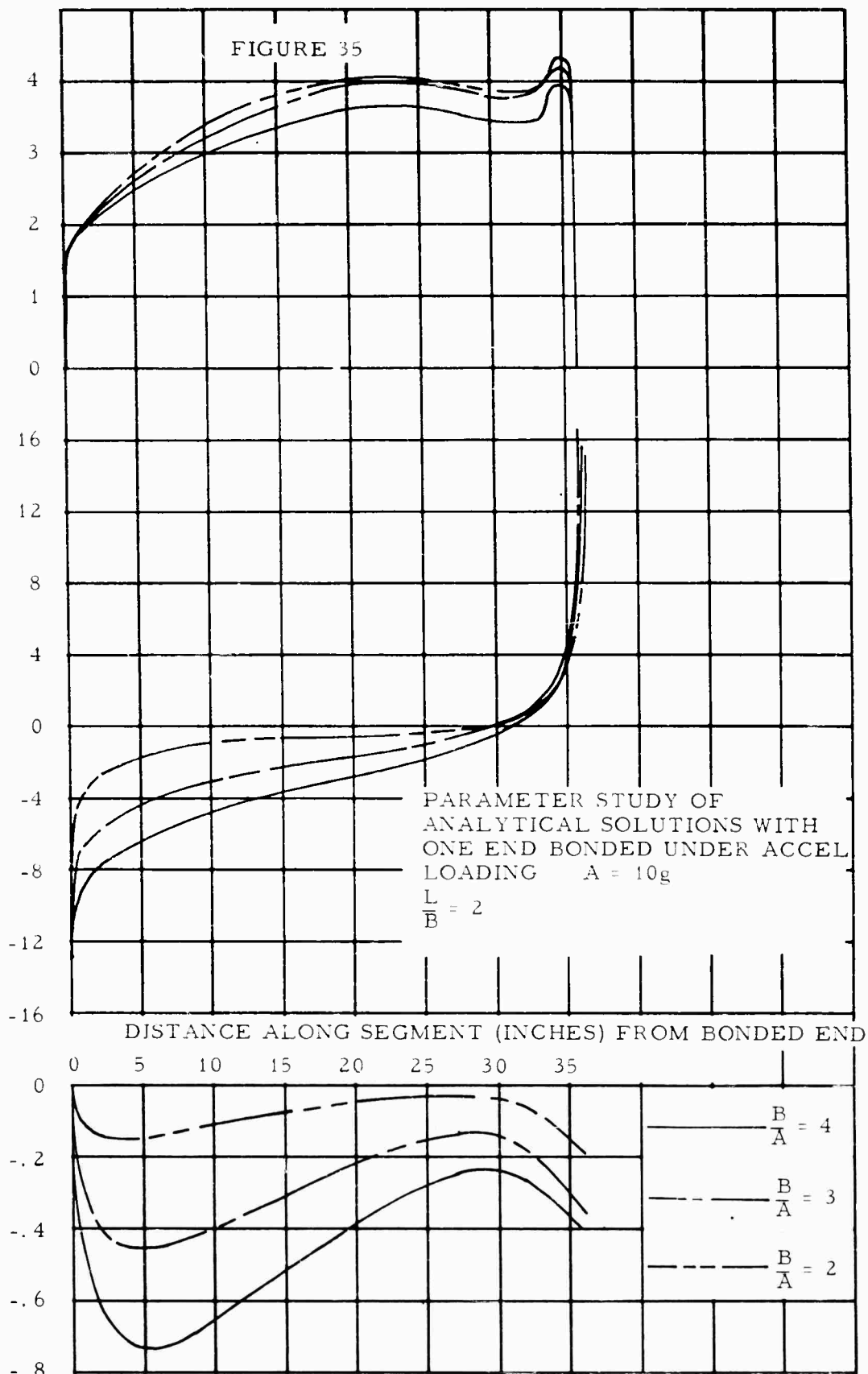


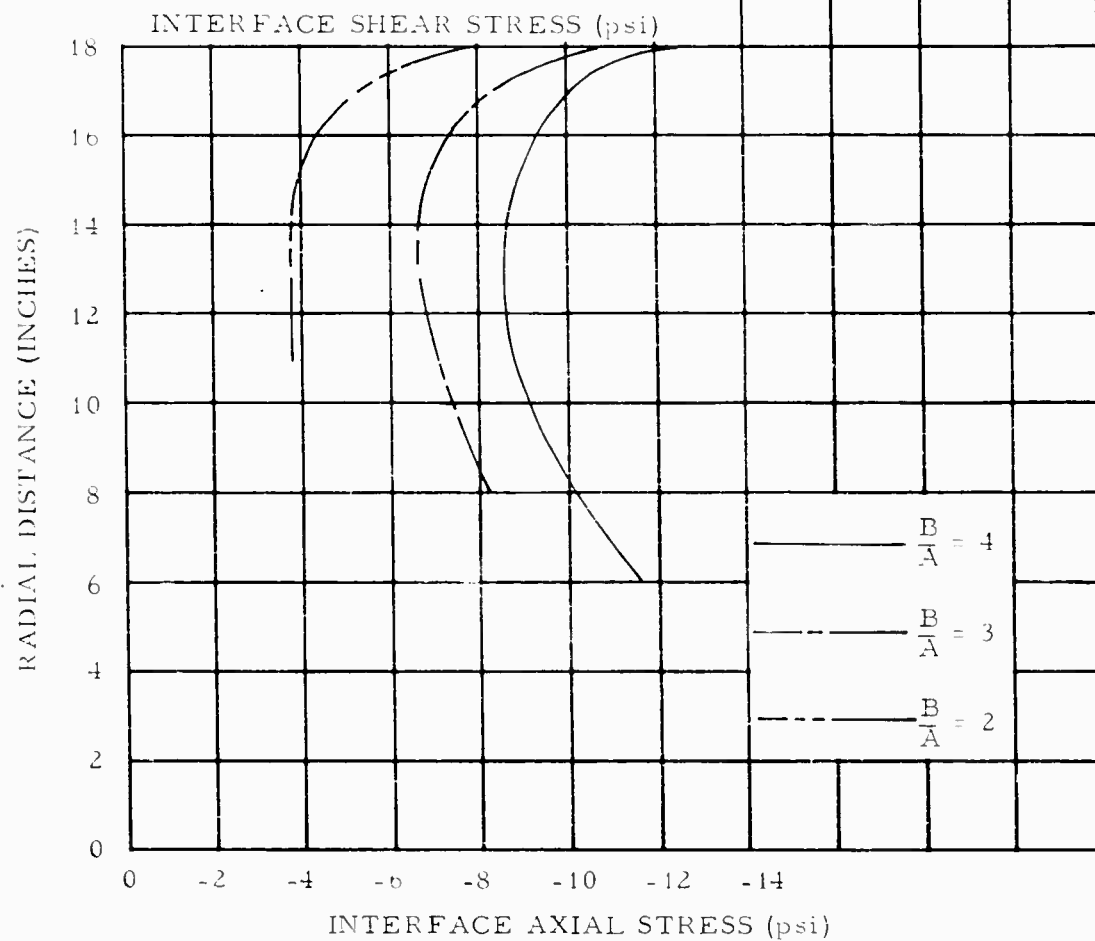
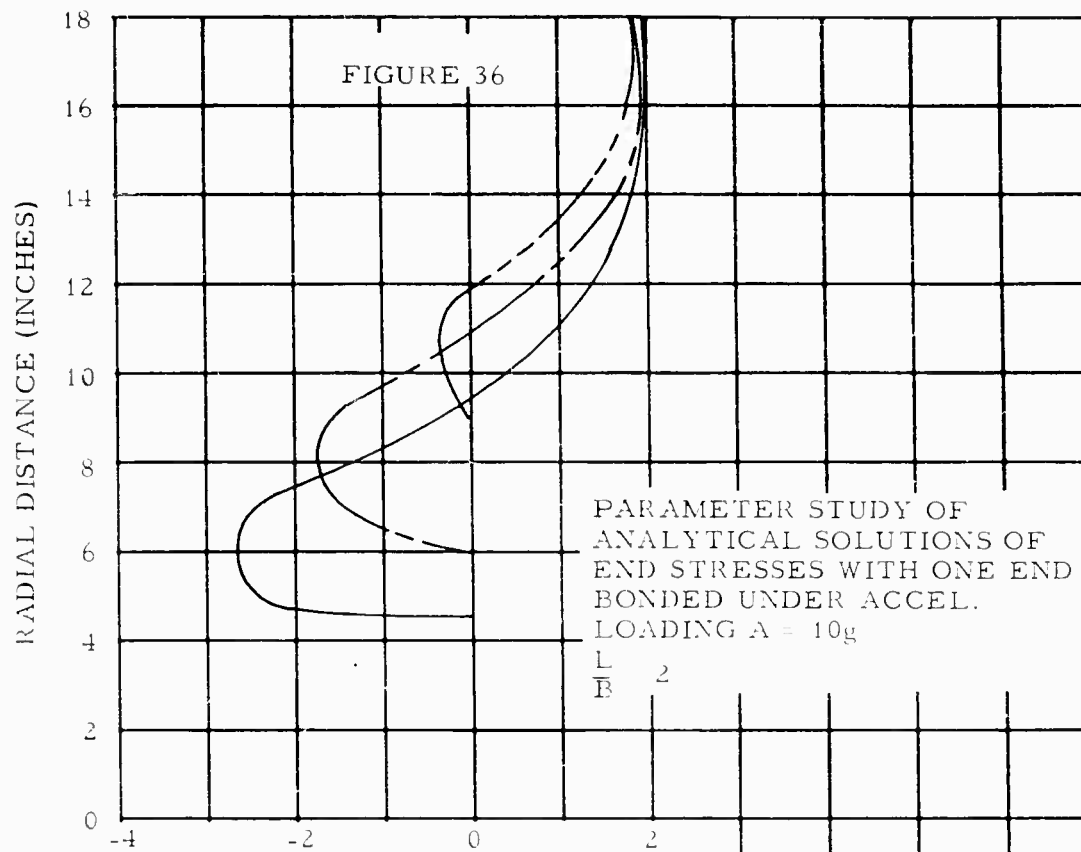
INTERFACE SHEAR STRESS
(psi)

INTERFACE RADIAL STRESS
(psi)

INNER BORE HOOP STRAIN
(%)

FIGURE 35



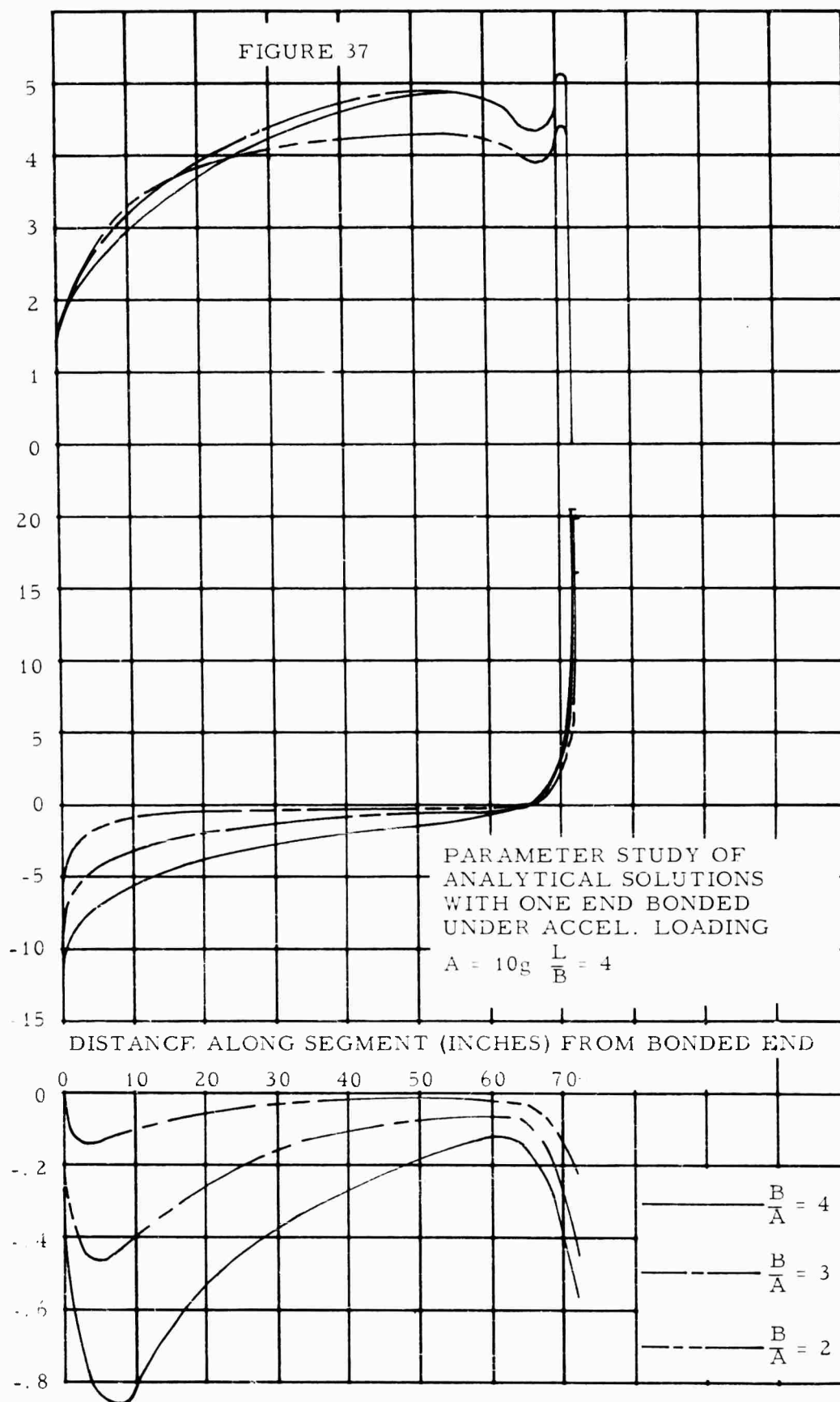


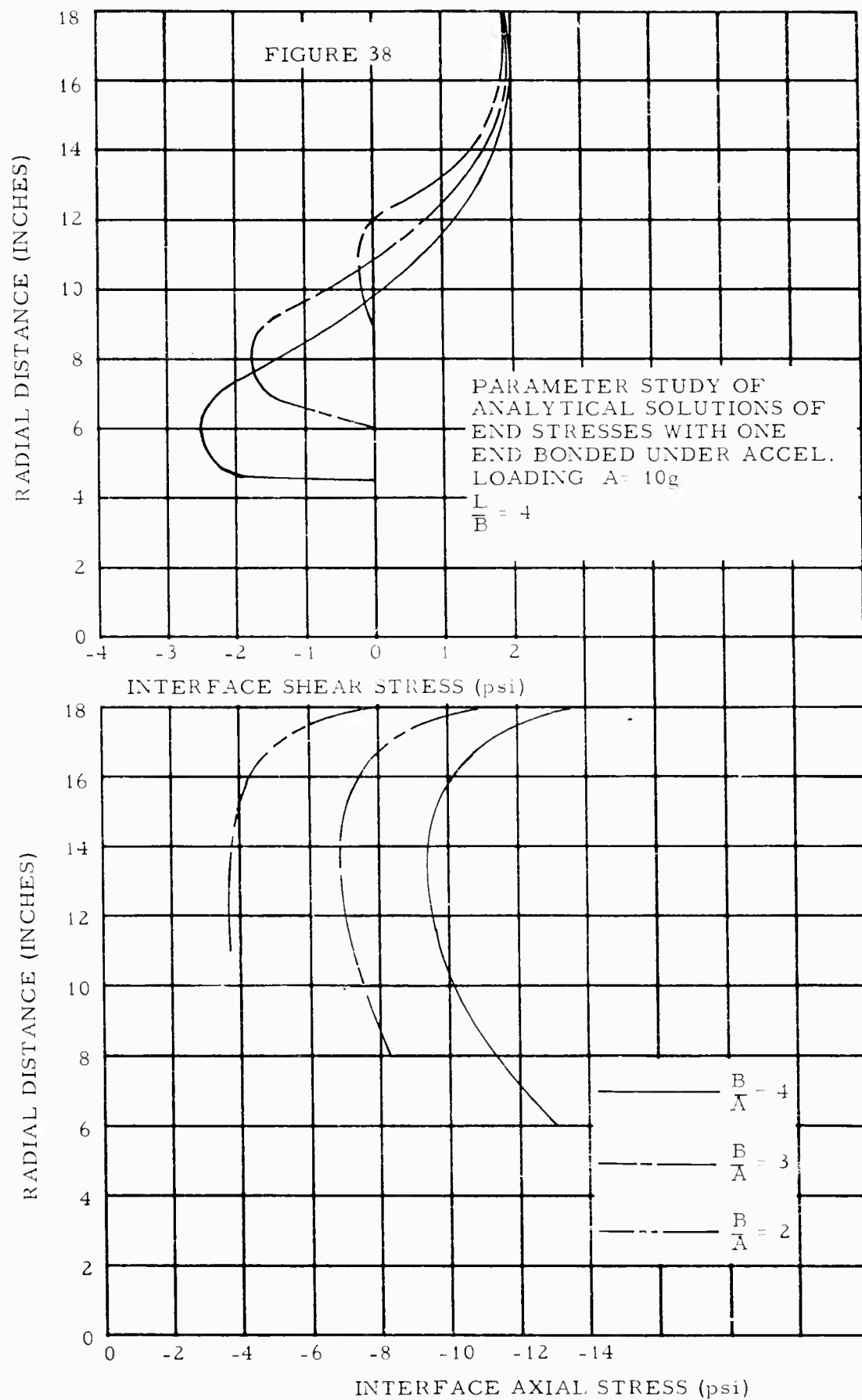
INTERFACE SHEAR STRESS
(psi)

INTERFACE RADIAL STRESS
(psi)

INNER BORE HOOP STRAIN
(%)

FIGURE 37



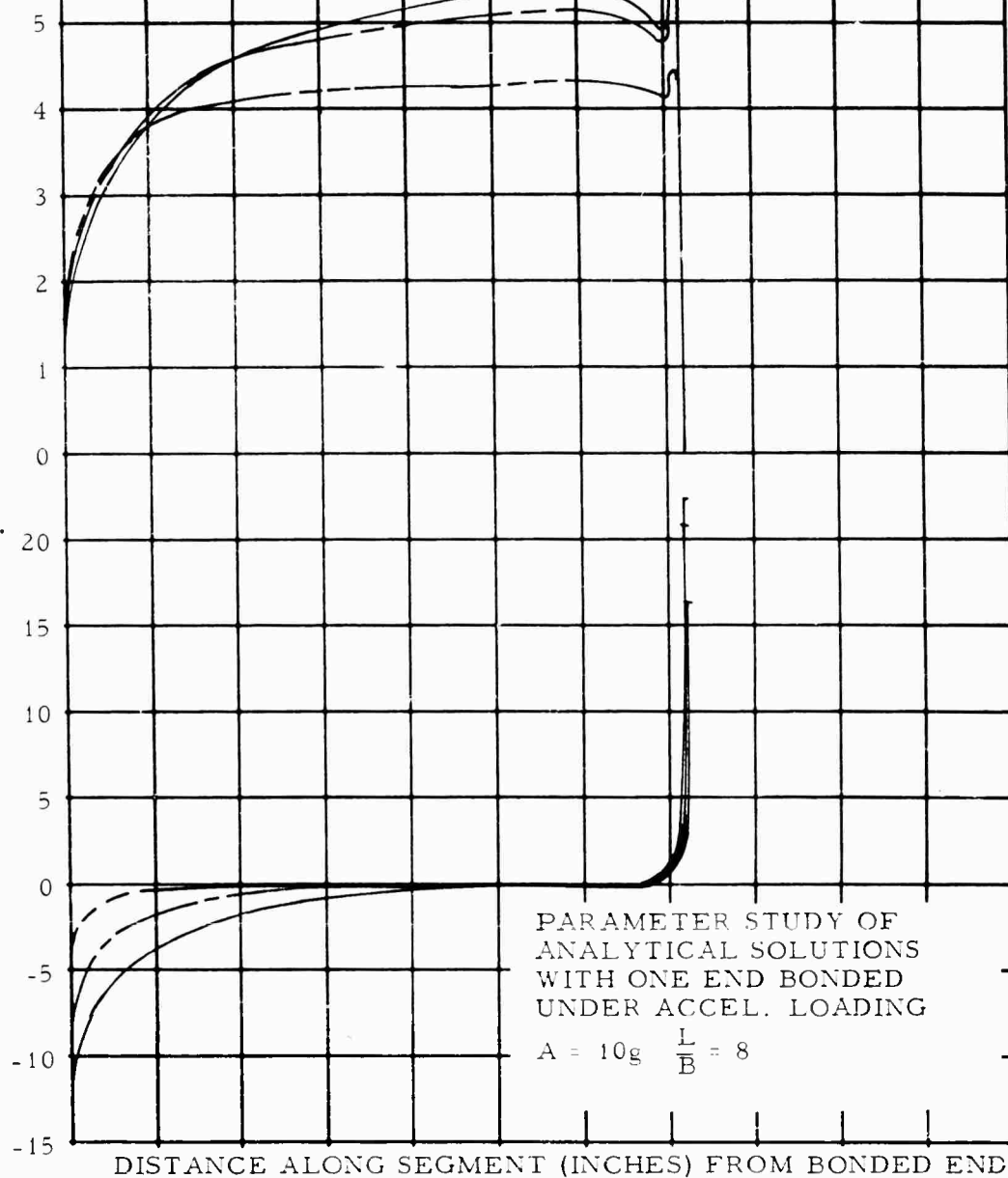


INTERFACE SHEAR STRESS
(psi)

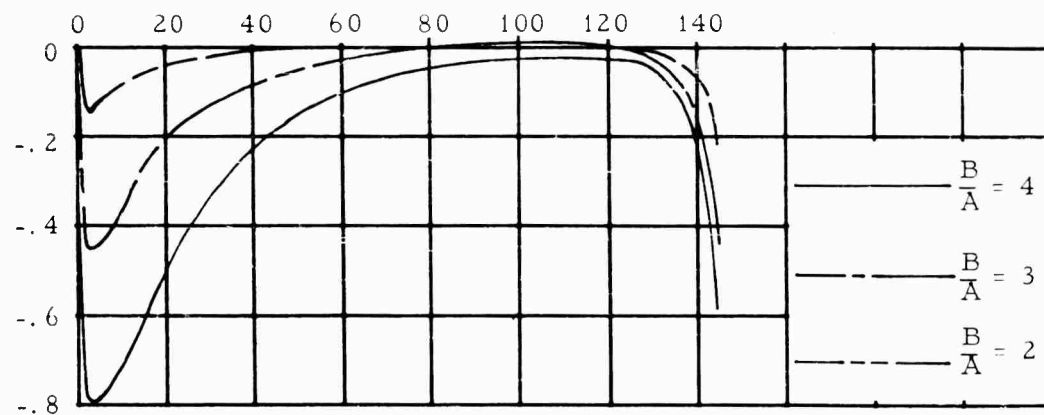
INTERFACE RADIAL STRESS
(psi)

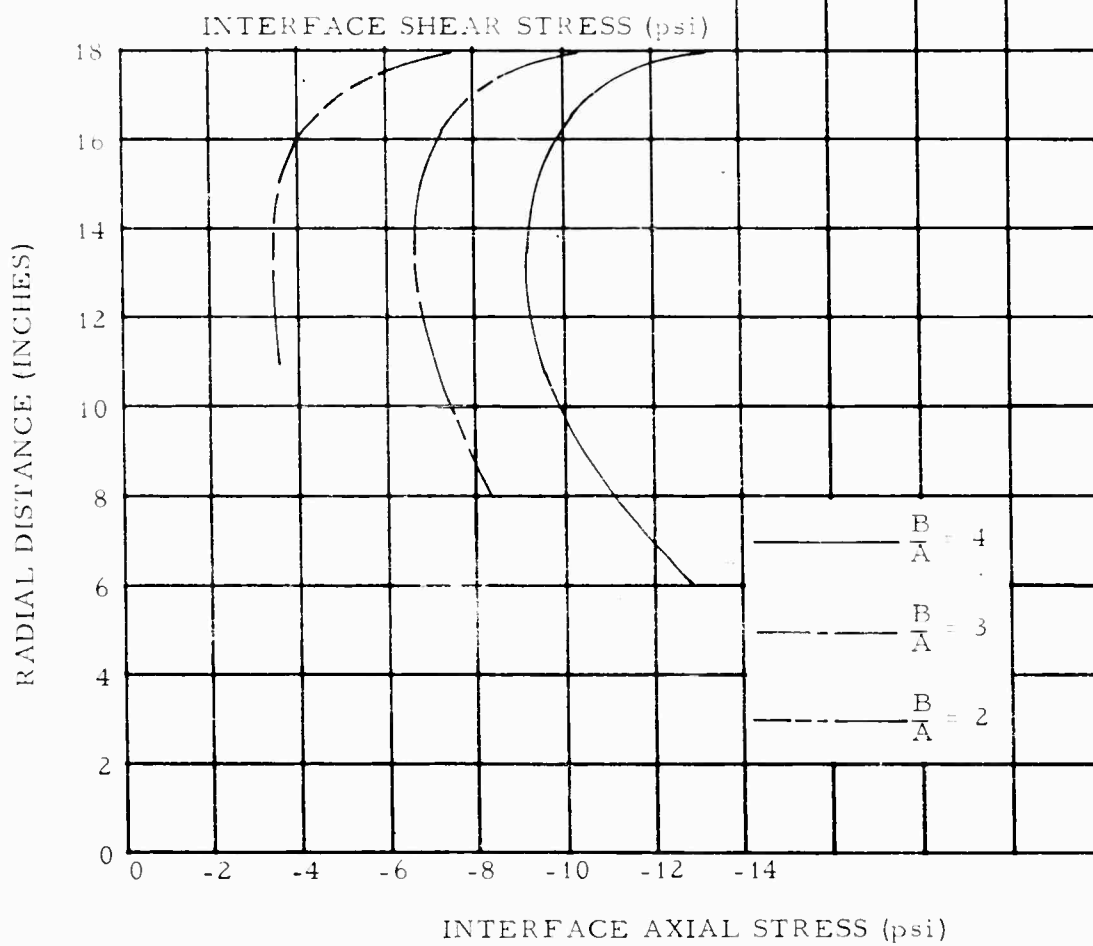
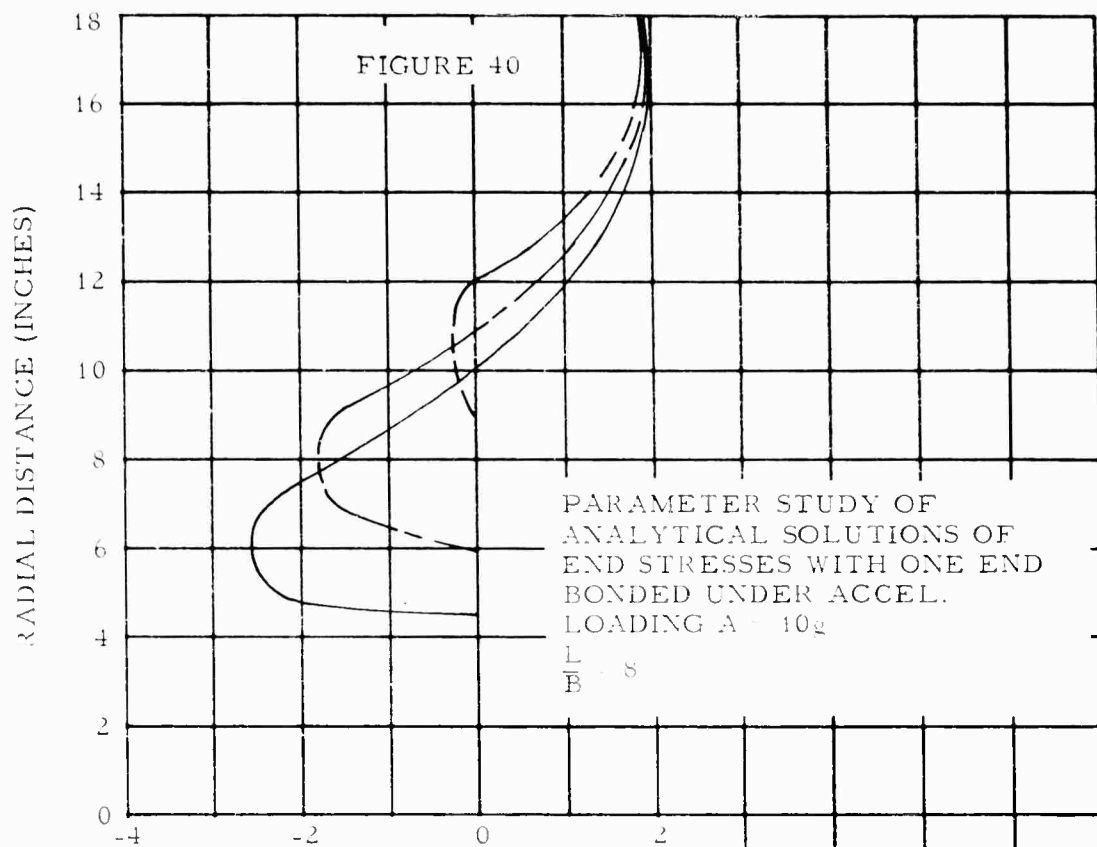
INNER BORE HOOP STRAIN
(%)

FIGURE 39

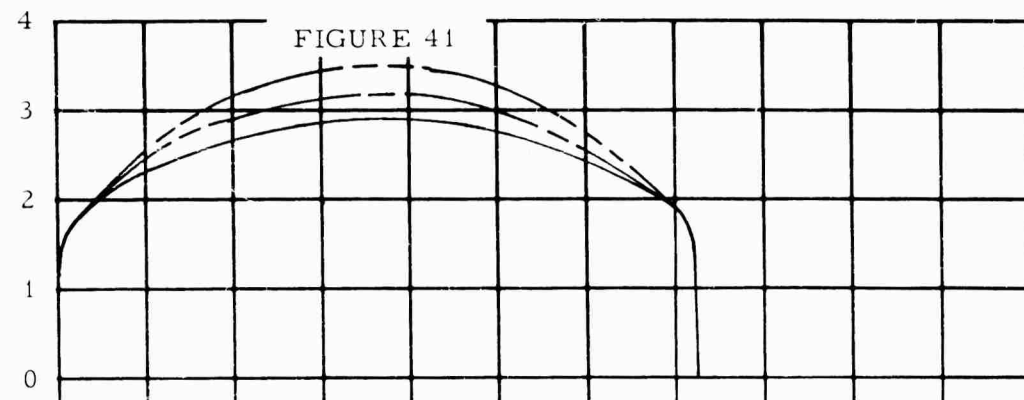


DISTANCE ALONG SEGMENT (INCHES) FROM BONDED END

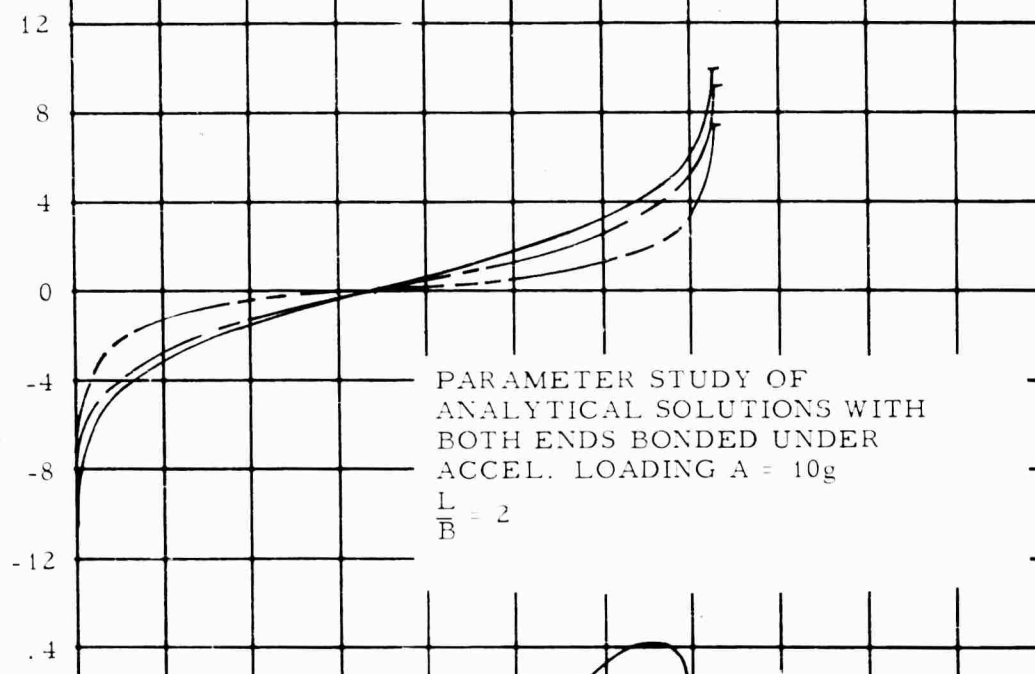




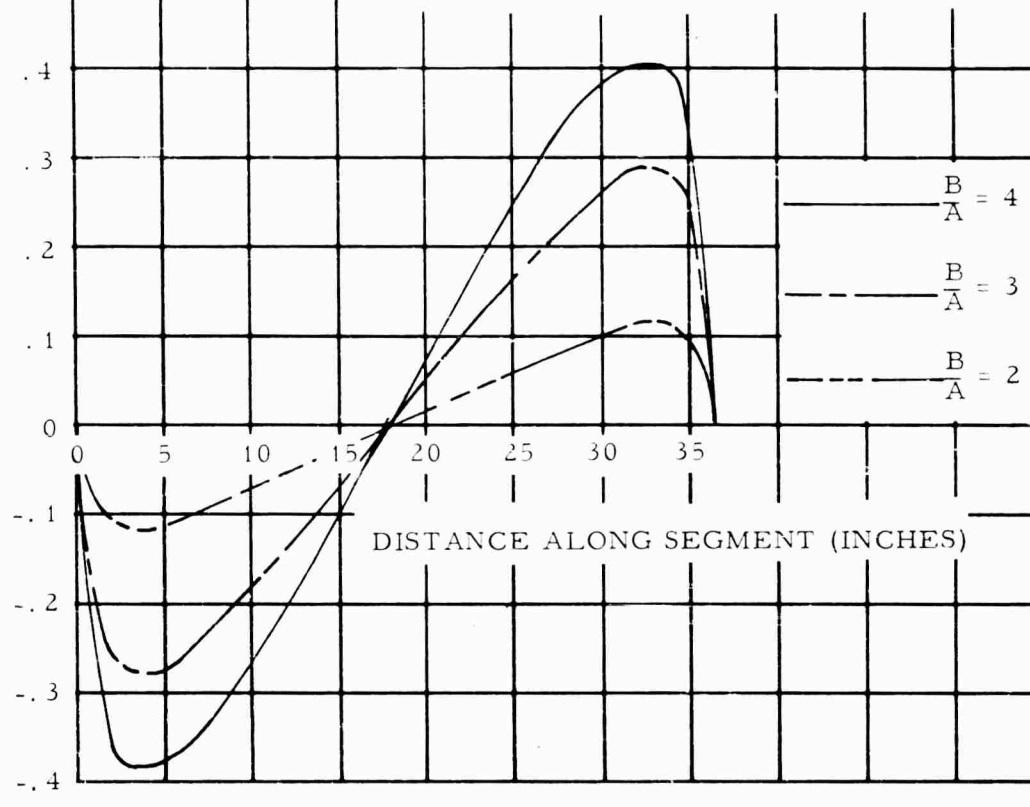
INTERFACE SHEAR STRESS
(psi)

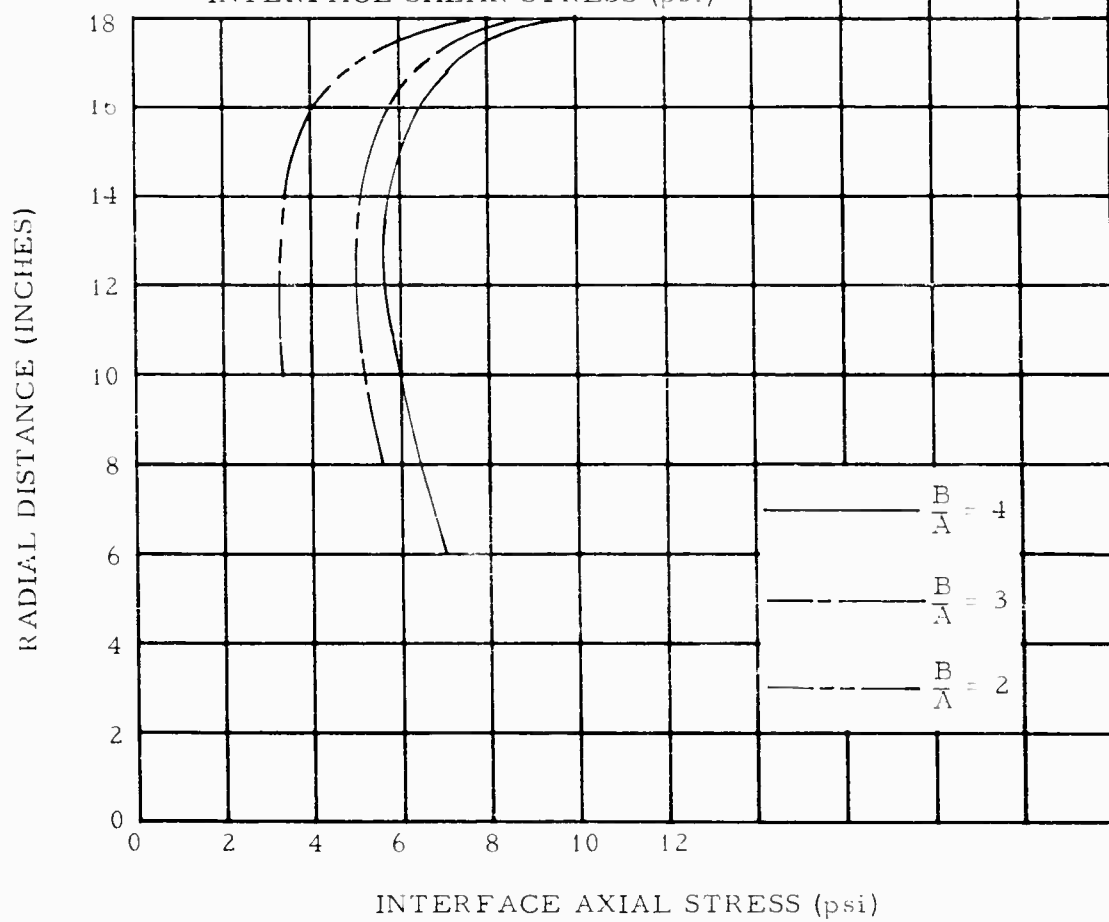
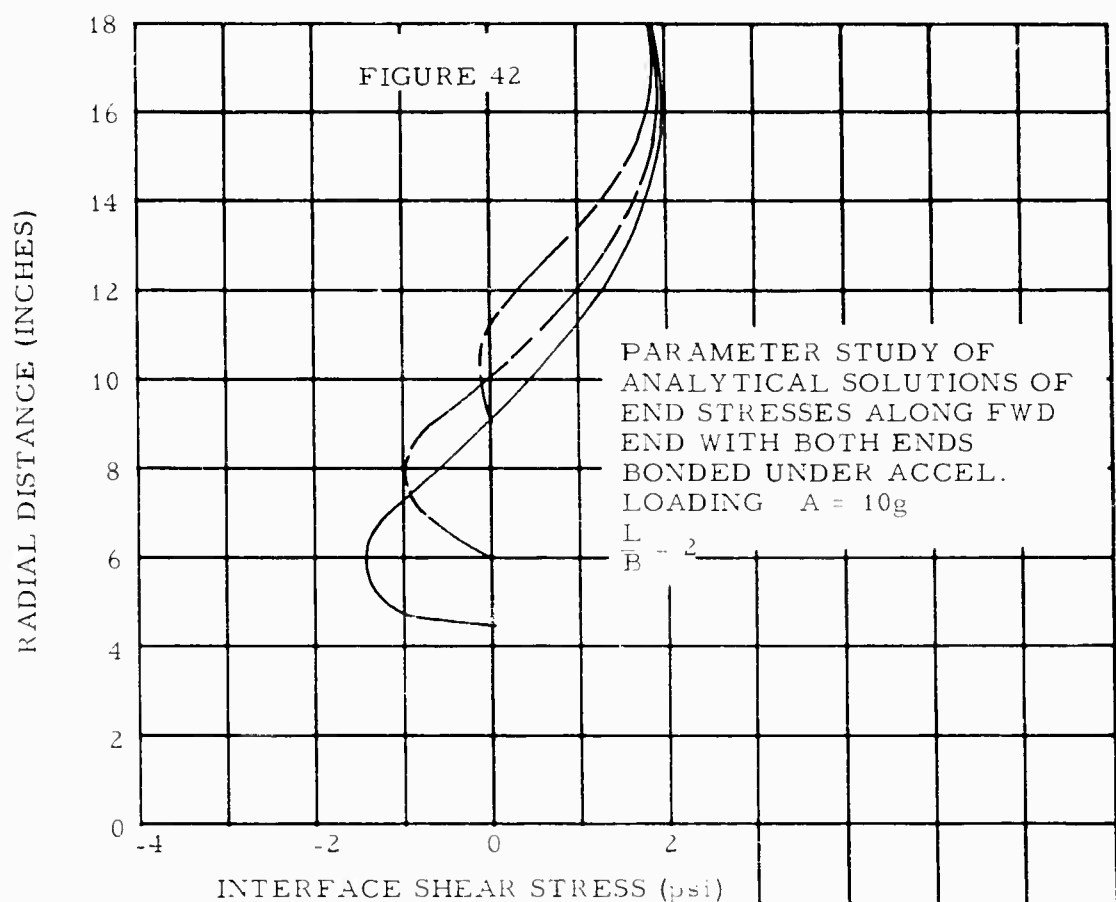


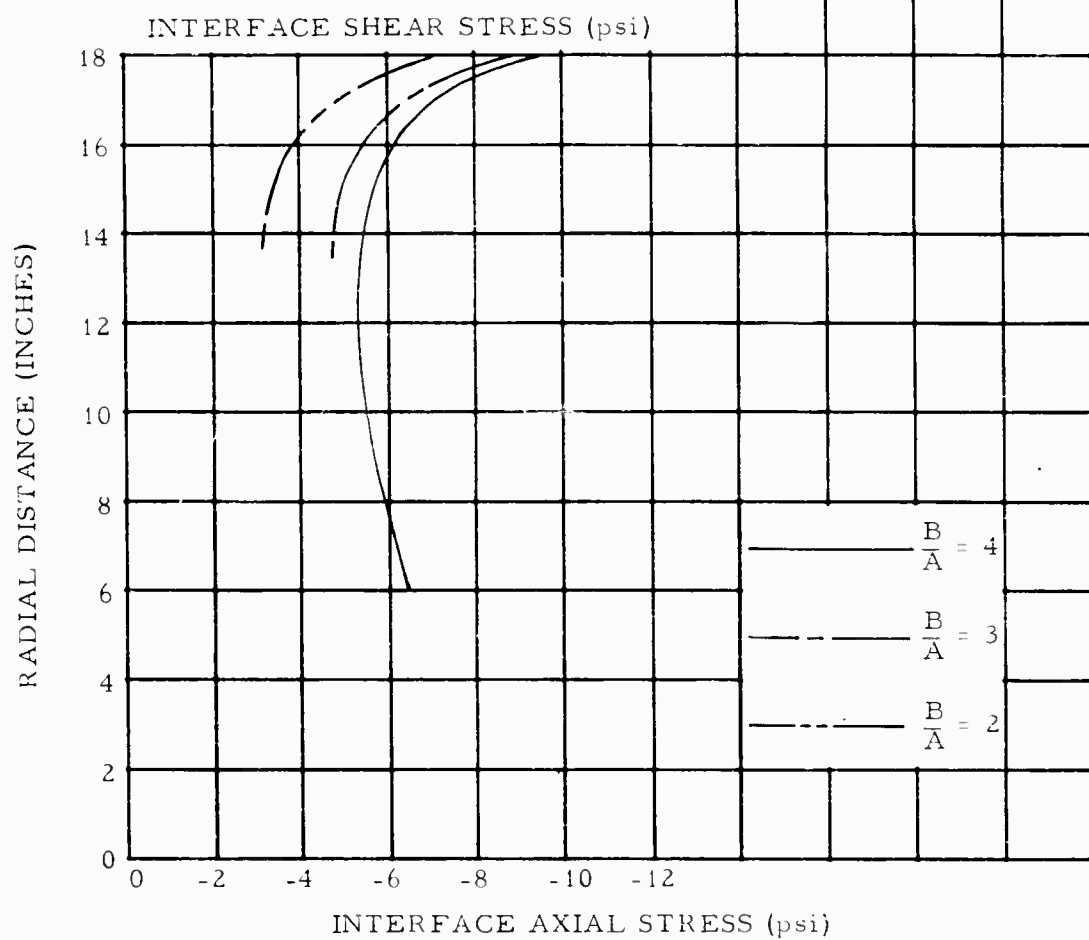
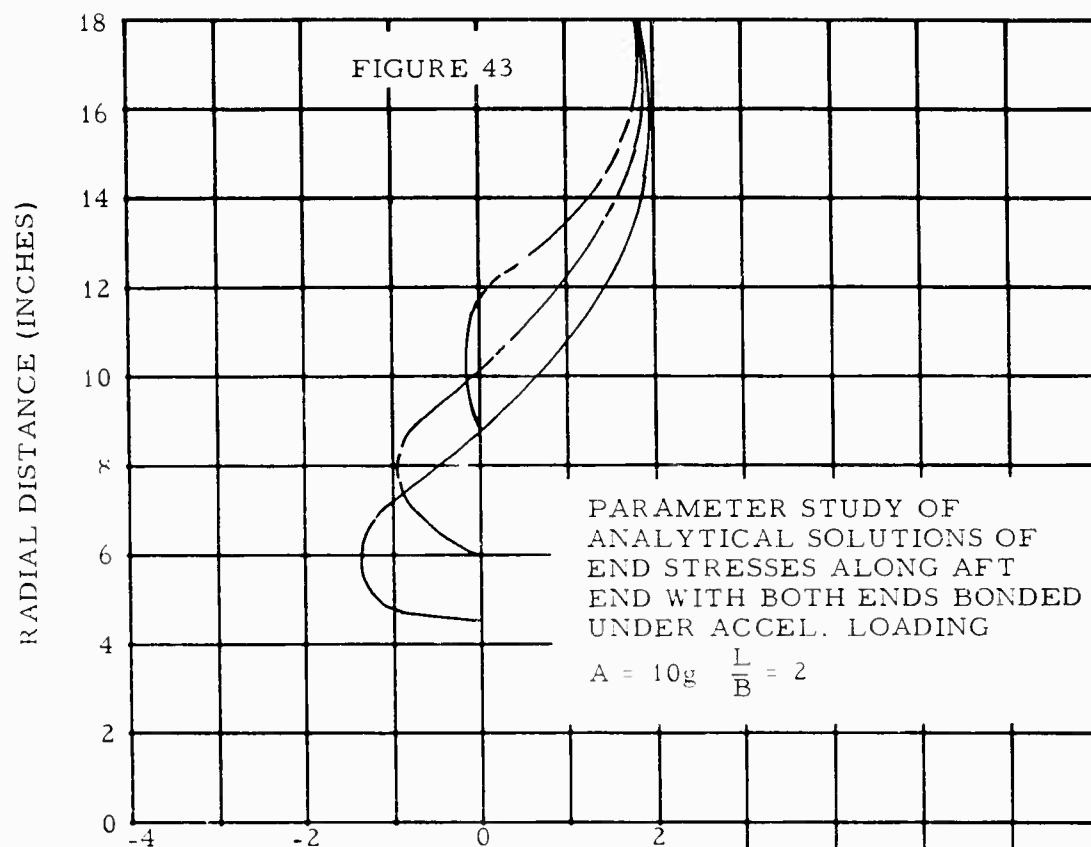
INTERFACE RADIAL STRESS
(psi)



INNER BORE HOOP STRAIN
(%)





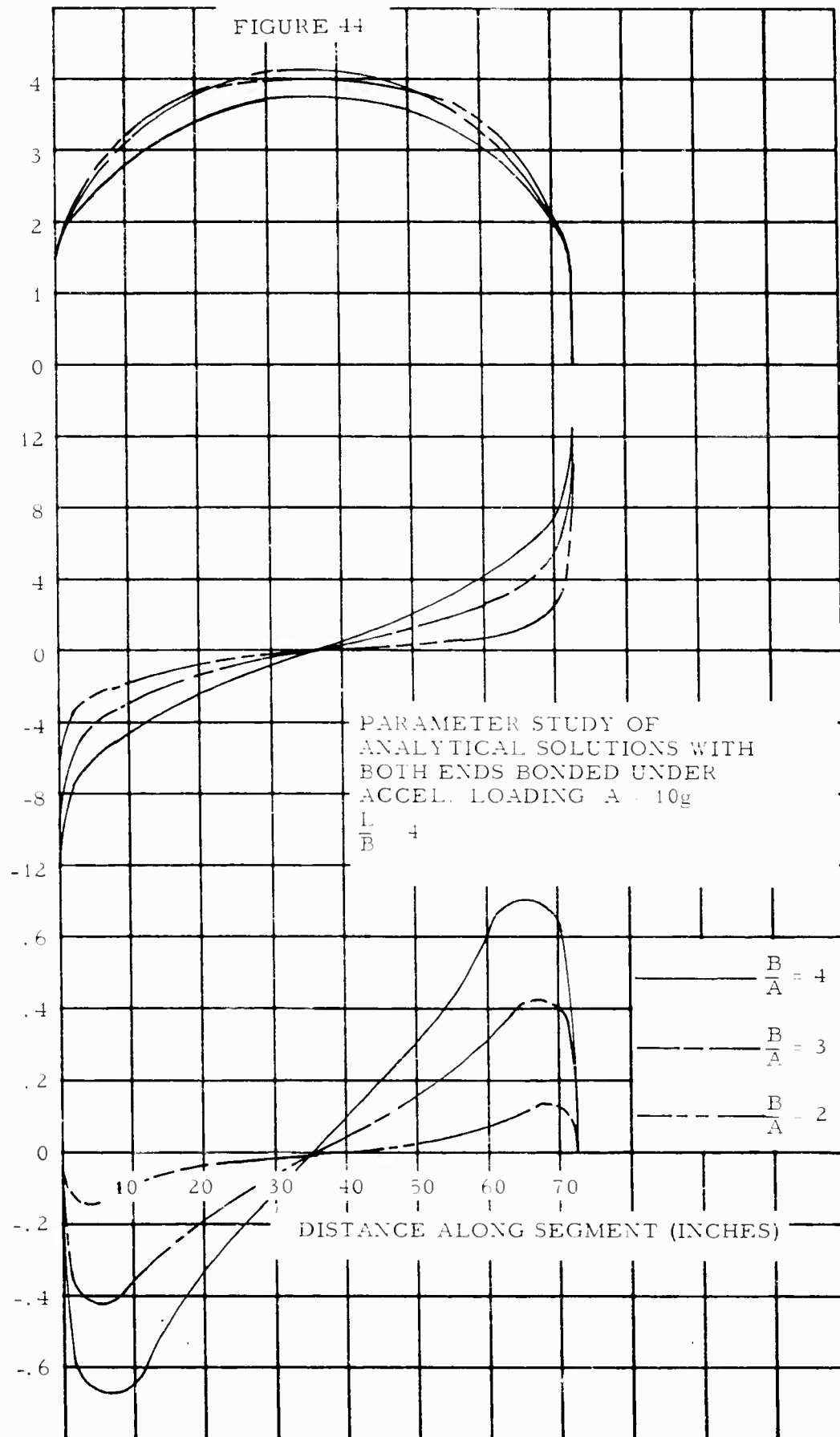


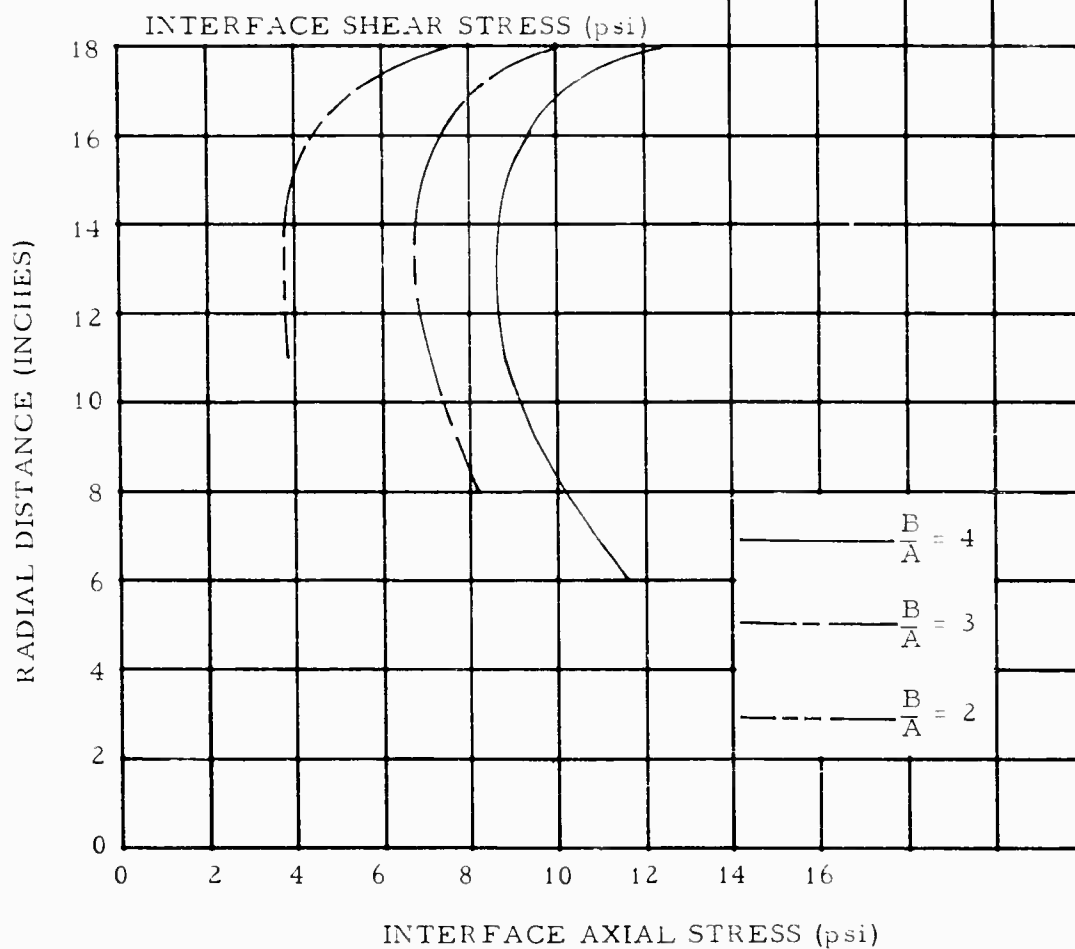
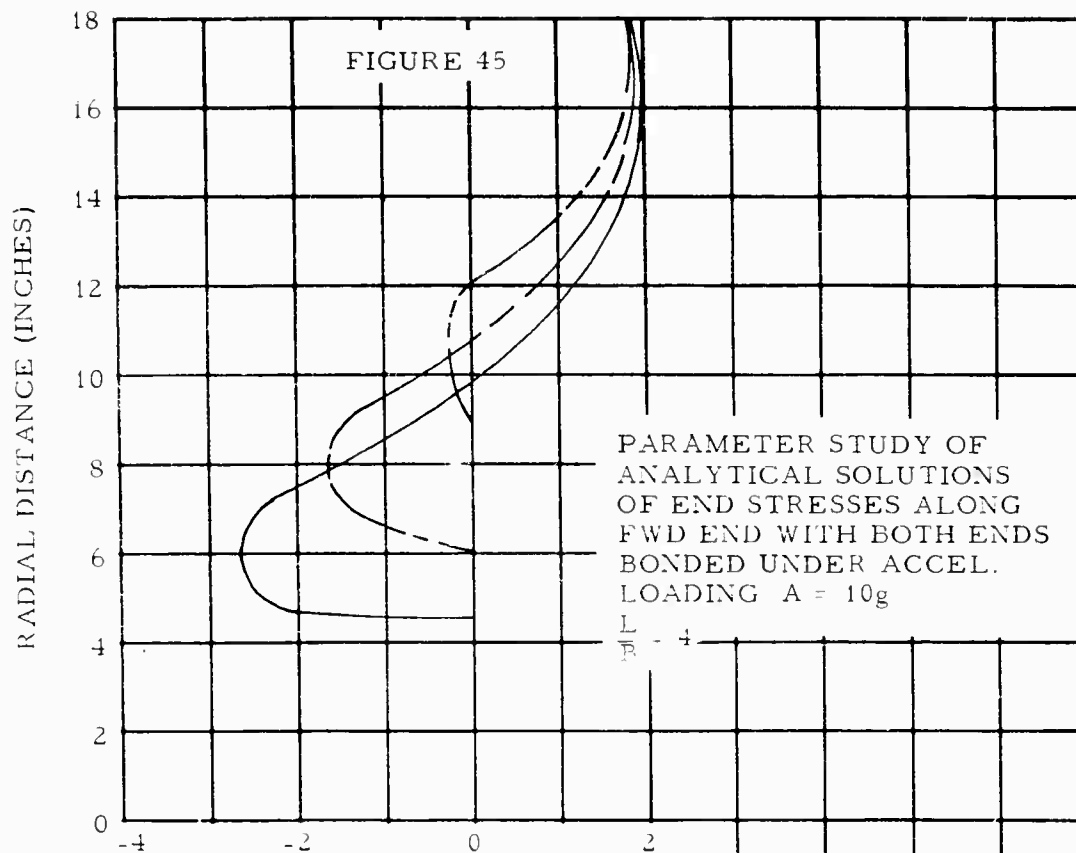
INTERFACE SHEAR STRESS
(psi)

INTERFACE RADIAL STRESS
(psi)

INNER BORE HOOP STRAIN
(%)

FIGURE 44





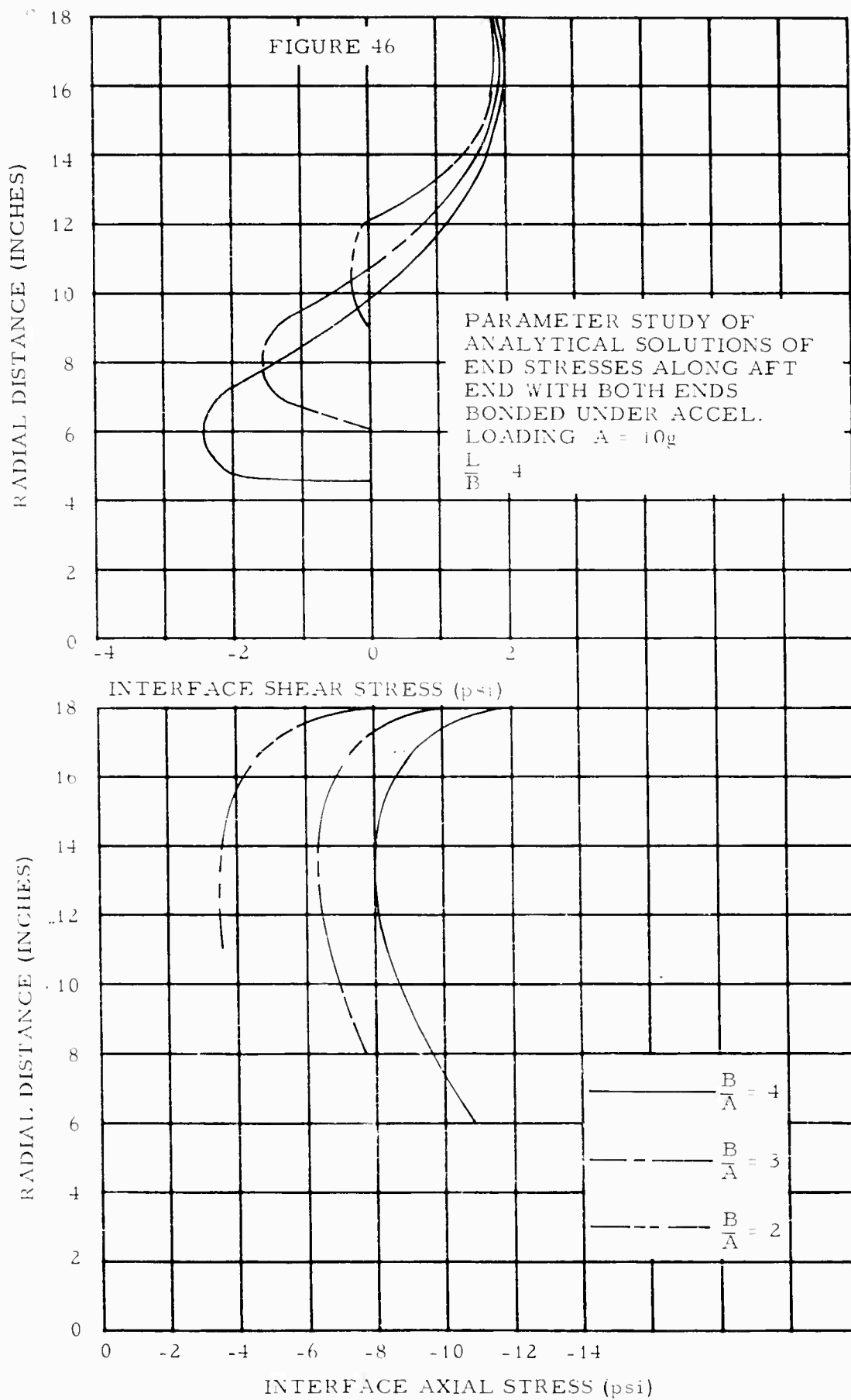
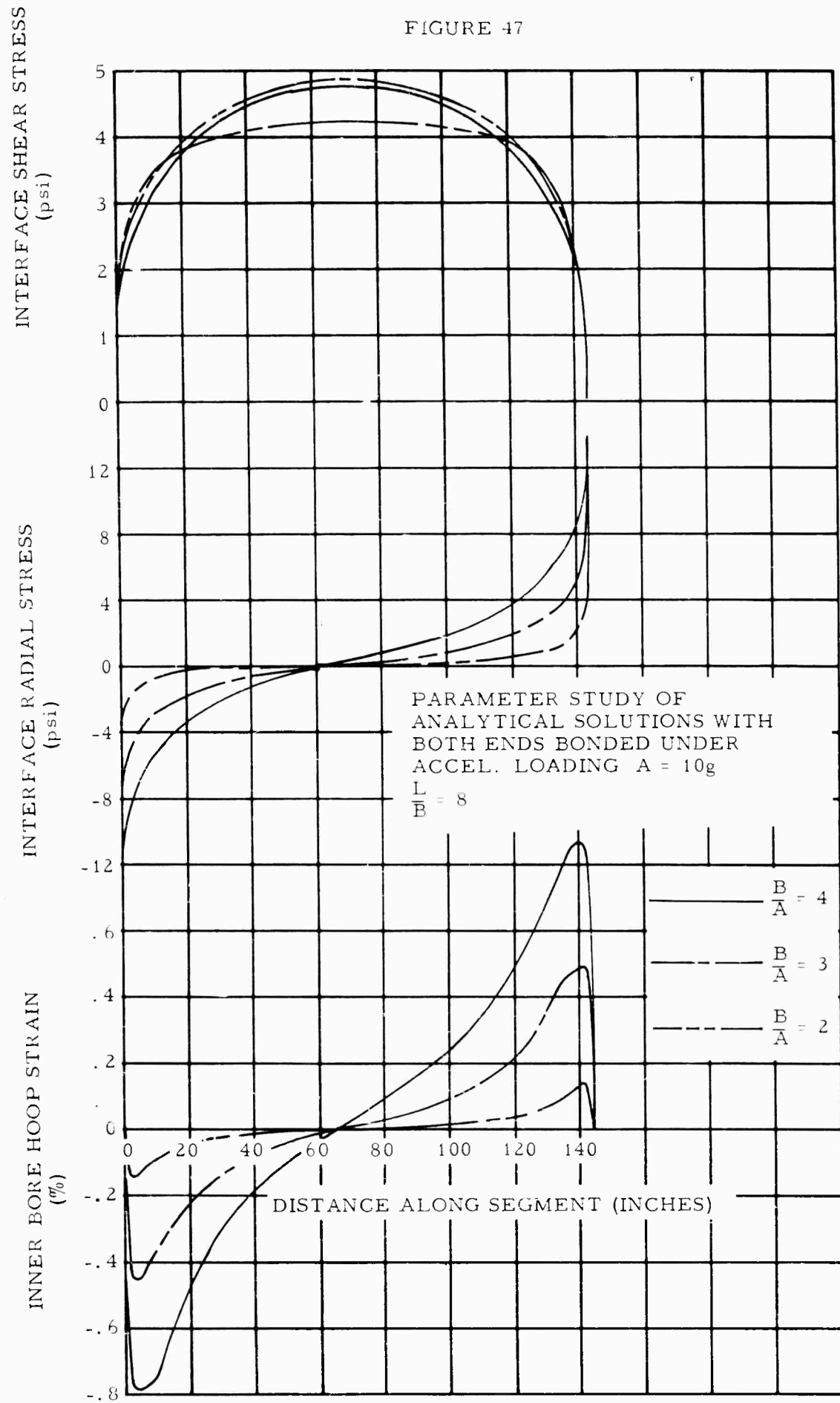
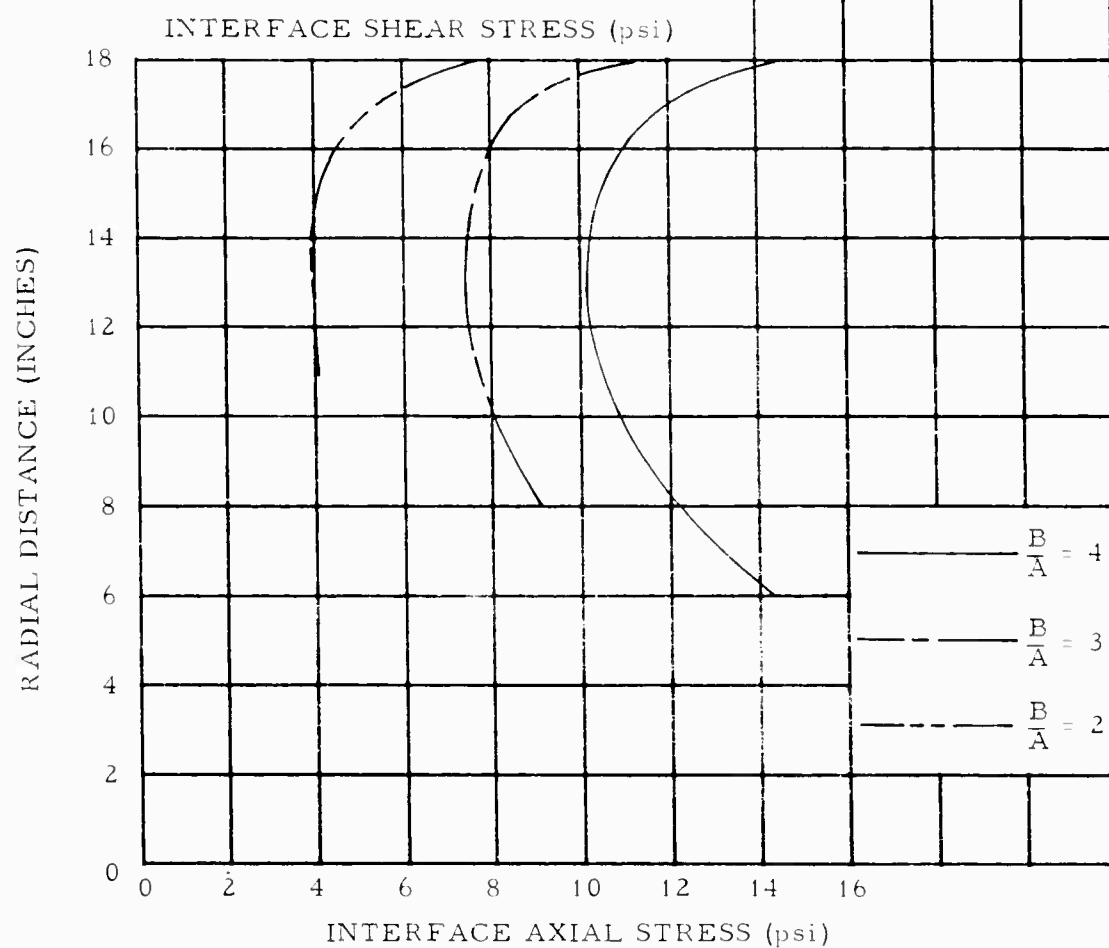
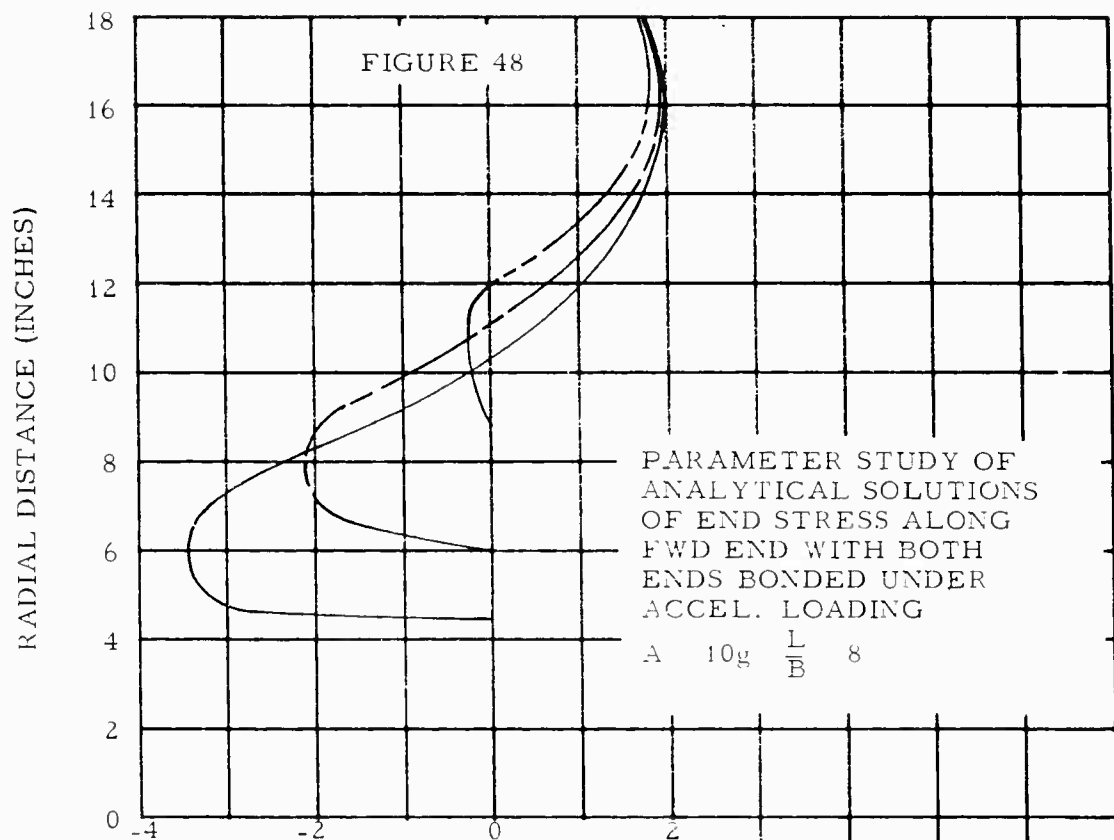
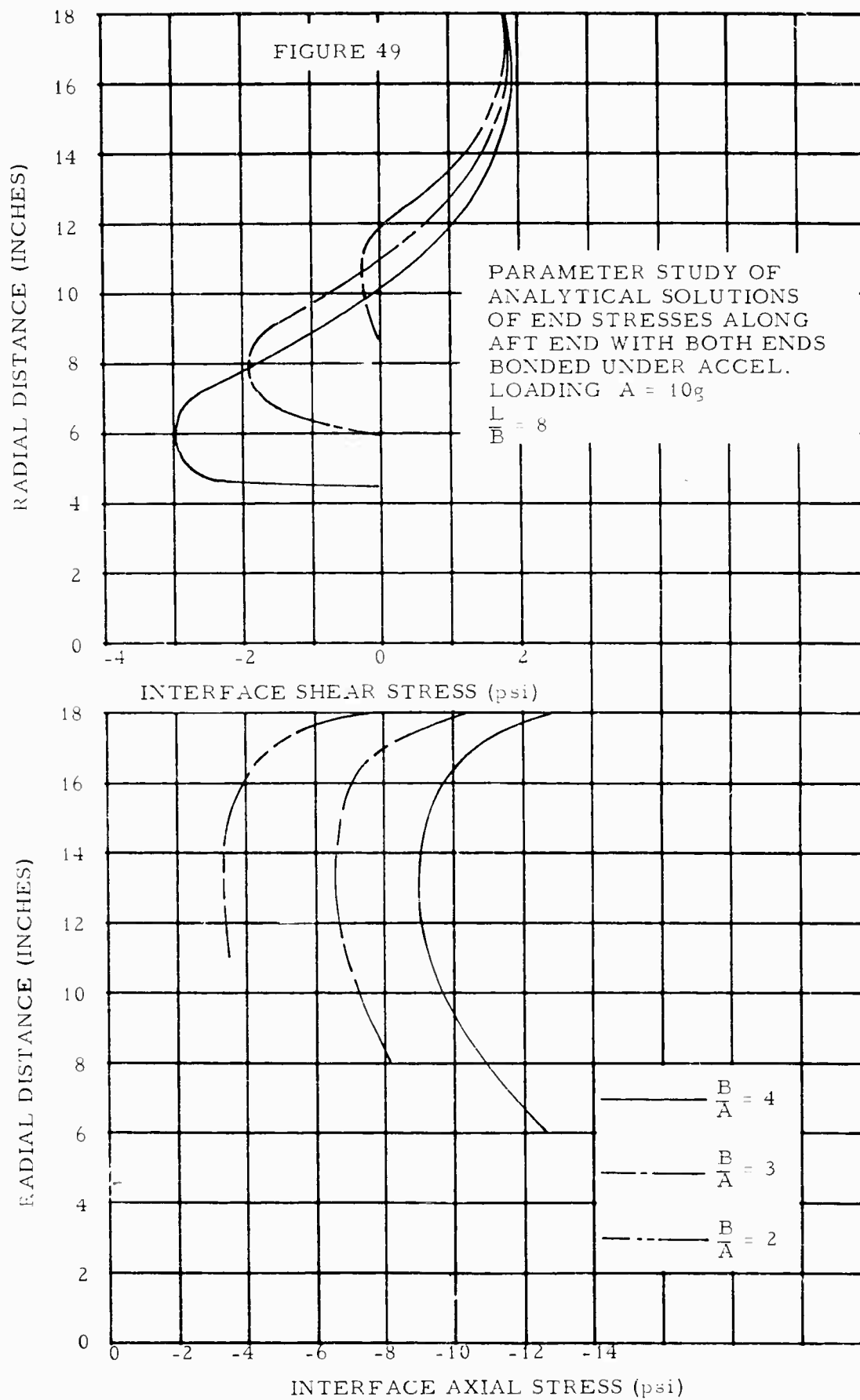


FIGURE 47







APPENDIX D

STRESS ANALYSIS OF PROPELLANT GRAINS
USING DISPLACEMENT EQUATIONS

by

R. M. Toms and J. E. Vinson
Structural Research Department
Aerojet-General Corporation

NOMENCLATURE

r, θ, z — Cylindrical coordinates.

$\sigma_r, \sigma_\theta, \sigma_z$ — Normal stress.

$\tau_{rz}, \tau_{\theta z}, \tau_{r\theta}$ — Shear stress.

u — Radial displacement.

w — Axial displacement.

a — Inner radius of cylinder.

b — Outer radius of cylinder.

l — Half length of cylinder.

h — Thickness of casing enclosing cylinder.

λ, μ — Lamé constants.

ν — Poisson's ratio.

E — Elastic modulus.

Note: Symbols subscripted by c refer to the casing.

I. INTRODUCTION

The determination of stress and strain fields in solid rocket motors was studied in terms of displacements. Two solutions were examined. The first was a method for obtaining the stresses and displacements expressed as linear combinations of products of the functions of r and the functions of z .

The second method was a finite-difference approach to the solution of the displacement equations. Calculations were performed on several stress problems where pressure was applied to the inner bore and ends of the grain. The propellant grain was assumed to be bonded to a thin, elastic shell on all or part of its outer surface and its ends. The geometry of the grain is shown in figure 1. The numerical work was carried out on an IBM 7090 computer.

II. GENERAL EQUATIONS

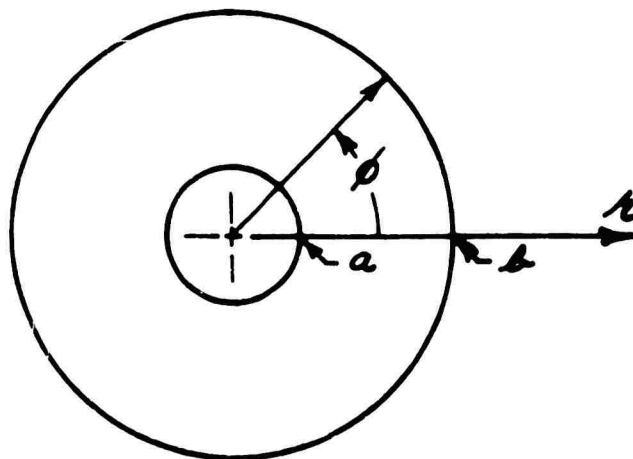
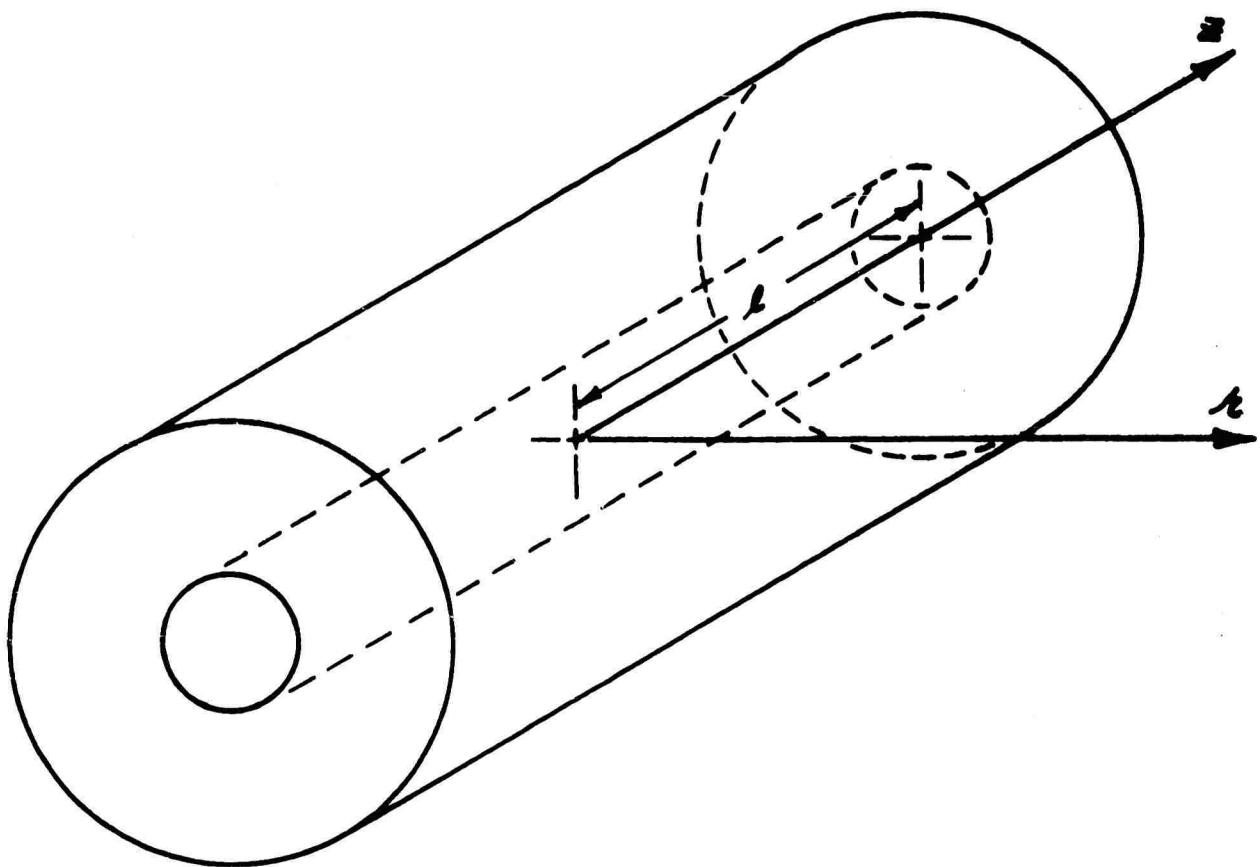
The classical stress-displacement relations for the axisymmetric loading conditions under consideration are given by: (Reference 3, page 3.)*

$$\tau_{r\phi} = \tau_{\phi z} = 0 \quad (1a)$$

$$\sigma_r = (\lambda + 2\mu) \frac{\partial u}{\partial r} + \lambda \left(\frac{\partial w}{\partial z} + \frac{u}{r} \right) \quad (1b)$$

$$\sigma_\phi = (\lambda + 2\mu) \frac{u}{r} + \lambda \left(\frac{\partial w}{\partial z} + \frac{\partial u}{\partial r} \right) \quad (1c)$$

* A list of symbols appears on Page D-ii.



CYLINDER GEOMETRY

figure 1

$$\sigma_z = (\lambda + 2\mu) \frac{\partial w}{\partial z} + \lambda \left(\frac{u}{r} + \frac{\partial u}{\partial r} \right) \quad (1d)$$

$$\tau_{rz} = \mu \left(\frac{\partial u}{\partial z} + \frac{\partial w}{\partial r} \right) \quad (1e)$$

The displacement equations of equilibrium of the grain in cylindrical coordinates are: (Reference 3, Page 4.)

$$(\lambda + 2\mu) \left[\frac{\partial^2 u}{\partial r^2} + \frac{1}{r} \frac{\partial u}{\partial r} - \frac{u}{r^2} \right] + (\lambda + \mu) \frac{\partial^2 w}{\partial r \partial z} + \mu \frac{\partial^2 u}{\partial z^2} = 0 \quad (2a)$$

$$\frac{\mu}{r} \frac{\partial}{\partial r} \left(r \frac{\partial w}{\partial r} \right) + (\lambda + 2\mu) \frac{\partial^2 w}{\partial z^2} + \frac{(\lambda + \mu)}{r} \frac{\partial}{\partial r} \left(r \frac{\partial u}{\partial z} \right) = 0 \quad (2b)$$

These elliptic partial differential equations can be solved simultaneously or combined into the single fourth-order equation,

$$\left(\frac{\partial}{\partial r} + \frac{1}{r} \frac{\partial}{\partial r} r + \frac{\partial^2}{\partial z^2} \right)^2 u = 0 \quad (3)$$

where the terms in the parentheses represent an operator operating on the displacement u .

The complete set of boundary conditions is:

Inner radius ($r = a$)

$$\left. \begin{aligned} \sigma_r(a, z) &= f_1(z) \\ \tau_{rz}(a, z) &= f_2(z) \end{aligned} \right\} \quad (4a)$$

Outer radius ($r = b$)

$$\left. \begin{aligned} u(b, z) &= u_c(z) & \sigma_r(b, z) &= \sigma_{rc}(z) \\ w(b, z) &= w_c(z) & \tau_{rz}(b, z) &= \tau_{rzc}(z) \end{aligned} \right\} \quad (4b)$$

Ends ($z = \pm l$)

bonded

$$\left. \begin{aligned} w(r, \pm l) &= w_c(r) & \sigma_z(r, \pm l) &= \sigma_{zc}(r) \\ u(r, \pm l) &= u_c(r) & \tau_{rz}(r, \pm l) &= \tau_{rzc}(r) \end{aligned} \right\} \quad (4c)$$

free

$$\sigma_z(r, \pm l) = f_3(r) \quad \tau_{rz}(r, \pm l) = f_4(r) \quad (4d)$$

where f_1 , f_2 , f_3 and f_4 are prescribed functions. The subscript c refers to quantities associated with the case.

Under the assumption that the axial force in the case and the shear load on the case are negligible, the governing differential equation for the radial displacement u_c is: (Reference 3, Page 33.)

$$\frac{d^4 u_c}{dz^4} + 4\theta^4 u_c = -\frac{\sigma_r(b, z)}{D} \quad (5a)$$

with

$$\theta^4 = \frac{3(1-\nu_c^2)}{b^3 h^3} \quad \text{and} \quad D = \frac{E_c h^3}{12(1-\nu_c^2)} \quad (5b)$$

The axial displacement of the case is given by: (Reference 3, Page 38.)

$$\frac{dw_c}{dz} + \frac{\nu_c}{b} u_c = 0 \quad (6)$$

Generally, the end plates offer an elastic support to the case; however, for simplicity, two limiting conditions are considered:

$$\text{Simple supports} \quad u_c(\pm l) = \frac{d^2 u_c(\pm l)}{dz^2} = 0 \quad (7a)$$

$$\text{Fixed supports} \quad u_c(\pm l) = \frac{du_c(\pm l)}{dz} = 0 \quad (7b)$$

The solution of the thermal problem can also be obtained from the above equations. Equations (1a), (1e), (2a), (2b) and (3), are unchanged, but the quantity $(3\lambda + 2\mu)\alpha T$, must be subtracted from the right-hand side of Equations (1b), (1c) and (1d). The quantity T is the temperature measured from an arbitrary reference value and α is the coefficient of thermal expansion.

Since the problem is linear, the displacements can be decomposed into two parts, (1) the displacements denoted by the subscripts 1, which are due to stresses and (2) the thermal displacements. Therefore, for the grain,

$$u = u_1 + \int_0^r \alpha T dr \quad (8a)$$

$$w = w_1 + \int_0^z \alpha T dz \quad (8b)$$

and for the case,

$$u_c = u_{c1} + \int_0^r \alpha_c T_c dr \quad (9a)$$

$$w_c = w_{c1} + \int_0^z \alpha_c T_c dz \quad (9b)$$

where u_1 , w_1 , u_{c1} and w_{c1} are determined by substituting them for u , w , u_c and w_c , respectively, in Equations (2a), (2b), (3), (5a) and (6).

III. THE ANALYTIC SOLUTION

A. DERIVATION

Discussion of the analytic solution will be restricted to the uniform internal pressurization of a thick-walled cylinder with unbonded ends and longitudinal symmetry. The boundary conditions become:

$$\left. \begin{array}{l} \tau_{rz}(r, \pm l) = 0 \\ \sigma_z(r, \pm l) = -P \end{array} \right\} \quad \begin{array}{l} \text{Unbonded ends} \\ \end{array} \quad (10a)$$

$$\left. \begin{array}{l} \tau_{rz}(a, z) = 0 \\ \sigma_r(a, z) = -P \end{array} \right\} \quad \begin{array}{l} \text{Inner bore} \\ \end{array} \quad (10b)$$

$$\left. \begin{array}{l} u(b, z) = u_c(z) \\ w(b, z) = w_c(z) \end{array} \right\} \quad \begin{array}{l} \text{Outer boundary} \\ \end{array} \quad (10c)$$

where P is the magnitude of the applied pressure, and $u_c(z)$ and $w_c(z)$ are as defined by (5a) and (6).

A solution of the governing differential equation which is sufficiently general to satisfy these boundary conditions is

$$\begin{aligned} u(r, z) = & c_1^0 r + c_2^0 r \log r + c_3^0 r + \frac{c_4^0}{r} + (c_5^0 r + \frac{c_6^0}{r}) z^2 \\ & + \sum_{n=1}^{\infty} \left\{ c_1^{\alpha_n} \frac{I_1(\alpha_n r)}{I_1(\alpha_n b)} + c_2^{\alpha_n} \frac{K_0(\alpha_n r)}{K_1(\alpha_n b)} + c_3^{\alpha_n} \frac{I_0(\alpha_n r)}{b I_0(\alpha_n b)} + c_4^{\alpha_n} \frac{r K_0(\alpha_n r)}{b K_0(\alpha_n b)} \right\} \cos(\alpha_n z) \\ & + \sum_{m=1}^{\infty} \left\{ c_1^{\beta_m} \frac{\cosh(\beta_m z)}{\cosh(\beta_m l)} + c_2^{\beta_m} \frac{z \sinh(\beta_m z)}{l \sinh(\beta_m l)} \right\} J_1(\beta_m r) \end{aligned} \quad (11)$$

where the I 's, J 's and K 's are Bessel functions. The α_n and β_m are eigenvalues of the problem which are generated by

$$\sin(\alpha_n l) = 0 \quad \text{and} \quad J_1(\beta_m b) = 0 \quad (12)$$

The c_1^0 , $c_1^{\alpha_n}$ and $c_1^{\beta_m}$ are constants to be determined by the boundary conditions (0 , α_n and β_m are used as superscripts to distinguish the three sets of constants).

The axial displacements w are obtained in terms of the c 's by substituting the expressions for u and its partial derivatives into Equations (2a) and (2b). Similarly, the stresses are obtained in terms of the c 's from Equations (1b), (1c), (1d) and (1e).

The resulting expressions for the displacements and stresses are substituted into the boundary conditions, yielding six equations, each involving only one of the two variables, r and z . All functions of z are expanded in Fourier series over the interval $(0, l)$ while the functions of r are expanded in Fourier-Bessel series over the interval $(0, b)$. Each of the six equations can then be written in one of the forms,

$$A_0 + \sum_{n=1}^{\infty} [A_n \cos(\alpha_n z) + B_n \sin(\alpha_n z)] = 0 \quad (13)$$

or

$$D_0 + \sum_{m=1}^{\infty} D_m J_1(\beta_m r) = 0 \quad (14)$$

Since these equations are valid for all values of r and z in the intervals $(0, b)$ and $(0, l)$, respectively, it follows (References 5 and 6) that

$$\left. \begin{aligned} A_0 &= 0, & A_n &= 0, & B_n &= 0 \\ D_0 &= 0, & D_n &= 0 \end{aligned} \right\} n=1, 2, 3, \dots \quad (15)$$

The A 's, B 's and D 's are expressions which are free of variables; however, they do involve the constants c_1^0 , $c_1^{\alpha_n}$ and $c_1^{\beta_m}$. Thus system (15) constitutes an infinite system of linear equations in the infinite set of

unknown constants, c_1^0 , $c_1^{\alpha_n}$ and $c_1^{\beta_m}$, which, in theory, uniquely determines these constants and thus completes the solution of the boundary value problem. In practice, however, this infinite system cannot be solved; hence, it is necessary to approximate the exact solution by the solution of the system,

$$\left. \begin{aligned} A_0 &= 0, & A_n &= 0, & B_n &= 0 & n &= 1, 2, \dots, N \\ D_0 &= 0, & D_m &= 0 & m &= 1, 2, \dots, M \end{aligned} \right\} \quad (16)$$

In general, the approximation improves with increasing N and M . However, the sizes of N and M are restricted by the storage space of the computer. A measure of the accuracy of the approximate solution can be obtained by solving the system (16) for several sets of values of N and M .

P. DISCUSSION

The most difficult aspect of this problem thus far has been that of obtaining the coefficients in the Fourier-Bessel expansions of functions. For the Fourier-Bessel expansion of $f(r)$,

$$f(r) = \sum_{m=1}^{\infty} d_m J_1(\beta_m r) \quad (17)$$

the coefficients are given by

$$d_m = \frac{2}{b^2 [J_0(\beta_m b)]^2} \int_0^b r f(r) J_1(\beta_m r) dr \quad (18)$$

These coefficients have been evaluated by numerical integration, which has involved two difficulties: (1) computer time required - the number of integrals to be evaluated and the large number of points at which it is

necessary to compute each integrand in order to achieve reasonable accuracy in the integration has made it necessary to expend considerable effort in optimizing the program to make it feasible as far as computer running time is concerned; (2) computation of function values - subroutines were not available for computing values of K_0 and K_1 , the modified Bessel functions of the second kind of orders zero and one, and the power series for these functions converge too slowly to be of use. Polynomial expressions (Reference 1) analogous to those used in existing subroutines for computing other Bessel functions proved very satisfactory, both in accuracy and in computer time required.

A sufficient number of the Fourier-Bessel coefficients have been evaluated to provide input data for the solution of the system (16) for $N \leq 10$ and $M \leq 15$. The system (16) will be solved for two or three sets of values of N and M meeting these restrictions. If the approximate solutions obtained are not sufficiently accurate, it will be necessary to calculate more Fourier-Bessel coefficients.

IV. THE FINITE-DIFFERENCE SOLUTION

A. FINITE-DIFFERENCE EQUATIONS

For a finite-difference solution it is convenient to work with the pair of displacement equations of equilibrium (2a) and (2b) rather than the single fourth-order equation (3).

The longitudinal cross-section of the motor is first divided into rectangular regions by means of a rectangular gridwork. A constant spacing is used but the spacing in the radial directions may be different from the spacing in the axial direction. By symmetry only one-half of the longitudinal cross-section need be considered. A typical gridwork is shown in Fig. 2.

At each mesh point, or node, the governing equations and boundary conditions are written in finite-difference form. A typical second-order,

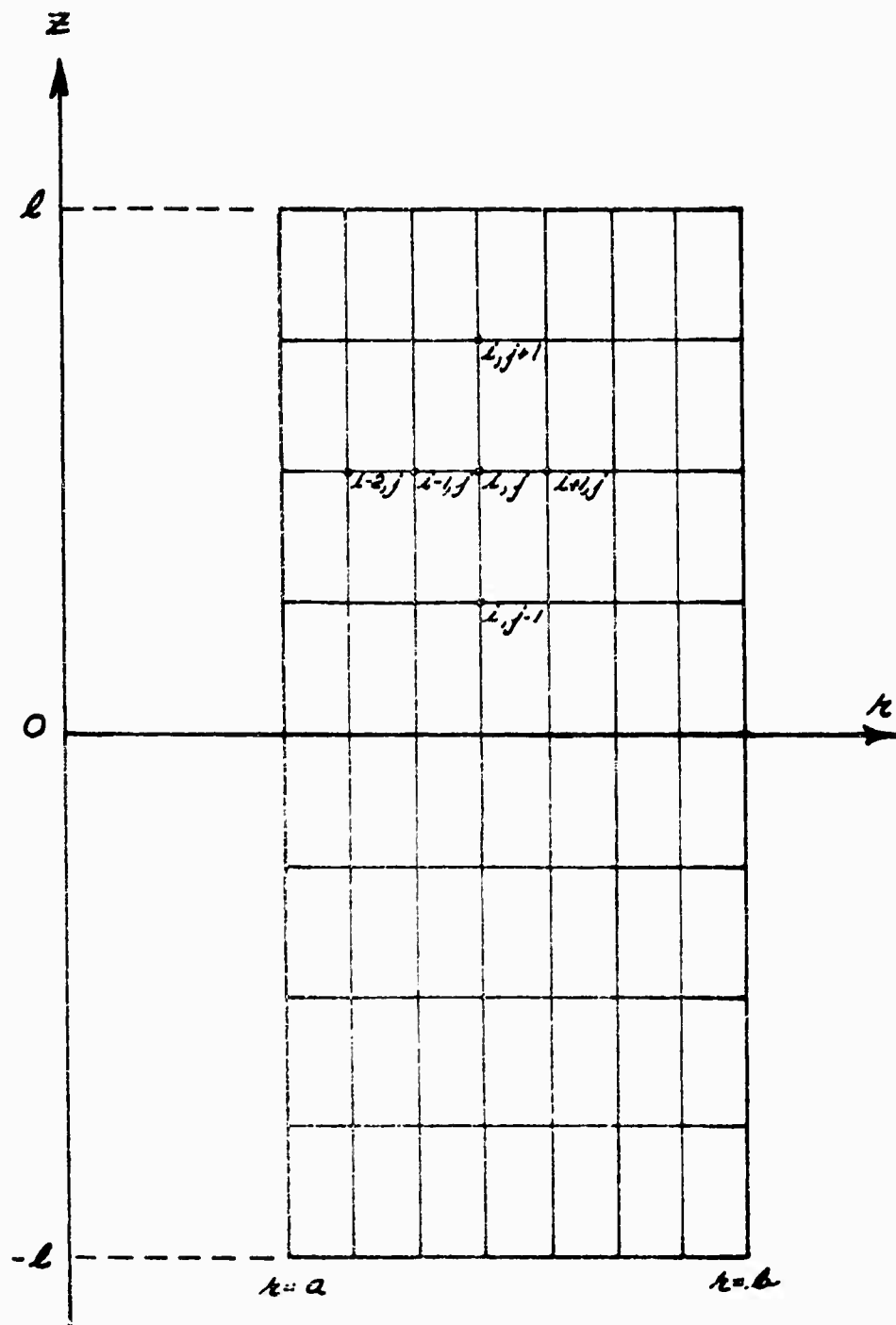


figure 2

finite-difference form for a first derivative at the point $r = i, z = j$, is:

$$\left. \frac{\partial u}{\partial r} \right|_{ij} = \frac{u_{i+1,j} - u_{i-1,j}}{2K} + O(K^2) \quad (19)$$

where K is the grid spacing in the radial direction.

The symbol $O(K^2)$ means that the error inherent in the approximations decreases with the square of K . Equation (19) is called a "central difference formula" since it is symmetrically centered about the point (i, j) . Such a formula is impractical at a nodal point which lies on the boundary; therefore, the so-called "forward" and "backward" difference formulas are used.

Forward difference formula

$$\left. \frac{\partial u}{\partial r} \right|_{ij} = \frac{-3u_{ij} + 4u_{i+1,j} - u_{i+2,j}}{2K} + O(K^2) \quad (20)$$

Backward difference formula

$$\left. \frac{\partial u}{\partial r} \right|_{ij} = \frac{u_{i-2,j} - 4u_{i-1,j} + 3u_{ij}}{2K} + O(K^2) \quad (21)$$

Similar finite-difference equations can be written for derivatives in the z direction, higher derivatives and mixed derivatives. Further discussion of finite-difference formulas is given by Hildebrand (Reference 2) or Salvadori and Baron (Reference 4).

At a node which is not on the boundary, the governing Equations (2a) and (2b) are written in finite-difference form. This leads to two linear equations at each internal node. At a boundary node the appropriate boundary conditions are written in finite-difference form making use of forward and backward difference formulas. Since there are two boundary conditions at each node, this also leads to two linear equations. If there are m

horizontal mesh lines and n vertical mesh lines the above procedure results in a system of $2mn$ linear algebraic equations in $2mn$ unknowns. The simultaneous solution to this linear system yields the values of the displacements u and w at each node. As the number of nodes increases, the accuracy of the finite-difference approximations increases. However, present computer facilities limit the number of nodes that can be introduced.

7. THE COMPUTER PROGRAM

The computer program which has been developed to handle this approach,* permits the determination of the necessary finite-difference forms and it solves the resulting set of equations. At each node the values of the displacements, stresses, strains, principal stresses, direction of principal stress and maximum shear stress are calculated and pointed out.

The program has been formulated to handle stress boundary conditions, displacement boundary conditions or mixed-boundary conditions. This allows end-bonded and partially-released grain configurations to be treated. The thermal stress problem has also been programmed into the routine but has not yet been checked out.

At the outer radius of the grain, the boundary condition (5a) presents some difficulties. At present, computer subroutines used to generate the necessary finite-difference equations can handle only first and second derivatives. A numerical value is chosen for the quantity $\frac{d^4 u_c}{dz^4}$ in the boundary condition and the problem is solved. Using the computed values for u_c and σ_r a new value of $\frac{d^4 u_c}{dz^4}$ is then calculated and the procedure repeated until the value of $\frac{d^4 u_c}{dz^4}$ stabilizes.

* The computer program is also discussed under Program DIFUV in Appendix E

C. NUMERICAL RESULTS AND DISCUSSION

To check out the computer program, a series of test cases were investigated. The following parameters were common to all cases.

$$\begin{aligned} 2\ell &= 143 \text{ in.} & E_c &= 30 \times 10^6 \text{ psi} \\ a &= 37 \text{ in.} & \nu_c &= 0.3 \\ b &= 70 \text{ in.} & h &= 0.5 \text{ in.} \\ E &= 1500 \text{ psi} & P &= 530 \text{ psi} \\ 13 \text{ longitudinal grid lines} & & 10 \text{ radial grid lines} & \end{aligned}$$

Case 1

The grain was subjected to a uniform pressure on its ends, inner bore and outer bore. A Poisson's ratio of $\nu = 0.45$ was used. The boundary conditions for this case are:

$$\left. \begin{aligned} \sigma_z(r, \pm \ell) &= -P & \sigma_r(u, z) &= \sigma_r(b, z) = -P \\ \tau_{rz}(r, \pm \ell) &= 0 & \tau_{rz}(u, z) &= \tau_{rz}(b, z) = 0 \end{aligned} \right\} \quad (22)$$

The analytic solution to this problem is:

$$\left. \begin{aligned} u &= - \frac{(1-2\nu)}{E} P r \\ w &= - \frac{(1-2\nu)}{E} P z \end{aligned} \right\} \quad (23)$$

The results of the analytic solution and the finite-difference solution agree at all nodal points to five significant digits.

Case 2

In this case the grain was subjected to uniform pressure on its ends and inner bore. Boundary conditions determined by the case displacements were used. The ends of the case were considered to be fixed. Some of the results for a Poisson's ratio of 0.3 are plotted in Figs. 3 and 4. Since there is an analytic singularity in the stresses at the corner, the curves were not extended into

this region. It was conjectured that the corner boundary condition and the value of ν would have considerable effect on the interface shear stress pattern.

Case 3

In this case a higher Poisson's ratio of 0.45 was used. It should be noted that at the outside corners are several possible boundary conditions which could be applied to the node. It was decided to try the following corner condition:

$$\left. \begin{aligned} u(b, \pm \ell) &= 0 \\ \tau_{rz}(b, \pm \ell) &= 0 \end{aligned} \right\} \quad (24)$$

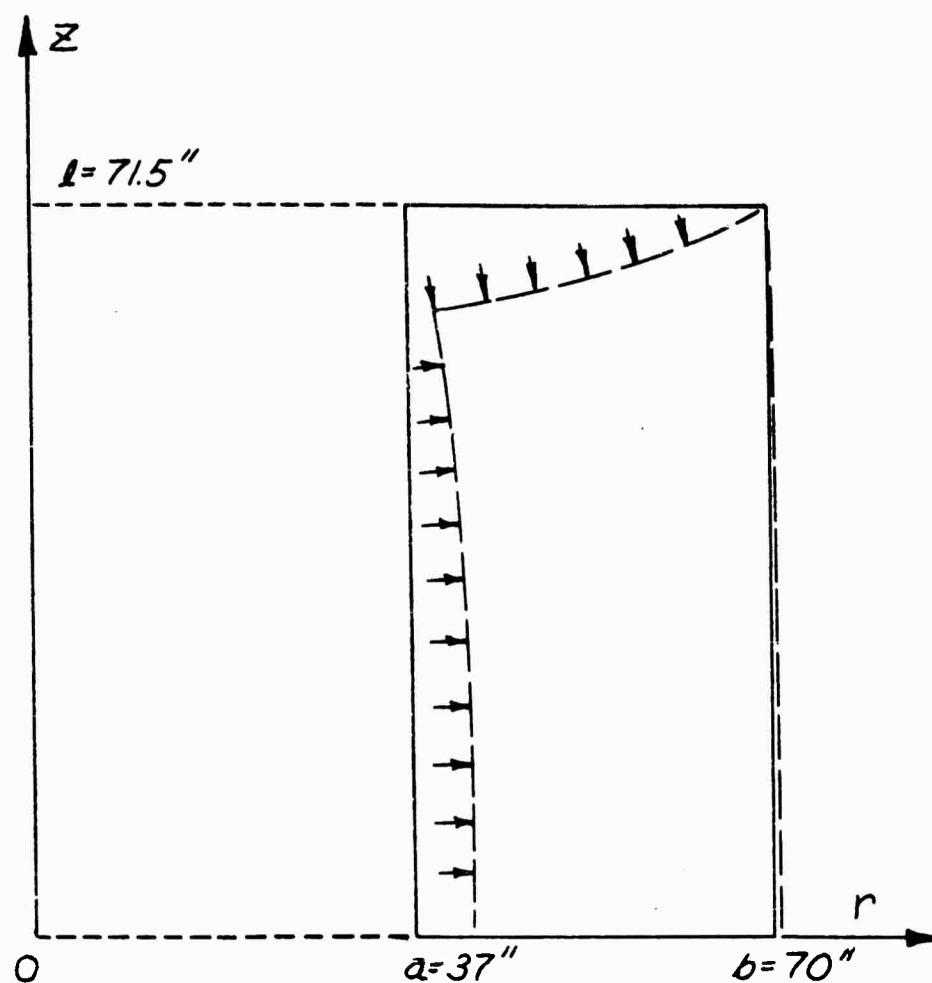
These changes had a marked effect on the shear stress pattern (Fig. 5). It should be noted that the maximum shear may be higher when a finer mesh is used in the corner.

Case 4

The conditions for this case are the same as those in Case 3. However, a slightly different approach for its solution was utilized. It was noted that due to the symmetry of the problem only the upper half of the cross-section of Fig. 2 need be considered. Symmetry considerations lead to the boundary conditions

$$\left. \begin{aligned} w(r, 0) &= 0 \\ \tau_{rz}(r, 0) &= 0 \end{aligned} \right\} \quad (25)$$

along the edge $z = 0$. The net effect of this procedure was to reduce the axial mesh size by one-half. The change in stress values was insignificant, but it was noted that all stresses were reduced in the third digit. It could be inferred then, that the stresses computed for the uniform pressure problem,



*Grain Displacement Due To A Uniform
Pressure Of 530 PSI -
 $\nu = .3$*

figure 3

INTERFACE STRESSES

CASE 2

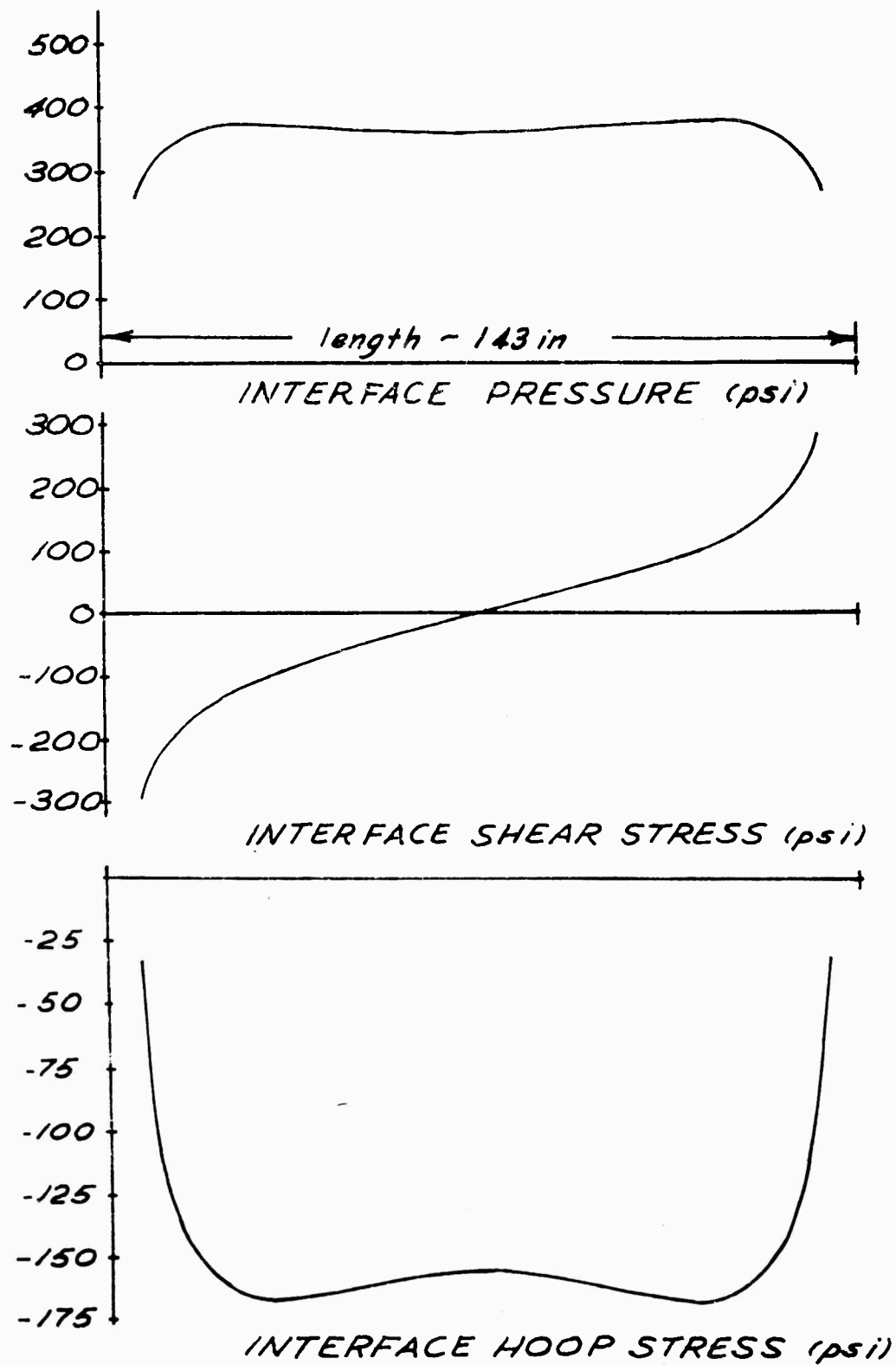


figure 4

INTERFACE STRESSES CASE 3

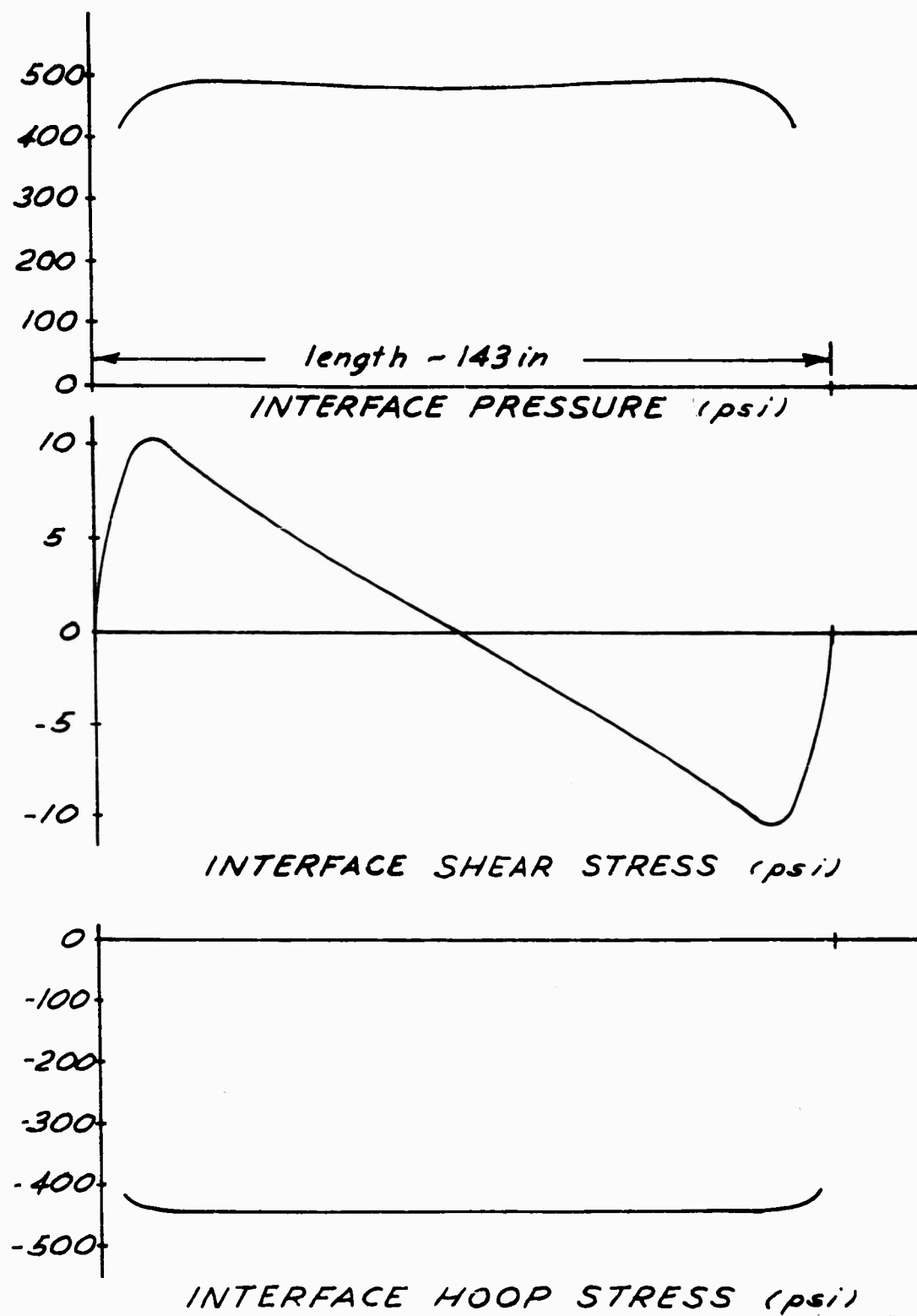


figure 5

are upper bounds of the stresses which satisfy the equilibrium conditions.

The above test cases indicate that significant results can be obtained with present computer capabilities. However, before any generalizations can be made, certain studies should be initiated. Namely, the subroutines used to generate finite-difference formulas should be altered to handle (1) higher derivatives; (2) finite-difference equations of higher-order accuracy and (3) variable grid spacing. The effect of the suggested changes on the inherent error in finite-difference approximations should be studied most carefully. As noted above, the appropriate formulation of the boundary condition at the interface corner should be investigated thoroughly.

With a solution improved by the above changes, parameter studies can be initiated to ascertain the effect of mechanical properties, web thickness, length, and various bonding conditions on stress pattern in propellant grains.

REFERENCES

1. Allen, E. E. "Polynomial Approximations to some Modified Bessel Functions", Mathematical Tables & other Aids to Computation, Vol. 10, p. 163, July 1956.
2. Hildebrand, F. P. Introduction to Numerical Analysis, McGraw-Hill Book Co., New York, pp. 128-180, 1956.
3. Hilton, H. H. & Murthy, P. N. "The Analysis of Elastic or Visco-elastic Finite Length Thick-Walled Cylinders Encased by Elastic Shells & Exposed to Internal Pressure, Thermal Cycling or Vertical Storage", AGO: SP61-1, May 1961.
4. Salvadori, M. G. & Baron, M. L. Numerical Methods in Engineering, Prentice-Hall, Inc., New York, 1952.
5. Watson, G. N. Theory of Bessel Functions, 2d Ed., Cambridge University Press, p. 651, 1944.
6. Zygmund, Antoni Trigonometrical Series, Dover Publications, New York, N. Y., p. 274, 1955.

APPENDIX E

FINITE DIFFERENCE SOLUTION OF ORDINARY AND
PARTIAL DIFFERENTIAL EQUATIONS

by

R. D. Glauz

Computing Services Division
Aerojet-General Corporation

Finite Difference Solution of Ordinary
and
Partial Differential Equations

By

R. D. Glauz

INTRODUCTION

The numerical solution of ordinary and partial differential equations is studied here from the standpoint of the use of finite-difference methods. These methods are applicable to ordinary differential equations which have boundary conditions specified at more than one point, the so-called two-point or jury type boundary conditions. For partial differential equations the finite difference approach is primarily used for equations of elliptic type. As the methods for partial differential equations are a simple generalization of those used for the ordinary differential equation a more or less unified treatment is possible. The basic concepts are developed for the ordinary differential equation and then those modifications necessary for the extension to more dimensions indicated.

The development of the tools necessary for solving this type of problem numerically could proceed in the following sequence:

- (a) description of the finite difference method
- (b) abstract generalization and unification using matrix methods
- (c) construction of computer programs utilizing these concepts
- (d) application of these programs to engineering problems.

As this sequence is valuable from both a reference and development or understanding of the material it is followed in this report.

I. Finite Difference Method

The solution of two-point boundary problems is quite different from that for one-point boundary problems. In the one-point boundary problem one starts at a specified point where sufficient information is available to enable the construction of the solution outward from that point. However, in the two-point boundary problem insufficient information is available at any one point to permit the construction of the solution. Thus, rather than building the solution out from one point, the solution over the entire interval must be found simultaneously.

The methods developed for "marching" problems were applicable to both linear and non-linear differential equations. In contrast, the two-point boundary problem is readily solved only for linear differential equations. Iterative methods have been developed for the non-linear case, however, there is no guarantee that they will work in every case. The general linear differential equation of second order can be written

$$\frac{d^2 y}{dx^2} + f(x) \frac{dy}{dx} + g(x)y = h(x) \quad (1)$$

with boundary conditions of the form

$$a \frac{dy}{dx} + by = c \quad (2)$$

The method of attack is to replace the differential equation by a finite difference equation at the interior points of the region. The boundary conditions are also replaced by their finite difference equivalent. Thus a large set of simultaneous equations in the unknown function values y_i are obtained. These equations are solved for the set of y_i . The method for solving simultaneous equations applicable to a sparse set of equations is very good here as each equation contains just a few unknowns. Sets of equations exceeding 500 arising from this type of problem have been solved exactly in minutes on a modern high speed computer.

The method of solution is illustrated first for the case of a single second order differential equation. Let us consider, for example, the problem

$$\frac{d^2 y}{dx^2} - \frac{dy}{dx} - 2y = x \quad y(0) = 2, \quad y(1) = 1$$

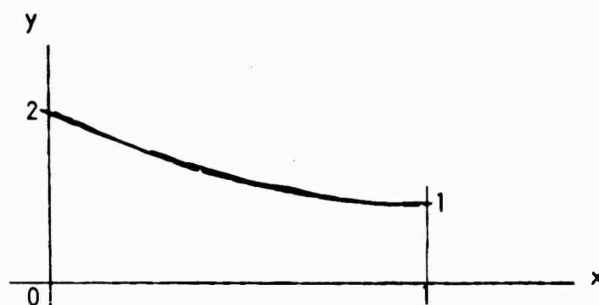


FIGURE 1

In the interval $0 \leq x \leq 1$ we are looking for a function $y(x)$ which takes on the values 2, 1 at the end-points and satisfies the differential equation everywhere in the interval. In finding a numerical solution first subdivide the interval by a set of points x_1, x_2, x_3, x_4 :

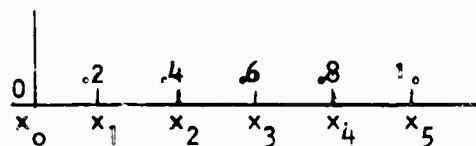


FIGURE 2

At each point we shall find the value y . At each of the interior points x_1, x_2, x_3, x_4 we need a representation for the differential equation. The function y will take the values y_1, y_2, y_3, y_4 at these points. However, we further need $\frac{d^2 y}{dx^2}, \frac{dy}{dx}$ in terms of y_0, y_1, y_2, \dots at each point. These relations can be found using Taylor's series.

The function y can be expanded in a Taylor's series about the point x_n

$$y(x) = y(x_n) + \left(\frac{dy}{dx}\right)_n (x-x_n) + \left(\frac{d^2y}{dx^2}\right)_n \frac{(x-x_n)^2}{2!} + \dots$$

or

$$y = y_n + y_n' (x-x_n) + y_n'' \frac{(x-x_n)^2}{2!} + y_n''' \frac{(x-x_n)^3}{3!} + y_n^{IV} \frac{(x-x_n)^4}{4!} + \dots \quad (3)$$

In particular, at x_{n+1} letting $x_{n+1} - x_n = h$ we have

$$y_{n+1} = y_n + y_n' h + y_n'' \frac{h^2}{2} + y_n''' \frac{h^3}{6} + y_n^{IV} \frac{h^4}{24} + \dots \quad (4)$$

Similarly at x_{n-1} we have $x_{n-1} - x_n = -h$ and

$$y_{n-1} = y_n - y_n' h + y_n'' \frac{h^2}{2} - y_n''' \frac{h^3}{6} + y_n^{IV} \frac{h^4}{24} - \dots \quad (5)$$

Adding equations (4), (5) we have

$$y_{n+1} + y_{n-1} = 2y_n + y_n'' h^2 + y_n^{IV} \frac{h^4}{12} + \dots \quad (6)$$

Solving for y_n''

$$y_n'' h^2 = y_{n+1} - 2y_n + y_{n-1} - y_n^{IV} \frac{h^4}{12} + \dots$$

or

$$\left(\frac{d^2y}{dx^2}\right)_n = \frac{y_{n+1} - 2y_n + y_{n-1}}{h^2} - \frac{y_n^{IV} h^2}{12} + \dots \quad (7)$$

Similarly by subtracting equations (4) and (5)

$$y_{n+1} - y_{n-1} = 2y_n' h + y_n''' \frac{h^3}{3} + \dots \quad (8)$$

and solving for y_n'

$$y_n' = \frac{y_{n+1} - y_{n-1}}{2h} - \frac{y_n'' h^2}{3} + \dots \quad (9)$$

We thus have approximately

$$\left(\frac{d^2 y}{dx^2}\right)_n \cong \frac{y_{n+1} - 2y_n + y_{n-1}}{h^2} \quad (10)$$

$$\left(\frac{dy}{dx}\right)_n \cong \frac{y_{n+1} - y_{n-1}}{2h} \quad (11)$$

At each point in the interval the differential equation can be written

$$\left(\frac{d^2 y}{dx^2}\right)_n - \left(\frac{dy}{dx}\right)_n - 2y_n = x_n \quad (12)$$

and using the finite difference expressions (10), (11) for the derivatives

$$\frac{y_{n+1} - 2y_n + y_{n-1}}{h^2} - \frac{y_{n+1} - y_{n-1}}{2h} - 2y_n = x_n \quad (13)$$

or multiplying by h^2

$$\left(1 - \frac{h}{2}\right) y_{n+1} - (2 + 2h^2) y_n + \left(1 + \frac{h}{2}\right) y_{n-1} = h^2 x_n \quad (14)$$

The equation (14) must be satisfied at each interior point in the interval:

$x_1, x_2, x_3, x_4.$

With $h = .2$ equation (14) becomes

$$.9 y_{n+1} - 2.08 y_n + 1.1 y_{n-1} = .04 x_n \quad (15)$$

At each interior point of the interval therefore

$$n = 1, x = .2 \quad .9y_2 - 2.08 y_1 + 1.1y_0 = .008 \quad (16)$$

$$n = 2, x = .4 \quad .9y_3 - 2.08 y_2 + 1.1y_1 = .016 \quad (17)$$

$$n = 3, x = .6 \quad .9y_4 - 2.08 y_3 + 1.1y_2 = .024 \quad (18)$$

$$n = 4, x = .8 \quad .9y_5 - 2.08 y_4 + 1.1y_3 = .032 \quad (19)$$

In addition we have the two boundary conditions

$$\begin{aligned} y_0 &= 2 \\ y_5 &= 1 \end{aligned} \quad (20)$$

Thus we have a set of six simultaneous equations in the six unknowns

$y_0, y_1, y_2, y_3, y_4, y_5$. These simultaneous equations are easily solved by elimination of variables yielding

x	Finite Difference	Exact Solution	Error
0	$y_0 = 2.0$	2.0	.0
.2	$y_1 = 1.6415 \ 9912$	1.6408 \ 9399	.0007 \ 0513
.4	$y_2 = 1.3583 \ 6241$	1.3573 \ 3843	.0010 \ 2398
.6	$y_3 = 1.1507 \ 0531$	1.1496 \ 9588	.0010 \ 0943
.8	$y_4 = 1.0258 \ 5377$	1.0251 \ 7709	.0006 \ 7668
1.0	$y_5 = 1.0$	1.0	.0

TABLE 1

The accuracy is quite good even with coarse spacing ($h = .2$)

The error can be reduced by using a smaller spacing h . This reduces the error in replacing the exact derivative by its finite differences approximation, i.e., reducing the truncation error. Setting $h = .1$ in equation (14) yields the finite

difference approximation applicable in the interior of the region:

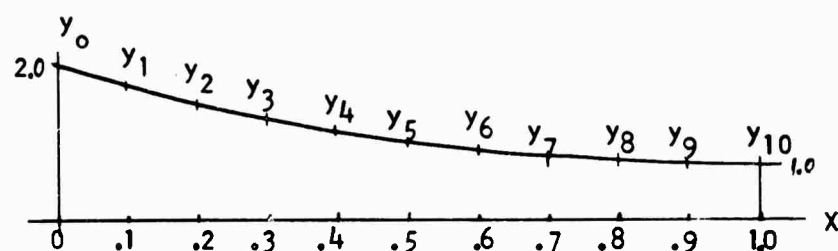


FIGURE 3

$$.95y_{n+1} - 2.02y_n + 1.05y_{n-1} = .01x_n \quad (21)$$

Putting n equal to $1, 2, \dots, 9$ yields the nine interior equations and with the two boundary equations

$$y_0 = 2 \quad y_{10} = 1$$

forms a set of eleven equations to be solved for the eleven unknowns y_0, y_1, \dots, y_{10} .

The values of y obtained at the even abscissas are tabulated in table 2 with the corresponding error.

x	Finite Differences	Exact Solution	Error
0	$y_0 = 2.0$	2.0	.0
.2	$y_2 = 1.6410 \ 7165$	1.6408 \ 9399	.0001 \ 7766
.4	$y_4 = 1.3575 \ 9649$	1.3573 \ 3843	.0002 \ 5806
.6	$y_6 = 1.1499 \ 5037$	1.1496 \ 9588	.0002 \ 5449
.8	$y_8 = 1.0253 \ 4779$	1.0251 \ 7709	.0001 \ 7070
1.0	$y_{10} = 1.0$	1.0	.0

TABLE 2

Note the reduction of error of the $h = .1$ spacing compared to the $h = .2$ case. The error has been reduced by approximately the factor four. This is to be expected from an inspection of the error term of the finite difference approximation used. The error term was of order h^2 , thus reducing the spacing h by a factor two reduced the error by a factor four. The error could be made as small as desired by reducing the spacing h . The practical limitation of this procedure is in the solution of the large number of simultaneous equations arising from a very small h . In practice one desires the most accurate answer for a fixed amount of labor. Other methods which will yield a more accurate answer with less labor are the error corrections methods and the use of a more accurate finite difference approximation in the differential equation. These two methods are closely connected and yield similar results.

Difference Correction

In the numerical solution of differential equations we have introduced error by approximately writing derivatives using finite difference expressions. Difference correction is a method for reducing the error introduced by using finite difference approximation. The exact central difference representation for the first and second derivatives is given by the equations:

$$y'_n = \frac{1}{h} (\mu\delta - \frac{1}{6} \mu\delta^3 + \frac{1}{30} \mu\delta^5 - \frac{1}{140} \mu\delta^7 + \frac{1}{630} \mu\delta^9 - \dots) y_n \quad (22)$$

$$y''_n = \frac{1}{h^2} (\delta^2 - \frac{1}{12} \delta^4 + \frac{1}{90} \delta^6 - \frac{1}{560} \delta^8 + \frac{1}{3150} \delta^{10} - \dots) y_n \quad (23)$$

In using these central difference equation we do not make any approximation if an infinite number of terms are retained. It is in the truncating of the series that errors are introduced. Thus if we retain as many terms as possible,

good accuracy is attainable. Let us replace the first difference inside the parenthesis by its Lagrangian representation in terms of functional values of y_i . Equations (22), (23) then become:

$$y'_n = \frac{-y_{n-1} + y_{n+1}}{2h} + \frac{1}{h} \left(-\frac{1}{6} \mu \delta^3 + \frac{1}{30} \mu \delta^5 - \frac{1}{140} \mu \delta^7 + \frac{1}{630} \mu \delta^9 - \dots \right) y_n$$

$$y'_n = \frac{-y_{n-1} + y_{n+1}}{2h} + \frac{1}{h} C_1 y_n \quad (24)$$

$$C_1 y_n = -\frac{1}{6} \mu \delta^3 y_n + \frac{1}{30} \mu \delta^5 y_n - \frac{1}{140} \mu \delta^7 y_n + \frac{1}{630} \mu \delta^9 y_n - \dots \quad (25)$$

$$y''_n = \frac{y_{n-1} - 2y_n + y_{n+1}}{h^2} + \frac{1}{h^2} \left(-\frac{1}{12} \delta^4 + \frac{1}{90} \delta^6 - \frac{1}{560} \delta^8 + \frac{1}{3150} \delta^{10} - \dots \right)$$

$$y''_n = \frac{y_{n-1} - 2y_n + y_{n+1}}{h^2} + \frac{1}{h^2} (C_2 y_n) \quad (26)$$

$$C_2 y_n = -\frac{1}{12} \delta^4 y_n + \frac{1}{90} \delta^6 y_n - \frac{1}{560} \delta^8 y_n + \frac{1}{3150} \delta^{10} y_n - \dots \quad (27)$$

The terms $\frac{C_1 y_n}{h}$, $\frac{C_2 y_n}{h^2}$ are the error or correction terms which must be included to have an exact representation of the derivatives. This correction term is included in the equations using an iteration technique. We solve the system as previously by neglecting the correction term. Using this solution, a difference table is constructed and the correction term evaluated based on the initial y_i . The system is again solved including the correction term, thus yielding corrected y_i . Successive application of this procedure converges to a more accurate solution to the original problem. The natural restriction on this procedure is in the requirement that the difference table converge, that is, higher differences decrease in value so that higher differences can be neglected. It is usual practice when

working with eight significant figures to retain up to the sixth or eighth difference and neglect higher differences. If the difference table does not converge it is necessary to reduce the spacing h .

In constructing the difference table it is necessary to have values of y_i outside the original range of values found. These additional values at both ends of the interval are found by successive application of the finite difference equation. Thus applying the finite difference equation for $n = 0$ will yield an equation in which y_{-1} is the only unknown quantity. For $n = -1$ we have an equation which is used to compute y_{-2} , etc.

As an example illustrating the difference correction method let us consider the first problem solved in this chapter. Additional values of y at the end-points of the interval and beyond are readily computed, for use in constructing the difference table.

Example: Apply difference correction to $y'' - y' - 2y = x$, $y(0) = 2$, $y(1) = 1$, $h = .2$.

Solution: We have the solution for the y_i as $y_0 = 2.0$, $y_1 = 1.64159912$, $y_2 = 1.35836241$, $y_3 = 1.15070531$, $y_4 = 1.02585377$, $y_5 = 1.0$.

For additional points at the ends of the interval we have

$$\begin{array}{ll} n = 0: & .9y_1 - 2.08y_0 + 1.1y_{-1} = 0 \quad \text{yields } y_{-1} = 2.43869163 \\ n = -1: & .9y_0 - 2.08y_{-1} + 1.1y_{-2} = .008 \quad \text{yields } y_{-2} = 2.96770781 \\ n = 5: & .9y_6 - 2.08y_5 + 1.1y_4 = .040 \quad \text{yields } y_6 = 1.10173428 \\ n = 6: & .9y_7 - 2.08y_6 + 1.1y_5 = .048 \quad \text{yields } y_7 = 1.37734145 \end{array}$$

The differential equation in finite difference form including correction terms is

$$\frac{y_{n-1} - 2y_n + y_{n+1}}{h^2} + \frac{c_2 y_n}{h^2} - \left[\frac{-y_{n-1} + y_{n+1}}{2h} + \frac{c_1 y_n}{h} \right] - 2y_n = x_n$$

$$\left(1 + \frac{h}{2}\right)y_{n-1} - (2+2h^2)y_n + \left(1 - \frac{h}{2}\right)y_{n+1} = -c_2 y_n + h c_1 y_n + h^2 x_n$$

with $h = .2$

$$1.1 y_{n-1} - 2.08 y_n + .9 y_{n+1} = -c_2 y_n + .2 c_1 y_n + .04 x_n$$

Retaining up to sixth differences in the correction terms yields

$$c_2 y_n \cong -\frac{1}{12} \delta^4 y_n + \frac{1}{90} \delta^6 y_n$$

$$c_1 y_n \cong -\frac{1}{6} \mu \delta^3 y_n + \frac{1}{30} \mu \delta^5 y_n$$

Using the values for the various differences from table 3 the corrections are calculated as

$c_2 y_1 = - .0004 \ 5479$	$c_1 y_1 = .0004 \ 2432$
$c_2 y_2 = - .0005 \ 5768$	$c_1 y_2 = - .0005 \ 7971$
$c_2 y_3 = - .0007 \ 3301$	$c_1 y_3 = - .0018 \ 5839$
$c_2 y_4 = - .0010 \ 1245$	$c_1 y_4 = - .0035 \ 8640$

The finite difference equation including corrector terms when evaluated at $n = 1, 2, 3, 4$ is

$$.9 y_2 - 2.08 y_1 + 1.1 y_0 = .0085 \ 3965$$

$$.9 y_3 - 2.08 y_2 + 1.1 y_0 = .0164 \ 4174$$

$$.9 y_4 - 2.08 y_3 + 1.1 y_2 = .0243 \ 6133$$

$$.9 y_5 - 2.08 y_4 + 1.1 y_3 = .0322 \ 9517$$

TABLE 3

	y	δ	δ^2	δ^3	δ^4	δ^5	δ^6
y_{-2}	2.9677 0781						
y_{-1}	2.4386 9163	--.5290 1618	.0903 2455				
y_0	2.0	--.4386 9163	.0802 9075	--.0100 3380	.0049 0722		
y_1	1.6415 9912	--.3584 0088		--.0051 2658		.0006 3480	
y_2	1.3583 6241	--.2832 3671	.0751 6417	--.0023 5557	.0055 4202	.0009 5164	.0006 3369
y_3	1.1507 0531	--.2076 5710	.0755 7961	.0004 1544		.0012 6849	
y_4	1.0258 5377	--.1248 5154	.0828 0556	.0038 2070	.0068 1051	.0017 1212	.0008 8726
y_5	1.0	--.0258 5377	.0989 9777	.0072 2595	.0089 6626	.0021 5575	.0012 7606
y_6	1.1017 3428	.1017 3428	.1275 8805	.0161 9221	.0123 9807	.0034 3181	.0018 6468
y_7	1.3773 4145	.2756 0717	.1738 7289	.0223 9124	.0176 9456	.0043 6415	
				.0285 9028		.0052 9649	
				.0462 8484			

The boundary condition equations remain the same. The solution of the equations is

y_i	y_i exact	error
2.0	2.0	0.0
1.6409 0054	1.6408 9399	.0000 0655
1.3573 4753	1.3573 3843	.0000 0910
1.1497 0445	1.1496 9588	.0000 0857
1.0251 8256	1.0251 7709	.0000 0547
1.0	1.0	0.0

TABLE 6

The reduction in error is quite significant, a factor of over 100. The same reduction in error could have been obtained by reducing the spacing h . However it would take a large decrease in h to obtain a comparable accuracy. Thus the use of the error correction technique has yielded a considerable increase in accuracy with only a doubling in the amount of computation necessary. Actually less computational effort has been expended in solving the set of simultaneous equations twice than was required in solving the set of equations for $h = .1$. The answers are considerably better however.

If the boundary conditions contain derivatives then it is also necessary to include the difference correction in them. In the case of retaining up to sixth differences in the correction it would be necessary to include three external points, that is, compute y_{-3} in addition to those already obtained.

In the example shown the difference table is very slowly convergent, thus it is surprising that such good results are obtained. To obtain eight significant figures of accuracy in the answer it would be necessary to reduce the value of h to .1 and apply the difference correction. The smaller value of h yields better convergence in the difference table.

The difference correction method is applicable to any order equation. It has been usefully applied to both first and fourth order equations in addition to the second order equation as in the examples. Although a decision must be made as to whether or not the difference table is convergent or not, easily done visually, but more difficult on a high speed computer, the method can still be mechanized with good results. It is possible that general purpose programs for solving single or sets of simultaneous differential equations could be written using this method. In the solution of partial differential equations using finite difference equations, it is necessary to use a difference correction technique as the number of simultaneous equations and their size prohibits the use of more accurate finite difference equations. For ordinary differential equations the use of more accurate finite difference approximations directly has lead to the best answers for a minimum amount of computer time.

High Order Approximations

In the computer solution of two point boundary problems it is desirable to obtain the most accurate answer for a fixed amount of computer time, or, what is equivalent - a fixed amount of dollars. Normally a program will be set up which requires the solution of many similar problems. In this case it is economical to make a preliminary study of the accuracy of various approximations and to obtain the method and corresponding spacing which yields the desired accuracy. It has been found that for the solution of ordinary differential equations with two point boundary conditions an economical approach is the use of high order finite difference approximations for the differential equations and boundary conditions. Thus finite difference approximations with $O(h^4)$ and $O(h^6)$ error terms have been used with good results. The use of these more accurate approximations increases the size or length

of each of the simultaneous equations but does not increase the number of equations. As the time for the computer solution increases rapidly with number of equations, it is thus advantageous to avoid increasing the number of equations. In fact, examples worked using $O(h^2)$ approximation and $O(h^6)$ approximation indicate an appreciable saving in machine time using the $O(h^6)$ approximation for a fixed number of significant figures of accuracy.

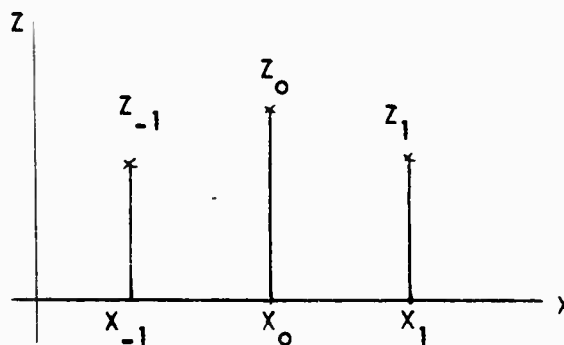
The use of higher order approximations can be done in two ways. The more accurate finite difference equations can be used directly thus yielding longer equations to solve simultaneously, or a difference correction procedure can be used.

II. FINITE DIFFERENCE AND INTERPOLATION EQUATIONS

Matrix theory can be used to give a systematic approach to the derivation of finite difference equations. Finite difference equations of any desired order of accuracy can be derived in a neat straightforward manner. As an introductory example consider the case of a quadratic interpolating function:

$$z = a_1 + a_2x + a_3x^2 \quad (28)$$

If we are given three points in the x, z plane as in the figures:



Then the coefficients a_i in the given function for z are completely determined by a set of equations:

$$\begin{aligned} z_{-1} &= a_1 + a_2 x_{-1} + a_3 x_{-1}^2 \\ z_0 &= a_1 + a_2 x_0 + a_3 x_0^2 \\ z_1 &= a_1 + a_2 x_1 + a_3 x_1^2 \end{aligned} \quad (29)$$

Once the coefficients a_i are determined it is then possible to find z for any desired value of x and also find the derivatives of z for any x since:

$$\begin{aligned} \frac{dz}{dx} &= a_2 + 2a_3 x \\ \frac{d^2z}{dx^2} &= 2a_3 \end{aligned} \quad (30)$$

Let us formulate the above procedure in a matrix form. The set of equations (29) written in matrix form become

$$Z = CA \quad (31)$$

with the matrices defined as

$$\begin{pmatrix} z_{-1} \\ z_0 \\ z_1 \end{pmatrix} = \begin{pmatrix} 1 & x_{-1} & x_{-1}^2 \\ 1 & x_0 & x_0^2 \\ 1 & x_1 & x_1^2 \end{pmatrix} \times \begin{pmatrix} a_1 \\ a_2 \\ a_3 \end{pmatrix} \quad (32)$$

The equation $Z = CA$ is solved for A by multiplying on the left with C^{-1} yielding:

$$A = C^{-1}Z \quad (33)$$

The equation $z = a_1 + a_2x + a_3x^2$ written in matrix form is

$$(z) = (1 \ x \ x^2) \begin{pmatrix} a_1 \\ a_2 \\ a_3 \end{pmatrix} \quad (34)$$

or

$$(z) = XA \quad (35)$$

Thus the value of (z) is obtained by combining (35) and (33)

$$(z) = XA = XC^{-1}Z \quad (36)$$

We also note that the derivatives of z are written in matrix form as

$$\frac{dz}{dx} = (a_2 + 2a_3x) = (0 \ 1 \ 2x) \begin{pmatrix} a_1 \\ a_2 \\ a_3 \end{pmatrix} = \frac{dX}{dx} \cdot A = \frac{dX}{dx} C^{-1}Z \quad (37)$$

$$\frac{d^2z}{dx^2} = \frac{d^2X}{dx^2} \cdot A = \frac{d^2X}{dx^2} \cdot C^{-1}Z \quad (38)$$

Example: In the previous analysis let the three values of x be $-h, 0, h$

$$\begin{array}{ccc} | & | & | \\ -h & 0 & h \end{array}$$

then the matrix C becomes

$$C = \begin{pmatrix} 1 & -h & h^2 \\ 1 & 0 & 0 \\ 1 & h & h^2 \end{pmatrix} \quad (39)$$

which has as inverse

$$C^{-1} = \begin{pmatrix} 0 & 1 & 0 \\ \frac{-1}{2h} & 0 & \frac{1}{2h} \\ \frac{1}{2h^2} & \frac{-1}{h^2} & \frac{1}{2h^2} \end{pmatrix} \quad (40)$$

Hence

$$(z) = (1 \ x \ x^2) \begin{pmatrix} 0 & 1 & 0 \\ \frac{1}{2h} & 0 & \frac{1}{2h} \\ \frac{1}{2h^2} & \frac{-1}{h^2} & \frac{1}{2h^2} \end{pmatrix} \begin{pmatrix} z_{-1} \\ z_0 \\ z_1 \end{pmatrix} \quad (41)$$

If we let $x = 0$ then

$$(z)_{x=0} = (1 \ 0 \ 0) \begin{pmatrix} 0 & 1 & 0 \\ \frac{-1}{2h} & 0 & \frac{1}{2h} \\ \frac{1}{2h^2} & \frac{-1}{h^2} & \frac{1}{2h^2} \end{pmatrix} \begin{pmatrix} z_{-1} \\ z_0 \\ z_1 \end{pmatrix} = (0 \ 1 \ 0) \begin{pmatrix} z_{-1} \\ z_0 \\ z_1 \end{pmatrix} = (z_0) \quad (42)$$

The derivative $\frac{dz}{dx}$ is obtained as

$$\left(\frac{dz}{dx}\right) = (0 \ 1 \ 2x) \begin{pmatrix} 0 & 1 & 0 \\ \frac{-1}{2h} & 0 & \frac{1}{2h} \\ \frac{1}{2h^2} & \frac{-1}{h^2} & \frac{1}{2h^2} \end{pmatrix} \begin{pmatrix} z_{-1} \\ z_0 \\ z_1 \end{pmatrix} \quad (43)$$

which evaluated at $x = 0$ yields

$$\left(\frac{dz}{dx}\right)_{x=0} = \begin{pmatrix} 0 & 1 & 0 \\ -\frac{1}{2h} & 0 & \frac{1}{2h} \\ \frac{1}{2h^2} & -\frac{1}{h^2} & \frac{1}{2h^2} \end{pmatrix} \begin{pmatrix} z_{-1} \\ z_0 \\ z_1 \end{pmatrix} = \begin{pmatrix} -\frac{1}{2h} & 0 & \frac{1}{2h} \end{pmatrix} \begin{pmatrix} z_{-1} \\ z_0 \\ z_1 \end{pmatrix} \quad (44)$$

or

$$\left(\frac{dz}{dx}\right)_{x=0} = \frac{z_1 - z_{-1}}{2h} \quad (45)$$

which is a useful finite difference expression for the first derivative.

The equation (41) for (z) is used for interpolating merely by substituting in the given value of x . Similarly equation (43) can be used for obtaining finite difference equations for the first derivative at various points.

The above procedure has been programmed for the case of three and seven equally spaced points. This corresponds to a second and sixth degree interpolating polynomial. Thus the computation of finite difference equations is mechanized so that any derivative (in the present programs up to fourth) can be approximated at any point with accuracy of up to sixth differences. Subroutines are available which

- (a) construct a matrix whose rows are $x, \frac{dx}{dx}, \frac{d^2x}{dx^2}, \frac{d^3x}{dx^3}, \frac{d^4x}{dx^4}$
- (b) multiply the above matrix by C^{-1} to generate the finite difference coefficients.

The generalization to several dimensions is in concept merely the multiple application of similar operators in different dimensions. The interpolating polynomial in several dimensions can be written in the form:

$$u = (a_0 + a_1x + a_2x^2 + \dots)(b_0 + b_1y + b_2y^2 \dots)(\dots) \quad (46)$$

In two dimensions with quadratic interpolation this simplifies to

$$\mu = (a_0 + a_1x + a_2x^2)(b_0 + b_1y + b_2y^2) \quad (47)$$

The basic equations in terms of matrices are modified as it is necessary to obtain a two dimensional array as the final result. The three dimensional case would lead to a three dimensional array of influence coefficients.

In deriving the finite difference approximations in two dimensions one is led to equations which are successive applications of the difference operators in the different coordinate directions.

Example: Obtain the finite difference equation for the derivative $\frac{\partial^2 u}{\partial x \partial y}$.

$$\begin{aligned} \text{Solution: } \frac{\partial^2 u}{\partial x \partial y} &= \frac{\partial}{\partial x} \left(\frac{\partial u}{\partial y} \right) = \frac{\partial}{\partial y} \left(\frac{\partial u}{\partial x} \right) \approx \frac{\partial}{\partial y} \left[\frac{u_{i+1,j} - u_{i-1,j}}{2h} \right] \\ &= \frac{\left[\frac{u_{i+1,j+1} - u_{i-1,j+1}}{2h} \right] - \left[\frac{u_{i+1,j-1} - u_{i-1,j-1}}{2h} \right]}{2k} \\ &= \frac{1}{4hk} [u_{i+1,j+1} - u_{i-1,j+1} - u_{i+1,j-1} + u_{i-1,j-1}] \end{aligned} \quad (48)$$

Note the successive application of the first derivative operator in each coordinate direction.

Formulating this in matrix notation:

$$(u) = (YB)^T (XA) U \quad (49)$$

$$\frac{\partial^{i+j} u}{\partial x^i \partial y^j} = \left(\frac{\partial^j Y}{\partial y^j} B \right)^T \left(\frac{\partial^i X}{\partial x^i} A \right) U \quad (50)$$

with

$$U = \begin{pmatrix} u_{i-1,j-1} & u_{i,j-1} & u_{i+1,j-1} \\ u_{i-1,j} & u_{i,j} & u_{i+1,j} \\ u_{i-1,j+1} & u_{i,j+1} & u_{i+1,j+1} \end{pmatrix} \quad \begin{array}{c} \xrightarrow{x} \\ \downarrow y \end{array} \quad (51)$$

In two dimensions we have

$$\begin{aligned} X &= (1 \ x \ x^2) & Y &= (1 \ y \ y^2) \\ \frac{dX}{dx} &= (0 \ 1 \ 2x) & \frac{dY}{dy} &= (0 \ 1 \ 2y) \\ \frac{d^2X}{dx^2} &= (0 \ 0 \ 2) & \frac{d^2Y}{dy^2} &= (0 \ 0 \ 2) \end{aligned} \quad (52)$$

The choice of an interpolating polynomial with the x, y terms isolated enables the use of the previous one dimensional analysis. The terms for the x and y direction are computed separately and a final row-column matrix multiplication generates the required finite difference approximation.

The extension to higher dimensions is handled similarly.

III. Computer Programs

In order to mechanize the construction of finite difference equations and their solution several computer programs have been written. This avoids the hand generation of finite difference equations and automates the solution of two-point boundary problems and elliptic partial differential equations.

The following programs have been constructed:

Ordinary differential equations

DIFF2 : Solves one second order differential equation

DIFFA : Solves two simultaneous second order differential equations

DIFF4 : Solves one fourth order differential equation

Partial differential equations - elliptic type

DIFXY : Solves one second order partial differential equation in two variables

DIFUV : Solves two simultaneous second order partial differential equations in two independent variables.

In all of these programs the boundary conditions include derivatives of order one less than the order of the equation. The coefficients of the differential equations can be functions of x or x,y as these coefficients are calculated at each point separately.

In general the procedure in using these programs is to

- (1) compute coefficients in differential equations
- (2) call the subroutine (subprogram)
- (3) use or print the results.

The basic data and technical usage of the above programs is described for each program in the following pages. As certain matrix operations are common to all of the programs they have been separately programmed and are used in conjunction with these programs (e.g. POLYX, DERIVX, etc.)

IDENTIFICATION:

DIFF2 - Second order differential equation solver using sixth differences

PURPOSE:

To solve a second order differential equation with a boundary condition at each end using sixth differences.

RESTRICTIONS:

$N \leq 100$

METHOD:

Central sixth differences are used to replace the differential equation by a finite difference equation and the resulting simultaneous equations are solved.

USAGE:

The entry is

CALL DIFF2 (C, F1, F2, F3, F4, F, DF, H, N, M, KON, IDP)

C(6) = first location of boundary condition coefficients: C(I)

$$\text{left end } C_1 \frac{df}{dx} + C_2 f = C_3$$

$$\text{right end } C_4 \frac{df}{dx} + C_5 f = C_6$$

$\left. \begin{array}{l} F1(N) \\ F2(N) \\ F3(N) \\ F4(N) \end{array} \right\}$ = location of differential equation coefficients
$$F1 \frac{d^2 f}{dx^2} + F2 \frac{df}{dx} + F3 f = F4$$

F(N) = location of function values - answers

DF(N) = location of derivatives - answers

H = length of finite difference jumps $H = \frac{X_R - X_L}{N - 1}$

N = number of points

M = 0 find function values only: F(N)
 = 1 find derivatives also: F(N), DF(N)

DIFF2 contd.

KON = SIMSD error return (Section 5.041 of FORTRAN Manual).
 If this is not zero, it is written out as KON = .

IDP = 0 no dump
 = 1 dump equations

CODING INFORMATION:

DIFF2 uses 575 storage cells and requires SIMSD, DERIVX, and POLYX as well as the IOH pack of subroutines.

NOMENCLATURE
(other than calling sequence)

ACC(I) - coefficients of finite difference equations

A1 to A3 - same as C1 to C3

B1 to B3 - same as C4 to C6

CON(I) - same as C1 to C6

K(I) - identification of unknowns

NA } Codes used to distinguish derivative
NB } and function computations

NX - X as a fixed point number

PX(I,J) - output from POLYX

XNX - X as a floating point number

IDENTIFICATION

DIFFA - Two simultaneous second order ordinary differential equations solver using sixth differences

PURPOSE

To solve two simultaneous second order differential equations with boundary conditions at each end using sixth differences.

RESTRICTIONS

$$N \leq 100$$

METHOD

Central sixth differences are used to replace the differential equations by finite difference equations and these simultaneous equations are solved.

USAGE

The entry is

CALL DIFFA (C,FC, F, DF, H, N, M, KON, IDP)

C(5,4) location of boundary condition coefficients. Each column is one equation of the form

$$C(1,i) \frac{df}{dx} + C(2,i) \frac{dg}{dx} + C(3,i)f + C(4,i)g = C(5,i) \quad i = 1 \text{ to } 4$$

FC(7, 2N) location of differential equation coefficients where for the kth point

$$A(1, 2K+1) \frac{d^2 f}{dx^2} + A(2, 2K+1) \frac{d^2 g}{dx^2} + A(3, 2K+1) \frac{df}{dx} + A(4, 2K+1) \frac{dg}{dx}$$

$$+ A(5, 2K+1)f + A(6, 2K+1)g = A(7, 2K+1)$$

$$A(1, 2K+2) \frac{d^2 f}{dx^2} + A(2, 2K+2) \dots \dots K = 2 \text{ to } N - 1$$

F(2N) location of function values (the set of g values follows the set of f values) - answers

DF(2N) location of derivatives - answers

H length of finite difference jump $H = \frac{X_R - X_L}{N - 1}$

N number of points

DIFFA contd.

M = 0 find function values only F(N)
 = 1 find derivatives also F(N), DF(N)

KON = SIMSD error return (Section 5.041 of FORTRAN Manual).
 If this is not zero it is written out as KON =

IDP = 0 no dump
 = 1 dump equations

CODING INFORMATION

DIFFA uses 1034 storage cells and requires SIMSD, DERIVX, AND POLYX as well as the IO pack of subroutines.

NOMENCLATURE

(other than calling sequence)

ACC(15) coefficients of finite difference equations

FX coefficient of differential equation term

IN I + N

K(15) identification of unknowns

KE number of equation

KI KK+N

KK K(J)

KL order of term

NA } codes used to distinguish derivative and function
NB } computation

NX X as a fixed point number

PX(I,J) output from POLYX

XNX X as a floating point number

IDENTIFICATION

DIFF4 - Fourth order differential equation solver using sixth differences

PURPOSE:

To solve a fourth order ordinary differential equation with two boundary conditions at each end using sixth differences.

RESTRICTIONS:

$N \leq 100$

METHOD:

Central sixth differences are used to replace the differential equation by a finite difference equation and the resulting simultaneous equations are solved. If desired, the first three derivatives are computed at each point using sixth differences.

USAGE:

The entry is

CALL DIFF4 (C, F1, F2, F3, F4, F5, F6, F, DF, D2F, D3F, M, K0N, H, N, IDP)

With

C(20) = location of boundary condition coefficients

$$\text{left end } C_1 \frac{d^3 y}{dx^3} + C_2 \frac{d^2 y}{dx^2} + C_3 \frac{dy}{dx} + C_4 y = C_5$$

$$C_6 \frac{d^3 y}{dx^3} + C_7 \frac{d^2 y}{dx^2} + C_8 \frac{dy}{dx} + C_9 y = C_{10}$$

$$\text{right end } C_{11} \frac{d^3 y}{dx^3} + C_{12} \frac{d^2 y}{dx^2} + C_{13} \frac{dy}{dx} + C_{14} y = C_{15}$$

$$C_{16} \frac{d^3 y}{dx^3} + C_{17} \frac{d^2 y}{dx^2} + C_{18} \frac{dy}{dx} + C_{19} y = C_{20}$$

$\left. \begin{array}{l} F1(N) \\ F2(N) \\ F3(N) \\ F4(N) \\ F5(N) \\ F6(N) \end{array} \right\}$ = location of coefficients of differential equation

$$F_1(x) \frac{d^4 y}{dx^4} + F_2(x) \frac{d^3 y}{dx^3} + F_3(x) \frac{d^2 y}{dx^2} + F_4(x) \frac{dy}{dx} + F_5(x) y = F_6(x)$$

DIFF4 contd.

$F(N)$	}	= location of answers at each point	F = function values
$DF(N)$			$DF = \frac{dy}{dx}$ values
$D2F(N)$			
$D3F(N)$			

$$D2F = \frac{d^2y}{dx^2}$$

$$D3F = \frac{d^3y}{dx^3}$$

M = 0 find function values only: $F(N)$
= 1 find derivatives also : $F(N)$, $DF(N)$, $D2F(N)$, $D3F(N)$

$K\emptyset N$ SIMSD error return (Section 5.041 of FORTRAN Manual)
if this is not zero, it is written out as $K\emptyset N =$.

H = length of finite difference jump $H = \frac{X_R - X_L}{N-1}$

N = number of points

IDP = 0 no dump
= 1 dump equations

IDENTIFICATION

DIFXY - Elliptic partial differential equation solver using second differences with sixth difference corrections

PURPOSE

To solve a second order elliptic partial differential equation using second differences with iterations to obtain sixth difference correction.

RESTRICTIONS

$M \cdot N \leq 225$

METHOD

Second differences are used to replace the differential equation by a finite difference equation and the simultaneous equations are solved. A correction term is then computed to obtain sixth difference corrections. This step may be repeated with sixth difference solutions as the limiting case. If desired, function values and first partials are then calculated for all input points using sixth differences.

USAGE

The entry is

CALL DIFXY (N, M, EH, EK, F, NCOR, IDP, KERR, KDER)

N	number of points in x direction
M	number of points in y direction
EH	length of finite difference jump in x direction $EH = \frac{X_R - X_L}{N - 1}$
EK	length of finite difference jump in y direction
F(N.M)	first location of function values at grid points - answers
NCOR	number of times corrections are to be applied (≥ 0) this is destroyed
IDP	<ul style="list-style-type: none">= 0 no dump= 1 dump
KERR	SIMSD error return (Section 5.041 of FORTRAN Manual)
KDER	<ul style="list-style-type: none">= 0 find only function values at grid points F(N.M)= 1 find function values and first partials at input points also. F(N.M), DFX(N.M), DFY(N.M), Z(N.M)

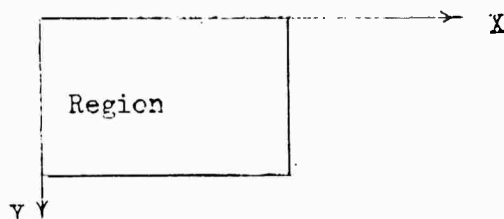
DIFXY contd.

In addition, erasable tapes 89 (21) and 810 (22) must be mounted (density optional). Tape 89 must contain:

X, Y, A(7) at each input point

x,y coordinates of point relative to corner of grid in units of EH and EK respectively

$$A(7) \quad A_1 \frac{\partial^2 f}{\partial x^2} + A_2 \frac{\partial^2 f}{\partial x \partial y} + A_3 \frac{\partial^2 f}{\partial y^2} + A_4 \frac{\partial f}{\partial x} + A_5 \frac{\partial f}{\partial y} + A_6 f = A_7$$



COMMON reads as follows:

V, DFX, DFY, Z -- answers

V(500) dummy to allow for DIFCOR

DFX(225) } first location of $\frac{\partial f}{\partial x}$, $\frac{\partial f}{\partial y}$ at input points
DFY(225) }

Z(225) first location of f at input points

CODING INFORMATION

DIFXY uses 1465 storage cells and 76475 to 75233 and requires SIMSD, DERXY, DIFCOR, No. 6, 7, 10, and 15, and the 10 pack of subroutines.

DUMP

Second differences:

X, Y, RX, RY, A(I), ACC(I)

L, NX, MY, NXN, MYM, K(I)

Sixth differences:

L, JK, NX, MY, K(I)

X, Y, ACC(I)

DIFXY contd.

Derivative calculations:

DFX, DFY, Z (ACC(10), ACC(11), ACC(12))

NON DUMP

Correction values followed by function values.

NOMENCLATURE
(except for descriptions under USAGE)

ACC(12)	finite difference coefficients and temporary storage for DFX, DFY, Z
JK	upper left hand corner of 7 x 7 grid for DIFCOR
K(10)	unknown identification
KDEN	determines if equations or partial derivatives
KDIF	are being found
KQ	tape reference number = 22
KXD	subscript for DFX, DFY, and Z
L	maximum order of derivatives needed from DIFCOR
LQ	tape reference number = 21
MN	M*N
MY	used to generate JK, RY, and a new Y
MYM	
ND	used to find K(I)
NX } NXN }	used to generate JK, RX, and a new X
PY(N.M)	correction values for F
RX } RY }	fractional parts of X and Y

IDENTIFICATION

DIFUV - Two simultaneous elliptic partial differential equation solver using second differences with sixth difference corrections.

PURPOSE

To solve two simultaneous elliptic partial differential equations using second differences with iteration to obtain sixth difference correction.

RESTRICTIONS

$M \cdot N \leq 225$

METHOD

Second differences are used to replace the differential equations by finite difference equations and the simultaneous equations are solved. A correction term is then computed to obtain sixth difference correction. This step may be repeated with sixth difference solutions as the limiting case. Desired function values and the first partials are then calculated for all input points using sixth differences.

USAGE

The entry is

CALL DIFUV (N, M, EH, EK, F, NCOR, IDP, KERR, KDER)

N number of points in X direction

M number of points in Y direction

EH length of finite difference jump in X direction

$$EH = \frac{X_R - X_L}{N - 1}$$

EK length of finite difference jump in Y direction

F(2.N.M) first location of function values at grid points (all answers are stored with f from 1 to N.M and g from N.M+1 to 2.N.M) - answers

NCOR number of times corrections are to be applied (≥ 0) this is destroyed

IDP = 0 no dump
 = 1 dump

KERR SIMSD error return (Section 5.04 of FORTRAN Manual)

DIFUV contd.

KDER = 0 find only function values at grid points F(.2.N.M)
 = 1 find function values and first partials at input points
 also F(2.N.M), DFX(2.N.M), Z(2.N.M)

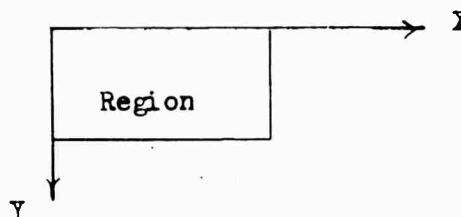
In addition erasable tapes B9 (21) and B10 (22) must be mounted (density optional). Tape B9 must contain

X,Y, A(13) A¹(13) at each input point

X,Y coordinates of point relative to corner of grid in units
 of EH and EK respectively

$$\begin{aligned} A(13) \quad & A_1 \frac{\partial^2 f}{\partial X^2} + A_2 \frac{\partial^2 g}{\partial X^2} + A_3 \frac{\partial^2 f}{\partial X \partial Y} + A_4 \frac{\partial^2 g}{\partial X \partial Y} + A_5 \frac{\partial^2 f}{\partial Y^2} \\ & + A_6 \frac{\partial^2 g}{\partial Y^2} + A_7 \frac{\partial f}{\partial X} + A_8 \frac{\partial g}{\partial X} + A_9 \frac{\partial f}{\partial Y} + A_{10} \frac{\partial g}{\partial Y} \\ & + A_{11} f + A_{12} g = A_{13} \end{aligned}$$

A'(13) second equation



COMMON reads as follows

V, DFX, DFY, Z - answers

V(500) dummy to allow for DIFCNG

DFX(450) first location of $\frac{\partial}{\partial X}$ at input points

DFY(450) first location of $\frac{\partial}{\partial Y}$ at input points

Z(450) first location of f at input points

CODING INFORMATION

DIFUV uses 2257 storage cells and 76475 to 73767 and requires SIMSD, DERXY, DIFCNG, #6, 7, 10, and 15, and the IO pack of subroutines.

DUMP

Second differences:

X, Y, RX, RY, A(I), ACC(I)

L, NX, MY, NXN, MYM, K(I)

Sixth differences:

L, JK, NX, MY, K(I)

X, Y, ACC (I)

Derivative calculations:

$\frac{\partial f}{\partial X}, \frac{\partial g}{\partial X}, \frac{\partial f}{\partial Y}, \frac{\partial g}{\partial Y}, f, g, (ACC (19) \text{ to } ACC (24))$

NON DUMP

Correction values followed by function values

NOMENCLATURE

(except for descriptions under usage)

ACC (24)	finite difference coefficients and temporary storage for DFX, DFY, Z
JK	upper left hand corner of 7 x 7 grid for DIFCNG
K(19)	unknown identification
KDEN } KDIF }	determines if equations or partial derivatives are being found
KQ	tape reference number = 22
KXD	subscripts for DFX, DFY, and Z (first dependent variable)
KXY	subscripts for DFX, DFY, and Z (second dependent variable)
L	maximum order of derivatives needed for DIFCNG
LQ	tape reference number = 21
MN	M*N
MN2	M*N*2

DIFUV contd.

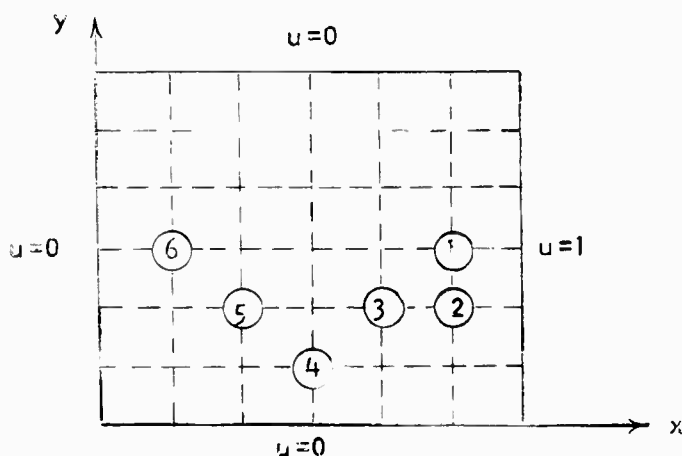
MY } MYM }	used to generate JK, RY, and a new Y
ND	used to find K(I)
NEQ	indicates which equation is being manipulated (1st or 2nd)
NX } NXN }	used to generate JK, RX, and a new X
PY (2.N.M)	correction values for F
RX } RY }	fractional parts of X and Y

IV. Error Analysis

In order to evaluate the feasibility and advantages of using high order difference approximation and difference correction in the solution using finite difference methods, several programs have been written applying the methods to problems with known analytic answers. This enables the development of an idea of the accuracy to be expected in applying these methods to other physical problems. One cannot directly generalize to other problems and say the accuracy is the same. However, it is reasonable to assume that for similar problems similar accuracy is to be expected.

The comparison between using finite difference equations of second order and those of sixth order indicates the distinct advantage of the higher order approximation.

A significant test was made solving Laplace's equation $\nabla^2 u = 0$ in a unit square. Laplace's equation was solved at the points shown below by means of DIFXY. The following table compares the analytic solution with the results obtained for 7 X 7 and 13 X 13 grids with various numbers of sixth difference corrections



Analytic Solution

$$u(x,y) = \left(\sum_{n=1}^{\infty} \frac{\sinh(n\pi x/a)}{\sinh n\pi} \frac{\sin(n\pi y/a)}{n} \right) \frac{4}{\pi}$$

n odd

<u>POINT</u>	<u>COORDINATES</u>	<u>ANALYTIC VALUE</u>	<u>NUMBER CORR.</u>	<u>VALUE</u>	<u>PER CENT ERROR</u>	<u>VALUE</u>	<u>PER CENT ERROR</u>
1	(5/6, 1/2)	.67831997	0	.66942501	-1.329	.67587935	-.361
			1	.67594250	- .352	.67821377	-.016
			2	.67689509	- .210	.67830834	-.0017
			3	.67700572	- .194		
2	(5/6, 1/3)	.63865374	0	.62922493	-1.476	.63577815	-.452
			1	.63527304	- .532	.63831901	-.052
			2	.63608025	- .405	.63851265	-.022
			3	.63616964	- .390		
3	(2/3, 1/3)	.38071831	0	.37878788	- .509	.38018971	-.139
			1	.38043677	- .074	.38069849	-.0052
			2	.38064198	- .020	.38071737	-.0002
			3	.38065840	- .016		
4	(1/2, 1/6)	.13071832	0	.13461538	2.981	.13178720	.811
			1	.13166914	.727	.13076561	.036
			2	.13118878	.360	.13072376	.0042
			3	.13112355	.310		
5	(1/3, 1/3)	.11928166	0	.12121212	1.618	.11981028	.443
			1	.11956343	.236	.11930139	.017
			2	.11935802	.064	.11928253	.0007
			3	.11934160	.050		
6	(1/6, 1/2)	.060243302	0	.061344211	1.827	.060546220	.503
			1	.060719263	.790	.060254870	.019
			2	.060727355	.803	.060243983	.0011
			3	.060751691	.836		

This test yielded an indication of the reduction error that can be expected for

- (a) increasing the number of grid points (reducing h)
- (b) applying difference correction
- (c) both reducing grid spacing and applying difference correction.

The solutions given without difference correction are those obtained using second differences. It would be expected that halving the grid interval would reduce the error by a factor of $(\frac{1}{2})^2$ or $\frac{1}{4}$. This is clearly followed by comparison of the results for no difference corrections. With the application of several difference corrections the finite difference solution approaches that obtained by using sixth differences. The effect of halving the interval with sixth differences is a reduction in error of $(\frac{1}{2})^6$ or $\frac{1}{64}$. A comparison of the results for 2 corrections shows an error reduction of this order of magnitude.

The reduction in error in going from no corrections to two or three corrections is significant and clearly illustrates the superiority of including difference correction.

An error analysis was performed of the finite difference solution to one dimensional plane strain. The boundary conditions were the inside boundary pressurized and the outside boundary fixed. The error analysis was performed to study several important factors in finite difference solutions.

- (a) comparison of second and sixth order approximations
- (b) effect of varying coefficients in the boundary conditions
- (c) effect of changing the geometry (location of boundary conditions)

The ordinary differential equation of axisymmetric plane strain can be put in dimensionless form as

$$\frac{d^2 u}{dr^2} + \frac{1}{r} \frac{du}{dr} - \frac{u}{a^2} = 0$$

with boundary conditions

$$u(1) = 0$$

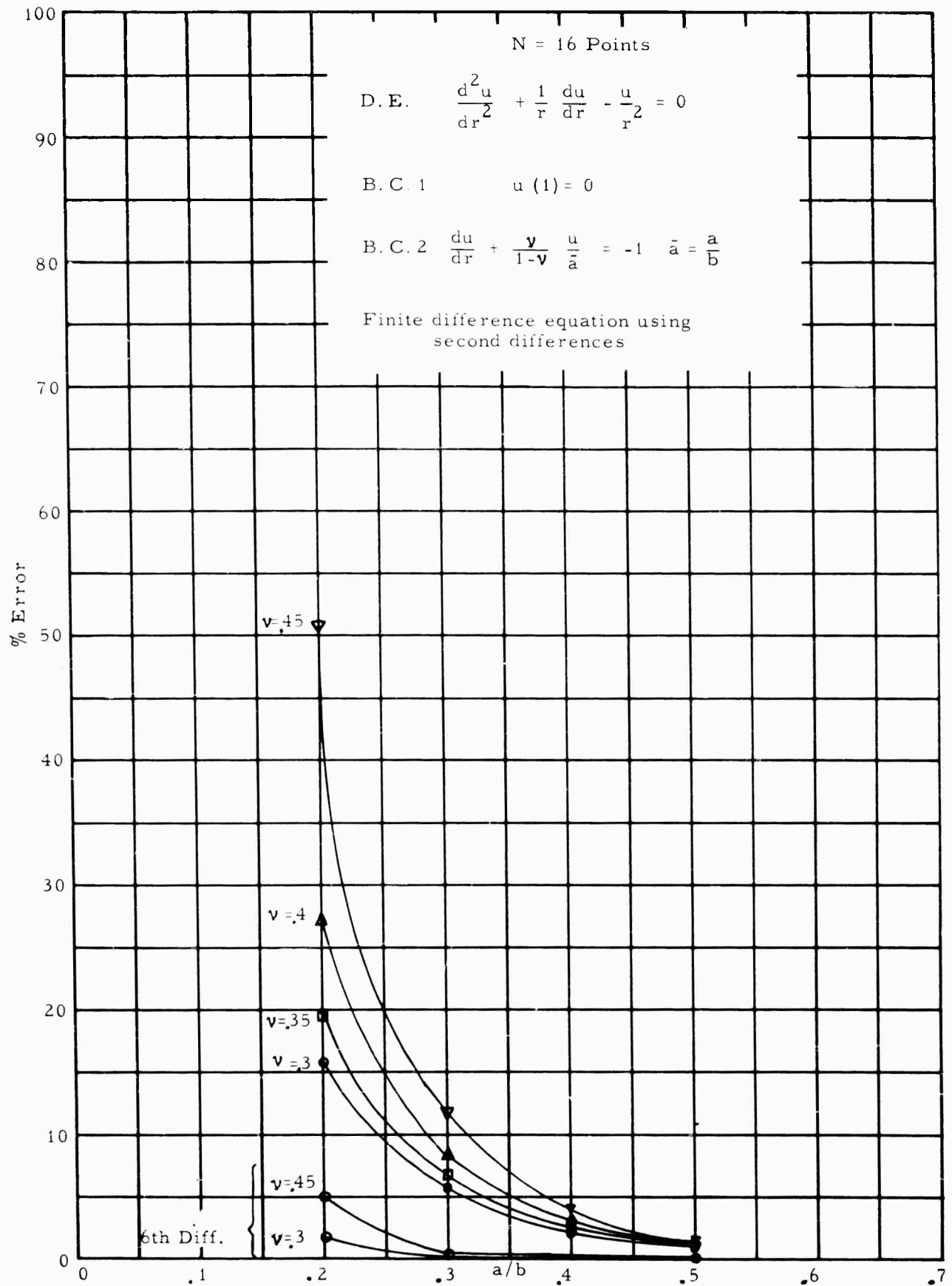
$$\frac{du}{dr} + \frac{1}{1-\nu} \frac{u}{a} = -1$$

The geometry has been scaled so that the outer boundary is at 1 and $\bar{a} = \frac{a}{b}$ the functional radial distance of the inner boundary. The value of Poisson's ratio ν and \bar{a} were varied to study their effect on the error. A fixed number of grid points $N = 16$ was used. The results are shown in the graph of Figure 4.

The graph shows the variation of % error with γ and a/b . The large variation in error illustrates the importance of the boundary conditions in the error analysis. It is large variations such as this that illustrate the difficulty in predicting the error in a particular problem.

A possible method of estimating the error for a particular problem utilizes the variation in error with grid spacing. A problem run with a particular grid spacing is rerun with the grid spacing cut in half. This reduction in grid spacing should reduce the error by a factor $\frac{1}{4}$ with second differences and a factor $\frac{1}{64}$ using sixth differences. Comparison of the two solutions will yield an estimate of the error. The practical limitation of this procedure is in the rapid increase in simultaneous equations to be solved.

Figure 4: ERROR IN FINITE DIFFERENCE SOLUTION



V. APPLICATIONS

The application of the sub=programs to engineering problems is similar for all cases. The steps to be followed in the numerical solution are:

- (a) read in input data and boundary conditions
- (b) generate coefficients of differential equation at each interior grid point and generate coefficients for the boundary conditions at boundary points
- (c) call the subroutine to
 - (1) set-up finite difference equations
 - (2) solve the set of equations
 - (3) compute derivatives at each point
- (d) compute desired output in terms of function values and derivatives.

This procedure can become complicated in individual problems. The complexity arises primarily in the mass of detail required to keep track of the grid points, boundary conditions and where applied, output desired and required output format, etc.

The applications which have been programmed include both ordinary and partial differential equations. A short list would include:

Ordinary differential equations

- (a) plane strain stress analysis
- (b) tapered shell stress analysis

Partial differential equations

- (a) Laplace's equation in one and two dependent variables
- (b) Rectangular plate stress analysis
- (c) Finite cylinder stress analysis
 - (1) displacement solution
 - (2) with thermal term
 - (3) with external elastic shell boundary condition.
- (d) Star grain stress analysis.

In order to give a picture of the type of problem which has been solved examples of the above problems are discussed from an engineering standpoint, that is, the physical problem is described, basic equations used, boundary conditions available, output, etc.

RECTANGULAR PLATE

The displacements of a thin rectangular plate satisfy the partial differential equations

$$B \frac{\partial^2 u}{\partial x^2} + (A + \mu) \frac{\partial^2 w}{\partial x \partial y} + \mu \frac{\partial^2 u}{\partial y^2} + F_x = 0$$

$$\mu \frac{\partial^2 w}{\partial x^2} + (A + \mu) \frac{\partial^2 u}{\partial x \partial y} + B \frac{\partial^2 w}{\partial y^2} + F_y = 0$$

with

$$B = \frac{E}{(1-\nu)(1+\nu)}, \quad \mu = \frac{E}{2(1+\nu)}, \quad A + \mu = \frac{E}{2(1-\nu)}$$

The stresses and strains are related to the displacements by the equations

$$\epsilon_{xx} = \frac{\partial u}{\partial x}, \quad \epsilon_{yy} = \frac{\partial w}{\partial y}, \quad \epsilon_{xy} = \frac{1}{2} \left(\frac{\partial w}{\partial x} + \frac{\partial u}{\partial y} \right)$$

$$\tau_{xx} = B \frac{\partial u}{\partial y} + A \frac{\partial w}{\partial y}, \quad \tau_{yy} = A \frac{\partial u}{\partial x} + B \frac{\partial w}{\partial y}, \quad \tau_{xy} = \mu \left(\frac{\partial w}{\partial x} + \frac{\partial u}{\partial y} \right)$$

In solving this problem a large variety of boundary conditions are possible. Those considered here are

$$\left. \begin{array}{l} u = \text{constant} \\ w = \text{constant} \\ \tau_{xx} = \text{constant} \\ \tau_{yy} = \text{constant} \\ \tau_{xy} = \text{constant} \end{array} \right\} \text{ on any side of the rectangular plate.}$$

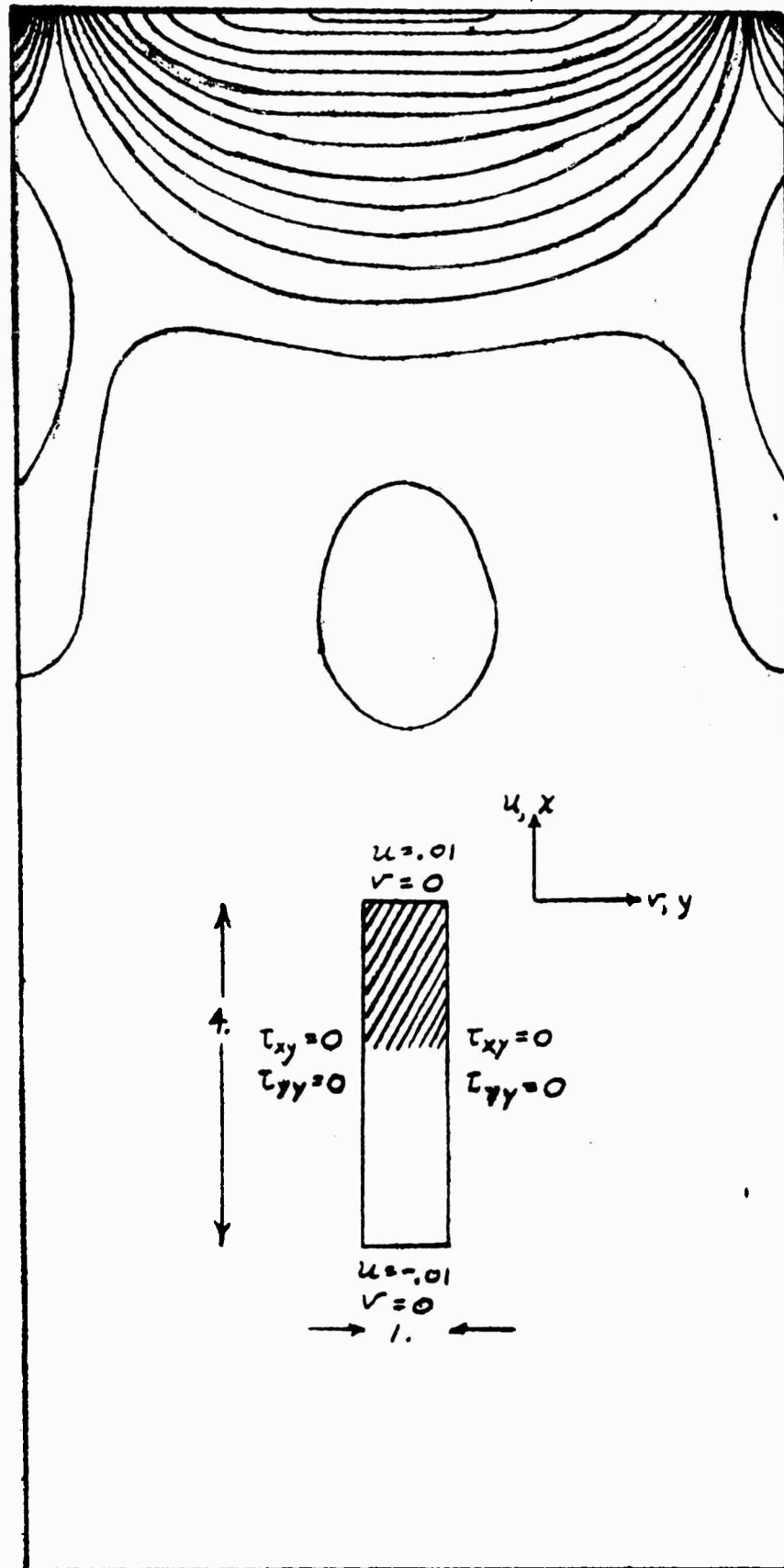
In specifying the boundary conditions it is necessary to give two boundary conditions on each edge of the plate.

The output from the program includes at each point:

$$u, w, \epsilon_{xx}, \epsilon_{yy}, \epsilon_{xy}, \tau_{xx}, \tau_{xy}, \tau_{yy}, \alpha, \tau_{\max}.$$

A plot of equal τ_m contours is shown in Figure 5. This corresponds to the photostress pattern obtainable experimentally.

Figure 5 Maximum Shear Stress on Rectangular Plate



FINITE CYLINDER

The thermal stress analysis of a finite cylinder using displacement partial differential equations requires the solution of

$$(\lambda + 2G) \frac{\partial^2 u}{\partial r^2} + G \frac{\partial^2 u}{\partial z^2} + (\lambda + G) \frac{\partial^2 w}{\partial r \partial z} + (\lambda + 2G) \frac{1}{r} \frac{\partial u}{\partial r} - (\lambda + 2G) \frac{u}{r^2} + F_r - \frac{E\alpha}{1-2\nu} \frac{\partial T}{\partial r} = 0$$

$$G \frac{\partial^2 w}{\partial r^2} + (\lambda + 2G) \frac{\partial^2 w}{\partial z^2} + \frac{G}{r} \frac{\partial w}{\partial r} + (\lambda + G) \frac{\partial^2 u}{\partial r \partial z} + (\lambda + G) \frac{1}{r} \frac{\partial u}{\partial z} + F_z - \frac{E\alpha}{1-2\nu} \frac{\partial T}{\partial z} = 0$$

with

$$\lambda = \frac{\nu E}{(1+\nu)(1-2\nu)}$$

$$G = \frac{E}{2(1+\nu)}$$

The stresses and strains are obtained from the displacements using the relations

$$\epsilon_r = \frac{\partial u}{\partial r}, \quad \epsilon_\theta = \frac{u}{r}, \quad \epsilon_z = \frac{\partial w}{\partial z}, \quad \epsilon_{rz} = \frac{\partial u}{\partial z} + \frac{\partial w}{\partial r}$$

$$\sigma_r = \lambda \left(\frac{\partial u}{\partial r} + \frac{u}{r} + \frac{\partial w}{\partial z} \right) + 2G \frac{\partial u}{\partial r} - \frac{E\alpha T}{1-2\nu}$$

$$\sigma_\theta = \lambda \left(\frac{\partial u}{\partial r} + \frac{u}{r} + \frac{\partial w}{\partial z} \right) + 2G \frac{u}{r} - \frac{E\alpha T}{1-2\nu}$$

$$\sigma_z = \lambda \left(\frac{\partial u}{\partial r} + \frac{u}{r} + \frac{\partial w}{\partial z} \right) + 2G \frac{\partial w}{\partial z} - \frac{E\alpha T}{1-2\nu}$$

$$\tau_{rz} = G \left(\frac{\partial u}{\partial z} + \frac{\partial w}{\partial r} \right)$$

The boundary conditions possible in this program include the specification of displacements or stresses on any side of the finite cylinder. A modification of the program allows the boundary condition corresponding to an elastic shell on the outer boundary. The output consists of all displacements, stresses, strains, maximum shearing stress at grid points.

As an illustration of the results the maximum shearing stress has been plotted in Figure 6. This corresponds well with a photoelastic test photograph.

PLANE STRAIN

As a test program and to perform various error analyses the one-dimensional elastic plane strain problem was programmed. The differential equation for the displacement in dimensionless form is given by

$$\frac{\partial^2 u}{\partial r^2} + \frac{1}{r} \frac{\partial u}{\partial r} - \frac{u}{r^2} = 0$$

$$u(b) = 0, \quad \frac{\partial u}{\partial r} + \frac{\nu}{1-\nu} \frac{u}{a} = -1 \quad \text{at } r = a$$

The analytic solution is given by

$$u(a) = C_2 \left(\frac{b}{a} - \frac{a}{b} \right) \quad C_2 = \frac{1}{1 + \left(\frac{b}{a}\right)^2 + \frac{\nu}{1-\nu} \left[1 - \left(\frac{b}{a}\right)^2 \right]}$$

The stresses at the inner surface are obtained from

$$\sigma_{rb} = -C_2 \cdot C_1 (1-\nu)$$

$$\sigma_{\theta b} = -C_2 \cdot C_1 \nu$$

$$C_1 = \frac{2}{(1+\nu)(1-2\nu)}$$

$$\sigma_{\theta a} = C_2 \left[-\frac{C_1}{2} + \frac{1}{(1+\nu)(a/2b)^2} \right]$$

A comparison of the analytic and finite difference solutions was made and values of u_a , σ_{rb} , $\sigma_{\theta b}$, $\sigma_{\theta a}$ computed with their per cent error using second differences and sixth differences. The computation yielded interesting results with regard to the effect of varying ν and the a/b ratio. The error was found to be highly dependent on the variation of both of those quantities. The values are plotted in the section on error analysis. The results suggest the importance of further investigation into the finite difference method. The transformation of the original differential equation to remove the effect of the $\frac{1}{r}$ term might yield further increases in accuracy.



BIBLIOGRAPHY

1. Fox, L. "Numerical Solution of Two-Point Boundary Problems in Ordinary Differential Equations" Oxford, 1957.
2. Glauz, R. D. "Notes on Matrix Theory", Computing Services Report Number 16, Aerojet-General Corporation, February 2, 1961.
3. Sokolnikoff, I. S. "Mathematical Theory of Elasticity", McGraw-Hill, 1956.
4. Timoshenko, S., and Goodier, J. N., "Theory of Elasticity", McGraw-Hill, 1951.

APPENDIX F

STUDIES RELATING TO STRUCTURAL ANALYSIS
OF SOLID PROPELLANTS

by

S. B. Dong, L. R. Herrman, K. S. Pister,
and R. L. Taylor
Institute of Engineering Research
University of California
Berkeley, California

TABLE OF CONTENTS

INTRODUCTION	1
PART I: ELASTIC AND VISCOELASTIC ANALYSIS OF ORTHOTROPIC CYLINDERS	
INTRODUCTION	3
LINEAR ELASTIC ANALYSIS OF ORTHOTROPIC SOLIDS	5
1. Recapitulation of the Linear Thermo- elastic Field Equations for Orthotropic Solids with Temperature-Independent Material Properties	5
2. Axisymmetrically Loaded Cylinders	8
3. Examples	12
LINEAR VISCOELASTIC ANALYSIS OF ORTHOTROPIC SOLIDS	19
4. Correspondence Principle for Anisotropic Viscoelasticity	19
5. Viscoelastic Solution for the Pres- surization of a Cylinder	20
6. Asymptotic Solutions	24
NONLINEAR ELASTIC ANALYSIS OF CYLINDERS WITH CYLINDRICAL ORTHOTROPY	28
7. Fundamental Equations for Solids in Plane Strain Subjected to Axisymmetric Loads	28
8. Solution for a Thick-Walled Cylinder Subjected to Internal and External Pressure	30
REFERENCES	38
PART II: BILINEAR ELASTICITY WITH APPLICATIONS TO THICK-WALLED CYLINDERS	
INTRODUCTION	41
NOTATION	44
BILINEAR ELASTIC THEORY	47
1. Bilinear Constitutive Equations	47
2. Elementary Solutions	50

3. Model Fitting Considerations for a Particular Material	63
4. Numerical Example	65
APPENDIX	68
5. Derivation of Bilinear Constitutive Equations	68
6. Derivation of Elementary Solutions	75
7. Proposed Generalization of the Bilinear Elastic Theory	91
REFERENCES	94
FIGURES	95

PART III: SOLUTION METHOD FOR NONLINEAR ELASTIC PROBLEMS WITH APPLICATIONS TO THICK-WALLED CYLINDERS

INTRODUCTION	107
FINITE ELASTIC THEORY	110
1. Summary of Notations and Formulas	110
2. Derivation of Constitutive Equations for Incompressible Thermoelasticity	114
3. Governing Equations for Thick-walled Cylinders	118
SECOND ORDER ELASTIC THEORY	128
4. General Theory	128
A SOLUTION METHOD FOR FINITE ELASTICITY	135
5. Outline of Method	135
6. Compressible Response	140
Uniaxial Test	
Thermal Stressing of a Thick-walled Cylinder	
Pressure Loading of a Thick-walled Cylinder	
Vertical Gravity Loading of a Thick-walled Cylinder	
7. Incompressible Response	161
Uniaxial Test	
Uniform Temperature Drop of a Thick-walled Cylinder	
Pressurization of a Thick-walled Cylinder	

8. Near-incompressible Response	168
Uniaxial Test	
Pressure Loading of a Thick-walled Cylinder	
9. An Approximate Solution Scheme	181
10. Numerical Examples	185
REFERENCES	189
FIGURES	190

PART IV: THERMAL DEFORMATION OF VISCOELASTIC MATERIALS

INTRODUCTION	201
GENERAL THEORY	202
1. Field Equations for Thermorheologically Simple Viscoelastic Materials	202
2. Displacement Equations of Equilibrium	210
APPLICATIONS	211
3. Specialization for Axisymmetric Plane Strain of Infinite Cylinders	211
4. Slowly Varying Uniform Temperature Fields	213
5. Infinite Cylinder Rigidly Encased	214
6. Numerical Solutions of Infinite Cylinder Rigidly Encased	220
7. Infinite Cylinder Bonded to a Thin Elastic Case	222
REFERENCES	225
FIGURES	226

INTRODUCTION

The continuing increase in the size of solid propellant motors has placed a concomitant demand upon the analyst to develop suitable techniques for predicting grain structural integrity. In the absence, at present, of a general continuum theory of mechanical behavior which is both realistic and tractable, it has been necessary to attempt to classify grain structural integrity problems into categories and treat each class of problems with less general, yet reasonably satisfactory methods (in the engineering sense). To give examples we cite the following.

In recent years, an extensive propellant-centered literature in linear temperature-independent viscoelastic theory has arisen. Recently, work on linear thermoviscoelasticity has begun to appear. At the same time the importance of nonlinear behavior has been recognized, and Rivlin-type elastic theory has been applied to grain analysis. More recently recognition has been given to the necessity for taking into account the initiation of strain-induced anisotropy resulting from the dewetting phenomenon. Finally, the importance of introducing appropriate failure criteria, as a companion to stress and deformation analysis, has been noted.

This report, consisting of four parts, is but another contribution to the "categorized" treatment of solid propellant mechanics. It is hoped, however, that the ideas presented will stimulate the development of a suitable nonlinear, non-homogeneous, anisotropic viscoelastic theory for propellant structural analysis.

The authors are indebted to Dr. J. L. Sackman, Assistant Professor of Civil Engineering, for assistance in the conduct of portions of the research leading to this report.

PART I

ELASTIC AND VISCOELASTIC ANALYSIS
OF ORTHOTROPIC CYLINDERS

by

S. B. DONG

INTRODUCTION

Stress analysis of cylindrical grains within the framework of linear isotropic elasticity and viscoelasticity has received considerable attention to date. An extensive body of information of this type has been reported by Williams, Blatz, and Schapery [1]. It is well-known, however, that filled propellants evince substantially different mechanical behavior in the presence of tensile stress fields than is found in compressive stress fields. This effect is a result of the presence of voids and the pullaway of the binder from the filler particles. Accordingly, a type of stress-induced anisotropy is developed in the propellant, necessitating consideration of anisotropic constitutive equations. The general problem involves the solution of boundary value problems for each subdomain of the body, defined by a particular state of stress, and the subsequent piecing-together of the solutions at common interfaces. In each instance the solution required will be that appropriate to an anisotropic body. The degree of stress-induced anisotropy encountered is at most orthotropy, thus the general discussion throughout this report will be restricted to this form of anisotropy. The analysis of bodies with a greater degree of anisotropy has been presented in [2]. Much of the present work has been drawn from Lekhnitskii [3] who, in addition to his own contributions, has summarized previous work in the field.

In view of the viscoelastic behavior of solid propellants under many circumstances, attention is drawn to the correspondence principle, first proposed by Alfrey for incompressible isotropic media [4] and generalized by Lee [5]. This principle was later extended for anisotropic bodies by Biot [6]. The forms of solution for many associated anisotropic elastic problems, however, are not readily invertible to recover the time-dependent viscoelastic response, although the

inversion of the solution for an orthotropic thick-walled cylinder has been demonstrated by Spillers [7]. An alternative method of solution is to begin with the viscoelastic field equations and formulate a governing equation in both space and time. This governing partial differential equation may then be solved by a suitable technique. The investigation of an orthotropic cylinder following this approach is discussed.

Due to a characteristically low rigidity in solid propellants, large deformations may be sustained under loading and environmental conditions. Stress analysis of solids based on a non-linear theory must be adopted to account for these large deformations. A solution for the pressurization of an elastic orthotropic thick-walled cylinder is presented to illustrate the particular features of such an analysis.

LINEAR ELASTIC ANALYSIS OF ORTHOTROPIC SOLIDS

1. Recapitulation of the Linear Thermoelastic Field Equations for Orthotropic Solids with Temperature-Independent Material Properties

Since many solid propellant configurations involve cylindrical geometries, the fundamental thermoelastic field equations will be summarized in cylindrical coordinates.

Stress Equations of Equilibrium

$$\begin{aligned}\frac{\partial \sigma_r}{\partial r} + \frac{1}{r} \frac{\partial \tau_{r\theta}}{\partial \theta} + \frac{\partial \tau_{rz}}{\partial z} + \frac{\sigma_r - \sigma_\theta}{r} + R &= 0 \\ \frac{\partial \tau_{r\theta}}{\partial r} + \frac{1}{r} \frac{\partial \sigma_\theta}{\partial \theta} + \frac{\partial \tau_{\theta z}}{\partial z} + \frac{2\tau_{r\theta}}{r} + \theta &= 0 \\ \frac{\partial \tau_{rz}}{\partial r} + \frac{1}{r} \frac{\partial \tau_{\theta z}}{\partial \theta} + \frac{\partial \sigma_z}{\partial z} + \frac{\tau_{rz}}{r} + Z &= 0\end{aligned}\tag{1.1}$$

where R , θ , and Z are body force components per unit of volume.

Strain-Displacement Relations

$$\begin{aligned}\epsilon_r &= \frac{\partial u}{\partial r} & \gamma_{\theta z} &= \frac{\partial v}{\partial z} + \frac{1}{r} \frac{\partial w}{\partial \theta} \\ \epsilon_\theta &= \frac{1}{r} \frac{\partial v}{\partial \theta} + \frac{u}{r} & \gamma_{rz} &= \frac{\partial w}{\partial r} + \frac{\partial u}{\partial z} \\ \epsilon_z &= \frac{\partial w}{\partial z} & \gamma_{r\theta} &= \frac{1}{r} \frac{\partial u}{\partial \theta} + \frac{\partial v}{\partial r} - \frac{v}{r}\end{aligned}\tag{1.2}$$

where u , v , w are the components of the displacement vector

in the r , θ , z directions.

Strain Compatibility Equations

$$\left[\frac{1}{r^2} \frac{\partial^2}{\partial \theta^2} - \frac{1}{r} \frac{\partial}{\partial r} \right] \epsilon_r + \left[\frac{\partial^2}{\partial r^2} + \frac{2}{r} \frac{\partial}{\partial r} \right] \epsilon_\theta = \frac{1}{r} \frac{\partial}{\partial \theta} \left[\frac{\partial}{\partial r} + \frac{1}{r} \right] \gamma_{r\theta}$$

$$\frac{\partial^2 \epsilon_r}{\partial z^2} + \frac{\partial^2 \epsilon_z}{\partial r^2} = \frac{\partial^2 \gamma_{rz}}{\partial r \partial z}$$

$$\frac{\partial^2 \epsilon_\theta}{\partial z^2} + \left[\frac{1}{r^2} \frac{\partial^2}{\partial \theta^2} + \frac{1}{r} \frac{\partial}{\partial r} \right] \epsilon_z = \frac{1}{r} \frac{\partial^2 \gamma_{\theta z}}{\partial \theta \partial z} + \frac{1}{r} \frac{\partial \gamma_{rz}}{\partial z}$$

$$\frac{2}{r} \frac{\partial^2 \epsilon_r}{\partial \theta \partial z} = \left(\frac{\partial}{\partial r} + \frac{2}{r} \right) \left[\frac{\partial \gamma_{r\theta}}{\partial z} + \frac{1}{r} \frac{\partial \gamma_{rz}}{\partial \theta} - \left(\frac{\partial}{\partial r} + \frac{1}{r} \right) \gamma_{\theta z} \right] \quad (1.3)$$

$$+ \left[\frac{2}{r} \frac{\partial}{\partial r} + \frac{2}{r^2} \right] \gamma_{\theta z} - \frac{2}{r^2} \frac{\partial \gamma_{rz}}{\partial \theta}$$

$$2 \left[\frac{\partial^2 \epsilon_\theta}{\partial r \partial z} + \frac{1}{r} \frac{\partial}{\partial \theta} (\epsilon_\theta - \epsilon_r) \right] = \frac{1}{r} \frac{\partial}{\partial \theta} \left[\frac{\partial \gamma_{r\theta}}{\partial z} - \frac{1}{r} \frac{\partial \gamma_{rz}}{\partial \theta} + \left(\frac{\partial}{\partial r} + \frac{1}{r} \right) \gamma_{\theta z} \right]$$

$$\frac{2}{r} \frac{\partial}{\partial \theta} \left[\frac{\partial}{\partial r} - \frac{1}{r} \right] \epsilon_z = \frac{\partial}{\partial z} \left[\left(\frac{\partial}{\partial r} - \frac{1}{r} \right) \gamma_{\theta z} + \frac{1}{r} \frac{\partial \gamma_{rz}}{\partial \theta} - \frac{\partial \gamma_{r\theta}}{\partial z} \right]$$

The constitutive equation for a solid with cylindrical orthotropy written in matrix form* is

* The individual matrices in Eq. (1.4) have been partitioned. The null submatrices in the off diagonal positions of the S_{ij} matrix indicate that extensional effects occur independently of shearing effects, i.e. they are uncoupled. For more general forms of anisotropy such coupling does occur, see, for example, [12].

$$\begin{bmatrix} \epsilon_r \\ \epsilon_\theta \\ \epsilon_z \\ \gamma_{\theta z} \\ \gamma_{rz} \\ \gamma_{r\theta} \end{bmatrix} = \begin{bmatrix} s_{11} & s_{12} & s_{13} & 0 & 0 & 0 \\ s_{12} & s_{22} & s_{23} & 0 & 0 & 0 \\ s_{13} & s_{23} & s_{33} & 0 & 0 & 0 \\ \hline 0 & 0 & 0 & s_{44} & 0 & 0 \\ 0 & 0 & 0 & 0 & s_{55} & 0 \\ 0 & 0 & 0 & 0 & 0 & s_{66} \end{bmatrix} \begin{bmatrix} \sigma_r \\ \sigma_\theta \\ \sigma_z \\ \tau_{\theta z} \\ \tau_{rz} \\ \tau_{r\theta} \end{bmatrix} + \begin{bmatrix} \alpha T \\ \alpha T \\ \alpha T \\ 0 \\ 0 \\ 0 \end{bmatrix} \quad (1.4)$$

The symmetric s_{ij} matrix defines the elastic compliances of the material. Thermal effects are accounted for by αT , where α is the coefficient of thermal expansion and T is the temperature change in the solid. Thermal isotropy has been assumed. The temperature function T must satisfy the heat conduction equation for a given problem.

It is sometimes convenient to deal with the inverse form of Eq. (1.4) given by

$$\begin{bmatrix} \sigma_r \\ \sigma_\theta \\ \sigma_z \\ \tau_{\theta z} \\ \tau_{rz} \\ \tau_{r\theta} \end{bmatrix} = \begin{bmatrix} c_{11} & c_{12} & c_{13} & 0 & 0 & 0 \\ c_{12} & c_{22} & c_{23} & 0 & 0 & 0 \\ c_{13} & c_{23} & c_{33} & 0 & 0 & 0 \\ \hline 0 & 0 & 0 & c_{44} & 0 & 0 \\ 0 & 0 & 0 & 0 & c_{55} & 0 \\ 0 & 0 & 0 & 0 & 0 & c_{66} \end{bmatrix} \begin{bmatrix} \epsilon_r - \alpha T \\ \epsilon_\theta - \alpha T \\ \epsilon_z - \alpha T \\ \gamma_{\theta z} \\ \gamma_{rz} \\ \gamma_{r\theta} \end{bmatrix} \quad (1.5)$$

The c_{ij} in Eq. (1.5) are called the elastic moduli of the material and are related to the s_{ij} by a matrix inverse.

$$[c_{ij}] = [s_{ij}]^{-1} \quad (1.6)$$

Boundary conditions will be discussed in connection with specific problems

2. Axisymmetrically Loaded Cylinders

Consider a finite hollow circular cylinder whose inner and outer radii are a and b , respectively. In the instance this cylinder is loaded by a system of forces and subjected to a temperature change, both of which are independent of the generatrix, the three dimensional problem reduces to one of plane strain. If further, the cylinder is loaded axisymmetrically, the dependent variables become independent of θ and the governing equations become ordinary differential equations in the variable r . In the case of plane strain ϵ_z may be taken as a constant:

$$\epsilon_z = K \text{ (a constant)} \quad (2.1)$$

Therefore from the strain-stress relations (1.4) there results

$$\sigma_z = \frac{1}{s_{33}} \left[K - s_{13}\sigma_r - s_{23}\sigma_\theta - \alpha T \right] \quad (2.2)$$

The remaining normal components of strain become

$$\epsilon_r = \beta_{11}\sigma_r + \beta_{12}\sigma_\theta + \left(1 - \frac{s_{13}}{s_{33}}\right)\alpha T + \frac{s_{13}}{s_{33}} K \quad (2.3)$$

$$\epsilon_\theta = \beta_{12}\sigma_r + \beta_{22}\sigma_\theta + \left(1 - \frac{s_{23}}{s_{33}}\right)\alpha T + \frac{s_{23}}{s_{33}} K$$

$$\text{where } \beta_{ij} = s_{ij} - \frac{s_{i3}s_{j3}}{s_{33}} \quad (i, j = 1, 2) \quad (2.4)$$

The relevant equilibrium and compatibility equations for torsionless axisymmetry take the following form

$$\sigma_{\theta} = \frac{d}{dr}(r\sigma_r) \quad (2.5)$$

$$\epsilon_r = \frac{d}{dr}(r\epsilon_{\theta}) \quad (2.6)$$

From Eqs. (2.5) and (2.6) with the help of Eq. (2.3), a differential equation in terms of σ_r can be formulated.

$$\begin{aligned} & \beta_{22} r^2 \frac{d^2 \sigma_r}{dr^2} + 3\beta_{22} r \frac{d\sigma_r}{dr} + (\beta_{22} - \beta_{11}) \sigma_r \\ & = \left[\frac{s_{13}}{s_{33}} - 1 \right] \alpha r \frac{dT}{dr} + \left[\frac{s_{13} - s_{23}}{s_{33}} \right] \alpha T + \left[\frac{s_{13} - s_{23}}{s_{33}} \right] K \end{aligned} \quad (2.7)$$

The boundary conditions for Eq. (2.7) are

$$\begin{aligned} \sigma_r(a) &= h_1 \\ \sigma_r(b) &= h_2 \end{aligned} \quad (2.8)$$

where h_1 and h_2 are prescribed constants.

By using Eq. (2.1) in the stress-strain relations (1.5) and the strain-displacement relations which, in the case of torsionless axisymmetry, are

$$\begin{aligned} \epsilon_r &= \frac{du}{dr} \\ \epsilon_{\theta} &= \frac{u}{r} \end{aligned} \quad (2.9)$$

a governing equation in terms of the displacement u may be obtained:

$$C_{11} \frac{d^2 u}{dr^2} + C_{11} \frac{1}{r} \frac{du}{dr} - C_{22} \frac{u}{r^2} = -\alpha(C_{11} + C_{12} + C_{13}) \frac{dT}{dr} - \alpha \left[C_{11} + C_{13} - C_{22} - C_{23} \right] \frac{1}{r} T + \left[C_{23} - C_{13} \right] K \quad (2.10)$$

The boundary conditions are given by the displacement u and the derivative of the displacement u . The exact expression depends on whether a displacement or a stress boundary condition is specified.

When a cylinder is pressurized internally and externally and subjected to an extensional force at the ends, the governing equation (2.7) must be solved with the following boundary conditions: on the lateral surfaces

$$\sigma_r(a) = -p \quad \sigma_r(b) = -q \quad (2.11)$$

where p and q are the prescribed values of the applied pressures and on the ends

$$2\pi \int_a^b \sigma_z(r) r dr = P \quad (\text{a prescribed value}) \quad (2.12)$$

The solution to Eq. (2.7) is

$$\sigma_r(r) = C_1 r^{-1-k} + C_2 r^{-1+k} + f(r) + \frac{S_{13} - S_{23}}{S_{33}(\beta_{22} - \beta_{11})} K \quad (2.13)$$

where

$$k = \sqrt{\frac{\beta_{11}}{\beta_{22}}} \quad (2.14)$$

and $f(r)$ is the particular solution for the non-homogeneous part of the differential equation for the terms involving T . C_1 and C_2 are constants of integration. For brevity, let

$$F(r) \equiv f(r) + \frac{S_{13} - S_{23}}{S_{33}(\beta_{22} - \beta_{11})} K \quad (2.15)$$

Evaluating C_1 and C_2 from the boundary conditions (2.11) there results

$$C_1 = \frac{[q + F(b)] ba^k - [p + F(a)] ab^k}{\left(\frac{b}{a}\right)^k - \left(\frac{a}{b}\right)^k} \quad (2.16)$$

$$C_2 = \frac{[p + F(a)] ab^{-k} - [q + F(b)] ba^{-k}}{\left(\frac{b}{a}\right)^k - \left(\frac{a}{b}\right)^k}$$

The remaining components of stress are

$$\sigma_\theta(r) = -C_1 kr^{-1-k} + C_2 kr^{-1+k} + \frac{d}{dr}(rF(r)) \quad (2.17)$$

$$\begin{aligned} \sigma_z(r) = \frac{1}{S_{33}} & \left[(kS_{23} - S_{13})C_1 r^{-1-k} - (S_{13} + kS_{23})C_2 r^{-1+k} \right. \\ & \left. - S_{23} \frac{d}{dr}(rF) - S_{13}F + K - \alpha T \right] \end{aligned} \quad (2.18)$$

The value K may be found by substituting Eq. (2.18) into the end boundary condition (2.12). If an explicit expression for σ_z is known, the integral may be evaluated, giving an algebraic relationship between K and P . As the temperature field is not given explicitly, no attempt will be made here to obtain a general relationship, since this step of the solution is straight-forward for a given problem.

The displacement u is found from the stress-strain-displacement relations (2.3) and (2.9).

$$u(r) = C_1(\beta_{12} - k\beta_{22})r^{-k} + C_2(\beta_{12} + k\beta_{22})r^k + \frac{S_{23}^K}{S_{33}} r + \beta_{22} r \frac{d}{dr}(rF) + \beta_{12}(rF) + (1 - \frac{S_{23}}{S_{33}})r\alpha T \quad (2.19)$$

The appearance of the independent variable r raised to non-integral powers containing the elastic coefficients is noteworthy, particularly with reference to the dependence of the displacement and stress distributions on the elastic coefficients. This, of course, has additional implications with respect to the solution of anisotropic viscoelasticity problems.

In the instance an orthotropic cylinder is subjected to torsion the problem of determining the stress and displacement distributions is exactly the same as that for the isotropic case. The reciprocal of the compliance S_{44} takes the place of the usual isotropic shear modulus. Since the solution of the torsion of cylinders may be found in any standard strength of materials text, no further consideration will be given here as the transition from isotropy to orthotropy is straightforward.

3. Examples

a. Internal Pressurization of a Cylinder of Hexagonal Material

Stress analysis of a thick-walled cylinder with hexagonal material properties was conducted to assess the effect of this particular kind of anisotropy which is characteristic of **stress-induced anisotropy** for a pressurized propellant cylinder in plane strain. The term hexagonal refers to a special form of orthotropy in which two of the three elastic compliances, S_{11} , S_{22} , and S_{33} , corresponding to radial, tangential, and axial directions, are identical. With this form of elastic symmetry,

it is possible to reduce the number of independent elastic compliances from nine (for orthotropy) to five, viz.: S_{11} , S_{22} , S_{12} , S_{13} , S_{44} . The parameters S_{12} , S_{13} are associated with cross-effects while S_{44} is a shear compliance.

The values of the parameters adopted for the study are:

$$\begin{aligned} S_{11} = S_{33} = \frac{1}{540} ; S_{22} = \frac{1}{300} ; S_{13} = \frac{-1}{1080} ; S_{12} = S_{23} \\ \bar{k}_1 = \frac{S_{11}}{S_{22}} = 0.556 ; \bar{k}_2 = \frac{-S_{13}}{S_{22}} = 0.278 ; \bar{k}_3 = \frac{-S_{12}}{S_{22}} \end{aligned} \quad (3.1)$$

The parameter \bar{k}_3 will be varied to obtain a family of curves. This parameter is essentially a measure of the cross-effect between the r and θ or the z and θ directions. No value was assigned to S_{44} since it does not appear in the expressions for the stresses given by Eqs. (2.13), (2.17), and (2.18). A plot of $\sigma_\theta(a)$ versus b/a for internal pressure only is shown in Fig. (3.1). The close proximity of the family of curves with \bar{k}_3 as a parameter discloses that the cross-effect has a negligible influence on the maximum stress for a particular value of \bar{k}_1 . Thus, it is seen that the major factor in the difference between the maximum stress in the isotropic and hexagonal cases is the parameter \bar{k}_1 , the ratio of the radial and tangential compliances. For solid propellants, which exhibit stress-induced orthotropy, \bar{k}_1 is less than unity. Consequently, the maximum stress lies below that for an isotropic cylinder for all values of b/a . The upper curve in the figure, corresponding to $\bar{k}_1 = 1.80$ and $\bar{k}_2 = \bar{k}_3 = 0.90$, is included to show the effect of interchanging the values of radial and tangential compliances.

b. Pressurization of a Cylinder with Stress-Induced Hexagonal Material Properties

When a cylinder is subjected to both internal and external

pressure, the tangential stress σ_θ crosses over from tension to compression at some radius between the values of b and a. If the criterion for the change of values of the compliances is taken at the instance when one principal stress goes from tension to compression, then it is possible to solve this problem as two concentric cylinders, one of which is isotropic and one with hexagonal material properties. The theory of bilinear solids is presented in Part II of this report by Herrmann, who discussed a number of classes of bilinear materials with different cross-over criteria. The problem presented herein is a special case in one of the classes discussed, where the cross-over point is taken to be zero stress.

The following steps are taken for the solution of this bilinear elastic problem:

- (1) Solve the following two boundary value problems:

isotropy

$$\frac{d^2 \sigma_{r1}}{dr^2} + \frac{3}{r} \frac{d\sigma_{r1}}{dr} = 0 \quad (3.2)$$

with

$$\sigma_{r1}(b) = -q \quad \sigma_{\theta1}(x) = 0$$

and hexagonality

$$\beta_{22} r^2 \frac{d^2 \sigma_{rh}}{dr^2} + 3\beta_{22} r \frac{d\sigma_{rh}}{dr} + (\beta_{22} - \beta_{11}) \sigma_{rh} = 0 \quad (3.3)$$

with

$$\sigma_{rh}(a) = -p \quad \sigma_{\theta h}(x) = 0$$

where x is the radius at which σ_θ crosses over. In Eqs. (3.2) and (3.3), K and the thermal effects have been neglected. The solution for this step is

$$\sigma_{ri}(r) = - \frac{qb^2}{x^2 + b^2} \left[\left(\frac{x}{r} \right)^2 + 1 \right] \quad (3.4a)$$

$$\sigma_{\theta i}(r) = \frac{qb^2}{x^2 + b^2} \left[\left(\frac{x}{r} \right)^2 - 1 \right] \quad (3.4b)$$

$$\begin{aligned} \sigma_{rh}(r) &= - \frac{pa}{\left(\frac{x}{a} \right)^k + \left(\frac{x}{a} \right)^{-k}} \frac{1}{r} \left[\left(\frac{x}{r} \right)^k + \left(\frac{x}{r} \right)^{-k} \right] \\ &= - \frac{pa}{\cosh \left[k \ln \frac{x}{a} \right]} \frac{1}{r} \cosh k \ln \left(\frac{x}{r} \right) \end{aligned} \quad (3.5a)$$

$$\begin{aligned} \sigma_{\theta h}(r) &= \frac{pak}{\left(\frac{x}{a} \right)^k + \left(\frac{x}{a} \right)^{-k}} \frac{1}{r} \left[\left(\frac{x}{r} \right)^k - \left(\frac{x}{r} \right)^{-k} \right] \\ &= \frac{pak}{\cosh \left[k \ln \frac{x}{a} \right]} \frac{1}{r} \sinh k \ln \frac{x}{r} \end{aligned} \quad (3.5b)$$

(2) Determine the value of x by equating the radial stresses of both sub-domains at the interface $r = x$.

$$\sigma_{ri}(x) = \sigma_{rh}(x) \quad (3.6)$$

Substituting Eqs. (3.4a) and (3.5a) into Eq. (3.6) gives:

$$\frac{qb^2}{x^2 + b^2} = \frac{pa}{x \left[\left(\frac{x}{a} \right)^k + \left(\frac{x}{a} \right)^{-k} \right]} \quad (3.7a)$$

or

$$pa(x^2 + b^2) = 2qb^2x \cosh \left[k \ln \left(\frac{x}{a} \right) \right] \quad (3.7b)$$

The solution of the transcendental equation (3.7b) gives the value of x .

In many problems of interest it is not the external pressure q which is prescribed, but rather a displacement boundary condition. Hence it is necessary to relate the external pressure to the displacement at the outer boundary. The displacements for the individual sub-domains may be found from Eqs. (2.3) and (2.9).

$$u_i(r) = -\frac{qb^2}{x^2 + b^2} \left[(\beta_{22_i} - \beta_{12_i}) \left(\frac{x}{r}\right)^2 - (\beta_{22_i} + \beta_{12_i}) \right] \quad (3.8)$$

$$u_h(r) = \frac{pa}{2 \cosh \left[k_h \ln \left(\frac{x}{a} \right) \right]} \left[(k_h \beta_{22_h} - \beta_{12_h}) \left(\frac{x}{r}\right)^{k_h} - (\beta_{12_h} + k_h \beta_{22_h}) \left(\frac{x}{r}\right)^{-k_h} \right] \quad (3.9)$$

where the subscripts h and i in the elastic coefficients distinguish them between hexagonal and isotropic properties. As an example consider the outer case to be rigid, i.e. $u_i(b) = 0$; then from Eq. (3.8) there results

$$\frac{x}{b} = \sqrt{\frac{\beta_{22_i} + \beta_{12_i}}{\beta_{22_i} - \beta_{12_i}}} \quad (3.10)$$

Eq. (3.10) shows that for a rigid outer case, the value of x/b is a constant, indicating that the value of x is independent of the ratio b/a and of the internal pressure (i.e., once the cylinder is pressurized, a cross-over point is immediately established and remains at that position as long as a pressure is maintained). To determine q in terms of p , substitute Eq. (3.10) into Eq. (3.7b)

$$q = \frac{pa}{b \cosh \left[k_h \ln \frac{b}{a} \sqrt{\frac{\beta_{22_i} + \beta_{12_i}}{\beta_{22_i} - \beta_{12_i}}} \right]} \left[\frac{\beta_{22_i}}{\beta_{22_i} - \beta_{12_i}} \right] \sqrt{\frac{\beta_{22_i} + \beta_{12_i}}{\beta_{22_i} - \beta_{12_i}}} \quad (3.11)$$

As a check, the displacements of both sub-domains must be the same at the interface, $u_i(x) = u_h(x)$. Equating Eqs. (3.8) and (3.9) for $r = x$ gives

$$q = \frac{pa}{b \cosh \left[k_h \ln \frac{b}{a} \sqrt{\frac{\beta_{22_i} + \beta_{12_i}}{\beta_{22_i} - \beta_{12_i}}} \right]} \left[\frac{\beta_{22_i}}{\beta_{22_i} - \beta_{12_i}} \right] \sqrt{\frac{\beta_{22_i} + \beta_{12_i}}{\beta_{22_i} - \beta_{12_i}}} \left[\frac{\beta_{12_h}}{\beta_{12_i}} \right] \quad (3.12)$$

Comparing Eqs. (3.11) and (3.12) shows that they are equal only if

$$\beta_{12_h} = \beta_{12_i} \quad (3.13)$$

Eq. (3.13) shows that there are only three relevant elastic constants instead of four in this type of stress-induced orthotropy. This relationship is a natural consequence of the cross-over criterion employed and may be seen more clearly in the direct formulation of the constitutive equations for a bilinear material as shown in Part II. Reflecting upon Eq. (3.10) it is reasonable to expect that x should depend on the elastic properties of both sub-domains.

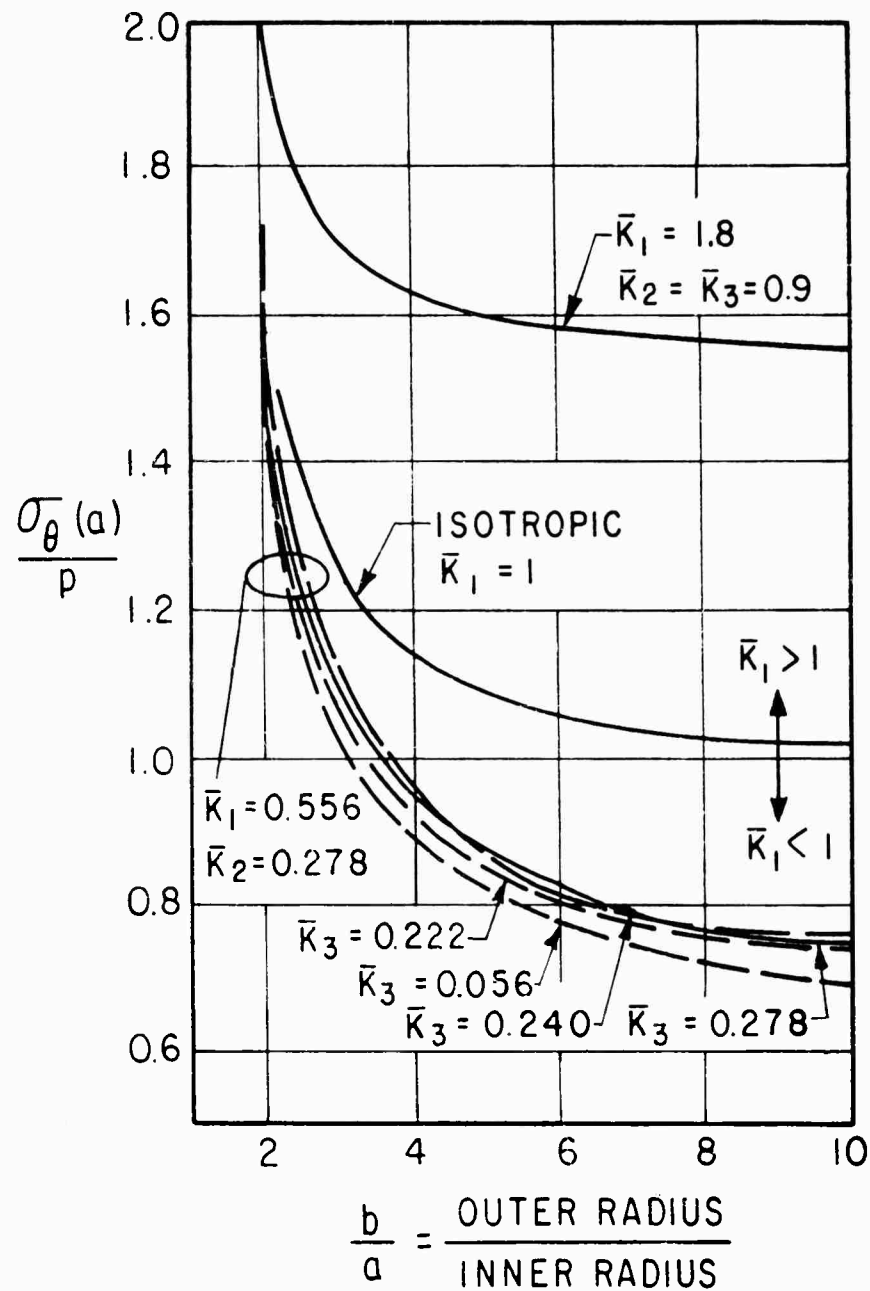


FIG.3-1 $\sigma_{\theta}(a)$ vs $\frac{b}{a}$ FOR INTERNAL PRESSURE

LINEAR VISCOELASTIC ANALYSIS OF ORTHOTROPIC SOLIDS

4. Correspondence Principle for Anisotropic Viscoelasticity

In linear isotropic viscoelasticity a useful analogy exists for the solution of boundary value problems. The correspondence principle has been repeatedly used for many isotropic problems. Following this principle an associated elastic problem with the proper boundary conditions in Laplace or Fourier transform space is inverted to obtain the viscoelastic response. This principle can be formally extended for anisotropic solids by replacing the elastic constitutive equations, (1.4) and (1.5), by viscoelastic constitutive equations

$$\sigma_{ij} = Q_{ij}^{kl} \epsilon_{kl} \quad (\text{summation on repeated indices}) \quad (4.1)$$

where Q_{ij}^{kl} is an operational tensor. Special forms of this tensor appear in [6] and [8].

The Laplace transform of Eq. (4.1) along with similar transforms of the equilibrium and compatibility equations, strain-displacement relations and boundary conditions are necessary to complete the formal analogy.

Using the correspondence principle and by inverting term by term the Mittag-Leffler expansion of the solution for the associated elastic orthotropic cylinder, Spillers has recovered the viscoelastic response [7]. In general the solution of viscoelastic problems may not be obtained in this straightforward manner. Recall from the solution of the cylinder problem in Section 2 that the independent variable r appears raised to a fractional power containing elastic coefficients. Although the viscoelastic response was obtained directly from the correspondence principle, the form of this solution seems

to indicate that other orthotropic problems may not be readily invertible. An alternative method of solution is applied to the same orthotropic cylinder in the next section. The approach, however, is valid for other orthotropic viscoelastic problems.

5. Viscoelastic Solution for the Pressurization of a Cylinder

The problem of the pressurization of a cylinder is intended to illustrate a method of solution which does not involve the correspondence principle. The governing equation in stress σ_r Eq. (2.7) is

$$\beta_{22} r^2 \frac{\partial^2 \sigma_r}{\partial r^2} + 3\beta_{22} r \frac{\partial \sigma_r}{\partial r} + (\beta_{22} - \beta_{11}) \sigma_r = \left[\frac{S_{13} - S_{33}}{S_{33}} \right] \alpha_r \frac{\partial T}{\partial r} + \left[\frac{S_{13} - S_{23}}{S_{33}} \right] \alpha_T + \left[\frac{S_{13} - S_{23}}{S_{33}} \right] K \quad (5.1)$$

where $\beta_{1j} = S_{1j} - \frac{S_{13}S_{j3}}{S_{33}}$ are now viscoelastic operators. The material properties are also assumed temperature independent. The theory of viscoelastic materials with temperature-dependent properties has been discussed by Muki and Sternberg [9] and the thermal deformation of viscoelastic cylinders with such materials properties is given in Part IV. The boundary and initial conditions for Eq. (5.1) are

$$\begin{aligned} \sigma_r(a, t) &= -pH(t) \\ \sigma_r(b, t) &= -qH'(t) \end{aligned} \quad (5.2)$$

$$\sigma_r(r, 0) = 0$$

(5.3)

$$\frac{\partial \sigma_r}{\partial t}(r, 0) = 0$$

where $H(t)$ is the Heaviside step function.

The solution of Eq. (5.1) is composed of two parts:

$$\sigma_r(r, t) = \sigma_{r1}(r, t) + \sigma_{r2}(r, t) \quad (5.4)$$

where σ_{r2} is any arbitrary function chosen specifically to satisfy boundary conditions, but, in general, not satisfying the differential equation. Techniques of selecting this function for specific purposes will be discussed in the sequel. Eq. (5.1) is thus recast in the following form with homogeneous boundary conditions:

$$\beta_{22} r^2 \frac{\partial^2 \sigma_{r1}}{\partial r^2} + \beta_{22} r \frac{\partial \sigma_{r1}}{\partial r} + (\beta_{22} - \beta_{11}) \sigma_{r1} = f(r, t) \quad (5.5)$$

where

$$f(r, t) = \left[\frac{S_{13} - S_{33}}{S_{33}} \right] \alpha r \frac{\partial T}{\partial r} + \left[\frac{S_{13} - S_{23}}{S_{33}} \right] \alpha T + \left[\frac{S_{13} - S_{23}}{S_{33}} \right] K \quad (5.6)$$

$$- \left[\beta_{22} r^2 \frac{\partial^2 \sigma_{r2}}{\partial r^2} + \beta_{22} r \frac{\partial \sigma_{r2}}{\partial r} + (\beta_{22} - \beta_{11}) \sigma_{r2} \right]$$

with

$$\sigma_{r1}(a, t) = 0 \quad (5.7)$$

$$\sigma_{r1}(b, t) = 0$$

$$\sigma_{r1}(r, 0) = \frac{\partial \sigma_{r1}(r, 0)}{\partial t} = 0 \quad (5.8)$$

A separation of variables technique on the homogeneous equation (5.5) is possible. Let

$$\sigma_{r1_h}(r, t) = R(r)\psi(t) \quad (5.9)$$

Substitution of Eq. (5.9) into Eq. (5.5) leads to the following two ordinary differential equations.

$$r^3 \frac{d^2 R}{dr^2} + 3r^2 \frac{dR}{dr} - \lambda r R = 0 \quad (5.10)$$

with

$$R(a) = R(b) = 0 \quad (5.11)$$

and

$$\left[\beta_{11} - (1 + \lambda) \beta_{22} \right] \psi(t) = 0 \quad (5.12)$$

with

$$\psi(0) = \frac{d\psi(0)}{dt} = 0 \quad (5.13)$$

where λ is a separation constant.

Eq. (5.10) with homogeneous boundary conditions (5.11) is a Sturm-Liouville differential equation. From that system of equations a complete set of characteristic functions and the corresponding characteristic values may be generated. Any arbitrary function in the variable r may now be expanded in terms of this set of characteristic functions. The solution to Eq. (5.10) is

$$R(r) = A_1 r^{-1-\sqrt{1+\lambda}} + A_2 r^{-1+\sqrt{1+\lambda}} \quad (5.14)$$

Evaluating the constants A_1 and A_2 from the boundary conditions leads to the following characteristic equation, the roots of which are the characteristic values.

$$\left(\frac{a}{b}\right)^{2\sqrt{1+\lambda}} = 1 \quad (5.15)$$

The characteristic values are

$$\lambda_n = - \left(1 + \frac{\pi^2 n^2}{\gamma^2}\right) \quad (5.16)$$

where

$$\gamma = \ln \frac{a}{b} \text{ and } n \text{ is an integer.} \quad (5.17)$$

The corresponding characteristic functions are

$$R_n = \frac{1}{r} \sin\left(\frac{\pi n}{\gamma} \ln \frac{r}{a}\right) \quad (5.18)$$

The solution of Eq. (5.12) with homogeneous initial conditions (5.13) is identically zero.

However, with the complete set of characteristic functions at our disposal, the non-homogeneous term of Eq. (5.5) can be expanded in an infinite series.

$$f(r, t) = \sum_{n=1}^{\infty} C_n(t) R_n(r) \quad (5.19)$$

where

$$C_n(t) = \frac{1}{N^2} \int_a^b f(r, t) R_n(r) r dr \quad (5.20)$$

$$N^2 = \int_a^b R_n^2 r dr \quad (5.21)$$

A particular solution may now be obtained using a mode superposition method. Let

$$\sigma_{rl_p} = \sum_{n=1}^{\infty} \psi_{n_p}(t) R_n(r) \quad (5.22)$$

where $\psi_{n_p}(t)$ are undetermined coefficients. Substitution of

Eqs. (5.22) and (5.19) into Eq. (5.5) gives .

$$\sum_{n=1}^{\infty} \lambda_n \psi_{n_p} R_n + (1 - \frac{\beta_{22}}{\beta_{11}}) \psi_{n_p} R_n = \sum_{n=1}^{\infty} C_n R_n \quad (5.23)$$

Therefore the solutions to the typical equation in time gives the coefficients of the series solution.

$$\lambda_n \psi_{n_p}(t) + (1 - \frac{\beta_{22}}{\beta_{11}}) \psi_{n_p}(t) = C_n(t) \quad (5.24)$$

6. Asymptotic Solutions

The selection of σ_{r2} can be made judiciously to minimize the error in using only a finite number of terms of the series for σ_{r1_p} . For the purpose of discussion consider a Maxwell-type response. If a solution for early times is desired, σ_{r2} should be taken as the elastic response multiplied by the Heaviside unit function. Since the major contribution at early times is attributed to the elastic response, the series solution for σ_{r1_p} will represent only the deviation from this effect due to viscoelastic properties of the body. These viscoelastic effects will be small in comparison to σ_{r2} , hence early termination of the infinite series will incur no major error in the total solution.

On the other hand, if a long time solution is needed, σ_{r2} should be taken as the steady creep solution in the case of a Maxwell-type response. To obtain such an expression, it is necessary to substitute the viscosity coefficients in place of the elastic coefficients in the differential equation and seek a solution. This steady creep solution represents the

bulk of the total response at very long times, and consequently the series σ_{r1_p} in this case is the deviation from this effect due to elasticity of the body. Again terminating the infinite series early will incur no major error in the total response. The roles of σ_{r2} and σ_{r1_p} for early and long times are thus interchanged.

The foregoing discussion on the selection of the function to satisfy boundary conditions need not be restricted to Maxwell-type responses. The qualitative approach used previously can be achieved systematically by examining the asymptotic forms of the constitutive equations. When a form of the constitutive equations is given, it is possible to predict the behavior of a solid at early or long times by reducing these equations to their asymptotic forms. A procedure of accomplishing this is to examine the Laplace transform of the constitutive equations. If t is the time variable and s is the transform variable, then as $s \rightarrow \infty$, $t \rightarrow 0$ and as $s \rightarrow 0$, $t \rightarrow \infty$. Performing the limiting process gives the asymptotic forms of these equations for early and long times. It is then possible to use this simplified form of the equations to obtain an asymptotic solution which will be used for σ_{r2} . Precaution should be taken in arriving at sensible relationships, i.e., for a limiting elastic response, a stress-strain relation should be obtained and for a limiting creep condition a stress-strain rate relation should be obtained.

A similar asymptotic process may be applied to the solution for σ_{r1_p} . A method for solving Eq (5.24) is by Laplace transform. The ultimate form of a typical equation for the particular value of the parameter λ_n prior to the Laplace inversion is

$$\frac{1}{2\pi i} \int_{\gamma-i\infty}^{\gamma+i\infty} \frac{a_m s^m + a_{m-1} s^{m-1} + \dots + a_0}{s [b_m s^m + b_{m-1} s^{m-1} + \dots + b_0]} e^{st} ds \quad (6.1)$$

It is possible to obtain an inversion for this expression by the method of partial fractions. However, for a high degree polynomial, the work involved is quite cumbersome. Since σ_{rlp} represents only a small portion of the total response for a selected time interval it is justifiable to use an approximate solution. Recall that $s \rightarrow 0$ and $s \rightarrow \infty$ is equivalent to $t \rightarrow \infty$ and $t \rightarrow 0$, respectively; the limiting process may again be applied. Consider the fraction

$$\frac{a_m s^m + a_{m-1} s^{m-1} + \dots + a_0}{s [b_m s^m + b_{m-1} s^{m-1} + \dots + b_0]} \quad (6.2)$$

As $s \rightarrow 0$, the lower order terms $a_0, a_1, \dots, b_0, b_1, \dots$ govern the value of the fraction. Hence the higher order terms in s may be neglected. The number of terms neglected depends on the accuracy of the desired solution. As an example, neglect all terms except a_0, a_1, b_0, b_1 ; then the asymptotic form is

$$\frac{a_1 s + a_0}{s [b_1 s + b_0]} \quad (6.3)$$

Such an expression is easily invertible. Should more accuracy be needed, include a_2 and b_2 . The expression in this case is

$$\frac{a_2 s^2 + a_1 s + a_0}{s [b_2 s^2 + b_1 s + b_0]} \quad (6.4)$$

which is still a relatively easy inversion. Such an argument may be continued until the desired accuracy is attained.

A similar argument may be used when $s \rightarrow \infty$. The higher order coefficients predominate and it is justifiable to neglect the lower order terms. An example of this asymptotic form is

$$\frac{a_n s^n + a_{n-1} s^{n-1}}{s [b_n s^n + b_{n-1} s^{n-1}]} = \frac{a_n s + a_{n-1}}{s [b_n s + b_{n-1}]} \quad (6.5)$$

This expression is equivalent to Eq. (6.3) which was noted to be readily invertible. For more accuracy additional terms must be included. By the foregoing techniques, a fairly accurate solution may be obtained with a minimum of computational effort.

Before eluding from this section attention is called to some other approximate methods of Laplace transform inversion. Schapery [10] has developed techniques which are applicable to stress analysis problems in quasi-static linear viscoelasticity. To use these methods it is only necessary to have knowledge of the associated elastic solution, either numerically or analytically. The principles underlying these techniques come from Irreversible Thermodynamics and a mathematical property of the Laplace Transform.

NON LINEAR ELASTIC ANALYSIS OF CYLINDERS
WITH CYLINDRICAL ORTHOTROPY

7. Fundamental Equations for Solids in Plane Strain Subjected to Axisymmetric Loads

Tensor notation will be used in this section; the reader is referred to [11] for more details. Adopting suitable convected coordinates

$$x^i = (r, \theta, z) , i = 1, 2, 3 \quad (7.1)$$

the line elements in the undeformed and the deformed states are, respectively

$$\begin{aligned} (ds_o)^2 &= g_{ij} dx^i dx^j \\ (ds)^2 &= G_{ij} dx^i dx^j \end{aligned} \quad (7.2)$$

where the metric tensors g_{ij} and G_{ij} are

$$g_{ij} = \begin{bmatrix} 1 & 0 & 0 \\ 0 & r^2 & 0 \\ 0 & 0 & 1 \end{bmatrix} \quad G_{ij} = \begin{bmatrix} (1 + \frac{du}{dr})^2 & 0 & 0 \\ 0 & r^2 (1 + \frac{u}{r})^2 & 0 \\ 0 & 0 & 1 \end{bmatrix} \quad (7.3)$$

The mixed form of the strain tensor is defined by

$$e_j^i = \frac{1}{2} (G_{ik} - g_{ik}) g^{kj} \quad (7.4)$$

The strain-displacement relations are

$$e_{ij}^1 = \begin{bmatrix} \frac{du}{dr} + \frac{1}{2} \left(\frac{du}{dr} \right)^2 & 0 & 0 \\ 0 & \frac{u}{r} + \frac{1}{2} \left(\frac{u}{r} \right)^2 & 0 \\ 0 & 0 & 0 \end{bmatrix}$$

According to Green and Adkins [11] the strain energy density for curvilinear anisotropy must be expressed in terms of the physical components of strain. In anisotropy it is necessary to account for both the changes in geometry and in the preferred directions of curvilinear anisotropy. For a solid with cylindrical orthotropy the strain energy density may be expressed as

$$W = W(e_1^1, e_2^2, e_3^3, e_2^1 e_1^2, e_3^1 e_1^3, e_3^2 e_2^3, e_2^1 e_3^2, e_3^1 e_2^3) \quad (7.6)$$

For a second order theory, the explicit form of W is

$$\begin{aligned} W = & k_1 (e_1^1)^2 + k_2 e_1^1 e_2^2 + k_3 e_1^1 e_3^3 + k_4 (e_2^2)^2 + k_5 e_2^2 e_3^3 \\ & + k_6 (e_3^3)^2 + k_7 e_2^1 e_1^2 + k_8 e_3^1 e_1^3 + k_9 e_3^2 e_2^3 + k_{10} (e_1^1)^3 \\ & + k_{11} (e_1^1)^2 e_2^2 + k_{12} (e_1^1)^2 e_3^3 + k_{13} (e_2^2)^2 e_1^1 + k_{14} (e_2^2)^3 \\ & + k_{15} (e_2^2)^2 e_3^3 + k_{16} (e_3^3)^2 e_1^1 + k_{17} (e_3^3)^2 e_2^2 + k_{18} (e_3^3)^3 \\ & + k_{19} e_1^1 e_2^2 e_3^3 + k_{20} e_1^1 e_2^1 e_1^2 + k_{21} e_1^1 e_3^2 e_2^3 + k_{22} e_1^1 e_3^1 e_1^3 \\ & + k_{23} e_2^2 e_1^2 e_1^1 + k_{24} e_2^2 e_3^2 e_2^3 + k_{25} e_2^2 e_3^1 e_1^3 + k_{26} e_3^3 e_2^1 e_1^2 \\ & + k_{27} e_3^3 e_3^2 e_2^3 + k_{28} e_3^3 e_3^1 e_1^3 + k_{29} e_2^1 e_3^2 e_1^3 \end{aligned} \quad (7.7)$$

The stresses referred to the deformed space are given by

$$\sigma_{ii} = \frac{\bar{G}_i^1}{\sqrt{I_3}} \frac{\partial W}{\partial e_i^1} \quad (\text{no sum on } i) \quad (7.8)$$

where

$$(\sigma_{11}, \sigma_{22}, \sigma_{33}) \equiv (\sigma_r, \sigma_\theta, \sigma_z) \quad (7.9)$$

$$\bar{G}_i^1 = g_{ii} G^{ii} = g^{ii} G_{ii} \quad (7.10)$$

$$I_3 = \frac{G}{g} = (1 + \frac{du}{dr})^2 (1 + \frac{u}{r})^2 \quad (7.11)$$

8. Solution for a Thick-Walled Cylinder Subjected to Internal and External Pressure

The problem of the pressurization of an orthotropic cylinder is governed by the following non-linear differential equation

$$\frac{d\sigma_r}{dr} + \frac{\sigma_r - \sigma_\theta}{r} + \frac{u}{r} \frac{d\sigma_r}{dr} + \frac{du}{dr} \left(\frac{\sigma_r - \sigma_\theta}{r} \right) = 0 \quad (8.1)$$

with the following boundary conditions

$$\sigma_r(a) = -p_a \quad \sigma_r(b) = -p_b \quad (8.2)$$

A method of solution is by a perturbation scheme. For details of this method, the reader is referred to Part III where a number of problems in nonlinear isotropic elasticity are treated by this perturbation scheme. Only the results for the orthotropic cylinder will be stated here.

The radial displacement is given by

$$\begin{aligned}
 u(r) = & ap_a \left[x_1 \left(\frac{r}{a} \right)^{m_1 + m_2} + x_2 c^{m_1 + m_2 - 1} \left(\frac{r}{a} \right)^{m_1 - m_2} \right] \\
 & - ap_b \left[x_1 c^{m_1 - m_2 - 1} \left(\frac{r}{a} \right)^{m_1 + m_2} + x_2 \left(\frac{r}{a} \right)^{m_1 - m_2} \right] \\
 & + ax_1^2 (p_a - p_b c^{m_1 - m_2 - 1})^2 \left[\frac{x_6}{x_{12}} \left(\frac{r}{a} \right)^{m_1 + m_2} + \frac{x_9}{x_{12}} \left(\frac{r}{a} \right)^{m_1 - m_2} - \frac{D_1}{x_3} \left(\frac{r}{a} \right)^{2m_1 + 2m_2 - 1} \right] \\
 & + 2ax_1 x_2 (p_a - p_b c^{m_1 - m_2 - 1}) (p_a c^{m_1 + m_2 - 1} - p_b) \left[\frac{x_7}{x_{12}} \left(\frac{r}{a} \right)^{m_1 + m_2} + \frac{x_{10}}{x_{12}} \left(\frac{r}{a} \right)^{m_1 - m_2} \right. \\
 & \left. - \frac{D_2}{x_4} \left(\frac{r}{a} \right)^{2m_1 - 1} \right] + ax_2^2 (p_a c^{m_1 + m_2 - 1} - p_b)^2 \left[\frac{x_8}{x_{12}} \left(\frac{r}{a} \right)^{m_1 + m_2} \right. \\
 & \left. + \frac{x_{11}}{x_{12}} \left(\frac{r}{a} \right)^{m_1 - m_2} - \frac{D_3}{x_5} \left(\frac{r}{a} \right)^{2m_1 - 2m_2 - 1} \right] \quad (8.3)
 \end{aligned}$$

The stresses are given by

$$\begin{aligned}
 \begin{pmatrix} \sigma_r \\ \sigma_\theta \\ \sigma_z \end{pmatrix} = & a^2 p_a \left[x_1 \begin{pmatrix} k_2 + 2k_1 (m_1 + m_2) \\ 2k_4 + k_2 (m_1 + m_2) \\ k_3 + k_5 (m_1 + m_2) \end{pmatrix} \left(\frac{r}{a} \right)^{m_1 + m_2 - 1} \right. \\
 & \left. + x_2 c^{m_1 + m_2 - 1} \begin{pmatrix} k_2 + 2k_1 (m_1 - m_2) \\ 2k_4 + k_2 (m_1 - m_2) \\ k_3 + k_5 (m_1 + m_2) \end{pmatrix} \left(\frac{r}{a} \right)^{m_1 - m_2 - 1} \right] \quad (8.4)
 \end{aligned}$$

$$\begin{aligned}
& - a^2 p_b \left[x_1 c^{m_1 - m_2 - 1} \begin{pmatrix} k_2 + 2k_1(m_1 + m_2) \\ 2k_4 + k_2(m_1 + m_2) \\ k_3 + k_5(m_1 + m_2) \end{pmatrix} \left(\frac{r}{a}\right)^{m_1 + m_2 - 1} \right. \\
& + x_2 \begin{pmatrix} k_2 + 2k_1(m_1 - m_2) \\ 2k_4 + k_2(m_1 - m_2) \\ k_3 + k_5(m_1 - m_2) \end{pmatrix} \left(\frac{r}{a}\right)^{m_1 - m_2 - 1} \Big] \\
& + a^2 x_1^2 (p_a - p_b c^{m_1 - m_2 - 1}) \left[\frac{x_6}{x_{12}} \begin{pmatrix} k_2 + 2k_1(m_1 + m_2) \\ 2k_4 + k_2(m_1 + m_2) \\ k_3 + k_5(m_1 + m_2) \end{pmatrix} \left(\frac{r}{a}\right)^{m_1 + m_2 - 1} \right. \\
& + \frac{x_9}{x_{12}} \begin{pmatrix} k_2 + 2k_1(m_1 - m_2) \\ 2k_4 + k_2(m_1 - m_2) \\ k_3 + k_5 \end{pmatrix} \left(\frac{r}{a}\right)^{m_1 - m_2 - 1} - \frac{D_1}{x_3} \begin{pmatrix} k_2 + 2k_1(2m_1 + 2m_2 - 1) \\ 2k_4 + k_2(2m_1 + 2m_2 - 1) \\ k_3 + k_5(2m_1 + 2m_2 - 1) \end{pmatrix} \left(\frac{r}{a}\right)^{2m_1 + 2m_2 - 2} \Big] \\
& + 2a^2 x_1 x_2 (p_a - p_b c^{m_1 - m_2 - 1}) (p_a c^{m_1 + m_2 - 1} - p_b) \left[\frac{x_7}{x_{12}} \begin{pmatrix} k_2 + 2k_1(m_1 + m_2) \\ 2k_4 + k_2(m_1 + m_2) \\ k_3 + k_5(m_1 + m_2) \end{pmatrix} \left(\frac{r}{a}\right)^{m_1 + m_2 - 1} \right. \\
& + \frac{x_{10}}{x_{12}} \begin{pmatrix} k_2 + 2k_1(m_1 - m_2) \\ 2k_4 + k_2(m_1 - m_2) \\ k_3 + k_5(m_1 - m_2) \end{pmatrix} \left(\frac{r}{a}\right)^{m_1 - m_2 - 1} - \frac{D_2}{x_4} \begin{pmatrix} k_2 + 2k_1(2m_1 - 1) \\ 2k_4 + k_2(2m_1 - 1) \\ k_3 + k_5(2m_1 - 1) \end{pmatrix} \left(\frac{r}{a}\right)^{2m_1 - 2} \Big]
\end{aligned}$$

(8.4)

Cont.

$$+ a^2 x_2^2 (p_a c^{m_1 + m_2 - 1} - p_b)^2 \left[\frac{x_8}{x_{12}} \begin{pmatrix} k_2 + 2k_1(m_1 + m_2) \\ 2k_4 + k_2(m_1 + m_2) \\ k_3 + k_5(m_1 + m_2) \end{pmatrix} \left(\frac{r}{a} \right)^{m_1 + m_2 - 1} \right]$$

$$+ \frac{x_{11}}{x_{12}} \begin{pmatrix} k_2 + 2k_1(m_1 - m_2) \\ 2k_4 + k_2(m_1 - m_2) \\ k_3 + k_5(m_1 - m_2) \end{pmatrix} \left(\frac{r}{a} \right)^{m_1 - m_2 - 1} - \frac{D_3}{x_5} \begin{pmatrix} k_2 + 2k_1(2m_1 - 2m_2 - 1) \\ 2k_4 + k_2(2m_1 - 2m_2 - 1) \\ k_3 + k_5(2m_1 - 2m_2 - 1) \end{pmatrix} \left(\frac{r}{a} \right)^{2m_1 - 2m_2 - 2} \Big]$$

$$+ a^4 \begin{pmatrix} 3k_{10} + 3k_1 \\ k_{11} - \frac{k_2}{2} \\ k_{12} - \frac{k_3}{2} \end{pmatrix} \left[p_a \left\{ x_1(m_1 + m_2) \left(\frac{r}{a} \right)^{m_1 + m_2 - 1} + x_2(m_1 - m_2) c^{m_1 + m_2 - 1} \left(\frac{r}{a} \right)^{m_1 - m_2 - 1} \right\} \right. \\ \left. - p_b \left\{ x_1(m_1 + m_2) c^{m_1 - m_2 - 1} \left(\frac{r}{a} \right)^{m_1 + m_2 - 1} + x_2(m_1 - m_2) \left(\frac{r}{a} \right)^{m_1 - m_2 - 1} \right\} \right]^2$$

$$+ a^4 \begin{pmatrix} k_{13} - \frac{k_2}{2} \\ 3k_4 + 3k_{14} \\ k_{15} - \frac{k_5}{2} \end{pmatrix} \left[p_a \left\{ x_1 \left(\frac{r}{a} \right)^{m_1 + m_2} + x_2 c^{m_1 + m_2 - 1} \left(\frac{r}{a} \right)^{m_1 - m_2} \right\} \right. \quad (8.4) \\ \left. - p_b \left\{ x_1 c^{m_1 - m_2 - 1} \left(\frac{r}{a} \right)^{m_1 + m_2} + x_2 \left(\frac{r}{a} \right)^{m_1 - m_2} \right\} \right]^2$$

cont.

$$+ a^4 \begin{pmatrix} 2k_{11} - 2k_1 + k_2 \\ 2k_{13} - 2k_4 + k_2 \\ k_{19} - k_3 - k_5 \end{pmatrix} \left[p_a \left\{ x_1(m_1 + m_2) \left(\frac{r}{a} \right)^{m_1 + m_2 - 1} + x_2(m_1 - m_2) c^{m_1 + m_2 - 1} \left(\frac{r}{a} \right)^{m_1 - m_2 - 1} \right\} \right. \\ \left. - p_b \left\{ x_1 c^{m_1 - m_2 - 1} \left(\frac{r}{a} \right)^{m_1 + m_2} + x_2 \left(\frac{r}{a} \right)^{m_1 - m_2} \right\} \right]^2$$

$$\begin{aligned}
& - p_b \left\{ x_1 (m_1 + m_2) c^{m_1 - m_2 - 1} \left(\frac{r}{a}\right)^{m_1 + m_2 - 1} + x_2 (m_1 - m_2) \left(\frac{r}{a}\right)^{m_1 - m_2 - 1} \right\} \left[p_a \left\{ x_1 \left(\frac{r}{a}\right)^{m_1 + m_2} \right. \right. \\
& \left. \left. + x_2 c^{m_1 + m_2 - 1} \left(\frac{r}{a}\right)^{m_1 - m_2} \right\} - p_b \left\{ x_1 c^{m_1 - m_2 - 1} \left(\frac{r}{a}\right)^{m_1 + m_2} + x_2 \left(\frac{r}{a}\right)^{m_1 - m_2} \right\} \right]
\end{aligned} \tag{8.4}$$

where

$$c = \frac{b}{a} \tag{8.5}$$

$$m_1 = \frac{k_2 - 2k_1}{k_1} \quad m_2 = \sqrt{(k_2 - 2k_1)^2 + 4k_1 k_4} \tag{8.6}$$

$$x_1 = \frac{3k_2 - 4k_1 - 2\sqrt{4(k_2 - 2k_1)^2 + 4k_1 k_4}}{(5k_2^2 - 8k_1 k_2 - 16k_1 k_4) (c^{m_1 - m_2 - 1} - c^{m_1 + m_2 - 1})} \tag{8.7}$$

$$x_2 = \frac{3k_2 - 4k_1 + 2\sqrt{4(k_2 - 2k_1)^2 + 4k_1 k_4}}{(5k_2^2 - 8k_1 k_2 - 16k_1 k_4) (c^{m_1 - m_2 - 1} - c^{m_1 + m_2 - 1})}$$

$$x_3 = 2C_2 \left[2(m_1 + m_2)^2 - 3(m_1 + m_2) + 1 \right] + (C_1 + C_7) \left[2m_1 + 2m_2 - 1 \right] + (C_6 - C_1)$$

$$x_4 = 2C_2 \left[2m_1^2 - 3m_1 + 1 \right] + (C_1 + C_7) (2m_1 - 1) + (C_6 - C_1)$$

$$x_5 = 2C_2 \left[2(m_1 - m_2)^2 - 3(m_1 - m_2) + 1 \right] + (C_1 + C_7) \left[2m_1 - 2m_2 - 1 \right] + (C_6 - C_1)$$

$$x_6 = K_1 \left[\{C_1 + (m_1 - m_2)C_2\} c^{2m_1 - 2m_2 - 2} - \{C_1 + (m_1 - m_2)C_2\} c^{m_1 - m_2 - 1} \right]$$

$$x_7 = K_2 \left[\{C_1 + (m_1 - m_2)C_2\} c^{2m_1 - 2} - \{C_1 + (m_1 - m_2)C_2\} c^{m_1 - m_2 - 1} \right]$$

$$x_8 = K_3 \left[\{C_1 + (m_1 - m_2)C_2\} c^{2m_1 - 2m_2 - 2} - \{C_1 + (m_1 - m_2)C_2\} c^{m_1 - m_2 - 1} \right]$$

$$x_9 = K_1 \left[C_1 + (m_1 + m_2)C_2 \right] \left[c^{m_1 + m_2 - 1} - c^{2m_1 + 2m_2 - 2} \right]$$

$$x_{10} = K_2 \left[C_1 + (m_1 + m_2)C_2 \right] \left[c^{m_1 + m_2 - 1} - c^{2m_1 - 2} \right]$$

$$x_{11} = K_3 \left[C_1 + (m_1 + m_2)C_2 \right] \left[c^{m_1 + m_2 - 1} - c^{2m_1 - 2m_2 - 2} \right]$$

$$x_{12} = (5k_2^2 - 8k_1k_2 - 16k_1k_4) (c^{m_1 - m_2 - 1} - c^{m_1 + m_2 - 1})$$

$$K_1 = C_3 (m_1 + m_2)^2 + C_4 + C_5 (m_1 + m_2) - \frac{D_1}{X_3} \{C_1 + (2m_1 + 2m_2 - 1)C_2\}$$

$$K_2 = C_3 (m_1^2 - m_2^2) + C_4 + C_5 m_1 - \frac{D_2}{X_4} \{C_1 + (2m_1 - 1)C_2\} \quad (8.8)$$

$$K_3 = C_3 (m_1 - m_2)^2 + C_4 + C_5 (m_1 - m_2) - \frac{D_3}{X_5} \{C_1 + (2m_1 - 2m_2 - 1)C_2\}$$

$$\begin{aligned}
D_1 = & (m_1 + m_2)^2 \{ c_2 + c_5 + c_7 + c_8 + 2c_2(m_1 + m_2 - 1) \} \\
& + (m_1 + m_2) \{ c_1 - c_2 + 2c_4 - c_5 + c_6 + c_{10} + c_5(m_1 + m_2 - 1) \} \\
& + (c_9 - c_1 - 2c_4)
\end{aligned}$$

$$\begin{aligned}
D_2 = & (m_1^2 + m_2^2)(c_2 + c_5) + a(c_1 - c_2 + 2c_4 - 2c_5 + c_6 + c_{10}) \\
& + (m_1^2 - m_2^2) \{ c_5 + c_7 + c_8 + 2c_3(m_1 - 1) \} \quad (8.9)
\end{aligned}$$

$$\begin{aligned}
D_3 = & (m_1 - m_2)^2 \{ c_2 + c_5 + c_7 + c_8 + 2c_2(m_1 - m_2 - 1) \} \\
& + (m_1 - m_2) \{ c_1 - c_2 + 2c_4 - c_5 + c_6 + c_{10} + c_5(m_1 - m_2 - 1) \} \\
& + (c_9 - 2c_4 - c_1)
\end{aligned}$$

$$\begin{aligned}
c_1 &= k_2 & c_6 &= k_2 - 2k_4 \\
c_2 &= 2k_1 & c_7 &= 2k_1 - k_2 \quad (8.10) \\
c_3 &= 3k_{10} + 3k_1 & c_8 &= 3k_{10} + k_1 - k_{11} + \frac{3k_2}{2} \\
c_4 &= k_{13} - \frac{k_2}{2} & c_9 &= k_{13} - \frac{3k_2}{2} - k_4 - 3k_{14} \\
c_5 &= 2k_{11} - 2k_1 + k_2 & c_{10} &= 2k_{11} - 2k_1 - 2k_{13} + 2k_4
\end{aligned}$$

The stresses and displacement when substituted back into the differential equation (8.1) will satisfy it within the degree of accuracy of the second order terms. Computation of numerical values of stress and displacement is contingent upon the knowledge of the strain energy function which can only be determined from experiments.

REFERENCES

1. Williams, M.L., Blatz, P.J., Schapery, R.A., "Fundamental Studies Relating to Systems Analysis of Solid Propellants," Final Report-GALCIT 101, California Institute of Technology, February 1961.
2. Dong, S.B., Pister, K.S., "Stress Analysis of Anisotropic Elastic and Viscoelastic Solids," 20th Meeting Bulletin, JANAF-ARPA-NASA Panel on Physical Properties of Solid Propellants, Vol. I, November 1961.
3. Lekhnitskii, S.G., Theory of Elasticity of an Anisotropic Body, Gosudarstvennoe Izdatel'stvo Tekhniko-Teoreticheskoi Literaturi, Moscow-Leningrad, 1950 (in Russian).
4. Alfrey, T., "Non-homogeneous Stresses in Visco-elastic Media," Quart. of Applied Math., Vol. II, No. 1, pp. 113-119, April 1944.
5. Lee, E.H., "Stress Analysis in Visco-Elastic Bodies," Quart. of Applied Math., Vol. 13, No. 2, pp. 183-190, July 1955.
6. Biot, M.A., "Dynamics of Viscoelastic Anisotropic Media," Proceedings of the Second Midwestern Conference on Solid Mechanics, pp. 94-108, 1955.
7. Spillers, W.R., "Orthotropic Viscoelastic Thick-Walled Tube," ONR Contract Nonr 266(78) Technical Report No. 9, Department of Civil Engineering and Engineering Mechanics, Columbia University, September 1961.
8. Hilton, H.H., "Anisotropic Nonhomogeneous Linear Viscoelastic Analysis," Report No. TD-16, Solid Rocket Plant of Aerojet-General Corporation, Sacramento, California, July 1961.
9. Muki, R., Sternberg, E., "On Transient Thermal Stresses in Viscoelastic Materials with Temperature-Dependent Properties," Journal of Applied Mechanics, Vol. 28, No. 2, pp. 193-207, June 1961.
10. Schapery, R.A., "Two Simple Approximate Methods of Laplace Transform Inversion for Viscoelastic Stress Analysis," GALCIT 119 Contract No. AF33(616)-8399, California Institute of Technology, Pasadena, California, Nov. 1961.

11. Green, A.E. and Adkins, J.E., Large Elastic Deformations, Oxford at the Clarendon Press, 1960.
12. Hearmon, R.F.S., An Introduction to Applied Anisotropic Elasticity, Oxford University Press, 1961.

PART II

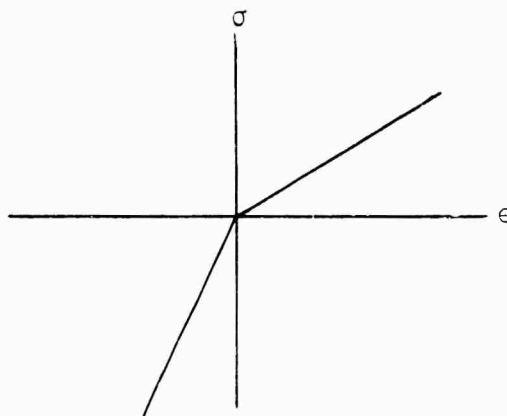
BILINEAR ELASTICITY WITH APPLICATIONS
TO THICK-WALLED CYLINDERS

by

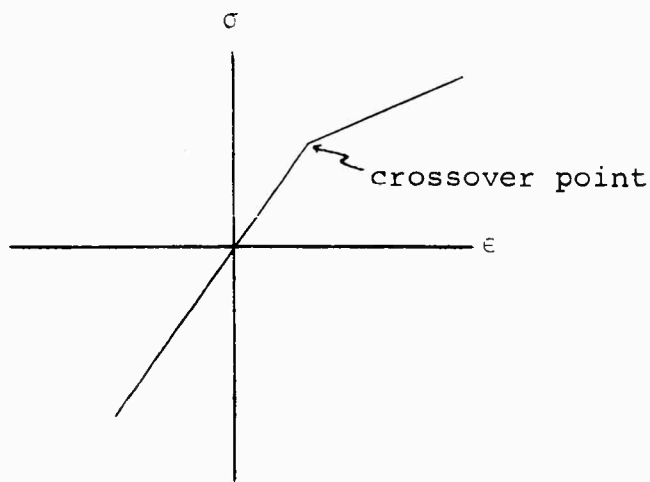
L. R. HERRMANN

INTRODUCTION

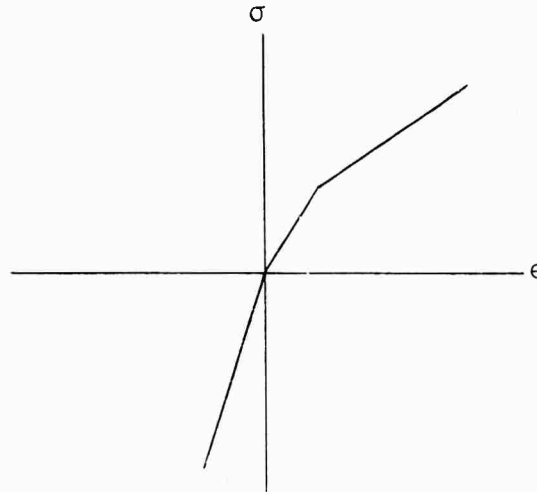
This investigation was initiated to attempt to approximate the behavior of propellants that exhibit different mechanical behavior in tension and compression. For example, one might experimentally obtain a uniaxial stress-strain curve of the form shown below:



We shall refer to the point of discontinuous rate of action as the "crossover point". In our study we have allowed this crossover point to occur at states other than the zero stress state; thus, we are able to accommodate a uniaxial stress-strain curve as shown below:



This generalization was made with the phenomenon of dewetting in mind, as it appears that dewetting usually occurs at some finite strain state. The following analysis may be easily extended to include trilinear materials without any conceptual difficulties, i.e., one might obtain a uniaxial stress-strain curve of the form:

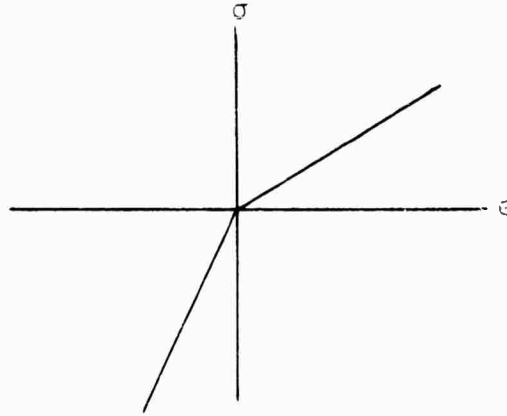


It should be noted that the crossover point in reality need not be a sharply defined point as we have pictured it **above** but the phenomenon must be capable of being approximately represented by a series of linear steps. Thus we may have a bilinear fit of experimental data as is illustrated in Figure 2. In reality what we are doing is approximating a nonlinear material response by a series of zones of linear action; thus, more appropriately this analysis might be called "elastic zone analysis". The nonlinear aspects of the problem will in general be manifested in a nonlinear algebraic equation whose solution locates the zone boundaries, see for example Eq.(2.18). Therefore, although the resulting theories are for infinitesimal strains, superposition is in general no longer valid as the resulting equations are bilinear, not linear.

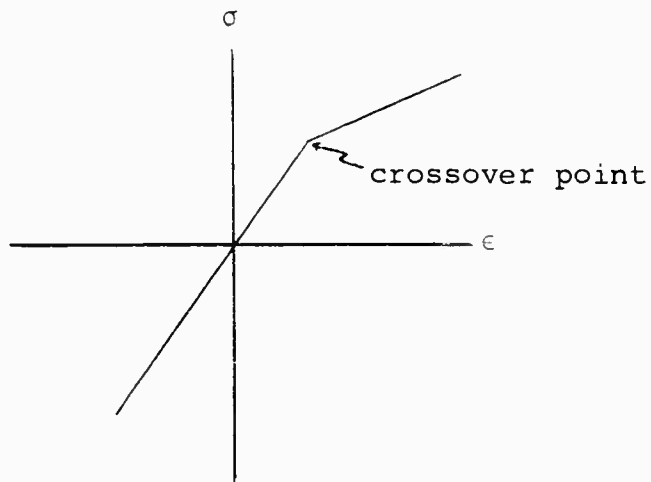
There are many ways to hypothesize a bilinear material depending on the criterion selected to define the crossover

INTRODUCTION

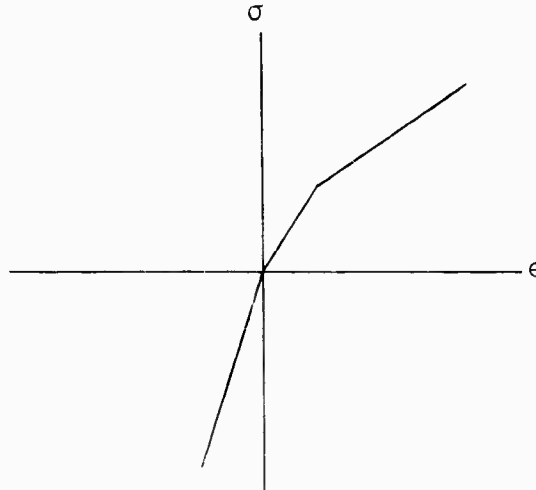
This investigation was initiated to attempt to approximate the behavior of propellants that exhibit different mechanical behavior in tension and compression. For example, one might experimentally obtain a uniaxial stress-strain curve of the form shown below:



We shall refer to the point of discontinuous rate of action as the "crossover point". In our study we have allowed this crossover point to occur at states other than the zero stress state; thus, we are able to accommodate a uniaxial stress-strain curve as shown below:



This generalization was made with the phenomenon of dewetting in mind, as it appears that dewetting usually occurs at some finite strain state. The following analysis may be easily extended to include trilinear materials without any conceptual difficulties, i.e., one might obtain a uniaxial stress-strain curve of the form:



It should be noted that the crossover point in reality need not be a sharply defined point as we have pictured it above but the phenomenon must be capable of being approximately represented by a series of linear steps. Thus we may have a bilinear fit of experimental data as is illustrated in Figure 2. In reality what we are doing is approximating a nonlinear material response by a series of zones of linear action; thus, more appropriately this analysis might be called "elastic zone analysis". The nonlinear aspects of the problem will in general be manifested in a nonlinear algebraic equation whose solution locates the zone boundaries, see for example Eq.(2.18). Therefore, although the resulting theories are for infinitesimal strains, superposition is in general no longer valid as the resulting equations are bilinear, not linear.

There are many ways to hypothesize a bilinear material depending on the criterion selected to define the crossover

point; i.e., it is somewhat analogous to the yield condition in plasticity. We shall consider three simple classes of bilinear elastic materials corresponding to the following crossover criteria:

- I) Principal strain criterion
- II) Principal stress criterion
- III) Mean stress criterion.

For the class I material we shall consider that the material passes from one linear phase of response to another as one of the principal strains passes through a critical value. We shall refer to this critical value as the "threshold" value. The first two criteria lead to the prediction of strain- or stress-induced anisotropy. This anisotropy is clearly apparent when one views the resulting constitutive equations Eqs (1.1) and (1.2). It will be noted that the preferred directions coincide with the principal stress directions and thus for that class of problems for which we do not know a priori the directions of the principal stresses, the governing equations for the class I and II materials become nearly intractable. The particular criterion that should be used to characterize a given material, of course, needs to be determined by experimental means; for example, one might analyze several different stress states as given by simple tests (see Sections 2 and 3).

It is to be noted that although we might have expected to be able to independently specify two or three elastic constants in each zone we have in totality only three independent elastic constants, as may be seen in Eqs. (1.1), (1.2) and (1.3). This restriction is not present in the proposed generalized theory of Section 7. The relationships relating the remaining constants, as found in a uniaxial test, are given by Eqs. (2.1), (2.2) and (2.3). They are different for each of the three classes of materials that we have considered and may be used as a guide in selecting the particular model to represent a given material, see Section 3.

NOTATION

(Additional notation will be explained as introduced.)

ϵ_i	Principal strain
ϵ_j^i	Strain
$e_j^i = \epsilon_j^i - \epsilon_m \delta_j^i$	Deviatoric strain
ϵ_r	Radial strain in cylindrical coordinates
ϵ_θ	Tangential strain in cylindrical coordinates
ϵ_z	Longitudinal strain in cylindrical coordinates
$\epsilon_m = \frac{1}{3} \epsilon_i^i$	Mean strain
$\theta = \epsilon_i^i$	First strain invariant
u	Radial displacement in cylindrical coordinates
σ_i	Principal stress
τ_j^i	Stress
$S_j^i = \tau_j^i - \sigma_m \delta_j^i$	Deviatoric stress
σ_r	Radial stress in cylindrical coordinates
σ_θ	Tangential stress in cylindrical coordinates
σ_z	Longitudinal stress in cylindrical coordinates

$\theta = \tau_i^i$	First stress invariant
$\sigma_m = \frac{1}{3}\tau_i^i$	Mean stress
k_i	Elastic modulus
c_i	Elastic compliance
B	Bulk modulus
μ	Shear modulus
n	Class III elastic constant
E	Young's modulus
ν	Poisson's ratio
$\bar{\mu}$	Shear modulus of the motor case
$\bar{\nu}$	Poisson's ratio of the motor case
α	Thermal coefficient of linear expansion (assumed temperature independent)
e	Principal strain threshold value
s	Principal stress threshold value
h	Mean stress threshold value
T	Absolute temperature
T_o	Reference temperature

$T^*=T-T_o$	Relative temperature
T_a	Inner wall temperature
T_b	Outer wall temperature
a	Inner radius of thick-walled cylinder
b	Outer radius of thick-walled cylinder
$c = \frac{b}{a}$	Radii ratio
t	Thickness of motor case
P_i	Pressure on inner wall of thick-walled cylinder
P'	Interface pressure between thick-walled cylinder and motor case
x	Radial location of zone boundary
m_i	Exponent in anisotropic solution
β	Exponent in anisotropic solution
δ_j^i	Kronecker delta

BILINEAR ELASTIC THEORY

1. Bilinear Constitutive Equations

The equilibrium and strain displacement equations remain unchanged from classical elasticity and therefore need not be considered here. The constitutive equations* for class I material become (see Section 5):

$$\text{Zone 1} \quad \epsilon_1 \leq e, \epsilon_2 \leq e, \epsilon_3 \leq e$$

$$\sigma_1 = c_1 \epsilon_1 + c_2 \epsilon_2 + c_2 \epsilon_3$$

$$\sigma_2 = c_2 \epsilon_1 + c_1 \epsilon_2 + c_2 \epsilon_3$$

$$\sigma_3 = c_2 \epsilon_1 + c_2 \epsilon_2 + c_1 \epsilon_3$$

$$\text{Zone 2} \quad \epsilon_1 \geq e, \epsilon_2 \leq e, \epsilon_3 \leq e$$

$$\sigma_1 = c_3 \epsilon_1 + c_2 \epsilon_2 + c_2 \epsilon_3 + e(c_1 - c_3)$$

(1.1)

$$\sigma_2 = c_2 \epsilon_1 + c_1 \epsilon_2 + c_2 \epsilon_3$$

$$\sigma_3 = c_2 \epsilon_1 + c_2 \epsilon_2 + c_1 \epsilon_3$$

$$\text{Zone 3} \quad \epsilon_1 \geq e, \epsilon_2 \geq e, \epsilon_3 \leq e$$

$$\sigma_1 = c_3 \epsilon_1 + c_2 \epsilon_2 + c_2 \epsilon_3 + e(c_1 - c_3)$$

$$\sigma_2 = c_2 \epsilon_1 + c_3 \epsilon_2 + c_2 \epsilon_3 + e(c_1 - c_3)$$

$$\sigma_3 = c_2 \epsilon_1 + c_2 \epsilon_2 + c_1 \epsilon_3$$

(continued)

*For simplicity of presentation the temperature terms have been omitted, but in subsequent sections we shall include them.

Zone 4 $\epsilon_1 \geq e$, $\epsilon_2 \geq e$, $\epsilon_3 \geq e$

$$\begin{aligned}\sigma_1 &= c_3 \epsilon_1 + c_2 \epsilon_2 + c_2 \epsilon_3 + e(c_1 - c_3) \\ \sigma_2 &= c_2 \epsilon_1 + c_3 \epsilon_2 + c_2 \epsilon_3 + e(c_1 - c_3) \\ \sigma_3 &= c_2 \epsilon_1 + c_2 \epsilon_2 + c_3 \epsilon_3 + e(c_1 - c_3)\end{aligned}\tag{1.1}$$

The constitutive equations for class II material are (see Section 5):

Zone 1 $\sigma_1 \leq s$, $\sigma_2 \leq s$, $\sigma_3 \leq s$

$$\begin{aligned}\epsilon_1 &= k_1 \sigma_1 + k_2 \sigma_2 + k_2 \sigma_3 \\ \epsilon_2 &= k_2 \sigma_1 + k_1 \sigma_2 + k_2 \sigma_3 \\ \epsilon_3 &= k_2 \sigma_1 + k_2 \sigma_2 + k_1 \sigma_3\end{aligned}$$

Zone 2 $\sigma_1 \geq s$, $\sigma_2 \leq s$, $\sigma_3 \leq s$

$$\begin{aligned}\epsilon_1 &= k_3 \sigma_1 + k_2 \sigma_2 + k_2 \sigma_3 + s(k_1 - k_3) \\ \epsilon_2 &= k_2 \sigma_1 + k_1 \sigma_2 + k_2 \sigma_3 \\ \epsilon_3 &= k_2 \sigma_1 + k_2 \sigma_2 + k_1 \sigma_3\end{aligned}\tag{1.2}$$

Zone 3 $\sigma_1 \geq s$, $\sigma_2 \geq s$, $\sigma_3 \leq s$

$$\epsilon_1 = k_3 \sigma_1 + k_2 \sigma_2 + k_2 \sigma_3 + s(k_1 - k_3)$$

(continued)

$$\begin{aligned}\epsilon_2 &= k_2 \sigma_1 + k_3 \sigma_2 + k_2 \sigma_3 + s(k_1 - k_3) \\ \epsilon_3 &= k_2 \sigma_1 + k_2 \sigma_2 + k_1 \sigma_3\end{aligned}\quad (1.2)$$

$$\text{Zone 4} \quad \sigma_1 \geq s, \quad \sigma_2 \geq s, \quad \sigma_3 \geq s$$

$$\begin{aligned}\epsilon_1 &= k_3 \sigma_1 + k_2 \sigma_2 + k_2 \sigma_3 + s(k_1 - k_3) \\ \epsilon_2 &= k_2 \sigma_1 + k_3 \sigma_2 + k_2 \sigma_3 + s(k_1 - k_3) \\ \epsilon_3 &= k_2 \sigma_1 + k_2 \sigma_2 + k_3 \sigma_3 + s(k_1 - k_3)\end{aligned}$$

For any given zone above we may write

$$\epsilon^{ij} = k_{km}^{ij} \tau^{km} + D^{ij},$$

then for an arbitrary set of orthogonal axes in that particular zone

$$\bar{\epsilon}^{ij} = \bar{k}_{km}^{ij} \bar{\tau}^{km} + \bar{D}^{ij}$$

where we may obtain \bar{k}_{km}^{ij} and \bar{D}^{ij} from k_{km}^{ij} and D^{ij} by means of fourth and second rank tensor transformations respectively; we set

$$k_{km}^{ij} = 0 \quad \text{for } i \neq j \quad \text{or } k \neq m \quad \text{and } D^{ij} = 0 \quad \text{for } i \neq j.$$

The constitutive equations for class III materials are (see Section 5):

$$\text{Zone 1} \quad \sigma_m \leq h$$

$$\tau_j^i = (B - \frac{2\mu}{3}) \theta \delta_j^i + 2\mu \epsilon_j^i$$

or

$$\epsilon_j^i = \frac{1}{3} \left(\frac{1}{3B} - \frac{1}{2\mu} \right) \theta \delta_j^i + \frac{1}{2\mu} \tau_j^i$$

Zone 2

$$\sigma_m \geq h$$

$$\tau_j^i = (nB - \frac{2}{3}\mu) \theta \delta_j^i + 2\mu \epsilon_j^i + h(1 - n) \delta_j^i \quad (1.3)$$

or

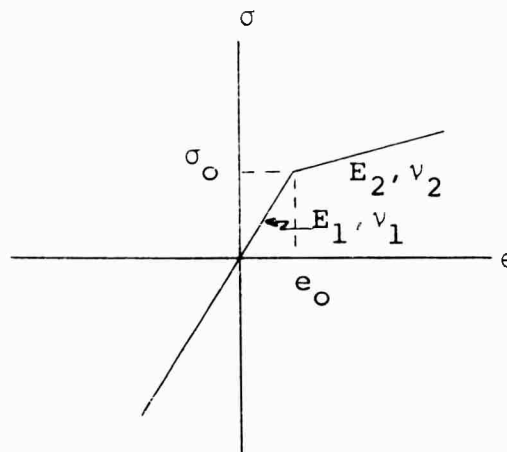
$$\epsilon_j^i = \frac{1}{3} \left(\frac{1}{3nB} - \frac{1}{2\mu} \right) \theta \delta_j^i + \frac{1}{2\mu} \tau_j^i - \frac{h(1 - n)}{3nB} \delta_j^i$$

2. Elementary Solutions

We shall assume for simplicity that $s > 0$, $e > 0$ and $h > 0$.

We first consider the analysis of some simple tests that may be used to determine the proper threshold criterion and the appropriate elastic constants for a given material; for example, see Section 3.

Uniaxial Test



Class I

$$c_1 = \frac{(1 - v_1) E_1}{(1 - 2v_1)(1 + v_1)}$$

$$c_2 = \frac{v_1 E_1}{(1 - 2v_1)(1 + v_1)}$$

$$c_3 = \frac{E_2(1 - v_2)}{(1 - 2v_2)(1 + v_2)}$$

$$e = e_o$$

In addition for a Class I representation from continuity requirements the following relationship must be valid (see Section 5)

$$\frac{E_2 v_2}{(1 - 2v_2)(1 + v_2)} = \frac{E_1 v_1}{(1 - 2v_1)(1 + v_1)} \quad (2.1)$$

Class II

$$k_1 = \frac{1}{E_1}$$

$$k_3 = \frac{1}{E_2}$$

$$k_2 = -\frac{v_1}{E_1}$$

$$s = \sigma_o$$

In addition for a Class II representation as a result of continuity requirements the following relationship must be valid (see Section 5):

$$\frac{\nu_1}{E_1} = \frac{\nu_2}{E_2} \quad (2.2)$$

Class III

$$\mu_1 = \frac{E_1}{2(1 + \nu_1)}$$

$$B_1 = \frac{E_1}{3(1 - 2\nu_1)}$$

$$n = \frac{E_2}{3B_1(1 - 2\nu_2)}$$

$$h = \frac{\sigma_o}{3}$$

Additionally for a Class III representation from continuity the following relationship must be valid:

$$\frac{E_1}{2(1 + \nu_1)} = \frac{E_2}{2(1 + \nu_2)} \quad (2.3)$$

Biaxial Test

$$(\sigma_1 = \sigma_2, \sigma_3 = 0)$$

Class I

Zone I

$$\epsilon_1 \leq e$$

$$\epsilon_3 = -\frac{2c_2}{c_1} \epsilon_1$$

$$\sigma_1 = (c_1 + c_2 - \frac{2c_2^2}{c_1}) \epsilon_1$$

Zone 3

$$\epsilon_1 \geq e$$

$$\epsilon_3 = -\frac{2c_2}{c_1} \epsilon_1$$

$$\sigma_1 = (c_3 + c_2 - \frac{2c_2^2}{c_1}) \epsilon_1 + e(c_1 - c_3)$$

Class II

Zone 1

$$\sigma_1 \leq s$$

$$\epsilon_1 = (k_1 + k_2) \sigma_1$$

$$\epsilon_3 = 2k_2 \sigma_1$$

Zone 3

$$\sigma_1 \geq s$$

$$\epsilon_1 = (k_3 + k_2) \sigma_1 + s(k_1 - k_3)$$

$$\epsilon_3 = 2k_2 \sigma_1$$

Class III

Zone 1

$$\sigma_1 \leq \frac{3h}{2}$$

$$\epsilon_1 = \frac{1}{3} \left(\frac{2}{3B} + \frac{1}{2\mu} \right) \sigma_1$$

$$\epsilon_3 = \frac{2}{3} \left(\frac{1}{3B} - \frac{1}{2\mu} \right) \sigma_1$$

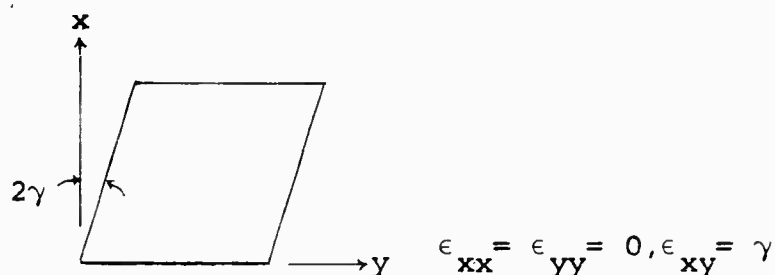
Zone 2

$$\sigma_1 \geq \frac{3h}{2}$$

$$\epsilon_1 = \frac{1}{3} \left(\frac{2}{3nB} + \frac{1}{2\mu} \right) \sigma_1 - \frac{h(1-n)}{3nB}$$

$$\epsilon_3 = \frac{2}{3} \left(\frac{1}{3nB} - \frac{1}{2\mu} \right) \sigma_1 - \frac{h(1-n)}{3nB}$$

Pure Shear Strain Test (see Section 6)



Class II

Zone 1

$$\sigma_1 \leq s \quad \text{or} \quad \gamma \leq (k_1 - k_2)s$$

$$\tau_{xx} = \tau_{yy} = 0$$

$$\tau_{xy} = \frac{1}{k_1 - k_2} \gamma$$

Zone 2

$$\sigma_1 \geq s \quad \text{or} \quad \gamma \geq (k_1 - k_2)s \quad (2.4)$$

$$\begin{aligned} \tau_{xx} = \tau_{yy} &= \frac{2(k_3 - k_1)((k_1 - k_2)s - \gamma)}{4k_1k_3 - k_2(k_1 + k_3 + 2k_2)} \\ \tau_{xy} &= \frac{s(k_3 - k_1)(2k_1 + k_2) + 2\gamma(k_1 + k_3 + k_2)}{4k_1k_3 - k_2(k_1 + k_3 + 2k_2)} \end{aligned}$$

Thus the threshold value of γ is

$$\gamma_c = (k_1 - k_2)s.$$

Class III Only one zone possible, $\sigma_m \leq s$ (as $\sigma_m \equiv 0$)

$$\tau_{xx} = \tau_{yy} = 0 \quad (2.5)$$

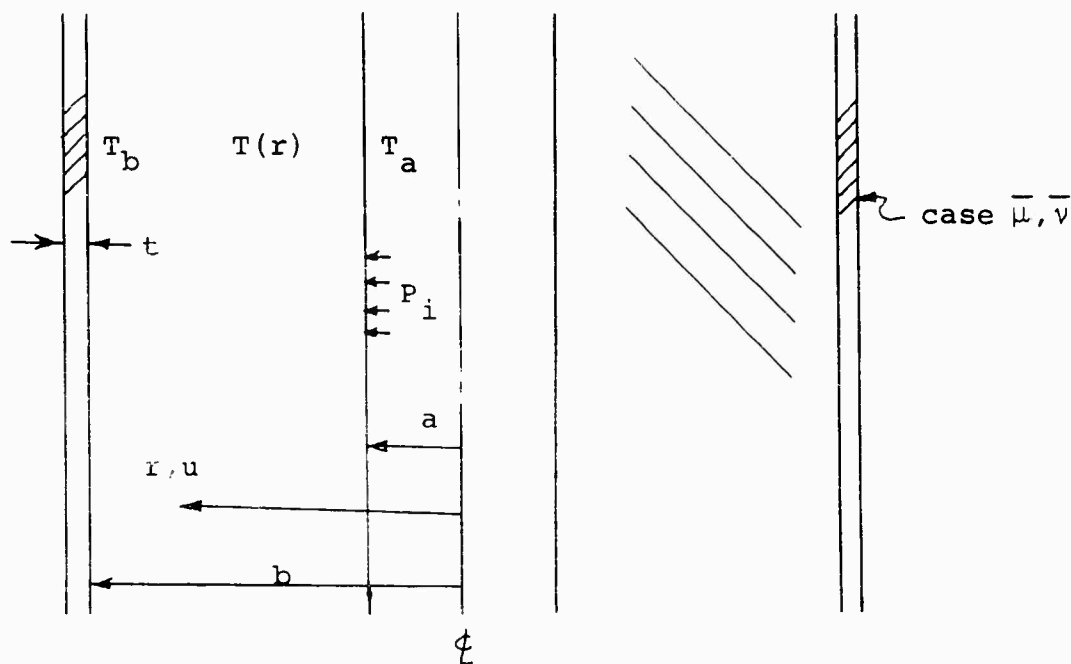
$$\tau_{xy} = 2\mu\gamma$$

Inspecting Eqs. (2.4) and (2.5) we see that the results of a pure shear strain test would clearly show whether or not stress-induced anisotropy is present in a given material.

Axially Symmetric Plane Strain Thick-walled Cylinder Problems

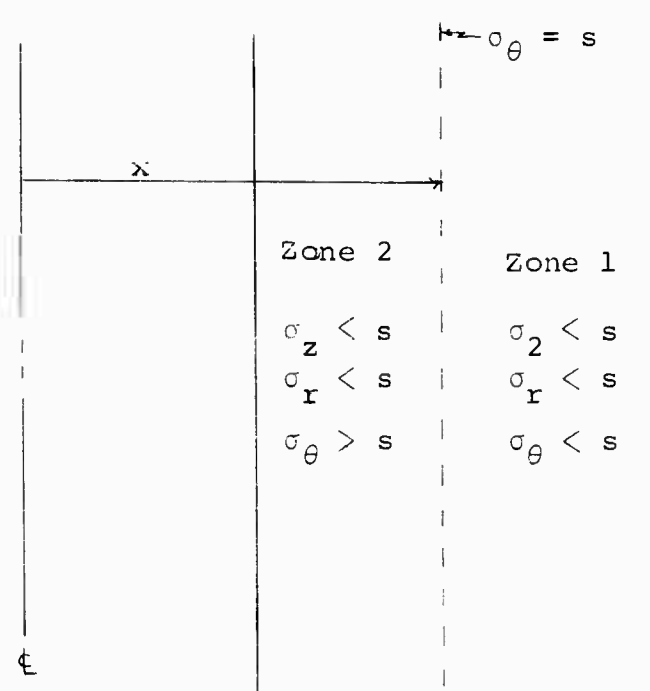
A case-bonded thermoelastic cylinder in plane strain is shown below with identifying notation. As shall be shown later, Class I material appears to be a very poor model for **actual** propellants, therefore in the sequel we shall consider only Classes II and III. Depending upon the relative magnitudes of the various material parameters we may have an arbitrary distribution of zones; thus, one cannot anticipate all situations that may arise in a given physical problem. Therefore, we shall only be able to consider a few sample problems

to illustrate the solution procedure that needs to be applied in a given problem.



Class II Material

Pressurization of a thick-walled cylinder, $\bar{\mu} = \bar{\nu} = 0$, with constant temperature, $T_a = T_b = T(r) = T_o$. For small internal pressure P_i , i.e., $P_i \leq P_c$, σ_r , σ_θ and σ_z are all less than the threshold value s ; hence, the body behaves isotropically and the solution is well known [1]. At $P_i = P_c$, $\sigma_\theta(a) = s$ and a zone boundary arises at $r = a$ and propagates through the cylinder as P_i increases above P_c , i.e., we have



This state exists (assuming that $E_1 \leq E_2$, see Section 6) if

$$s \left(\frac{1}{2} c^{-m_2} + \frac{1}{2} c^{-m_1} - 1 \right) \leq P_i \leq s \frac{c^2 - 1}{c^2 + 1}.$$

The resulting stress distributions will be as follows:

Zone 2: $a \leq r \leq x$

$$\sigma_r = - (P_i + s) \frac{\left(\frac{r}{x}\right)^{m_1} + \left(\frac{r}{x}\right)^{m_2}}{\left(\frac{a}{x}\right)^{m_1} + \left(\frac{a}{x}\right)^{m_2}} + s$$

$$\sigma_\theta = \sigma_r + r \frac{d\sigma_r}{dr}$$

$$u = r(k_2 - \frac{k_2^2}{k_1})\sigma_r + r(k_3 - \frac{k_2^2}{k_1})\sigma_\theta + s(k_1 - k_3)r$$

$$m_1 = -1 - \beta$$

$$m_2 = -1 + \beta$$

where

$$\beta = \sqrt{\frac{k_1^2 - k_2^2}{k_1 k_3 - k_2^2}}$$

Zone 1: $x \leq r \leq b$

$$\sigma_r = s \frac{1}{(\frac{b}{x})^2 + 1} \left[1 - (\frac{b}{r})^2 \right]$$

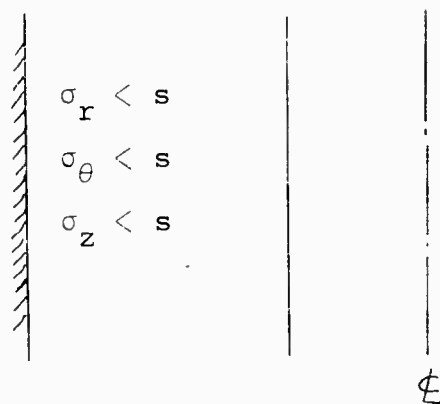
$$\sigma_\theta = \sigma_r + r \frac{d\sigma_r}{dr}$$

$$u = r(k_2 - \frac{k_2^2}{k_1})\sigma_r + r(k_1 - \frac{k_2^2}{k_1})\sigma_\theta$$

where x is determined from the equation

$$\frac{c^2}{(\frac{x}{a})^2 + c^2} = \frac{\frac{P_i}{s} + 1}{(\frac{a}{x})^{m_1} + (\frac{a}{x})^{m_2}}$$

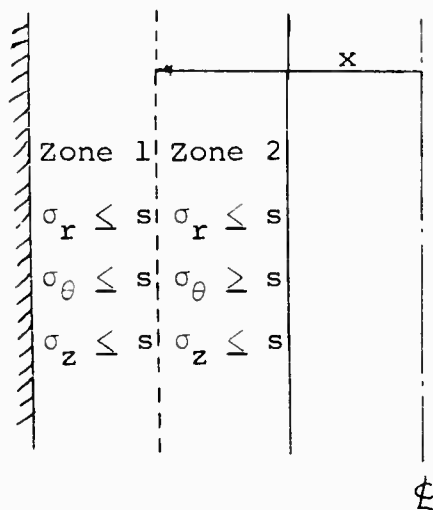
Uniform temperature drop of a thick-walled cylinder bonded to a rigid case, $\bar{\mu} = \infty$, $T_a = T_b = T(r) = T$. Let $T^* = T - T_0$. For $T^* \geq T_1$ we have



The material behaves isotropically and the solution is well known. When $T^* = T_1$, $\sigma_\theta(a) = s$ hence, a zone boundary arises (see Section 6) when

$$T^* = T_1 = -\frac{s}{2\alpha} \left[\frac{k_1}{c} + (k_1 + 2k_2) \right]$$

For $T_2 \leq T^* \leq T_1$, we have



In Zone 1

$$\sigma_{\theta} = A - \frac{D}{r^2} \quad (2.6)$$

$$\sigma_r = A + \frac{D}{r^2} \quad (2.7)$$

$$\sigma_z = -\frac{1}{k_1} (\alpha T^* + 2k_2 A) \quad (2.8)$$

$$u = (k_2 + k_1 - 2 \frac{k_2^2}{k_1}) Ar + (k_2 - k_1) \frac{D}{r} + \alpha T^* r (1 - \frac{k_2}{k_1}) \quad (2.9)$$

$$D = x^2 (A - s) \quad (2.10)$$

$$A = \frac{k_1 s (\frac{x}{b})^2 + \alpha T^*}{k_1 (\frac{x}{b})^2 - (k_1 + 2k_2)} \quad (2.11)$$

In Zone 2

$$\sigma_r = \frac{F}{r^{\beta+1}} + H r^{\beta-1} + s \quad (2.12)$$

$$\sigma_{\theta} = -\frac{\beta F}{r^{\beta+1}} + \beta H r^{\beta-1} + s \quad (2.13)$$

$$u = \left[k_2 - \beta k_3 + (\beta - 1) \frac{k_2^2}{k_1} \right] \frac{F}{r^{\beta}} + \left[k_2 + \beta k_3 - (\beta + 1) \frac{k_2^2}{k_1} \right] H r^{\beta} + s \left[k_2 + k_1 - 2 \frac{k_2^2}{k_1} \right] r + \alpha T^* (1 - \frac{k_2}{k_1}) r \quad (2.14)$$

$$F = Hx^{2\beta} \quad (2.15)$$

$$H = - \frac{as}{a^\beta + x^{2\beta} a^{-\beta}} \quad (2.16)$$

$$\beta = \sqrt{\frac{k_1^2 - k_2^2}{k_1 k_3 - k_2^2}} \quad (2.17)$$

$$T_2 = s \left[\frac{2k_2}{c(c^{-\beta} + c^\beta)} - (2k_2 + k_1) \right]$$

where one finds x from the equation

$$\frac{k_1 s \left(\frac{x}{b}\right)^2 + \alpha T^*}{k_1 \left(\frac{x}{b}\right)^2 - (k_1 + 2k_2)} + \frac{\left(\frac{x}{b}\right)^{\beta-1} \frac{s}{c}}{c^{-\beta} + \left(\frac{x}{b}\right)^{2\beta} c^\beta} = s. \quad (2.18)$$

Class III Material

Pressurization of a case-bonded cylinder. When $\sigma_m \leq h$, (see Section 6) we have the usual classical solution, [1]. When $\sigma_m \geq h$, i.e., $P_i \geq P_c$, we have a second zone of action (for this particular problem the whole cylinder passes from one zone to the other at the same time), where

$$P_c = \frac{\frac{\mu(c^2 - 1)h}{c^2} \left[3x_1 - \frac{(1-n)}{3nB} \right] - \frac{h(1-n)}{c^2 + 3nBx_1} + \frac{3(1-\bar{\nu})b\mu nBx_1}{\bar{\mu}t}}{\frac{1}{c^2} - \frac{\left(\frac{1}{3nBx_1} + 1\right)}{\mu(c^2 - 1) \left[\frac{c^2 + 3nBx_1}{3nBx_1\mu(c^2 - 1)} + \frac{(1-\bar{\nu})b}{\bar{\mu}t} \right]}}$$

$$x_1 = \frac{1}{3} \left(\frac{1}{3nB} + \frac{1}{\mu} \right)$$

$$\sigma_r = A + \frac{D}{r^2}$$

$$\sigma_\theta = A - \frac{D}{r^2}$$

$$u = \frac{r}{x_1} \left[\frac{1}{6\mu} \left(\frac{1}{3nB} - \frac{1}{2\mu} \right) \sigma_r + \frac{1}{6\mu} \left(\frac{2}{3nB} + \frac{1}{2\mu} \right) \sigma_\theta - \frac{h(1-n)}{6\mu nB} \right]$$

$$A = \frac{P_i - c^2 P'}{c^2 - 1}$$

$$D = \frac{b^2}{c^2 - 1} (P' - P_i)$$

$$P' = \frac{\frac{P_i}{(c^2 - 1)} \left[\frac{1}{3nBx_1} + 1 \right] - \frac{h(1-n)}{3nBx_1}}{\frac{c^2 + 3nBx_1}{3nBx_1(c^2 - 1)} + \frac{\mu(1-\bar{\nu})b}{\bar{\mu}t}}$$

Uniform temperature drop of a thick-walled cylinder bonded to a rigid case, $\bar{\mu} = \infty$. Again for $T^* \geq T_c$ we have the usual classical solution. As $T^* \rightarrow T_c$ the whole cylinder passes from one linear mode of action to another and we find

$$\sigma_r = A + \frac{D}{r^2} \quad (2.19)$$

$$\sigma_{\theta} = A - \frac{D}{r^2} \quad (2.20)$$

$$u = \frac{3}{2(\mu + 3nB)} Ar - \frac{1}{2\mu} \frac{D}{r} + \left(\alpha T^* - \frac{h(1-n)}{3nB} \right) \frac{9nBr}{2(\mu + 3nB)} \quad (2.21)$$

$$D = -a^2 A \quad (2.22)$$

$$A = \frac{h(1-n) - 3\alpha T^* nB}{1 + \frac{1}{3c^2} \left(1 + \frac{3nB}{\mu} \right)} \quad (2.23)$$

$$T_c = -\frac{h}{\alpha} \frac{\frac{1}{\mu} + \frac{1}{3B}}{1 + \frac{3B}{\mu \left[1 + \frac{1}{3c^2} \left(1 + \frac{3B}{\mu} \right) \right]}}$$

3. Model Fitting Considerations for a Particular Material

The plotted points in Figures 1 and 2 represent experimental data for a typical propellant that apparently experiences the dewetting phenomenon. The solid lines represent bilinear approximation of the uniaxial response. We find

$$\begin{array}{ll} B_1 = 74,600 \text{ psi} & k_1 = 1.243 \times 10^{-3} \text{ in}^2/\text{lb} \\ B_2 = 8,920 \text{ psi} & \text{which yields } k_2 = -.621 \times 10^{-3} \text{ in}^2/\text{lb} \\ E_1 = 805 \text{ psi} & k_3 = 1.276 \times 10^{-3} \text{ in}^2/\text{lb.} \\ E_2 = 714 \text{ psi} & \end{array}$$

As the curves yielding B_1 , B_2 and E_1 are very easy to place accurately, we select these values as fundamental and calculate E_2 from the continuity relationships* (2.1), (2.2) and (2.3) respectively. We thus obtain for

$$\text{Class I} \quad E_2 = 6090 \text{ psi}$$

$$\text{Class II} \quad E_2 = 784 \text{ psi}$$

$$\text{Class III} \quad E_2 = 797 \text{ psi.}$$

Comparing these values of E_2 with the experimental value of E_2 in Fig. 1, we see that the Class II and III models fit the experimental results much better than the Class I model. It is also apparent that the results from one simple test are not sufficient to select a crossover criterion for a given material. For example the results of the uniaxial test reported above would indicate that the above material may be represented by either a Class II or Class III model, but as we shall see in the next section, the two models give very different results when utilized in the solution of another problem. Thus it must be emphasized that one needs to examine the results of more than one stress state. If one were to perform a biaxial test ($\sigma_1 = \sigma_2 = \sigma$ and $\sigma_3 = 0$) on the above material and if it were to behave as a Class II material we would obtain Figures 3 and 4 whereas if it were to behave as a Class III material we would obtain Figures 5 and 6. The volume changes for the two postulated behaviors are compared in Figure 7. Although we do not have any biaxial test data taken from the same material as the uniaxial data presented

* We have called these equations continuity relationships since they arise from the fact that we have required a continuous action across the zone boundaries.

in Figures 1 and 2 we do have some biaxial test data taken from a somewhat similar propellant, as given in Figure 8. It will be noted that if we represent this data by a bilinear response, the crossover point would be much lower than predicted by the Class II representation (see Figure 4) for the first type of propellant. The crossover point would be slightly higher than that given by the Class III representation (see Figure 6), for the first propellant. If we make the crossover occur at the value as given by the Class III biaxial test (see Figure 6) the fit is still rather good (see Figure 9). From these very crude data, tentatively, it appears that the bilinear phenomenon may be represented by the Class III criterion. However it must be emphasized that the above conclusion is a mere conjecture as it is based upon only two types of tests performed upon slightly different propellant formulations, tests which were not equilibrium tests and therefore are not a true indication of the elastic equilibrium action (also the accuracy of the tests is somewhat in question). It should be noted that the biaxial volume changes are about ten times greater than expected, see Figures 6 and 8; this may be due to one of the following causes: (1) different propellant formulations, (2) rate effects and/or (3) experimental inaccuracies. In light of these considerations it must be pointed out that the above analysis is merely indicative of the type of analysis and experiments that must be made to characterize the bilinear action of a given propellant.

4. Numerical Example

Making use of the elastic constants, obtained by fitting first a Class II then a Class III model to the uniaxial test data of Figures 1 and 2, we have evaluated some of the dependent

variables that arise in the problem of the uniform temperature drop of a thick-walled cylinder bonded to a rigid case using the results from Section 2. The results are plotted in Figures 10 - 19. For the Class II representation the material behaves isotropically down to a temperature of 39.6°F at which time $\sigma_{\theta}(a) = s$, hence a zone boundary arises at $r = a$. As the material is further cooled this zone boundary moves across the cylinder and reaches the outer boundary at $T = 0^{\circ}\text{F}$ (see Figure 10), at this point $\sigma_z(b) = s$; thus a new zone boundary arises and proceeds toward $r = a$. Although the action within a given zone is linear, the fact that the zone boundary is moving results in a nonlinear response (see Figure 15).

One will note that the effects of the stress-induced anisotropy for this problem are very small and the results are nearly coincidental with the results obtained by assuming isotropic behavior throughout (see the dotted lines in Figures 11 - 15).

For the Class III representation of the same material the zone boundary arises throughout the cylinder at $T = 53^{\circ}\text{F}$ and thus the response is in two linear segments, see Figure 16. In this case the resulting response is considerably different from that obtained by ignoring bilinear effects (see the dotted lines). Comparing Figures 11 - 15 to Figures 16 - 19, respectively, one will see the considerable difference in results obtained by considering that the material behaves as a Class II or Class III model. As a uniaxial test tended to indicate that either model would suitably represent the material, the above results once again emphasize the need to consider several stress states in selecting an appropriate model for a given material. The data used in the previous calculations were as follows:

$c = 2.5, 10$ (as indicated on the Figures)

$\bar{\mu} = \infty$

$\bar{\alpha} = 0$

$\alpha = 6.0 \times 10^{-5} \text{ in/in}^{\circ}\text{F}$

$B = 74,600 \text{ psi}$

$n = .1195$

$\mu = 268 \text{ psi}$

$h = 30 \text{ psi}$

$k_1 = 1.243 \times 10^{-3} \text{ in}^2/\text{lb}$

$k_2 = -.621 \times 10^{-3} \text{ in}^2/\text{lb}$

$k_3 = 1.276 \times 10^{-3} \text{ in}^2/\text{lb}$

$s = 90 \text{ psi}$

APPENDIX

5. Derivation of Bilinear Constitutive Equations

As the derivation of the constitutive equations for a Class I material is exactly paralleled by the derivation of the constitutive equations for a Class II material we shall only present the latter.

In the derivation of the governing field equations for a Class II bilinear material we shall assume that the material is at all time phenomenologically continuous and that within each zone of action it is linearly elastic and homogeneous. Thus the equilibrium equations and strain displacement relations are identical to those for classical elasticity.

Let the criterion for passage from one mode of action to another be the passage of the value of one of the principal stresses through the threshold value s . Thus we identify four zones, i.e.,

$$1. \quad \sigma_1 < s, \sigma_2 < s, \sigma_3 < s$$

$$2. \quad \sigma_1 > s, \sigma_2 < s, \sigma_3 < s$$

$$3. \quad \sigma_1 > s, \sigma_2 > s, \sigma_3 < s$$

$$4. \quad \sigma_1 > s, \sigma_2 > s, \sigma_3 > s.$$

Zones 1 and 4 will be isotropic; zones 2 and 3 will be anisotropic. Thus we may write

$$\begin{aligned} \text{Zone 1} \quad & \sigma_1 < s, \sigma_2 < s, \sigma_3 < s \\ & \epsilon_1 = k_1 \sigma_1 + k_2 \sigma_2 + k_2 \sigma_3 \\ & \epsilon_2 = k_2 \sigma_1 + k_1 \sigma_2 + k_2 \sigma_3 \\ & \epsilon_3 = k_2 \sigma_1 + k_2 \sigma_2 + k_1 \sigma_3 \end{aligned} \tag{5.1}$$

$$\begin{aligned}
\text{Zone 2} \quad & \sigma_1 > s, \sigma_2 < s, \sigma_3 < s \\
& \epsilon_1 = k_3\sigma_1 + k_4\sigma_2 + k_4\sigma_3 + D_1 \\
& \epsilon_2 = k_4\sigma_1 + k_5\sigma_2 + k_6\sigma_3 + D_2 \\
& \epsilon_3 = k_4\sigma_1 + k_6\sigma_2 + k_5\sigma_3 + D_3
\end{aligned}$$

$$\begin{aligned}
\text{Zone 3} \quad & \sigma_1 > s, \sigma_2 > s, \sigma_3 < s \\
& \epsilon_1 = k_7\sigma_1 + k_8\sigma_2 + k_9\sigma_3 + D_3 \\
& \epsilon_2 = k_8\sigma_1 + k_7\sigma_2 + k_9\sigma_3 + D_3 \\
& \epsilon_3 = k_9\sigma_1 + k_9\sigma_2 + k_{10}\sigma_3 + D_4
\end{aligned} \tag{5.1}$$

$$\begin{aligned}
\text{Zone 4} \quad & \sigma_1 > s, \sigma_2 > s, \sigma_3 > s \\
& \epsilon_1 = k_{11}\sigma_1 + k_{12}\sigma_2 + k_{12}\sigma_3 + D_5 \\
& \epsilon_2 = k_{12}\sigma_1 + k_{11}\sigma_2 + k_{12}\sigma_3 + D_5 \\
& \epsilon_3 = k_{12}\sigma_1 + k_{12}\sigma_2 + k_{11}\sigma_3 + D_5.
\end{aligned}$$

To insure a continuous* passage from one mode of action to another we must obtain relationships for the "interzone" (i.e. when $\sigma_i = s$) which are independent of the path traveled in reaching the interzone, i.e., the relations of Zone 1 as $\sigma_1 \rightarrow s^-$ must be identical to those of Zone 2 as $\sigma_1 \rightarrow s^+$, etc. Equating the constitutive equations of Zone 1 and Zone 2

* A proposed generalization of the bilinear theory in which this condition is relaxed is outlined in Section 7.

as $\sigma_1 \rightarrow s$ we obtain

$$k_4 = k_2 \quad (5.2)$$

$$D_1 = s(k_1 - k_3) \quad (5.3)$$

$$k_5 = k_1 \quad (5.4)$$

$$k_6 = k_2 \quad (5.5)$$

$$D_2 = 0. \quad (5.6)$$

Equating the constitutive equations of Zone 2 and Zone 3 as $\sigma_2 \rightarrow s$ and using Equations (5.2) to (5.6), we obtain

$$k_7 = k_3 \quad (5.7)$$

$$k_9 = k_2 \quad (5.8)$$

$$k_8 = k_2 \quad (5.9)$$

$$D_3 = s(k_1 - k_3) \quad (5.10)$$

$$D_4 = 0 \quad (5.11)$$

$$k_{10} = k_1. \quad (5.12)$$

Equating the constitutive equations of Zone 3 and Zone 4 as $\sigma_3 \rightarrow s$ we obtain

$$\begin{aligned} k_{11} &= k_3 \\ k_{12} &= k_2 \end{aligned} \quad (5.13)$$

$$D_5 = s(k_1 - k_3).$$

Using the above relationships we may write Equation (5.1) as

$$\text{Zone 1} \quad \sigma_1 \leq s, \sigma_2 \leq s, \sigma_3 \leq s$$

$$\epsilon_1 = k_1 \sigma_1 + k_2 \sigma_2 + k_2 \sigma_3$$

$$\epsilon_2 = k_2 \sigma_1 + k_1 \sigma_2 + k_2 \sigma_3$$

$$\epsilon_3 = k_2 \sigma_1 + k_2 \sigma_2 + k_1 \sigma_3$$

$$\text{Zone 2} \quad \sigma_1 \geq s, \sigma_2 \leq s, \sigma_3 \leq s$$

$$\epsilon_1 = k_3 \sigma_1 + k_2 \sigma_2 + k_2 \sigma_3 + s(k_1 - k_3)$$

$$\epsilon_2 = k_2 \sigma_1 + k_1 \sigma_2 + k_2 \sigma_3$$

$$\epsilon_3 = k_2 \sigma_1 + k_2 \sigma_2 + k_1 \sigma_3$$

(5.14)

$$\text{Zone 3} \quad \sigma_1 \geq s, \sigma_2 \geq s, \sigma_3 \leq s$$

$$\epsilon_1 = k_3 \sigma_1 + k_2 \sigma_2 + k_2 \sigma_3 + s(k_1 - k_3)$$

$$\epsilon_2 = k_2 \sigma_1 + k_3 \sigma_2 + k_2 \sigma_3 + s(k_1 - k_3)$$

$$\epsilon_3 = k_2 \sigma_1 + k_2 \sigma_2 + k_1 \sigma_3$$

$$\text{Zone 4} \quad \sigma_1 \geq s, \sigma_2 \geq s, \sigma_3 \geq s$$

$$\epsilon_1 = k_3 \sigma_1 + k_2 \sigma_2 + k_2 \sigma_3 + s(k_1 - k_3)$$

$$\epsilon_2 = k_2 \sigma_1 + k_3 \sigma_2 + k_2 \sigma_3 + s(k_1 - k_3)$$

$$\epsilon_3 = k_2 \sigma_1 + k_2 \sigma_2 + k_3 \sigma_3 + s(k_1 - k_3).$$

We shall now consider the stress-strain relations for arbitrary directions. Let y^i be principal axes (along which τ^{ii} acts) and x^i be arbitrary axes (along which $\bar{\tau}^{\alpha\beta}$ acts); both systems are assumed orthogonal.

Now
$$\bar{\epsilon}^{\alpha\beta} = \epsilon^{ij} \frac{\partial x^\alpha}{\partial y^i} \frac{\partial x^\beta}{\partial y^j}$$

but
$$\epsilon^{ij} = 0 \quad \text{for } i \neq j.$$

thus
$$\bar{\epsilon}^{\alpha\beta} = \epsilon^{ii} \frac{\partial x^\alpha}{\partial y^i} \frac{\partial x^\beta}{\partial y^i}$$

from (5.14) we may write

$$\epsilon^{ii} = k_{jj}^{ii} \tau^{jj} + D^{ii}$$

also
$$\tau^{jj} = \frac{\tau^{\gamma\lambda}}{\tau} \frac{\partial y^j}{\partial x^\gamma} \frac{\partial y^i}{\partial x^\lambda}$$

thus
$$\bar{\epsilon}^{\alpha\beta} = (k_{jj}^{ii} \frac{\tau^{\gamma\lambda}}{\tau} \frac{\partial y^j}{\partial x^\gamma} \frac{\partial y^j}{\partial x^\lambda} + D^{ii}) \frac{\partial x^\alpha}{\partial y^i} \frac{\partial x^\beta}{\partial y^i}$$

$$\bar{\epsilon}^{\alpha\beta} = k_{jj}^{ii} \frac{\partial y^j}{\partial x^\gamma} \frac{\partial y^j}{\partial x^\lambda} \frac{\partial x^\alpha}{\partial y^i} \frac{\partial x^\beta}{\partial y^i} \frac{\tau^{\gamma\lambda}}{\tau} + D^{ii} \frac{\partial x^\alpha}{\partial y^i} \frac{\partial x^\beta}{\partial y^i} \quad (5.15)$$

therefore
$$\bar{k}_{\gamma\lambda}^{\alpha\beta} = k_{jj}^{ii} \frac{\partial y^j}{\partial x^\gamma} \frac{\partial y^j}{\partial x^\lambda} \frac{\partial x^\alpha}{\partial y^i} \frac{\partial x^\beta}{\partial y^i}, \quad \bar{D}^{\alpha\beta} = D^{ii} \frac{\partial x^\alpha}{\partial y^i} \frac{\partial x^\beta}{\partial y^i}$$

or if we define $k_{jm}^{ik} = 0$ for $i \neq k$ or $j \neq m$ or both, then k_{km}^{ij} is a fourth rank tensor; similarly D^{ij} is a rank two tensor.

In the derivation of the constitutive equations for a Class III material we shall assume that the criterion for passage from one mode of action to another is governed by the passage of the mean stress σ_m through the threshold value h .

For the criterion of $\sigma_m = h$ we have two possible zones of action, i.e., Zone 1 ($\sigma_m \leq h$) and Zone 2 ($\sigma_m \geq h$). We shall let the quantities of Zone 1 be denoted by a subscript, e.g., B_1 etc.

Thus for Zone 1 $\sigma_m \leq h$

$$\sigma_m = 3B_1 \epsilon_m$$

$$s_j^i = 2\mu_1 e_j^i$$

Zone 2

$$\sigma_m \geq h$$

$$\sigma_m = 3B_2 \epsilon_m + D_m$$

$$s_j^i = 2\mu_2 e_j^i + D_j^i$$

Considering the interzone as in the previous derivation we have for

$$\sigma_m \rightarrow h^-$$

$$h = 3B_1 \epsilon_m$$

$$s_j^i = 2\mu_1 e_j^i$$

$$\sigma_m \rightarrow h^+$$

$$h = 3B_2 \epsilon_m + D_m$$

$$s_j^i = 2\mu_2 e_j^i + D_j^i.$$

Thus we must have the following relations

$$\mu_1 = \mu_2$$

$$D_j^i = 0$$

$$D_m = h(1 - \frac{B_2}{B_1}).$$

Using the above equations we may write the constitutive equations as (let $n = \frac{B_2}{B_1}$ and $B = B_1$)

$$\text{Zone 1} \quad \sigma_m \leq h$$

$$\tau_j^i = (B - \frac{2}{3}\mu) \theta \delta_j^i + 2\mu \epsilon_j^i$$

$$\text{or} \quad \epsilon_j^i = \frac{1}{3}(\frac{1}{3B} - \frac{1}{2\mu}) \theta \delta_j^i + \frac{1}{2\mu} \tau_j^i$$

$$\text{Zone 2} \quad \sigma_m \geq h$$

$$\tau_j^i = (nB - \frac{2}{3}\mu) \theta \delta_j^i + 2\mu \epsilon_j^i + h(1 - n) \delta_j^i$$

$$\text{or} \quad \epsilon_j^i = \frac{1}{3}(\frac{1}{3nB} - \frac{1}{2\mu}) \theta \delta_j^i + \frac{1}{2\mu} \tau_j^i - \frac{h(1 - n)}{3Bn} \delta_j^i.$$

6. Derivation of Elementary Solutions

A. Analysis of a pure shear strain test ($\tau_{zz} = 0$) for a Class II material when $\sigma_1 \geq s$, $\epsilon_{xx} = \epsilon_{yy} = 0$, and $\epsilon_{xy} = \gamma$. For pure shear strain the principal axes will be at 45° to the x and y axis. Using Equation (5.15)

$$\epsilon_{xx} = 0 = (k_3 + 2k_2 + k_1)\tau_{xx} + 2(k_3 - k_1)\tau_{xy} + (k_3 + k_1)\tau_{yy} + 2s(k_1 - k_3) \quad (6.1)$$

$$\epsilon_{yy} = 0 = (k_3 + k_1)\tau_{xx} + 2(k_3 - k_1)\tau_{xy} + (k_3 + 2k_2 + k_1)\tau_{yy} + 2s(k_1 - k_3)$$

$$4\epsilon_{xy} = 4\gamma = (k_3 - k_1)\tau_{xx} + 2(k_1 + k_3 - 2k_2)\tau_{xy} + (k_3 - k_1)\tau_{yy} + 2s(k_1 - k_3). \quad (6.2)$$

From Equation (6.1)

$$\tau_{xx} = \tau_{yy} = \frac{2(k_3 - k_1)[(k_1 - k_2)s - \gamma]}{4k_1k_3 - k_2(k_1 + k_3 + 2k_2)}$$

and from Equation (6.2)

$$\tau_{xy} = \frac{s(k_3 - k_1)(2k_1 + k_2) + 2\gamma(k_1 + k_3 + k_2)}{4k_1k_3 - k_2(k_1 + k_3 + 2k_2)}.$$

Thus,

$$\sigma_1 = \frac{(k_3 - k_1)(4k_1 - k_2)s + 2(2k_1 + k_2)\gamma}{4k_1k_3 - k_2(k_1 + k_3 + 2k_2)}.$$

As we assumed that $\sigma_1 \geq s$, we find that when $\sigma_1 = s$,

$$\gamma_c = (k_1 - k_2)s.$$

B. Pressurization of a hollow cylinder* under plane strain for a Class II material.

The appropriate field equations are:

(1) equilibrium equation

$$\frac{d\sigma_r}{dr} + \frac{\sigma_r - \sigma_\theta}{r} = 0 \quad (6.3)$$

(2) strain-displacement equations

$$\epsilon_r = \frac{du_r}{dr}$$

$$\epsilon_\theta = \frac{u_r}{r} \quad (6.4)$$

$$\epsilon_z = 0$$

The constitutive equations are given by Equations (5.14). We shall consider loading conditions such that the following zones are present:

a		
x		
b		
	Zone 2	Zone 1
	$\sigma_z \leq s$	$\sigma_z \leq s$
	$\sigma_r \leq s$	$\sigma_r \leq s$
	$\sigma_\theta \geq s$	$\sigma_\theta \leq s$

*The anisotropic thick-walled cylinder solutions are given in Part I and may be used to construct the bilinear solutions for a thick-walled cylinder where $s = 0$. However, we are here considering the situation where $s \neq 0$ and thus we shall construct the necessary anisotropic solutions as needed.

Thus in Zone 2, $a \leq r \leq x$

$$\begin{aligned}\epsilon_{\theta} &= k_2 \sigma_r + k_3 \sigma_{\theta} + k_2 \sigma_z + s(k_1 - k_3) \\ \epsilon_r &= k_1 \sigma_r + k_2 \sigma_{\theta} + k_2 \sigma_z \\ \epsilon_z &= k_2 \sigma_r + k_2 \sigma_{\theta} + k_1 \sigma_z\end{aligned}\tag{6.5}$$

Combining Equations (6.3), (6.4) and (6.5) and solving the resulting differential equation we obtain

$$\sigma_r = Ar^{m_1} + Dr^{m_2} + s\tag{6.6}$$

$$\sigma_z = -\frac{k_2}{k_1}(\sigma_r + \sigma_{\theta})$$

$$u = r(k_2 - \frac{k_2^2}{k_1})\sigma_r + r(k_3 - \frac{k_2^2}{k_1})\sigma_{\theta} + s(k_1 - k_3)r$$

$$\sigma_{\theta} = A(1 + m_1)r^{m_1} + D(1 + m_2)r^{m_2} + s\tag{6.7}$$

where

$$m_1 = -1 - \beta\tag{6.8}$$

$$m_2 = -1 + \beta$$

and

$$\beta = \sqrt{\frac{k_1^2 - k_2^2}{k_1 k_3 - k_2^2}}.\tag{6.9}$$

The boundary conditions for this zone may be written as:

$$\begin{aligned}r = a & \quad \sigma_r = -P_i \\ r = x & \quad \sigma_{\theta} = s\end{aligned}\tag{6.10}$$

Applying the boundary conditions to Equations (6.6) and (6.7) we obtain

$$A = \frac{-(P_i + s)(1 + m_2)x^{m_2}}{a^{m_1}(1 + m_2)x^{m_2} - a^{m_2}(1 + m_1)x^{m_1}}$$

$$D = \frac{(P_i + s)(1 + m_1)x^{m_1}}{a^{m_1}(1 + m_2)x^{m_2} - a^{m_2}(1 + m_1)x^{m_1}}.$$

Thus Equation (6.6) becomes

$$\sigma_r = -(P_i + s) \left[\frac{\left(\frac{r}{x}\right)^{m_1} + \left(\frac{r}{x}\right)^{m_2}}{\left(\frac{a}{x}\right)^{m_1} + \left(\frac{a}{x}\right)^{m_2}} \right] + s. \quad (6.11)$$

In Zone 1

$$\epsilon_r = \frac{du_r}{dr} = k_1 \sigma_r + k_2 \sigma_\theta + k_2 \sigma_z$$

$$\epsilon_\theta = \frac{u_r}{r} = k_2 \sigma_r + k_1 \sigma_\theta + k_2 \sigma_z \quad (6.12)$$

$$\epsilon_z = 0 = k_2 \sigma_r + k_2 \sigma_\theta + k_1 \sigma_z$$

Thus

$$\sigma_z = -\frac{k_2}{k_1} (\sigma_r + \sigma_\theta)$$

Combining Equations (6.3), (6.4) and (6.12) and solving the resulting differential equation we obtain

$$\sigma_r = A + \frac{D}{r^2} \quad (6.13)$$

$$\sigma_\theta = \sigma_r + r \frac{d\sigma_r}{dr} = A - \frac{D}{r^2}, \quad (6.14)$$

The boundary conditions may be written as

$$r = x \quad \sigma_\theta = s$$

$$r = b \quad \sigma_r = 0.$$

Applying the above boundary conditions to Equations (6.13) and (6.14) we find

$$D = - \frac{sb^2x^2}{b^2 + x^2}$$

$$A = \frac{sx^2}{b^2 + x^2}.$$

Then Equation (6.13) becomes

$$\sigma_r = \frac{sx^2}{b^2 + x^2} \left(1 - \frac{b^2}{r^2}\right). \quad (6.15)$$

To find x we set $\sigma_r(x^-) = \sigma_r(x^+)$. Using Equation (6.11) and (6.15) we obtain

$$\frac{s(x^2 - b^2)}{x^2 + b^2} = - (P_i + s) \left[\frac{2}{\left(\frac{a}{x}\right)^{m_1} + \left(\frac{a}{x}\right)^{m_2}} \right] + s$$

or

$$\frac{\left(\frac{b}{a}\right)^2}{\left(\frac{x}{a}\right)^2 + \left(\frac{b}{a}\right)^2} = \frac{\frac{P_i}{s} + 1}{\left(\frac{a}{x}\right)^{m_1} + \left(\frac{a}{x}\right)^{m_2}}. \quad (6.16)$$

We shall now investigate the pressure range for which the assumed zone configuration will exist. One limit will be when $x = b$; from Equation(6.16) we find

$$\frac{(\frac{b}{a})^2}{(\frac{b}{a})^2 + (\frac{b}{a})^2} = \frac{\frac{P_1}{s} + 1}{(\frac{a}{b})^{m_1} + (\frac{a}{b})^{m_2}}$$

or

$$P_1 = s \left[\frac{1}{2}(\frac{a}{b})^{m_2} + \frac{1}{2}(\frac{a}{b})^{m_1} - 1 \right] .$$

The other limit will be when $x = a$. To find this critical pressure we set $x = a$ in Equation (6.16)

$$\frac{s(a^2 - b^2)}{a^2 + b^2} = - P_2$$

or

$$P_2 = s \frac{(\frac{b}{a})^2 - 1}{(\frac{b}{a})^2 + 1} .$$

The assumption that $\sigma_r \leq s$ is obviously true. We also have assumed that $\sigma_z \leq s$; thus we must now impose this condition (it may be easily shown to be true in Zone 1) now (for $a \leq x \leq b$, $x \geq r \geq a$)

$$\sigma_z = - \frac{k_2}{k_1}(\sigma_r + \sigma_\theta) = - \frac{k_2}{k_1}(2\sigma_r + r \frac{d\sigma_r}{dr}).$$

Therefore we have

$$s \geq -\frac{k_2}{k_1} \left[-(P_i + s) \left[\frac{(2 + m_1) \left(\frac{r}{x}\right)^{m_1} + (2 + m_2) \left(\frac{r}{x}\right)^{m_2}}{\left(\frac{a}{x}\right)^{m_1} + \left(\frac{a}{x}\right)^{m_2}} \right] + 2s \right].$$

Using Equations (6.8) and (6.16) we have (note $-\frac{k_2}{k_1} = \nu_1$, see Section 2)

$$(1 - 2\nu_1) \geq \frac{\nu_1 \left(\frac{b}{a}\right)^2 \left(\frac{x}{r}\right)}{\left(\frac{x}{a}\right)^2 + \left(\frac{b}{a}\right)^2} \left[(\beta-1) \left(\frac{x}{r}\right)^\beta - (\beta+1) \left(\frac{r}{x}\right)^\beta \right]$$

but

$$(1 - 2\nu_1) \geq 0$$

$$\nu_1 > 0$$

$$\frac{\left(\frac{b}{a}\right)^2 \left(\frac{x}{r}\right)}{\left(\frac{x}{a}\right)^2 + \left(\frac{b}{a}\right)^2} > 0.$$

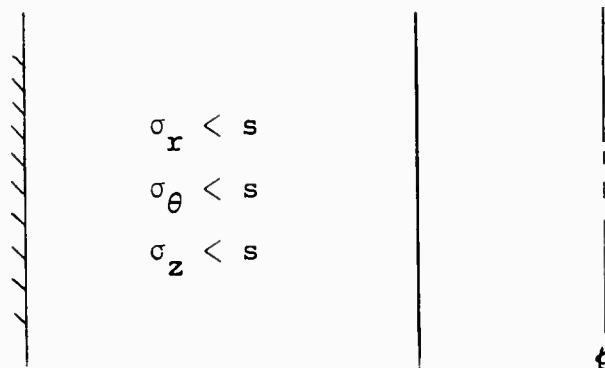
Also if $E_2 \leq E_1$, see Section 3, then $\beta \leq 1$ from Equation (6.9) and

$$\left[(\beta - 1) \left(\frac{x}{r}\right)^\beta - (\beta + 1) \left(\frac{r}{x}\right)^\beta \right] < 0$$

thus,

$$\sigma_z \leq s.$$

C. Uniform temperature drop of a thick-walled cylinder bonded to a rigid case. Class II material. Let $T^* = T - T_0$. For $0 \geq T^* \geq T_1$ we have



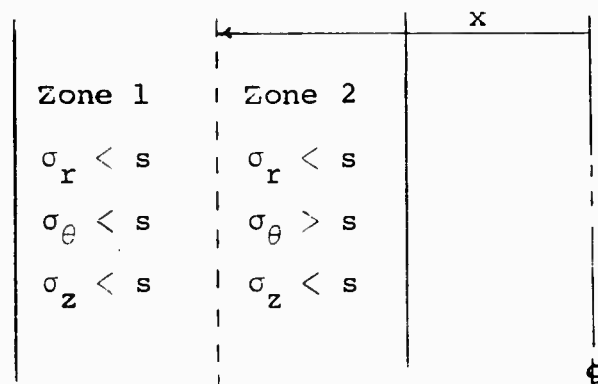
The material remains isotropic and the solution is well known, see Part III. A zone boundary will arise at $r = a$ when $\sigma_\theta = s$; from Part III we find

$$\sigma_\theta(a) = s = - \frac{6\alpha T_1 B}{1 + \frac{1}{3c^2}(1 + \frac{3B}{\mu})}$$

or

$$T_1 = \frac{-s \left[1 + \frac{1}{3c^2}(1 + \frac{3B}{\mu}) \right]}{6\alpha B} \quad (6.17)$$

For $T_2 \leq T^* \leq T_1$, we have



The equilibrium equation is given by Equation (6 3), the strain-displacement equation by Equation (6 4) and the constitutive equation* by Equation (5 14) where we add to each equation the term αT^* . Combining the resulting equations and solving we obtain for Zone 1

$$\sigma_{\theta} = A - \frac{D}{r^2} \quad (6.18)$$

$$\sigma_r = A + \frac{D}{r^2} \quad (6.19)$$

$$\sigma_z = -\frac{1}{k_1}(\alpha T^* + 2k_2 A) \quad (6.20)$$

$$u = (k_2 + k_1 - 2\frac{k_2^2}{k_1})Ar + (k_2 - k_1)\frac{D}{r} + \alpha T^* r(1 - \frac{k_2}{k_1}), \quad (6.21)$$

The boundary conditions may be written as

$$\begin{aligned} r = b & \quad u = 0 \\ r = x & \quad \sigma_{\theta} = s \end{aligned}$$

hence $D = x^2(A - s) \quad (6.22)$

$$A = \frac{k_1 s \frac{x^2}{b^2} + \alpha T^*}{k_1 \frac{x^2}{b^2} - (k_1 + 2k_2)}. \quad (6.23)$$

*At present we are not in possession of any experimental data which would indicate whether the linear coefficient of thermal expansion changes value as we pass from one zone of action to another or remains a constant; for simplicity we have assumed that it remains a constant.

For Zone 2

$$\sigma_r = \frac{F}{r^{\beta+1}} + Hr^{\beta-1} + s \quad (6.24)$$

$$\sigma_\theta = -\frac{\beta F}{r^{\beta+1}} + \beta Hr^{\beta-1} + s \quad (6.25)$$

$$\sigma_z = -\frac{\alpha T^*}{k_1} - \frac{k_2}{k_1} \left[2s + (\beta + 1)Hr^{\beta-1} + (1-\beta) \frac{F}{r^{\beta+1}} \right] \quad (6.26)$$

$$u = \left[k_2 - \beta k_3 + (\beta-1) \frac{k_2^2}{k_1} \right] \frac{F}{r^\beta} + \left[k_2 + \beta k_3 - (\beta+1) \frac{k_2^2}{k_1} \right] Hr^\beta + s \left[k_2 + k_1 - 2 \frac{k_2^2}{k_1} \right] r + \alpha T^* \left(1 - \frac{k_2}{k_1} \right) r \quad (6.27)$$

where
$$\beta = \sqrt{\frac{k_1^2 - k_2^2}{k_1 k_3 - k_2^2}} \quad (6.28)$$

The boundary conditions for Zone 2 may be written as

$$r = x, \quad \sigma_\theta = s$$

$$r = a, \quad \sigma_r = 0$$

which yields

$$F = Hx^{2\beta} \quad (6.29)$$

$$H = -\frac{as}{a^\beta + x^{2\beta} a^{-\beta}} \quad (6.30)$$

The zone boundary x may be found from

$$\sigma_z(x^-) = \sigma_z(x^+)$$

Using Equations (6 18) (6 22) (6 23) (6 24) (6 29) and (6 30) we obtain

$$\frac{k_1 s \frac{x^2}{b^2} + \alpha T^*}{k_1 \frac{x^2}{b^2} - (k_1 + 2k_2)} + \frac{\left(\frac{x}{b}\right)^{\beta-1} \frac{s}{c}}{c^{-\beta} + \left(\frac{x}{b}\right)^{2\beta} c^{\beta}} = s. \quad (6.31)$$

T_2 may be found by setting $x = b$ in Equation (6 31):

$$\frac{k_1 s + \alpha T_2}{k_1 - (k_1 + 2k_2)} + \frac{\frac{s}{c}}{c^{-\beta} + c^{\beta}} = s$$

or

$$T_2 = \frac{s}{\alpha} \left[\frac{2k_2}{c(c^{-\beta} + c^{\beta})} - (2k_2 + k_1) \right]$$

It is now necessary to consider the assumption that $\sigma_z \leq s$ (as $\sigma_z = \text{constant}$ in Zone 1 we see that the maximum σ_z in Zone 2 will at least have to be equal to σ_z in Zone 1 as $\sigma_z(x^-) = \sigma_z(x^+)$; thus we need only consider Zone 2) Now in Zone 2

$$\sigma_z = -\frac{\alpha T^*}{k_1} - \frac{k_2}{k_1} \left[2s + \frac{Hx^{\beta}}{r} \left[(1 + \beta) \left(\frac{r}{x}\right)^{\beta} + (1 - \beta) \left(\frac{x}{r}\right)^{\beta} \right] \right].$$

We seek a maximum of this function in the interval $a \leq r \leq x$, thus setting

$$\frac{d\sigma_z}{dr} = 0 = \frac{-k_2}{k_1} H x^\beta \left[\frac{(1+\beta)}{x^\beta} (\beta-1) r^{\beta-2} - (1-\beta) x^\beta (\beta+1) r^{-\beta-2} \right]$$

or

$$r^{2\beta} = -x^{2\beta}.$$

Accordingly, no maximum occurs in this interval. It will be necessary to check the end points of the interval in each particular problem.

Now

$$\sigma_z(x) = -\frac{\alpha T^*}{k_1} - \frac{k_2}{k_1} (2s + 2H x^{\beta-1}) \quad (6.32)$$

$$\sigma_z(a) = -\frac{\alpha T^*}{k_1} - \frac{k_2}{k_1} \left[2s + \frac{Hx^\beta}{a} \left[(1+\beta) \left(\frac{a}{x}\right)^\beta + (1-\beta) \left(\frac{x}{a}\right)^\beta \right] \right] \quad (6.33)$$

D. Uniform temperature drop of a thick-walled cylinder bonded to a rigid case, Class III material. From the classical elastic solution, see Part III, we see that the mean stress is a constant, thus the mean stress will reach its threshold value h throughout the cylinder at the same critical temperature T_1 . Let us consider the case when $T^* \leq T_1$. Combining the equilibrium equation (6.3), the strain displacement equation (6.4) and the Zone 2 constitutive equation (1.3) and solving we obtain

$$\sigma_r = A + \frac{D}{r^2}$$

$$\sigma_\theta = A - \frac{D}{r^2}$$

$$\sigma_m = \frac{3nB\mu}{\mu+3nB} \left[\frac{A}{\mu} - \alpha T^* + \frac{h(1-n)}{3nB} \right]$$

$$u = \frac{3}{2(\mu+3nB)} Ar - \frac{1}{2\mu} \frac{D}{r} + \left(\alpha T^* - \frac{h(1-n)}{3nB} \right) \frac{9nB}{2(\mu+3nB)} r.$$

The boundary conditions are

$$\begin{aligned} r = b, u &= 0 \\ r = a, \sigma_r &= 0 \end{aligned}$$

which yield

$$D = -a^2 A$$

$$A = \frac{h(1-n) - 3\alpha T^* nB}{1 + \frac{1}{3c^2} \left(1 + \frac{3nB}{\mu} \right)}.$$

Note that the constitutive equations for Zone 1, see Equation (13), may be obtained from the constitutive equations for Zone 2 by letting $h = 0$ and $n = 1$ in the latter; thus we may obtain the solution for Zone 1 (i.e. $T^* \geq T_1$) by setting $h = 0$ and $n = 1$ in the above solution. For example, in Zone 1

$$u = \frac{3}{2(\mu + 3B)} Ar + \frac{1}{2\mu} \frac{a^2 A}{r} + \frac{a\alpha T^* B}{2(\mu + 3B)} r$$

$$A = \frac{-3\alpha T^* B}{1 + \frac{1}{3c^2} \left(1 + \frac{3B}{\mu} \right)}$$

$$\sigma_m = \frac{3B\mu}{\mu + 3B} \left[\frac{A}{\mu} - \alpha T^* \right].$$

Now to find T_1 we set $\sigma_m = h$ and $T^* = T_c$ in the above equation i.e.

$$h = \frac{3B\mu}{\mu + 3B} \left[- \frac{3\alpha T_c B}{\mu \left[1 + \frac{1}{3c^2} \left(1 + \frac{3B}{\mu} \right) \right]} - \alpha T_c \right]$$

$$\text{or } T_c = \frac{-(\mu + 3B)h}{3B\mu\alpha} \cdot \frac{1}{1 + \frac{3B}{\mu \left[1 + \frac{1}{3c^2} \left(1 + \frac{3B}{\mu} \right) \right]}}$$

E. Pressurization of a thick-walled cylinder (Class III material) bonded to an elastic case. As in the previous problem the classical solution. see [1], shows us that the complete cylinder passes from the first zone of action to the second at the instant that $P_i = P_c$. We find from Equations (6.3), (6.4) and (1.3) (for Zone 2)

$$\sigma_r = A + \frac{D}{r^2} \quad (6.34)$$

$$\sigma_\theta = A - \frac{D}{r^2} \quad (6.35)$$

$$\sigma_z = - 2 \frac{k_2}{k_1} A \quad (6.36)$$

$$u_r = r \left(k_2 - \frac{k_2^2}{k_1} \right) \left(A + \frac{D}{r^2} \right) + r \left(k_1 - \frac{k_2^2}{k_1} \right) \left(A - \frac{D}{r^2} \right) - \frac{h(1-n)}{3Bn} \left(1 - \frac{k_2}{k_1} \right)$$

$$3\sigma_m = \frac{A + \frac{h(1-n)}{3nB}}{k_1} \quad (6.37)$$

where

$$k_1 = \frac{1}{3} \left(\frac{1}{3nB} + \frac{1}{\mu} \right)$$

$$k_2 = \frac{1}{3} \left(\frac{1}{3nB} - \frac{1}{2\mu} \right).$$

We may write the boundary conditions as

$$r = a, \quad \sigma_r = -P_i$$

$$r = b, \quad \sigma_r = -P'$$

which yield

$$D = -a^2(A + P_i)$$

$$A = \frac{a^2 P_i - b^2 P'}{b^2 - a^2}.$$

Hence

$$u_r = r \left[(k_2 + k_1 - \frac{2k_2^2}{k_1}) \frac{a^2 P_i - b^2 P'}{b^2 - a^2} - (1 - \frac{k_2}{k_1}) \frac{h(1-n)}{3nB} \right] + \frac{(k_2 - k_1) a^2 b^2 (P' - P_i)}{r(b^2 - a^2)}. \quad (6.38)$$

The displacement of the motor case will be

$$\bar{u}_r = \frac{(1 - \bar{\nu}^2)}{\bar{E}} \frac{b^2 P'}{t} \quad (6.39)$$

and equating Equations (6.38) and (6.39) with $r = b$, we obtain

$$\frac{(1 - \bar{\nu}^2)}{\bar{E}} \frac{b^2 P'}{t} = b \left[(k_2 + k_1 - \frac{2k_2^2}{k_1}) \frac{a^2 P_i - b^2 P'}{b^2 - a^2} - (1 - \frac{k_2}{k_1}) \frac{h(1-n)}{3nB} \right] + \frac{(k_2 - k_1) a^2 b^2 (P' - P_i)}{b(b^2 - a^2)}$$

$$\text{or } P' = \frac{\frac{2}{b^2 + 3nBk_1 a^2}}{3nBk_1 \mu (b^2 - a^2) + \frac{(1-\bar{\nu})b}{\bar{\mu}t}} \left[\frac{a^2 P_i}{2\mu (b^2 - a^2) \left[\frac{1}{3nBk_1} + 1 \right]} - \frac{h(1-n)}{6\mu nBk_1} \right]. \quad (6.40)$$

To determine the value of P_c we set $\sigma_m = h$. Note that as in the previous problem we obtain the Zone 1 solution by setting $n = 1$ and $h = 0$. Then

$$3hk_1 = \frac{a^2 P_c - b^2 P'}{\mu (b^2 - a^2)}$$

and using Equation (6.40)

$$3hk_1 = \frac{a^2 P_c}{\mu (b^2 - a^2)} - \frac{b^2}{\mu (b^2 - a^2)} \frac{\frac{2}{b^2 + 3Bk_1 a^2}}{3Bk_1 \mu (b^2 - a^2) + \frac{(1-\bar{\nu})b}{\bar{\mu}t}}.$$

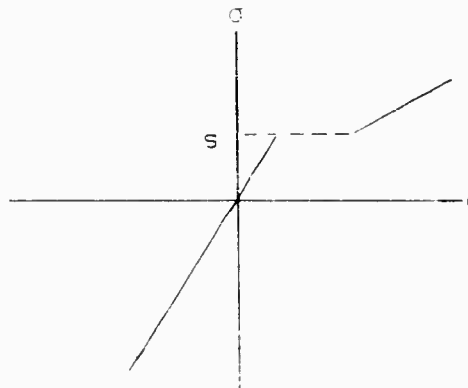
$$\frac{a^2 P_c}{2\mu (b^2 - a^2) \left[\frac{1}{3Bk_1} + 1 \right]}$$

or

$$P_c = \frac{3hk_1 \mu (b^2 - a^2)}{a^2 - \frac{a^2 b^2 (3Bk_1 + 1)}{\mu (b^2 - a^2) \left[\frac{b^2 + 3Bk_1 a^2}{\mu (b^2 - a^2)} + \frac{3(1-\bar{\nu})bk_1 B}{\bar{\mu}t} \right]}}.$$

7. Proposed Generalization of the Bilinear Elastic Theory

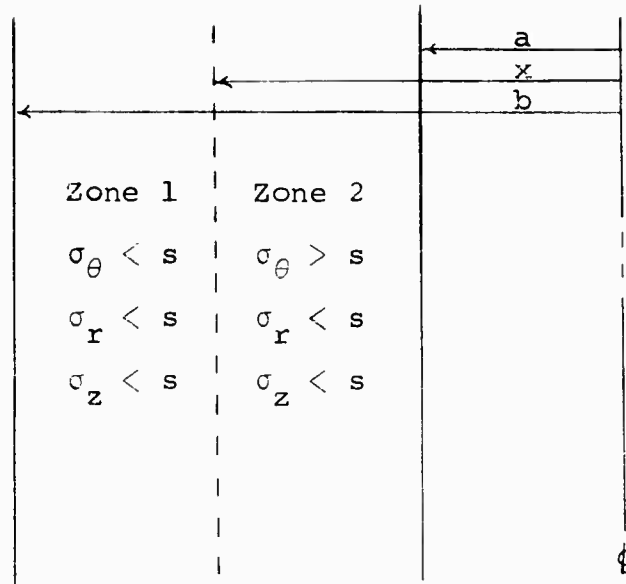
We shall now consider a generalization* of the bilinear elastic theory presented in Section 1. The generalization will be realized by allowing the constitutive equations to become discontinuous across the zone boundaries, whereas in the previous discussion we have only allowed the gradients of the constitutive equations to be discontinuous. Thus we would be able to accommodate a material which yields a uniaxial stress-strain curve of the form shown below, where the unloading curve is assumed to coincide with the loading curve.



Allowing the constitutive equations to be discontinuous at zone boundaries relieves us of the continuity conditions (2.1), (2.2) and (2.3) or their more general forms as given in Section 5 by Equations (5.2) through (5.13). Thus the general constitutive equations for a Class II material (where we allow discontinuous constitutive equations) are given by Equation (5.1). Similar considerations hold for Class I and Class III materials.

To illustrate the solution method that one would now employ we shall outline the method of solution for a simple problem, the pressurization of a thick-walled cylinder. Let us consider loading conditions compatible with the following:

*This generalization was suggested by Dr. Paul J. Blatz, California Institute of Technology.



As in Section 6 we would solve a separate problem for each zone, i.e., in Zone 1 we would use the Zone 1 constitutive equations, Equation (5.1) and the boundary conditions

$$r = b, \sigma_r^{(1)} = 0$$

$$r = x, \sigma_{\theta}^{(1)} = s.$$

The resulting solution will be in terms of an unknown parameter x . For Zone 2 we would use the Zone 2 constitutive equations and the results will be expressed in terms of three unknown constants, two constants of integration (A_1 and A_2) and the zone boundary x ; let this solution carry superscripts (2). The three unknown parameters A_1 , A_2 and x which appear in the two solutions are found from the following conditions

$$\sigma_r^{(2)}(a) = -P_i \text{ (Boundary condition)}$$

$$\sigma_r^{(2)}(x) = \sigma_r^{(1)}(x) \quad (\text{Equilibrium condition})$$

$$u^{(2)}(x) = u^{(1)}(x) \quad (\text{Geometric condition}).$$

Note that in Section 6 we were able to use the condition $\sigma_\theta^{(2)}(x) = s$, see Equation (6.10), but as we have no longer required continuity of the constitutive equations across the zone boundaries this condition is no longer valid. Finally we must establish limits upon the loading conditions (in this problem upon P_i) such that the assumed zone distribution exists.

The above theory was not presented in detail, as yet no experimental evidence has been produced to indicate the necessity of such a theory.

REFERENCES

- (1) Williams, M.L., Blatz, P.J. and Schapery, R.A., "Fundamental Studies Relating to Systems Analysis of Solid Propellants," GALCIT Report 101, California Institute of Technology, February 1961.

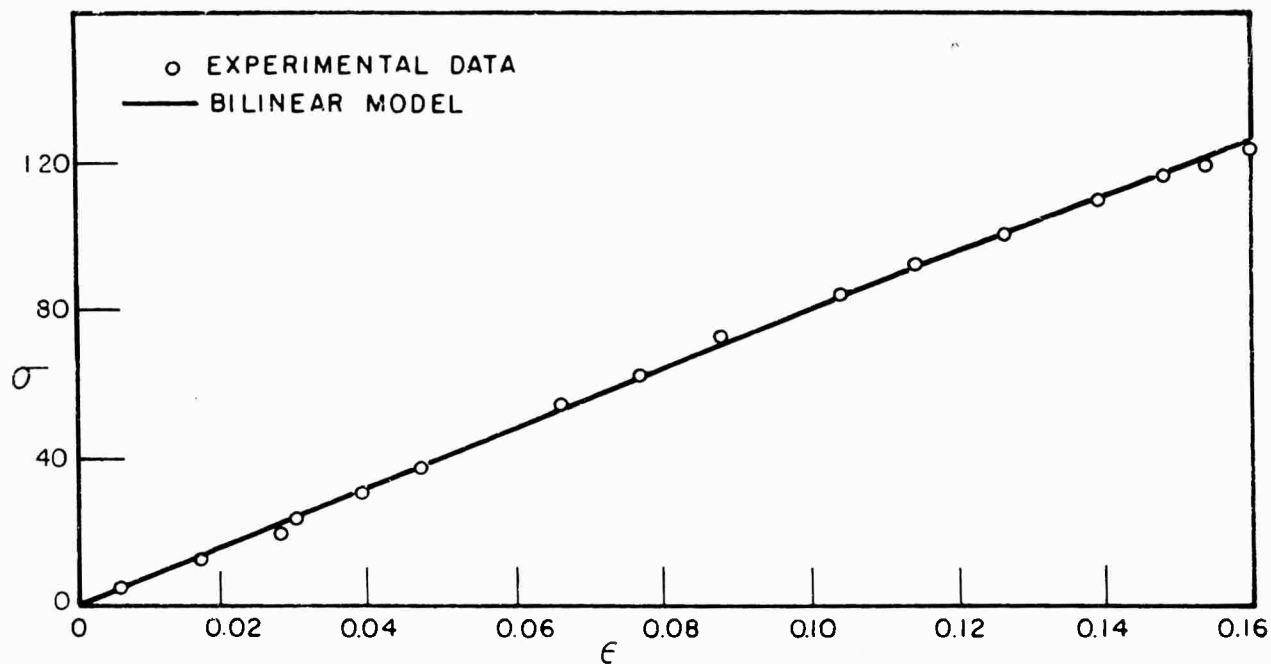


FIG.1 UNIAXIAL TEST OF A TYPICAL PROPELLANT

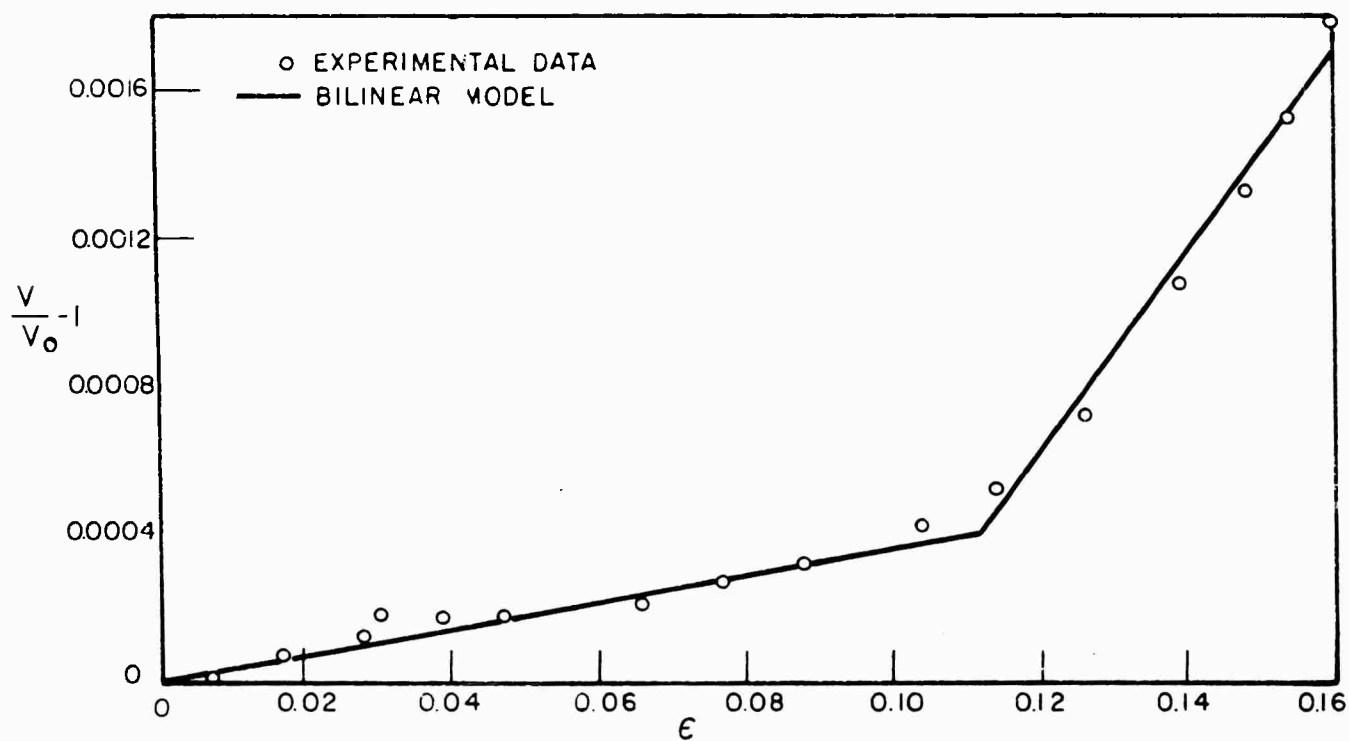


FIG. 2 UNIAXIAL TEST OF A TYPICAL PROPELLANT

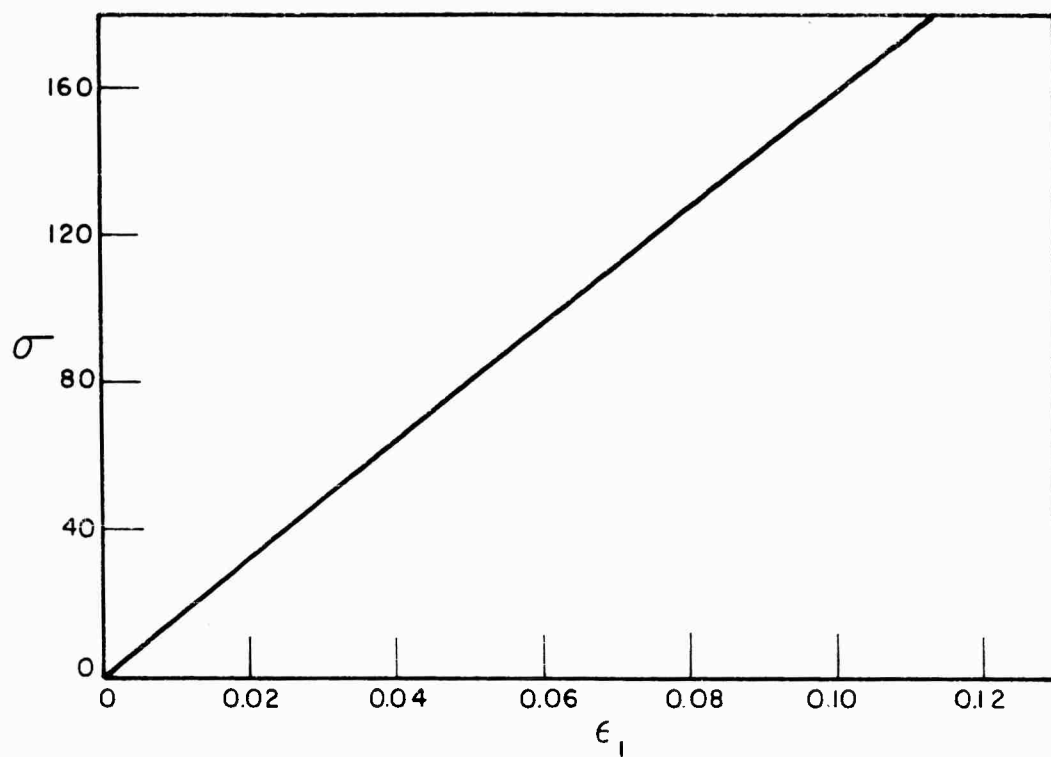


FIG.3 HYPOTHETICAL BIAXIAL TEST FOR A CLASS II MODEL

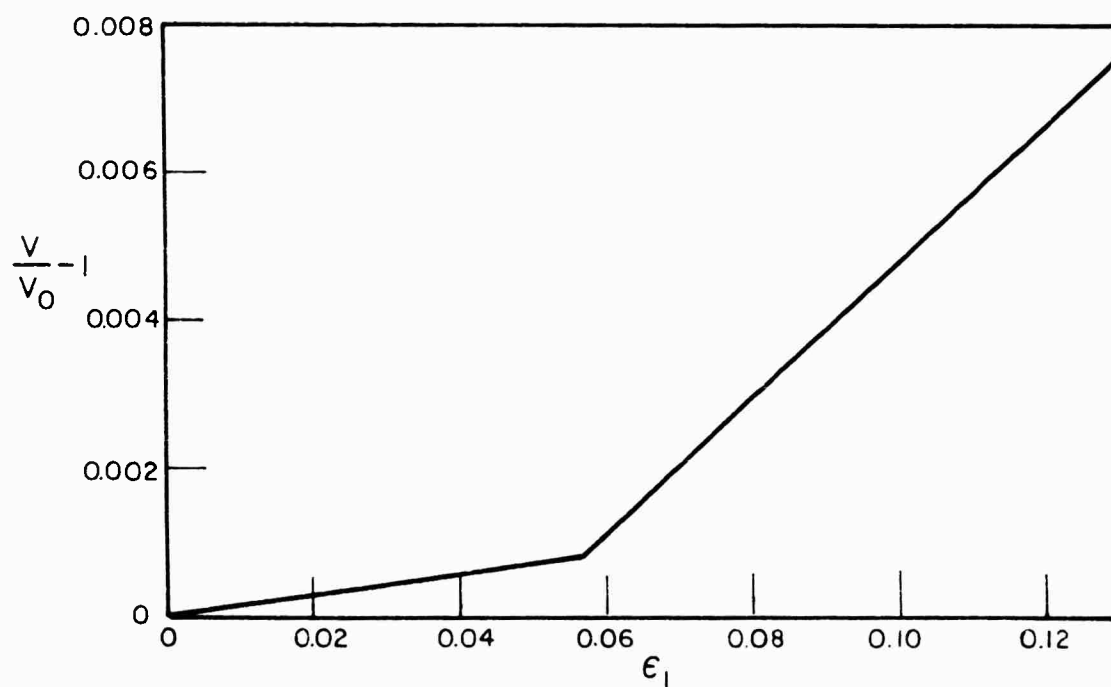


FIG.4 HYPOTHETICAL BIAXIAL TEST FOR A CLASS II MODEL

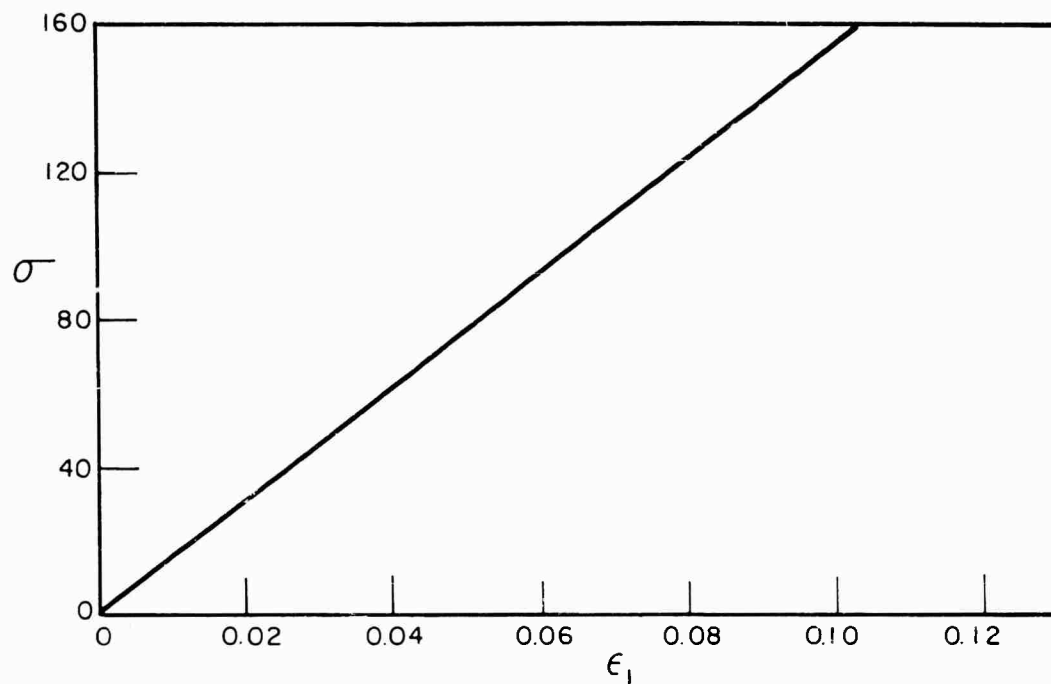


FIG. 5 HYPOTHETICAL BIAXIAL TEST FOR A CLASS III MODEL

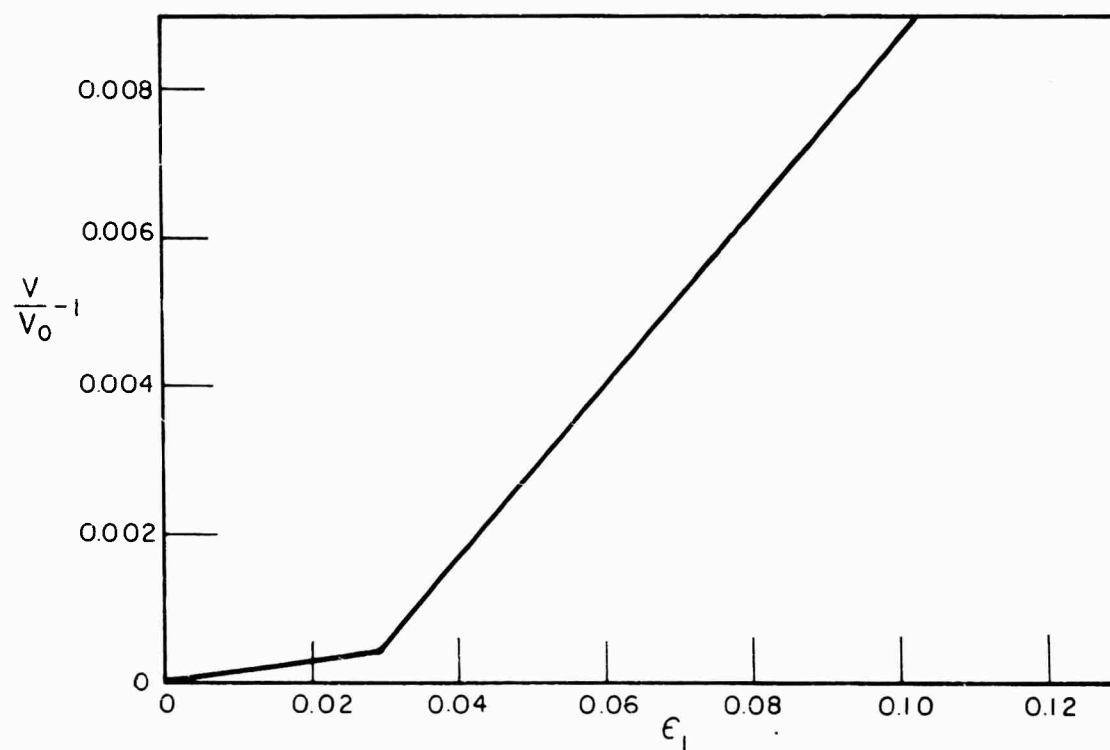


FIG. 6 HYPOTHETICAL BIAXIAL TEST FOR A CLASS III MODEL

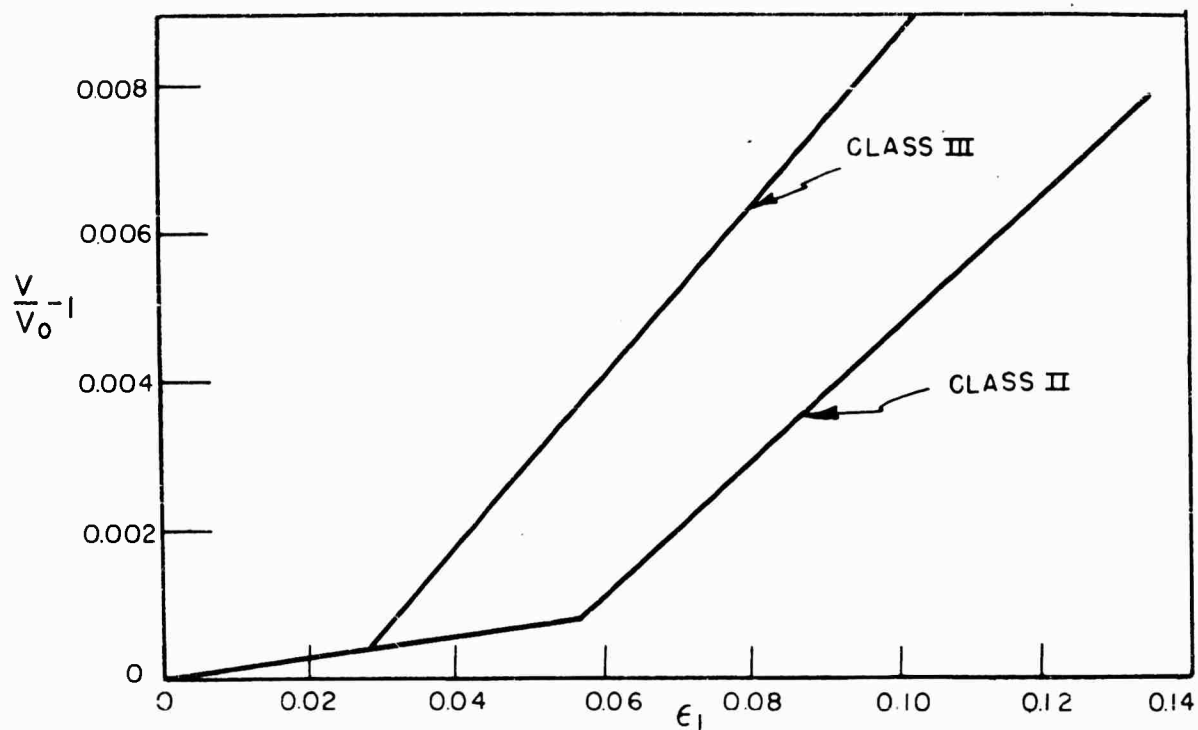


FIG. 7 COMPARISON OF HYPOTHETICAL BIAxIAL TEST
FOR CLASS II AND III MODELS

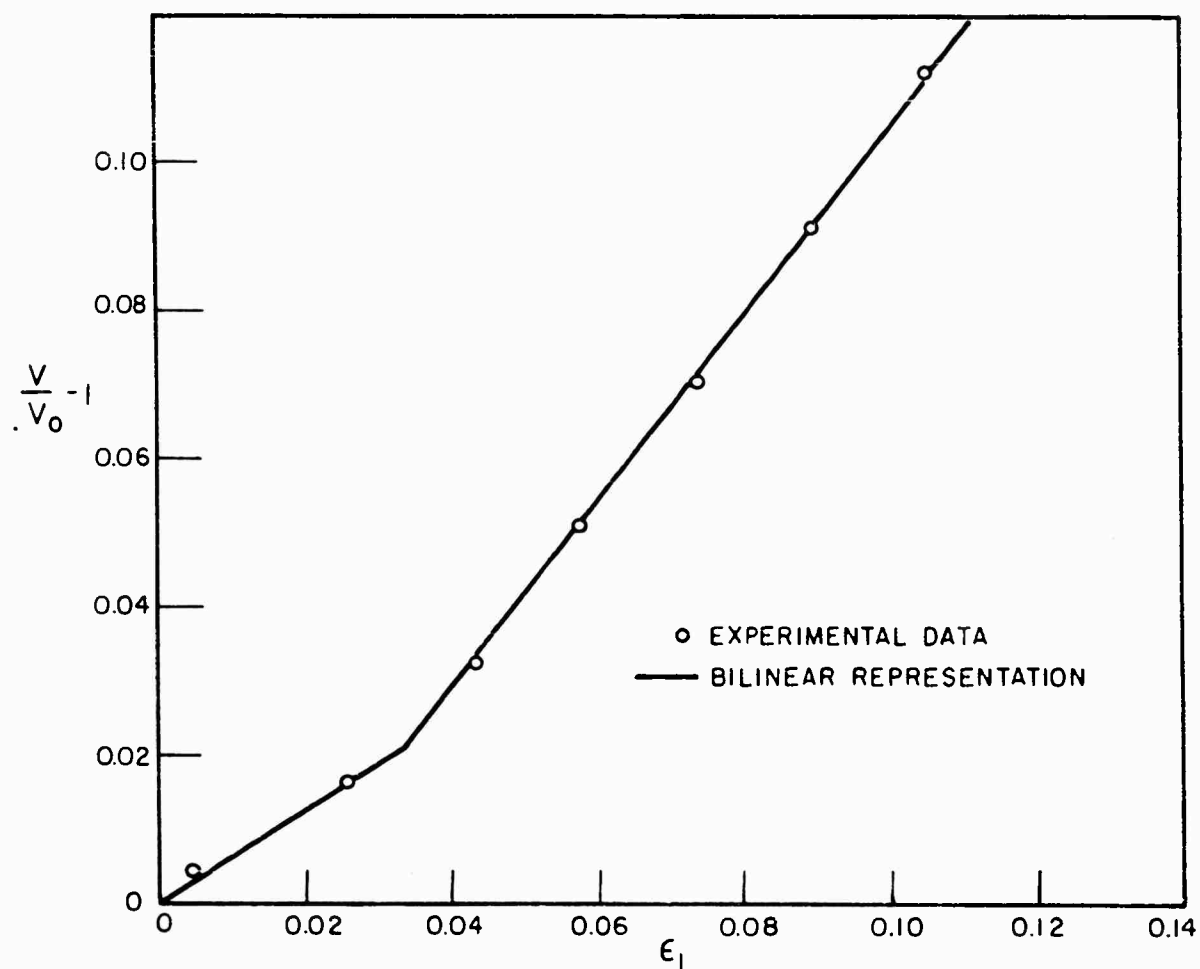


FIG. 8 BIAxIAL TEST OF A TYPICAL PROPELLANT

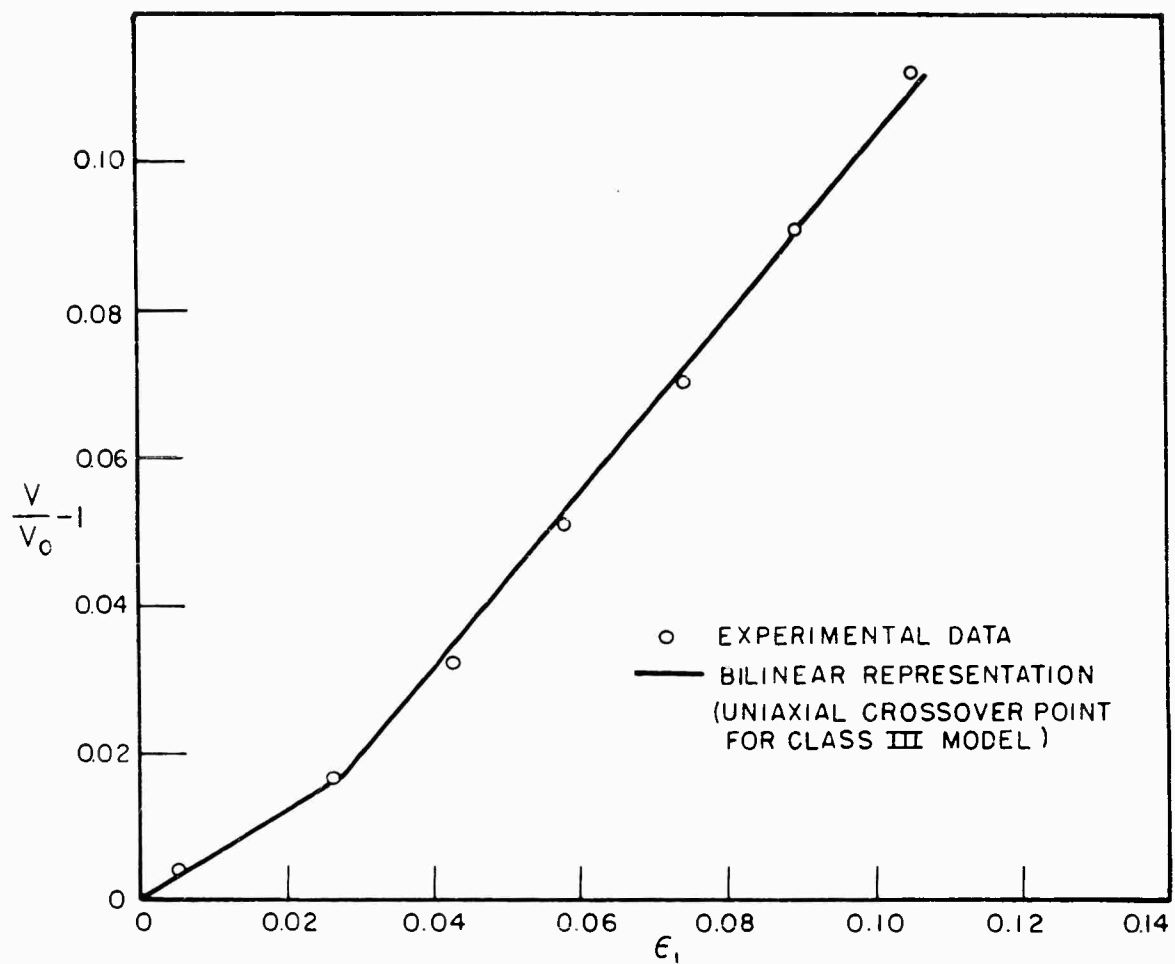


FIG.9 BIAxIAL TEST OF A TYPICAL PROPELLANT

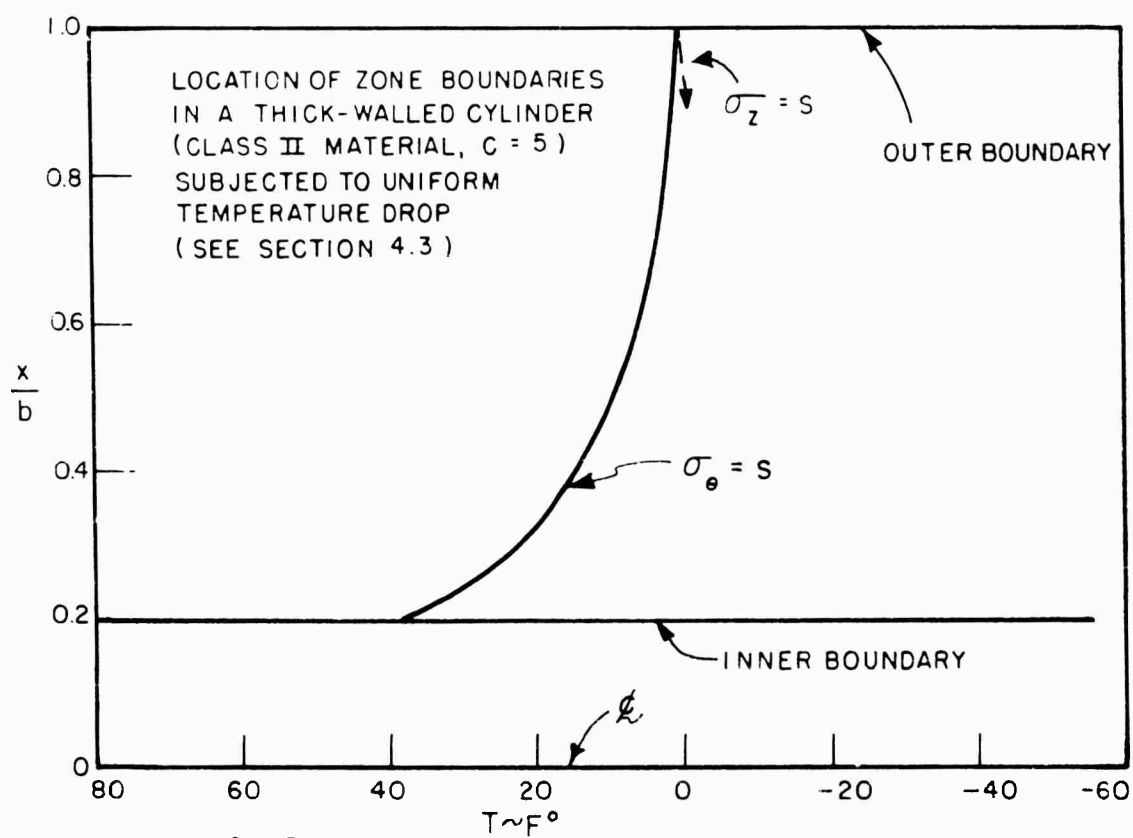


FIG.10

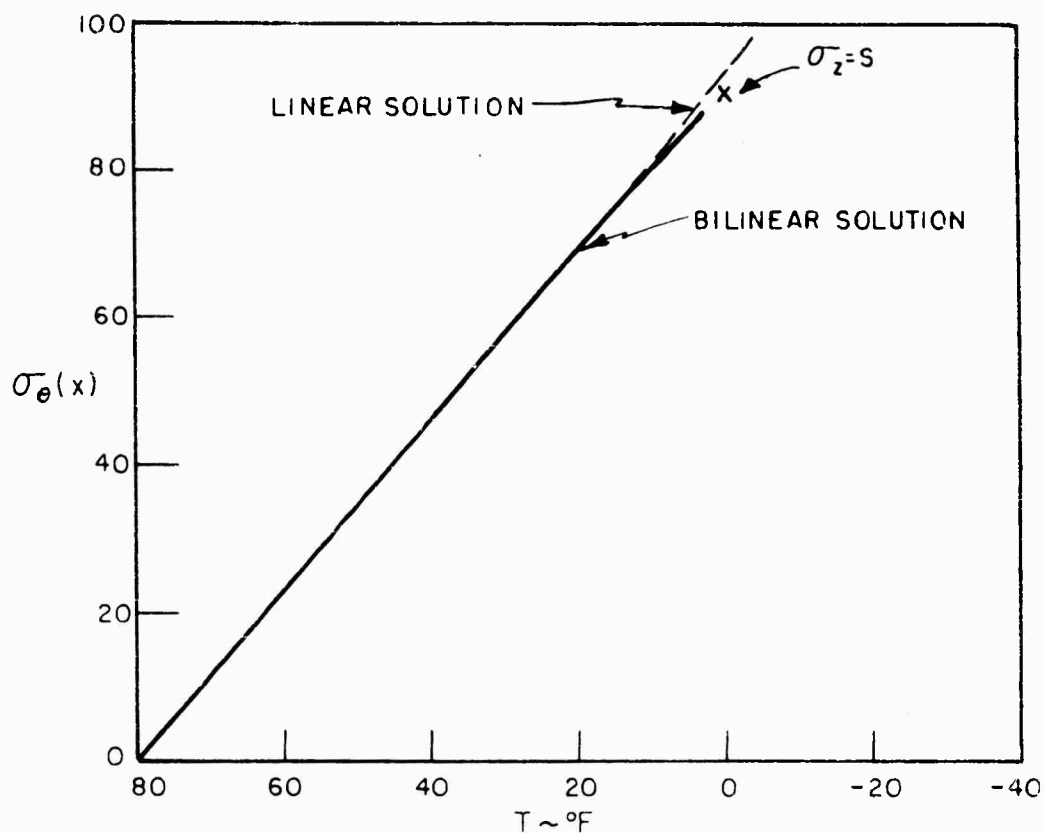


FIG.11 UNIFORM TEMPERATURE DROP OF A CLASS II THICK-WALLED CYLINDER, $C = 5$ (SEE SECTION 4.3)

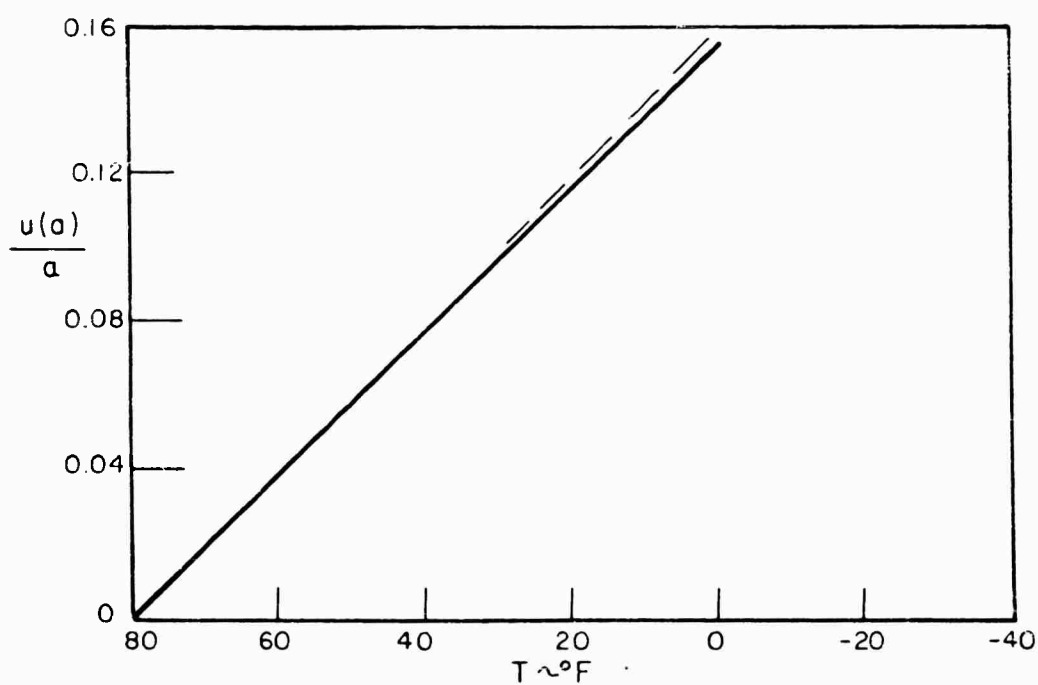


FIG.12 UNIFORM TEMPERATURE DROP OF A CLASS II THICK-WALLED CYLINDER, $C = 5$ (SEE SECTION 4.3)

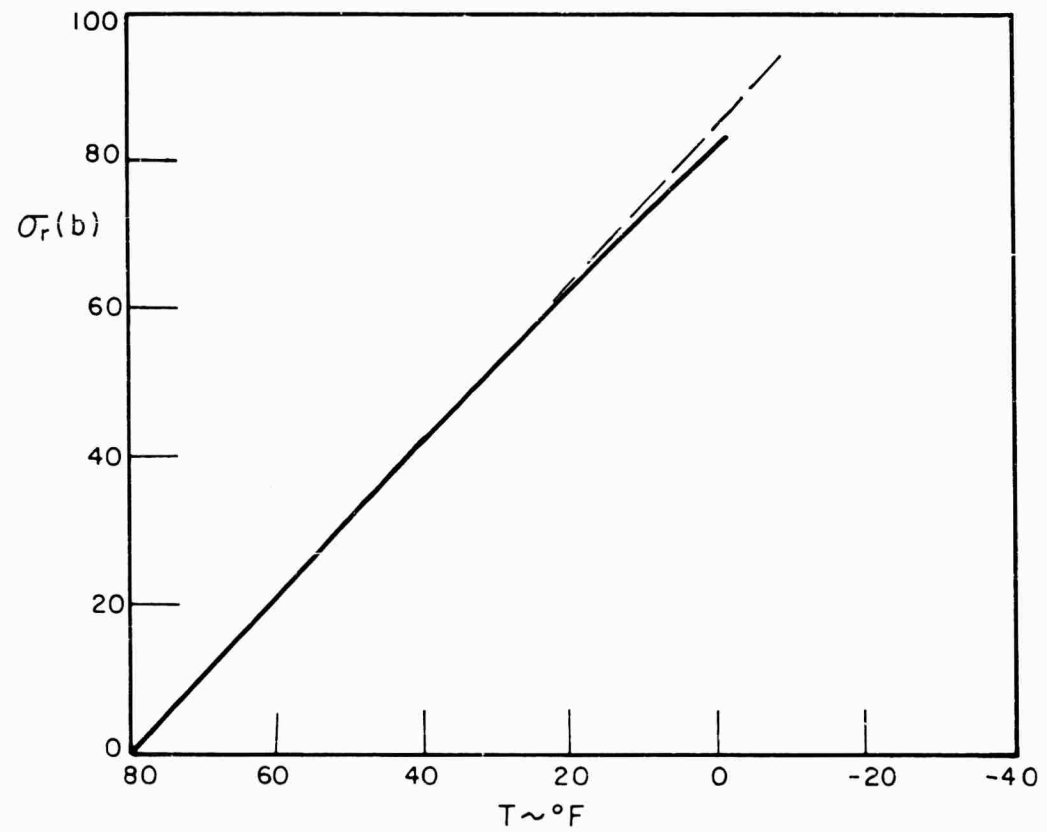


FIG. 13 UNIFORM TEMPERATURE DROP OF A
CLASS II THICK-WALLED CYLINDER
 $C = 5$ (SEE SECTION 4.3)

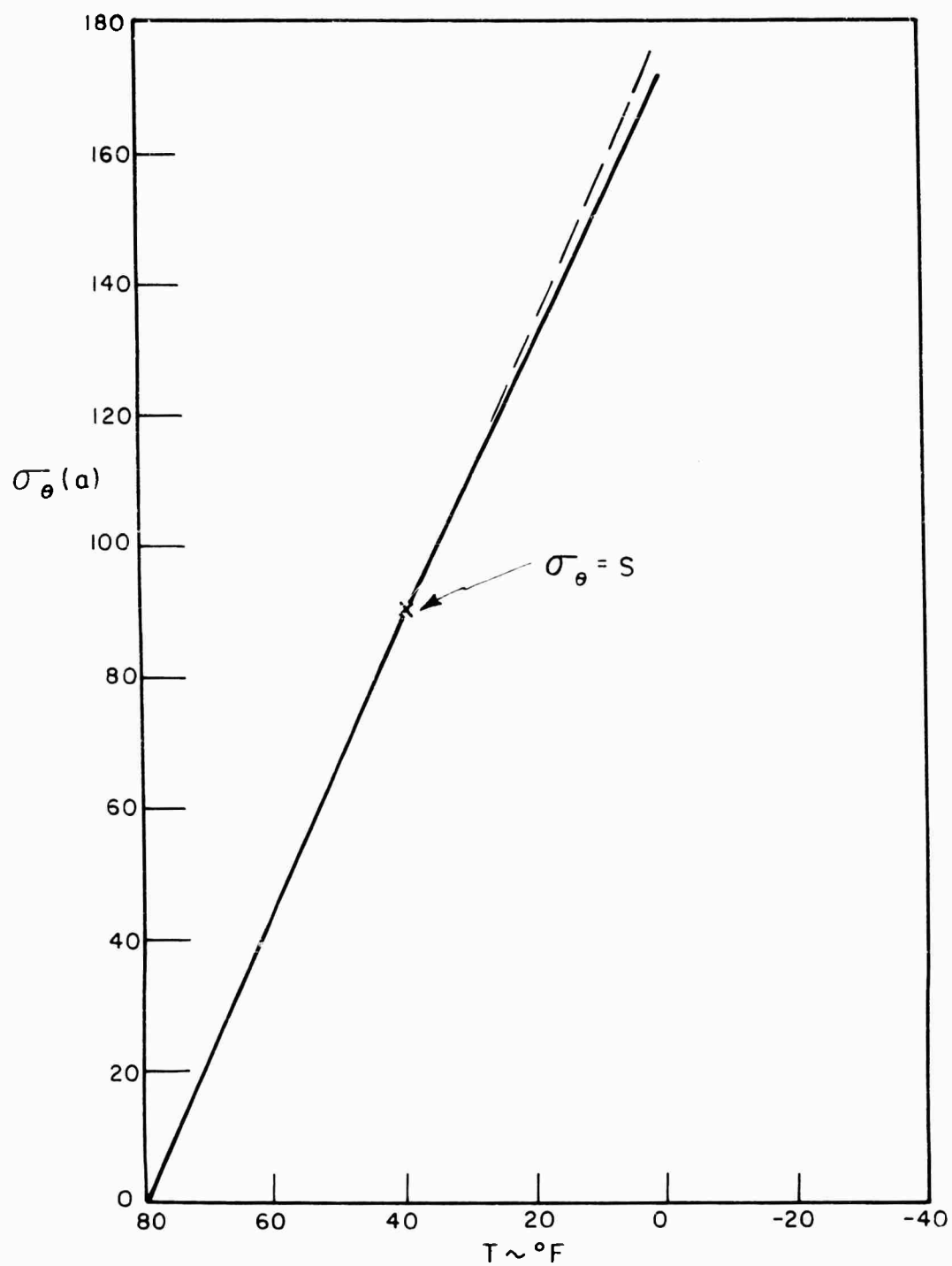


FIG. 14 UNIFORM TEMPERATURE DROP OF A
CLASS II THICK-WALLED CYLINDER,
 $C = 5$ (SEE SECTION 4.3)

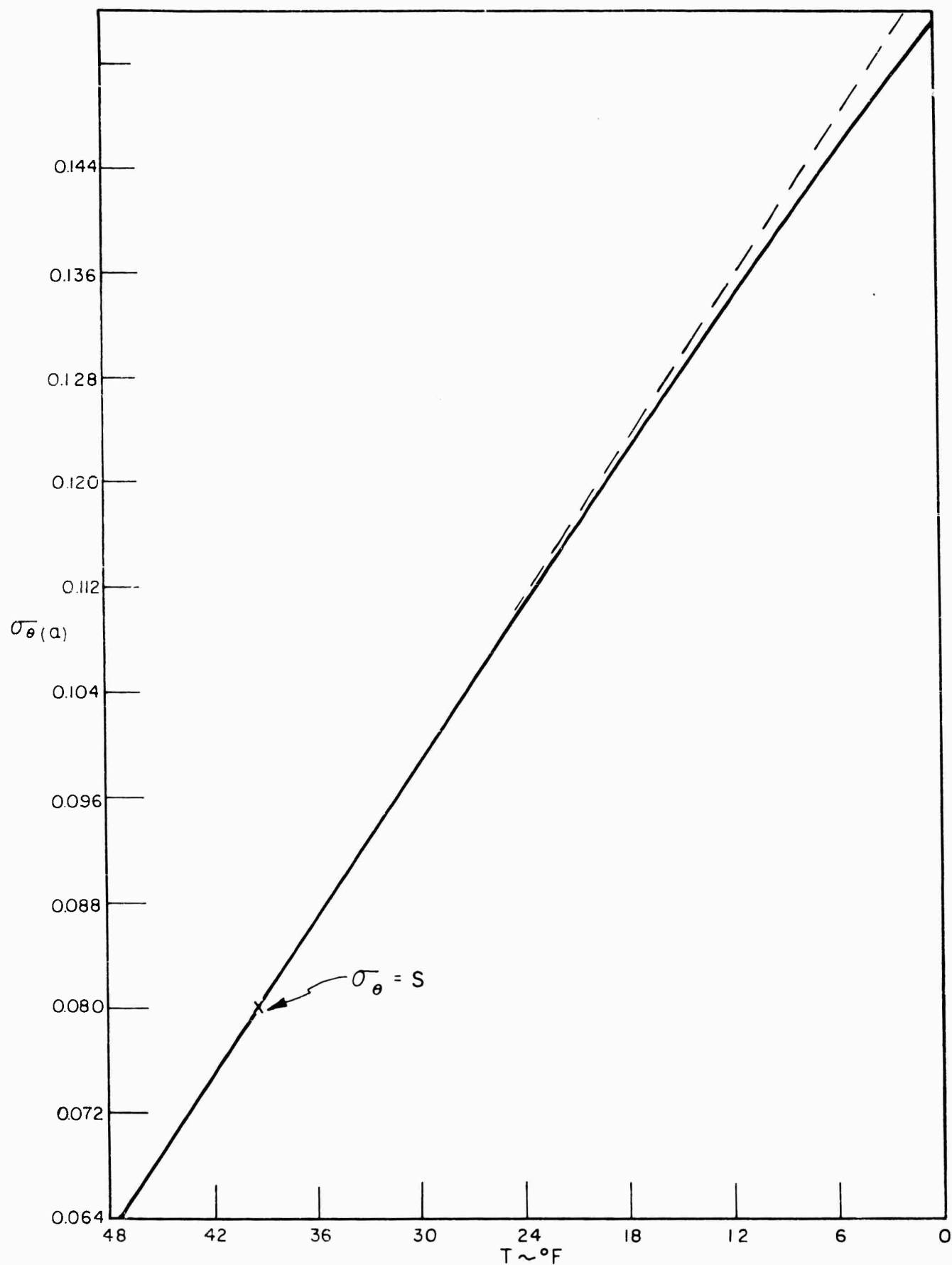


FIG.15 UNIFORM TEMPERATURE DROP OF A CLASS II THICK-WALLED CYLINDER, $C = 5$ ENLARGED PORTION OF FIG.14
(SEE SECTION 4.3)

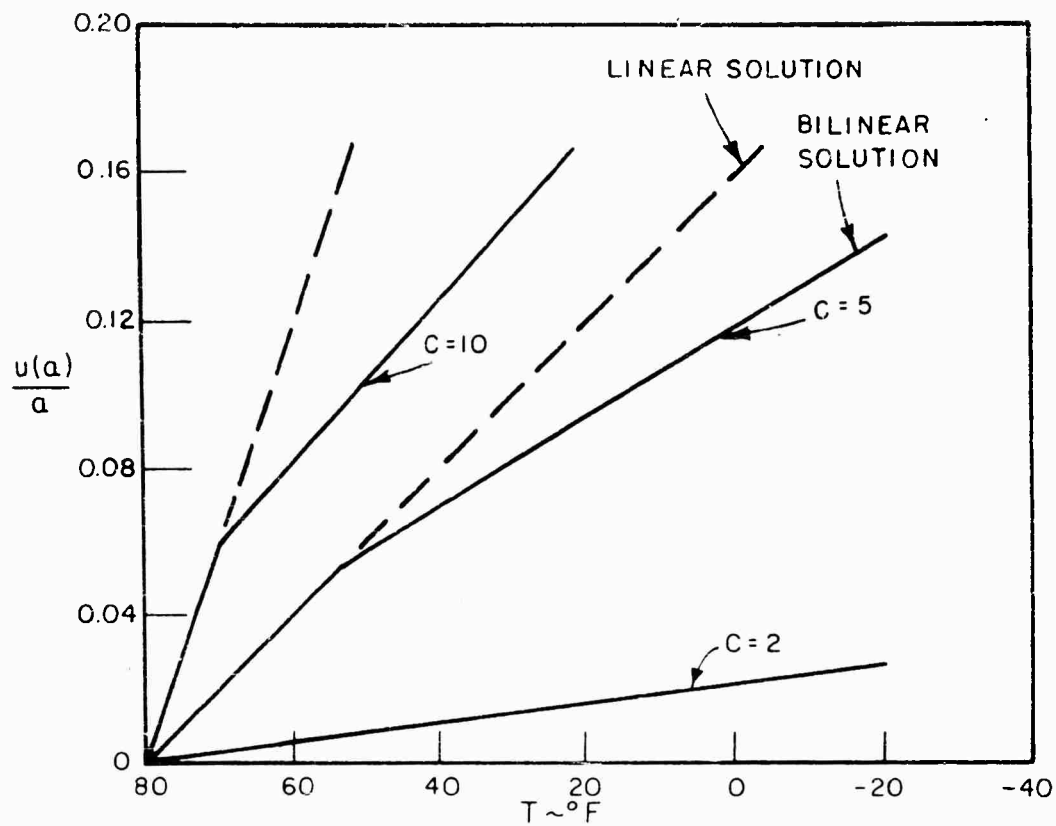


FIG.16 UNIFORM TEMPERATURE DROP OF A CLASS III THICK-WALLED CYLINDER (SEE SECTION 4.3)

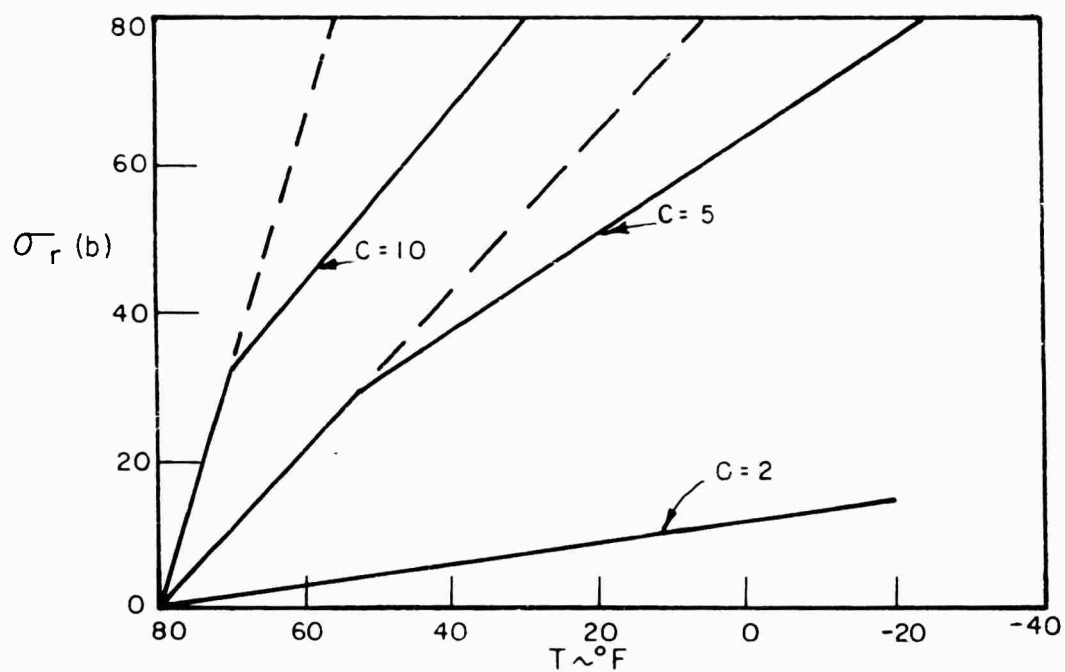


FIG.17 UNIFORM TEMPERATURE DROP OF A CLASS III THICK-WALLED CYLINDER (SEE SECTION 4.3)

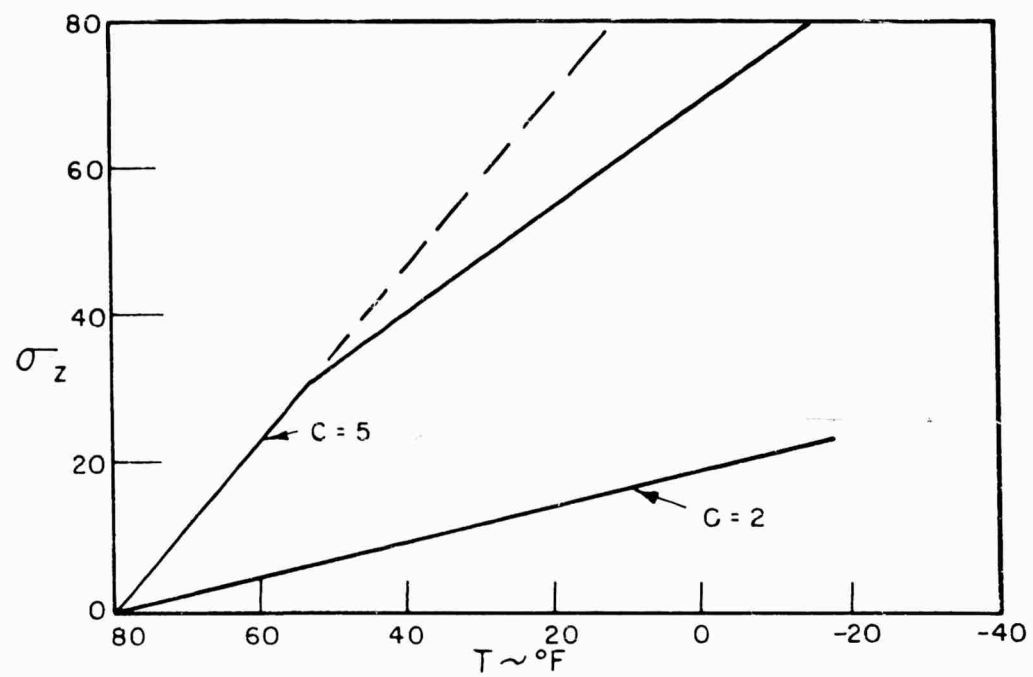


FIG.18 UNIFORM TEMPERATURE DROP OF A CLASS III THICK-WALLED CYLINDER (SEE SECTION 4.3)

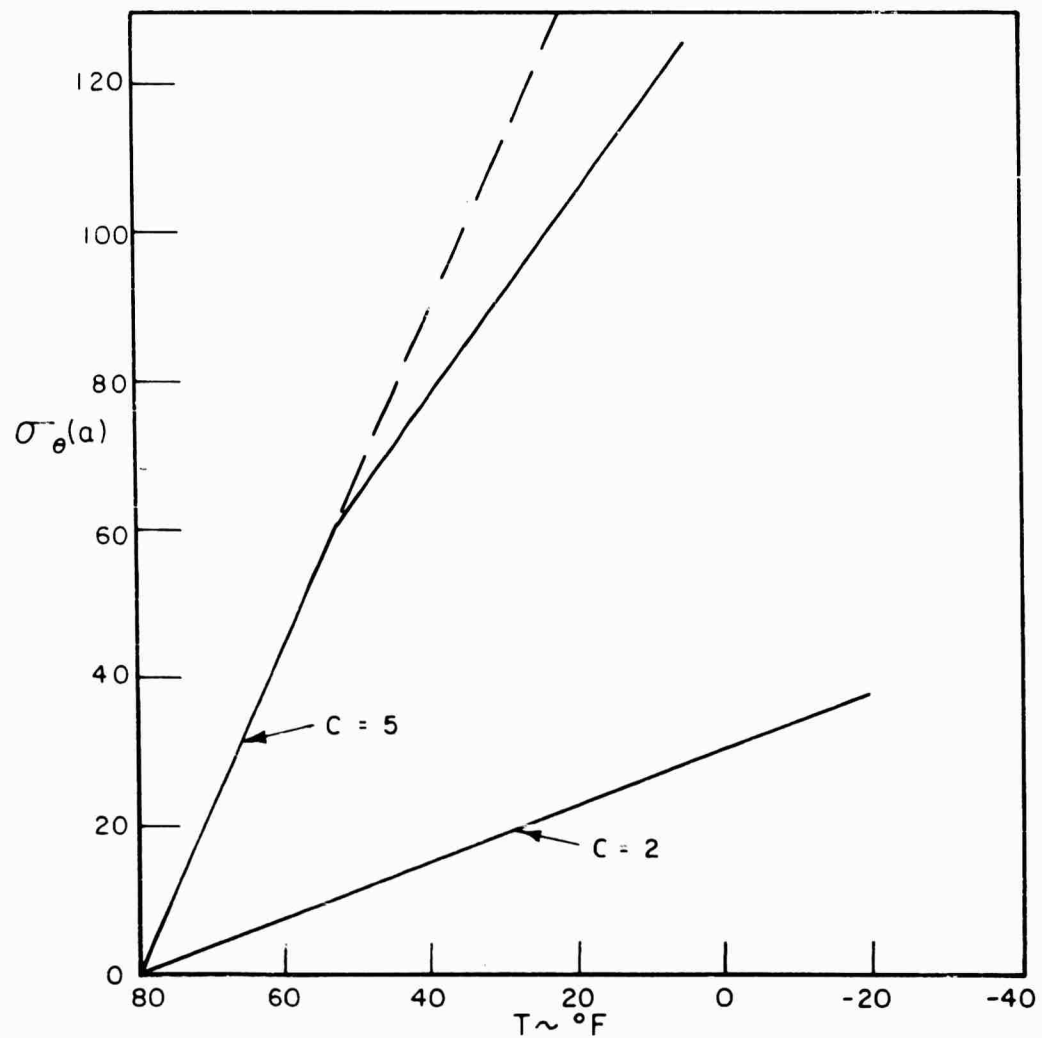


FIG.19 UNIFORM TEMPERATURE DROP OF A CLASS III THICK-WALLED CYLINDER (SEE SECTION 4.3)

PART III

SOLUTION METHOD FOR NONLINEAR ELASTIC PROBLEMS
WITH APPLICATIONS TO THICK-WALLED CYLINDERS

by

L. R. HERRMANN

INTRODUCTION

The state of stress and deformation existing in an elastic body is governed by the finite elastic field equations [1] i.e., equilibrium equations, strain-displacement equations, and stress-strain laws (constitutive equations). These equations will in general be a set of non-linear partial differential equations. Classical elasticity (or first order elasticity) treats those boundary value problems for which this set of non-linear equations may be approximated by a linear set obtained from the finite elastic equations by (1) neglecting all powers of the displacement gradients in the equilibrium equations as compared to unity and neglecting second powers of the displacement gradients as compared to the first power in the strain-displacement relationships and (2) showing by experiment that for the range of strain of interest the constitutive equations are approximately linear. (This may be considered as one of the postulates for classical elasticity). The first assumption is justified if the strain is small. We shall consider a class of problems for which the above two assumptions are no longer justified but in which the strains are still relatively small; we shall base our theory on the following two conditions: (1) the displacement gradients are of such a magnitude that we may neglect their second powers as compared to unity and their first powers in the equilibrium equations and (2) the constitutive equations may be approximated by a truncated series of the second order (the extension to third and higher order theories will be obvious and offers no conceptual difficulties). We shall consider a theory in which the strains are still relatively small, since most problems susceptible to elastic analysis that occur in rocket motor analysis fall into this category.

The best way to treat the constitutive equations is the derivation of their general form experimentally [6], as it

is then apparent how to obtain approximations for the range of strain of interest. Until such expressions have been found for solid propellants, we shall postulate that it is possible to approximate the constitutive equations by a truncated series of a given order. This method of approximating the constitutive equations by a truncated series for a second order theory has previously been used numerous times (see for example Rivlin [3], also Green [2]).

In problems involving strains which are still relatively small and the solution as given by classical theory still approximately valid, it is natural to seek a series solution using the classical solution as a first approximation (note that this method is not directly applicable to the problem of elastic stability). Several such series solutions have been developed; for example Rivlin's second order theory [3] and Green's successive approximation method [2]. The principal advantages of such series solutions are (1) the effects of the non-linearities (i.e. deviations from the classical solution) are clearly illustrated and (2) the higher order solutions may be found immediately if a general solution of the classical problem is known (where body forces are included). The solution for each term of the series merely involves the solution of the classical problem with a nonhomogeneous part depending upon the previous terms (Note: we shall extend the solution method to include those problems for which the classical solution is not known). We shall illustrate yet a third series solution method i.e. solution by perturbation. We have chosen this method for two reasons (1) the method of application is entirely straightforward and (2) we believe that it reduces the algebraic complexities in many problems. The reduction in algebraic complexity is chiefly achieved in two ways, first by deriving the governing equations for each individual problem and second by judiciously selecting the appropriate level of approximation at which to apply certain of the boundary conditions. To be able to apply perturbation theory two conditions

must exist [5]; first there must exist a state, near to the one sought, that has an exact solution. Second, the passage from this state to the one in question must take place in a smooth manner (thus excluding stability problems). These conditions are met for the class of problems considered as the actual solution may be reached after a smooth transition from the solution of the classical elastic equations. Although the foundation upon which our perturbation theory is based depends upon the existence of the classical solution its application does not require knowledge of this solution, as was pointed out above.

We shall consider three general types of material response: compressible, incompressible, and near-incompressible. A near-incompressible material is defined as one for which in the classical region Poisson's ratio is very nearly equal to one-half. We shall discriminate materials that are nearly incompressible for three reasons: (1) to effect a reduction in algebra, (2) to isolate the effects of compressibility, and (3) to illustrate some of the difficulties that arise as $\nu \rightarrow 0.5$.

We shall exhibit a general solution scheme but we shall not derive general equations as it appears to be simpler to derive the governing equations separately for each individual class of problems. Thus our procedure will be to illustrate the method for several simple examples occurring in rocket motor design, including a consideration of the thick-walled cylinder subjected to various loads and thermal effects.

The following treatment consists of two parts: (1) a preliminary consideration of the general finite elastic theory (including some extension necessary for the following work) and (2) illustration of the general solution scheme.

FINITE ELASTIC THEORY

1. Summary of Notations and Formulas (We shall employ curvilinear tensor notation; see [1] and [4])

Notations

x^i	Material coordinates (i.e. coordinates fixed in the body)
y^i	Spatial coordinates (i.e. coordinates fixed in space)
g_{ij}	Covariant components of the metric tensor for the material coordinates in the undeformed space
h_{ij}	Covariant components of the metric tensor for the spatial coordinates
G_{ij}	Covariant components of the metric tensor for the material coordinate system (Green's deformation tensor) in the deformed space
\parallel	Indicates covariant differentiation with respect to the deformed material coordinate system (example $\tau^{ij}{}_{\parallel 1}$)
$\bar{\Gamma}^i_{jk}$	Christoffel three index symbols of the second kind taken with respect to the deformed material coordinate system
τ^{ij}	Contravariant tensor components of stress in the deformed body referred to the deformed base vectors
σ_{ij}	Physical components of stress in the deformed body per unit of deformed area referred to the deformed base vectors
s^{ij}	Contravariant tensor components of stress in the deformed body per unit of undeformed area, referred to the deformed base vectors
η^i	Contravariant tensor components of the displacements in the direction of the undeformed material base vectors ($\eta^{(1)}$ are the physical components)
ξ^i	Contravariant tensor components of the displacement in the direction of the deformed material base vectors ($\xi^{(1)}$ are the physical components)

E^{ij}	Contravariant tensor components of strain
θ_i	Strain invariants
I_i	Alternate form of strain invariants
A	Helmholtz free energy per unit of initial volume
E	Internal energy per unit of initial volume
S	Entropy per unit of initial volume
K	Thermal coefficient of conduction (assumed as temperature and strain independent)
C_E	Specific heat at constant deformation
T_a	Absolute temperature
T	Relative temperature ratio
T_o	Reference temperature
α	Linear coefficient of thermal expansion
$C = O(a)$	Indicates C is of the order of magnitude of a
B	Bulk modulus
ν	Poisson's ratio
μ	Shear modulus
ρ	Density per unit of deformed volume
ρ_o	Density per unit of undeformed volume
V	Deformed volume
V_o	Undeformed volume
F^i	Contravariant components of the body force per unit of mass, referred to the deformed base vectors.

Governing equations:

Equilibrium equations

$$\tau^{ij}{}_{||i} + \rho F^j = 0 \quad (1.1)$$

Strain-displacement relations

$$E_j^i = \frac{1}{2}(G^{*i}{}_j - \delta_j^i) \quad (1.2)$$

where $G_j^{*i} = g^{ik} G_{jk}$ (1.3)

also $\theta_1 = \frac{1}{1!} \delta_{ij} E_i^j = 0(E_j^i)$ (1.4)

$$\theta_2 = \frac{1}{2!} \delta_{km}^{ij} E_i^k E_j^m = 0(E_j^i)^2 \quad (1.5)$$

$$\theta_3 = \frac{1}{3!} \delta_{omn}^{ijk} E_i^o E_j^m E_k^n = 0(E_j^i)^3 \quad (1.6)$$

$$I_1 = 2\theta_1 + 3 \quad (1.7)$$

$$I_2 = 4\theta_2 + 4\theta_1 + 3 \quad (1.8)$$

$$I_3 = 8\theta_3 + 4\theta_2 + 2\theta_1 + 1 = \left(\frac{dv}{dv_0}\right)^2 = \frac{|G_{ij}|}{|g_{ij}|}. \quad (1.9)$$

Form of the Helmholtz free energy

$$A = E - T_a S. \quad (1.10)$$

For an isotropic body

$$A = A(\theta_1, \theta_2, \theta_3, T) \quad (1.11)$$

where

$$T = \frac{T_a - T_0}{T_0} \quad (1.12)$$

Stress-strain laws for compressible material

$$\tau^{ij} = \frac{1}{\sqrt{I_3}} \frac{\partial A}{\partial E_{ij}} = \frac{s^{ij}}{\sqrt{I_3}} \quad (1.13)$$

Noting the above representation for A, see (1.11), we may alternatively write Equation (1.13) for an isotropic compressible material as

$$\tau^{ij} = \frac{1}{\sqrt{I_3}} \left[g^{ij} \frac{\partial A}{\partial \theta_1} + \left(\frac{1}{2} B^{ij} - g^{ij} \right) \frac{\partial A}{\partial \theta_2} + \frac{1}{4} (g^{ij} - B^{ij} + I_3 G^{ij}) \frac{\partial A}{\partial \theta_3} \right] \quad (1.14)$$

where

$$B^{ij} = I_1 g^{ij} - g^{ir} g^{js} G_{rs}. \quad (1.15)$$

Heat conduction equation

$$(KG^{ij} T_a)_{||j} = \rho (C_E \dot{T}_a - \frac{T_a}{\rho_0} \frac{\partial s_{ij}}{\partial T_a} \dot{E}_{ij}) \quad (1.16)$$

where

$$C_E = - \frac{\partial^2 A}{\partial T_a^2} T_a.$$

Physical components

$$\sigma_{ij} = \sqrt{\frac{G_{jj}}{G_{ii}}} \tau^{ij} \quad (\text{no sum}) \quad (1.17)$$

$$\eta^{(i)} = \sqrt{g_{ii}} \eta^i \quad (\text{no sum}) \quad (1.18)$$

$$\xi^{(i)} = \sqrt{G_{ii}} \xi^i \quad (\text{no sum}) \quad (1.19)$$

2. Derivation of Constitutive Equations for Incompressible Thermoelasticity.

Incompressible thermoelasticity describes materials that are mechanically incompressible (i.e., due to stresses) but thermally compressible. We shall consider an incompressible body subjected to certain temperatures and forces such that at some internal point the state of the body is characterized by an absolute temperature T_a (or relative temperature ratio T , see [4]) and displacements η^i . We shall now subject the body to virtual displacements $\delta\eta^i$ (the restrictions placed on $\delta\eta^i$ will be considered below) at constant temperature (i.e., $\delta T = 0$). If we now consider the virtual work performed on some arbitrary volume V during the virtual displacements, we find that

$$V.W. = \iiint_V \tau^{ij} \delta E_{ij} dv \quad (\text{see [1] p.71}). \quad (2.1)$$

This virtual work in an elastic body must equal the change in value of the Helmholtz free energy function (see [4]), $A^* = A^*(E_{ij}, T)$ where A^* is the Helmholtz free energy per unit of deformed volume. Thus,

$$V.W. = \iiint_V \delta A^* dv \quad (2.2)$$

In the formulation of δA^* the variations of δE_{ij} are not arbitrary but must satisfy the additional constraint

$$I_3 - \left(\frac{dv}{dv_0}\right)^2 = 0, \text{ see Eq. (1.9).}$$

where $\left(\frac{dv}{dv_0}\right)$ is a function of T only. Defining a Lagrange

multiplier h' we form

$$L = A^* \frac{h'}{2} \left[I_3 - \left(\frac{dv}{dv_0} \right)^2 \right]$$

Thus $\delta A^* = \delta L$ and $I_3 - \left(\frac{dv}{dv_0} \right)^2 = 0$ where we may now treat the δE_{ij} as independent. We obtain

$$\delta L = \delta A^* = \frac{\partial A^*}{\partial E_{ij}} \delta E_{ij} + \frac{h'}{2} \frac{\partial I_3}{\partial E_{ij}} \delta E_{ij}, \text{ where } I_3 = \left(\frac{dv}{dv_0} \right)^2. \quad (2.3)$$

From Eqs. (2.1), (2.2), and (2.3), we obtain

$$\iiint_V \left[\tau^{ij} - \frac{\partial A^*}{\partial E_{ij}} - \frac{h'}{2} \frac{\partial I_3}{\partial E_{ij}} \right] \delta E_{ij} dv = 0.$$

Treating the δE_{ij} as arbitrary and in view of the arbitrariness of the volume integral we obtain

$$\tau^{ij} = \frac{h'}{2} \frac{\partial I_3}{\partial E_{ij}} + \frac{\partial A^*}{\partial E_{ij}}.$$

Expressing the above equation in terms of the Helmholtz free energy per unit of undeformed volume A ,

$$A^* = \frac{dv_0}{dv} A = \frac{1}{\sqrt{I_3}} A, \text{ see (1.9),}$$

thus

$$\tau^{ij} = \frac{h'}{2} \frac{\partial I_3}{\partial E_{ij}} + \frac{1}{\sqrt{I_3}} \frac{\partial A}{\partial E_{ij}}$$

also

$$\frac{\partial I_3}{\partial E_{1j}} = 2G^{ij}I_3, \quad (\text{see } \square 1 \square, \text{ p. 75}), \quad (2.4)$$

and

$$\tau^{ij} = hG^{ij} + \frac{1}{\sqrt{I_3}} \frac{\partial A}{\partial E_{ij}}, \quad \text{where } I_3 = \left(\frac{dv}{dv_0}\right)^2 \quad (2.5)$$

Letting

$$\sqrt{I_3} - 1 = \frac{dv - dv_0}{dv_0} = f(T) \quad (2.6)$$

we may write

$$\tau^{ij} = hG^{ij} + \frac{1}{1+f(T)} \frac{\partial A}{\partial E_{ij}}, \quad \text{where } I_3 = 1+2f(T)+f^2(T) \quad (2.7)$$

For an isotropic material $A = A(\theta_1, \theta_2, \theta_3, T)$, see Equation (1.11), or noting the relationship between θ_1 and I_3 , Equation (1.9), we may write

$$A = A(\theta_2, \theta_3, I_3 - 1 - 2f(T) - f^2(T), T)$$

If we let

$$\bar{I}_3 = I_3 - 1 - 2f(T) - f^2(T) \quad (2.8)$$

then

$$A = A(\theta_2, \theta_3, \bar{I}_3, T) \quad (2.9)$$

The condition of incompressibility is now expressed by $\bar{I}_3 = 0$.

Let

$$A|_{\bar{I}_3=0} = \bar{A}(\theta_2, \theta_3, T) \quad (2.9a)$$

now
$$\frac{\partial A}{\partial E_{ij}} = \frac{\partial A}{\partial \theta_2} \frac{\partial \theta_2}{\partial E_{ij}} + \frac{\partial A}{\partial \theta_3} \frac{\partial \theta_3}{\partial E_{ij}} + \frac{\partial A}{\partial \bar{I}_3} \frac{\partial \bar{I}_3}{\partial E_{ij}}$$

but
$$\frac{\partial \bar{I}_3}{\partial E_{ij}} = \frac{\partial I_3}{\partial E_{ij}} = 2I_3 G^{ij}, \text{ see (2.4),}$$

$$\left. \frac{\partial A}{\partial \theta_2} \right|_{\bar{I}_3=0} = \frac{\partial \bar{A}}{\partial \theta_2}$$

$$\left. \frac{\partial A}{\partial \theta_3} \right|_{\bar{I}_3=0} = \frac{\partial \bar{A}}{\partial \theta_3}$$

$$\frac{\partial A}{\partial \bar{I}_3} = \text{scalar} = h''$$

thus
$$\left. \frac{\partial A}{\partial E_{ij}} \right|_{\bar{I}_3=0} = \frac{\partial \bar{A}}{\partial \theta_2} \frac{\partial \theta_2}{\partial E_{ij}} + \frac{\partial \bar{A}}{\partial \theta_3} \frac{\partial \theta_3}{\partial E_{ij}} + 2h'' I_3 G^{ij} \quad (2.10)$$

or
$$\left. \frac{\partial A}{\partial E_{ij}} \right|_{\bar{I}_3=0} = \frac{\partial \bar{A}}{\partial E_{ij}} + 2h'' I_3 G^{ij}, \quad (2.11)$$

hence

$$\tau^{ij} = H G^{ij} + \frac{1}{\sqrt{I_3}} \frac{\partial \bar{A}}{\partial E_{ij}} \quad \text{and} \quad \bar{I}_3 = 0, \quad (2.12)$$

Alternatively

$$\tau^{ij} = H G^{ij} + \frac{1}{1+f(T)} \frac{\partial \bar{A}}{\partial E_{ij}} \quad \text{and} \quad I_3 = 1+2f(T)+f^2(T), \quad (2.13)$$

where

$$H = h + 2 \sqrt{I_3} h'' ,$$

or from Equation (1.14)

$$\tau^{ij} = H G^{ij} + \frac{1}{1+f(T)} \left[\left(\frac{1}{2} B^{ij} - g^{ij} \right) \frac{\partial \bar{A}}{\partial \theta_2} + \frac{1}{4} (g^{ij} - B^{ij} + I_3 G^{ij}) \frac{\partial \bar{A}}{\partial \theta_3} \right] , \quad (2.14)$$

where

$$B^{ij} = I_1 g^{ij} - g^{ir} g^{js} G_{rs} .$$

3. Governing Equations for Thick-walled Cylinders.

Consider the behavior of an infinitely long thick-walled cylinder subjected to axially symmetrical forces and temperature distribution. In order to illustrate two fundamental approaches to the formulation of the finite elastic equations we shall consider two distinctly different types of displacement fields; first we shall consider the effects of pressure and temperature which will cause motion only in the radial direction, and secondly we shall consider the effects of a vertical gravity loading which shall give rise to both a longitudinal and radial motion. In the first problem we shall select our material coordinate system such that in the initial state it coincides with the cylindrical coordinate system (r, θ, z) and in the second problem we shall select our material coordinate system such that in the final state it coincides with the cylindrical coordinate system (r, θ, z) . Thus if we compute the

stress at the point $r = r_0$, $\theta = \theta_0$ and $z = z_0$, we have for the first problem found the state of stress of the material that initially occupied the point (r_0, θ_0, z_0) while in the second problem we have found the state of stress for the material that occupies (r_0, θ_0, z_0) in its deformed position.

Pressure and Temperature Loading of a Thick-walled Cylinder

We shall describe the initial state in cylindrical coordinates (r, θ, z) . The material coordinates shall be selected such that in the initial state they coincide with these cylindrical coordinates, i.e.,

$$(x^1, x^2, x^3) = (r, \theta, z) \quad (3.1)$$

then $(ds_0)^2 = g_{ij} dx^i dx^j$

where
$$g_{ij} = \begin{bmatrix} 1 & & \\ & (x^1)^2 & \\ & & 1 \end{bmatrix} \quad (3.2)$$

The spatial coordinate system will be chosen as a cylindrical coordinate system also, thus

$$(ds)^2 = h_{\alpha\beta} dy^\alpha dy^\beta$$

where
$$h_{\alpha\beta} = \begin{bmatrix} 1 & & \\ & (y^1)^2 & \\ & & 1 \end{bmatrix}$$

The displacement field will be

$$\eta^1 = \eta^{(1)} = u(x^1) = u(r)$$

$$\eta^2 = 0$$

$$\eta^3 = 0.$$

In the deformed state the material coordinates will be related to the spatial coordinate system as follows

$$y^1 = x^1 + u(x^1) = r + u(r)$$

$$y^2 = x^2 = \theta$$

$$y^3 = x^3 = z.$$

The Green's deformation tensor is given by

$$G_{ij} = h_{\alpha\beta} \frac{\partial y^\alpha}{\partial x^i} \frac{\partial y^\beta}{\partial x^j}$$

or

$$G_{ij} = \begin{bmatrix} (1 + \frac{du}{dr})^2 & & \\ & (r+u)^2 & \\ & & 1 \end{bmatrix} \quad (3.3)$$

also

$$G^{*i}_j = g^{ik} G_{jk}$$

or

$$G^{*i}_j = \begin{bmatrix} (1 + \frac{du}{dr})^2 & & \\ & (1 + \frac{u}{r})^2 & \\ & & 1 \end{bmatrix} \quad (3.4)$$

The Christoffel symbols of the second kind may be found from

$$\bar{\Gamma}^{i}_{jk} = \frac{G^{in}}{2} \left[\frac{\partial G_{jn}}{\partial x^k} + \frac{\partial G_{kn}}{\partial x^j} - \frac{\partial G_{jk}}{\partial x^n} \right]$$

$$\bar{\Gamma}^1_{11} = \frac{\frac{d^2 u}{dr^2}}{(1 + \frac{du}{dr})}$$

$$\bar{\Gamma}^3_{13} = \bar{\Gamma}^1_{12} = \bar{\Gamma}^1_{13} = \bar{\Gamma}^2_{11} = \bar{\Gamma}^3_{11} = \bar{\Gamma}^1_{33} = 0$$

$$\bar{\Gamma}^2_{12} = \frac{(1 + \frac{du}{dr})}{(r + u)}$$

$$\bar{\Gamma}^1_{22} = - \frac{(r + u)}{(1 + \frac{du}{dr})}.$$

The equations of equilibrium in material coordinates, Equation (1.1), are

$$\tau^i_{j||i} - \rho F_j = 0$$

The non-trivial equation for this problem is, for $j = 1$,

$$\tau_{1||1}^1 = 0$$

$$\text{or } \frac{\partial \tau_1^1}{\partial x^1} + \tau_1^1 [\bar{\Gamma}_{11}^1 + \bar{\Gamma}_{21}^2 + \bar{\Gamma}_{31}^3] - \tau_1^1 \bar{\Gamma}_{11}^1 - \tau_2^2 \bar{\Gamma}_{21}^2 - \tau_3^3 \bar{\Gamma}_{31}^3 = 0$$

$$\text{Noting that } \tau_1^1 = \sigma_{11} = \sigma_r, \quad \tau_2^2 = \sigma_{22} = \sigma_\theta,$$

$$\frac{d\sigma_r}{dr} + \frac{\sigma_r - \sigma_\theta}{r} + \frac{u}{r} \frac{d\sigma_r}{dr} + \frac{du}{dr} \frac{\sigma_r - \sigma_\theta}{r} = 0. \quad (3.5)$$

The strain components, Equation (1.2), are

$$E_j^1 = \frac{1}{2} (G^{*i}_j - \delta_j^1)$$

$$\text{or } E_j^i = \begin{bmatrix} \frac{du}{dr} + \frac{1}{2} \left(\frac{du}{dr} \right)^2 \\ \frac{u}{r} + \frac{1}{2} \left(\frac{u}{r} \right)^2 \\ 0 \end{bmatrix} \quad (3.6)$$

leading to the invariants

$$\theta_1 = E_1^1 + E_2^2 \quad (3.7)$$

$$\theta_2 = E_1^1 E_2^2$$

$$\theta_3 = 0$$

$$I_3 = 1 + 2E_1^1 + 2E_2^2 + 4E_1^1 E_2^2$$

The heat conduction equation, Equation (1.16), is

$$(KG^{ij}T_{a||j})_{||i} = \rho(C_E \dot{T}_a - \frac{T_a}{\rho_0} \frac{\partial s^{ij}}{\partial T_a} \dot{E}_{ij}).$$

For our problem we note K and T_0 are constants and consider only steady state conditions. Thus,

$$G^{ij}T_{||ij} = 0$$

$$\text{or} \quad G^{11} \frac{d^2 T}{d(x^1)^2} - \frac{dT}{dx^1} [G^{11}\Gamma_{11}^1 + G^{22}\Gamma_{22}^1 + G^{33}\Gamma_{33}^1] = 0$$

$$\begin{aligned} \text{or} \quad \frac{d^2 T}{dr^2} + \frac{1}{r} \frac{dT}{dr} + \left\{ \left(\frac{u}{r} + \frac{du}{dr} \right) \frac{d^2 T}{dr^2} - \left(r \frac{d^2 u}{dr^2} - 2 \frac{du}{dr} \right) \frac{1}{r} \frac{dT}{dr} \right\} \\ + \left\{ \frac{u}{r} \frac{du}{dr} \frac{d^2 T}{dr^2} - \left[u \frac{d^2 u}{dr^2} - \left(\frac{du}{dr} \right)^2 \right] \frac{1}{r} \frac{dT}{dr} \right\} = 0 \end{aligned} \quad (3.8)$$

Governing Equations for Vertical Slump of a Thick-walled Cylinder

Selecting material coordinates (x^i) such that in the deformed body they coincide with the cylindrical coordinates (r, θ, z) , the material metric tensor is

$$G_{ij} = \begin{bmatrix} 1 & & \\ & (x^1)^2 & \\ & & 1 \end{bmatrix} \quad (3.9)$$

Let (y^i) be cylindrical coordinates, therefore

$$h_{ij} = \begin{bmatrix} 1 & & \\ & (y^1)^2 & \\ & & 1 \end{bmatrix}$$

The displacement field will be

$$\xi^1 = \xi^{(1)}(x^1) = u(r)$$

$$\xi^2 = 0$$

$$\xi^3 = \xi^{(3)}(x^1) = w(r).$$

Thus, $y^1 = x^1 - u^1 = r - u(r)$

$$y^2 = x^2$$

$$y^3 = x^3 - u^3 = z - w(r).$$

Now

$$g_{ij} = h_{kn} \frac{\partial y^k}{\partial x^i} \frac{\partial y^n}{\partial x^j}$$

or

$$g_{ij} = \begin{bmatrix} (1 - \frac{du}{dr})^2 + (\frac{dw}{dr})^2 & 0 & -\frac{dw}{dr} \\ 0 & (r - u)^2 & 0 \\ -\frac{dw}{dr} & 0 & 1 \end{bmatrix} \quad (3.10)$$

Also g^{ij} may be found from $g^{ij}g_{ik} = \delta_k^i$

$$g^{ij} = \begin{bmatrix} \frac{1}{(1 - \frac{du}{dr})^2} & 0 & \frac{\frac{dw}{dr}}{(1 - \frac{du}{dr})^2} \\ 0 & \frac{1}{(r - u)^2} & 0 \\ \frac{\frac{dw}{dr}}{(1 - \frac{du}{dr})^2} & 0 & 1 + \frac{\frac{dw}{dr}}{(1 - \frac{du}{dr})^2} \end{bmatrix} \quad (3.11)$$

and

$$I_3 = \frac{|G_{ij}|}{|g_{ij}|} = \frac{1}{(1 - \frac{u}{r})^2 (1 - \frac{du}{dr})^2} \quad (3.12)$$

The equilibrium equations are the usual equations for cylindrical coordinates,

$$\frac{d\sigma_r}{dr} + \frac{\sigma_r - \sigma_\theta}{r} = 0$$

(3.13)

and

$$\frac{d\tau_{rz}}{dr} + \frac{1}{r} \tau_{rz} + \rho g = 0$$

From Equations (1.9) and (3.12),

$$\frac{\rho}{\rho_0} = \frac{1}{\sqrt{I_3}} = (1 - \frac{u}{r}) (1 - \frac{du}{dr})$$

(3.14)

thus

$$\frac{d\tau_{rz}}{dr} + \frac{1}{r} \tau_{rz} + \rho_0 (1 - \frac{u}{r}) (1 - \frac{du}{dr}) g = 0.$$

The deformation tensor is

$$G^{*i}_{\ j} = \begin{bmatrix} \frac{1}{(1 - \frac{du}{dr})^2} & 0 & \frac{\frac{dw}{dr}}{(1 - \frac{du}{dr})^2} \\ 0 & \frac{r^2}{(r - u)^2} & 0 \\ \frac{\frac{dw}{dr}}{(1 - \frac{du}{dr})^2} & 0 & 1 + \frac{(\frac{dw}{dr})^2}{(1 - \frac{du}{dr})^2} \end{bmatrix}$$

leading to strain displacement equations

$$E_j^i = \frac{1}{2} \begin{bmatrix} \frac{1}{(1 - \frac{du}{dr})^2} - 1 & 0 & \frac{\frac{dw}{dr}}{(1 - \frac{du}{dr})^2} \\ 0 & \frac{1}{(1 - \frac{u}{r})^2} - 1 & 0 \\ \frac{\frac{dw}{dr}}{(1 - \frac{du}{dr})^2} & 0 & \frac{(\frac{dw}{dr})^2}{(1 - \frac{du}{dr})^2} \end{bmatrix} \quad (3.15)$$

SECOND ORDER ELASTIC THEORY

4. General Theory.

In the remainder of this section, we shall assume that the magnitude of strains is such that we need retain only first and second order terms in our final equations. It must be emphasized that when the resulting solutions are applied to a specific problem, the numerical results must justify the above assumption.

For example the strain-displacement relations, Equation (3.15), for a second order theory, would be written as follows:

$$E_j^i = \begin{bmatrix} \frac{du}{dr} + \frac{3}{2} \left(\frac{du}{dr} \right)^2 & 0 & \frac{1}{2} \frac{dw}{dr} + \frac{du}{dr} \frac{dw}{dr} \\ 0 & \frac{u}{r} + \frac{3}{2} \left(\frac{u}{r} \right)^2 & 0 \\ \frac{1}{2} \frac{dw}{dr} + \frac{du}{dr} \frac{dw}{dr} & 0 & \left(\frac{dw}{dr} \right)^2 \end{bmatrix}.$$

The form of the Helmholtz free energy function which determines the form of the constitutive equations will now be determined for a second order elastic theory. The energy datum is taken at the reference temperature T_0 . For a compressible material, assuming that T is of the order of magnitude of E_j^1 , we expand A in a power series in θ_1 and T and retain terms of third order or less. The range of validity of the second order theory needs to be considered in light of the relative size of the coefficients of the neglected terms as compared to the

terms retained in the expansion, a comparison which can best be made by finding the total expression for A by experimental means. Accordingly,

$$A = k_1(\theta_2 + k_2\theta_1^2 + k_3\theta_1\theta_2 + k_4\theta_1^3 + k_5\theta_3 + k_6T\theta_1 + k_7T\theta_1^2 + k_8T\theta_2 + k_9T^2\theta_1 + k_{10}T^2 + k_{11}T^3). \quad (4.1)$$

In classical elasticity only the first and second order terms are retained, i.e.,

$$A = k_1(\theta_2 + k_2\theta_1^2 + k_6T\theta_1 + k_{10}T^2)$$

which when compared to the usual notation [4] is written

$$A = -2\mu \left[\theta_2 - \frac{1-\nu}{2(1-2\nu)} \theta_1^2 + \frac{(1+\nu)\alpha T_0}{1-2\nu} \theta_1 T + k_{10}T^2 \right].$$

Comparing terms we find (note k_{10} and k_{11} need not be evaluated)

$$k_1 = -2\mu$$

$$k_2 = -\frac{1-\nu}{2(1-2\nu)} \quad (4.2)$$

$$k_6 = \frac{1+\nu}{1-2\nu} \alpha T_0$$

or

$$\mu = -\frac{k_1}{2}$$

$$\nu = \frac{1 + 2k_2}{1 + 4k_2} \quad (4.3)$$

$$\alpha = -\frac{k_6}{2T_0(1 + 3k_2)}$$

In incompressible elasticity we need the function $\bar{A}(\theta_2, \theta_3, T)$, Equation (2.9a), which, in light of the above reasoning, shall be taken as

$$\bar{A} = c_1(\theta_2 + c_2\theta_3 + c_3T\theta_2 + c_4T^2 + c_5T^3) \quad (4.4)$$

It is also necessary to have an expression for $\frac{dv - dv_0}{dv_0}$ as a

function of T . For a second order incompressible theory, Equation (2.6) is written

$$\frac{dv - dv_0}{dv_0} = \beta_1 T + \beta_2 T^2 = f(T) \quad (4.5)$$

For classical thermoelasticity we have $\frac{dv - dv_0}{dv_0} = 3\alpha T_0 T$; thus

$\beta_1 = 3\alpha T_0$. Hence, the incompressibility condition $\bar{I}_3 = 0$,

from Equation (2.8) yields

$$I_3 = \left[1 + f(T)\right]^2 = 0 \quad (4.6)$$

Substituting for I_3 .

$$1 + 2\theta_1 + 4\theta_2 + 8\theta_3 - 1 - 2f(T) - f^2(T) = 0$$

$$\text{or} \quad (4.7)$$

$$\theta_1 + 2\theta_2 + 4\theta_3 = \beta_1 T + (\beta_2 + \frac{1}{2}\beta_1^2)T^2$$

$$\text{Now let} \quad (\beta_2 + \frac{1}{2}\beta_1^2) = \beta_2^* \quad (4.8)$$

$$\text{then} \quad \theta_1 + 2\theta_2 + 4\theta_3 = \beta_1 T + \beta_2^* T^2. \quad (4.9)$$

In order to relate the coefficients appearing in Equations (4.1) and (4.4) it is necessary to express A in terms of $\theta_2, \theta_3, \bar{I}_3$ and T. Noting that

$$\bar{I}_3 = 2\theta_1 + 4\theta_2 + 8\theta_3 - 2\beta_1 T - 2\beta_2^* T^2$$

we may write Equation (4.1) as

$$\begin{aligned} A = k_1 \left\{ \theta_2 + k_5 \theta_3 + \left[-4\beta_1 k_2 + k_3 \beta_1 - 2k_6 + k_8 \right] T \theta_2 + \frac{k_2}{4} \bar{I}_3^2 \right. \\ + \left[k_2 \beta_1 + \frac{k_6}{2} \right] \bar{I}_3 T + \frac{k_4}{8} \bar{I}_3^3 + \left[\frac{3\beta_1 k_4}{4} + \frac{k_7}{4} \right] \bar{I}_3^2 T \\ \left. + \left[k_2 \beta_2^* + \frac{3k_4 \beta_1^2}{2} + \beta_1 k_7 + \frac{k_9}{2} \right] \bar{I}_3 T^2 + \left[-2k_2 + \frac{k_3}{2} \right] \bar{I}_3 \theta_2 + h(T) \right\}. \end{aligned}$$

Thus

$$A|_{I_3=0} = \bar{A} = k_1 \left\{ \theta_2 + k_5 \theta_3 + \left[-4\beta_1 k_2 + k_3 \beta_1 - 2k_6 + k_8 \right] r \theta_2 + h(T) \right\}$$

which, when compared with Equation (4.4), yields

$$\begin{aligned} c_1 &= k_1 \\ c_2 &= k_5 \\ c_3 &= \left[-4\beta_1 k_2 + k_3 \beta_1 - 2k_6 + k_8 \right]. \end{aligned} \tag{4.10}$$

To obtain the constitutive equations we need merely apply either Equation (1.14) or (2.14). For example, for the pressure and temperature loading of a compressible cylinder we will make use of Equation (1.14) where, (see Equations (3.2), (3.3) and (3.7)),

$$g^{11} = 1$$

$$B^{11} = 2\theta_1 + 3 - G_{11}$$

$$G_{11} = 2E_1^1 + 1$$

$$G^{11} = \frac{1}{1 + 2E_1^1}$$

$$\theta_1 = E_1^1 + E_2^2$$

$$\theta_2 = E_1^1 E_2^2$$

$$\theta_3 = 0$$

Thus,

$$\tau^{11} = \frac{k_1}{\sqrt{I_3}} \left[2k_2(E_1^1 + E_2^2) + k_3 E_1^1 E_2^2 + 3k_4(E_1^1 + E_2^2)^2 + k_6 T \right. \\ \left. + 2k_7 T(E_1^1 + E_2^2) + k_9 T^2 + k_3 E_2^2(E_1^1 + E_2^2) + k_8 E_2^2 T + E_2^2 \right].$$

Utilizing Equations (1.2), (1.17), and (2.4), we can write

$$\sigma_r = G_{11} \tau^{11} = (2E_1^1 + 1) \tau^{11},$$

or

$$\sigma_r = k_1 \left[(1+2k_2)E_2^2 + 2k_2 E_1^1 + k_6 T + E_1^1 E_2^2 (2k_3 + 6k_4 + 1) + (E_1^1)^2 (3k_4 + 2k_2) \right. \\ \left. + (E_2^2)^2 (k_3 + 3k_4 - 1 - 2k_2) + E_1^1 T (2k_7 + k_6) + E_2^2 T (2k_7 + k_8 - k_6) + k_9 T^2 \right]$$

Likewise

$$\sigma_r - \sigma_\theta = k_1 \left\{ (E_2^2 - E_1^1) + [(E_1^1)^2 - (E_2^2)^2] (4k_2 + 1 - k_3) + (E_1^1 - E_2^2) T (2k_6 - k_8) \right\}.$$

Making use of Equation (3.6),

$$\sigma_r = k_1 \left[(1+2k_2) \frac{u}{r} + 2k_2 \frac{du}{dr} + k_6 T + (k_3 + 3k_4 - \frac{1}{2} - k_2) \left(\frac{u}{r} \right)^2 \right. \\ \left. + (k_2 + 3k_4 + 2k_2) \left(\frac{du}{dr} \right)^2 + (2k_3 + 6k_4 + 1) \frac{u}{r} \frac{du}{dr} + (2k_7 + k_6) T \frac{du}{dr} \right. \\ \left. + (2k_7 + k_8 - k_6) T \frac{u}{r} + k_9 T^2 \right] \quad (4.11)$$

and

$$\sigma_r - \sigma_\theta = k_1 \left(\frac{u}{r} - \frac{du}{dr} \right) \left[1 + \left(k_3 - \frac{1}{2} - 4k_2 \right) \left(\frac{u}{r} + \frac{du}{dr} \right) + (k_8 - 2k_6) T \right]. \quad (4.12)$$

A SOLUTION METHOD FOR FINITE ELASTICITY

5. Outline of Method.

In order to cast the governing equations for pressure and temperature problems into a form susceptible to a perturbation solution (i.e., into a form where the relative magnitude of the various terms is apparent) we shall make the following change of variables; (A somewhat similar method of introducing a perturbation parameter for thick cylindrical shell theory is given in [9]).

$$v = \frac{u}{u_{\max}} \quad (5.1)$$

$$\rho = \frac{r}{a} , \quad (5.2)$$

where a is the inner radius of the cylinder.

Thus

$$\left| \frac{v}{\rho} \right| \leq 1$$

and

$$\frac{u}{r} = \frac{v u_{\max}}{\rho a}$$

Let

$$\frac{u_{\max}}{a} = \delta \quad (\text{For a second order theory } |\delta| < 1.) \quad (5.3)$$

Therefore,

$$\frac{u}{r} = \delta \frac{v}{\rho}$$

Also let

$$\sigma_r = k_1 \delta s_\rho \quad (5.4)$$

$$\sigma_\theta = k_1 \delta s_\theta$$

$$T = \delta T^* \quad (5.5)$$

Making the above change of variables the governing equations (3.5), (3.8), (4.11) and (4.12) may be written

$$\frac{ds_\rho}{d\rho} + \frac{s_\rho - s_\theta}{\rho} = - \delta \left[\frac{v}{\rho} \frac{ds_\rho}{d\rho} + \frac{dv}{d\rho} \frac{s_\rho - s_\theta}{\rho} \right]$$

$$\begin{aligned} \frac{d^2 T^*}{d\rho^2} + \frac{1}{\rho} \frac{dT^*}{d\rho} = & - \delta \left[\left(\frac{v}{\rho} + \frac{dv}{d\rho} \right) \frac{d^2 T^*}{d\rho^2} - \left(\rho \frac{d^2 v}{d\rho^2} - 2 \frac{dv}{d\rho} \right) \frac{1}{\rho} \frac{dT^*}{d\rho} \right] - \delta^2 \left\{ \frac{v}{\rho} \frac{dv}{d\rho} \frac{d^2 T^*}{d\rho^2} \right. \\ & \left. - \left[v \frac{d^2 v}{d\rho^2} - \left(\frac{dv}{d\rho} \right)^2 \right] \frac{1}{\rho} \frac{dT^*}{d\rho} \right\} \end{aligned}$$

$$\begin{aligned} s_\rho = & (1+2k_2) \frac{v}{\rho} + 2k_2 \frac{dv}{d\rho} + k_6 T^* + \delta \left[(k_3+3k_4 - \frac{1}{2} - k_2) \left(\frac{v}{\rho} \right)^2 + 3(k_4 \right. \\ & \left. + k_2) \left(\frac{dv}{d\rho} \right)^2 + (2k_3 + 6k_4 + 1) \frac{v}{\rho} \frac{dv}{d\rho} + (2k_7 + k_6) T^* \frac{dv}{d\rho} + (2k_7 \right. \\ & \left. + k_8 - k_6) T^* \frac{v}{\rho} + k_9 T^{*2} \right] \quad (5.6) \end{aligned}$$

$$s_\rho - s_\theta = \frac{v}{\rho} - \frac{dv}{d\rho} + \delta \left\{ (k_3 - \frac{1}{2} - 4k_2) \left[\left(\frac{v}{\rho} \right)^2 - \left(\frac{dv}{d\rho} \right)^2 \right] + (k_8 - 2k_6) T^* \left(\frac{v}{\rho} - \frac{dv}{d\rho} \right) \right\}.$$

As $\delta \rightarrow 0$ the above equations approach the classical elastic equations; thus, we have established the conditions that are prerequisite to a solution by perturbation, i.e., (1) a near state for which an exact solution is known (as $\delta \rightarrow 0$ we have the state as defined by the classical field equations) and (2) the transition from this near state to the desired state should proceed in a smooth manner (as previously indicated we shall not consider stability problems). It should be noted that the perturbation parameter δ is merely a device used in obtaining a solution and as such will not appear in the final solution. To effect a solution by perturbation we expand the dependent variables in a perturbation series, i.e.,

$$T^* = T^{*(0)} + \delta T^{*(1)} + \dots$$

$$v = v^{(0)} + \delta v^{(1)} + \dots$$

$$s_\rho = s_\rho^{(0)} + \delta s_\rho^{(1)} + \dots$$

$$s_\theta = s_\theta^{(0)} + \delta s_\theta^{(1)} + \dots$$

(5.7)

where $v^{(0)}$ is the solution of the near state (first approximation), $v^{(1)}$ is the first corrective term, etc. Substitution of the above expressions into the governing equations and equating coefficients of δ we obtain the following systems of equations;

First system

$$\frac{d^2 T^{*(0)}}{d\rho^2} + \frac{1}{\rho} \frac{dT^{*(0)}}{d\rho} = 0$$

$$\frac{ds_{\rho}^{(0)}}{d\rho} + \frac{s_{\rho}^{(0)} - s_{\theta}^{(0)}}{\rho} = 0$$

(5.8)

$$s_{\rho}^{(0)} - (1 + 2k_2) \frac{v^{(0)}}{\rho} - 2k_2 \frac{dv^{(0)}}{d\rho} - k_6 T^{*(0)} = 0$$

$$s_{\rho}^{(0)} - s_{\theta}^{(0)} - \frac{v^{(0)}}{\rho} + \frac{dv^{(0)}}{d\rho} = 0 ,$$

Second system

$$\frac{d^2 T^{*(1)}}{d\rho^2} + \frac{1}{\rho} \frac{dT^{*(1)}}{d\rho} = - \left(\frac{v^{(0)}}{\rho} + \frac{dv^{(0)}}{d\rho} \right) \frac{d^2 T^{*(0)}}{d\rho^2} + \left(\rho \frac{d^2 v^{(0)}}{d\rho^2} \right.$$

$$\left. - 2 \frac{dv^{(0)}}{d\rho} \right) \frac{1}{\rho} \frac{dT^{*(0)}}{d\rho}$$

$$\frac{ds_{\rho}^{(1)}}{d\rho} + \frac{s_{\rho}^{(1)} - s_{\theta}^{(1)}}{\rho} = \frac{1}{\rho} \left(\frac{v^{(0)}}{\rho} - \frac{dv^{(0)}}{d\rho} \right)^2 \quad (5.9)$$

$$s_{\rho}^{(1)} - (1 + 2k_2) \frac{v^{(1)}}{\rho} - 2k_2 \frac{dv^{(1)}}{d\rho} - k_6 T^{*(1)} = (k_3 + 3k_4 - \frac{1}{2}$$

$$- k_2) \left(\frac{v^{(0)}}{\rho} \right)^2$$

Continued

$$\begin{aligned}
& + 3(k_4 + k_2) \left(\frac{dv^{(0)}}{d\rho} \right)^2 + (2k_3 + 6k_4 + 1) \frac{v^{(0)}}{\rho} \frac{dv^{(0)}}{d\rho} + (2k_7 + k_6) T^{*(0)} \frac{dv^{(0)}}{d\rho} \\
& + (2k_7 + k_8 - k_6) T^{*(0)} \frac{v^{(0)}}{\rho} + k_9 (T^{*(0)})^2 \\
s_\rho^{(1)} - s_e^{(1)} - \left(\frac{v^{(1)}}{\rho} - \frac{dv^{(1)}}{d\rho} \right) &= (k_3 - 4k_2 - \frac{1}{2}) \left[\left(\frac{v^{(0)}}{\rho} \right)^2 - \left(\frac{dv^{(0)}}{d\rho} \right)^2 \right] \\
& + (k_8 - 2k_6) T^{*(0)} \left(\frac{v^{(0)}}{\rho} - \frac{dv^{(0)}}{d\rho} \right).
\end{aligned}$$

The first set of equations is that of classical elasticity. The left hand side of the two systems of equations are identical. Whereas the first system is homogeneous (in the absence of body forces and temperature sources) the second system has non-homogeneous parts composed of non-linear terms derived from the solution of the first system of equations; hence, the non-homogeneous parts of the second system are known functions once we have solved the first system of equations.

It is to be pointed out that, although the perturbation solution method leads to an infinite series, for a second order theory we need only consider the first two terms of this series. If we used perturbation to solve a problem described by a third order theory we would need three terms, etc., since neglecting the third and higher terms of the series introduces errors of the same magnitude as those introduced by neglecting third and higher powers of strain in the formulation of a second order theory.

6. Compressible Response.

Uniaxial Test

The uniaxial test is analyzed since it is the most common test performed upon material samples. Although it is preferable to obtain elastic properties using an experimental approach as outlined in [6], it is possible to obtain results from a uniaxial test. For a description of a uniaxial test where thermal effects are included, see [7]. The solution of the uniaxial problem may be considered from a perturbation standpoint.

We shall select material coordinates x^1 to coincide with rectangular cartesian coordinates in the initial state. Choosing the spatial coordinates y^1 as rectangular cartesian coordinates we thus find

$$g_{ij} = \delta_{ij} = h_{ij}.$$

The displacement field will be given by

$$\eta^1 = e_1 x^1 \quad (\text{no sum}),$$

and as

$$y^1 = x^1 + \eta^1$$

or

$$y^1 = (1 + e_1) x^1 \quad (\text{no sum})$$

Hence,

$$G_{ij} = G_{ij}^* = \begin{bmatrix} (1 + e_1)^2 & & \\ & (1 + e_2)^2 & \\ & & (1 + e_3)^2 \end{bmatrix}$$

and

$$E_j^i = \begin{bmatrix} e_1 + \frac{1}{2}e_1^2 & & \\ & e_2 + \frac{1}{2}e_2^2 & \\ & & e_3 + \frac{1}{2}e_3^2 \end{bmatrix},$$

Utilizing Eqs. (1.15), (1.7), (1.9), (4.1) and (1.5) we find

$$g^{11} = 1$$

$$B^{11} = I_1 - G_{11} = I_1 - (1 + e_1)^2$$

$$G^{11} = \frac{1}{(1 + e_1)^2}$$

$$I_1 = 2\theta_1 + 3 ,$$

$$I_3 = 1 + 2\theta_1 + 4\theta_2 + 8\theta_3 ,$$

$$\frac{\partial A}{\partial \theta_1} = k_1 (2k_2\theta_1 + k_3\theta_2 + 3k_4\theta_1^2 + k_6T + 2k_7T\theta_1 + k_9T^2)$$

$$\frac{\partial A}{\partial \theta_2} = k_1 (1 + k_3\theta_1 + k_8T)$$

$$\frac{\partial A}{\partial \theta_3} = k_1 k_5 ,$$

$$\theta_1 = e_1 + e_2 + e_3 + \frac{1}{2} e_1^2 + \frac{1}{2} e_2^2 + \frac{1}{2} e_3^2$$

$$\theta_2 = e_1 e_2 + e_1 e_3 + e_2 e_3.$$

From Eq. (1.13)

$$\begin{aligned} s^{11} = k_1 & \left[2k_2 e_1 + (2k_2 + 1)(e_2 + e_3) + (k_2 + 3k_4) e_1^2 + (k_2 + \frac{1}{2} + 3k_4 \right. \\ & + k_3)(e_2^2 + e_3^2) + (2k_3 + 6k_4)(e_1 e_2 + e_1 e_3) + (3k_3 + k_5 \\ & \left. + 6k_4) e_2 e_3 + k_6 T + 2k_7 e_1 T + (2k_7 + k_8) T(e_2 + e_3) + k_9 T^2 \right] \end{aligned}$$

likewise

$$\begin{aligned} s^{22} = k_1 & \left[2k_2 e_2 + (2k_2 + 1)(e_1 + e_3) + (k_2 + 3k_4) e_2^2 + (k_2 + \frac{1}{2} + 3k_4 \right. \\ & + k_3)(e_1^2 + e_3^2) + (2k_3 + 6k_4)(e_1 e_2 + e_2 e_3) + (3k_3 + k_5 + 6k_4) e_1 e_3 \\ & \left. + k_6 T + 2k_7 e_2 T + (2k_7 + k_8) T(e_1 + e_3) + k_9 T^2 \right]. \end{aligned}$$

For a uniaxial test of an isotropic material

$$e_2 = e_3 \text{ and}$$

$$s^{11} = k_1 \left[2k_2 e_1 + 2(2k_2 + 1)e_2 + (k_2 + 3k_4)e_1^2 + (2k_2 + 1 + 12k_4 + 5k_3 + k_5)e_2^2 + 2(2k_3 + 6k_4)e_1 e_2 + k_6 T + 2k_7 e_1 T + 2(2k_7 + k_8)Te_2 + k_9 T^2 \right]$$

$$s^{22} = k_1 \left[(4k_2 + 1)e_2 + (2k_2 + 1)e_1 + (2k_2 + \frac{1}{2} + 12k_4 + 3k_3)e_2^2 + (k_2 + \frac{1}{2} + 3k_4 + k_3)e_1^2 + (5k_3 + 12k_4 + k_5)e_1 e_2 + k_6 T + (4k_7 + k_8)Te_2 + (2k_7 + k_8)Te_1 + k_9 T^2 \right].$$

From Eqs. (1.13), (1.17) and the above

$$\sigma_{11} = \frac{1 + e_1}{(1 + e_2)^2} s^{11}$$

or

$$\begin{aligned} \sigma_{11} = k_1 \left[2k_2 e_1 + 2(2k_2 + 1)e_2 + 3(k_2 + k_4)e_1^2 + (12k_4 + 5k_3 - 6k_2 - 3 + k_5)e_2^2 + 2(2k_3 + 6k_4 + 1)e_1 e_2 + k_6 T + (2k_7 + k_6)e_1 T \right. \\ \left. + 2(2k_7 + k_8 - k_6)Te_2 + k_9 T^2 \right]. \end{aligned} \quad (6.1)$$

Let σ_{1n} be the nominal stress (i.e., per unit of initial area)

$$\text{then } \sigma_{1n} = (1 + e_1)s^{11}$$

$$\begin{aligned}
\text{or } \sigma_{1n} = k_1 & \left[2k_2 e_1 + 2(2k_2 + 1)e_2 + 3(k_2 + k_4)e_1^2 + (2k_2 + 1 + 12k_4 + k_5 \right. \\
& + 5k_3)e_2^2 + 2(2k_2 + 1 + 2k_3 + 6k_4)e_1 e_2 + k_6 T + (2k_7 + k_6)e_1 T \\
& \left. + 2(2k_7 + k_8)Te_2 + k_9 T^2 \right] \quad (6.2)
\end{aligned}$$

also $\sigma_{22} = s_{22} = 0$, hence

$$\begin{aligned}
0 = k_1 & \left[(4k_2 + 1)e_2 + (2k_2 + 1)e_1 + (2k_2 + \frac{1}{2} + 12k_4 + 3k_3)e_2^2 \right. \\
& + (k_2 + \frac{1}{2} + 3k_4 + k_3)e_1^2 + (5k_3 + 12k_4 + k_5)e_1 e_2 + k_6 T \\
& \left. + (4k_7 + k_8)Te_2 + (2k_7 + k_8)Te_1 + k_9 T^2 \right]. \quad (6.3)
\end{aligned}$$

Thermal Stressing of a Thick-walled Cylinder

The first of Eqs. (5.8) may be written

$$\frac{d}{d\rho} \left[\rho \frac{dT^{*(0)}}{d\rho} \right] = 0$$

whose solution is

$$T^{(0)} = C^{(0)} \ln \rho + D^{(0)} \quad (6.4)$$

Noting the above results and using the third and fourth of Eqs. (5.8) we may write the second of Eq. (5.8) as

$$\frac{d}{d\rho} \left\{ \frac{1}{\rho} \frac{d}{d\rho} [\rho v^{(0)}] \right\} = - \frac{k_6}{2k_2} C^{(0)} \frac{1}{\rho}$$

whose solution is

$$v^{(0)} = \bar{A}^{(0)} \frac{1}{\rho} + B^{(0)} \frac{1}{\rho} - \frac{k_6}{4k_2} C^{(0)} \rho \left(\ln \rho - \frac{1}{2} \right). \quad (6.5)$$

Thus,

$$T^{*(0)} = C^{(0)} \ln \rho + D^{(0)}$$

$$v^{(0)} = A^{(0)} \rho + B^{(0)} \frac{1}{\rho} - \frac{k_6}{4k_2} C^{(0)} \rho \ln \rho \quad (6.6)$$

$$s_{\rho}^{(0)} = (1 + 4k_2) A^{(0)} + k_6 D^{(0)} - \frac{k_6}{2} C^{(0)} + B^{(0)} \frac{1}{\rho^2} - \frac{k_6}{4k_2} C^{(0)} \ln \rho.$$

From the above solution to the first system of equations we are able to calculate the nonhomogenous part of the second system of equations. Thus, we are able to integrate the second system. The resulting expression for $T^{*(1)}$ is

$$T^{*(1)} = C^{(1)} \ln \rho + D^{(1)} + B^{(0)} C^{(0)} \frac{1}{\rho^2}$$

while the expressions for the remaining dependent variables may be similarly obtained. The constants $A^{(0)}$, $B^{(0)}$, $C^{(0)}$, $D^{(0)}$, $A^{(1)}$, $B^{(1)}$ etc., are evaluated from the boundary conditions.

In order to avoid the rather involved algebra we shall consider the problem of a uniform temperature drop T of a thick-walled cylinder bonded to a rigid case. The inner and outer cylinder radii are a and b respectively. The boundary conditions are

$$\text{at } r = a, \rho = 1 \quad \left\{ \begin{array}{l} T^*(0) = T^* = \frac{T}{\delta} \\ T^*(1) = 0 \\ s_{\rho}^{(0)} = 0 \\ s_{\rho}^{(1)} = 0 \end{array} \right. \quad (6.7)$$

$$\text{and at } r = b, \quad \left\{ \begin{array}{l} T^*(0) = T^* \\ T^*(1) = 0 \\ v^{(0)} = 0 \\ v^{(1)} = 0. \end{array} \right. \\ \rho = \frac{b}{a} = c$$

Applying the above boundary conditions to Eq. (6.6) we obtain

$$C^{(0)} = 0$$

$$D^{(0)} = T^*$$

$$A^{(0)} = \frac{k_6 T^*}{c^2 - (1 + 4k_2)} \quad (6.8)$$

$$B^{(0)} = -c^2 A^{(0)}$$

Let

$$X_1 = \frac{k_6}{c^2 - (1 + 4k_2)}$$

then

$$T^{(0)} = T^*$$

$$v^{(0)} = T^* X_1 \left(\rho - \frac{c^2}{\rho} \right) \quad (6.9)$$

$$s_{\rho}^{(0)} = T^* \left\{ X_1 \left[(1+4k_2) - \frac{c^2}{\rho^2} \right] + k_6 \right\}.$$

The second of Eq. (6.7) yields $C^{(1)} = D^{(1)} = 0$. The above first order solution and Eqs. (5.9) yields

$$\frac{d}{d\rho} \left\{ \frac{1}{\rho} \frac{d}{d\rho} [\rho v^{(1)}] \right\} = \frac{(T^* X_1)^2}{k_2} (4k_2 - 1 - 2k_3) \frac{c^4}{\rho^5}.$$

The solution is

$$v^{(1)} = \frac{(T^* X_1)^2}{8k_2} (4k_2 - 1 - 2k_3) \frac{c^4}{\rho^3} + A^{(1)} \rho + B^{(1)} \frac{1}{\rho}. \quad (6.10)$$

The third of Eq. (5.9) becomes

$$\begin{aligned}
s_{\rho}^{(1)} = & (1 + 4k_2)A^{(1)} + B^{(1)} \frac{1}{\rho^2} - (X_1 T^*)^2 \left[\left(\frac{1 + 2k_3 + 4k_2}{8k_2} \right) \frac{c^4}{\rho^4} \right. \\
& \left. - (1 + 8k_2 - 2k_3) \frac{c^2}{\rho^2} - (3k_3 + 12k_4 + \frac{1}{2} + 2k_2) \right] \\
& + X_1 (T^*)^2 \left[(4k_7 + k_8) + (2k_6 - k_8) \frac{c^2}{\rho^2} \right] + k_9 (T^*)^2.
\end{aligned} \tag{6.11}$$

Applying the second boundary condition in Eq. (6.7) to the above equations we find that

$$A^{(1)} = X_2 (T^*)^2 \tag{6.12}$$

$$B^1 = X_3 (T^*)^2$$

where

$$X_2 = \frac{c^2 X_4 - X_5}{c^2 - (1 + 4k_2)} \tag{6.13}$$

$$X_3 = \frac{c^2 [X_5 - X_4 (1 + 4k_2)]}{c^2 - (1 + 4k_2)} \tag{6.14}$$

$$X_4 = - \frac{X_1^2 (4k_2 - 1 - 2k_3)}{8k_2} \tag{6.15}$$

$$\begin{aligned}
X_5 = X_1^2 & \left[\frac{1 + 2k_3 + 4k_2}{8k_2} c^4 - (1 + 8k_2 - 2k_3) c^2 - (3k_3 + 12k_4 + \frac{1}{2} \right. \\
& \left. + 2k_2) \right] - X_1 \left[(4k_7 + k_8) + (2k_6 - k_8) c^2 \right] - k_9
\end{aligned} \tag{6.16}$$

$$X_1 = \frac{k_6}{c^2 - (1 + 4k_2)} \tag{6.17}$$

$$c = \frac{b}{a}.$$

Making use of Eqs. (6.10), (6.11), (6.12), (5.1), (5.2), (5.3), (5.4), and (5.7), we may express our results as follows

$$\begin{aligned}
\sigma_r = k_1 T & \left\{ X_1 \left[(1 + 4k_2) - \frac{b^2}{r^2} \right] + k_6 \right\} + k_1 T^2 \left\{ (1 + 4k_2) X_2 + X_3 \frac{a^2}{r^2} \right. \\
& - X_1^2 \left[\left(\frac{1 + 2k_3 + 4k_2}{8k_2} \right) \frac{b^4}{r^4} - (1 + 8k_2 - 2k_3) \frac{b^2}{r^2} - (3k_3 + 12k_4 + \frac{1}{2} \right. \\
& \left. + 2k_2) \right] + X_1 \left[(4k_7 + k_8) + (2k_6 - k_8) \frac{b^2}{r^2} \right] + k_9 \left. \right\}
\end{aligned} \tag{6.18}$$

$$u = TX_1 \left(r - \frac{b^2}{r} \right) + T^2 \left[X_2 r + X_3 \frac{a^2}{r} - X_4 \frac{b^4}{r^3} \right]. \tag{6.19}$$

The very important fact that the results do not depend upon δ (as δ is only a numerical indicator of the relative

sizes of the various terms appearing in the governing equations) is clearly illustrated in the above results.

Pressure Loading of a Thick-walled Cylinder

Setting $T^{*(0)} = 0$ in Eq. (6.6) we find that

$$v^{(0)} = A^{(0)} \rho + B^{(0)} \frac{1}{\rho} \quad (6.20)$$

$$s_{\rho}^{(0)} = (1 + 4k_2) A^{(0)} + B^{(0)} \frac{1}{\rho^2}.$$

Using the first and fourth of Eq. (5.9) we may write the third Eq. (5.9) as

$$\frac{d}{d\rho} \left\{ \frac{1}{\rho} \frac{d}{d\rho} [\rho v^{(1)}] \right\} = \frac{1}{k_2} (4k_2 - 2k_3 - 1) (B^{(0)})^2 \frac{1}{\rho^5}.$$

The solution is

$$v^{(1)} = A^{(1)} \rho + B^{(1)} \frac{1}{\rho} + \frac{1}{8k_2} (4k_2 - 2k_3 - 1) \frac{(B^{(0)})^2}{\rho^3} \quad (6.21)$$

hence from Eq. (5.9)

$$\begin{aligned} s_{\rho}^{(1)} = & (1 + 4k_2) A^{(1)} + B^{(1)} \frac{1}{\rho^2} + (3k_3 + 12k_4 + 2k_2 + \frac{1}{2}) (A^{(0)})^2 \\ & - \frac{4k_2 + 2k_3 + 1}{8k_2} \frac{(B^{(0)})^2}{\rho^4} + (2k_3 - 8k_2 - 1) A^{(0)} B^{(0)} \frac{1}{\rho^2}. \end{aligned} \quad (6.22)$$

Let us now consider the specific problem of a thick-walled cylinder subjected to an internal pressure P_i , the boundary conditions will be:

At $r = a \ (\rho = 1); \ \sigma_r = -P_i$

or $s_\rho = s_\rho^{(0)} = -\frac{P_i}{k_1 \delta}$

Let $\bar{P} = \frac{P_i}{k_1 \delta}$

then $s_\rho^{(0)} = -\bar{P}$

and $s_\rho^{(1)} = 0 \quad (6.23)$

and at $r = b (\rho = \frac{b}{a} = c); \quad s_\rho^{(0)} = 0 = s_\rho^{(1)} \quad (6.24)$

Applying the above boundary conditions to Eq. (6.20) we find

$$A^{(0)} = \frac{\bar{P}}{(c^2-1)(1+4k_2)}$$

$$B^{(0)} = -\frac{c^2 \bar{P}}{c^2-1} \quad (6.25)$$

Noting the above results and applying the remaining boundary

conditions to Eq. (6.22) we find

$$A^{(1)} = (\bar{P})^2 X_1 \quad (6.26)$$

$$B^{(1)} = (\bar{P})^2 X_2$$

where

$$X_1 = - \frac{1}{(c^2-1)^2 (1+4k_2)^2} \left[\frac{(3k_3 + 12k_4 + 2k_2 + \frac{1}{2})}{(1+4k_2)} + \frac{c^2(4k_2 + 2k_3 + 1)(1+4k_2)}{8k_2} \right] \quad (6.27)$$

$$X_2 = \frac{c^2}{(c^2-1)^2 (1+4k_2)} \left[\frac{(c^2+1)(4k_2 + 2k_3 + 1)(1+4k_2)}{8k_2} + (2k_3 - 8k_2 - 1) \right]. \quad (6.28)$$

Using the above notation we may write our solution from Eqs. (6.20), (6.21), and (6.22) as

$$\sigma_r = \frac{P_i}{c^2-1} \left[1 - \frac{b^2}{r^2} \right] - \frac{(P_i)^2 (4k_2 + 2k_3 + 1)}{8k_1 k_2 (c^2-1)^2} \left[c^2 - (c^2+1) \frac{b^2}{r^2} + \frac{b^4}{r^4} \right]$$

$$u = \frac{P_i}{k_1 (1+4k_2) (c^2-1)} \left[r - (1+4k_2) \frac{b^2}{r} \right] + \frac{P_i^2}{k_1^2} \left[X_1 r + X_2 \frac{a^2}{r} + \frac{(4k_2 - 2k_3 - 1)}{8k_2 (c^2-1)^2} \frac{b^4}{r^3} \right]. \quad (6.29)$$

We shall now consider an externally case bonded thick-walled cylinder subjected to internal pressure. Let the elastic properties of the thin case be $\bar{\nu}$ and \bar{E} and denote its thickness by t . The motion of the case is given by

$$\bar{u} = \frac{(1 - \bar{\nu}^2)}{\bar{E}} \frac{b^2 P'}{t} \quad (6.30)$$

where P' is the interface pressure. We shall consider the situation when the case is very rigid in comparison to the thick-walled cylinder, i.e., we must consider the material of the thick-walled cylinder as rather compressible. (See Section 8 for a discussion of compressibility effects.) The displacement at the interface will be of second order as compared to the displacement at the inner radius (in the application to a specific problem one must verify this assumption). We may thus illustrate one of the methods for reducing the algebraic complexities of a given problem, i.e., introducing various boundary conditions at different levels of approximation. We employ the following boundary conditions:

$$\text{At } \rho = 1; \quad s_{\rho}^{(0)} = -\bar{P} \quad \text{where} \quad \bar{P} = \frac{P_i}{k_1 \delta} \quad (6.31)$$

$$s_{\rho}^{(1)} = 0$$

and at

$$\rho = c; \quad v^{(0)} = 0$$

$$v^{(1)} = \bar{w} \quad \text{where} \quad \bar{w} = \frac{\bar{u}}{a\delta^2}. \quad (6.32)$$

The interface pressure P' is found from the continuity condition

$$\sigma_r(b) = -P' \quad (6.33)$$

$$\text{i.e.} \quad k_1 \delta \left[s_{\rho}^{(0)} + \delta s_{\rho}^{(0)} \right]_{r=b} = -P'$$

The above boundary conditions when applied to Eqs. (6.20), (6.21), and (6.22) give

$$A^{(0)} = - \frac{\bar{P}}{1 + 4k_2 - c^2}$$

$$B^{(0)} = \frac{c^2 \bar{P}}{1 + 4k_2 - c^2}$$

$$A^{(1)} = \bar{P}^2 X_6$$

$$B^{(1)} = \bar{P}^2 X_7$$

where

$$X_6 = \frac{\bar{X}_1 - cX_2 - \frac{c\bar{u}k_1^2}{aP_i^2}}{1 + 4k_2 - c^2} \quad (6.34)$$

$$X_7 = \frac{c(1 + 4k_2) \left[\frac{\bar{u}k_1^2}{aP_i^2} + X_2 \right] - c^2 \bar{X}_1}{1 + 4k_2 - c^2}$$

$$x_1(r) = - \frac{1}{(1 + 4k_2 - c^2)^2} \left[(3k_3 + 12k_4 + 2k_2 + \frac{1}{2}) - \frac{(4k_2 + 2k_3 + 1)}{8k_2} \frac{b^4}{r^4} \right. \\ \left. - (2k_3 - 8k_2 - 1) \frac{b^2}{r^2} \right] \quad (6.35)$$

$$\bar{X}_1 = x_1(r = a)$$

$$x_2 = - \frac{c(4k_2 - 2k_3 - 1)}{8k_2(1 + 4k_2 - c^2)^2}$$

$$\bar{u} = \frac{(1 - \bar{v}^2)}{\bar{E}} \frac{b^2 P'}{t},$$

We now evaluate P' from Eqs. (6.30), (6.32), and (6.33):

$$P' = \frac{-4k_1 k_2 c P_i + X_4 (P_i)^2}{X_5} \quad (6.36)$$

where

$$X_4 = \frac{X_3 c}{1 + 4k_2 - c^2} + 4k_2 c \bar{X}_1 - (1 + 4k_2)(c^2 - 1)X_2 \\ X_5 = \frac{k_1 c [k_1 (1 + 4k_2)(c^2 - 1)(1 - \bar{v}^2)b - \bar{E}t(1 + 4k_2 - c^2)]}{\bar{E}t} \quad (6.37)$$

$$X_3 = k_3 + 12k_4 + 10k_2 + 1 - \frac{2k_3 + 1}{8k_2}. \quad (6.37)$$

Using the above notation we find

$$\begin{aligned} \sigma_r = & \frac{P_i}{1+4k_2-c^2} \left[\frac{b^2}{r^2} - (1+4k_2) \right] + \frac{P_i^2}{k_1} (1+4k_2) X_6 + \frac{P_i^2 X_7}{k_1} \frac{a^2}{r^2} - \frac{P_i^2}{k_1} X_1(r) \\ u = & \frac{P_i}{k_1(1+4k_2-c^2)} \left[\frac{b^2}{r} - r \right] + \frac{P_i^2 X_6}{k_1^2} r + \frac{P_i^2 X_7}{k_1^2} \frac{a^2}{r} \\ & + \frac{(4k_2-2k_3-1)P_i^2}{8k_2k_1^2(1+4k_2-c^2)} \frac{b^4}{r^3}. \end{aligned} \quad (6.38)$$

Vertical Gravity Loading of a Thick-walled Cylinder

Consider now the deformation of a vertical case bonded thick-walled cylinder subjected to gravity loading. We shall assume that the case is sufficiently rigid so that longitudinal case motion may be neglected. The classical solution [8] of this problem yields the results that the radial displacement u is zero, hence $u^{(0)}$ is zero and $u = \delta u^{(1)}$. From this result we see that the radial motion will be an order smaller than the vertical motion, i.e., $u = \delta u^{(1)}$ compared to $w = w^{(0)} + \delta w^{(1)}$. Therefore, we need to include only the first order terms of the radial displacement. The solution of the classical problem serves as a valuable guide to the relative magnitude of various terms occurring in the second order solution. The set of govern-

ing equations, Eqs. (3.13), (3.14), (3.15), and (4.1) is:

$$E_j^i = \begin{bmatrix} \frac{du}{dr} & 0 & \frac{1}{2} \frac{dw}{dr} \\ 0 & \frac{u}{r} & 0 \\ \frac{1}{2} \frac{dw}{dr} & 0 & \frac{1}{2} \left(\frac{dw}{dr} \right)^2 \end{bmatrix} \quad (6.39)$$

$$\frac{d\sigma_r}{dr} + \frac{\sigma_r - \sigma_\theta}{r} = 0 \quad (6.40)$$

$$\frac{d\tau_{rz}}{dr} + \frac{1}{r} \tau_{rz} + \rho_0 g = 0 \quad (6.41)$$

$$A = k_1(\theta_2 + k_2\theta_1^2 + k_3\theta_1\theta_2 + k_4\theta_1^3 + k_5\theta_3), \quad (6.42)$$

The deformed boundaries are located at $r = a + u|_{\text{inner radius}}$ and $r = b + u|_{\text{outer radius}}$. The displacements enter into the boundary conditions since material coordinates were selected to coincide with the cylindrical coordinates in the final state. Inasmuch as we are only retaining first order terms of u (corresponding to the classical solution) we consider the boundaries as located at $r = a$ and $r = b$ respectively. From Eq. (6.42) we find

$$\frac{\partial A}{\partial \theta_1} = k_1 [2k_2 \theta_1 + k_3 \theta_2 + 3k_4 \theta_1^2]$$

$$\frac{\partial A}{\partial \theta_2} = k_1 [1 + k_3 \theta_1]$$

$$\frac{\partial A}{\partial \theta_3} = k_1 k_5.$$

Kinematic variables needed to complete the formulation of the solution are recorded below:

$$\theta_1 = \frac{du}{dr} + \frac{u}{r} + \frac{1}{2} \left(\frac{dw}{dr} \right)^2$$

$$\theta_2 = -\frac{1}{4} \left(\frac{dw}{dr} \right)^2$$

$$\theta_3 = 0$$

$$g^{11} = \left(1 + 2 \frac{du}{dr} \right)$$

$$B^{11} = 2 \left(1 + \frac{u}{r} + 2 \frac{du}{dr} \right)$$

$$G^{11} = 1$$

$$\frac{1}{\sqrt{I_3}} = 1 - \frac{u}{r} - \frac{du}{dr}.$$

Placing the above results into Eq. (1.14) we find

$$\sigma_r = k_1 \left[2k_2 \frac{du}{dr} + (2k_2 + 1) \frac{u}{r} + (k_2 - \frac{k_3}{4}) \left(\frac{dw}{dr} \right)^2 \right] \quad (6.43)$$

$$\sigma_\theta = k_1 \left[(2k_2 + 1) \frac{du}{dr} + 2k_2 \frac{u}{r} + (k_2 - \frac{k_3}{4} + \frac{1}{2} - \frac{k_5}{4}) \left(\frac{dw}{dr} \right)^2 \right] \quad (6.44)$$

$$\tau_{rz} = - \frac{k_1}{2} \frac{dw}{dr}. \quad (6.45)$$

The above equations, because of their simplicity, may be integrated directly without resorting to a perturbation solution. Identical results may be obtained by perturbation. Integration of Eq. (6.41) gives

$$\tau_{rz} = - \rho_o g \frac{r}{2} + \frac{A}{r}$$

and applying the boundary condition $\tau_{rz}(a) = 0$ we find

$$\tau_{rz} = \frac{\rho_o g}{2} \left(\frac{a^2}{r} - r \right). \quad (6.46)$$

Substitution of the above expression into Eq. (6.45) and integrating we obtain

$$w = - \frac{\rho_o g}{k_1} \left(a^2 \ln r - \frac{r^2}{2} \right) + B$$

Applying the boundary condition $w(b) = 0$, we obtain

$$w = \frac{\rho_o g}{k_1} \left[a^2 \ln \frac{b}{r} - \frac{b^2 - r^2}{2} \right]. \quad (6.47)$$

Substitution of the above results into Eqs. (6.43), (6.44), and (6.40) we obtain

$$\frac{d}{dr} \left[\frac{1}{r} \frac{d}{dr} (ru) \right] = \frac{\rho_o^2 g^2}{2k_2 k_1^2} \left[\left(\frac{1}{2} - \frac{k_5}{4} \right) \left(\frac{a^4}{r^3} - 2 \frac{a^2}{r} + r \right) + 2 \left(k_2 - \frac{k_3}{4} \right) \left(\frac{a^4}{r^3} - r \right) \right],$$

which upon integration is

$$u = Ar + B \frac{1}{r} - \frac{\rho_o^2 g^2}{2k_2 k_1^2} \left\{ \left(\frac{1}{2} - \frac{k_5}{4} \right) \left[\frac{a^2}{2} \frac{\ln r}{r} + \frac{a^2}{2} (2 \ln r - 1) - \frac{r^2}{8} \right] + 2 \left(k_2 - \frac{k_3}{4} \right) \left(\frac{a^4}{2} \frac{\ln r}{r} + \frac{r^3}{8} \right) \right\}. \quad (6.48)$$

Thus, Eq. (6.43) becomes

$$\begin{aligned} \sigma_r = k_1 \left[(4k_2 + 1)A + \frac{B}{r^2} \right] - \frac{\rho_o^2 g^2}{k_1} \left[\left(\frac{1}{2} - \frac{k_5}{4} \right) \left(\frac{a^2}{2r^2} + 2a^2 \ln r - \frac{r^2}{2} \right) + 2a^2 \left(k_2 - \frac{k_3}{4} \right) \right] - \frac{\rho_o^2 g^2}{2k_2 k_1^2} \left\{ \left(\frac{1}{2} - \frac{k_5}{4} \right) \left[\frac{a^2}{2} \frac{\ln r}{r^2} + \frac{a^2}{2} (2 \ln r - 1) - \frac{r^2}{8} \right] + 2 \left(k_2 - \frac{k_3}{4} \right) \left(\frac{a^4}{2} \frac{\ln r}{r^2} + \frac{r^2}{8} \right) \right\}. \end{aligned} \quad (6.49)$$

The constants A and B may be evaluated from appropriate boundary conditions, which, for a rigid case are

$$\begin{aligned} \sigma_r(a) &= 0 \\ u(b) &= 0 \end{aligned} \quad (6.50)$$

7. Incompressible Response.

No real material is truly incompressible. Therefore, whenever we represent a material as incompressible, we are only approximating its true behavior. It is very desirable to utilize such an approximation, when justified, because of the resulting substantial reduction in algebraic difficulties. The assumption of incompressibility is very often made in finite elasticity as most of the materials capable of finite elastic deformations are very nearly incompressible. The question of whether the actual stress and strain state is well approximated by the incompressible state (for a given nearly incompressible material) will depend upon the type of boundary conditions (as shall be illustrated later). We must avoid those problems that approach the physically contradictory problem of enforcing displacement boundary conditions which prescribes a net change in volume of an incompressible material. For this type of problem a singularity arises and thus for problems of this type the solution will be very sensitive to the actual amount of compressibility present. A further consideration of this problem will be presented in Section 8, including some numerical indications of the range of validity of such a theory.

Uniaxial Test

Equations (2.12), (2.14), and (4.4) become, upon specialization for uniaxial stress field in an incompressible material,

$$\sigma_{11} = H + k_1 \left[2e_2 + (k_5 - 3)e_2^2 + 2e_1e_2 + 2c_3Te_2 \right] \quad (7.1)$$

$$\sigma_{22} = 0 = H + k_1 \left[e_2 + e_1 + \frac{1}{2}e_2^2 - \frac{1}{2}e_1^2 + (k_5 - 1)e_1e_2 + c_8Te_2 + c_8Te_1 \right] \quad (7.2)$$

and from Eq. (4.9)

$$\beta_1 T + \beta_2^* T^2 = e_1 + 2e_2 + \frac{1}{2} e_1^2 + 3e_2^2 + 4e_1 e_2. \quad (7.3)$$

Uniform Temperature Drop of a Thick-walled Cylinder

Noting Eq. (4.5) we may write Eq. (2.13) as

$$\tau^{ij} = H G^{ij} + \frac{1}{1 + \beta_1 T + \beta_2 T^2} \frac{\partial \bar{A}}{\partial E_{ij}}.$$

In a manner similar to the derivation given in Section 4, we find

$$\sigma_r = H + k_1 \left[\frac{u}{r} + \frac{1}{2} \left(\frac{u}{r} \right)^2 + 2 \frac{u}{r} \frac{du}{dr} + (c_3 - \beta_1) T \frac{u}{r} \right] \quad (7.4)$$

$$\sigma_r - \sigma_\theta = k_1 \left[\frac{u}{r} - \frac{du}{dr} + \frac{1}{2} \left(\frac{u}{r} \right)^2 - \frac{1}{2} \left(\frac{du}{dr} \right)^2 + (c_3 - \beta_1) T \left(\frac{u}{r} - \frac{du}{dr} \right) \right].$$

The incompressibility condition as given by Eq. (4.9) becomes

$$0 = \frac{du}{dr} + \frac{u}{r} - \beta_1 T + \frac{1}{2} \left(\frac{u}{r} \right)^2 + 2 \frac{u}{r} \frac{du}{dr} + \frac{1}{2} \left(\frac{du}{dr} \right)^2 - \beta_2^* T^2. \quad (7.5)$$

Applying the perturbation scheme, as outlined in Section 5 we find the following two systems of equations (where $H = k_1 \delta(h^{(0)} + \delta h^{(1)} + \dots)$):

First system

$$\frac{d^2 T^*(0)}{d\rho^2} + \frac{1}{\rho} \frac{dT^*(0)}{d\rho} = 0$$

$$\frac{ds_{\rho}^{(0)}}{d\rho} + \frac{s_{\rho}^{(0)} - s_{\theta}^{(0)}}{\rho} = 0 \quad (7.6)$$

$$s_{\rho}^{(0)} = h^{(0)} + \frac{v^{(0)}}{\rho}$$

$$s_{\rho'}^{(0)} - s_{\theta}^{(0)} = \frac{v^{(0)}}{\rho} - \frac{dv^{(0)}}{d\rho}$$

$$\frac{dv^{(0)}}{d\rho} + \frac{v^{(0)}}{\rho} - \beta_1 T^*(0) = 0$$

Second system

$$\frac{d^2 T^*(1)}{d\rho^2} + \frac{1}{\rho} \frac{dT^*(1)}{d\rho} = - \left(\frac{v^{(0)}}{\rho} + \frac{dv^{(0)}}{d\rho} \right) \frac{d^2 T^*(0)}{d\rho^2} + \left(\rho \frac{d^2 v^{(0)}}{d\rho^2} \right.$$

$$\left. - 2 \frac{dv^{(0)}}{d\rho} \right) \frac{1}{\rho} \frac{dT^*(0)}{d\rho}$$

$$\frac{ds_{\rho}^{(1)}}{d\rho} + \frac{s_{\rho}^{(1)} - s_{\theta}^{(1)}}{\rho} = \frac{1}{\rho} \left(\frac{v^{(0)}}{\rho} - \frac{dv^{(0)}}{d\rho} \right)^2$$

$$s_{\rho}^{(1)} = h^{(1)} + \frac{v^{(1)}}{\rho} + \frac{1}{2} \left(\frac{v^{(0)}}{\rho} \right)^2 + 2 \frac{v^{(0)}}{\rho} \frac{dv^{(0)}}{d\rho} + (c_3 - \beta_1) T^*(0) \frac{v^{(0)}}{\rho}$$

(7.7)

$$s_{\rho}^{(1)} - s_{\theta}^{(1)} = \frac{v^{(1)}}{\rho} - \frac{dv^{(1)}}{d\rho} + \frac{1}{2} \left(\frac{v^{(0)}}{\rho} \right)^2 - \frac{1}{2} \left(\frac{dv^{(0)}}{d\rho} \right)^2 + (c_3 - \beta_1) T^{*(0)} \left(\frac{v^{(0)}}{\rho} - \frac{dv^{(0)}}{d\rho} \right)$$

$$\frac{dv^{(1)}}{d\rho} + \frac{v^{(1)}}{\rho} - \beta_1 T^{*(1)} = - \frac{1}{2} \left(\frac{v^{(0)}}{\rho} \right)^2 - 2 \frac{v^{(0)}}{\rho} \frac{dv^{(0)}}{d\rho} - \frac{1}{2} \left(\frac{dv^{(0)}}{d\rho} \right)^2 + \beta_2^* (T^{*(0)})^2$$

The solution of the first system of equations, recalling that we are considering a uniform temperature drop, is given by

$$\begin{aligned} v^{(0)} &= A^{(0)} \frac{1}{\rho} + \frac{\beta_1}{2} T^* \rho \\ s_{\rho}^{(0)} &= B^{(0)} + \frac{A^{(0)}}{\rho^2} + \frac{\beta_1 T^*}{2} \\ s_{\rho}^{(0)} - s_{\theta}^{(0)} &= 2 \frac{A^{(0)}}{\rho^2} \\ h^{(0)} &= B^{(0)} \end{aligned} \tag{7.8}$$

The boundary conditions for zero pressure at the inner radius and a rigid case at the outer radius are

at

$$\rho = 1 \quad s_{\rho}^{(0)} = 0 = s_{\rho}^{(1)} \tag{7.9}$$

and at

$$\rho = c \quad v^{(0)} = 0 = v^{(1)}$$

Thus,

$$\begin{aligned}
 v(0) &= \frac{\beta_1 T^*}{2} \left(\rho - \frac{c^2}{\rho} \right) \\
 s_\rho^{(0)} &= \frac{\beta_1 T^* c^2}{2} \left(1 - \frac{1}{\rho^2} \right) \\
 s_\rho^{(0)} - s_\theta^{(0)} &= -\beta_1 T^* \frac{c^2}{\rho^2} \\
 h(0) &= -\frac{\beta_1 T^*}{2} (1 - c^2).
 \end{aligned} \tag{7.10}$$

Noting the above results, Eq. (4.8), and the boundary conditions (7.9) we may integrate Eqs. 7.7, thus obtaining

$$\begin{aligned}
 s_\rho^{(1)} &= \frac{T^{*2} c^2 (1 - \frac{1}{\rho^2})}{2} \left\{ \beta_1^2 \left[\frac{3c^2}{4} \left(1 + \frac{1}{\rho^2} \right) - 1 \right] + c_3 \beta_1 + \beta_2 \right\} \\
 s_\rho^{(1)} - s_\theta^{(1)} &= \frac{T^{*2} c^2}{\rho^2} \left[\beta_1^2 - c_3 \beta_1 - \frac{\beta_1^2}{2} \frac{c^2}{\rho^2} - \beta_2 \right] \\
 v^{(1)} &= \left(\frac{\beta_1 T^*}{2} \right)^2 \frac{c}{2} \left[2 \frac{c}{\rho} - \frac{c^3}{\rho^3} - \frac{\rho}{c} \right] + \frac{\beta_2 T^{*2} c}{2} \left[\frac{\rho}{c} - \frac{c}{\rho} \right].
 \end{aligned} \tag{7.11}$$

Combining the above two systems and writing the results in terms of the original variables we obtain

$$\begin{aligned}
 u &= \frac{\beta_1 T}{2} \left(r - \frac{b^2}{r} \right) + \left(\frac{\beta_1 T}{2} \right)^2 \frac{b}{2} \left[2 \frac{b}{r} - \frac{b^3}{r^3} - \frac{r}{b} \right] + \frac{\beta_2 T^2 b}{2} \left[\frac{r}{b} - \frac{b}{r} \right] \\
 \sigma_r &= \frac{\beta_1 k_1 T c^2}{2} \left(1 - \frac{a^2}{r^2} \right) + \frac{T^2 k_1 c^2 (1 - \frac{a^2}{r^2})}{2} \left\{ \beta_1^2 \left[\frac{3c^2}{4} \left(1 + \frac{a^2}{r^2} \right) - 1 \right] + c_3 \beta_1 + \beta_2 \right\}
 \end{aligned} \tag{7.12}$$

Comparing the above results with Eqs. (6.18) and (6.19) we see the substantial reduction in algebra effected by the assumption of incompressibility. The validity of this assumption will be discussed in Section 8.

Pressurization of a Thick-walled Cylinder

From Eq. (7.8) we see that the solution to the first system is

$$v^{(0)} = \frac{A^{(0)}}{\rho}$$

$$s_{\rho}^{(0)} = B^{(0)} + \frac{A^{(0)}}{\rho^2} \quad (7.13)$$

$$h^{(0)} = B^{(0)}.$$

Noting these results the solution of Eq. (7.7) is

$$v^{(1)} = \frac{A^{(1)}}{\rho} - \frac{(A^{(0)})^2}{2\rho^3}$$

$$s_{\rho}^{(1)} = B^{(1)} + \frac{A^{(1)}}{\rho^2} - \frac{3}{2} \frac{(A^{(0)})^2}{\rho^4}. \quad (7.14)$$

Considering the internally pressurized unbonded cylinder we have for boundary conditions

at

$$\rho = 1 \quad s_{\rho}^{(0)} = - \frac{P_i}{k_i \delta} = - \bar{P}$$

$$s_{\rho}^{(1)} = 0 \quad (7.15)$$

and at $\rho = c$ $s_{\rho}^{(0)} = s_{\rho}^{(1)} = 0$

The above boundary conditions yield

$$A^{(0)} = - \frac{c^2 \bar{P}}{c^2 - 1}$$

$$B^{(0)} = \frac{\bar{P}}{c^2 - 1}$$

$$B^{(1)} = - \frac{3c^2 \bar{P}^2}{2(c^2 - 1)^2}$$

$$A^{(1)} = \frac{3c^2 (c^2 + 1) \bar{P}^2}{2(c^2 - 1)^2}$$

Thus our final results are

$$u = - \frac{P}{k_1 (c^2 - 1)} \frac{b^2}{r} + \frac{b^2 P^2}{k_1^2 2(c^2 - 1)^2 r} \left[3(c^2 + 1) - \frac{b^2}{r^2} \right] \quad (7.16)$$

$$\sigma_r = \frac{P}{c^2 - 1} \left[1 - \frac{b^2}{r^2} \right] - \frac{3c^2 P^2}{2k_1 (c^2 - 1)^2} \left[1 - \frac{b^2 + a^2}{r^2} + \frac{b^2 a^2}{r^4} \right]$$

Once again comparing the above solution with Eq. (6.29) we see the substantial reduction of labor made possible by the incompressibility assumption.

8. Near-Incompressible Response.

The following considerations were motivated by two characteristics of the incompressible assumption, as indicated in the introductory remarks to the previous section: simplification in the mathematical description of the problem and introduction of large errors for certain types of boundary conditions. We hope to achieve two goals in the following investigation: to be able to extend this simplification of description to a larger class of problems (i.e., to those materials which exhibit compressibility) by introducing a corrective term that will account for the actual compressibility and to obtain a numerical indication of the error introduced in a given problem by the incompressibility assumption. We shall first obtain a series representation (by means of perturbation) of the classical field equations, where the first approximation is the set of classical incompressible field equations and subsequent terms account for the actual compressibility of the material. Subsequently we shall solve a uniform temperature drop problem, first with boundary conditions that exemplify the merits of the solution method, and second for boundary conditions that will cause the solution method to break down for certain values of ν and c (as the actual state will not be near the incompressible state). Lastly we shall derive the governing equations for a near-incompressible second order elastic theory.

Writing the classical stress (τ_j^i) and strain (ϵ_j^i) tensors in terms of their deviatoric (\bar{s}_j^i and e_j^i) and isotropic (θ and θ) components one obtains

$$\tau_j^i = \bar{s}_j^i + \frac{\Theta}{3} \delta_j^i \quad (8.1)$$

$$\epsilon_j^i = e_j^i + \frac{\Theta}{3} \delta_j^i$$

where

$$\Theta = \tau_i^i \quad (8.2)$$

$$\Theta = \epsilon_i^i.$$

The classical constitutive equations may be written as

$$\bar{s}_j^i = 2\mu e_j^i \quad (8.3)$$

$$\Theta = 3B(\theta - 3\alpha T_0 T).$$

We shall now define a parameter ϵ as follows

$$\epsilon = \frac{\bar{B}}{B}. \quad (8.4)$$

Where \bar{B} is of the order of magnitude of μ ; thus ϵ is small since $B \gg \mu$ for a nearly incompressible material. For classical elasticity it is most convenient to let $\bar{B} = \mu$ then $\epsilon = \frac{\mu}{B} = \frac{3(1-2\nu)}{2(1+\nu)}$.

Thus we may write

$$\theta = \frac{3\bar{B}}{\epsilon}(\theta - 3\alpha T_0 T) \quad (8.5)$$

Combining Eqs. (8.4), (8.1), and (8.5) we obtain

$$\epsilon_j^i = \frac{1}{2\mu}(\tau_j^i - \frac{\Theta}{3} \delta_j^i) + \frac{\epsilon}{9B} \Theta \delta_j^i + \alpha T_0 T \delta_j^i. \quad (8.6)$$

Solving for τ_j^i we find

$$\tau_j^i = 2\mu \epsilon_j^i + \frac{\theta}{3} \delta_j^i - \epsilon \frac{2\mu}{9\bar{B}} \theta \delta_j^i - 2\mu \alpha T_O T \delta_j^i \quad (8.7)$$

and inverting Eq. (8.5) we obtain

$$\theta = \epsilon \frac{\theta}{3\bar{B}} + 3\alpha T_O T. \quad (8.8)$$

We have now established the condition for a perturbation solution for a class of problems determined by the size of ν and the type of boundary conditions. Expanding our dependent variables in series in ϵ , substituting into the above equations, and equating coefficients, we obtain the following systems of constitutive equations

$$\tau_j^{i(0)} = 2\mu \epsilon_j^{i(0)} + \frac{\theta^{(0)}}{3} \delta_j^i - 2\mu \alpha T_O T^{(0)} \delta_j^i \quad (8.9)$$

$$\theta^{(0)} = 3\alpha T_O T^{(0)}$$

and for $n \geq 1$

$$\tau_j^{i(n)} = 2\mu \epsilon_j^{i(n)} + \frac{\theta^{(n)}}{3} \delta_j^i - 2\mu \alpha T_O T^{(n)} \delta_j^i - \frac{2\mu}{9\bar{B}} \theta^{(n-1)} \delta_j^i \quad (8.10)$$

$$\theta^{(n)} = 3\alpha T_O T^{(n)} + \frac{\theta^{(n-1)}}{3\bar{B}}.$$

The equilibrium equations may likewise be written in series form,

i.e.,

$$\tau_j^i|_i^{(0)} + \rho F_j^{(0)} = 0 \quad (8.11)$$

$$\tau_j^i|_i^{(n)} + \rho F_j^{(n)} = 0 \quad n \geq 1$$

Substitution of the constitutive equations (8.9) and (8.10) into the above equations, we obtain the following displacement equations of equilibrium

$$\nabla^2 u_j^{(0)} + \frac{1}{\mu} \left(\frac{1}{3} \theta|_j^{(0)} + \rho F_j^{(0)} \right) + \alpha T_o T|_j^{(0)} = 0 \quad (8.12)$$

where
$$u^i|_i^{(0)} = 3\alpha T_o T^{(0)}$$

and for

$$n \geq 1 \quad \nabla^2 u_j^{(n)} + \frac{1}{\mu} (\rho F_j^{(n)} + \frac{1}{3} \theta|_j^{(n)} + \frac{\mu}{9B} \theta|_j^{(n-1)}) + \alpha T_o T|_j^{(n)} = 0 \quad (8.13)$$

where
$$u^i|_i^{(n)} = \frac{\theta^{(n-1)}}{3B} + 3\alpha T_o T^{(n)}.$$

The solution of each system of the above equations is equivalent to the solution of a nonhomogeneous incompressible problem.

We shall now consider the uniform temperature drop of a thick-walled cylinder in light of the above equations introducing a dimensionless temperature $T^{(0)} = \frac{\Delta T}{T_o}$. Solving the

first system of equations we obtain (where $\bar{B} = \mu$)

$$u^{(0)} = \frac{A^{(0)}}{r} + \frac{3\alpha}{2} r \Delta T$$

$$\sigma_r^{(0)} = -2\mu \frac{A^{(0)}}{r^2} + \frac{C^{(0)}}{3} + \mu \alpha \Delta T \quad (8.14)$$

$$\theta^{(0)} = C^{(0)},$$

Noting the above results, the solution to the second system of equations becomes

$$u^{(1)} = \frac{A^{(1)}}{r} + \frac{C^{(0)}}{6\mu} r$$

$$\sigma_r^{(1)} = -2\mu \frac{A^{(1)}}{r^2} + \frac{C^{(1)}}{3} + \frac{C^{(0)}}{9}. \quad (8.15)$$

Let us first consider the specific problem where we have no external case; thus, the boundary conditions become (note that no restrictions are placed on volume change)

$$\text{at } r = a \quad \sigma_r^{(0)} = \sigma_r^{(1)} = 0$$

$$\text{and at } r = b \quad \sigma_r^{(0)} = \sigma_r^{(1)} = 0$$

Using the above boundary conditions we find

$$u^{(0)} = \frac{3\alpha\Delta T}{2} r$$

$$u^{(1)} = -\frac{\alpha\Delta T r}{2} = \left(-\frac{1}{3}\right)u^{(0)} \quad (8.16)$$

$$\sigma_r^{(0)} = \sigma_r^{(1)} = 0.$$

Noting Eq. (8.16) and the general equations (8.13) for the n^{th} term we see that $u^{(n)} = -\frac{1}{3} u^{(n-1)}$, and noting that $\epsilon = \frac{\mu}{B}$ we find that

$$u = \frac{3\alpha\Delta T}{2} r \left[1 - \frac{\mu}{3B} + \left(\frac{\mu}{3B}\right)^2 - \dots \right] \quad (8.17)$$

$$\sigma_r = 0.$$

For illustration let us consider the exact solution, which may be written as

$$u = \frac{3\alpha\Delta T}{2} r \left(\frac{1}{1 + \frac{\mu}{3B}} \right) \quad (8.18)$$

or for small $\frac{\mu}{3B}$

$$u = \frac{3\alpha\Delta T}{2} r \left[1 - \frac{\mu}{3B} + \left(\frac{\mu}{3B}\right)^2 - \dots \right] \quad (8.19)$$

Let us now consider the range of validity of the above approximation. To use only the first term (i.e., assume incompressibility) let us make $\frac{\mu}{3B} \leq 0.05$ (which is equivalent to $\nu \geq 0.428$). To use only the first two terms let us make $(\frac{\mu}{3B})^2 \leq 0.05$ which is equivalent to $\nu \geq 0.226$). Thus with only one corrective term to the incompressible solution we may consider very compressible materials. We shall now consider the specific problem where the thick-walled cylinder is bonded to a rigid case. Thus the boundary conditions are

$$\text{at } r = a \quad \sigma_r^{(0)} = \sigma_r^{(1)} = 0 \quad (8.20)$$

$$\text{and at } r = b \quad u^{(0)} = u^{(1)} = 0$$

Note that we now have a boundary condition $u(b) = 0$ that tends to specify a volume change that is physically impossible for as $a \rightarrow 0$ the condition that $u(b) = 0$ means that the volume must remain a constant whereas a change in temperature demands a volume change, thus we shall find the solution to be very sensitive to the actual amount of compressibility as $a \rightarrow 0$. Noting the above boundary condition we find that

$$\begin{aligned} u^{(0)} &= \frac{3\alpha\Delta T}{2} \left(r - \frac{b^2}{r} \right) \\ \sigma_r^{(0)} &= 3\mu\alpha\Delta T \left(\frac{b^2}{r^2} - c^2 \right) \\ u^{(1)} &= \frac{\alpha\Delta T(1 + 3c^2)}{2} \left(\frac{b^2}{r} - r \right) \\ \sigma_r^{(1)} &= \alpha\mu\Delta T(1 + 3c^2) \left(c^2 - \frac{b^2}{r^2} \right). \end{aligned} \quad (8.21)$$

As above we find that

$$u = \frac{3\alpha\Delta T}{2} \left(r - \frac{b^2}{r} \right) \left\{ 1 - \frac{\mu}{B} \left(\frac{1}{3} + c^2 \right) + \left[\frac{\mu}{B} \left(\frac{1}{3} + c^2 \right) \right]^2 + \dots \right\} \quad (8.22)$$

$$\sigma_r = 3\alpha\mu\Delta T \left(\frac{b^2}{r^2} - c^2 \right) \left\{ 1 - \frac{\mu}{B} \left(\frac{1}{3} + c^2 \right) + \dots \right\}.$$

For $\left| \frac{\mu}{B} \left(\frac{1}{3} + c^2 \right) \right| < 1$ the above series may be summed to yield

$$u = \frac{3\alpha\Delta T \left(r - \frac{b^2}{r} \right)}{2 \left[1 + \frac{\mu}{B} \left(\frac{1}{3} + c^2 \right) \right]} \quad (8.23)$$

$$\sigma_r = \frac{3\alpha\mu\Delta T \left(\frac{b^2}{r^2} - c^2 \right)}{1 + \frac{\mu}{B} \left(\frac{1}{3} + c^2 \right)}.$$

For $\left| \frac{\mu}{B} \left(\frac{1}{3} + c^2 \right) \right| \geq 1$ we see that the above series does not converge. Letting v_c be the critical value of v that determines the boundary of the region of convergence, we find that for

$$c = 2 \quad v_c = .393$$

$$c = 10 \quad v_c = .495$$

We shall now consider the range of validity of the above approximation, Eq. (8.21). To use only the first term (i.e., assume incompressibility) let us make

$$\frac{\mu}{B} \left(\frac{1}{3} + c^2 \right) \leq .05 \quad \text{then} \quad c = 2 \quad v \geq .494$$

$$c = 10 \quad v \geq .49975$$

To use only the first two terms let us make

$$\left[\frac{\mu}{B} \left(\frac{1}{3} + c^2 \right) \right]^2 \leq .05 \quad \text{then} \quad c = 2 \quad \nu \geq .4746$$

$$c = 10 \quad \nu \geq .4989$$

It is to be noted that, for certain problems, although the series may not converge for $\nu \leq \nu_c$ it is possible that if the series may be summed for $\nu > \nu_c$ the resulting expression may be valid for $\nu \leq \nu_c$ (as was the case above), this of course would need to be investigated for each individual problem.

Let us now establish a near-incompressible second order elastic theory. We shall base it upon the assumption that the compressibility effects are of the same order of magnitude as the second order non-linear effects. For illustrative purposes we shall consider the governing equations for the pressurization of a thick-walled cylinder.

Proceeding as before we can separate the problem into two systems, i.e.,

$$s_{\rho} = s_{\rho}^{(0)} + \delta s_{\rho}^{(1)} \quad (8.24)$$

We shall now express the governing equations for $s_{\rho}^{(0)}$ (the classical equations) as was done for near-incompressible classical elasticity, see Eqs. (8.9) and (8.10).

Thus,

$$s_{\rho}^{(0)} = s_{\rho}^{(0)(0)} + \epsilon s_{\rho}^{(0)(1)} \quad (8.25)$$

where

$$\epsilon = \frac{\bar{B}}{B}.$$

Let us now choose \bar{B} such that $\epsilon \approx \delta$, whence

$$s_{\rho}^{(0)} = s_{\rho}^{(0)(0)} + \delta s_{\rho}^{(0)(1)} \quad (8.26)$$

Noting these expressions for the first system variables and referring to Eq. (5.9) we may write the equation for the second system as

$$\frac{ds_{\rho}^{(1)}}{d\rho} + \frac{s_{\rho}^{(1)} - s_{\theta}^{(1)}}{\rho} = \frac{1}{\rho} \left(\frac{v^{(0)(0)}}{\rho} - \frac{dv^{(0)(0)}}{d\rho} \right)^2 \text{ etc.} \quad (8.27)$$

Now let us write $s_{\rho}^{(1)} = s_{\rho}^{(1)(0)} + \delta s_{\rho}^{(1)(1)}$ where $s_{\rho}^{(1)(0)}$ is the effect if the material were incompressible and $s_{\rho}^{(1)(1)}$ is the compressible effect. Thus,

$$s_{\rho} = s_{\rho}^{(0)(0)} + \delta s_{\rho}^{(1)(0)} + \delta^2 s_{\rho}^{(1)(1)} \quad (8.28)$$

For a second order theory we may neglect $s_{\rho}^{(1)(1)}$. To obtain the governing equations for $s_{\rho}^{(1)(0)}$ we use the equations derived in incompressible finite elasticity except that in the constitutive equations I_3 is no longer equal to 1. Hence,

$$\begin{aligned} s_{\rho}^{(1)(0)} &= h^{(1)(0)} + \frac{v^{(1)(0)}}{\rho} - \frac{1}{2} \left(\frac{v^{(0)(0)}}{\rho} \right)^2 + \frac{dv^{(0)(0)}}{d\rho} \frac{v^{(0)(0)}}{\rho} \\ s_{\rho}^{(1)(0)} - s_{\theta}^{(1)(0)} &= \frac{v^{(1)(0)}}{\rho} \frac{dv^{(1)(0)}}{d\rho} - \frac{1}{2} \left(\frac{v^{(0)(0)}}{\rho} \right)^2 + \frac{1}{2} \left(\frac{dv^{(0)(0)}}{d\rho} \right)^2 \end{aligned} \quad (8.29)$$

$$\frac{dv^{(1)}(0)}{d\rho} + \frac{v^{(1)}(0)}{\rho} = -\frac{1}{2}\left(\frac{dv^{(0)}(0)}{d\rho}\right)^2 - \frac{1}{2}\left(\frac{v^{(0)}(0)}{\rho}\right)^2 - 2\frac{dv^{(0)}(0)}{d\rho}\frac{v^{(0)}(0)}{\rho}$$

$$\frac{ds_{\rho}^{(1)}(0)}{d\rho} + \frac{s_{\rho}^{(1)}(0) - s_{\theta}^{(1)}(0)}{\rho} = \frac{1}{\rho}\left(\frac{v^{(0)}(0)}{\rho} - \frac{dv^{(0)}(0)}{d\rho}\right)^2 \quad (8.29)$$

The system of equations governing $s_{\rho}^{(0)}(1)$ is obtained from the second term equations for near-incompressible classical elasticity, Eq. (8.10),

$$s_{\rho}^{(0)}(1) = -\frac{dv^{(0)}(1)}{d\rho} + \frac{\epsilon^{(0)}(1)}{3} + \frac{k_1}{9B}\epsilon^{(0)}(0)$$

$$s_{\rho}^{(0)}(1) - s_{\theta}^{(0)}(1) = \frac{v^{(0)}(1)}{\rho} - \frac{dv^{(0)}(1)}{d\rho}$$

(8.30)

$$\frac{v^{(0)}(1)}{\rho} + \frac{dv^{(0)}(1)}{d\rho} = \frac{k_1}{3B}\epsilon^{(0)}(0)$$

$$\frac{ds_{\rho}^{(0)}(1)}{d\rho} + \frac{s_{\rho}^{(0)}(1) - s_{\theta}^{(0)}(1)}{\rho} = 0.$$

As both $s_{\rho}^{(1)}(0)$ and $s_{\rho}^{(0)}(1)$ are second order terms, we shall combine them, letting

$$\bar{s}_{\rho}^{(1)} = s_{\rho}^{(1)}(0) + s_{\rho}^{(0)}(1), \quad (8.31)$$

Adding the system of equations (8.29) and (8.30) and rearranging terms slightly we obtain the following governing system of equations for the second order solution:

$$\left(\text{Let } \frac{\bar{\theta}^{(0)}(0)}{3} = \bar{h}^{(0)}\right)$$

$$\bar{s}_{\rho}^{(1)} = -\frac{d\bar{v}^{(1)}}{d\rho} + \bar{h}^{(1)} + \frac{1}{2}\left(\frac{\bar{v}^{(0)}}{\rho}\right)^2 + \frac{k_1}{3\bar{B}} \bar{h}^{(0)}$$

$$\bar{s}_{\rho}^{(1)} - \bar{s}_{\theta}^{(1)} = \frac{\bar{v}^{(1)}}{\rho} - \frac{d\bar{v}^{(1)}}{d\rho} \quad (8.32)$$

$$\frac{d\bar{v}^{(1)}}{d\rho} + \frac{\bar{v}^{(1)}}{\rho} = \left(\frac{\bar{v}^{(0)}}{\rho}\right)^2 + \frac{k_1}{\bar{B}} \bar{h}^{(0)}$$

$$\frac{d\bar{s}_{\rho}^{(1)}}{d\rho} + \frac{\bar{s}_{\rho}^{(1)} - \bar{s}_{\theta}^{(1)}}{\rho} = \frac{4}{\rho} \left(\frac{\bar{v}^{(0)}}{\rho}\right)^2$$

where $\bar{s}_{\rho}^{(0)}(0) = \bar{s}_{\rho}^{(0)}$. The governing equations for the first term are identical to those of incompressible elasticity and are given by Eq. (7.6).

Uniaxial Test

Because of the dependence of the near-incompressible theory, as developed above, upon the notion of perturbation it will be

expedient to consider the uniaxial test in the same manner. The uniaxial test for a compressible or incompressible solid may be similarly treated.

$$\text{Let} \quad e_1 = e_1^{(0)} + e_1^{(1)} \quad (8.33)$$

where $e_1^{(1)}$ is the deviation from classical incompressibility, etc.

$$\sigma_1 = (\sigma_1^{(0)} + \sigma_1^{(1)}) \quad (8.33)$$

Using Eqs. (8.9), (8.10), (7.1) and (7.2) we proceed as above and obtain

$$\begin{aligned} \sigma_1^{(0)} &= -\frac{3k_1}{2} e_1^{(0)} \\ \sigma_1^{(1)} &= k_1 \left[e_2^{(1)} - e_1^{(1)} + \frac{3}{4} \left(k_2 - \frac{5}{2} \right) (e_1^{(0)})^2 \right] \\ 0 &= e_1^{(1)} + 2e_2^{(1)} - \frac{k_1}{B} e_2^{(0)} - \frac{3}{4} (e_1^{(0)})^2 \end{aligned} \quad (8.34)$$

Pressure Loading of a Thick-walled Cylinder

The solution of the system of Eqs. (7.6) and (8.32) with the boundary condition $\sigma_r(a) = -P$, $\sigma_r(b) = 0$ yields

$$u = - \frac{P}{k_1(c^2 - 1)} \frac{b^2}{r} + \frac{1}{B} \frac{P}{2(c^2 - 1)} r + \frac{b^2 P^2}{2k_1^2(c^2 - 1)r} \left[3(c^2 + 1) - \frac{b^2}{r^2} \right]$$

(8.35)

$$\sigma_r = \frac{P}{c^2 - 1} \left[1 - \frac{b^2}{r^2} \right] - \frac{3c^2 P^2}{2k_1(c^2 - 1)^2} \left[1 - \frac{b^2 + a^2}{r^2} + \frac{b^2 a^2}{r^4} \right]$$

It will be noted that the above solution retains the algebraic simplicity of the incompressible solution, Eq. (7.16). The second term in the expression for u is the corrective term for compressibility.

9. An Approximate Solution Scheme.

As pointed out previously in the Introduction, the perturbation solution method depends upon the existence of the classical solution, not upon the knowledge of this solution. Thus the two sets of equations developed by the perturbation method govern the problem whether or not we are able to solve the classical problem. We might use some approximate solution scheme to solve the two systems of equations but practically this is rather poor, because the nonhomogeneous parts of the second system depend upon the solution of the first system; thus any errors in the solution of the first system of equations tend to be magnified. In order to avoid this magnification of error it is necessary to slightly modify the system of equations before we apply an approximate solution scheme to each.

The modified system of equations that we shall develop will not only allow us to solve approximately each system of equations without reflecting the errors of the solution to the

first system of equations into the second system of equations but will actually contain in the second solution a correction to improve the approximate solution of the first system.

We may use any approximate solution method applicable in classical elasticity to solve each of the systems of equations, e.g., minimum potential energy, collocation, numerical schemes, etc., because we may view each system merely as a mathematical problem identical to some classical elastic problem. It is apparent that we may use any approximate method that is valid for classical elasticity.

We shall only consider the form of the equilibrium equation for a thick-walled cylinder and the form of the σ_r boundary condition. We will not derive any of the other thick-walled cylinder equations, as this one example will serve to illustrate the method. Although at this point we will solve no examples, we will point to two previously obtained solutions which may be viewed in this light.

Let us now consider the derivation of the equilibrium equation for a thick-walled cylinder. From Eq. (5.6)

$$\frac{ds_\rho}{d\rho} + \frac{s_\rho - s_\theta}{\rho} = -\delta \left[\frac{v}{\rho} \frac{ds_\rho}{d\rho} + \frac{dv}{d\rho} \frac{s_\rho - s_\theta}{\rho} \right] \quad (9.1)$$

Referring to Eq. (5.7)

$$\begin{aligned} s_\rho &= s_\rho^{(0)} + \delta s_\rho^{(1)} \\ s_\theta &= s_\theta^{(0)} + \delta s_\theta^{(1)} \\ v &= v^{(0)} + \delta v^{(1)} \end{aligned} \quad (9.2)$$

and substituting the above expressions into Eq. (9.1) we obtain

$$\left[\frac{ds_{\rho}^{(0)}}{d\rho} + \frac{s_{\rho}^{(0)} - s_{\theta}^{(0)}}{\rho} \right] + \delta \left[\frac{ds_{\rho}^{(1)}}{d\rho} + \frac{s_{\rho}^{(1)} - s_{\theta}^{(1)}}{\rho} + \frac{v^{(0)}}{\rho} \frac{ds_{\rho}^{(0)}}{d\rho} + \frac{dv^{(0)}}{d\rho} \frac{s_{\rho}^{(0)} - s_{\theta}^{(0)}}{\rho} \right] + \dots = 0 \quad (9.3)$$

As before the first system equilibrium equation is

$$\frac{ds_{\rho}^{(0)}}{d\rho} + \frac{s_{\rho}^{(0)} - s_{\theta}^{(0)}}{\rho} = 0 \quad (9.4)$$

If, for example, we only approximately solve the problem, we might, instead of satisfying the above equation, have

$$\frac{ds_{\rho}^{(0)}}{d\rho} + \frac{s_{\rho}^{(0)} - s_{\theta}^{(0)}}{\rho} = \bar{g}(\rho) \quad (9.5)$$

Assuming that the error function $\bar{g}(\rho)$ is small (compared to $s_{\rho}^{(0)}$ and $s_{\theta}^{(0)}$) we may write $\bar{g}(\rho) = \epsilon g(\rho)$ where $g(\rho)$ is of the order of magnitude of $s_{\rho}^{(0)}$ and $s_{\theta}^{(0)}$ and $\epsilon \ll 1$. If ϵ is of the order of magnitude of δ we shall take $\epsilon = \delta$, thus $\bar{g}(\rho) = \delta g(\rho)$ (note if $\epsilon = O(\delta^2)$ then, as we shall see, the second system of equations remains unchanged) or

$$\frac{ds_{\rho}^{(0)}}{d\rho} + \frac{s_{\rho}^{(0)} - s_{\theta}^{(0)}}{\rho} = \delta g(\rho) \quad (9.6)$$

Noting the above results Eq. (9.3) becomes

$$\begin{aligned}
& -\delta g(\rho) + \delta \left[\frac{ds_{\rho}^{(1)}}{d\rho} + \frac{s_{\rho}^{(1)} - s_{\theta}^{(1)}}{\rho} + \frac{v^{(0)}}{\rho} \frac{ds_{\rho}^{(0)}}{d\rho} + \frac{dv^{(0)}}{d\rho} \frac{s_{\rho}^{(0)} - s_{\theta}^{(0)}}{\rho} \right] \\
& + \delta^2 \left[\dots \right] + \dots = 0
\end{aligned}$$

The second system equilibrium equation is now

$$\frac{ds_{\rho}^{(1)}}{d\rho} + \frac{s_{\rho}^{(1)} - s_{\theta}^{(1)}}{\rho} = - \left[\frac{v^{(0)}}{\rho} \frac{ds_{\rho}^{(0)}}{d\rho} + \frac{dv^{(0)}}{d\rho} \frac{s_{\rho}^{(0)} - s_{\theta}^{(0)}}{\rho} + g(\rho) \right] \quad (9.7)$$

A similar consideration may be applied to the remaining field equations. An example of such a solution (i.e., when the field equations are only approximately solved) is the finite near-incompressible theory of the previous section, for there we approximately solve the first system by an incompressibility approximation, introduce an error function into the second approximation by means of the compressibility terms and lastly approximately solve the second system.

Similarly we might have a boundary condition of the form

$$s_{\rho} \big|_{\rho=c} = \bar{P}$$

from Eq. (9.2)

$$s_{\rho}^{(0)} \big|_{\rho=c} + \delta s_{\rho}^{(1)} \big|_{\rho=c} + \dots = \bar{P} \quad (9.8)$$

The boundary condition of the first system of equations is

$$s_{\rho}^{(0)} \big|_{\rho=c} = \bar{P} \quad (9.9)$$

Let us assume that we only approximately satisfy this boundary condition, i.e., we set

$$s_{\rho}^{(0)}|_{p=c} = \bar{\bar{P}} \quad \text{where} \quad \bar{P} - \bar{\bar{P}} = \delta P \quad (9.10)$$

and $\bar{\bar{P}}$ is of the order of magnitude of $s_{\rho}^{(0)}$. Thus Eq. (9.8) becomes

$$\delta s_{\rho}^{(1)}|_{p=c} + \dots = \bar{P} - \bar{\bar{P}} = \delta P$$

and the second boundary condition becomes

$$s_{\rho}^{(1)}|_{p=c} = P \quad (9.11)$$

Equation (6.38) is a solution of this type, i.e., we solved the first system using the approximation that the case was rigid, then we corrected the error in the second approximation.

10 Numerical Examples.

As an example of the numerical results that may be expected when one evaluates the analytical solutions presented in the previous sections we shall consider the pressurization problem for a thick-walled cylinder bonded to an elastic case (see Section 6 and Fig. 1). The resulting solution merely involves algebraic operations, thus the results may be obtained extremely rapidly by means of an electronic computer.*

* Sincere appreciation is expressed to R.F. Nickell who programmed the solution.

The nonlinearities in a finite elastic problem are due to two causes; (1) nonlinear geometric effects and (2) nonlinear constitutive equations. The nonlinear effects introduced by the constitutive equations depend both upon the magnitude of the strains and also upon the relative magnitudes of the elastic constants that appear in the constitutive equation, whereas the nonlinear effects introduced by geometry depend only upon the magnitude of the strains. Thus one must determine the range of validity of a given approximation for each particular material used. For our material, as we shall see later, the magnitude of the second order constants ($k_1 k_3$, $k_1 k_4$ and $k_1 k_5$) is substantially larger than the magnitude of the first order constants (k_1 and $k_1 k_2$); thus we would expect the range of validity of the first order solution to be rather restricted. The proper way to judge the range of validity for a given approximation is to inspect the size of the subsequent term in the series. Thus as we have obtained the second order solution we are able to investigate the range of validity of the first order solution. Likewise to be able to consider the accuracy of our second order solution we would need to inspect the third order solution; as this has not been done it may be possible that some of the results presented herein for large pressures may fall beyond the domain of the second order solution.

In deriving the solution in Section 6 the following assumptions were made in order to consider the case as rigid in the first approximation. (If these assumptions were not true we could not set $v^{(0)}(c) = 0$); (1) the case is very rigid in comparison to the thick-walled cylinder and (2) the thick-walled cylinder is relatively compressible. In order to satisfy the above assumptions we have restricted our calculations to large \bar{E} , small $\frac{b}{t}$, small k_1 , and small k_2 (k_2 is a measure of the compressibility, see Eq. (4.2)).

As the finite elastic response of propellants has not been suitably characterized it was necessary for us to obtain the elastic constants for a typical propellant by fitting the second order equations governing a uniaxial test from Section 6 to an experimental curve. The resulting elastic properties should be viewed as very tentative as the method of curve fitting was not entirely satisfactory and as there were some questions as to the accuracy of the experimental data. Depending upon how we choose to fit the uniaxial expressions of Section 6 to the experimental data we could obtain a substantial range in values of the elastic constants, these ranges are indicated in Figures 7, 10, 11 and 14 by the vertical dashed lines. The seemingly best fit yielded the following values

$$k_1 = - 558 \text{ psi}$$

$$k_2 = - 8.01$$

$$k_3 = - 25.8$$

$$k_4 = 72.8$$

$$k_5 = 4.11$$

The pressurization solution as presented in Section 6 depends upon the following parameters \bar{E} , $\bar{\nu}$, $\frac{b}{t}$, c , k_1 , k_2 , k_3 and k_4 . We selected the following values for our "standard" solution.

$$\bar{E} = 30 \times 10^6 \text{ psi}$$

$$\bar{\nu} = 0.3$$

$$\frac{b}{t} = 100$$

$$c = 2$$

$$k_1 = - 558 \text{ psi} \qquad k_3 = - 25.8$$

$$k_2 = - 8.01 \qquad k_4 = 72.8$$

The results as presented in Figures 2 - 14 are for the above parametric values unless the values of the parameter are specifically indicated; i.e., in Figure 5, for example, we are studying the effect upon the "standard" solution when \bar{E} varies from the value given above.

The case was so stiff compared to the thick-walled cylinder that we nearly obtained hydrostatic compression of the thick-walled cylinder as may be seen in Figure 3, 4, 9, 10 and 13 where we see that the stresses are nearly equal to the applied pressure. For small pressures the solution differs only slightly from the first order solution (shown by the dotted lines in Figure 2) but as the pressure is increased the nonlinearities become more and more important, thus in Figures 12 and 14 we see that for small pressure the solution is nearly independent of the second order constants. Also in Figure 9, whereas for low pressures $\sigma_r(a)$ is a linear function of the first order constant k_1 , we see that for higher pressures it becomes a nonlinear function of k_1 . As the strains are much larger at the inner surface of the thick-walled cylinder than at the outer (we found $\frac{u(b)}{b} < .001$) we should expect the nonlinearities to be far more pronounced at the inner surface than at the outer. This prediction is readily verified by comparing Figures 3 and 4 and by noting from Figure 13 that $\sigma_r(b)$ is essentially independent of the second order constants even for large values of the applied pressure.

REFERENCES

1. Green, A.E. and Zerna, W., Theoretical Elasticity, Oxford University Press, England, 1954.
2. Green, A.E. and Adkins, J.E., Large Elastic Deformations, Oxford University Press, England, 1960.
3. Rivlin, R.S., "The Solution of Problems in Second Order Elasticity Theory" J. Rat. Mech. Anal. v.2, 1953, pp 53.
4. Weiner, J.H. and Boley, B.A., "Basic Concepts of the Thermodynamics of Continuous Media" Technical Report, U.S.A.F., ARDC, Wright-Patterson Air Force Base, Ohio, June 1957.
5. Morse, P.M., and Feshbach, H., Methods of Theoretical Physics, McGraw-Hill Book Company, New York, 1953.
6. Rivlin, R.S. and Saunders, D.W., "Large Elastic Deformations of Isotropic Materials VII. Experiments on the Deformations of Rubber" Phil. Trans. Roy. Soc. London, v.A243, 1953, pp 251.
7. Anthony R.L., Caston, R.H., and Guth, E., "Equations of State for Natural and Synthetic Rubber-Like Materials," J. Phy. Chem., v.46, 1942, pp 826.
8. Williams, M.L., Blatz, P.J. and Schapery, R.A., "Fundamental Studies Relating to Systems Analysis of Solid Propellants" Final Report-GALCIT 101, California Institute of Technology, February 1961.
9. Johnson, M.W. and Reissner E., "On the Foundations of the Theory of Thin Elastic Shells" J. Math. and Physics, v.37, 1959, pp 371.

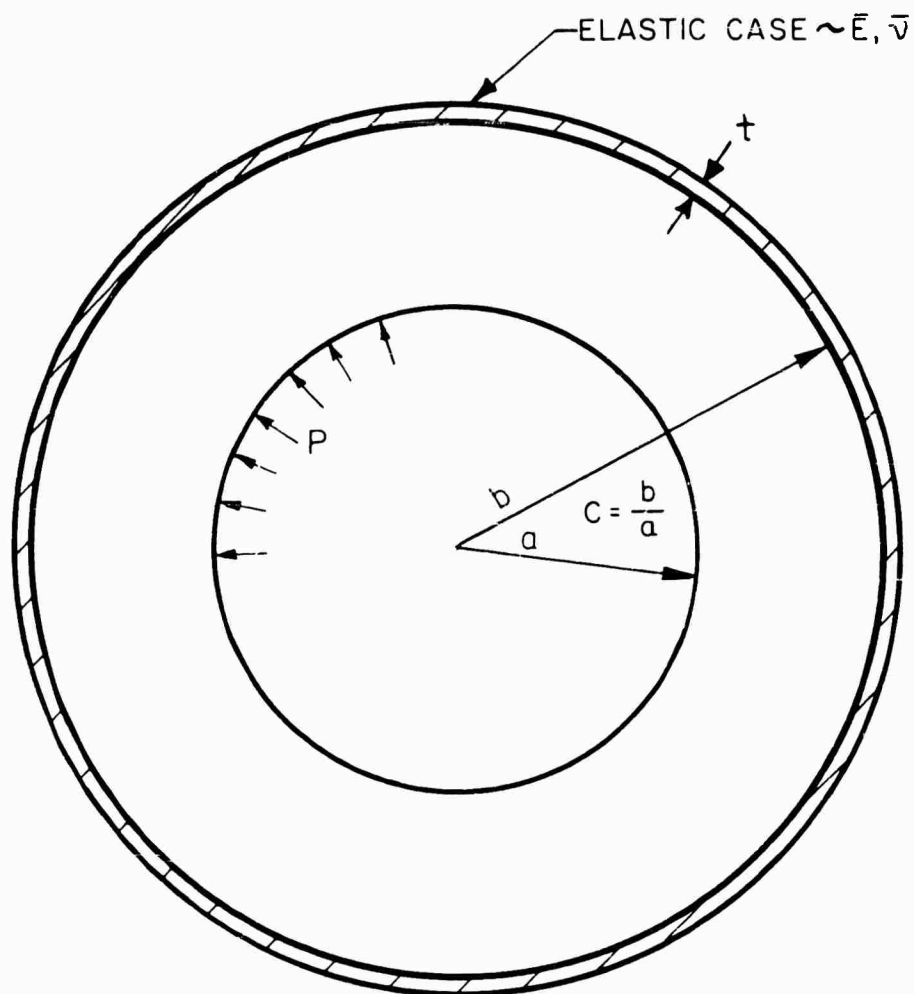


FIG.1 PRESSURIZATION OF A THICK-WALLED CYLINDER
BONDED TO AN ELASTIC CASE
(SEE SECTIONS 6 AND 10)

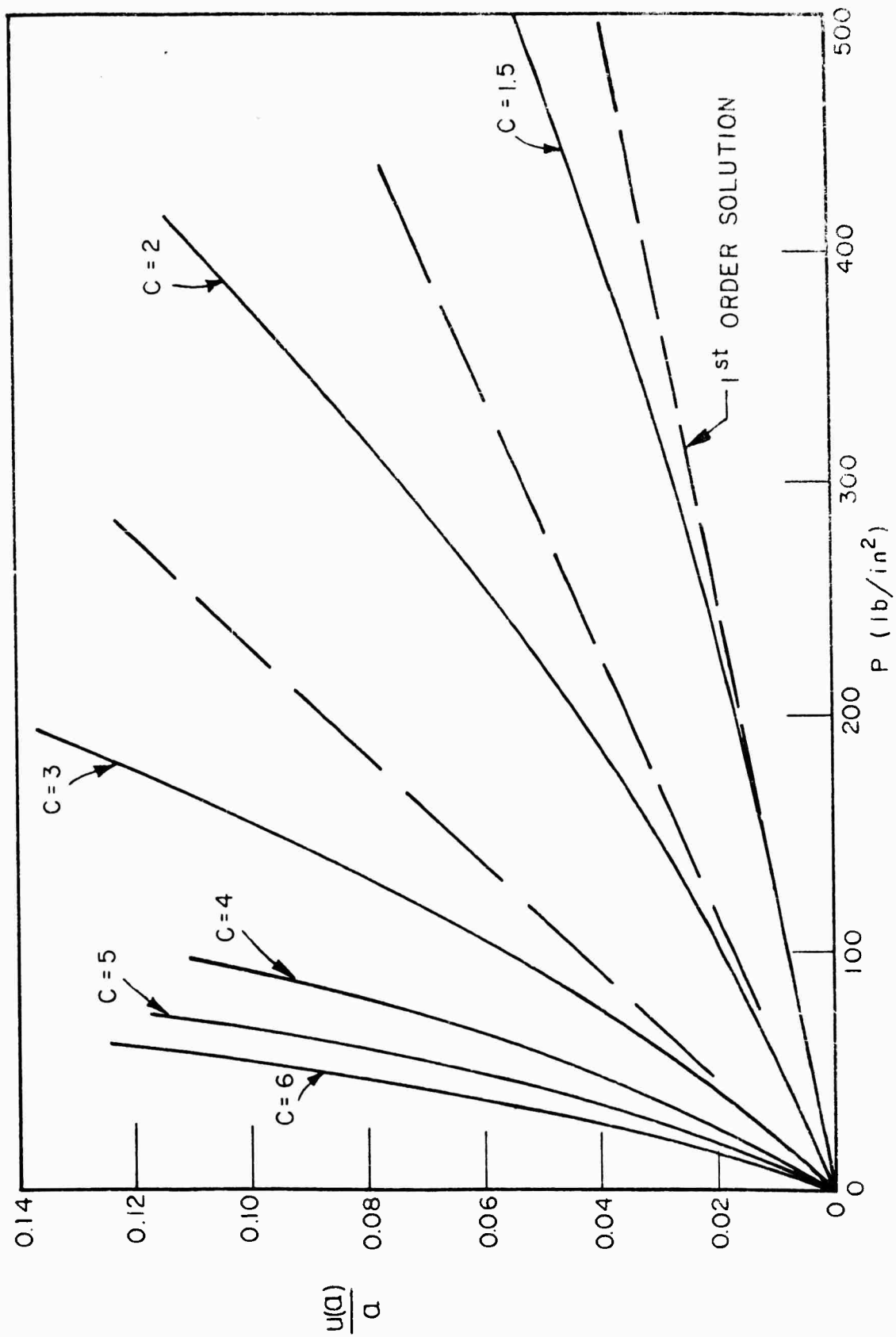


FIG.2 INNER BORE DISPLACEMENT - PRESSURE AS A FUNCTION OF CYLINDRICAL RADII RATIO.

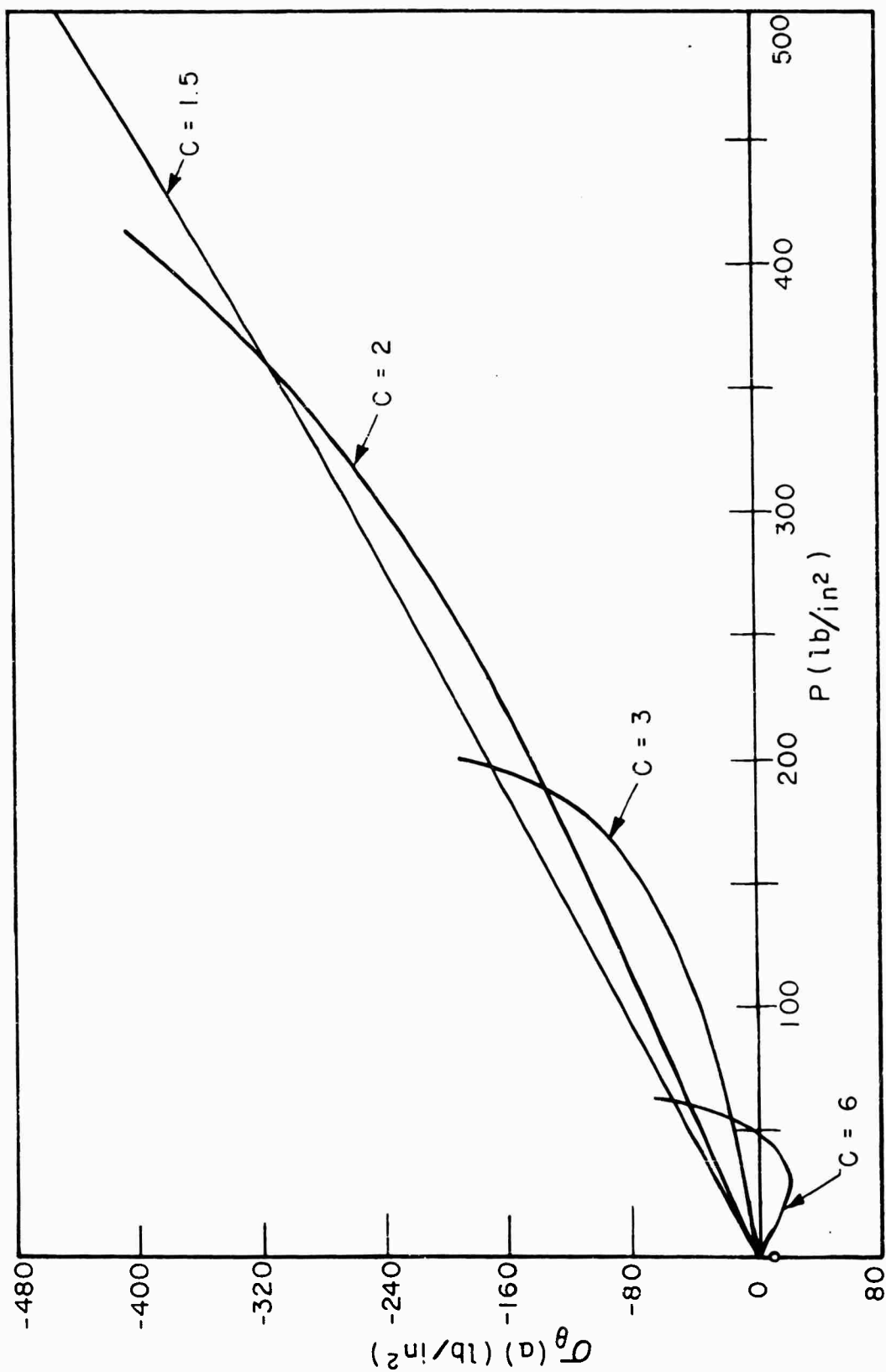


FIG. 3 INNER BORE TANGENTIAL STRESS - PRESSURE AS A FUNCTION
OF CYLINDRICAL RADII RATIO

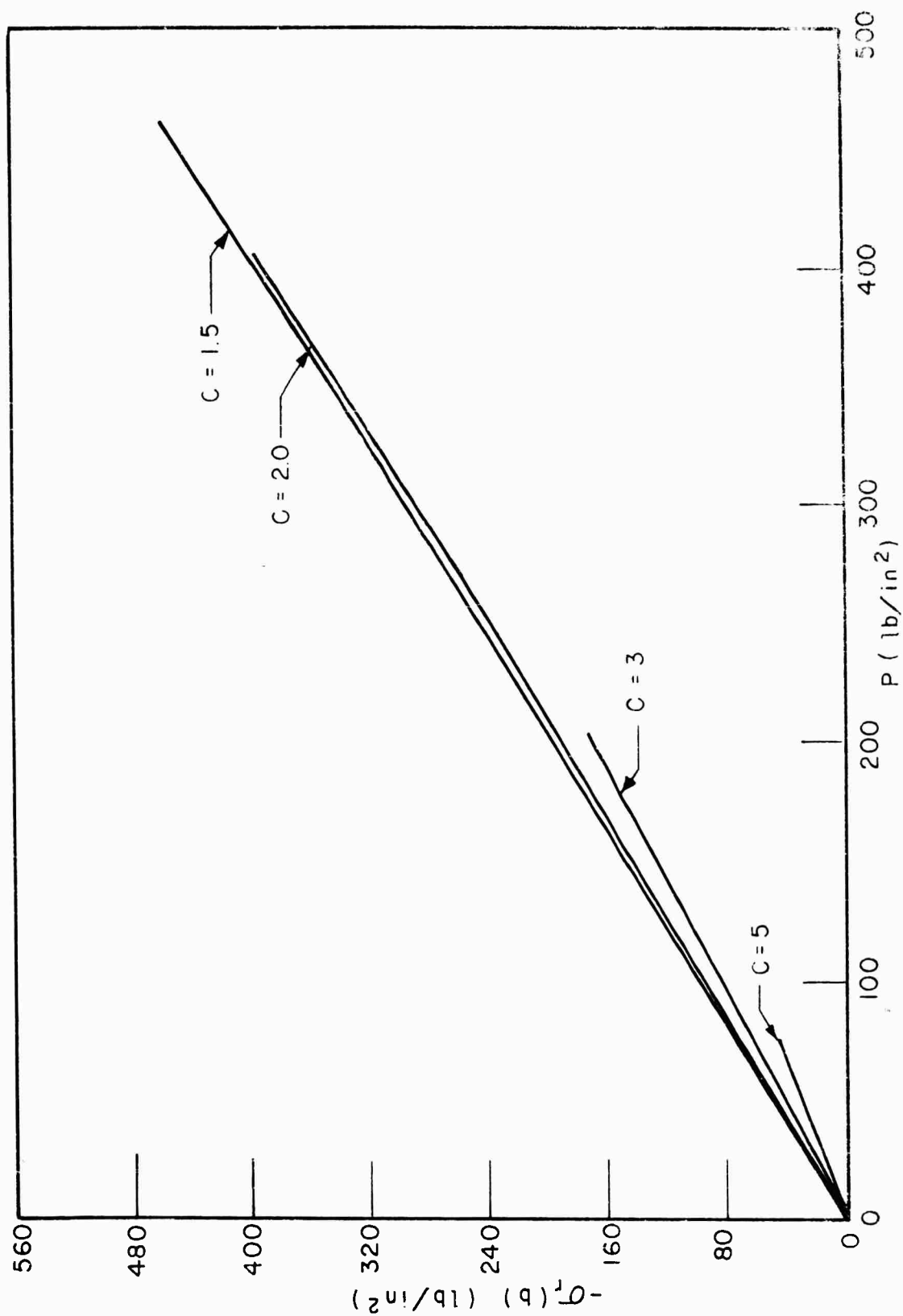


FIG. 4 CASE PRESSURE — PRESSURE AS A FUNCTION OF CYLINDRICAL RADII RATIO

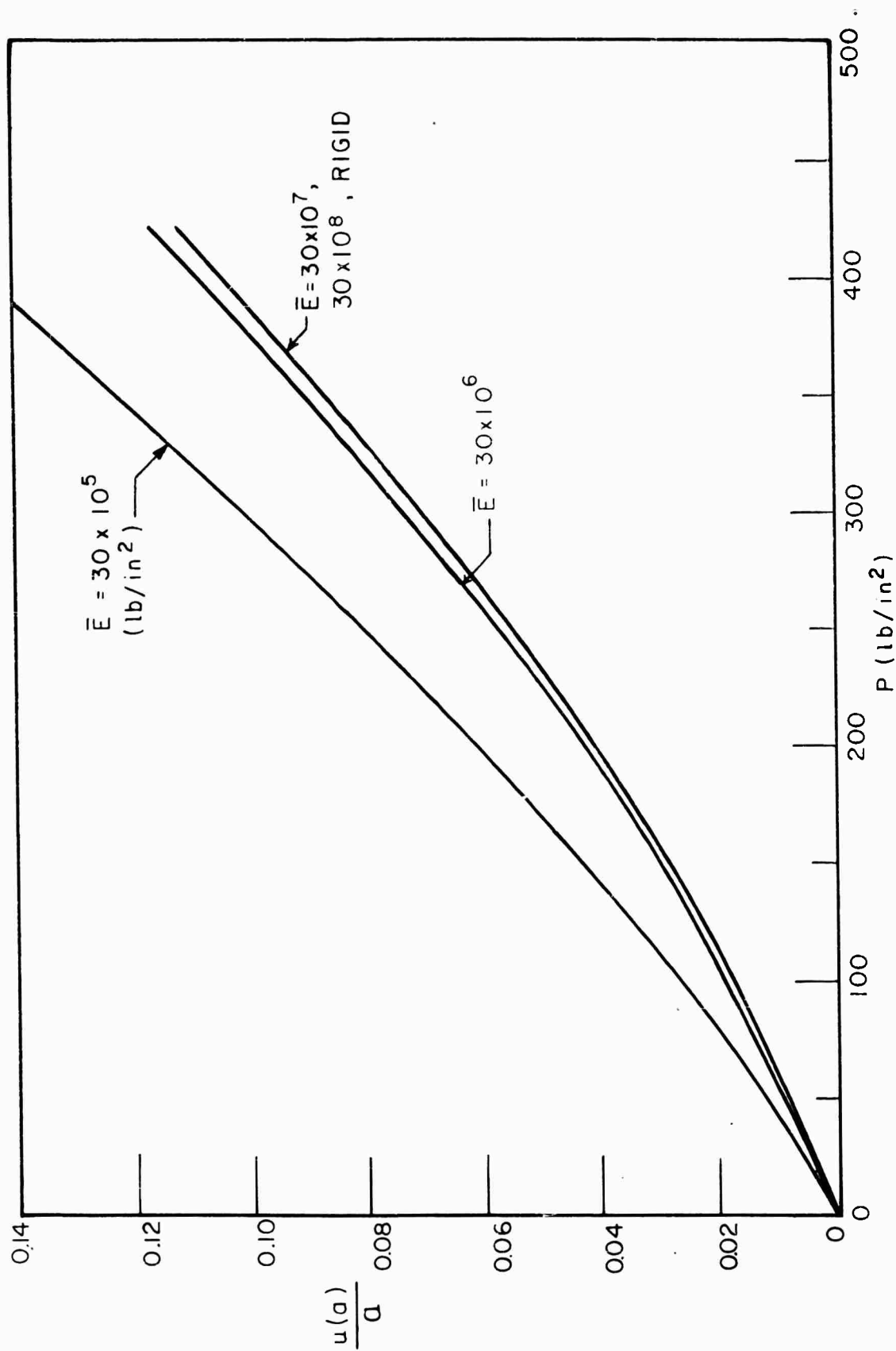


FIG.5 INNER BORE DISPLACEMENT - PRESSURE AS A FUNCTION OF CASE STIFFNESS ($b/t = 100$)

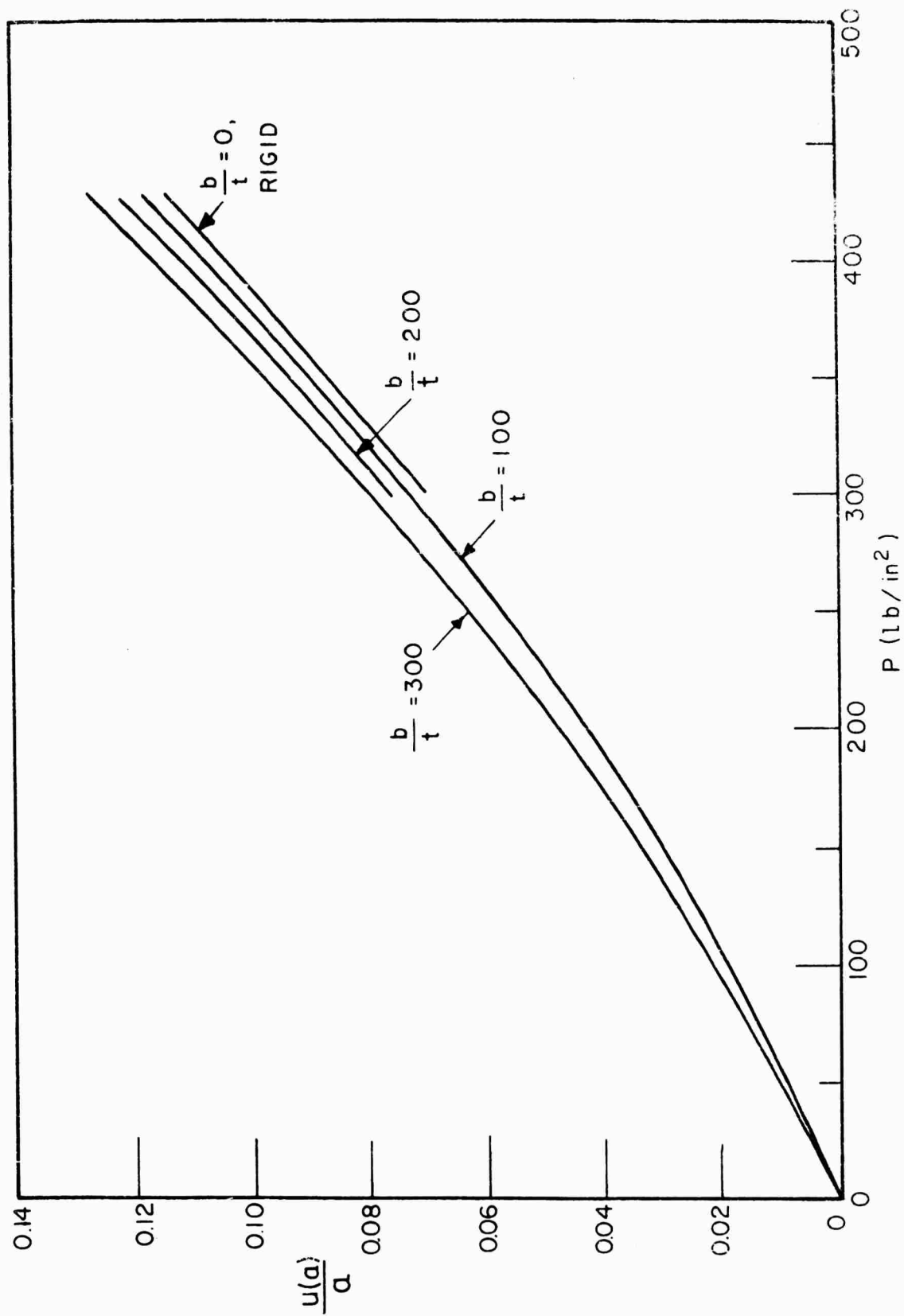


FIG.6 INNER BORE DISPLACEMENT - PRESSURE AS A FUNCTION OF CASE STIFFNESS ($\bar{E} = 30 \times 10^6$)

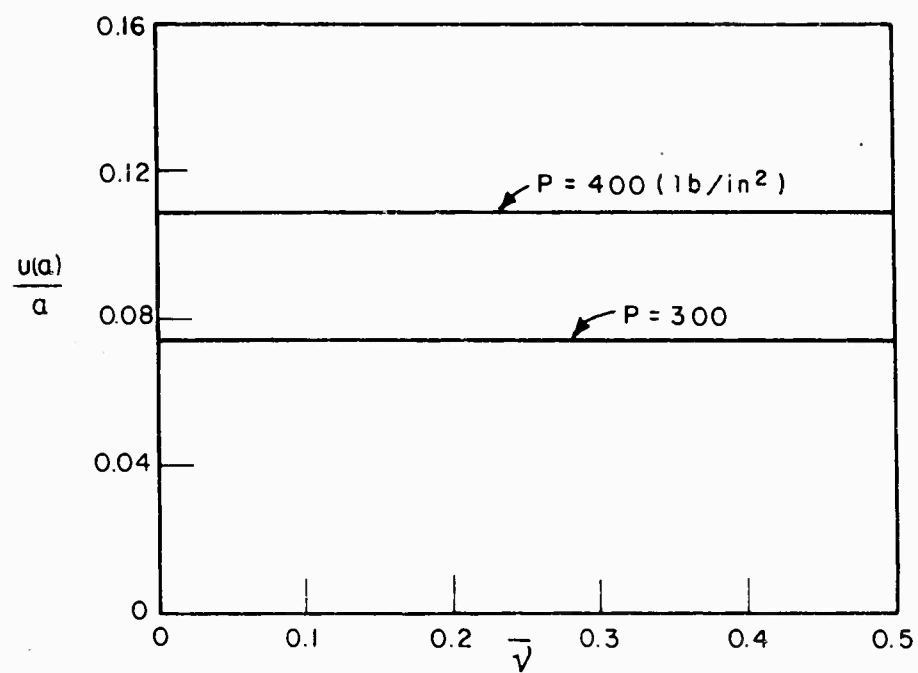


FIG.7 INNER BORE DISPLACEMENT - CASE POISSON'S RATIO

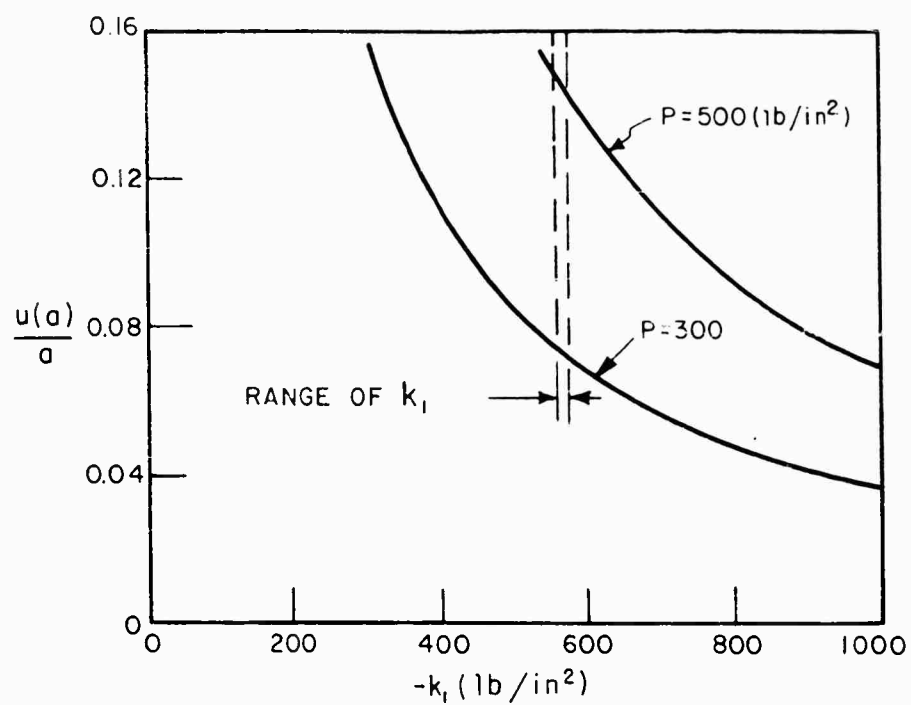


FIG.8 INNER BORE DISPLACEMENT - ELASTIC MATERIAL PARAMETER

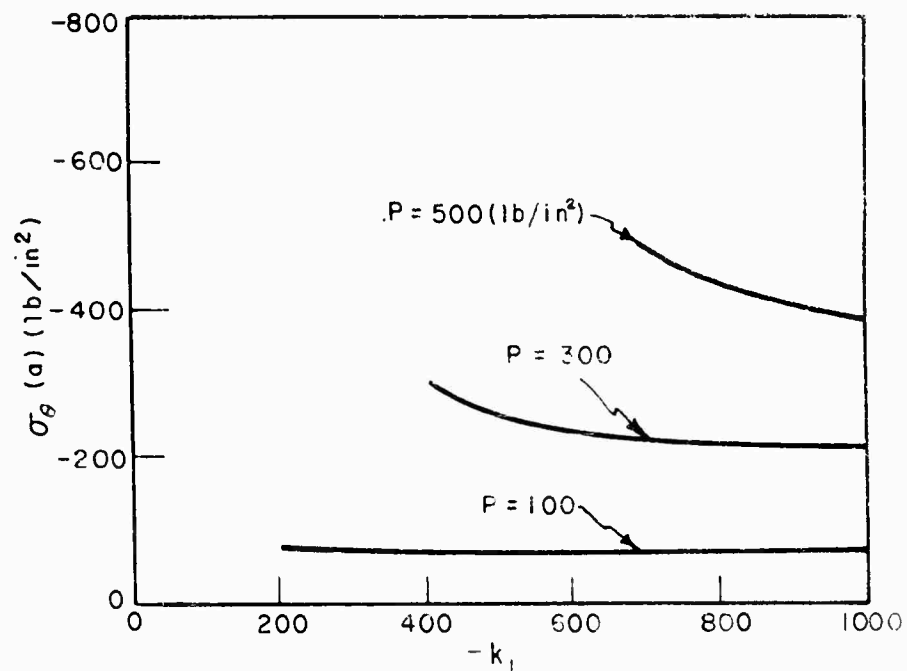


FIG. 9 INNER BORE TANGENTIAL STRESS — ELASTIC MATERIAL PARAMETER

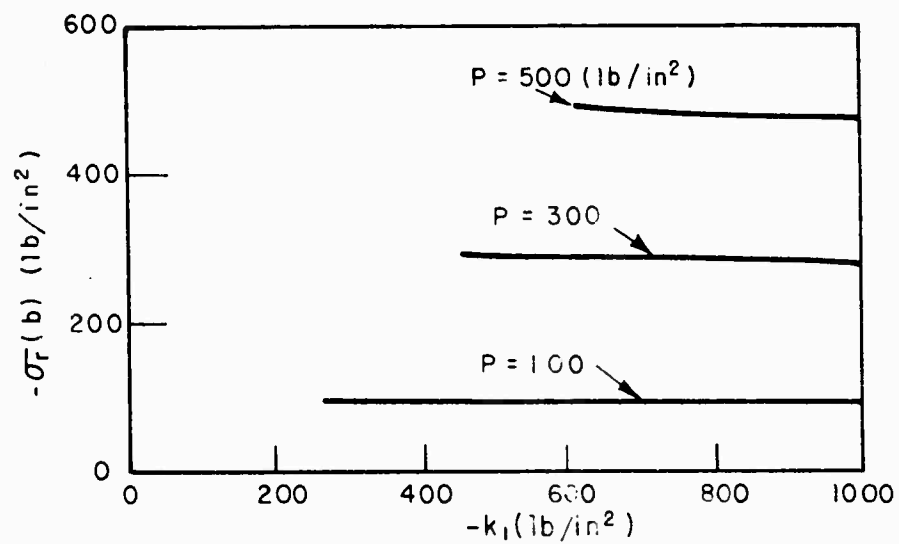


FIG. 10 CASE PRESSURE — ELASTIC MATERIAL PARAMETER

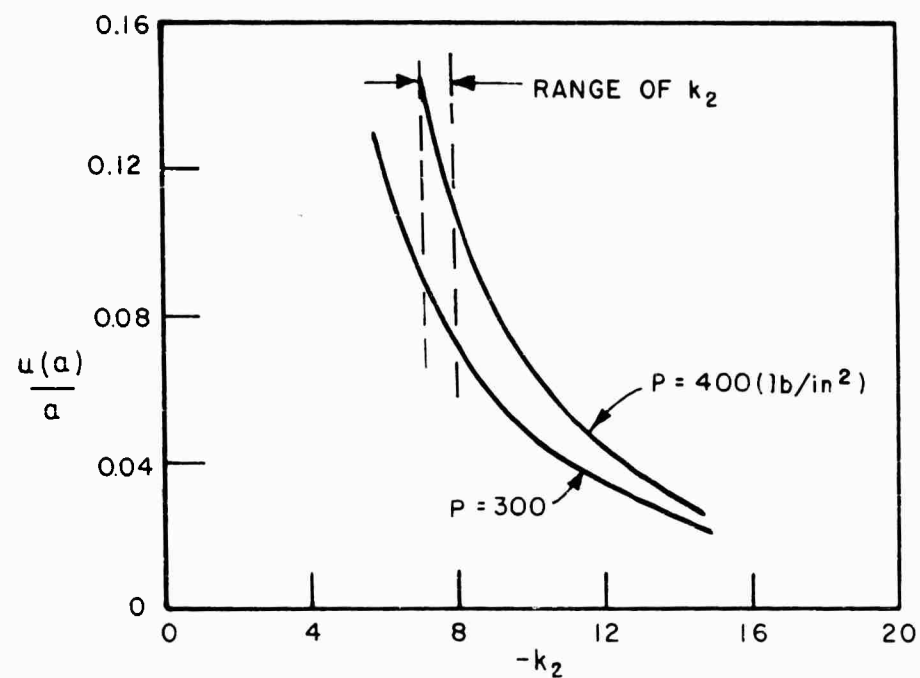


FIG.11 INNER BORE DISPLACEMENT -
ELASTIC MATERIAL PARAMETER

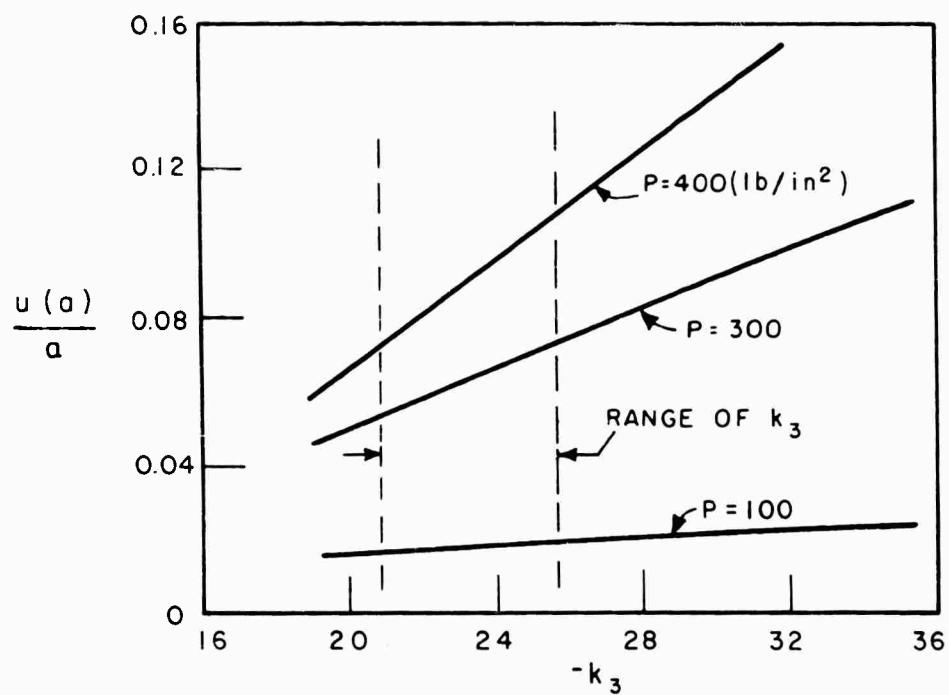


FIG.12 INNER BORE DISPLACEMENT -
ELASTIC MATERIAL PARAMETER

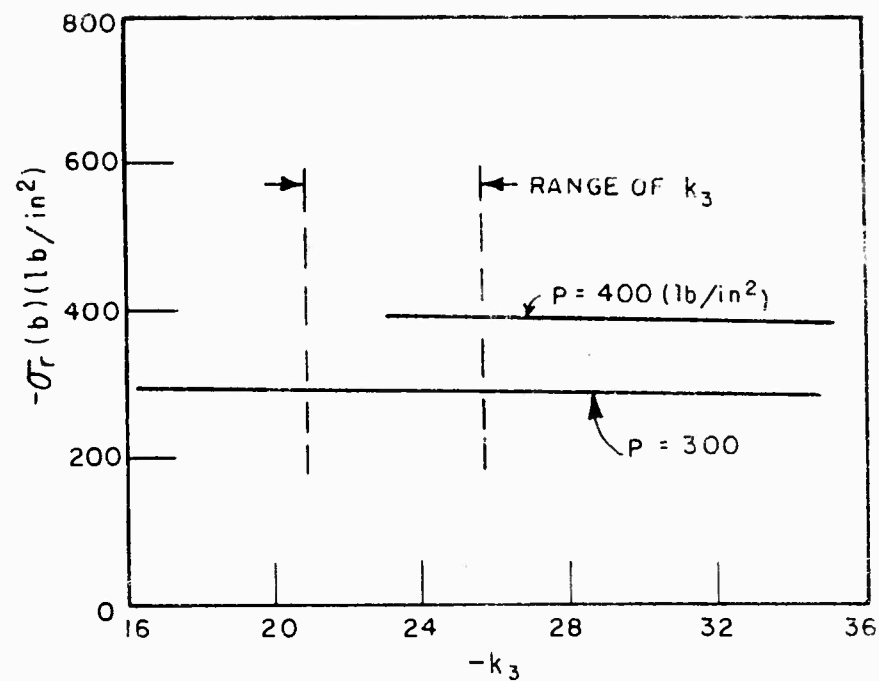


FIG.13 CASE PRESSURE - ELASTIC MATERIAL PARAMETER

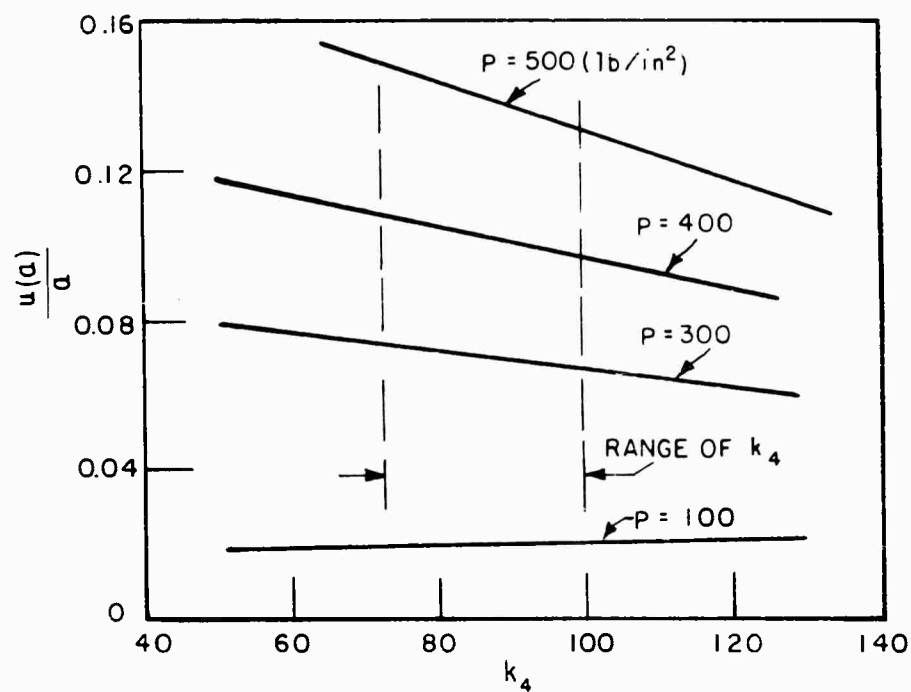


FIG. 14 INNER BORE DISPLACEMENT-ELASTIC MATERIAL PARAMETER

PART IV

THERMAL DEFORMATIONS OF VISCOELASTIC MATERIALS

by

R. L. TAYLOR

INTRODUCTION

It is well known that the response of stressed viscoelastic materials is influenced greatly by temperature changes in the transition range between the glassy and rubbery states. Any meaningful thermoviscoelastic analysis should reflect this behavior. One means of accounting for this type of response for a selected class of materials is the use of the time-temperature equivalence postulate: a change in temperature is equivalent to a shift in time. If the changes in response can be specified by a single time-temperature shift function, the material has been classified as "thermorheologically simple" by Schwarzl and Staverman [1]. In this part a solution method for a class of problems involving thermorheologically simple materials will be discussed.

GENERAL THEORY

1 Field Equations for Thermorheologically Simple Viscoelastic Materials.

With reference to an orthogonal curvilinear coordinate system, the linearized equilibrium equations in the absence of body forces and inertia terms are

$$\tau_j^1(x,t)_{,i} = 0 \quad (1.1)$$

where x denotes the curvilinear coordinate triad, (x^1, x^2, x^3) , while t denotes time. τ_j^1 are the mixed tensor components of stress, a repeated index appearing in a contravariant and covariant position implies summation, and a covariant index preceded by a comma implies covariant differentiation [5].

The linearized strain-displacement relations are

$$\epsilon_{ij}(x,t) = \frac{1}{2}(u_{i,j} + u_{j,i}) \quad (1.2)$$

where ϵ_{ij} and u_i are the covariant components of the linear strain tensor and the displacement vector respectively. In the subsequent analysis the mixed strain tensor will be needed. This is accomplished in the usual manner by raising an index to obtain the associated mixed strain tensor. Thus,

$$\epsilon_j^k = g^{ki} \epsilon_{ij} = \frac{1}{2}(u_{,j}^k + g^{k1} u_{j,i}) \quad (1.3)$$

where g^{ki} are the contravariant components of the metric tensor and u^k those of the displacement vector, respectively.

As is customary in isotropic viscoelastic analysis the stress and strain tensors are decomposed into their deviatoric and spherical components for convenience. Accordingly,

$$\tau_j^i = s_j^i + \delta_j^i \sigma \quad (1.4)$$

where $\sigma = \frac{1}{3} \tau_i^i$

and

$$\epsilon_j^i = e_j^i + \delta_j^i \epsilon \quad (1.5)$$

$$\epsilon = \frac{1}{3} \epsilon_i^i$$

In the above δ_j^i is the Kronecker delta, defined as

$$\delta_j^i = \begin{cases} 1, & i = j \\ 0, & i \neq j \end{cases} \quad (1.6)$$

Considering first the constitutive equations in the absence of thermal effects, it is known that the linear constitutive laws admit the differential-operator representation

$$P_1(D) s_j^i(x, t) = Q_1(D) e_j^i(x, t)$$

and

$$P_2(D) \sigma(x, t) = Q_2(D) \epsilon(x, t) \quad (1.7)$$

where

$$D \equiv \frac{\partial}{\partial t} ; P_i(D) = \sum_{n=0}^{N_i} p_i^{(n)} D^n$$

$$Q_i(D) = \sum_{m=0}^{M_i} q_i^{(m)} D^m$$

and

$$p_i^{(N_i)} \neq 0, \quad q_i^{(M_i)} \neq 0 \quad (i = 1, 2)$$

Thus P_i and Q_i are polynomial differential time operators of degree N_i and M_i respectively. The material properties are introduced through the $p_i^{(n)}$ and $q_i^{(m)}$ coefficients. The use of differential-operator representation is practically limited to media possessing finite and discrete relaxation spectra and retardation times. For this reason, it is convenient to consider the constitutive laws in integral form.

First, consider a mechanical test conducted at constant temperature. If an experiment is performed in which a constant strain (e.g., a constant deviator strain $\epsilon_{(0)j}^i$) is introduced at time zero and the material is assumed undisturbed for $t < 0$, then the time history of stress can be determined by measurement. Considering the stress-time history for the $\epsilon_{(0)j}^i$ deviator strain, the deviator-stress history s_j^i may be expressed through the relation

$$s_j^i(t) = G_1(t) \epsilon_{(0)j}^i \quad (1.8)$$

where $G_1(t)$ is defined as the deviatoric (shear) relaxation function and $\epsilon_{(0)j}^i$ is the constant strain introduced at $t = 0$. Subsequently, if the strain is a prescribed function of time, then the stress history may be determined by using the Boltzmann superposition principle. Thus, for example,

$$s_j^i(t) = \sum_{k=0}^{n-1} G_1(t_{(n)} - t_{(k)}) \left[e_{(k+1)j}^i - e_{(k)j}^i \right] \quad (1.9)$$

where $e_{(k)j}^i$ is the magnitude of the strain at the time $t_{(k)}$. If we now pass to the limit by letting $t_{(k+1)} - t_{(k)}$ tend to zero, then the sum becomes an integral and the relaxation integral laws in the absence of thermal effects are given by

$$s_j^i(x, t) = \int_0^t G_1(t-t') \frac{\partial}{\partial t'} e_j^i(x, t') dt'$$

and

$$\sigma(x, t) = \int_0^t G_2(t-t') \frac{\partial}{\partial t'} \epsilon(x, t') dt' \quad (1.10)$$

Similarly, the creep integral laws are given by

$$e_j^i(x, t) = \int_0^t J_1(t-t') \frac{\partial}{\partial t'} s_j^i(x, t') dt'$$

and

$$\epsilon(x, t) = \int_0^t J_2(t-t') \frac{\partial}{\partial t'} \sigma(x, t') dt' \quad (1.11)$$

where G_i and J_i , ($i = 1, 2$), are relaxation moduli and creep compliances respectively (in shear and dilatation).

Equations (1.10) and (1.11) vary slightly from the integral laws presented in Gross [3] in that instantaneous elastic and steady creep do not occur explicitly. However, in the above form, if the limits are taken from 0^- to t^+ then the discontinuities in the integrals between 0^- and 0^+ and t^- and t^+ will give rise to the two additional terms included in [3]. In evaluating any of the integrals which follows (unless otherwise indicated) these discontinuities must first be removed by evaluating the integrals from 0^- to 0^+ and t^- to t^+ .

The above constitutive laws were presented on the basis that the body remained isothermal for all time. Thus the material properties G_1 , J_1 , $p_1^{(n)}$ and $q_1^{(n)}$ must be regarded as having been determined for the temperature at which the material is being stressed. Mechanical properties of viscoelastic materials in the transition range between the glassy and the rubbery state show marked dependence upon the temperature. One method of accounting for temperature dependence is through the use of the time-temperature equivalence hypothesis in which a "reduced time" is introduced to account for both time and temperature variations. To exemplify the use of the "reduced time," consider the variation of the relaxation moduli G_1 with the temperature. Following the notation of Muki and Sternberg [6] let $G_1(t)$ be the relaxation modulus at the constant base temperature T_0 . We desire to account for variations of temperature from T_0 , say for any uniform temperature T . Let $\bar{G}_1(t, T)$ be the relaxation modulus at the temperature T , thus

$$\bar{G}_1(t, T_0) = G_1(t) = L_1(\log t) \quad (1.12)$$

The postulate of a single time-temperature equivalence function (i.e., the thermorheologically simple material) now assumes the form -

$$\bar{G}_i(t, T) = L_i \left[\log t + \log \phi(T) \right] = G_i \left[t \phi(T) \right] \quad (1.13)$$

where $\phi(T)$ is defined as the shift function. For uniform temperature, the product $t\phi(T)$ is defined as the "reduced time" ξ .

Once the shift function $\phi(T)$ is known, $\bar{G}_i(t, T)$ may be determined for other temperatures.

We next suppose the material to be subjected to non-uniform temperature $T(x, t)$. In extending the above concept, the reduced time must be generalized consistent with the postulated time-temperature equivalence and also the thermal expansion must be included in the constitutive law describing the dilatational behavior of the material. Moreland and Lee [4] stated these modifications and obtained general constitutive laws for a thermorheologically simple material as follows:

$$\begin{aligned} s_j^i(x, t) &= \int_0^t G_1(\xi - \xi') \frac{\partial}{\partial t'} e_j^i(x, t') dt' \\ \sigma(x, t) &= \int_0^t G_2(\xi - \xi') \frac{\partial}{\partial t'} \left[\epsilon(x, t') - \alpha_0 \theta(x, t') \right] dt' \end{aligned} \quad (1.14)$$

where the reduced time is now determined from

$$\xi = f(x, t) = \int_0^t \phi \left[T(x, t') \right] dt', \quad \xi' = f(x, t') \quad (1.15)$$

while the "pseudo-temperature" $\theta(x, t)$ is defined by

$$\theta(x, t) = \frac{1}{\alpha_0} \int_{T_0}^{T(x, t)} \alpha(T') dT', \quad \alpha_0 = \alpha(T_0) \quad (1.16)$$

$\alpha(T)$ is the temperature-dependent coefficient of thermal expansion. If α is temperature independent, then

$$\theta(x, t) = T(x, t) - T_0$$

where $T(x, t)$ is the solution of the Fourier heat conduction equation. The creep integral laws modified for the effects of temperature are given by

$$\begin{aligned} e_j^i(x, t) &= \int_0^t J_1(\xi - \xi') \frac{\partial}{\partial t'} s_j^i(x, t') dt' \\ \epsilon(x, t) &= \int_0^t J_2(\xi - \xi') \frac{\partial}{\partial t'} \sigma(x, t') dt' + \alpha_0 \theta(x, t) \end{aligned} \quad (1.17)$$

In order to make use of the Laplace transform it is convenient to remove from the field equations the explicit dependence upon the physical time. From Eq. (1.15), $f(x, t)$ can be inverted formally with respect to time to yield

$$t = g(x, \xi) \quad (1.18)$$

The explicit dependence upon time t in any function of space and time $F(x, t)$ is now removed by substituting Eq. (1.18) for t , thus,

$$F(x, t) = F[x, g(x, \xi)] \quad (1.19)$$

In order to avoid any ambiguity, we will define, following [6],

$$\hat{F}(x, \xi) = F(x, t) \quad (1.20)$$

It must be emphasized that $\hat{F}(x, \xi)$ is not the same function as $F(x, t)$ but has first been subjected to the transformation given by Eq. (1.18).

Substituting the results of Eq. (1.20) and making the appropriate changes in variables in the constitutive equations leads to the relaxation integral laws:

$$\begin{aligned} \hat{s}_j^i(x, \xi) &= \int_0^\xi G_1(\xi - \xi') \frac{\partial}{\partial \xi'} \hat{e}_j^i(x, \xi') d\xi' \\ \hat{\sigma}(x, \xi) &= \int_0^\xi G_2(\xi - \xi') \frac{\partial}{\partial \xi'} \left[\hat{\epsilon}(x, \xi') - \alpha_0 \hat{\theta}(x, \xi') \right] d\xi' \end{aligned} \quad (1.21)$$

and to the creep integral laws

$$\begin{aligned} \hat{e}_j^i(x, \xi) &= \int_0^\xi J_1(\xi - \xi') \frac{\partial}{\partial \xi'} \hat{s}_j^i(x, \xi') d\xi' \\ \hat{\epsilon}(x, \xi) &= \int_0^\xi J_2(\xi - \xi') \frac{\partial}{\partial \xi'} \hat{\sigma}(x, \xi') + \alpha_0 \hat{\theta}(x, \xi) \end{aligned} \quad (1.22)$$

The differential operator form of the constitutive equations modified for the effects of temperature and consistent with the time-temperature equivalence hypothesis may be determined most easily by taking the Laplace transform with respect to the reduced time in Eqs. (1.21) and (1.22). Substituting the relation between transforms of relaxation and creep functions

and the transforms of the corresponding differential operators, and finally inverting the resulting transforms results in the differential operator constitutive laws. These results are presented in [4] and [6] and are not repeated here since all subsequent discussion is based on integral laws.

2. Displacement Equations of Equilibrium.

The field equations for a thermorheologically simple material were presented in the previous section. In order to determine the stresses and displacements in the interior of a body when displacements or stresses are prescribed on its surface, it is desirable, when possible, to reduce the number of dependent variables. To this end, the strain-displacement relations are first substituted into the constitutive equations yielding,

$$s_j^i(x, t) = \int_0^t G_1(\xi - \xi') \frac{\partial}{\partial t'} \left\{ \frac{1}{2} [u_{,j}^i + g^{ik} u_{j,k}] - \frac{1}{3} \delta_j^i u_{,k}^k \right\} dt' \quad (2.1)$$

$$\sigma(x, t) = \int_0^t G_2(\xi - \xi') \frac{\partial}{\partial t'} \left\{ \frac{1}{3} u_{,k}^k - \alpha_o \theta \right\} dt'$$

Combining the deviatoric and spherical components of stress to obtain the components of the stress tensor in terms of the displacement components, we obtain

$$\tau_j^i = \int_0^t G_1(\xi - \xi') \frac{\partial}{\partial t'} \left\{ \frac{1}{2} [u_{,j}^i + g^{ik} u_{j,k}] - \frac{1}{3} \delta_j^i u_{,k}^k \right\} dt' \quad (2.2)$$

$$+ \frac{1}{3} \delta_j^i \int_0^t G_2(\xi - \xi') \frac{\partial}{\partial t'} [u_{,k}^k - 3\alpha_o \theta] dt'$$

Substituting the expression for stress into the equilibrium equation and assuming that the integration and differentiation may be interchanged, yields after regrouping terms,

$$\begin{aligned} & \int_0^t \left\{ \left[G_1(\xi - \xi') + 2G_2(\xi - \xi') \right] \frac{\partial}{\partial t'} (u_{,j}^i) + 3G_1(\xi - \xi') \frac{\partial}{\partial t'} (g^{ik} u_{j,k}) \right\}_{,i} dt' \\ & - 6 \int_0^t \left\{ G_2(\xi - \xi') \frac{\partial}{\partial t'} (\alpha_0 \theta) \right\}_{,j} dt' + 2 \int_0^t \left[(G_1(\xi - \xi') - G_2(\xi - \xi')) \right]_{,i} \frac{\partial}{\partial t'} (u_{,j}^i) dt' \\ & - 2 \int_0^t \left[G_1(\xi - \xi') - G_2(\xi - \xi') \right]_{,j} \frac{\partial}{\partial t'} (u_{,i}^j) dt' = 0 \end{aligned} \quad (2.3)$$

The covariant derivatives of the material properties will no longer vanish due to the non-homogeneity introduced by the variable temperature field; thus, the last two integrals include terms which do not exist in the homogeneous linear viscoelastic analysis which has been presented to date in the literature.

APPLICATIONS

3. Specialization for Axisymmetric Plane Strain of Infinite Cylinders.

For axisymmetric plane strain, the only non-zero displacement component is the radial component u^1 . Furthermore, the only variations in the radial displacement will be in the radial coordinate x^1 . Thus two of the displacement equations of equilibrium are satisfied identically and the third is given by

$$\int_0^t \left\{ \left[G_1(\xi - \xi') + 2G_2(\xi - \xi') \right] \frac{\partial}{\partial t'} (u^1_{,1}) + 3G_1(\xi - \xi') \frac{\partial}{\partial t'} (g^{ik} u_{1,k}) \right\}_{,1} dt' \\ - 6 \int_0^t \left\{ G_2(\xi - \xi') \frac{\partial}{\partial t'} (\alpha_0 \theta) \right\}_{,1} dt' = 0 \quad (3.1)$$

The evaluation of the covariant derivatives yields upon regrouping and expressing in terms of the contravariant displacement component,

$$\int_0^t \left(\frac{\partial}{\partial x^1} \left\{ \left[2G_1(\xi - \xi') + G_2(\xi - \xi') \right] \frac{\partial^2}{\partial t' \partial x^1} (u^1) \right\} \right. \\ + \left[2G_1(\xi - \xi') + G_2(\xi - \xi') \right] \frac{\partial^2}{\partial t' \partial x^1} \left(\frac{1}{x^1} u^1 \right) - 3 \frac{\partial}{\partial x^1} G_1(\xi - \xi') \frac{\partial}{\partial t'} \left(\frac{u^1}{x^1} \right) \\ \left. - 3 \frac{\partial}{\partial x^1} \left[G_2(\xi - \xi') \frac{\partial}{\partial t'} \alpha_0 \theta(t') \right] \right) dt' = 0 \quad (3.2)$$

The solution for u^1 proves to be very difficult since in general the variable coefficients are dependent upon the x^1 coordinate in a very complex manner. For this reason, we turn our attention to approximations which might give some significant results. The analysis to follow will pertain to instances in which the temperature is varying slowly enough that it can be assumed to be uniform throughout the entire cylinder. This forms one limit case to the analysis. The other limit, that of the temperature varying with radius but time independent has been investigated previously for cylinders

by Moreland and Lee [4]. The elastic-viscoelastic analogy is extended for the above two limit cases in [8]. The intermediate case where temperature varies in both space and time, while it may be the most important part of any analysis, remains for the present intractable.

4. Slowly Varying Uniform Temperature Fields.

For slowly varying temperatures independent of the spatial coordinates, the reduced time also becomes independent of the spatial coordinates and, consequently, we may write Eq. (3.1) in the simple form

$$\int_0^t \left\{ \left[2G_1(\xi - \xi') + G_2(\xi - \xi') \right] \frac{\partial}{\partial t'} u^i_{,il}(x, t') \right\} dt' = 0 \quad (4.1)$$

For which a solution exists when

$$u^i_{,il} = 0 \quad (4.2)$$

The evaluation of the covariant derivatives leads to

$$\frac{\partial u^1}{\partial x^1 \partial x^1} + \frac{1}{x^1} \frac{\partial u^1}{\partial x^1} - \frac{u^1}{x^1 x^1} = 0 \quad (4.3)$$

In the above instance, the contravariant radial displacement tensor component is the same as the physical component, hence we may write the above equation in the more familiar notation of u and r (for u^1 and x^1 respectively) as

$$\frac{\partial^2 u}{\partial r^2} + \frac{1}{r} \frac{\partial u}{\partial r} - \frac{u}{r^2} = 0 \quad (4.4)$$

for which the general integral is

$$u(r, t) = C_1(t) r + C_2(t) \frac{1}{r} \quad (4.5)$$

5. Infinite Cylinder Rigidly Encased.

Considering now an infinite cylinder with a stress-free inner boundary and fixed outer boundary (i.e., enclosed by a rigid case) where a and b are the inner and outer radii respectively the constants of integration will be evaluated from

$$\begin{aligned} u(b, t) &= 0 \\ \tau_1^1 &= \sigma_r(a, t) = 0 \end{aligned} \quad (5.1)$$

Satisfying the first boundary condition gives from Eq. (4.5)

$$C_2(t) = -b^2 C_1(t) \quad (5.2)$$

and hence

$$u^1(r, t) = u(r, t) = C_1(t) \left[r - \frac{b^2}{r} \right] = -C_1(t) \left[\frac{b^2 - r^2}{r} \right] \quad (5.3)$$

Upon noting that for $r = a$,

$$u_{,k}^k = \frac{\partial u}{\partial r} + \frac{u}{r} = 2C_1(t)$$

and

(5.4)

$$u_{,1}^1 = g^{1k} u_{1,k} = \frac{\partial u}{\partial r} = C_1(t) \left[1 + \frac{b^2}{a^2} \right]$$

The second boundary condition yields, upon using Eq. (2.2),

$$\sigma_r(a, t) = 0 = \int_0^t \left\{ G_1(\xi - \xi') \frac{\partial}{\partial t'} \left[C_1(t') \left(1 + \frac{b^2}{a^2} \right) - \frac{2}{3} C_1(t') \right] \right. \\ \left. + \frac{1}{3} G_2(\xi - \xi') \frac{\partial}{\partial t'} \left[2C_1(t') - 3\alpha_0 \theta(t') \right] \right\} dt' \quad (5.5)$$

or

$$\int_0^t \left[\left\{ a^2 \left[G_1(\xi - \xi') + 2G_2(\xi - \xi') \right] + 3b^2 G_1(\xi - \xi') \right\} \frac{\partial}{\partial t'} (C_1(t')) \right. \\ \left. - 3a^2 G_2(\xi - \xi') \frac{\partial}{\partial t'} (\alpha_0 \theta(t')) \right] dt' = 0 \quad (5.6)$$

Subjecting $C_1(t)$ and $\theta(t)$ to the transformation Eq. (1.18) and taking the Laplace transform⁺ yields

$$\hat{C}_1^* = \frac{3a^2 G_2^* \alpha_0 \hat{\theta}^*}{a^2 (G_1^* + 2G_2^*) + 3b^2 G_1^*} \quad (5.7)$$

⁺ An asterisk denotes the Laplace transform of the function with respect to the reduced time.

If the ratio of radii is defined as

$$c = \frac{b}{a} , \quad (5.8)$$

then after representing the functional dependence of the material properties by

$$pR^*(p) = \frac{G_2^*}{(G_1^* + 2G_2^*) + 3c^2 G_1^*} , \quad (5.9)$$

$R(\xi)$ may be determined by clearing fractions and inverting using the convolution integral. Thus, $R(\xi)$ is given by

$$\int_0^\xi R(\xi') \frac{\partial}{\partial (\xi - \xi')} \left[(1 + 3c^2) G_1(\xi - \xi') + 2G_2(\xi - \xi') \right] d\xi' = G_2(\xi) \quad (5.10)$$

Now, the formal inversion of the problem may be performed, yielding

$$C_1(t) = 3 \int_0^t R(\xi - \xi') \frac{\partial}{\partial t'} (\alpha_0 \theta(t')) dt' \quad (5.11)$$

Numerical inversions of similar functions are given in [2], [6], and [7]. Finally we may write

$$u(r, t) = - 3 \left(\frac{b^2 - r^2}{r} \right) \int_0^t R(\xi - \xi') \frac{\partial}{\partial t'} (\alpha_0 \theta(t')) dt' \quad (5.12)$$

where $R(\xi)$ is defined by Eq. 5.10.

By combining Eq. (5.7) and the transform of Eq. (5.3) and clearing fractions before inversion we may write the solution in a different form, one which will not require the evaluation of $R(\xi)$:

$$\begin{aligned} & \int_0^t \frac{\partial}{\partial t'} \left\{ \left[G_1(\xi - \xi') + 2G_2(\xi - \xi') \right] + 3c^2 G_1(\xi - \xi') \right\} u(r, t') dt' \\ & = - 3 \left(\frac{b^2 - r^2}{r} \right) \int_0^t \frac{\partial}{\partial t'} \left[G_2(\xi - \xi') \right] \alpha_0 \theta(t') dt' \end{aligned} \quad (5.13)$$

The above expression is a Volterra integral equation, for which numerical solution techniques exist, one of which will be discussed subsequently.

The solution of the corresponding thermoelasticity problem is

$$u(r, t) = - \left(\frac{b^2 - r^2}{r} \right) \frac{(1 + \nu) \alpha_0 \theta(t)}{1 + (1 - 2\nu) c^2} \quad (5.14)$$

Thus, the solution is observed to be dependent only upon Poisson's ratio. It is easily verified that the material properties of the thermoviscoelastic problems also occur in combinations such that the solution is dependent only upon the time dependent Poisson's ratio. Since data available on the time and temperature dependence of Poisson's ratio are limited, it appears to be preferable to express the solution in terms of the extension modulus E and the bulk modulus K , quantities for which data are more readily available. If it is assumed that the volumetric behavior is purely elastic

and, hence, time independent, Eq. (5.13) may be modified so that the material properties G_1 and G_2 are expressed in terms of E and K , the extension modulus and bulk modulus respectively. After performing this modification and also removing the discontinuities in the integrals at times 0 and t , the time dependence of $u(r, t)$ is determined by solving the non-homogeneous Volterra equation of the second kind:

$$\begin{aligned} & \left(1 + \frac{c^2 E_G}{3K}\right) u(r, t) - \frac{c^2}{3K} \int_{0^+}^{t^-} \frac{\partial}{\partial t'} \left[E(\xi - \xi') \right] u(r, t') dt' \\ &= - \frac{3}{2} \left(\frac{b^2 - r^2}{r} \right) \left[\left(1 - \frac{E_G}{9K}\right) \alpha_0 \theta(t) + \frac{1}{9K} \int_{0^+}^{t^-} \frac{\partial}{\partial t'} \left[E(\xi - \xi') \right] \alpha_0 \theta(t') dt' \right] \end{aligned} \quad (5.15)$$

where E_G is the initial or glassy modulus. A common technique for solving Volterra equations is through the use of the Laplace transform; in the above example this requires a functional knowledge of E . However, if a numerical scheme of integration is introduced, the measured data are sufficient to determine the behavior of the system. Lee and Rogers [2] have proposed a finite difference solution which may be used. The time interval of interest is divided into n increments t_i , $i = 1, 2, \dots, n+1$, with $t_1 = 0$ and $t_{n+1} = t$ (the reduced time is also divided into n intervals ξ_i , $i = 1, 2, \dots, n+1$). As will be shown, the increments need not be the same over each interval. The integrals with limits 0^+ to t^- are also separated into n intervals

$$\int_{0^+}^{t^-} \left[\quad \right] dt' = \sum_{i=1}^n \int_{t_i}^{t_{i+1}} \left[\quad \right] dt'$$

The solution to the example problem now takes the form

$$(1 + \frac{c^2 E_G}{3K}) u(r, t_{n+1}) = \frac{c^2}{3K} \sum_{i=1}^n \int_{t_i}^{t_{i+1}} \frac{\partial}{\partial t'} \left[E(\xi_{n+1} - \xi') \right] u(r, t') dt' \quad (5.16)$$

$$- \frac{3}{2} \left(\frac{b^2 - r^2}{r} \right) \left[\left(1 - \frac{E_G}{9K} \right) \alpha_o \theta(t_{n+1}) + \frac{1}{9K} \sum_{i=1}^n \int_{t_i}^{t_{i+1}} \frac{\partial}{\partial t'} \left[E(\xi_{n+1} - \xi') \right] \alpha_o \theta(t') dt' \right]$$

If the functions $u(r, t')$ and $\theta(t')$ occurring under the integrals are approximated by

$$u(r, t') = \frac{1}{2} \left[u(r, t_{i+1}) + u(r, t_i) \right] \quad t_i < t' < t_{i+1} \quad (5.17)$$

$$\theta(t') = \frac{1}{2} \left[\theta(t_{i+1}) + \theta(t_i) \right]$$

the integrals may be evaluated, and lead to the result

$$\begin{aligned} (1 + \frac{c^2 E_G}{3K}) u(r, t_{n+1}) &\approx \frac{c^2}{3K} \sum_{i=1}^n \frac{1}{2} \left[u(r, t_{i+1}) + u(r, t_i) \right] \left[E(\xi_{n+1} - \xi_{i+1}) \right. \\ &- E(\xi_{n+1} - \xi_i) \left. \right] - \frac{3}{2} \left(\frac{b^2 - r^2}{r} \right) \left\{ \left(1 - \frac{E_G}{9K} \right) \alpha_o \theta(t_{n+1}) + \frac{1}{2} \alpha_o \left[\theta(t_{i+1}) \right. \right. \\ &+ \theta(t_i) \left. \right] \left[E(\xi_{n+1} - \xi_{i+1}) - E(\xi_{n+1} - \xi_i) \right] \left. \right\} \quad (5.18) \end{aligned}$$

The terms in this approximation occur in a form such that the error propagation is quickly attenuated. Using this intuitive argument, it may be anticipated that the above representation will be stable. The above simple formulation introduces no complications when the intervals $t_{i+1} - t_i$ (or $\xi_{i+1} - \xi_i$) are varied. This may not be the case if more elaborate difference schemes are introduced.

The fact that an initial value problem has now replaced the original boundary value problem enhances the solution technique since the value at each succeeding time interval is dependent only on the preceding times and not on later ones as might be the case in other boundary value problems. The solution is now in a form for which the digital computer may be used to perform the final numerical steps. Some examples of the solution method are discussed [2].

6. Numerical Solutions of Infinite Cylinder Rigidly Encased.

A numerical analysis has been performed for two uniform temperature fields. The cylinder analyzed has a radii ratio $c = 4$. The bulk modulus was selected as 74,600 psi, the coefficient of thermal expansion $\alpha_0 = 6 \times 10^{-5}/^{\circ}\text{F}$ and the extension relaxation function and shift function as shown in Fig. 1.

First the problem in which the temperature is suddenly dropped 80°F at all points of the cylinder is investigated. Physically, this requires the cylinder to have a distributed sink such that heat may be instantaneously dissipated. However, the solution to this hypothetical problem may be utilized for the solution of other physically important problems. The solution has been carried out using Eq. (5.18); the time history of the inner boundary tangential strain $\frac{u}{a}$ is shown in Fig. 2. In addition the method of solution presented by Eqs. (5.9), (5.11), and (5.12) was carried out. After expressing

Eq. (5.9) in terms of the extension and bulk moduli, the first step in this solution is to perform the inversion. This may be performed by expressing the modified Eq. (5.9) as a convolution integral and using the finite difference technique of numerical integration. The functional dependence of $R(\xi)$ is shown in Fig. 3. For the constant uniform temperature field Eq. (5.12) may be integrated to yield

$$u(r,t) = - 3\left(\frac{b^2 - r^2}{r}\right)R(\xi)\alpha_0\theta \quad (6.1)$$

where θ represents the constant uniform temperature change.

For a temperature drop of 80°F and the properties of the cylinder cited previously, the inner boundary tangential strain is again as shown in Fig. 2. From Eq. (6.1), one observes that a constant uniform temperature drop may be used to generate the function $R(\xi)$.

The second example investigated is the slow temperature decrease of the rigidly encased cylinder used in the first example. The dependence of ξ upon t for a uniform cooling of 2°F/100 min. was determined from Eq. (1.15) and is shown in Fig. 4. The solution of Eq. (5.18) for this temperature decrease is shown in Fig. 5. The initial departure of the strain from a straight line is due to the crude time intervals selected for desk calculator computation. Using the kernel function $R(\xi)$ in Eq. (5.12), the solution was repeated, yielding again the results shown in Fig. 5. Once the function $R(\xi)$ is known the determination of the circumferential strain history requires the evaluation of the single integral which appears in Eq. (5.12). Thus, using this method, it appears to be easier to obtain solutions for various uniform temperature variations.

While the above calculations are for a cylindrical inner boundary, appropriate strain concentration factors may be used to approximate the maximum strain for different shaped inner configurations, utilizing information in [8], since the material is homogeneous.

7. Infinite Cylinder Bonded to a Thin Elastic Case.

We next turn our attention to an infinite cylinder bonded to a thin elastic case. Designating the displacement, stresses, and the temperature in the cylinder with subscript I's and those of the case by II's, the mechanical properties of the elastic case are specified by E_{II} , ν_{II} , and α_{II} ; its thickness by h , where it is assumed that $h/b \ll 1$; and its uniform temperature $\theta_{II}(t)$. The temperature of the case is allowed to differ from that of the cylinder since in many instances the temperature surrounding the system may drop suddenly, so that initially the case is at one temperature the cylinder at essentially another. This instance may prove to be one of particular interest in studying bond failures between the case and cylinder.

The boundary conditions are given by a stress free inner boundary

$$\sigma_{rI}(a, t) = 0 \quad (7.1)$$

and the continuity conditions at the interface

$$\sigma_{rI}(b, t) = \sigma_{rII}(b, t) \quad (7.2)$$

$$u_I(b, t) = u_{II}(b, t)$$

The general integral for u_I is given, as in the previous section, by Eq. (4.5). For a thin case, the solution for the displacement of an infinite case is

$$u_{II}(b, t) = -\left(\frac{1-\nu_{II}^2}{E_{II}}\right) \frac{b^2}{h} \sigma_{rII}(b, t) + (1+\nu_{II}) b \alpha_{II} \theta_{II}(t) \quad (7.3)$$

Satisfying the boundary conditions in an analogous manner as presented in the previous section and expressing the solution in terms of $E_I(t)$ and K_I , the displacement at the inner boundary of the cylinder is determined from

$$\begin{aligned} & 162 \frac{h}{b} \left(\frac{b^2}{b^2 - a^2} \right) \frac{E_{II} K_I^2}{(1+\nu_{II})} \frac{u_I(t)}{a} + 108 (1-\nu_{II}) K_I^2 \int_0^t \frac{\partial}{\partial t'} \left[E_I(\xi - \xi') \right] \frac{u_I(t')}{a} dt' \\ & + \frac{2h}{b} \left(\frac{b^2}{b^2 - a^2} \right) \frac{E_{II}}{1+\nu_{II}} \int_0^t \frac{\partial}{\partial t'} \left[\int_0^{t'} \frac{\partial}{\partial t''} (E_I(\xi'')) E_I(\xi - \xi' - \xi'') dt'' \right] \frac{u_I(t')}{a} dt' \\ & = - 81 \frac{h}{b} \left(\frac{E_{II}}{1+\nu_{II}} \right) K_I^2 \left[3 \alpha_{OI} \theta_I(t) - 2 (1+\nu_{II}) \left(\frac{b^2}{b^2 - a^2} \right) \alpha_{II} \theta_{II}(t) \right] \\ & + 18 K_I \int_0^t \frac{\partial}{\partial t'} E_I(\xi - \xi') \left\{ \left[9 K_I (1-\nu_{II}) - 3 \frac{h}{b} \right] \alpha_{OI} \theta_I(t') \right. \\ & \left. - 2 (1+\nu_{II}) \frac{h}{b} \left(\frac{E_{II}}{1+\nu_{II}} \right) \left(\frac{b^2}{b^2 - a^2} \right) \alpha_{II} \theta_{II}(t') \right\} dt' \quad (7.4) \end{aligned}$$

(Continued)

$$\begin{aligned}
 & -3 \int_0^t \frac{\partial}{\partial t'} \left(\int_0^{t'} \frac{\partial}{\partial t''} (E_I(\xi'')) E_I(\xi - \xi' - \xi'') dt'' \right) \left\{ \left[6K_I(1+v_{II}) \right. \right. \\
 & \left. \left. -2 \frac{h}{b} \left(\frac{E_{II}}{1+v_{II}} \right) \right] \alpha_{OI} \theta_I(t') - 2(1+v_{II}) \frac{h}{b} \left(\frac{E_{II}}{1+v_{II}} \right) \left(\frac{b^2}{b^2 - a^2} \right) \alpha_{II} \theta_{II}(t') \right\} dt'
 \end{aligned}
 \tag{7.4}$$

continued

A solution to this equation may be obtained by employing the finite difference technique of the preceding section.

REFERENCES

1. Schwarzl, F. and Staverman, A.J., "Time-temperature Dependence of Linear Viscoelastic Behavior," J. Appl. Phys., 23, 838-843, 1952.
2. Lee, E. H. and Rogers, T.G., "Solution of Viscoelastic Stress Analysis Problems Using Measured Creep or Relaxation Functions," Div. Appl. Math. Report DA-G-54/1, Brown University, 1961.
3. Gross, B., Mathematical Structure of the Theories of Viscoelasticity, Hermann and Cie, Paris, 1953.
4. Moreland, L.W. and Lee, E.H., "Stress Analyses for Viscoelastic Materials with Temperature Variation," Trans. Soc. of Rheology, 4, 233-263, 1960.
5. Sokolnikoff, I.S., Tensor Analysis, John Wiley & Sons, New York, 1951.
6. Muki, R. and Sternberg, E., "On Transient Thermal Stresses in Viscoelastic Materials with Temperature Dependent Properties," J. Appl. Mech., 28, 2, June 1961.
7. Schapery, R.A. "Two Simple Approximate Methods of Laplace Transform Inversion for Viscoelastic Stress Analyses," Calif. Inst. of Technology, GALCIT SM 61-23, November 1961.
8. Hilton, H.H. and Russell, H. G., "An Extension of Alfrey's Analogy to Thermal Stress Problems in Temperature Dependent Linear Viscoelastic Media," J. Mech. and Phys. of Solids, 9, April 1961.

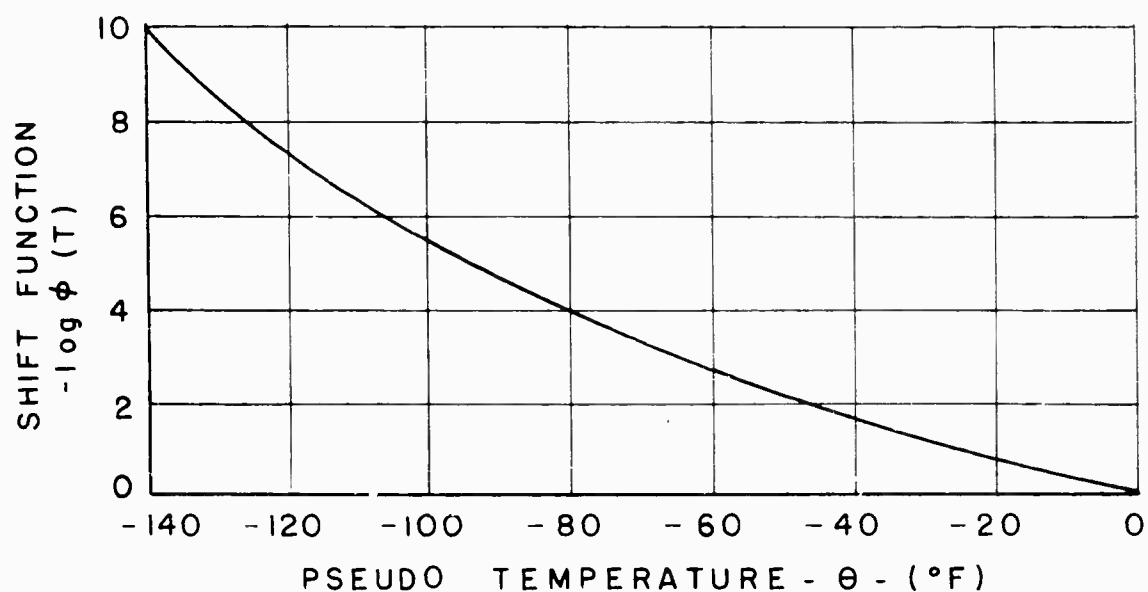
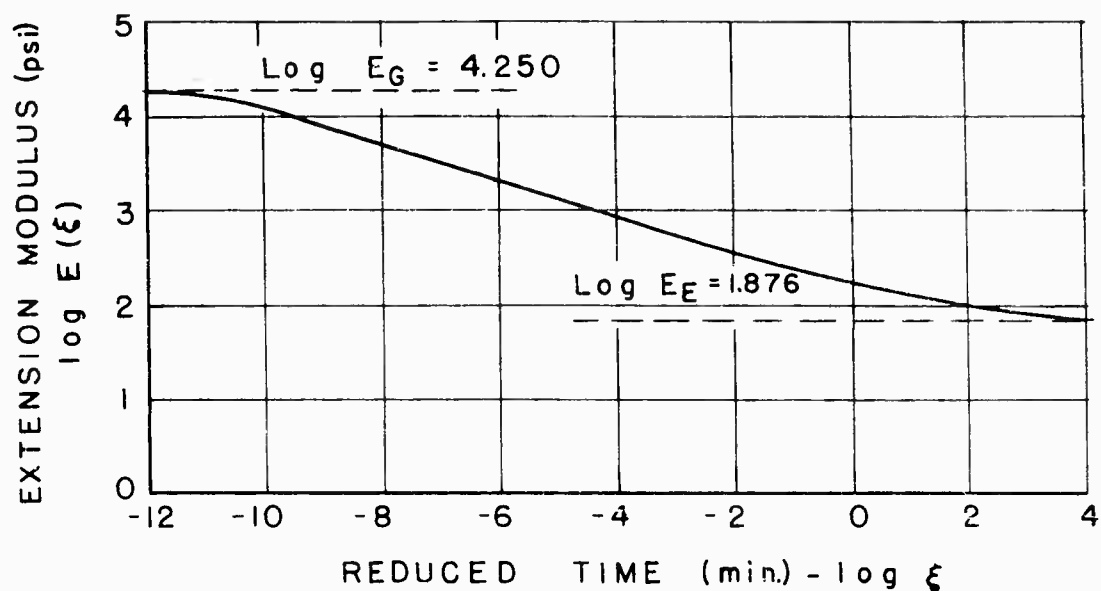


FIG. 1. - THERMOMECHANICAL TIME HISTORY FOR VISCOELASTIC MATERIAL OF EXAMPLE PROBLEMS, REFERENCE TEMPERATURE 77°F.

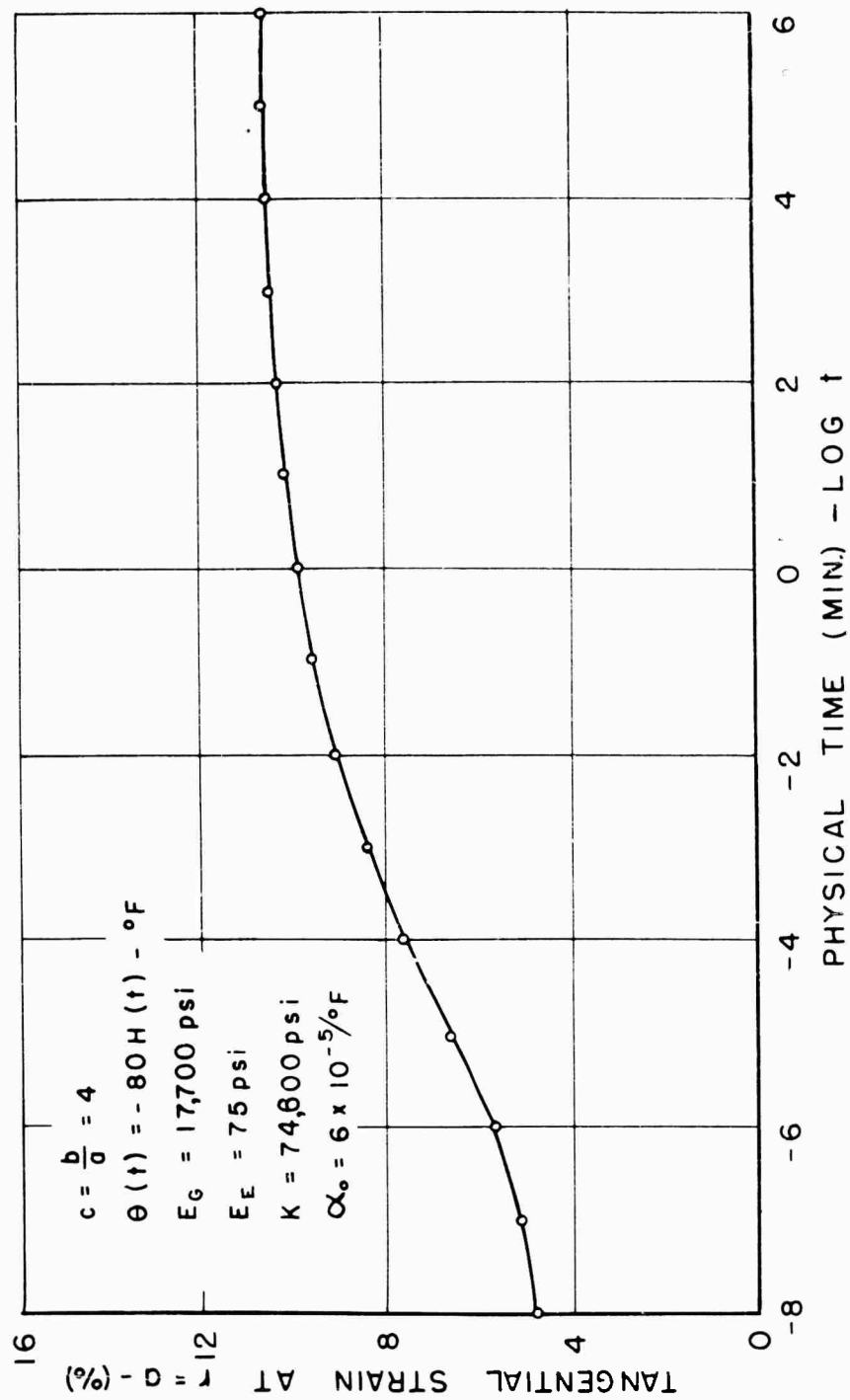


FIG. 2. TANGENTIAL STRAIN TIME HISTORY FOR A
 CYLINDER SUBJECTED TO A CONSTANT
 TEMPERATURE DECREASE AT $t = 0$

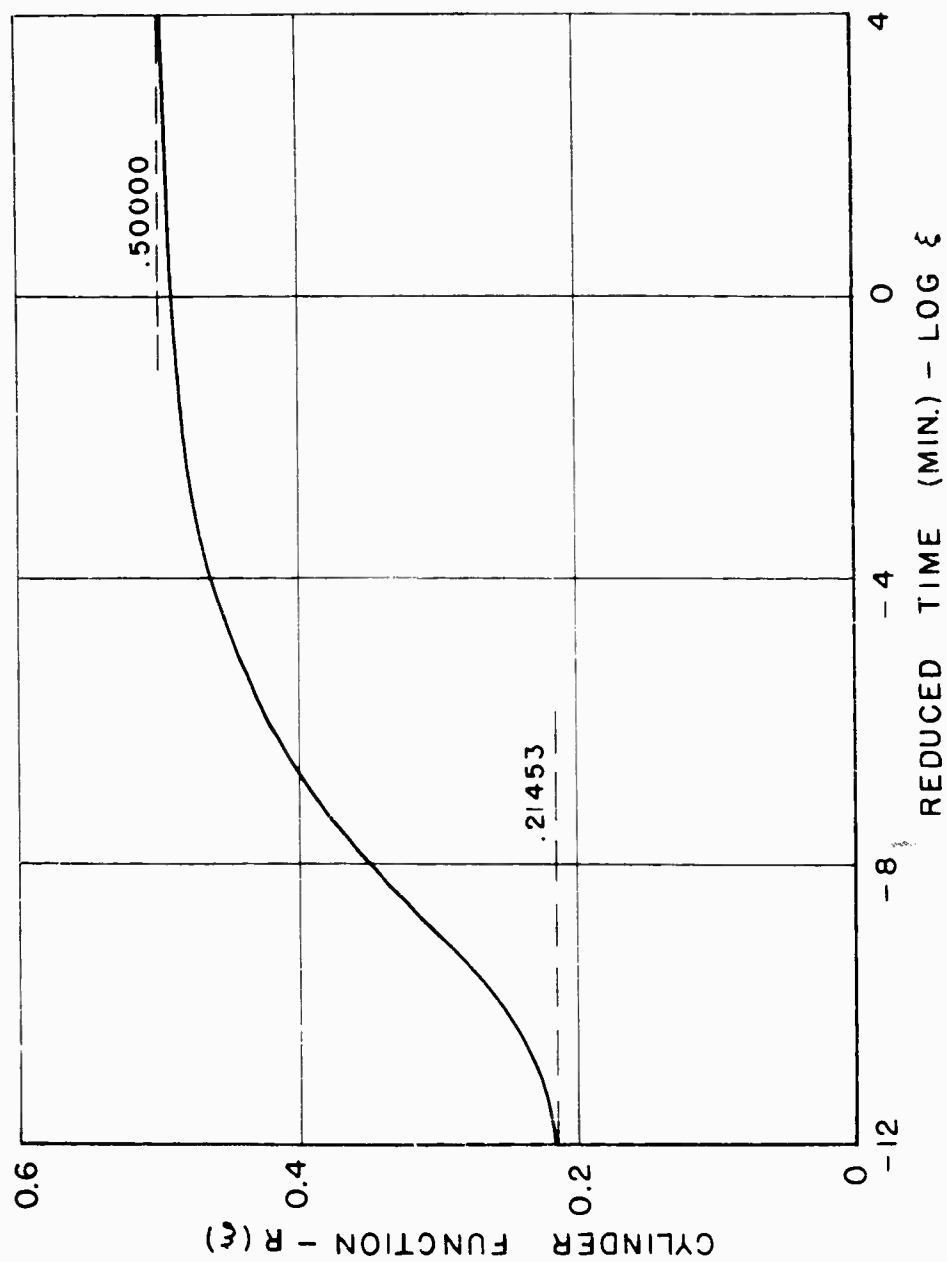


FIG. 3. CYLINDER FUNCTION FOR EQ. 5.12, $c = 4$

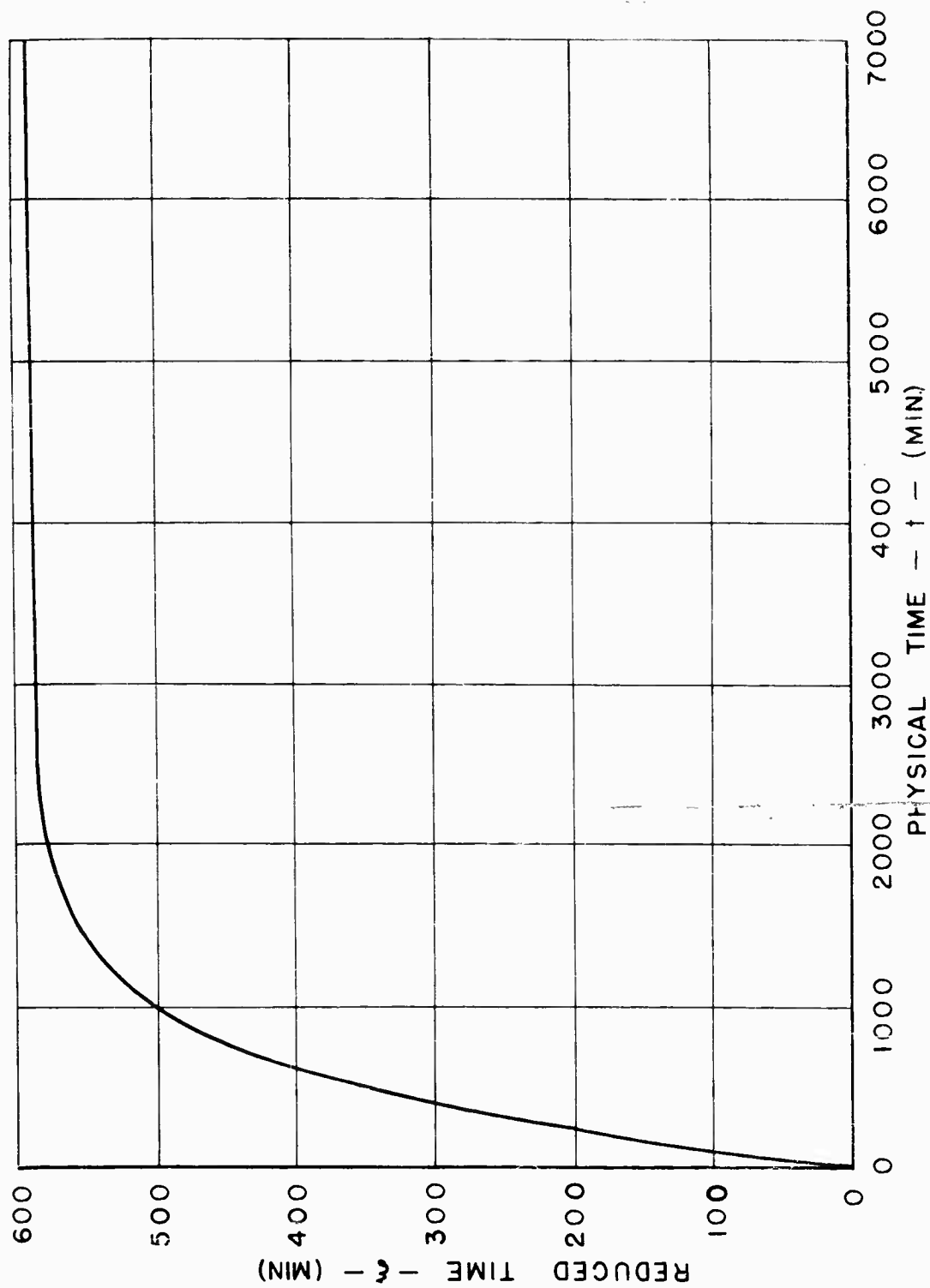


FIG 4. REDUCED TIME VS. PHYSICAL TIME FOR UNIFORM COOLING OF 2°F MIN AND SHIFT FUNCTION IN FIG. 1.

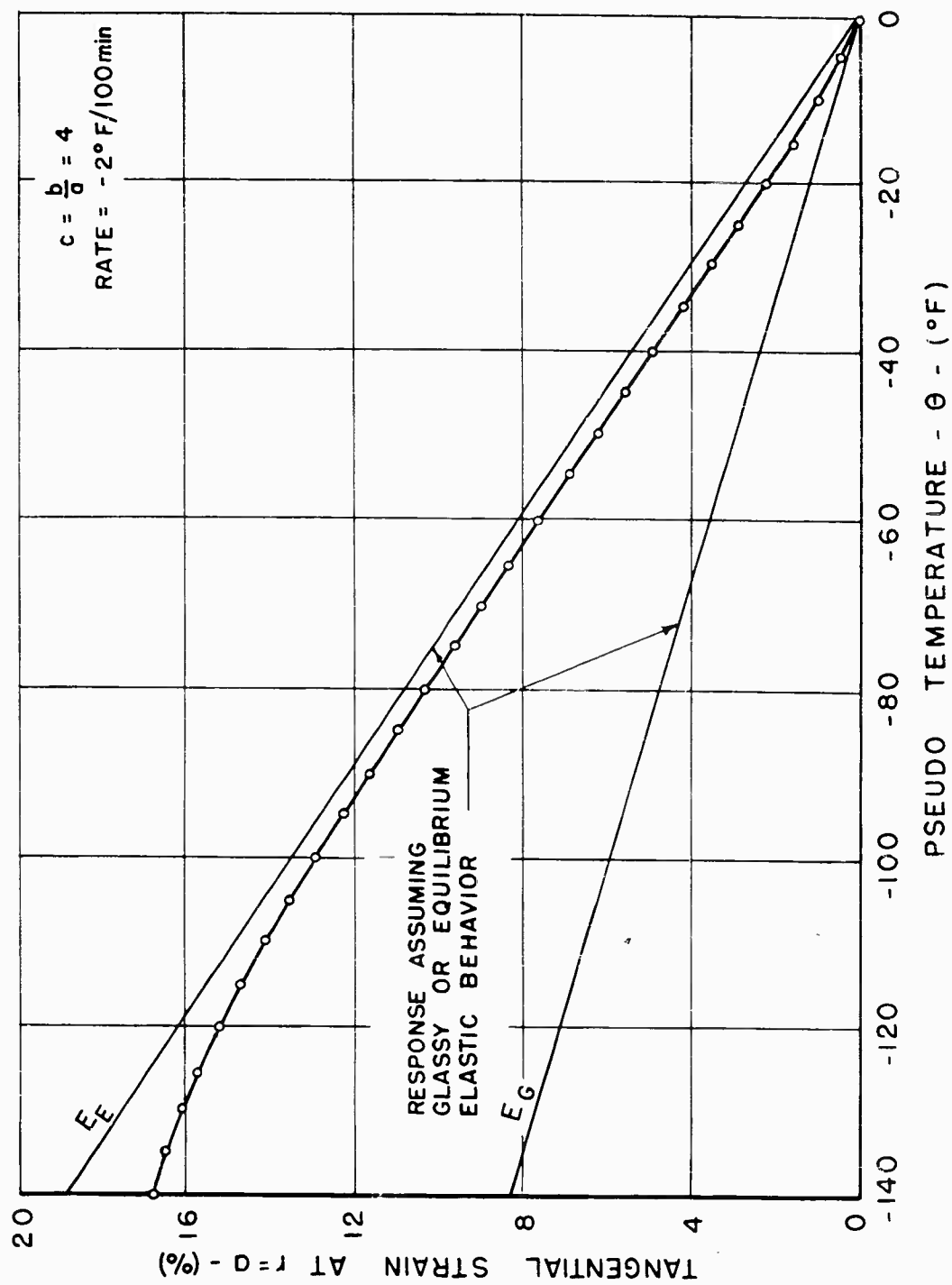


FIG. 5. — UNIFORM COOLING OF A THICK WALL CYLINDER

APPENDIX G

INVESTIGATION OF THE FAILURE OF SOLID FUELS
UNDER COMBINED STRESSES

by

G. S. Leon and F. A. McClintock
Department of Mechanical Engineering
Massachusetts Institute of Technology

Investigation of the Failure of Solid Fuels

Under Combined Stresses

I. Introduction

Everyone is agreed that understanding the failure of rubber filled with hard particles, specifically solid fuels, is important for rocket design. However, it is unlikely that anyone at this stage can specifically state the processes occurring during deformation and what particular stage constitutes failure.

To illustrate these points, the observed behavior of a tensile specimen of filled rubber can be used. The first noticeable change in property is a gradual decrease in the stiffness which is not recoverable unless the load is removed and time is allowed for the damage to heal.^{1*} It is possible, then, that a limiting value of stiffness might be considered as failure if the grain is expected to help the rocket case carry the internal loads. This decrease in stiffness results from a progressive unbonding of the particles and the rubber, creating voids in the material. This process is observed by the accompanying change in density of the material. Possibly a limiting value of porosity or increase in volume might be considered as a failure. For instance, an increase in porosity would increase the linear burning rate for a constant mass burning rate. This might lead to failure if a local band of high porosity material surrounded by bonded material permitted burning to penetrate into this band at a faster linear rate. The voids tend to agglomerate and regions of highly separated material become evident as the load on the specimen is increased. A maximum load is

* Superscripts refer to references at the back.

generally observed in uniaxial tension which must correspond to an instability. One particular cross-sectional region of the specimen undergoes very great local deformations and finally fractures. This peak load can certainly be considered as failure, particularly if the surrounding material makes the region unstable so that fracture follows without appreciable change in macroscopic deformation. From this discussion we can see that failure may mean a decrease in stiffness, an increase in volume, and instability and localization of deformation or complete fracture.

To gain insight into these phenomena, the aim of this investigation has been to develop a model analytically which would reproduce the behavior of the filled rubber in terms of the elastic properties of the rubber, the bonding strength between rubber and filler, and the amount of filler present. Along with this, experimental work is planned to help in the evaluation of such a model. It is hoped that even if only qualitatively, the model may point out the principal variables and if possible give a first approximation of behavior of the composite materials in terms of the variables just mentioned.

The advantage of having such a model can be illustrated by two samples. As a guide for designing composite materials, if the bond strength is high we can expect the stiffness to be maintained up to high values of stress but with accompanying small fracture strain (based on gage length). If elongation is desired but high strength is not essential, then a lower value of bond strength would be desirable. This effect can be seen from the data presented in Fig. 4 of Reference 1 which is shown schematically in Fig. 1. If a particular grain design is being analyzed and the stress and strain conditions at the root of the star are known, it should be possible to predict the order of magnitude of volume increase and the stability of

the region for crack formation. This would certainly be important for proper burning.

In the sections that follow the current state of the analysis in this investigation of failure is presented along with a discussion on the work that is necessary for its development. The status of the experimented work is also summarized.

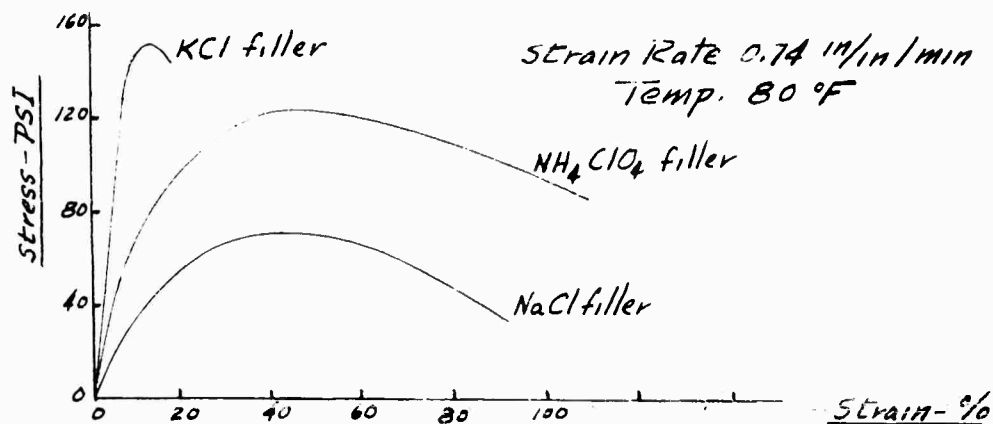


Fig. 1 Comparison on the Effect of Filler Upon the Mechanical Properties of a Polyurethane Propellant

II Summary of Analysis

To facilitate the presentation of this material, the resulting equations and general approach are presented in this section and the derivation of the equations is paralleled in the Appendix. This will permit understanding of the discussion which follows without having to be familiar with the detailed analysis.

This summary is presented in sections including the analysis of stress and strain between adjacent particles, the combination of particles into an orderly array, consideration of the disorder of the array on the bulk properties, and finally the effects of unbonding on the properties during a tensile test. Similar sections in the Appendix can be referred to for depth in detail.

A. Conditions Between Adjacent Particles

In considering the behavior of filled polymers it was first recognized that the critical regions for stiffness and failure were the ligaments of binder connecting the filler particles as shown in

Fig. 2. Regions of this type were represented by two spheres connected

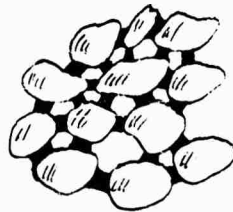


Fig. 2 Schematic of filled polymer showing ligaments

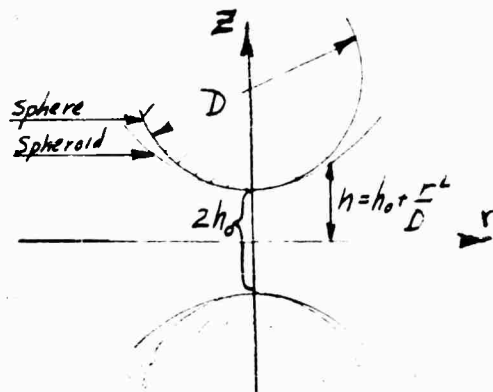


Fig. 3 Model for ligaments.

by the rubber. Since the critical region lies where the spheres are closest to each other, the significant terms of the expanded expression for the spherical surfaces were used. The resulting surface is a paraboloid of revolution as shown schematically in Fig. 3. The stress and strain conditions in this region were analyzed for a direct separation and for a shear displacement of the spheres. For each case, upper and lower bounds on the stiffness were found as well as a simple strength-of-materials solution. Because these solutions are close, (see Appendix, Fig. A-5, particularly as the

initial separation of the spheres approaches zero where they all converge, the use of the simple solution was justified. This is particularly true because most of the interest is in highly filled materials with the particles very close to each other.

For separation, the most significant stress is the hydrostatic component along the surface of the sphere which at the center is given by Eq. 1.

This relation is expressed in terms of the Young's modulus of the binder (where for a Poisson ration of 0.5, $3G = E$), the relative displacement $2W_0$ and the separation ratio $f = 2h_0/D$. This last term is important because it permits relating initial separation to volume density for any given arrangement of spheres.

$$P = - \frac{E W_0}{2 D} \left[\frac{(1+f)}{f^2(1+4f)} \right] \quad (1)$$

For shear, the most important stress is shear along the surface which is generally of a lower order of magnitude than the hydrostatic stress and not as likely to result in a pull-away.

3. Array of Particles- Elastic Constants of Filled Rubber Before Unbonding

The next step in the analysis was to group the spheres in some fashion to get the stiffness and stress conditions in terms of macroscopic scale- that is, for a sample of material containing many spheres. Two arrangements of spheres were investigated. First, to reduce complication and in the hope that the resulting model might adequately represent experimental evidence, a simple cubic array was used. Later, because the simple cubic array proved too crude, a face-centered cubic array was analyzed. The simple cubic array can have a maximum volume fraction of only 0.52 with only six nearest neighbors per sphere while the face-centered cubic can give a maximum 0.74 volume fraction of spheres which is close to or lighter than the packings used in solid fuels. This most densely packed arrangement also results in twelve nearest neighbors per sphere.

To compute the Young's modulus of a simple cubic array of hard spheres bonded to a rubbery matrix, the strain energy contribution for the different ligaments was added to a nominal strain energy contribution for the interstitial matrix for tension along a cube axis. This yielded the following expression:

$$\bar{E}_c^b = E \left\{ \left[\frac{3\pi}{16f(1+f)(1+4f)^2} \right] + \left[\frac{(0.293+f)^2}{(1+f)^2} + \frac{1.41(0.293+f)}{(1+f)(0.500+f)} + \frac{0.111}{(1+f)(0.293+f)} \right] \right\} \quad (2)$$

The second term in Eq. 2 relates to the interstitial volume and is very small for small values of relative separation, f , or for highly filled rubbers.

A similar expression for the face centered cubic array is given by Eq. 3 where the interstitial contribution is neglected:

$$\bar{E}_c^b = E \left\{ \left[\frac{\pi}{16\sqrt{2}f(1+f)(1+8f)} \right] \left[\frac{\{15+28f(1+8f)^2 \ln(\frac{1+8f}{8f})\} \{3+4f(1+8f)^2 \ln(\frac{1+8f}{8f})\}}{\{6+4f(1+8f)^2 \ln(\frac{1+8f}{8f})\}} \right] \right\} \quad (3)$$

Numerical comparison of the two expressions seems to indicate similar stiffnesses for the two arrays. It is only in comparing the shear moduli for the two arrays and, particularly, the averaged moduli that the differences become apparent.

Similar approaches were used for determining the shear moduli in the cube orientation for the two arrays. The simple cubic array gives:

$$\bar{G}_c^b = \frac{E}{3} \left\{ \left[\frac{\pi}{4(1+f)} \ln\left(\frac{1+4f}{4f}\right) \right] + \left[\frac{(0.293+f)^2}{(1+f)^2} + \frac{(0.293+f)}{(1+f)} \ln\left(\frac{1+f}{0.293+f}\right) + \frac{0.553}{(1+f)} \right] \right\} \quad (4)$$

where again the second term is for the interstitial volume. Since the only contribution to resisting shearing of the cube from the ligaments is from the shear of the ligaments since the ligaments are relatively soft in shear, the shear modulus in the simple cubic array is very small compared to the Young's modulus.

This is not the case for the shear modulus of the face-centered array in the cube orientation where shear of the cube involves separation as well as shear of the ligaments. The resulting shear modulus for this denser array is given below, again not including the interstitial contribution which is negligible:

$$\bar{G}_c^b = \frac{E}{3} \left\{ \left[\frac{\pi}{4\sqrt{2} f(1+f)(1+8f)} \right] \left[3 + 4f(1+8f)^2 \ln\left(\frac{1+8f}{8f}\right) \right] \right\} \quad (5)$$

C. Randomness of Orientation of the Array of Particles- Average Elastic Constants.

The values obtained in the previous section apply only to the bonded material (superscript b) and, since the spheres are rigid and the binder has a Poisson ratio of 1/2, the Poisson ratio of the composite must also be 1/2. However, the material is not isotropic since the required conditions for isotropy, $\bar{G}_c^b = \bar{E}_c^b/3$ is not satisfied by either array.

For both arrays the material has cubic symmetry for the elastic properties (superscript c referring to the cube axes) but if oriented in any direction other than a cube axis, a different set of elastic constants would have to be specified. The elastic constants in any direction relative to the cube axes can be found by a simple transformation procedure. The variation in \bar{E}^b is shown in Fig. 4. From this it is apparent that the f.c.c. array is very close to being isotropic.

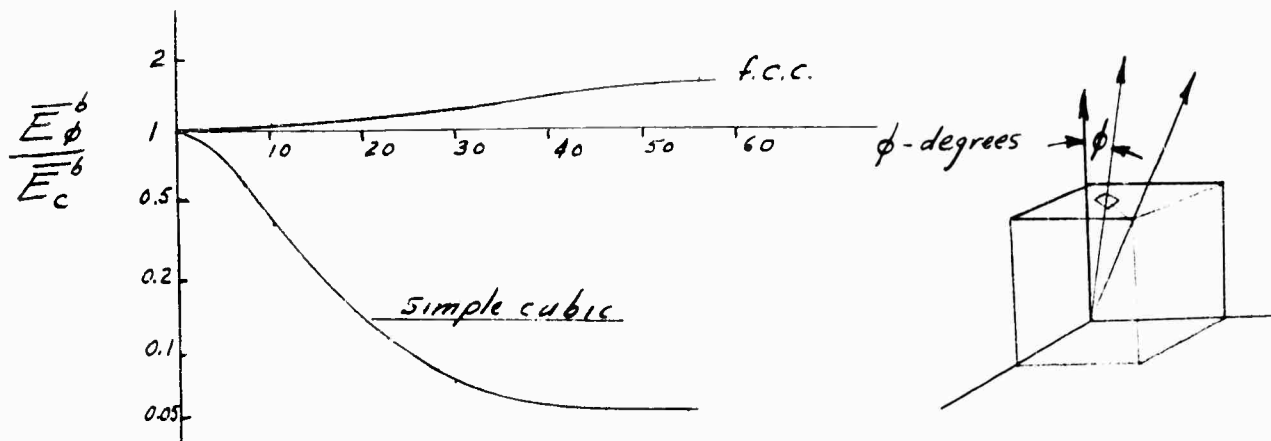


Fig. 4 Variation of Elastic Constants
With Orientation as Shown for $f = .01$

In a large piece of material we cannot expect the spheres to take up an orderly array. More likely there will be variations in the spacing. Even if the spacing were fairly uniform, regions would be found in which the clustered spheres would form cubic arrays oriented in every possible way. To find elastic constants for such a material requires an averaging of the elastic constants for all orientations of the cube. An exact solution to this problem is practically not possible, but upper and lower bounds can be found. The upper bound requires that all the elements undergo the same strain while the lower bound requires all elements to have the same stress. Strain energy obtained in each case is used to find the bounds of the average elastic constants. Naturally, each case violates either continuity of equilibrium and therefore is only approximate.

Solution of this problem for both arrays, since they both have cubic symmetry, yields:

$$\bar{E}_{upper\ bound}^b = 0.400 \bar{E}_c^b + 1.80 \bar{G}_c^b \quad (6)$$

$$\bar{E}_{lower\ bound}^b = \frac{\bar{E}_c^b \bar{G}_c^b}{0.400 \bar{G}_c^b + 0.200 \bar{E}_c^b} \quad (7)$$

The more closely the material satisfies the conditions of isotropy, the closer will be the bounds as shown in Fig. 5.

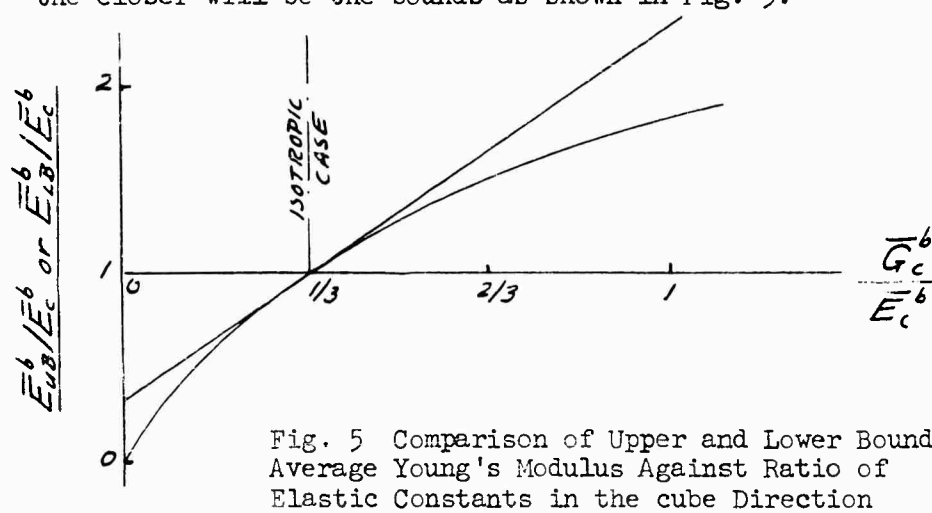


Fig. 5 Comparison of Upper and Lower Bound Average Young's Modulus Against Ratio of Elastic Constants in the cube Direction

The density can be expressed in terms of the volume ratio for either packing:

$$\begin{aligned} \frac{V_{\text{spheres}}}{V_{\text{total}}} &= \frac{0.524}{(1+f)^3} && \text{simple cubic} \\ &= \frac{0.740}{(1+f)^3} && \text{face centered cubic} \end{aligned} \quad (8)$$

This relation can be used to compare the averaged Young's modulus as found from the cube constants and the bounding relations (Eq. 6 and 7) in terms of the volume density. A better comparison is in terms of the relative volume density, that is the ratio of the actual to the maximum density for a given packing, which is the same for both packings.

$$\frac{V_{\text{spheres}}}{V_{\text{spheres max.}}} = \frac{1}{(1+f)^3} \quad (9)$$

Figure 6 shows the results of these calculations and indicates a very good agreement for the face-centered cubic array with experimental evidence obtained at Aerojet General Corporation.

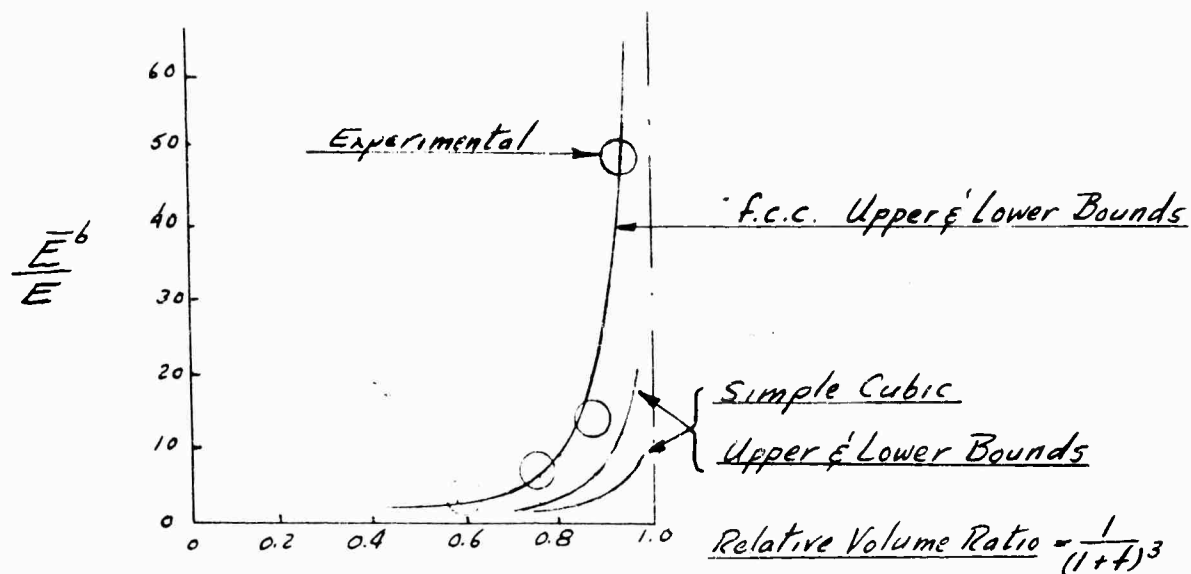


Fig. 3- Calculated variation of Young's modulus with relative volume density in terms of binder modulus E_0 , and compared with experimental data obtained at Aerojet General Corporation.

D. Grain Separation due to Varying Orientations

The upper and lower bound elastic constants obtained in Section C apply only as long as the bonds between the filler and matrix remain intact. As the stress or strain in a tensile specimen is increased, for regions of some orientation the bonding strength will be exceeded. The resultant material, after a fraction of regions have separated, is then made up in part by the stiffness of these separated regions as well as by the stiffness of the remaining bonded regions. Since the unbonded material is much softer than the bonded material, we can expect a decrease in the modulus and possibly a yield in the stress-strain curve. At higher stress, more regions would begin to separate. This spreading-out of the process of separation, leading to a rounding of the stress-strain curve, depends on the anisotropy of the material. It therefore turns out to be important for the hypothetical simple cubic array, but not important for the more realistic face-centered cubic array. For this reason,

although the analysis is presented here as a matter of record, it is not now considered as important as the effect of variability in particle spacing, for which an analysis has not yet been carried out.

Consider first what the stiffness of the separated material will be. The first region to separate will be where the surfaces of the spheres are closest together, where the hydrostatic tension is greatest. Once separated, the level of hydrostatic stress can no longer be maintained and further peeling back can be expected. A partial bonding between the sphere and the matrix will exist for some time but the mater-

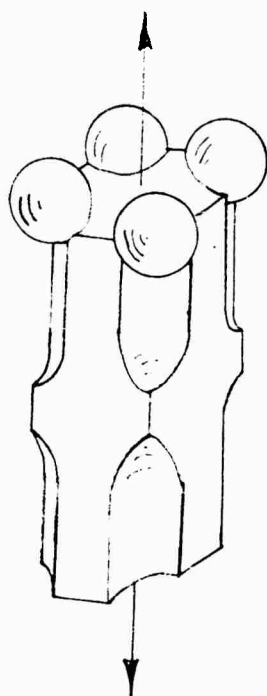


Fig. 7- Schematic of Single Cell of Deformed Material After Separation of the Spheres and Large Strains Along the Cube Axis.

ial will be weak since the hydrostatic stress which gave the high stiffness before separation no longer exists. In the limit, complete separation can be expected as indicated in Fig. 7. For an approximation the sphere can be assumed to be completely unbonded as soon as the bonding strength is exceeded and the resulting stiffness to be that of the unbonded matrix. This is hard to evaluate because of the interference between the matrix and spheres. If the interference of the spheres is neglected then the stiffness is that of a foam which can be estimated as shown in the Appendix.

The elastic constants computed for the foam practically satisfy the condition

of isotropy and also permit changes in volume. These constants were used for the separated regions in computing the net moduli for the partly separated material .

Referring to Fig. 6, the x direction can be considered as being the specimen direction which can take any possible orientation with respect to the cube directions of the sub-regions within the specimen. For each orientation of the cubes, the elastic constants will have a different value which can be expressed in terms of the cube constants already mentioned. However, it is only necessary to consider a stereographic triangle such as the one indicated since, from cubic

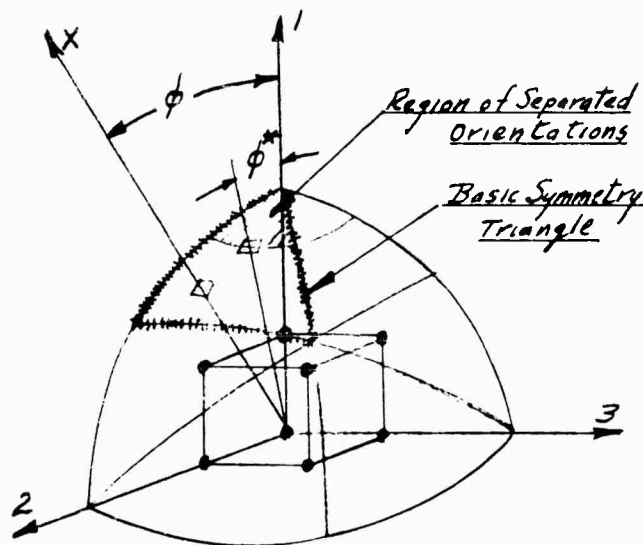


Fig. 6- Representation of Orientation of Loading Axis With Respect to Cube Axes Indicating Regions of Symmetry and Separated Material.

symmetry, the elastic constants would repeat in each triangle.

For either the upper or lower bound solution (i.e., specifying a uniform strain or stress field) those regions in which the cube axis coincides with the x axis will be the first to separate. As the stress or strain is increased, regions oriented within an arc formed by the angle ϕ^* will separate successively. The extent of the separated region as designated by the angle is related directly to the macroscopic stress or strain through the Eq. 1 shown in the Appendix.

To find the current elastic constants, it is necessary to find the

strain energy at the given loading for both the separated and bonded regions. This strain energy gives the elastic constants directly and from the lower bound also gives an expression for the volume change.

The equations which result from this calculation are of the form given here for the approximate upper bound solution:

$$\begin{aligned} \bar{E}_{UB} = & \bar{E}_{UB}^b - 3(\bar{E}_c^b - \bar{E}_c^u)/(1 - \cos \phi^*) \\ & - \frac{3}{20} \left\{ (1.5\bar{E}_c^b - 4.5\bar{G}_c^b) - (1 + 2\nu^u + \nu^{u2}) \left(\frac{\bar{E}_c^u}{(1 + \nu^u)} - 2\bar{G}_c^u \right) \right\} / (-8 + 5\cos \phi^* + 10\cos^3 \phi^* - 7\cos^5 \phi^*). \end{aligned} \quad (10)$$

As long as no bonds have broken, $\cos \phi^* = 1$, and \bar{E}_{UB} has the value of the bonded upper bound \bar{E}_{UB}^b . The angle ϕ^* is related to the bonding strength C , the macroscopic hydrostatic stress $\bar{\sigma}_{ext}$, the modulus of the binder E , the macroscopic strain $\bar{\epsilon}_{xx}$, and a function of the separation ratio \bar{K} , by

$$\cos \phi^* = \sqrt{\frac{2}{3} \frac{(C - \bar{\sigma}_{ext})}{E \bar{K} \bar{\epsilon}_{xx}}} + \frac{1}{3}. \quad (11)$$

As shown in the Appendix, $E\bar{\epsilon}_{ext}$ is the hydrostatic stress at the ligaments (see Eq. 1). When this hydrostatic stress is equal to the bonding strength $(C - \bar{\sigma}_{ext})$, then separation starts ($\cos \phi^* = 1$). This also gives the macroscopic strain $\bar{\epsilon}_{xx}$ at which separation starts. The angle ϕ^* can then be found for successively greater values of and the current value of the modulus \bar{E}_{UB} found from Eq. 10 as a function of the strain. To plot the stress-strain curve, the stress is found from the product of the strain and modulus for successive values of ϕ^* . A similar method is used for the lower bound solution.

The stress-strain relationship for the simple cubic array predicted by these relations for a tension test with gradual separation is shown in Fig. 9. As this figure shows, the upper and lower bounds cross over after initial separation. The reason for this, as explained in the Appendix, is that for the same stress or strain a different amount of unbonding exists in the two solutions. Therefore, the materials are not the same, and the solutions are not true upper and lower bounds but only approximate solutions.

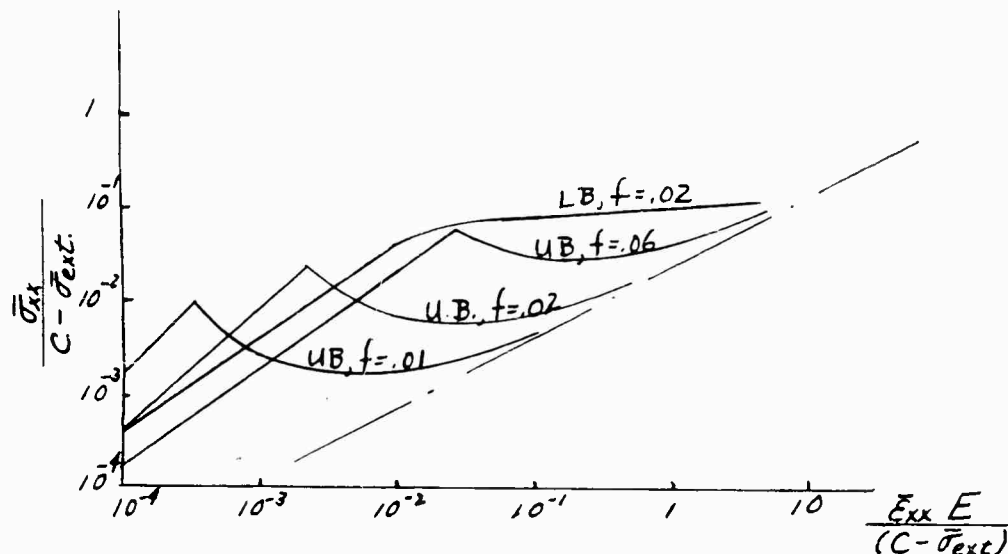


Fig. 9- Stress-Strain Curves Predicted by Analysis for a Simple Cubic Array Material in a Tension Test.

Besides the low initial modulus predicted by the simple cubic array in these curves (see Fig. 6) the peaks from the upper bound solution occur at stresses and strains that are much too low compared to the experimental evidence. Nominal values of the bonding strength, C , and the Young's modulus of the binder, E , can be used to compare these peaks with those shown in Fig. 1. Even if it is argued that the bonding strengths are much greater on the small scale of separation found in the material than is normally used for evaluating bond strengths, the difference cannot be fully accounted for. The peaks in these curves

correspond to the strain at which the initial separation occurs, which is certainly not true experimentally.

Inspection of the face-centered cubic model indicated that it would give an even more unrealistic result. the reason for this is that this dense array is more nearly isotropic and the strength of the sub-regions would have a much smaller dependence on orientation.

A more realistic approach for analysing the progressive unbonding must be based on recognition that the spacing of the particles is not uniform but varies according to some distribution about the mean value. In this manner, with the face-centered cubic array, the strength of the sub-regions would depend on the density of the cluster of particles in the region. The orientation of the sub-regions would be secondary. It would further have to be recognized that, when a sub-region becomes unbonded, the probability of propagation of the unbonding is dependent on whether there are relatively strong or weak sub-regions in the vicinity. Analysis in this direction might be based on the model proposed by Hashin².

E. Development of Sheets of Unbonded Material

We now turn to the next larger scale of phenomena, assuming that considerations of the preceding sections have led to a stress-strain behavior which for the uniaxial case can be idealized as shown in Fig. 10. Consider two extreme modes of elastic behavior, one with complete bonding between the filler and matrix and the other with no bonding. Between these two extremes, there may be intermediate forms of behavior, with unbonding in only one or two of the principal directions. In this section we will consider conditions for the localization of separated regions in thin sheets within a grain.

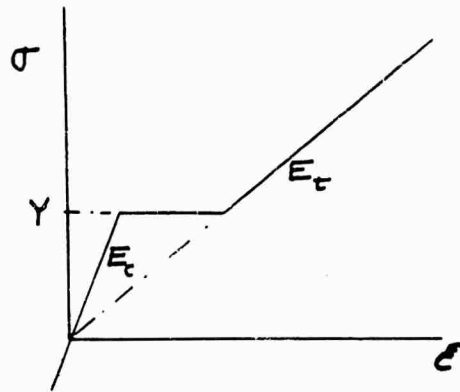


Fig. 10- Uniaxial Stress-Strain Curve for a Filled Elastomer

For the model shown in Fig.10, in compression, or with small amounts of tension, a modulus would have a relatively high value, E_c . At a critical value of the stress, Y , separation would occur, resulting in a very large increase in strain. Subsequently, the modulus would be much reduced, having a value E_t . The following

three-dimensional formulation arose out of a suggestion by Dr. Paul J. Blatz. Although they may not be exactly the formulation he proposed, they coincide for $Y=0$, corresponding to separation at zero stress.

The principal stresses are taken to be in the order

$$\sigma_{11} \geq \sigma_{22} \geq \sigma_{33} \quad (12)$$

When all normal components are less than Y , the usual isotropic elastic equations hold with a modulus of elasticity E_c , and Poisson's ratio ν_c . When just one principal stress component exceeds the critical value, there will be a reduced modulus in the direction of maximum normal stress. In addition, the terms involving one stressed and one transverse direction will have intermediate values:

$$\left. \begin{aligned} \epsilon_{11} &= \frac{\sigma_{11}}{E_t} - \frac{\nu_t \sigma_{22}}{E_c} - \frac{\nu_t \sigma_{33}}{E_c} \\ \epsilon_{22} &= -\frac{\nu_t \sigma_{11}}{E_c} + \frac{\sigma_{22}}{E_c} - \frac{\nu_c \sigma_{33}}{E_c} \\ \epsilon_{33} &= -\frac{\nu_t \sigma_{11}}{E_c} - \frac{\nu_c \sigma_{22}}{E_c} + \frac{\sigma_{33}}{E_c} \end{aligned} \right\} \text{ for } \sigma_{11} \geq Y \geq \sigma_{22} \geq \sigma_{33} \quad (13)$$

If two principal stresses exceed the critical strength, a similar set of equations will hold:

$$\left. \begin{aligned} \epsilon_{11} &= \frac{\sigma_{11}}{E_t} - \frac{\nu_t \sigma_{22}}{E_t} - \frac{\nu_t \sigma_{33}}{E_t} \\ \epsilon_{22} &= -\frac{\nu_t \sigma_{11}}{E_t} + \frac{\sigma_{22}}{E_t} - \frac{\nu_t \sigma_{33}}{E_t} \\ \epsilon_{33} &= -\frac{\nu_t \sigma_{11}}{E_t} - \frac{\nu_t \sigma_{22}}{E_t} + \frac{\sigma_{33}}{E_t} \end{aligned} \right\} \text{for } \sigma_{11} \geq \sigma_{22} \geq Y \geq \sigma_{33} \quad (14)$$

Finally, when all three normal components exceed the critical strength, the material is again isotropic with Young's modulus E_t and Poisson's ratio ν_t .

When a small region in such a solid first begins to unbond, the state of stress and strain will be complicated in its neighborhood. It seems reasonable to suppose, however, that the region of unbonding would spread in a direction normal to the maximum principal stress. If so, a thin sheet will develop across which certain of the components of stress and strain can be discontinuous but others must be continuous. In particular, the normal component of stress, σ_{11} , must be continuous. If the state of stress is relatively constant over large areas of the zone, then to prevent the development of large shear strain it is necessary that the two lateral components of normal strain be continuous. Using the superscript s to denote conditions in the sheet, these two requirements may be summarized as:

$$\sigma_{11} = \sigma_{11}^s ; \quad \epsilon_{22} = \epsilon_{22}^s , \quad \epsilon_{33} = \epsilon_{33}^s \quad . \quad (15)$$

We now inquire what restrictions these conditions impose on the transverse stress components in the deformation sheet, σ_{22}^s and σ_{33}^s . We first postulate that unbonding has occurred only on one plane in the sheet, so that Eq. 13 holds. Equating the transverse normal strains within and without the sheet, we obtain for $\sigma_{22} = \sigma_{33}$;

$$\epsilon_{22} = -\frac{\nu_c \sigma_{11}}{E_c} + \frac{\sigma_{22}}{E_c} - \frac{\nu_c \sigma_{33}}{E_c} = -\frac{\nu_c \sigma_{11}}{E_c} + \frac{\sigma_{22}^s}{E_c} - \frac{\nu_c \sigma_{33}^s}{E_c}$$

$$\text{or, } \sigma_{22}^s = \sigma_{22} + \frac{(\frac{\nu_c E_c}{E_i} - \nu_c)}{1 - \nu_c} \sigma_{11} \quad (16)$$

Taking account of the fact that $\sigma_{11} = Y$, for the transverse normal component of stress to be less than Y it is necessary that

$$Y \geq \sigma_{22}^s \quad \text{or,} \quad \sigma_{22} \leq Y \left(\frac{1 - \nu_c E_c / E_i}{1 - \nu_c} \right) \quad (17)$$

Similar equations will be obtained for the other transverse component of stress. Since the intermediate modulus of elasticity, E_i , is likely to be much less than the bonded modulus, E_c , in many cases a compressive transverse stress will be required to prevent unbonding. In any event, the transverse stress on unbonding will be less than the normal component of stress for unbonding in the first direction. The situation is illustrated in Fig. 11. If the maximum transverse stress is greater than the value given by Eq. 17, then the next stage of unbonding will occur, provided that E_c/E_i is greater than 1. In this case, the intermediate equations for partial unbonding are not needed and there is an abrupt transition from bonded to completely unbonded isotropic behavior.

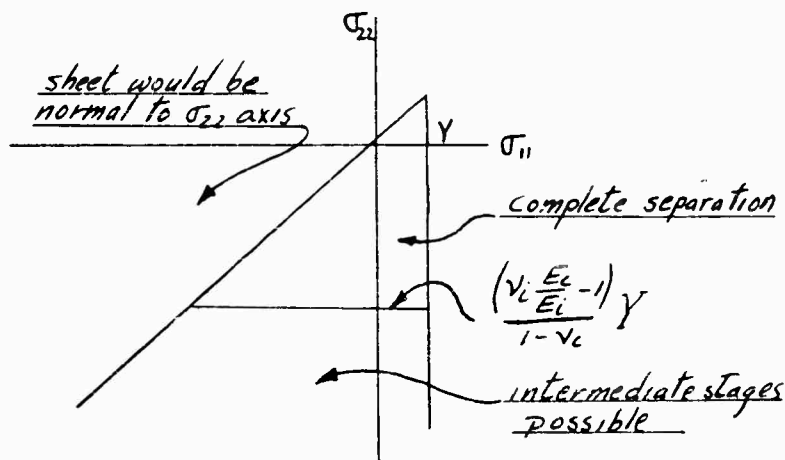


Fig. 11- Locus of Complete Unbonding in a Deformation Sheet

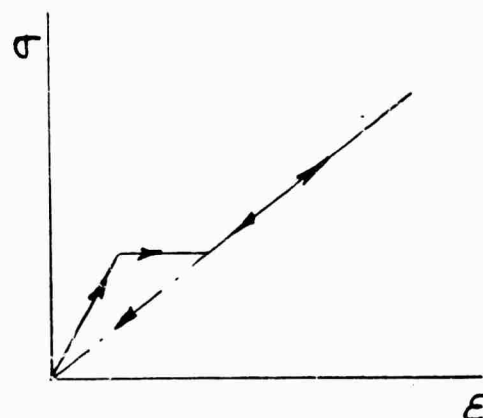


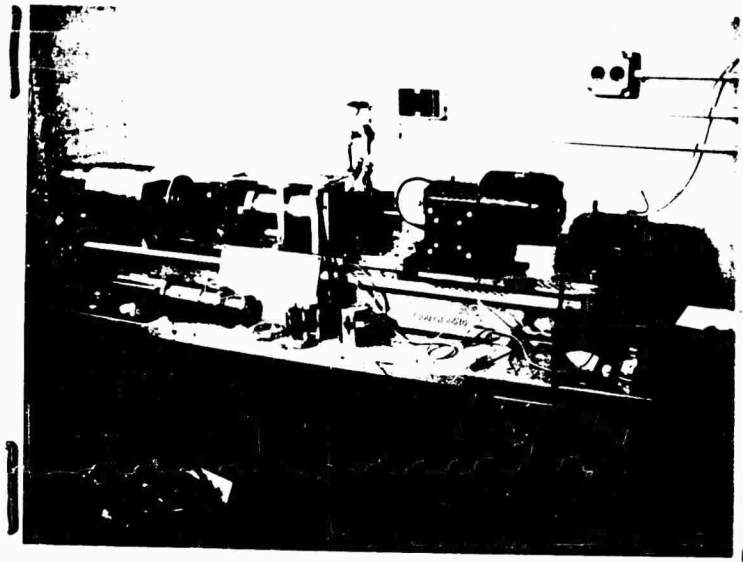
Fig. 12- Unloading Behavior of a Filled Elastomer After Unbonding

Applying these results to the tensile test, then, one would expect unbonding to occur in a thin sheet, within which complete unbonding occurs as soon as the sheet forms. As the yield sheet thickens, the transverse stress in it will drop, which might lead one to suspect a rebonding. In an actual material, however, the closure does not lead to rebonding until a considerable passage of time has allowed the bonds to reheal, so that, on decrease of stress, a path corresponding to that shown in Fig. 12 is followed.

III. Experimental

The importance of hydrostatic stress on the properties of filler polymers has been well established by the work of Mr. C. Surland at Aerojet General Corporation on tensile specimens under hydrostatic pressure. Data on the effect of shear and hydrostatic stress would add considerably to the understanding of fracture. The tensile hydrostatic loading is particularly important because under some combined loadings the hydrostatic component can be in tension and of a very significant magnitude. With this in mind, and also to be able to confirm the theoretical considerations with more than simple tension data, a test rig was built to investigate the effect of these combined loadings.

The equipment was designed to be able to superimpose hydrostatic stress (tension and compression) on distortion strains (shear). This is done by twisting a solid cylindrical specimen 6 inches in diameter and 2 inches long. At the same time, the specimen can be subjected to a hydrostatic pressure of up to 100 psi or a hydrostatic tension of up to 100 psi. The hydrostatic tension is obtained by spinning the



Photograph of Experimental Test Rig
Showing High Speed Motor on Left and Twisting Motor on Right

Figure 12

G-19a

specimen about its axis while holding its length constant. The relatively high bulk modulus of the material, prior to large amounts of unbonding, is directly responsible for this stress condition as can be found in Timoshenko and Goodier³.

Molds for making the cylindrical specimens as well as tension specimens, for comparison of results, have been prepared. No results can be reported because of difficulty encountered in mixing and preparation of adequate inert specimens.

IV. Results and Discussion

In this investigation a model was developed for interpreting test data on solid fuels which could ultimately relate uniaxial and combined load behavior and which would be useful for application to design problems. The model was built up of the principal constituent variables such as binder elastic properties, bond strengths, and filler densities. This approach was used in order to learn which factors determine the behavior.

The first step in the investigation was to develop the conditions existing in a region between a pair of adjacent particles. The results of this analysis, summarized above, indicate a very great magnification of the nominal stress in the ligament regions. This predicts that the bond strength will be overcome, in regions where the particles are very close together, at very low values of stress and strain. Due to the relative incompressibility of the material, the model also predicts that a macroscopic hydrostatic pressure has an effect equivalent to greater bond strengths. This implies that greater tensile loads and strains are possible prior to fracture when testing under pressure

which is directly supported by experimental results.

Putting these results together by grouping particles into orderly arrays, the elastic constants for the composite material were determined. Using the face-centered cubic array, which gives densities similar to those found in random packings, the dependence of the Young's modulus on the volume fraction of filler was found to correspond very well with available data.

From these considerations it was possible to develop the conditions for separation of a homogeneous region. By considering the face-centered cubic array as being fully isotropic, the limiting maximum principal strain that results in unbonding is given very closely by:

$$\bar{\epsilon}_1 = \frac{2W_0}{2h_0 + D} = \frac{2W_0}{D(1+f)} \quad (18)$$

Using this relation in conjunction with Eq. 1, modified for the f.c.c. array as mentioned in the Appendix, the tension across the ligament is given by:

$$p = - \frac{E\bar{\epsilon}_1}{4} (1+f) \left[\frac{(1+16f)}{f^2(1+8f)^2} \right] \quad (19)$$

Since the macroscopic hydrostatic stress adds directly to this, due to incompressibility, when the sum of these exceeds the bonding strength, \underline{C} , separation takes place.

$$-p + \frac{\bar{\sigma}_1 + \bar{\sigma}_2 + \bar{\sigma}_3}{3} = C \quad (20)$$

Using the stress-strain relations for the incompressible material,

$$\epsilon_1 = \frac{\bar{\sigma}_1}{E^b} - \frac{1}{2} \frac{(\bar{\sigma}_2 + \bar{\sigma}_3)}{E^b} = \frac{3}{2} \frac{\bar{\sigma}_1}{E^b} - \frac{(\bar{\sigma}_1 + \bar{\sigma}_2 + \bar{\sigma}_3)}{2E^b} \quad (21)$$

and combining with the previous relations, the locus for separation of a homogeneous region is found:

$$C = \frac{3E}{8E^b} \left[\frac{(1+f)(1+16f)}{f^2(1+8f)^2} \right] \bar{\sigma}_1 + \left\{ 1 - \frac{3E}{8E^b} \left[\frac{(1+f)(1+16f)}{f^2(1+8f)^2} \right] \right\} \frac{(\bar{\sigma}_1 + \bar{\sigma}_2 + \bar{\sigma}_3)}{3} \quad (22)$$

This locus is symmetrical about the principal stress directions and can be represented by a pyramid as shown in Fig. 13. The shape of the pyramid shows the dependence of the strength on the hydrostatic pressure. The location of the apex is controlled by the bond strength. It is interesting to note that this figure is analogous to that given by Dr. P. Blatz⁹ except that for an incompressible material the apex of his surface is infinitely high. Furthermore, the dependence of the fracture strain is here given in terms of other material properties.

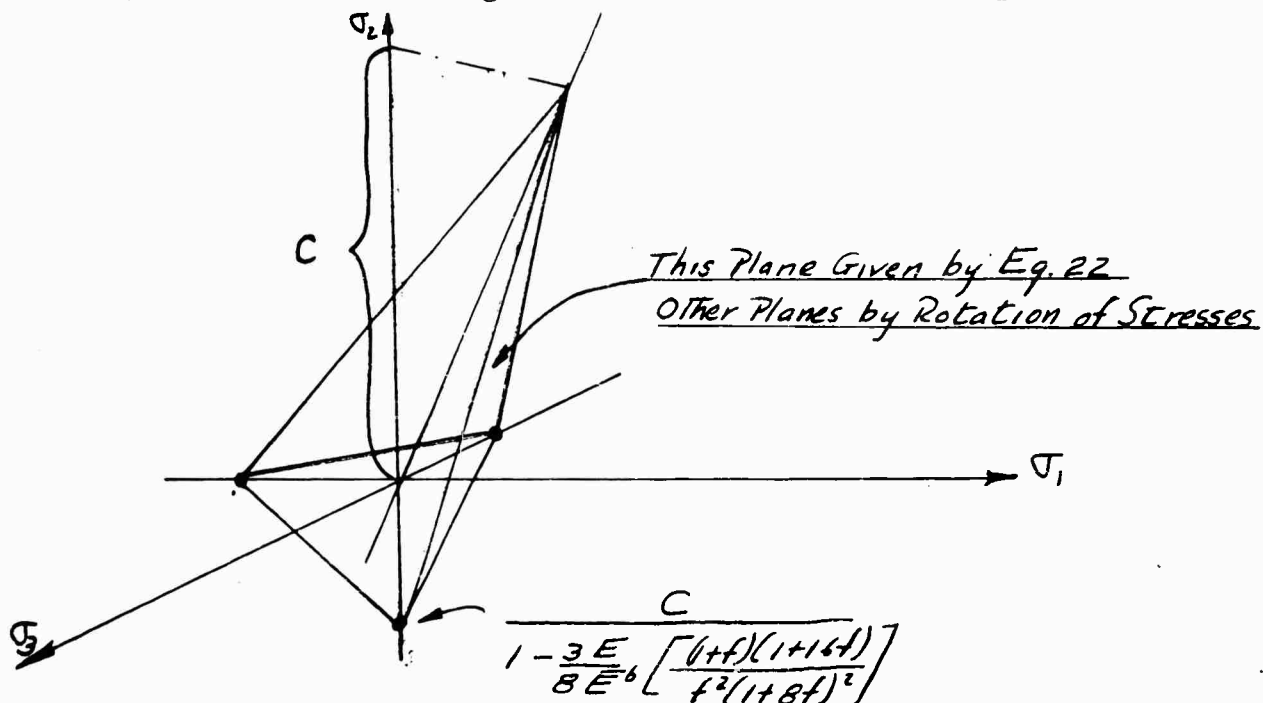


Fig. 13- Locus of Principal Stresses for Separation of a Uniform Region of Face-Centered Cubic Material.

Extension of this analysis to regimes of progressive unbonding, to predict load deflection and volume change phenomena, did not give satisfactory results. This portion of the analysis, particularly when modified for combined stresses, is the most important and also

the most challenging. It is felt that the building blocks are now available and that a realistic model of this behavior can now be described analytically. A first step in this direction would be to take into account variations in particle spacing and the statistical distribution of strength. This approach should explain the stability of the first regions to unbond, determining whether the unbonding becomes localized or spreads uniformly over the part.

The experimental results, when obtained, will add significantly to the limited information now available on the behavior of these materials under combined loads. Such data must be available to develop a theory of failure.

In the course of this investigation the importance of size effects in testing these materials became increasingly apparent. This is illustrated in the following arguments. They point out the need for having large enough specimens to be able to extend the data obtained from them to actual motor design.

It must be recognized that the material is non-homogeneous in the strength of sub-regions within it. If the specimen is small in any of its dimensions compared to any of these regions, different properties will be measured for the material. Any weak sub region which is first to unbond during loading will concentrate its share of the load on adjacent regions. The distribution of this load and the likelihood of propagation will depend on the extent of material around the unbonded zone. This is due not only to the existence of boundaries but also due to the statistical distribution of the strength of adjacent regions. Thus, tension tests on sheets would show different results from tests on a thicker block of material.

The importance of this size effect would be particularly apparent

in notch sensitivity experiments. If the test part is small and the stress gradients large compared to the size of the sub-regions, significant scatter can be expected. This would be attributable in large part to the lack of adequate statistical sampling of strengths in the high stress region of the notch. The results of such tests could not properly be extended to the design of the root of a star in an actual rocket motor where the size would be much greater.

Another important and related size effect can be deduced from the analysis presented in Section II-E of this report. As is shown by those results, the formation of bands of unbonded material across a tensile specimen depend on the restraint of the bonded regions next to the discontinuity. If the lateral dimensions of the specimen are not large compared with the thickness of the discontinuity then the restraints will be different and complete unbonding will not take place. The resulting stress-strain curves would indicate different mechanical properties.

These effects are important for interpretation and application of test results. It is strongly recommended that these effects be considered in the planning of tests and evaluation of data. It is further recommended that analytical and statistical studies be continued to better understand these size effects.

V. Conclusions

1.) The modulus of a filled rubbery material was estimated under the following assumptions:

- a) Closely spaced spherical particles,
- b) Simple cubic or face-centered cubic array,
- c) Incompressible matrix and rigid particles,
- d) Isotropic small-strain elastic behavior of the matrix.

- 2.) It was found that:
- a) The simple cubic array gave too high compliances for the given density,
 - b) The face-centered cubic array gave nearly isotropic behavior of reasonable elastic compliance,
 - c) The locus of fracture initiation for the face-centered cubic array takes the pyramidal form shown in Fig. 13,
 - d) A model to predict stress-strain behavior during unbonding gave an abrupt drop in the stress at very small values of strain,
 - e) Statistical variability in particle spacing will lead to a rounding out of the stress-strain curve on unbonding,
 - f) The statistical variability must be considered in predicting the performance of large parts from small components, and especially in predicting notch sensitivity.
- 3.) Experimental apparatus to study the effect of hydrostatic pressure has been built.
- 4.) The formation of sheets of unbonded material often leads to simultaneous unbonding in all three principal directions, as indicated in Fig. 12.

VI. APPENDIX

The individual steps and reasoning used in the analysis are presented here paralleling the material in the Summary. This is done to make it easier to look in detail at any step mentioned in the Summary.

A. Conditions Between Adjacent Particles:

I. Expression for Sphere Surface.

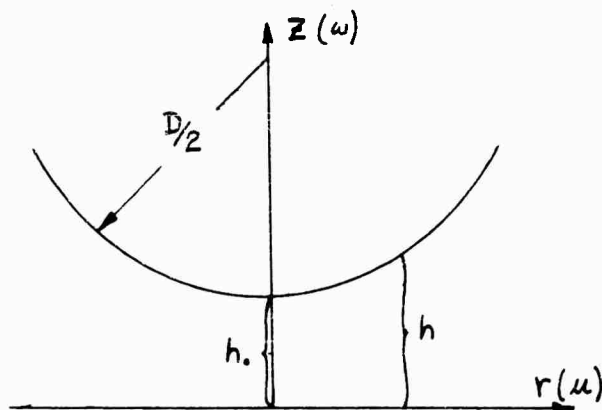


Fig. (A-1)

This expression is much easier to use and for small values of the radius, in the region of primary importance; the deviation from the sphere is small. At a radius of $D/2\sqrt{2}$ the error is about 15% in h for small values of h_0 .

In cylindrical coordinates the expression for the surface of the sphere shown in Fig. (A-1) is:

$$h = \left(\frac{D}{2} + h_0\right) - \sqrt{\left(\frac{D}{2}\right)^2 - r^2} \quad (\text{A-1})$$

The first significant terms of this function are:

$$h = h_0 + \frac{r^2}{D} \quad (\text{A-2})$$

II. Solution for Stresses and Strain Energy due to Separation of Two Spheres.

1. Approximate Solution:

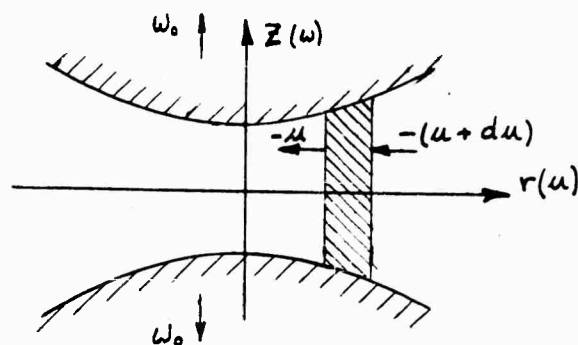


Fig. (A-2)

As the spheres are separated, because the matrix is incompressible, material must flow in from the sides to maintain constant volume.

If the spheres are close together, for a small displacement w_0 of the spheres, large displacements u can be expected. In fact to a first approximation, displacements w of the matrix can be neglected in considering the stress and strains resulting.

Following this argument, a displacement field can be found such as:

$$u = -\frac{3w_0}{4} \left(\frac{r}{h} \right) \left[1 - \left(\frac{z}{h} \right)^2 \right] \quad (A-3)$$

which satisfies continuity on the gross scale (i.e., for an annulus of height h , using the $z = 0$ plane as reference). This displacement field gives rise to a shear stress τ_{rz} found from

$$\tau_{rz} = G \gamma_{rz} = G \left(\frac{\partial u}{\partial z} + \frac{\partial w}{\partial r} \right) \quad (A-4)$$

If the spheres are close together and the region of highest stress is near the center, the derivative $\frac{\partial h}{\partial r}$ is negligible and equilibrium is satisfied by introducing a hydrostatic stress so that:

$$\frac{dp}{dr} = \frac{\partial \tau_{rz}}{\partial z} \quad \text{or, } p = -\frac{3Gw_0 D}{8h^2} + C = -\frac{E w_0}{2D \left[f + \frac{2r^2}{b^2} \right]^2} + C \quad (A-5)$$

The variation of this pressure with the radius is implicit through h . For small values of the separation ratio, f , the pressure drops extremely fast as shown in Fig. (A-3). Because of this rapid drop,

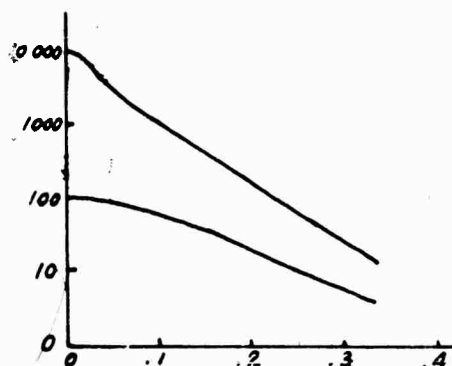
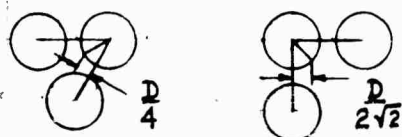


Fig. (A-3)

as long as the separation ratio is low, the pressure at the center is quite insensitive to the pressure at large radii or in the interstitial region. For this reason the pressure at $r = D/2\sqrt{2}$ was

taken as zero for the simple cubic array to evaluate the constant in Eq. (A-5) giving:

$$p = - \frac{E \omega_0 D}{8} \left[\frac{1}{h^2} - \frac{1}{(h_0 + \frac{D}{4})^2} \right] \quad (A-6)$$

A similar expression results for the face-centered cubic array taking the pressure equal to zero at $r = D/4$. In the following, the development used applies to the simple cubic array but is directly analogous to that for the denser packing.

Particularly, at the center where $h = h_0$, we have Eq. 1 of the Summary:

$$p = - \frac{E \omega_0}{2 D} \left[\frac{1 + 8f}{f^2(1 + 4f)^2} \right] \quad (A-7)$$

Since this is an approximate solution, its validity can be checked by comparing the strain energy in the ligament with upper and lower bounds of this energy. The strain energy given by this approximate solution is:

$$\begin{aligned} S.E. APPROX &= \frac{1}{2} \int_0^r \int_0^{h(r)} 2\pi r dr dz (\gamma^2 G) \\ &= \frac{\pi E \omega_0^2 D^2}{16 h_0} \left[\frac{h_0}{(h_0 + \frac{D}{4})^2} - 1 \right]^2 = \frac{\pi E \omega_0^2 D}{8 f} \left[\frac{-2(\frac{f}{5})^2}{f + 2(\frac{f}{5})^2} \right]^2 \end{aligned} \quad (A-8)$$

A plot of this function (Fig. A-4) shows that the strain energy

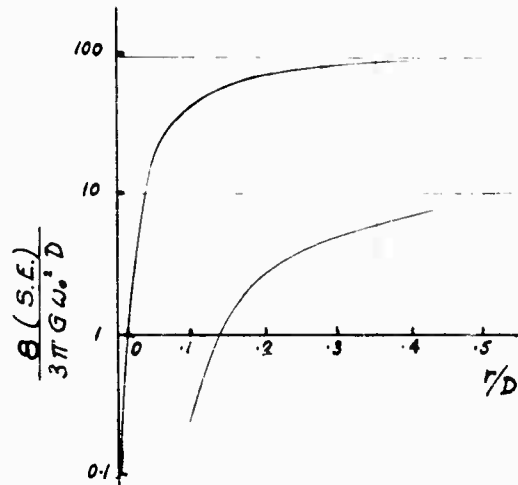


Fig. (A-4)

is small. This gives:

$$S.E. APPROX = \frac{\pi E \omega_0^2 D}{8 f (1 + 4f)^2} \quad (A-9)$$

levels off very quickly for small separation ratios. The energy is, therefore, dependent on what is occurring in the ligament.

Considering that the sphere surface flares out very quickly after $r = D/2\sqrt{2}$, the strain energy beyond this radius can be neglected as long as the separation ratio f

2. Bounds on Strain Energy of Separation:

Timoshenko and Goodier⁽³⁾ give the expressions for strain energy in terms of the stress or strain which, when Poisson's ratio is 1/2, reduce to:

$$\frac{d(S.E.)}{dV} = \frac{1}{4E} [(\sigma_x - \sigma_y)^2 + (\sigma_y - \sigma_z)^2 + (\sigma_z - \sigma_x)^2] + \frac{3}{2E} (\tau_{xy}^2 + \tau_{yz}^2 + \tau_{zx}^2) \quad (A-10)$$

$$\frac{d(S.E.)}{dV} = \frac{E}{3} (\epsilon_x^2 + \epsilon_y^2 + \epsilon_z^2) + \frac{E}{6} (\gamma_{xy}^2 + \gamma_{yz}^2 + \gamma_{zx}^2) \quad (A-11)$$

An upper bound on the strain energy of an exact solution can be found if a strain or displacement solution is known which satisfies the boundary displacement and continuity conditions but not necessarily equilibrium. Similarly a lower bound requires only that a stress solution satisfying equilibrium be known.⁽⁴⁾

A displacement field satisfying continuity and a stress field satisfying equilibrium, in cylindrical coordinates as indicated in Fig. (A-1), are:

$$u = -\frac{3\omega_0 r}{4h} \left[1 - \left(\frac{z}{h} \right)^2 \right] \quad (A-12)$$

$$v = 0$$

$$\omega = \frac{\omega_0}{2h^2} \left[3h_0 z + \frac{2z^3}{h} - \frac{3h_0 z^3}{h^2} \right]$$

$$\begin{aligned} \sigma_r = -p &= \frac{E\omega_0 D}{8} \left[\frac{1}{h^2} - \frac{1}{(h_0 + \frac{z}{h})^2} \right], & \tau_{rz} &= \frac{E}{2} \left(\frac{\omega_0}{h} \right) \left(\frac{r}{h} \right) \left(\frac{z}{h} \right) \\ \sigma_\theta = -p & & \tau_{r\theta} &= 0 \\ \sigma_z = -p + \frac{E}{4} \left(\frac{\omega_0}{h} \right) \left(\frac{z^2}{h^2} \right) \left[\frac{4h - 6h_0}{h} \right], & \tau_{\theta z} &= 0 \end{aligned} \quad (A-13)$$

The relations for equilibrium and continuity can be found in any advanced book in elasticity^(3,5,6). Using Eqs. (A-12) and

(A-13) with (A-10) and (A-11) the bounds on the strain energy can

be found as:

$$S.E._{UB} = \int_0^{r=D/2\sqrt{2}} \int_0^h \frac{d(S.E.)}{dV} 2\pi r dz dr \quad (A-14)$$

$$= \pi E \omega_0^2 D \left\{ \frac{1}{8f} \left[1 - 2 \left(\frac{4f}{1+4f} \right) + \left(\frac{4f}{1+4f} \right)^2 \right] + \frac{1}{10} \left[6 \ln \left(\frac{1+4f}{4f} \right) - 5 \left(\frac{4f}{1+4f} \right)^2 + 10 \left(\frac{4f}{1+4f} \right) - 5 \right] \right. \\ \left. + \frac{f}{10} \left(\frac{1+4f}{4f} \right) \left[-66 \left(\frac{4f}{1+4f} \right) \ln \left(\frac{1+4f}{4f} \right) + 11 \left(\frac{4f}{1+4f} \right)^3 - 58 \left(\frac{4f}{1+4f} \right)^2 + 17 \left(\frac{4f}{1+4f} \right) + 30 \right] \right\} \quad (A-15)$$

$$S.E._{LB} = \int_0^{r=D/2\sqrt{2}} \int_0^h \frac{d(S.E.)}{dV} 2\pi r dz dr$$

$$= \pi E \omega_0^2 D \left\{ \frac{1}{8f(1+4f)^2} + \frac{1}{40} \ln \left(\frac{1+4f}{4f} \right) - \frac{3(5+2f)}{320(1+4f)^2} \right\}$$

A comparison of the strain energy from Eqs. (A-9), and (A-14), and

(A-15) is shown in Fig. (A-5). As can be seen, the approximate

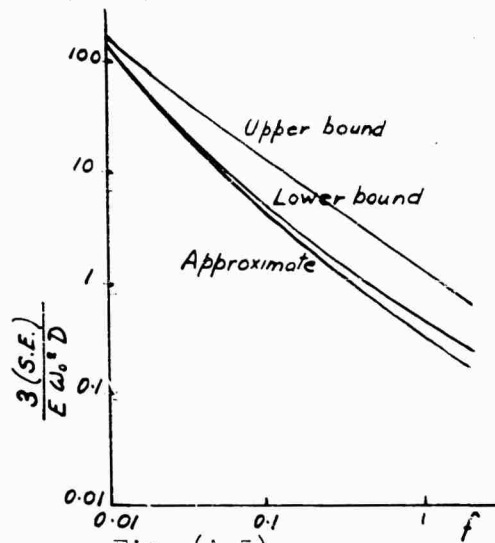


Fig. (A-5)

solution is close to the exact solu-

tion (somewhere between upper and

lower bounds) for small values of f

(high packing densities). In fact

not only do the strain energies con-

verge, but a comparison of the solu-

tions shows them to be identical in

the limit as f approaches zero. For

larger values of f , the strain energy

is small and the contribution of interstitial volumes becomes signi-

ficant in evaluating the overall stiffness of the material. At any

rate, the convergence of the solutions as shown in Fig. (A-5) justifies

the use of the approximate relations.

Analogous results are obtained for the face-centered array where

the integration is carried out to $r = D/4$.

III. Solution For Stresses and Strain Energy due to Shear between

Two Spheres:

The solution for this case is similar to the previous one for separation of spheres. An approximate solution was found and the strain energy compared with upper and lower bound solutions. Because of the similarity the equations are presented without much comment.

The main difference between this solution and the previous one is that there is no circular symmetry. The coordinates are shown in Fig. (A-6). The approximate solution consists simply of:

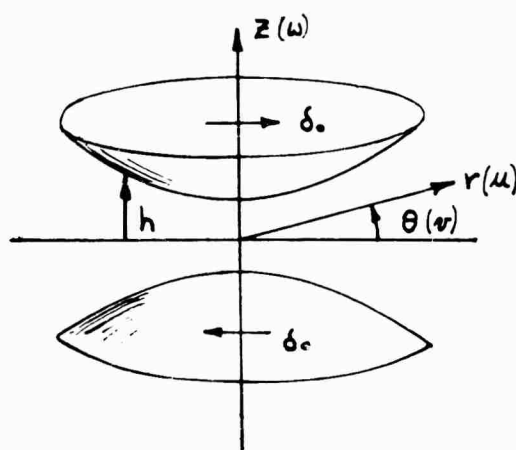


Fig. (A-6)

$$\begin{aligned}\tau_{rz} &= \frac{\delta_0 \cos \theta}{h} \frac{E}{3} \\ \tau_{z\theta} &= -\frac{\delta_0 \sin \theta}{h} \frac{E}{3}\end{aligned}\quad (A-16)$$

where all the other stresses are considered negligibly small. The strain energy within the radius $r = D/2\sqrt{2}$ is:

$$S.E._{APPROX} = \frac{\pi E \delta_0^2 D}{6} \left(\frac{1+4f}{4f} \right) \quad (A-17)$$

A displacement field and stress field, satisfying continuity and equilibrium respectively, for upper and lower bounds on the actual strain energy are:

$$\begin{aligned}\mu &= \delta_0 \cos \theta \left(\frac{z}{h} \right) \\ \nu &= -\delta_0 \sin \theta \left(\frac{z}{h} \right) \\ \omega &= \delta_0 \cos \theta \frac{(h_0 - h)}{r} \left[1 - \frac{z^2}{h^2} \right],\end{aligned}\quad (A-18)$$

$$\sigma_r = 0 \quad \tau_{rz} = \frac{E}{3} \left(\frac{\delta_0 \cos \theta}{h} \right) \quad (\text{A-19})$$

$$\sigma_\theta = 0 \quad \tau_{z\theta} = -\frac{E}{3} \left(\frac{\delta_0 \sin \theta}{h} \right)$$

$$\sigma_z = \frac{E}{3} \frac{\delta_0 \cos \theta}{h} \left(\frac{z}{h} \right) \left(\frac{2r}{D} \right) \quad \tau_{\theta r} = 0$$

The strain energy for these two solutions is:

$$S.E._{u\theta} = \frac{\pi E \delta_0^2 D}{6} \left\{ \ln \left(\frac{1+4f}{4f} \right) \left[1-f + \frac{2f^2}{5} \right] + \frac{2f}{5} + \frac{5}{48} \right\} \quad (\text{A-20})$$

$$S.E._{u\theta} = \frac{\pi E \delta_0^2 D}{6} \left\{ \ln \left(\frac{1+4f}{4f} \right) \left[1 - \frac{f}{9} \right] + \frac{1}{36} \right\} \quad (\text{A-21})$$

A comparison of the approximate solution and the bounds on the exact solution are shown in Table (A-7). Again the solutions converge as \underline{f} becomes small. Similar expressions and comparisons apply to the face-centered array where the integration is carried out to $r = D/4$ only.

Table (A-7)

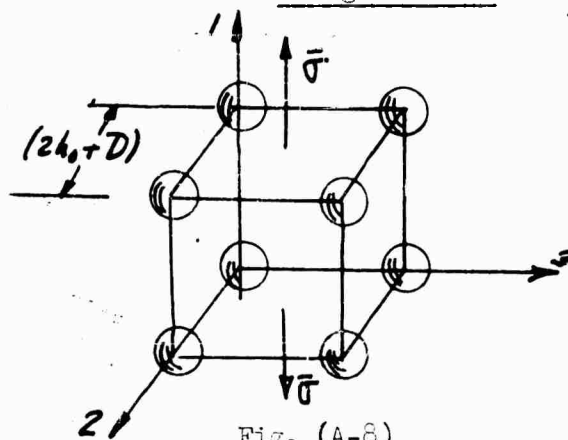
\underline{f}	$\frac{3(S.E.)_{u\theta}}{E \delta_0^2 D}$	$\frac{3(S.E.)_{u\theta}}{E \delta_0^2 D}$	$\frac{3(S.E.)_{Approx}}{E \delta_0^2 D}$
0.01	5.24	5.17	5.11
0.02	4.18	4.13	4.08
0.06	2.62	2.60	2.57
0.10	1.99	1.99	1.96
0.20	1.33	1.24	1.27
0.50	0.859	0.644	0.636
1.00	0.929	0.355	0.350

B. Elastic Constants for Arrays of Particles:

I. Simple Cubic Array.

The local stress solutions can be combined to give the elastic constants for a simple cubic array of spheres.

1. Youngs Modulus:



Referring to Fig. (A-8), if a tensile stress, $\bar{\sigma}$, is applied there will be a resulting strain $\bar{\epsilon}_{11} = -2\bar{\epsilon}_{22} = -2\bar{\epsilon}_{33}$ satisfying constant volume such that:

$$\bar{\epsilon}_{11} = \frac{\bar{\sigma}}{\bar{E}_c'} \quad (\text{A-22})$$

where \bar{E}_c' is the cubic constant for the bonded material. Also we have the strain energy in the unit cube:

$$S.E. = (\frac{1}{2} \bar{\sigma} \bar{\epsilon}_{11}) V_0 = \frac{\bar{\epsilon}_{11}^2 \bar{E}_c'}{2} D^3 (1+f)^3 \quad (\text{A-23})$$

However, since:

$$\bar{\epsilon}_{11} = \frac{2\omega_0}{2h_0 + D} = \frac{2\omega_0}{D(1+f)}, \quad (\text{A-24})$$

this strain energy can be written as:

$$S.E. = 2 \bar{E}_c' \omega_0^2 D (1+f) \quad (\text{A-25})$$

This energy must equal the strain energy within the elemental cube. In the vertical direction there are four ligaments stretched by an amount $2\omega_0$ and Eq. (A-8) is used for their contribution. However, this equation is for only half of the ligament (the bottom half is the same by symmetry) and the four ligaments are shared by

adjoining elemental cubes so that effectively only one ligament feels the full extension in the unit cube. In the horizontal direction, the strains are half as great and by a similar argument only two whole ligaments belong to the cube. The total strain energy in the ligaments is, therefore:

$$S.E. \text{ Ligaments} = \frac{\pi E W_0^2 D}{8f(1+4f)^2} \left[2 + 4 \times \frac{1}{4} \right] = \frac{3\pi E W_0^2 D}{8f(1+4f)^2} . \quad (A-26)$$

To this should be added the contribution of the material in the interstitial volume. Since this energy is negligible for a close spacing of spheres, all that is required is an approximate term which will satisfy the limiting conditions as the volume density of spheres goes to zero. This can be done as indicated in Fig. (A-9) by breaking the interstitial volume up into sections and attributing

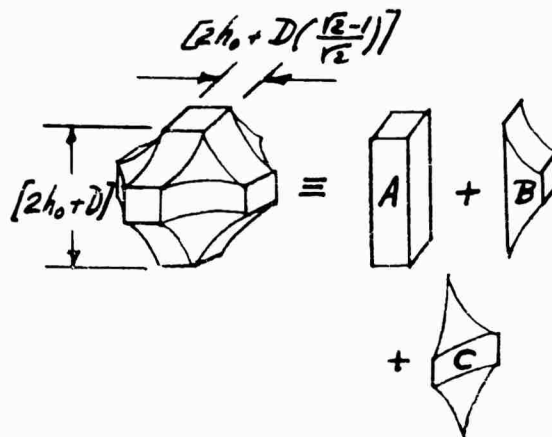


Fig. (A-9)

to each section the nominal deformation of the unit cube. For example, region "A" is assumed to have a uniform strain equal to the macroscopic strain of the unit cube. For the four regions "B" and "C" since their contribution is negligible for both limiting conditions, a rough estimate was made, the details of which are not significant enough to describe. The expressions derived for these regions are:

$$S.E._{INTERSTITIAL} \cong E \omega^2 D \left\{ \left[\frac{2(0.293+f)}{(1+f)} \right]^2_A + \left[\frac{2.82(0.293+f)}{(0.500+f)} \right]^2_B + \left[\frac{0.221}{(0.293+f)} \right]^2_C \right\}. \quad (A-27)$$

Inspection of this equation shows that as f becomes very large (low volume density) only the contribution of "A" is significant and that the equation becomes identical to Eq. (A-25) resulting in $\bar{E}_c^b = E$ as would be expected.

Equating the strain energies from Eq. (A-25) and the sum of Eqs. (A-26) and (A-27) permits solving for the elastic modulus of the filled rubber in the cube direction giving Eq. 2 of the Summary.

$$\bar{E}_c^b = E \left\{ \left[\frac{3\pi}{16f(1+f)(1+4f)} \right]^2 + \left[\frac{(0.293+f)^2}{(1+f)^2} + \frac{1.41(0.293+f)}{(1+f)(0.500+f)} + \frac{0.11}{(1+f)(0.293+f)} \right] \right\} \quad (2) \quad (A-28)$$

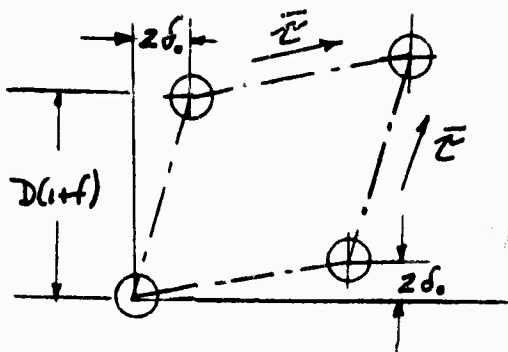
2. Shear Modulus:

To find the shear modulus, \bar{G}_c^b , for the simple cubic array in the cube orientation the procedure followed is essentially the same as for the Young's modulus. A macroscopic shear stress $\bar{\tau}$ is considered acting on the elemental cube giving rise to a shear strain $\bar{\gamma}$. The strain energy is expressed by:

$$S.E. = \left(\frac{1}{2} \bar{\tau} \bar{\gamma} \right) D^3 (1+f)^3 \quad (A-29)$$

Referring to Fig. (A-9) the relationship between $\bar{\gamma}$ and δ_o is evident:

$$\bar{\gamma} = \frac{4\delta_o}{D(1+f)} \quad (A-30)$$



(A-10)

Eq. (A-29) can then be written as:

$$S.E. = 8\delta_0^2 \bar{G}_c^b D(1+f) . \quad (A-31)$$

That the spheres do not rotate in pure shear can be demonstrated by considering equilibrium.

The strain energy internal to the unit cube consists of the contribution of the ligaments and of the interstitial volume. There are two ligaments per unit cube and using Eq. (A-17) which gives the strain energy for half a ligament in shear:

$$S.E. \text{ LIGAMENTS} = \frac{2\pi E \delta_0^2 D}{3} \ln\left(\frac{1+f}{1-f}\right) . \quad (A-32)$$

The contributions of the interstitial volume was estimated by approximating the shape of this volume as indicated in Fig. (A-10). This approximate shape was assumed to undergo a deformation as shown in the figure and strain energy calculated accordingly, giving:

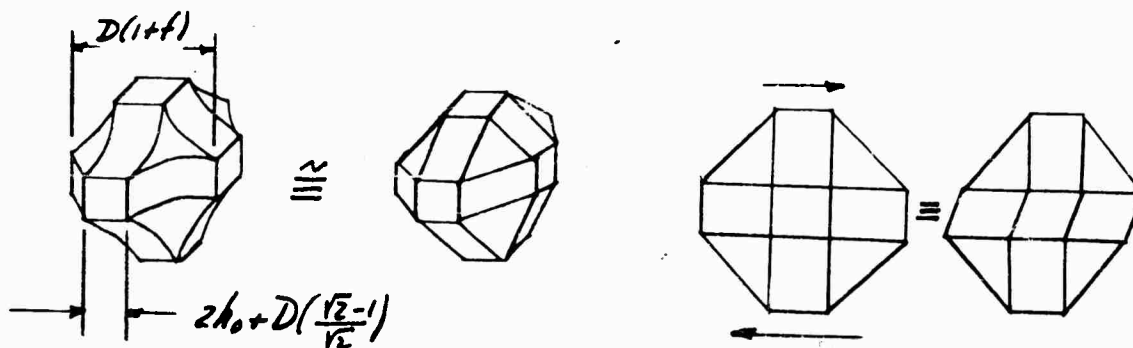


Fig. (A-11)

$$S.E._{INTERSTITIAL} = \frac{8 \int_0^2 E D}{3} \left\{ \frac{(0.293+f)^2}{(1+f)^2} + \frac{(0.293+f) \ln(1+f)}{0.293+f} + 0.353 \right\} \quad (A-33)$$

Summing the contributions of Eqs. (A-31), (A-32), and (A-33) permits solving for the shear modulus and results in Eq. 4 of the Summary.

$$\bar{G}_c^b = \frac{E}{3} \left\{ \left[\frac{\pi}{4(1+f)} \ln\left(\frac{1+f}{4f}\right) \right] + \left[\frac{(0.293+f)^2}{(1+f)^2} + \frac{(0.293+f) \ln(1+f)}{0.293+f} + 0.353 \right] \right\} \quad (A-34)$$

A comparison of \bar{E}_c^b and \bar{G}_c^b shows that only for very large values of f , when the elastic constants are essentially those of the matrix, is the condition of isotropy, $\bar{E}_c^b = 3 \bar{G}_c^b$ satisfied for the simple cubic array.

II. Face-Centered Cubic Array.

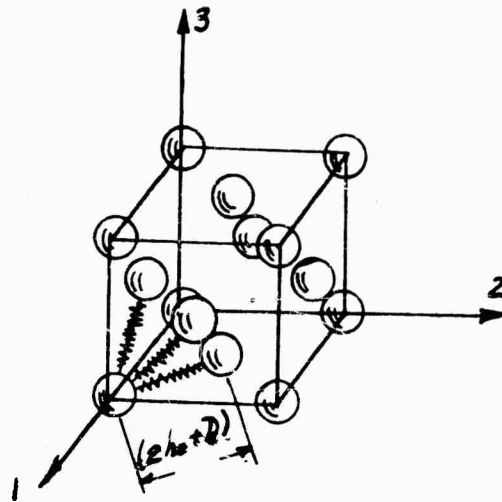
The method used for calculating the elastic constants of the face-centered cubic array, though based on the local stress and strain conditions between adjacent particles, is slightly different than that described for the simple cubic array. The ligaments between nearest neighbors were treated as springs able to resist separation and shear of the particles.

From the strain energy solution for the ligament the stiffness of the springs can be obtained.

Finally, the Young's and shear moduli for the cube can then be expressed in terms of all the springs between nearest neighbors,

Fig. (A-12). Although the strain energy contribution of the interstitial volume is not included because it is small, its presence is accounted for by restricting the deformation of the cube to give no volume changes. This means that the resulting elastic constants do not reduce

to the matrix constants for low volume density of filler but this restriction is not important in the range of volume fractions of interest.



By applying mechanics to the cube system the Young's and shear moduli in terms of the equivalent linear and shear springs of the ligament, K_T and K_S , is given by:

$$\bar{E}_c^h = \frac{3 K_T}{4\sqrt{2}D(1+f)} \left[\frac{(5+7\frac{K_S}{K_T})(1+\frac{K_S}{K_T})}{(2+\frac{K_S}{K_T})} \right] \quad (A-35)$$

Fig. (A-12)

$$\bar{G}_c^b = \frac{K_T}{\sqrt{2}D(1+f)} \left[1 + \frac{K_S}{K_T} \right] \cdot \quad (A-36)$$

Referring to Eq. (A-9), the strain energy for separation, for a ligament of radius $r = D/4$, is:

$$S.E. = \frac{\pi E \omega_0^2 D}{8f(1+8f)^2} \quad (A-37)$$

The spring rate, K_T , is then found from:

$$K_T = \frac{2 S.E.}{\omega_0^2} = \frac{\pi E D}{4f(1+8f)^2} \quad (A-38)$$

Similarly for the equivalent spring in shear; from Eq. (A-17) modified for a ligament of radius, $r = D/4$:

$$K_s = \frac{\pi E D}{3} \ln\left(\frac{1+8f}{8f}\right) \quad (A-39)$$

Substitution of these expressions in (A-35) and (A-36) results in Eqs. 3 and 5 of the Summary.

$$E_c^b = E \left\{ \left[\frac{\pi}{16\sqrt{2}f(1+f)(1+8f)^2} \right] \left[\frac{\{15+28f(1+8f)^2 \ln(\frac{1+8f}{8f})\}}{\{6+4f(1+8f)^2 \ln(\frac{1+8f}{8f})\}} \right] \right\} \quad (3)$$

(A-40)

$$\bar{G}_c^b = \frac{E}{3} \left\{ \left[\frac{\pi}{4\sqrt{2}f(1+f)(1+8f)^2} \right] \left[3 + 4f(1+8f)^2 \ln\left(\frac{1+8f}{8f}\right) \right] \right\} \quad (5)$$

(A-41)

It is interesting to note that the anisotropy of this array is small and for a value of the separation ratio close to $f = 0.2$ satisfies the condition for isotropy $E_c^b = 3\bar{G}_c^b$.

C. Randomness of Orientation of the Array of Particles

Average Elastic Constants

Since both arrays are anisotropic and in the large scale all possible orientations of the cube array would occur, it is necessary to find an average value for the elastic constants. In the averaging process the material becomes isotropic.

I. General Transformations

The general equations of elasticity can be expressed in terms of either influence coefficients S_{ijkl} or stiffness coefficients C_{ijkl} (called elastic moduli and elastic coefficients respectively by Jaeger⁽⁷⁾) where the subscript notation is that used by Hill⁽⁶⁾ and similar to that used by Sokolnikoff.⁽⁵⁾

$$\epsilon_{ij} = S_{ijkl} \sigma_{kl} \quad (A-42)$$

$$\sigma_{ij} = C_{ijkl} \epsilon_{kl} \quad (A-43)$$

The tensor transformation rules apply to the constants as well as to the stresses and strains. Thus, for example,

$$S_{abcd} = S_{ijkl} l_{ia} l_{jb} l_{kc} l_{ld} \quad (A-44)$$

$$\text{and} \quad \sigma_{ab} = \sigma_{ij} l_{ia} l_{jb} \quad (A-45)$$

where the "l"'s are the direction cosines between the subscripted coordinates.

With cubic symmetry only three independent constants exist and Poissons ratio $\nu = 1/2$. Using the subscripts 1, 2, 3 to refer to the cube axes, these are related to the general constants by,

$$\begin{aligned} \bar{S}_{1111}^b &= \frac{1}{E_c} = \bar{S}_{2222}^b, \text{ etc.} \\ \bar{S}_{2211}^b &= -\frac{\nu}{E_c} = \bar{S}_{3311}^b = \bar{S}_{1122}^b, \text{ etc.} \\ \bar{S}_{1212}^b &= \frac{1}{4G_c} = \bar{S}_{2121}^b = \bar{S}_{1313}^b, \text{ etc.} \\ \bar{C}_{1111}^b &= \frac{(1-\nu) E_c}{(1+\nu)(1-2\nu)} \\ \bar{C}_{2211}^b &= \frac{\nu E_c}{(1+\nu)(1-2\nu)} \\ \bar{C}_{1212}^b &= G_c \end{aligned} \quad (A-46)$$

$$(A-47)$$

In any coordinate orientation i, j, k, the elastic constants can be found in terms of the cube values through the transformation of Eq. (A-44).

The general transformation can be written in the form:

$$S_{ijkl} = \bar{S}_{1111}^b \delta_{ij} \delta_{kl} + \bar{S}_{1122}^b (\delta_{ik} \delta_{jl} + \delta_{il} \delta_{jk} - 2\delta_{ij} \delta_{kl}) - (\bar{S}_{1111}^b - \bar{S}_{1122}^b - 2\bar{S}_{1122}^b) (l_{1i} l_{1j} l_{2k} l_{2l} + l_{1i} l_{1j} l_{3k} l_{3l} + l_{2i} l_{2j} l_{3k} l_{3l} + l_{2i} l_{2j} l_{1k} l_{1l} + l_{3i} l_{3j} l_{1k} l_{1l} + l_{3i} l_{3j} l_{2k} l_{2l}) , \quad (A-48)$$

where the Kronecker delta is used.⁽⁵⁾ Specifically, the Young's modulus in any orientation is:

$$\bar{S}_{xxxx}^b = \bar{S}_{1111}^b - 2(\bar{S}_{1111}^b - \bar{S}_{1122}^b - 2\bar{S}_{1122}^b) (l_{1x}^2 l_{2x}^2 + l_{2x}^2 l_{3x}^2 + l_{3x}^2 l_{1x}^2). \quad (A-49)$$

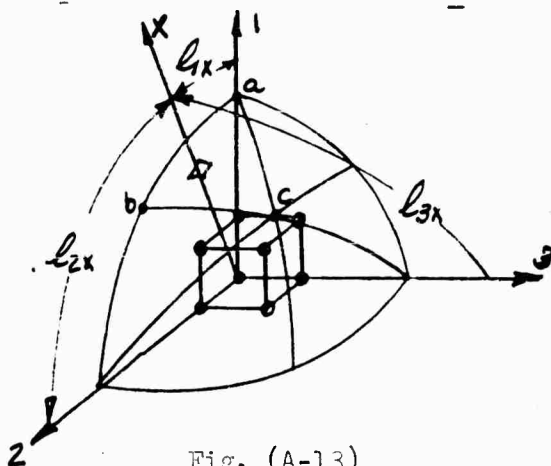
If the material is isotropic then $(\bar{S}_{1111}^b - \bar{S}_{1122}^b - 2\bar{S}_{1122}^b)$ is equal to zero and the constant is independent of orientation.

II. Lower Bound

To find the lower bound of the elastic constants, it is assumed that regions of cubic material exist in a tensile specimen in all orientations with equal probability. All the regions are assumed to have the same macroscopic stress $\bar{\sigma}_{xx}$ even though they will deform by different amounts and violate continuity unless the material is isotropic. The strain energy of any volume is:

$$\frac{d(S.E.)}{dV} = \frac{1}{2} \bar{\sigma}_{xx} \bar{E}_{xx} = \frac{1}{2} \bar{\sigma}_{xx}^2 \bar{S}_{xxxx}^b . \quad (A-50)$$

Fig. (A-13) shows a unit cube at a general orientation with respect to the tension axis \underline{x} . Because of cubic symmetry, it is possible



to get all values of \bar{S}_{xxxx}^b for orientations of the axis \underline{x} within the stereographic triangle "abc". The other triangles merely repeat the same values since the 1, 2, and

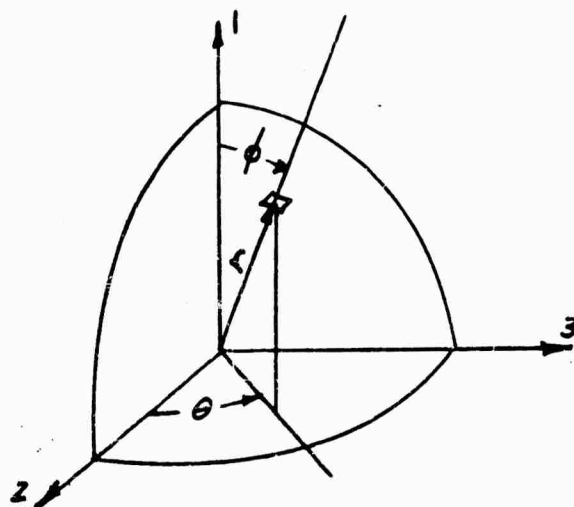


Fig. (A-14)

3 axes are interchangeable.

Using spherical coordinates as indicated in Fig. (A-14), the elemental surface of a unit sphere is:

$$dA = d\phi \cdot \sin\phi \cdot d\theta. \quad (A-51)$$

The average strain energy per unit volume for all possible

orientations can therefore be expressed as:

$$\text{avg. S.E. per unit vol.} = \frac{\int_0^{\pi/2} \int_0^{\pi/2} \frac{d(S.E.)}{dV} d\theta \sin\phi d\phi}{\text{Surface Area of Unit Sphere}} \quad (A-52)$$

Using the transformation from direction cosines to spherical coordinates: (8)

$$\begin{aligned} l_{1x} &= \cos\phi \\ l_{2x} &= \sin\phi \cos\theta \\ l_{3x} &= \sin\phi \sin\theta \end{aligned} \quad (A-53)$$

and from (A-49), (A-50), and (A-52) the average strain energy is found:

$$S.E. = \frac{\bar{\sigma}_{xx}^2}{2} \left\{ \bar{S}_{1111}^b - \frac{4}{\pi} \int_0^{\pi/2} \int_0^{\pi/2} (\bar{S}_{1111}^b - \bar{S}_{2222}^b - 2\bar{S}_{1212}^b) (\sin^2\phi \cos^2\theta \sin^2\theta + \sin^2\phi \cos^2\phi) d\theta d\phi \right\} \quad (A-54)$$

This strain energy can be written in terms of the average coefficient, \bar{S}_{1111LB}^b , with the lower bound subscript.

$$S.E. = \frac{\bar{\sigma}_{xx}^2}{2} \bar{S}_{1111}^b L.B. \quad (A-55)$$

Finally, equating the last two expressions and integrating:

$$\bar{S}_{1111}^b = \bar{S}_{1111}^b - \frac{2}{5} (\bar{S}_{1111}^b - \bar{S}_{1122}^b - 2 \bar{S}_{1212}^b) \quad (A-56)$$

Substituting according to (A-46) and recognizing that the material is incompressible:

$$\bar{E}_{LB}^b = \frac{\bar{E}_c^b \bar{G}_c^b}{0.400 \bar{G}_c^b + 0.200 \bar{E}_c^b} \quad \begin{matrix} (6) \\ (A-57) \end{matrix}$$

III. Upper Bound

A similar procedure is followed to find an upper bound for the elastic constants. In this case every cubic region is assumed to undergo the same macroscopic strain and, because of the different orientations the stresses are not in equilibrium. For the bonded material, with a Poisson ratio of $\nu = 1/2$ the strain in tension is $\bar{E}_{xx} = -\bar{E}_{yy}/\nu = -\bar{E}_{zz}/\nu$. This gives rise to three stresses according to Eq. (A-43).

$$\begin{aligned} \bar{\sigma}_{xx} &= C_{xxxx} \bar{E}_{xx} + C_{xxyy} \bar{E}_{yy} + C_{xxzz} \bar{E}_{zz} \\ \bar{\sigma}_{yy} &= C_{yyyy} \bar{E}_{yy} + C_{yyzz} \bar{E}_{zz} + C_{yyxx} \bar{E}_{xx} \\ \bar{\sigma}_{zz} &= C_{zzzz} \bar{E}_{zz} + C_{zzxx} \bar{E}_{xx} + C_{zzyy} \bar{E}_{yy} \end{aligned} \quad (A-58)$$

The strain energy unit volume is:

$$\begin{aligned} d(S.E.) &= \frac{1}{2} (\bar{\sigma}_{xx} \bar{E}_{xx} + \bar{\sigma}_{yy} \bar{E}_{yy} + \bar{\sigma}_{zz} \bar{E}_{zz}) \\ &= \frac{\bar{E}_{xx}^2}{2} \left\{ C_{xxxx} - \nu(C_{xxyy} + C_{xxzz}) - \nu(C_{yyxx} + C_{zzxx}) \right. \\ &\quad \left. + \nu^2(C_{yyyy} + C_{yyzz} + C_{zzyy} + C_{zzzz}) \right\}. \end{aligned} \quad (A-59)$$

Substitution for the stiffness coefficients in terms of the cube stiffnesses as in equation 41a and some algebra reduces this expression to:

$$d(S.E.) = \frac{\bar{E}_{xx}^2}{2} \left\{ (1+2\nu^2) C_{1111} - (4\nu-2\nu^2) C_{1122} \right. \\ \left. - 2(1+2\nu+\nu^2)(C_{1111}-C_{1122}-2C_{2212})(\ell_{1x}^2\ell_{2x}^2+\ell_{2x}^2\ell_{3x}^2+\ell_{3x}^2\ell_{1x}^2) \right\}. \quad (A-60)$$

Using the relation given in Eq. (A-47) and averaging for all orientations of the tension axis as was done for the lower bound gives the average strain energy per unit volume for the upper bound.

avg. S. E. per unit volume =

$$\frac{\bar{E}_{xx}^2}{2} \left\{ \bar{E}_c^b - \frac{2}{3}(1+2\nu+\nu^2) \left(\frac{\bar{E}_c^b}{(1+\nu)} - 2\bar{G}_c^b \right) \right\}. \quad (A-61)$$

This strain energy must equal the macroscopic value in terms of the average (upper bound) modulus.

$$S.E. = \frac{\bar{E}_{xx}^2}{2} \bar{E}_{u.B.}^b. \quad (A-62)$$

From these last two equations and noting that the material is incompressible, Eq. 6 of the Summary is obtained

$$\bar{E}_{u.B.}^b = 0.400 \bar{E}_c^b + 1.80 \bar{G}_c^b. \quad (A-63)$$

A comparison of the upper and lower bound values of the modulus is shown in Fig. 5 of the Summary.

D. Effect of Separation on the Elastic Properties During a Tension

Test in Terms of the Simple Cubic Array.

I. Conditions for Unbonding

For the particular case of simple tension, the change in the elastic constants can be estimated as the stress or strain conditions exceed the bond strength of the filler particles and matrix. Eq. (A-7) gives the hydrostatic stress between two spheres in terms of

the separation ($2w_0$) which in turn is related to the strain in the cube axis. Since the bonded material is assumed incompressible the strain in the cube direction is given by (3):

$$\bar{\epsilon}_{11} = \frac{2w_0}{D(1+f)} = \frac{3\bar{\sigma}_{11}'}{2\bar{E}_c} = \frac{3(\bar{\sigma}_{11} - \bar{\sigma})}{2\bar{E}_c} \quad (A-64)$$

where $\bar{\sigma}_{11}'$ is the macroscopic reduced stress and $\bar{\sigma}$ is the macroscopic hydrostatic stress. If all elements are assumed to have the same stress, $\bar{\sigma}_{xx}$, as for the lower bound solution, the stress in the cube orientation is:

$$\bar{\sigma}_{11}' = \bar{\sigma}_{xx} \ell_{1x}^2 - \frac{\bar{\sigma}_{xx}}{3} \quad (A-65)$$

These expressions, along with Eq. (A-7) give the hydrostatic stress in the ligaments in terms of the uniaxial stress at any orientation to the cube axis.

$$\begin{aligned} p &= - \left[\frac{3(1+f)(1+8f)}{8f^2(1+4f)^2 \bar{E}_c} E \right] (\bar{\sigma}_{xx} \ell_{1x}^2 - \frac{\bar{\sigma}_{xx}}{3}) \quad (A-66) \\ &= -K (\bar{\sigma}_{xx} \ell_{1x}^2 - \frac{\bar{\sigma}_{xx}}{3}) \end{aligned}$$

If C is the bonding strength and a superimposed hydrostatic stress, $\bar{\sigma}$ external, is permitted, the stress in the ligament will produce separation when:

$$-p = C - \bar{\sigma}_{external} - \frac{\bar{\sigma}_{xx}}{3} \quad (A-67)$$

Referring to Fig. (A-15), the direction cosine, ℓ_{1x} , is equal to $\cos \phi^*$. This cosine can be solved from Eqs. (A-66) and (A-67).

$$\cos \phi^* = \sqrt{\frac{(C - \bar{\sigma}_{ext} - \bar{\sigma}_{xx}/3)}{K \bar{\sigma}_{xx}}} + \frac{1}{3} \quad (A-68)$$

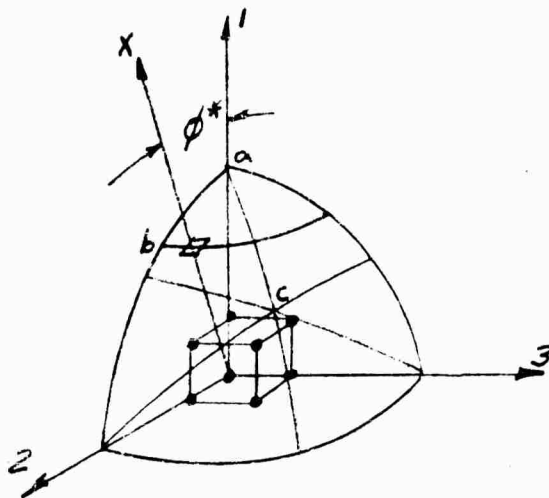


Fig. (A-15)

Further, ϕ^* increases indicating the region separated as in Fig. (A-15). Only the stereographic triangle "abc" needs to be considered since the other two axes are only repetitions of this orientation. As $\bar{\sigma}_{xx}$ becomes very large, $\cos \phi^*$ approaches a value of $1/\sqrt{3}$ which is the direction of the cube diagonal. Elements oriented in this direction relative to the tension axis separate when $\bar{\sigma}_{xx} = 3(C - \bar{\sigma}_{ext})$. It should also be noted that since K (Eq. (A-66)) is a function of the separation ratio, the macroscopic stress, $\bar{\sigma}_{xx}$, at which the bonding strength is overcome, depends on the volume density of filler.

If the macroscopic strains are specified for simple tension, as in the upper bound solutions, then the strains at which the bonds are broken can be expressed in terms of the strains. For a strain

$$\bar{\epsilon}_{xx} = -2\bar{\epsilon}_{yy} = -2\bar{\epsilon}_{zz} \text{ by the transformation rules:}$$

$$\begin{aligned} \bar{\epsilon}_{11} &= \bar{\epsilon}_{xx} \ell_{1x}^2 + \bar{\epsilon}_{yy} \ell_{1y}^2 + \bar{\epsilon}_{zz} \ell_{1z}^2 \\ &= \frac{\bar{\epsilon}_{xx}}{2} (3\ell_{1x}^2 - 1) = \frac{\bar{\epsilon}_{xx}}{2} (3\cos^2 \phi^* - 1) \end{aligned} \quad (\text{A-70})$$

Inspection of this equation reveals that as $\bar{\sigma}_{xx}$ is increased from zero, $\cos \phi^*$ has no meaning until $\bar{\sigma}_{xx}$ reaches the value for initial separation:

$$\bar{\sigma}_{xx} = \frac{3(C - \bar{\sigma}_{ext})}{2K + 1} \quad (\text{A-69})$$

At this point, $\cos \phi^* = 1$, so that the first elements to separate are orientated to coincide with the tension axis. As the stress is increased

From Eqs. (A-64) and (A-7) the hydrostatic pressure in the ligament can be written in terms of the strain.

$$p = -E \left[\frac{(1+f)(1+8f)}{4f^2(1+4f)^2} \right] \frac{\bar{E}_{xx}}{2} (3\cos\phi^* - 1) \quad (A-71)$$

$$= -E\bar{K} \frac{\bar{E}_{xx}}{2} (3\cos\phi^* - 1) .$$

When this pressure exceeds the bonding strength, separation of the material starts and the $\cos\phi^*$ can be found in terms of the strain

$$\cos\phi^* = \sqrt{\frac{2(C - \bar{\sigma}_{external})}{3E\bar{K}\bar{E}_{xx}}} + \frac{1}{3} \quad (A-72)$$

Inspection of this relation shows that as the strain is increased the material remains bonded until:

$$\bar{E}_{xx} = \frac{C - \bar{\sigma}_{external}}{\bar{K}E} \quad (A-73)$$

The first regions to separate are oriented with the tension axis.

As the strain is increased, the angle ϕ^* increases indicating the material separated.

II Elastic Constants in Unbonded Material

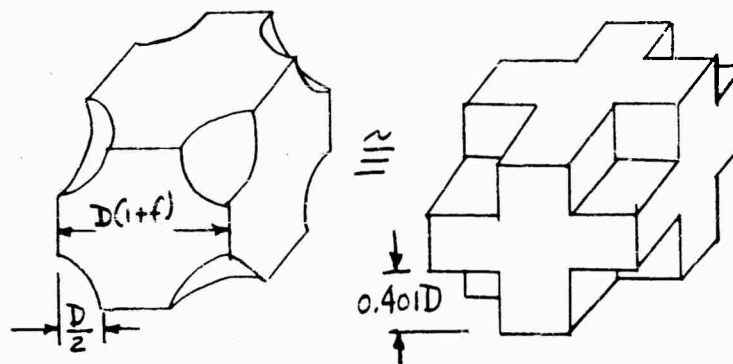
After the ligament separates from the spheres, the material in that region is relatively weak but can still carry some load. To obtain a modulus for the material having some separated regions it is necessary to average with the modulus of both the bonded and unbonded material. Right after separation at the ligaments the spheres undoubtedly have a partial bond and this would show up as anisotropy in a tensile specimen in the direction at right angles to the tension axis. However, the stiffness of the separated material will be very much smaller and eventually, as the strains increase,

the particles can be considered as totally unbonded. For this reason it is easier to estimate elastic constants assuming total separation of the spheres and to assume that this value obtains as soon as the ligament bond is broken.

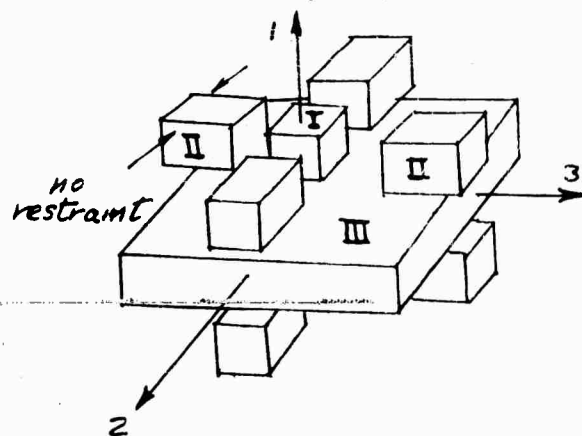
The estimate used for the elastic constants with no bonds neglects the interference of the spheres so that, in a sense, it is an estimate for the constants of a foam. This estimate was made by first taking the matrix volume per unit cube and considering a similar though simpler shape as shown in figure 14a which has the same volume. The material in this shape is broken up into sections

as shown in

Fig. (A-17). Under a tensile load, it was required that the load carried by sections I and II be equal to that in III,



(A-16)



(A-17)

that the strains of I and II be the same in the tensile direction, that the deformation across I and II in the 2 or 3 direction be the same as in element III (that faces remain plane), and that the net force on the sides be zero. Sections II are permitted to contract without restraint as indicated in the figure.

Solution of this model involves simple mechanics and gives the following constants with the superscript "u" for unbonded:

$$\bar{S}_{111}^u = \frac{1}{E} \left\{ 1 + \frac{1.04(2.21+f)}{(1+f)(0.195+f)[2(1+f)^2 + 4.03(1+f) + 3.24]} \right\} \quad (A-74)$$

$$\bar{S}_{112}^u = -\frac{1}{2E} \left\{ 1 + \frac{1.04}{(0.195+f)[2(1+f)^2 + 4.03(1+f) + 3.24]} \right\} \quad (A-75)$$

The ratio of these constants gives the Poisson ratio which varies from 1/2 for very light packing to about .35 for high volume densities.

For the shear stiffness, the volume shown in figure 14a was assumed to undergo a uniform shear strain, therefore estimating the modulus on the basis of volume.

$$\bar{S}_{1212}^u = \frac{3(1+f)^3}{4E[(1+f)^3 - 0.522]} \quad (A-76)$$

These constants practically satisfy the condition for isotropy, but for any other orientation the constants can be found as described previously. Particularly, the average values can be found from Eqs. (A-56) or (A-61).

III Approximate "Lower Bound" Solution

To find approximate solutions to the stress-strain behavior during a tensile test, two conditions were used. First, it was assumed that all the elements had the same stress and that as the stress increased regions would separate. By getting the strain

energy, the current stiffness could be found. In the second case it was assumed that all the elements had the same strain. These solutions are not true upper and lower bounds after the material starts to unbond since the material is changing in nature and at the same stress or strain the two solutions may not have equal amounts of unbonded material.

Referring to Fig. (A-18), if ϕ^* marks the limit of separated regions, the strain energy for a uniform stress, $\bar{\sigma}_{xx}$, is :

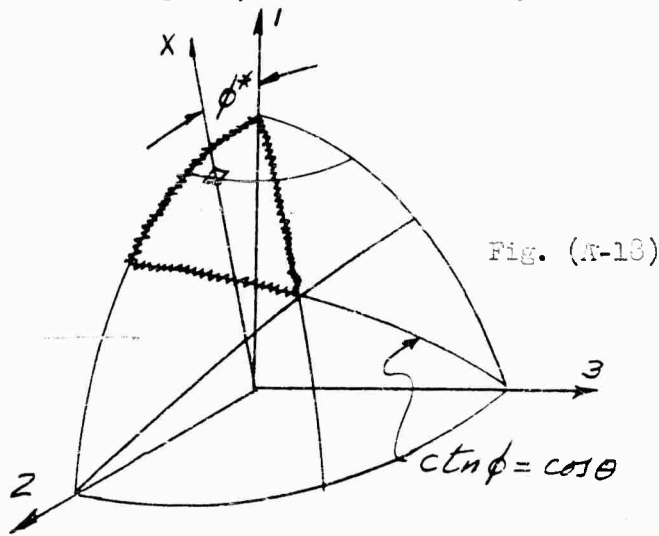


Fig. (A-18)

$$S.E. = \frac{\bar{\sigma}_{xx}^2}{2} \left\{ \frac{12}{\pi} \int_0^{\phi^*} \int_0^{\pi/4} \bar{S}_{xxxx} \sin \phi d\phi d\theta \right. \\ \left. + \frac{12}{\pi} \int_{\phi^*}^{\pi/4} \int_{\phi = ctn^{-1} \cot \theta}^{\pi/4} \bar{S}_{xxxx} \sin \phi d\phi d\theta \right\}.$$

(A-77)

Rearranging and substituting in terms of the elastic constants in the cube orientation, the current elastic constant \bar{S}_{IIILB} can be found.

$$\bar{S}_{IIILB} = \bar{S}_{IIILB}^b - \frac{12}{\pi} \int_0^{\pi/4} \int_0^{\phi^*} [(\bar{S}_{IIII}^b - \bar{S}_{IIII}^4) - 2(\bar{S}_{IIII}^b - \bar{S}_{IIII}^4 - \bar{S}_{II12}^b + \bar{S}_{II12}^4 - 2\bar{S}_{I121}^b + 2\bar{S}_{I121}^4) \\ (\sin^4 \phi \cos^2 \theta \sin^2 \theta + \sin^2 \phi \cos^4 \theta)] \sin \phi d\phi d\theta. \quad (A-78)$$

This integration, if carried beyond $\phi^* = 45^\circ$ must change the upper

limit on ϕ from ϕ^* to $\text{ctn}^{-1}(\cos \theta)$ since only one triangle is being used as indicated in Fig. (A-18).

Integration gives:

$$\begin{aligned} \bar{S}_{1111LB} = \bar{S}_{1111LB}^b - 3(\bar{S}_{1111}^b - \bar{S}_{1111}^u)(1 - \cos \phi^*) \\ - \frac{3}{20} [(\bar{S}_{1111}^b - \bar{S}_{1122}^b - 2\bar{S}_{1212}^b) - (\bar{S}_{1111}^u - \bar{S}_{1122}^u - 2\bar{S}_{1212}^u)] (-8 + 5\cos \phi^* + 10\cos^3 \phi^* - 7\cos^5 \phi^*). \end{aligned} \quad (\text{A-79})$$

The value of $\cos \phi^*$ is found from Eq. (A-68) so that for each value of stress $\bar{\sigma}_{xx}$, the current modulus $1/\bar{S}_{1111LB}$ is obtained in terms of the volume density (or \bar{f}), the elastic constant of the binder \underline{E} , and the bonding strength \underline{C} . The strain corresponding to the stress $\bar{\sigma}_{xx}$ can also be found and the stress-strain curve plotted.

IV Volume Change

From this analysis, the change in volume can also be estimated. For any element at any orientation the strain at right angles to the tension axis is:

$$\bar{E}_{yy} = \bar{S}_{yyxx}^{b \text{ or } u} \bar{\sigma}_{xx}, \quad \bar{E}_{zz} = \bar{S}_{zzxx}^{b \text{ or } u} \bar{\sigma}_{xx} \quad (\text{A-80})$$

The average of \bar{E}_{yy} and \bar{E}_{zz} can then be averaged for all orientations and from this total average strain and the stress, $\bar{\sigma}_{xx}$, the coefficient \bar{S}_{yyxxLB} can be found for any amount of unbonding.

$$\begin{aligned} \bar{S}_{yyxxLB} = -\frac{\bar{S}_{1111LB}^b}{2} + 3(\bar{S}_{1111}^b - \bar{S}_{1122}^u)(1 - \cos \phi^*) \\ - \frac{3}{40} [(\bar{S}_{1111}^b - \bar{S}_{1122}^b - 2\bar{S}_{1212}^b) - (\bar{S}_{1111}^u - \bar{S}_{1122}^u - 2\bar{S}_{1212}^u)] (-8 + 5\cos \phi^* + 10\cos^3 \phi^* - 7\cos^5 \phi^*). \end{aligned} \quad (\text{A-81})$$

Since the volume change is equal to the sum of the three principal strains:

$$\frac{\Delta V}{V} = \bar{E}_{xx} + \bar{E}_{yy} + \bar{E}_{zz} = (\bar{S}_{xxxxLB} + 2\bar{S}_{yyxxLB}) \bar{\sigma}_{xx} \quad (\text{A-82})$$

Substituting from (A-78) and (A-81) gives:

$$\frac{\Delta V}{V} = 3(\bar{S}_{111}^4 + 2\bar{S}_{112}^4) / (1 - \cos \phi^*) = \frac{3(12\nu^4)}{E_c^4} (1 - \cos \phi^*). \quad (\text{A-83})$$

The volume change is dependent on the stress, bonding strength, volume density of spheres, and elastic modulus of the binder.

V. Approximate "Upper Bound" Solution

The other solution, in which the strains are specified, is essentially the same. The expression arrived at is:

$$\begin{aligned} \bar{E}_{UB} = \bar{E}_{UB}^b - \frac{12}{\pi} \int_0^{\pi/4 \phi^*} \int_0^\pi \left\{ [\bar{E}_c^b - \bar{E}_c^4] - [2(1+2\nu^b + \nu^{4b}) \left(\frac{\bar{E}_c^b}{(1+\nu^b)} - 2\bar{G}_c^b \right) \right. \right. \\ \left. \left. - 2(1+2\nu^4 + \nu^{4^2}) \left(\frac{\bar{E}_c^4}{(1+\nu^4)} - 2\bar{G}_c^4 \right) \right] (\sin^4 \phi \cos^2 \theta \sin^2 \theta + \sin^2 \phi \cos^2 \phi) \right\} \sin \phi d\phi d\theta. \end{aligned} \quad (\text{A-84})$$

When integrated, the relationship is that given in the Summary:

$$\begin{aligned} \bar{E}_{UB} = \bar{E}_{UB}^b - 3(\bar{E}_c^b - \bar{E}_c^4)(1 - \cos \phi^*) \\ - \frac{3}{2G_c} \left\{ (1.5\bar{E}_c^b - 4.5\bar{G}_c^b) - (1+2\nu^4 + \nu^{4^2}) \left(\frac{\bar{E}_c^4}{(1+\nu^4)} - 2\bar{G}_c^4 \right) \right\} (-8 + 5\cos \phi^* + 10\cos^3 \phi^* - 7\cos^5 \phi^*). \end{aligned} \quad \begin{matrix} (\text{A-85}) \\ (10) \end{matrix}$$

From Eq. (A-72) the modulus \bar{E}_{UB} can be found in terms of the strain \bar{E}_{xx} and from this the stress-strain curve can be built up.

REFERENCES

- 1) "Study of Mechanical Properties of Solid Rocket Propellant," Aerojet General Corporation, Report No. 0411-100-1, 30 May, 1961.
- 2) "The Elastic Moduli of Heterogeneous Materials," by Z. Hashin, Harvard University, Division of Engineering and Applied Physics, Report No. 9, Contract Nonr 1062(02).
- 3) "Theory of Elasticity," by S. Timoshenko and J. N. Goodier, McGraw-Hill (Chp. 6, and pg. 10).
- 4) "Engineering Analysis," S. H. Crandall, McGraw-Hill.
- 5) "Mathematical Theory of Elasticity," E. S. Suhubi, McGraw-Hill (Chp. 3 and pg. 2).
- 6) "Mathematical Theory of Plasticity," R. Hill, Oxford (appendix).
- 7) "Elasticity, Fracture and Flow," J. C. Jaeger, Methuen (pp. 53-66).
- 8) "Advanced Calculus for Engineers," F. B. Hildebrand, Prentice Hall, (pg. 328).
- 9) "The Yield Surface in Normal Stress or Normal Strain Space," by P. J. Blatz, California Institute of Technology, Guggenheim Aeronautical Laboratory, CALCAP 54-10, August 1960.